

Lecture Notes in Civil Engineering

Dharamveer Singh
Lelitha Vanajakshi
Ashish Verma
Animesh Das *Editors*

Proceedings
of the Fifth
International
Conference
of Transportation
Research Group
of India

5th CTRG Volume 1

 Springer

Lecture Notes in Civil Engineering

Volume 218

Series Editors

Marco di Prisco, Politecnico di Milano, Milano, Italy

Sheng-Hong Chen, School of Water Resources and Hydropower Engineering,
Wuhan University, Wuhan, China

Ioannis Vayas, Institute of Steel Structures, National Technical University of
Athens, Athens, Greece

Sanjay Kumar Shukla, School of Engineering, Edith Cowan University, Joondalup,
WA, Australia

Anuj Sharma, Iowa State University, Ames, IA, USA

Nagesh Kumar, Department of Civil Engineering, Indian Institute of Science
Bangalore, Bengaluru, Karnataka, India

Chien Ming Wang, School of Civil Engineering, The University of Queensland,
Brisbane, QLD, Australia

Lecture Notes in Civil Engineering (LNCE) publishes the latest developments in Civil Engineering - quickly, informally and in top quality. Though original research reported in proceedings and post-proceedings represents the core of LNCE, edited volumes of exceptionally high quality and interest may also be considered for publication. Volumes published in LNCE embrace all aspects and subfields of, as well as new challenges in, Civil Engineering. Topics in the series include:

- Construction and Structural Mechanics
- Building Materials
- Concrete, Steel and Timber Structures
- Geotechnical Engineering
- Earthquake Engineering
- Coastal Engineering
- Ocean and Offshore Engineering; Ships and Floating Structures
- Hydraulics, Hydrology and Water Resources Engineering
- Environmental Engineering and Sustainability
- Structural Health and Monitoring
- Surveying and Geographical Information Systems
- Indoor Environments
- Transportation and Traffic
- Risk Analysis
- Safety and Security

To submit a proposal or request further information, please contact the appropriate Springer Editor:

- Pierpaolo Riva at pierpaolo.riva@springer.com (Europe and Americas);
- Swati Meherishi at swati.meherishi@springer.com (Asia - except China, and Australia, New Zealand);
- Wayne Hu at wayne.hu@springer.com (China).

All books in the series now indexed by Scopus and EI Compendex database!

More information about this series at <https://link.springer.com/bookseries/15087>

Dharamveer Singh · Lelitha Vanajakshi ·
Ashish Verma · Animesh Das
Editors

Proceedings of the Fifth International Conference of Transportation Research Group of India

5th CTRG Volume 1

 Springer

Editors

Dharamveer Singh
Department of Civil Engineering
Indian Institute of Technology Bombay
Mumbai, Maharashtra, India

Lelitha Vanajakshi
Department of Civil Engineering
Indian Institute of Technology Madras
Chennai, Tamil Nadu, India

Ashish Verma
Department of Civil Engineering
Indian Institute of Science Bangalore
Bengaluru, Karnataka, India

Animesh Das
Department of Civil Engineering
Indian Institute of Technology Kanpur
Kanpur, Uttar Pradesh, India

ISSN 2366-2557

ISSN 2366-2565 (electronic)

Lecture Notes in Civil Engineering

ISBN 978-981-16-9920-7

ISBN 978-981-16-9921-4 (eBook)

<https://doi.org/10.1007/978-981-16-9921-4>

© The Editor(s) (if applicable) and The Author(s), under exclusive license to Springer Nature Singapore Pte Ltd. 2022

This work is subject to copyright. All rights are solely and exclusively licensed by the Publisher, whether the whole or part of the material is concerned, specifically the rights of translation, reprinting, reuse of illustrations, recitation, broadcasting, reproduction on microfilms or in any other physical way, and transmission or information storage and retrieval, electronic adaptation, computer software, or by similar or dissimilar methodology now known or hereafter developed.

The use of general descriptive names, registered names, trademarks, service marks, etc. in this publication does not imply, even in the absence of a specific statement, that such names are exempt from the relevant protective laws and regulations and therefore free for general use.

The publisher, the authors and the editors are safe to assume that the advice and information in this book are believed to be true and accurate at the date of publication. Neither the publisher nor the authors or the editors give a warranty, expressed or implied, with respect to the material contained herein or for any errors or omissions that may have been made. The publisher remains neutral with regard to jurisdictional claims in published maps and institutional affiliations.

This Springer imprint is published by the registered company Springer Nature Singapore Pte Ltd. The registered company address is: 152 Beach Road, #21-01/04 Gateway East, Singapore 189721, Singapore

Preface

Transportation Research Group of India (TRG) is a not-for-profit registered society, which was established to bring all transportation researchers, academicians, and professionals on one platform to enable transportation research on problems faced in India and elsewhere and develop solutions for betterment. The TRG is celebrating completion of its 10 years.

TRG has brought this edited book titled *Proceedings of the Fifth International Conference of Transportation Research Group of India* in three volumes. Volume I of the book contains the papers on themes, TCT-A01: Pavements and materials, TCT-D01: Travel behaviour and transport demand, and TCT-H01: Emerging travel technology (ITS and IOT) Volume II contains the papers on the themes TCT-B01: Traffic flow theory, operations and facilities; TCT-C01: Transport planning, policy, economics and project finance, and TCT-I01: Other transportation modes (including NMT) and pedestrian. Likewise, Volume III contains the papers on the themes TCT-E01: Environment (including energy) and sustainability in transportation, TCT-F01: Transportation safety and security, and TCT-G01: Transport and mobility networks (including public transportation, freight and logistics). This book on conference proceedings is a compilation of quality research papers that are selected through a journal-style double-blind review process.

We acknowledge the support extended by Prof. Abdul Rawoof Pinjari and Prof. Gitakrishnan Ramadurai in managing the review process. This Volume I of the 5th Conference of TRG consists of 37 papers. Out of these, 31 papers are related to pavement and materials; 5 papers present works done in the travel behaviour and transport demand; and 1 paper has a focus on emerging travel technologies. Research areas covered under theme TCT-A01 include use of innovative materials, recycling and stabilization of highway materials, pavement managements and preservation techniques, characterization of binders, performance of various types of asphalt mixes, use of waste materials in asphalt mixes, concrete pavement, and innovative mixes. TCT-D01 covers new travel demand forecasting approaches, and TCT-H01 includes emerging technology for transportation application. We are quite hopeful that the papers contained in this volume, as well as in the other two volumes,

will be significantly useful to the future researchers in the area of Transportation Engineering.

Mumbai, India
Chennai, India
Bengaluru, India
Kanpur, India

Dharamveer Singh
Lelitha Vanajakshi
Ashish Verma
Animesh Das

About TRG and CTRG



Transportation Research Group of India (TRG) is a not-for-profit registered society with the mission to aid India's overall growth through focused transportation research, education, and policies in the country. It was formally registered on May 28, 2011, and has completed 10 years of its journey this year. The following are the vision and objectives of TRG.

Vision

- To provide a unique forum within India for the interchange of ideas among transportation researchers, educators, managers, policymakers from India and all over the world, with the intention of covering all modes and sectors of transport (road, rail, air, and water; public and private; motorized and non-motorized) as well as all levels (urban, regional, inter-city, and rural transport) and for both passenger and freight movement, in India, and at the same time to also address the transportation-related issues of safety, efficiency, economic and social development, local and

global environmental impact, energy, land-use, equity and access for the widest range of travellers with special needs, etc.

- To serve as a platform to guide and focus transportation research, education, and policies in India towards satisfying the country's needs and to assist in its overall growth.

Objectives

- To conduct a regular peer-reviewed conference in India so as to provide a dedicated platform for the exchange of ideas and knowledge among transportation researchers, educators, managers, and policymakers from India and all over the world, from a perspective which is multi-modal, multi-disciplinary, multi-level, and multi-sectoral, but with an India-centric focus. Initially, this conference will be held every two years; however, the frequency may change as per the decision of the society from time to time.
- To publish a peer-reviewed journal of good international standard that considers and recognizes quality research work done for Indian conditions, but which also encourages quality research focused on other developing and developed countries that can potentially provide useful learning lessons to address Indian issues.
- To conduct other activities such as seminars, training and research programs, meetings, discussions as decided by the society from time to time, towards fulfilling the mission and vision of the society.
- To identify pertinent issues of national importance, related to transportation research, education, and policy through various activities of the society and promote transportation researchers, educators, managers, and policymakers in an appropriate manner to address the same.
- To collaborate with other international societies and organizations like, WCTRS, ASCE, TRB, etc., in a manner that works towards fulfilling the mission and vision of the society.

The Conference of Transportation Research Group of India (CTRG) is the premier event of TRG. It is held every two years and traditionally moves around India. In the past, CTRG has been organized in Bangalore (December 2011), Agra (December 2013), Kolkata (December 2015), Mumbai (December 2017), Bhopal (December 2019), and Trichy (upcoming in December 2021 jointly with NIT Trichy, in association with IISc Bangalore, IIT Madras, IIT Palakkad and NATPAC). CTRG has been getting wide scale recognition from reputed Indian and international institutions/organizations like IIT Kanpur, IIT Kharagpur, IIT Guwahati, IIT Bombay (Mumbai), SVNIT Surat, MANIT Bhopal, NIT Trichy, TRB, WCTRS, CSIR-CRRI, ATPIO, T&DI-ASCE, EASTS, to name a few. CTRG is a large conference typically attended by around 400–500 participants, usually from 12 to 15 countries, with about 200 double-blind peer-reviewed technical papers being presented. The conference

provides a wide range of executive courses, tutorials, workshops, technical tours, keynote sessions, and special sessions.

Transportation in Developing Economies (TiDE) is the official journal of TRG and is published by Springer. TiDE was formally launched in 2014 and has so far published seven volumes.



Prof. Ashish Verma

Indian Institute of Science Bangalore
Founding and Immediate Past President, TRG



Prof. Akhilesh Kumar Maurya

Indian Institute of Technology Guwahati
Current President, TRG

List of Reviewers

Ramesh A., IIT Ropar
Rao A. Mohan, CRRI
Ganesh A. R., IIT Madras
Norhidayah Abdul Hassan, UTM Universiti Teknologi, Malaysia
Mukti Advani, CRRI
Amit Agarwal, IIT Roorkee
P. K. Agarwal, MANIT-Bhopal
Ruchika Agarwala, IIT Bombay
Juraidah Ahmad, Universiti Teknologi MARA
Notani Mohammad Ali, Purdue University
D. S. N. V. Amarkumar, Shell Bitumen, India
M. V. L. R. Anjaneyulu, NIT Calicut
Sabreena Anowar, University of Missouri
Uma Arepalli, Maine Department of Transportation
Shriniwas Arkatkar, NIT Surat
Ashutosh Arun, CSIR
Anil Kumar Bachu, IIT Patna
Rajneesh Bahari, Indian Army
Ranja Bandyopadhyaya, NIT Patna
Arunabha Banerjee, IIT Guwahati
Ipsita Banerji, IISc., Bangalore
Manik Barman, University of Minnesota, Duluth
Munwar Basha, IIT Hyderabad
Debasis Basu, IIT Bhubaneswar
Ambika Behl, CRRI
Ashik Bellary, KLS, VBIT
Reema Bera, IIT Kharagpur
P. R. Bhanumurthy, JNTU, Andhra Pradesh
Gottumukkala Bharath, CRRI
Ashish Bhaskar, Queensland University of Technology
Prithvi Bhat, Queensland University of Technology

Sudip Bhattacharjee, Alabama A&M University
 Tanmoy Bhowmik, University of Central Florida
 Sasanka Bhushan, VIT University, Vellore
 Prasanta Bhuyan, NIT-Rourkela
 Mehek Biswas, IISc., Bangalore
 Nomesw Bolia, IIT Delhi
 Bhaswati Bora, IIT Kanpur
 Anuj Budhkar, IEST Shibpur, West Bengal
 Anush Chandrappa, IIT Bhubaneswar
 Arti Chaudhary, CRRI
 Akhilesh Chepuri, Sreenidhi Institute of Science and Technology, Ph.D. from SVNIT
 Munavar Fairooz Cheranchery, TKM College of Engineering, Kerala
 BhargavaRama Chilukuri, IIT Madras
 Tanuj Chopra, Thapar Institute of Engineering and Technology
 Pushpa Choudhary, IIT Roorkee
 Rajan Choudhary, IIT Guwahati
 Venkaiah Chowdary, NIT Warangal
 Saurabh Dandapat, IIT Kharagpur
 Atasi Das, GR Infratech
 Bibhutibhusan Das, NIT Surathkal
 Pritikana Das, CSIR, CRRI
 Sanhita Das, IIT Guwahati
 Subasish Das, Texas A&M University
 Vivek R. Das, Dayanand Sagar College of Engineering, Kerala
 Venkata Santosh Kumar Delhi, IIT Bombay
 Ravi Deshpande, Indian Army
 Partha Pratim Dey, IIT Bhubaneswar
 P. V. Divya, IIT Palakkad
 Venkata Ramana Duddu, University of North Carolina, Charlotte
 Madhu Errampalli, CRRI
 Galkin Andrii, O. M. Beketov National University of Urban Economy in Kharkiv,
 Kharkiv, Ukraine
 Tejash Gandhi, Kao-Corporation
 Venu Garikapati, National Renewable Energy Laboratory, NREL
 G. S. Ghataora, University of Birmingham, UK
 Indrajit Ghosh, IIT Roorkee
 Kaniska Ghosh, IIT Kharagpur
 Ripunjoy Gogoi, Amity University
 S. S. V. Gopalaraju, MVGR College of Engineering
 Sutapa Goswami, University of Calcutta
 Bharath Gottumukkala, CRRI
 Shiva Kumar Govindaraju, University of Pisa UNIPI, Italy
 Bivina G. R., IIT Roorkee
 Pradip Gundaliya, L. D. College of Engineering, Gujarat
 Ankit Gupta, IIT BHU

Sanjay Gupta, School of Planning and Architecture, Delhi
Ayyanna Habal, IIT Bombay
Mohd. Rosli Hainin, UTM Universiti Teknologi, Malaysia
Md. Bashirul Haque, University of Leeds, UK
Shimul Haque, Queensland University of Technology
Gayathri Harihan, IISc., Bangalore
Vasant Havangi, CRRI
Simon Hesp, Queen's University, Canada
Praveen Idara, University of Missouri, USA
Suresh Immanuel, University of Evansville
Norfarah Nadia Ismail, International Islamic University, Malaysia
Abhijith Iyengar, IIT Madras
Nur Izzi, UKM National University of Malaysia
Bhavesh Jain, IIT Roorkee
Subham Jain, IIT Kanpur
Udit Jain, IIT Roorkee
Nataraju Jakkula, CSIR
Lalita Jangpangi, CSIR
Ashok Julaganti, NIT Warangal
Raghuram Kadali, Sri Vasavi Engineering College, Andhra Pradesh
Nurul Hidayah Kamaruddin, Universiti Tun Hussein Onn Malaysia, UTHM
Venkatesan Kanagaraj, IIT Kanpur
Siksha Kar, CRRI
Gunasekaran Karuppanan, Anna University, Tamil Nadu
Aniket Kataware, IIT Bombay
Ankit Kathuria, IIT Jammu
Ravinder Kayitha, CRRI
Ahmad Khan, Queen's University, UK
Durgarani Korlapati, Andhra University, Andhra Pradesh
Suhana Koting, University of Malaysia
Rajesh Krishnan, Imperial College of London, UK
Ambika Kuity, NIT Silchar
Venu Madhav Kukkapalli, University of North Carolina, Charlotte
Aditya Kumar, IIT Bombay
Anjan Kumar, IIT Guwahati
Anupam Kumar, Delft University
Binod Kumar, CRRI
Prabin Kumar, IIT Bombay
Rajiv Kumar, NIT Jalandhar
Ravindra Kumar, CRRI
Vasantha Kumar, VIT, Vellore
Molugaram Kumar, UCE, Osmania University, Hyderabad
Phani Kumar Patnala, Echelon Institute of Technology, Haryana
Kranti Kumar Kuna, IIT Kharagpur
Ganeshbabu K. V., Amaravati Development Corporation, Andhra Pradesh

Deepa L., TKM College of Engineering, Kerala
Sam Labi, Purdue University, USA
K. M. Laxmanrao, JNTUH College of Engineering, Hyderabad
Harikrishna M., NIT Calicut
Shashi M., Indian School of Mines
Manoj M., IIT Delhi
Nivedya M. K., Worcester Polytechnic Institute WPI, USA
Nagabhushana M. N., CRRI
Geetimukta Mahapatra, IIT Guwahati
Smruti Sourava Mohapatra, IIT-ISM Dhanbad
Saurabh Maheshwari, University of California, Davis
Ramesh Chandra Majhi, CRRI
Avijit Maji, IIT Bombay
Bandhan Majumdar, BITS Pilani, Hyderabad
Haritha Malladi, Lafayette College, NYC
C. Mallikarjuna, IIT Guwahati
Ajinkya Mane, University of North Carolina, Charlotte
Bappaditya Manna, IIT-Delhi
Samson Mathew, NIT Trichy
Gabriella Mazzulla, University of Calabria, Italy
Arpan Mehar, NIT Warangal
Prakash Mehta, Tawata Technology, Gujarat
Swati Mitra, IIT Kharagpur
Abhishek Mittal, CRRI
Mithun Mohan, NIT Karnataka
Ranju Mohan, IISc., Bangalore
Abhisek Mudgal, IIT BHU
Caleb Munigety, IISc., Bangalore
Dasaka Murty, IIT Bombay
Sai Kiran Myakuntla, IISc., Bangalore
Lohit Kumar Nainegali, IIT Dhanbad
Syam Nair, IIT Kanpur
Prakash Nanthagopalan, IIT Bombay
Binanda Narzary, Tezpur University
Akhandappagol Ningappa, NIT-K, Surathkal
Sangram Nirmale, IISc., Bangalore
Seckin Ozkul, University of South Florida
Rajesh Paleti, Pennsylvania State University
Pan Pan, Queen's University, Canada
Mahabir Panda, NIT Rourkela
Anurag Pande, California Polytechnic State University
Manoranjan Parida, IIT Roorkee
Purnima Parida, CBRI
Bhaskar Paul, IIT Kharagpur
Digvijay Pawar, IIT Hyderabad

Praveena Penmetsa, University of Alabama
Vedagiri Perumal, IIT Bombay
C. S. R. K. Prasad, NIT Warangal
Prashant Prasad, IIT Kharagpur
M. Lakshmi Vara Prasad, NIT Silchar
G. V. R. Prasadaraju, JNTU Kakinada, Andhra Pradesh
Sushma Prusty, IIT Bombay
Farzana Rahman, University of Asia-Pacific
Bharat Rajan, IIT Bombay
Sridhar Raju, BITS Pilani, Hyderabad
Gitakrishnan Ramadurai, IIT Madras
Ayothiraman Ramanathan, IIT Delhi
T. V. Ramanayya, NIT Warangal
G. D. Ransinchung, IIT Roorkee
K. Ramachandra Rao, IIT Delhi
Sita Rami Reddy, VNIT, Nagpur
Amaranatha Reddy, IIT Kharagpur
K. S. Reddy, IIT Kharagpur
Padma Rekha, SRM Institute of Science and Technology
S. Rokade, MANIT, Bhopal
Sandeepan Roy, IIT Bombay
Minal S. CRRI
Shankar Sabavath, NIT Warangal
Nikhil Saboo, IIT BHU
Romeil Sagwal, CSIR
Dulal Saha, University of Waterloo
Amarendra Kumar Sahoo, GMR Infrastructure Ltd.
Umesh Chandra Sahoo, IIT Bhubaneswar
Prasant Sahu, BITS Pilani, Hyderabad
Jagadish Prasad Sahu, IIT Roorkee
Subbarao Saladi, Mahindra Ecole College of Engineering, Hyderabad
Moses Santhakumar, NIT Trichy
Binu Sara, College of Engineering, Trivandrum
Goutham Sarang, VIT Vellore
Sajitha Sasidharan, IISc., Bangalore
Shobhit Saxena, IISc., Bangalore
Robert Schneider, School of Architecture and Urban Planning, University of Wisconsin, Milwaukee
Padma Seetharaman, CSIR
Ravi Sekhar, CSIR
Sathish Kumar Selvaraj, University of Melbourne
Yogesh Shah, IITRM Ahmedabad
K. V. R. Ravi Shankar, NIT Warangal
S. Shankar, NIT Warangal
Ravi Shankar S., CRRI

Niraj Sharma, CSIR
R. Shivashankar, NIT Surathkal
Burhan Showkat, IIT Bombay
Manoj Shukla, CRRI
Raj Sidharthan, University of Nevada
Gourab Sil, BITS Pilani
Bhupendra Singh, NIT Patna
Dharamveer Singh, IIT Bombay
Priyansh Singh, BITS Pilani
Rina Singh, CRRI
Varun Singh, MNNIT, Allahabad
Anil Kumar Sinha, CRRI
Kalaanidhi Sivagnanasundaram, Technion Israel Institute of Technology
M. Sivakumar, NIT Calicut
R. Sivananadan, IIT Madras
Anand Sreeram, Hong Kong Polytechnic University; Visiting Scholar at University of Texas
R. Srinivasakumar, Osmania University, Hyderabad
Karthik K. Srinivasan, IIT Madras
Y. Sudheerbabu, Nimra College of Engineering and Technology, Andhra Pradesh
Sanjeev Kr. Suman, NIT Patna
V. Sunitha, NIT Trichy
S. N. Suresha, NIT Karnataka
Mansha Swami, IIT Roorkee
Aravind Krishna Swamy, IIT Delhi
Subba Rao Swarna, Survey of India, Dehradun
Deprizon Syamsunur, UCSI University, Malaysia
Rahul T. M., IIT Ropar
Shams Tanvir, North Carolina State University
Manoj Tipnis, L&T
Devesh Tiwari, CRRI
Lelitha Vanajakshi, IIT Madras
Harsha Vajjarapu, IISc., Bangalore
Sudhir Varma, IIT Patna
Nagendra Velaga, IIT Bombay
K. Venkatarreddy, NIT Warangal
Veena Venudharan, IIT Palakkad
A. Veraragavan, IIT Madras
Ashish Verma, IISc., Bangalore
Meghna Verma, Ramaiah Institute of Management, Bangalore
Durgesh Vikram, BITS Pilani
V. Vinayaka Ram, BITS Pilani, Hyderabad
Guru Vittal, CRRI
Haryati Yaacob, Universiti Teknologi Malaysia
Shamsunnahar Yasmin, Queensland University of Technology, Australia

Contents

Experimental Studies on Bio-bitumen Produced Using Charcoal from Coconut Shell Waste	1
Nishant Garg, Tanuj Chopra, and Anush K. Chandrappa	
Planning for Demand Responsive Bus Service for Limited Area Using Simulation	21
Sharmeela Kale and Premjeet Das Gupta	
A Heuristic Method of Prioritizing Flexible Pavement Sections	51
V. S. Sanjay Kumar and Abin Joseph	
Effect of Compaction Levels on Moisture Susceptibility in Asphalt Mix	67
A. Jegan Bharath Kumar and Anoop. T. Vijayan	
Rutting Characterisation of EVA Modified Bitumen for High Modulus Asphalt Mixes (HiMA)	81
B. Anil Kumar, Gautam Gaurav, Kranthi Kuna, M. Amaranatha Reddy, and K. Sudhakar Reddy	
A Review on the Use of Alternative Materials as a Sustainable Approach in the Manufacture of Concrete Paver Blocks	93
Sumit Nandi and G. D. R. N. Ransinchung	
Activity-Based Model: Requisite for a New Travel Demand Forecasting Approach for India	109
Suchismita Nayak and Debapratim Pandit	
Analysis of Falling Weight Deflectometer (FWD) Data of a Flexible Pavement Using Two Different Programs	123
Shubham Mishra, Rakesh Kumar Srivastava, Pradeep Kumar, and Tanuj Chopra	

Understanding the Preferences and Attitudes of App-Based Taxi Users Toward Existing Modes	135
Punyabeet Sarangi, M. Manoj, and Geetam Tiwari	
Estimation of Trip Generation Rates for Different Landuses for an Indian City	155
Ashish Verma and Shubhayan Ukil	
Economic and Environmental Analysis of Adaptation Strategies to Mitigate Impact of Climate Change on Pavements	165
Megha Sharma, Sundeeep Inti, and Vivek Tandon	
Performance Analysis of Black Cotton Soil Treated with Dimensional Limestone (Kota Stone) Slurry Waste	179
Pradeep Kumar Gautam, Pravesh Saini, Pawan Kalla, Ajay Singh Jethoo, and Harshwardhan Singh Chouhan	
Experimental Investigation on the Feasibility of Using Construction Demolition Waste Materials for Subbase Layer in Flexible Pavement	193
R. Chandra Prathap and U. Salini	
Condition Assessment of Reinforced Concrete Bridge Deck Using Infrared Thermography	201
Vidhi Vyas, Ajit Pratap Singh, and Anshuman Srivastava	
A Purpose Based Trip Distribution Gravity Model for an Indian City	211
V. S. Sanjay Kumar and M. V. L. R. Anjaneyulu	
Effect of Jarosite as Partial Replacement of Fine Aggregate in Pavement Quality Concrete Mixes	223
Dinesh Ganvir and Binod Kumar	
Comparison of Various Approaches for Evaluation and Overlay Design of a Concrete Pavement	231
Shubham Mishra, Rakesh Kumar Srivastava, Pradeep Kumar, and Tanuj Chopra	
Investigating the Intention to Use Metro Services: A Behavioral Approach	247
Anshamol N. Rahim, Jomy Thomas, and Vishnu Baburajan	
Determining Optimum Antistripping Additive Content in Asphalt Mixtures Using Boil Test	263
Shivpal Yadav, Abhilash Kusam, Zahra M. Tayebali, and Akhtarhusein A. Tayebali	

Characterization of Nano-Alumina Modified Asphalt Binders and Mixtures 275
 Pubali Nazir, Rajan Choudhary, Abhinay Kumar, and Ankush Kumar

Soil Stabilization Using Waste Plastic 289
 Aiswarya Govind and Anjan Patel

Utilization of E-waste Plastic as Aggregate Replacement in Bituminous Concrete Mixes 299
 Abhitesh Sachdeva and Umesh Sharma

Investigation of Physical and Chemical Properties in RAP Materials ... 311
 Kajugaran Santhirasegaram, Wasantha Kumara Mamppearachchi, and Dharamveer Singh

Application of New-fangled Tools and Techniques in Data Collection for Asset Management System for Urban Road Network in India 319
 Bhavesh Jain, Manoranjan Parida, Devesh Tiwari, and Ramesh Anbanandam

Structural Design of the Pervious Concrete Pavements: A Computational Mechanics Approach 339
 Avishreshth Singh, M. Nithyadharan, Prasanna Venkatesh Sampath, and Krishna Prapoorna Biligiri

PG Grading of Bitumen Using Capillary and Brookfield Viscometers 351
 Akanksha Pandey, Sham S. Ravindranath, and Sridhar Raju

Studies on Temperature Differential for Different Types of Overlay Over Cement Concrete Pavement 365
 M. Varuna, Deepak Raikar, and S. Sunil

Utilization of Waste Materials for Productions of Sustainable Roller-Compacted Concrete Pavements—A Review 377
 Solomon Debbarma, G. D. Ransinchung R.N., Surender Singh, and Surya Kant Sahdeo

Design of Experimental Approach for Optimization of Foam Bitumen Characteristics 397
 Fadamoro Oluwafemi Festus, Siksha Swaroopa Kar, and Devesh Tiwari

Analysis of Short-Term Ageing Mechanism of Pyro-oil Modified Bitumen Compared to VG30 Based on FTIR Spectroscopy 413
 Hemantkumar P. Hadole and Mahadeo S. Ranadive

Impact on Resilient Modulus Values of the Bituminous Mixture Using Different Standard Methods	425
Aditya Singh, Devesh Tiwari, A. P. Singh, Tanuj Chopra, and Anush K. Chandrappa	
Selection of Bitumen in Indian Condition	439
Swapan Kumar Bagui, Atasi Das, and Yash Pandey	
Compaction Characteristics of Marshall Mould at Refusal Density	449
Swapan Kumar Bagui, Atasi Das, and Yash Pandey	
Experimental Investigation on the Effect of Microwave Heating Technique on the Healing Characteristics of Bituminous Concrete Mixtures	463
Satya Lakshmi Aparna Noojilla and Kusam Sudhakar Reddy	
Utilization of Waste Ethylene-Propylene-Diene-Monomer (EPDM) Rubber Modified Binder in Asphalt Concrete Mixtures	477
Ankush Kumar, Rajan Choudhary, and Abhinay Kumar	
Assessing the Suitability of Polyethylene Terephthalate (PET) in Bituminous Concrete Mixes	495
Mohit Chaudhary, Nikhil Saboo, and Ankit Gupta	
Experimental Investigation of Resilient Modulus of Various Bituminous Mixes	507
Swapan Kumar Bagui, Atasi Das, Yash Pandey, and Kishan Vachhani	

About the Editors

Dr. Dharamveer Singh is an Associate Professor in Department of Civil Engineering, Indian Institute of Technology Bombay. Dr. Singh graduated from MBM Engineering College Jodhpur, Rajasthan in 2000. He completed his M.Tech. in Transportation Engineering from IIT Kharagpur in 2004. Dr. Singh holds a Ph.D. from University of Oklahoma, Norman, USA. Dr. Singh actively works in areas of asphalt binder rheology, stabilized pavement layers, recycling of pavements, performance of asphalt mixes, and material and test protocol development. He has published over 100 referred journal papers. Dr. Singh is an active member of several committee of Indian Roads Congress. Dr. Singh has been Active Reviewer of several leading national and international journals, also he is serving as an editorial board member of leading journals.

Dr. Lelitha Vanajakshi is a Professor in the Transportation Division of the Department of Civil Engineering at IIT Madras. She holds a Ph.D. from Texas A&M University, USA. Her teaching and research interests are in the general area of transportation systems with emphasis on traffic flow modelling, traffic operations, and intelligent transportation systems. She has published more than 70 journal publications and more than 100 conference papers. She serves in various editorial boards and is Member of various national and international societies. She has been involved in 15 research projects and has graduated more than 10 M.S./Ph.D. scholars.

Dr. Ashish Verma is currently a Professor of Transportation Engineering in the Department of Civil Engineering and Centre for infrastructure, Sustainable Transportation, and Urban Planning (CiSTUP) and Robert Bosch Centre for Cyber Physical Systems (RBCCPS) at Indian Institute of Science (IISc), Bangalore, India. Before joining IISc, he served at IIT Guwahati, and Mumbai Metropolitan Region Development Authority. His research interests are in sustainable transportation planning, public transport planning and management, modeling and optimization of transportation systems, travel behavior, driver behavior and road safety, intelligent transportation system (ITS), traffic management etc. He has authored more than 120 research publications in the area of sustainable transportation and road safety. He is Associate

Editor of Springer journal *Urban Rail Transit*. He is Current and Founding President of Transportation Research Group of India.

Dr. Animesh Das is a Professor in the Department of Civil Engineering, IIT Kanpur. Dr. Das's area of expertise is pavement material characterization, analysis, design, and evaluation. He is interested in both theoretical as well as experimental studies. He has worked on problems related to characterization of asphalt mix and aggregates, asphalt recycling, asphalt micromechanics, microstructure and image analysis of asphaltic material, pavement design optimization, pavement surface characterization etc. He has published several papers in various journals and conference proceedings of repute.

Experimental Studies on Bio-bitumen Produced Using Charcoal from Coconut Shell Waste



Nishant Garg, Tanuj Chopra, and Anush K. Chandrappa

1 Introduction

In India, viscosity grade 30 (VG30) binder is most commonly used in pavement applications other than national and state highways. It is the last residue in the fractional distillation of crude petroleum and harder than VG10 and VG20 bitumen. Bitumen is a viscoelastic material having hydrocarbons, which softens gradually when heated and hardens at low temperature [1]. More than 80% of the highways are made of bituminous mixtures in the world [2]. During the last few years, many distress like pothole, edge cracking, corrugation, etc. were observed in the flexible pavement with rutting and fatigue cracking being the major distresses. These distresses are mainly due to repetitive overloaded commercial vehicles, high temperature, incorrect mix design, and climate conditions. The rutting of bituminous mixtures mainly involves subsidence/depression along the wheel path causing permanent deformation. Due to the depression of the surface, water get accumulates in ruts and this water further deteriorates the pavement. As a result, bituminous pavement possess insufficient structural adequacy before the end of design period and increase the maintenance cost of the pavement [3]. The other factor is the poor quality of bitumen and inadequate physical and rheological properties (resistance to rutting and fatigue cracking), which leads to structural and functional distresses. Several types of modifiers and additives are used to enhance the physical and rheological properties of the bituminous binder [4].

N. Garg · T. Chopra · A. K. Chandrappa (✉)
Department of Civil Engineering, Thapar Institute of Engineering and Technology, Patiala,
Punjab, India
e-mail: akc@iitbbs.ac.in

T. Chopra
e-mail: tchopra@thapar.edu

© The Author(s), under exclusive license to Springer Nature Singapore Pte Ltd. 2022
D. Singh et al. (eds.), *Proceedings of the Fifth International Conference of Transportation Research Group of India*, Lecture Notes in Civil Engineering 218,
https://doi.org/10.1007/978-981-16-9921-4_1

As bitumen shares 40% contribution to reduce rutting in bituminous mixtures [5], many organizations are studying modified bitumen with various additives such as polymers, crumb rubber, hydrated lime, and natural rubber to improve the performance ability of bitumen in mixtures [6]. However, high raw materials costs, high production costs, storage issues, and limitations in availability as per demands have seen reduced utilization of such modified binders. In order to find an alternative with sustainability considerations, modifiers derived from the bio-waste are gaining attention among the bitumen technologists. As bio-wastes are known to create environmental hazard by consuming land for filling and altering the properties of natural ground soil over time, a sustainable solution needs to be developed to utilize them effectively. Owing to their better compatibility with bitumen and lower cost, modification of bitumen using bio-wastes is gaining attention among bitumen technologists to investigate the influence of bio-wastes on performance of bitumen. Naturally occurring materials such as palm oil fuel ash and rice husk ash are used as additives to modify the base binder to enhance the rheological properties and performance of the bitumen [7]. Among several bio-waste materials, coconut shell charcoal powder has more potential of being one of the bio-waste modifiers due to high carbon content and fine nature for better dispersion. Coconut shell is an agricultural waste and is richly available; it is also discharged by various industries [8]. Among other countries, India is ranked third in production of coconut all over the world with an annual production of 21,500 million tons [9]. In India, more than 15 states and union territories produce coconuts. Tamil Nadu ranked on top with more than 31% share of the total production of coconut in India. Coconut shell is lightweight, extremely strong, rigid and eco-friendly due to biodegradability and emission of carbon dioxide is in low amount when burnt [8, 10] and microscopic image of the coconut shell reveals that the surface of coconut shell is very rough which increase the compressive strength in composite structure [11, 12].

The main aim of this paper is to utilize coconut shell waste as charcoal powder with their unique characteristics as additive in binder modification to investigate the physical and rheological properties of bio-bitumen by using dynamic shear rheometer (DSR).

2 Objective and Scope

The objective of this research was to evaluate rheological performance of the bitumen modified using charcoal powder and understand the permanent deformation characteristics using multiple stress creep-recovery (MSCR) test. The scope of the research study included:

- Modification of bitumen with charcoal powder at various percentages
- Determination of basic properties of modified bitumen
- Determination of complex shear modulus and phase angle

- Determining percent recovery and creep compliance of modified bitumen
- Understanding the stress sensitivity of modified bitumen

3 Materials and Methods

3.1 Bituminous Binder

Viscosity grade 30 (VG30) control bituminous binder was used in this research, which was procured from construction site in Barnala city, Punjab. For modification purpose, 750 g of control binder was taken for each percentage of coconut charcoal powder.

3.2 Preparation of Micromaterial

The coconut shell charcoal as shown in Fig. 1a was powdered in Los Angeles abrasion machine to produce the finer size particles. The crushed material was sieved through 75 μm sieve to obtain fine material for modification as shown in Fig. 1b.

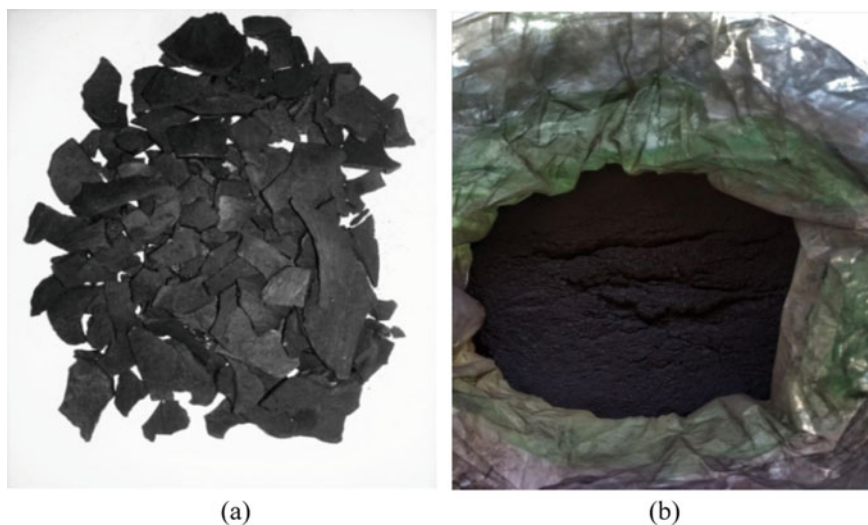


Fig. 1 a Coconut shell charcoal, b micro charcoal powder

Fig. 2 Blending machine

3.3 Blending Process

The microcharcoal powder was added at various percentages, which included 1, 2, 3, and 4% by weight of bitumen. The blending process was done with shear mixture having 1750 rpm at constant temperature of 150 °C for 60 min. The mixing time, temperature, and speed were tentatively chosen for uniform dispersion of charcoal powder in the bitumen. The blender used in the mixing process is shown in Fig. 2.

3.4 Basic Bitumen Property Tests

Penetration test

Penetration test is the simplest test to determine the consistency of the bitumen. The modified bitumen was heated up to pouring consistency while stirring continuously. The hot bitumen was poured on standard cup and allowed to cool at room temperature for 90 min. Further, it was conditioned in water bath maintained at 25 °C for 1 h. Penetration test was done as per IS 1203 [13].

Softening point

The softening point is an important test to determine the temperature at which bitumen changes phase from solid to flow-able phase. The test was conducted as per IS: 1205 [14] using ring and ball apparatus. Bitumen was heated between 100 and 110 °C or above until it was completely fluid and poured into the rings and allowed to cool down for 30 min in room temperature. The excess bitumen was trimmed with hot knife and placed on the metallic support. After that, trimmed sample was placed in the water bath maintained at 5 °C for 15 min, and then two steel balls having weight of 2.5 g with centering guide were placed on the each ring in the liquid and heated. The temperature at which the bitumen touches the base plate placed at distance of 25 mm below rings was recorded as softening point.

Storage stability test

The addition of modifiers in bitumen tends to settle at the bottom when stored for long duration. In addition, large differences in densities between bitumen and modifier may lead to issues in stability for storage. In order to determine the storage stability of bitumen modified with coconut charcoal powder, storage stability test was performed as per IS-15642 [15] and ASTM D5976 [16]. About 50–55 gm of modified bitumen was poured into the steel pipes having 1 mm thickness, diameter of pipe was 25.4 mm (1 in.) and height was 150 mm. The sealed steel pipes with modified bitumen were conditioned in oven for 24 h at 163 °C. Following this, hot modified bitumen was placed in the deep freezer for four hours. The steel pipes with frozen modified bitumen were cut into three equal parts. The softening points of top and bottom portion were tested to determine the softening temperature.

Strain sweep and oscillation tests

The bitumen being viscoelastic in nature has a characteristic region where applied oscillating shear stress is proportional to shear strain rate, which is referred to as linear viscoelastic region. In order to determine the linear viscoelastic region of unaged bitumen, strain sweep test was conducted at different strain levels of: 2, 4, 6, 8, 10, 12, 14, and 16%. The linear viscoelastic range was determined such that the reduction in complex shear modulus shall not be less than 0.95 times the complex shear modulus corresponding to 2% strain. Further, the oscillation test was carried out to determine the complex shear modulus and phase angle of bitumen within the determined LVR. The test was conducted as per AASHTO T-315 [17] on a 25 mm diameter sample and 1 mm thickness at a temperature of 65 °C; representing pavement surface temperature during peak summer and loading frequency was 1.57 Hz and 4% strain to ensure the measurement in linear viscoelastic region.

Multiple stress creep recovery (MSCR)

MSCR test was conducted to evaluate the stress sensitivity and recovery behavior at 65 °C, which gives an indication of resistance to permanent deformation. The test was conducted as per AASHTO TP70 [18, 19] which uses percentage recovery (%R) as shown in Eq. 1 and non-recoverable creep compliance (J_{nr}) as shown in Eq. 2 to describe the elastic and plastic state of the unaged bituminous binder using dynamic

shear rheometer (DSR). The sample was placed between the parallel plate assembly with 25 mm diameter and 1 mm gap between the plates. Ten creep-recovery cycles were run on each different stress levels of 0.1, 1, 2 and 3.2 kPa to understand the stress sensitivity of control and modified binders. One cycle in MSCR test consists of 1 s of creep loading followed by 9 s of recovery. Two parameters, which includes: percentage recovery (%R) indicating the amount of recovery achieved in binder during recovery period and non-recoverable creep compliance indicating the amount of residual strain left in the binder were calculated from the creep-recovery data.

- % Recovery equation:

$$\varepsilon_r = \frac{(\varepsilon_1 - \varepsilon_{10})}{\varepsilon_1} \times 100 \quad (1)$$

where,

- ε_r Percentage recovery.
- ε_1 Strain value at the end of creep portion.
- ε_{10} Strain value at the end of recovery portion.

- Non-recoverable creep compliance equation (J_{nr}) kPa^{-1} :

$$J_{nr} = \frac{\text{Non - recovered strain}}{\text{Stress}(0.1, 1, 2, 3.2\text{kPa})} \quad (2)$$

The different tests conducted on bitumen are shown in Fig. 3.

4 Results and Discussion

4.1 Penetration Test

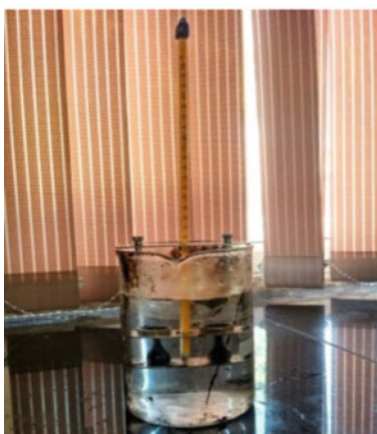
Table 1 shows that penetration value of modified binder decreases at certain limit as the addition of MCP content increases. The reductions in penetration value of modified binder were 19.07, 24.52, 17.1, and 14.99% as compared with control binder for 1%, 2%, 3% and 4% addition, respectively. The maximum reduction was 24.52% for 2% addition of MCP.

4.2 Softening Point

The softening point test results indicated that the softening point temperature initially showed an increasing trend up to 2% as shown in Table 1. The softening point of



(a)



(b)



(c)



(d)

Fig. 3 a Penetration test, b softening point test, c storage stability test, d dynamic shear rheometer (DSR)

Table 1 PI of C.B and modified binder

MCP (%)	Penetration test, 1/10th mm	Softening point test, °C	PI
0	61	47.5	-1.380
1	50	55.0	-0.045
2	46	57.5	0.325
3	51	58.0	0.656
4	52	58.0	0.721

control binder was 48 °C, whereas the softening point temperature at 2% addition was 58 °C indicating a 10 °C increase in softening point. After 2%, any further addition did not show significant increase in the softening point temperature.

4.3 Penetration Index (PI) or Temperature Susceptibility

The PI value for control and modified binder was calculated from Eq. 3 [8]. From Table 1, the PI value of control binder is less than -1 indicating that it is highly susceptibility to temperature. However for modified binders, the value of PI is approaching to + 1 and more than control binder indicating that addition of MCP, the modified binder has low susceptibility to temperature and resist the rutting and cracking in permanent deformation.

$$PI = \frac{(1951.4 - 500\log P - 20S.P)}{(50\log P - S.P - 120.14)} \quad (3)$$

where,

P Penetration value.

S.P Softening point value.

4.4 Storage Stability Test

Table 2 shows the results of storage stability test. It can be seen that the differences in the top and bottom portion of the specimen are within the prescribed limit. The addition of charcoal powder in bitumen does not lead to any storage stability concerns.

Table 2 Storage stability test

Microcharcoal powder (MCP) (%)	Difference between top and bottom parts specimen (°C)	Specification: <2.2 °C
1	1.2	Ok
2	0.9	Ok
3	1.4	Ok
4	1.0	Ok

4.5 Complex Shear Modulus (G^*)

Complex shear modulus is obtained from oscillation sweep test and is the ratio of maximum shear stress to maximum shear strain. It gives the total resistance of binder to deformation and also characterizes the elastic and viscous behavior of the binder at medium to high temperature. Higher complex shear modulus gives the better resistance to flow deformation and improves the rutting performance of the binder. Figure 4 shows the complex shear modulus (G^*) at different content of MCP, and it was observed that complex shear modulus was increasing as content of MCP increased. However, after 2% addition, the complex shear modulus starts to decrease. The probable reason for initial increase in complex shear modulus could be due to the fact that the charcoal powder was well dispersed up to certain level providing enhanced filler effect. However, increased addition might have cause flocculation leading to improper dispersion of modifier resulting in lack of synergistic effect. It implies that excessive addition of MCP reduces the performance of binder and decreases resistance to flow deformation. Sample containing 2% MCP gives the higher value of complex shear modulus and shows better resistance to deformation of binder as compared with control binder.

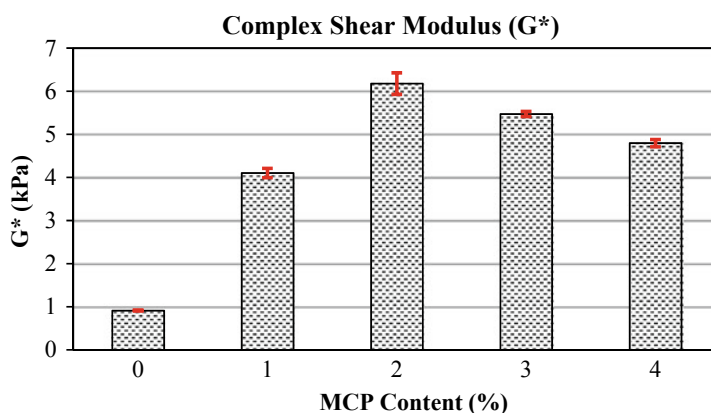


Fig. 4 Complex shear modulus at different MCP content. *Error bar indicates one standard deviation

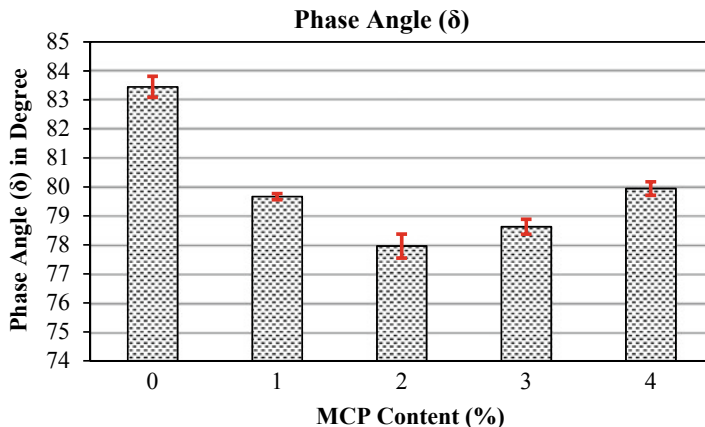


Fig. 5 Phase angle at different MCP content. *Error bar indicates one standard deviation

4.6 Phase Angle (Δ)

Phase angle is the time lag between shear strain and shear stress of binder under test condition. Along with complex modulus, phase angle is also the parameter which defines the viscous and elastic components of binder. Generally, binder having phase angle $0-45^\circ$ shows elastic nature and $45-90^\circ$ shows viscous nature [20]. Figure 5 shows that for control binder, the lag between shear strain and shear stress was more, indicating highly viscous property, but with the addition of MCP, the lag starts to decrease indicating better elastic property. The minimum time lag is obtained at 2% of MCP which helps to retard rutting parameter, while excessive addition of MCP increases the phase angle. The increase in phase angle beyond 2% addition may be due to the fact that the applied shear stress is shared more by the bitumen due to lack of proper dispersion of charcoal powder particles.

4.7 Loss Factor-Tan(δ)

Loss or damping factor is related to storage moduli (G') and loss moduli (G'') and defined as the ratio of viscous component of complex modulus and elastic component of complex modulus as shown in Eq. 4. It describes the average energy dissipation in continuous steady oscillation dynamic test. Figure 6 shows that the loss factor for control binder is higher than the modified binders. However, with the addition of MCP, loss factor starts decreasing resulting in reduction, thus showing elastic behavior [21]. Lower loss factor can easily correlate the binder with more rutting resistance performance and improve the elastic properties and vice versa. The minimum loss factor was achieved at 2% addition of MCP content.

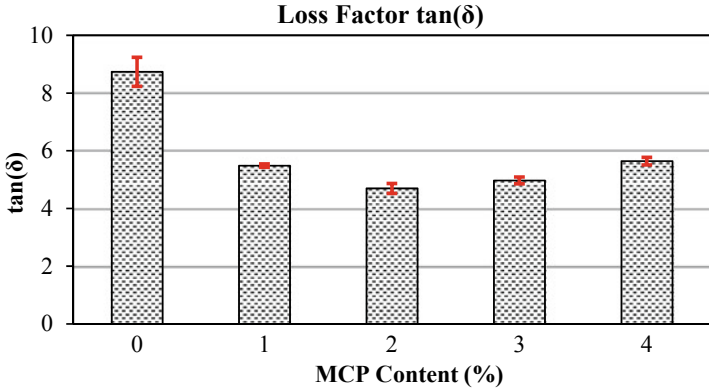


Fig. 6 Loss factor at different MCP content. *Error bar indicates one standard deviation

$$\tan \delta = \frac{G''}{G'} \tag{4}$$

4.8 Rutting Performance Indicator ($|G^*|/\sin(\delta)$)

Rutting performance indicator is considered as an important parameter to evaluate the rutting resistance and elastic property of the binder at 65 °C and 10 rad/s frequency [22]. From Fig. 7, addition of MCP causes the increase in rutting parameter as compared to the control binder. The highest value of ($|G^*|/\sin(\delta)$) was achieved at 2% of MCP content which means maximum resistance to permanent deformation of bituminous binder. Rutting parameter increases with MCP but after 2% content of

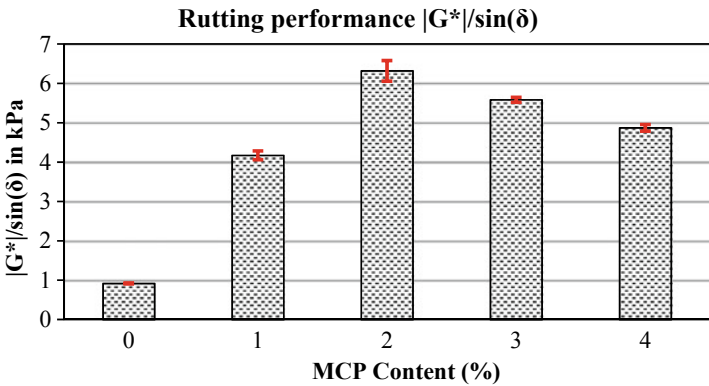


Fig. 7 Rutting performance at different MCP content. *error bar indicates one standard deviation

MCP, rutting parameter start decreasing. The analysis shows that it makes the binder stiff than the control binder by making the strong and cohesion bond between MCP and bituminous binder.

4.9 Multiple Stress Creep-Recovery Test (MSCR)

MSCR is a test in performance grading of binder performed according to AASHTO TP70 [18] which uses the high temperature to evaluate the rutting performance of the bituminous binder. This test analyzes the potential of binder to permanent deformation under creep loading and recovery, which are simulative of field loading. From Fig. 8, it is observed that control binder (CB) has higher creep strain for all creep stress levels. The addition of charcoal powder in the bitumen significantly improved the creep-recovery behavior of the bitumen indicating enhanced rutting performance. The %strain underwent by the modified binder for a given stress level reduced significantly when MCP was added in the bitumen. This can be mainly attributed to the filler effect of coconut charcoal powder, where the applied creep load is shared between charcoal powder and bitumen enhancing the stiffness of bitumen leading to lower strain.

The percentage recovery (% R) and non-recoverable creep compliance (J_{nr}) are calculated according to the AASHTO TP70 [18] using Eqs. 1 and 2 and are shown in Fig. 9. It can be seen that addition of coconut charcoal powder in bitumen initially increased the recovery and decreased the J_{nr} . But after 2% addition, there was decrease in recovery and increase in J_{nr} . This behavior can be due to the fact that as the content of coconut charcoal was increased initially, there was uniform and homogeneous distribution. However, after 2% addition, there is a possibility of agglomeration of charcoal powder leading to lack of homogeneous distribution where the effect of charcoal powder was reduced. In addition, an interesting observation was that the control binder showed negative recovery even at 0.1 kPa stress level indicating the control bitumen was highly rut susceptible [23]. The negative recovery can be either due to low quality bitumen, where after removal of creep load, the binder still experienced creep load or the equipment was not capable of unloading immediately at the end of creep cycle. As negative recovery was not observed in modified bitumen, it can be stated that the control binder had very low rut resistance. This clearly signifies the effect of charcoal addition, which improved the creep-recovery behavior. In all Figures from 9a–d, error bars indicate one standard deviation.

4.9.1 Stress Sensitivity

In addition to recovery and J_{nr} , another important parameter is stress sensitivity, which indicates behavior of bitumen for changes in stress levels. This is very important from field considerations as pavements are subjected to different type of loads,

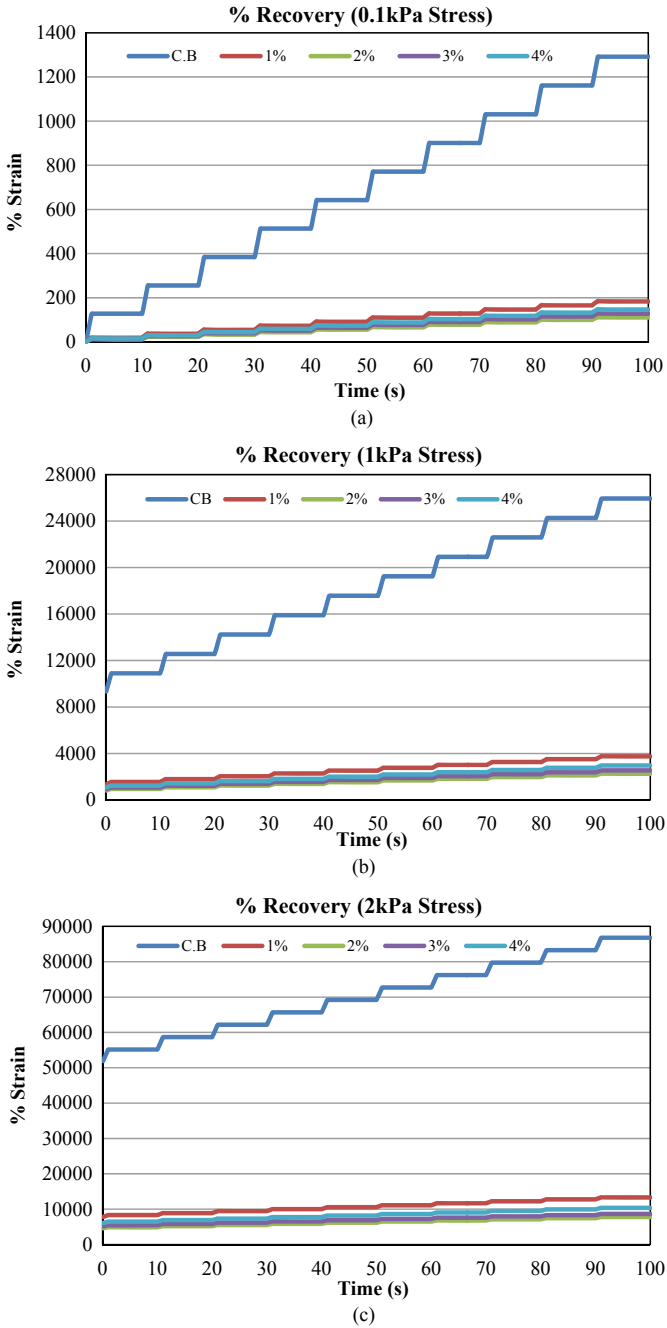


Fig. 8 Effect of different creep stresses on control and modified binder, %strain versus time graphs: **a** at 0.1 kPa creep stress, **b** at 1 kPa creep stress, **c** at 2 kPa creep stress, **d** at 3.2 kPa creep stress

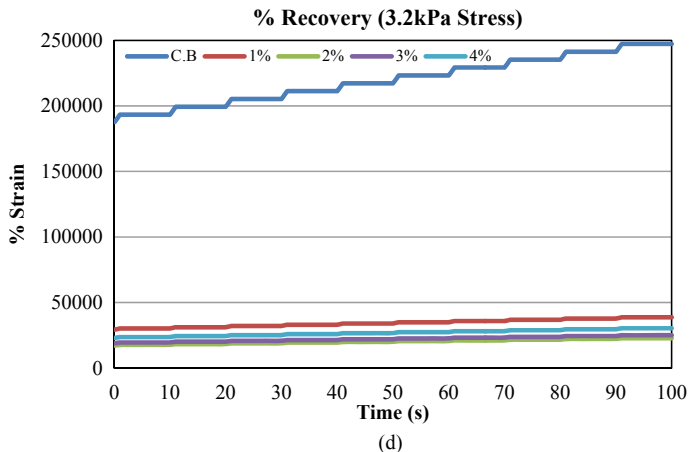


Fig. 8 (continued)

which may change bitumen property significantly, if it is stress sensitive. To understand the stress sensitivity, binders were subjected to different stress levels. Stress sensitivity indicates the behavior of binder when it is subjected to different magnitudes of stresses. A more stress sensitive binder may not perform intended function [24]. Figure 10 shows a plot of J_{nr} and %recovery for control binder and modified binder with 2% addition of MCP. It is seen that for control binder, J_{nr} increasing drastically, when creep stress change from 0.1 to 1.0 kPa. However, in case of binder with 2% MCP, no significant increase in J_{nr} was found when creep stress levels were increased. This behavior of binder modified with MCP clearly indicates that it is less stress sensitive and does not yield for changes in stress levels even at high temperatures such as 65 °C.

5 Discussions

Based on the above rheological tests, it can be observed that at the addition of 2% coconut shell, charcoal powder by weight maximized the desirable properties of bitumen to resist permanent deformation. It was postulated that the homogeneous dispersion of charcoal powder at 2% addition might be the reason for the typical observation. In order to investigate this further, image of bitumen consisting of different percentage of charcoal powder was taken at microscopic level using scanning electron microscope (SEM). The modified bitumen was initially super-cooled in liquid nitrogen to break the bitumen without disturbing the dispersion of particles inside the bitumen. The SEM images of bitumen at different percentages of coconut shell charcoal are shown in Fig. 11. The images shown are the fractured surface of bitumen when it is super-cooled with liquid nitrogen. It can be seen that

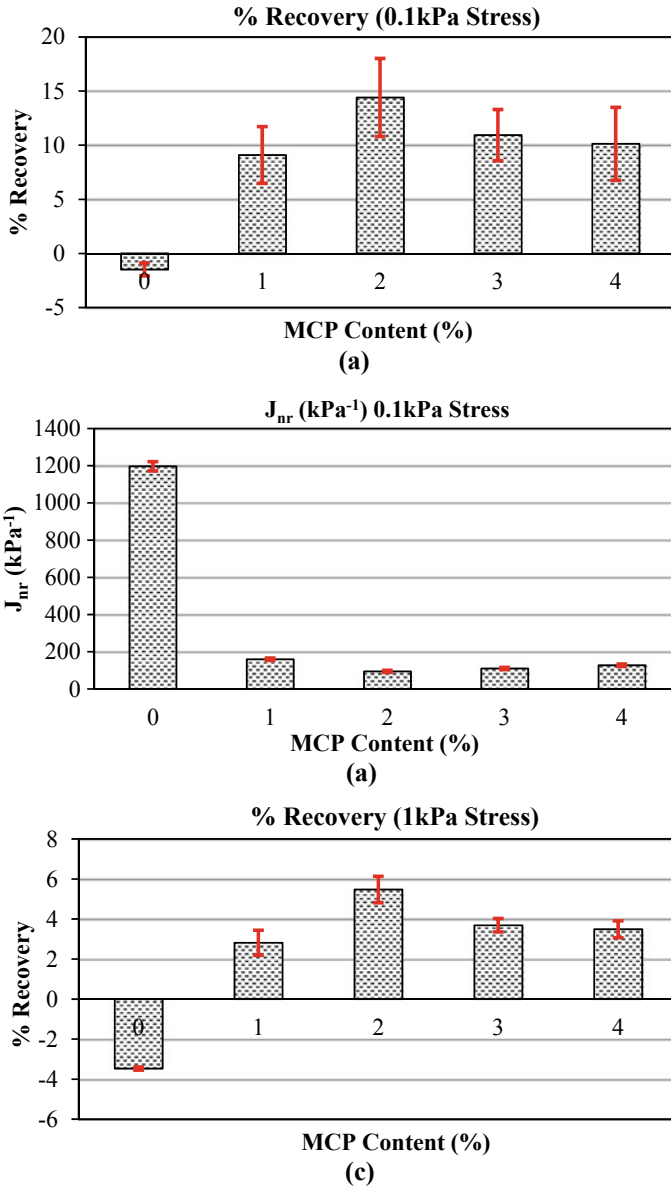


Fig. 9 Effect of different creep stresses on control and modified binder on %recovery and J_{nr} : **a** at 0.1 kPa creep stress, **b** at 1 kPa creep stress, **c** at 2 kPa creep stress, **d** at 3.2 kPa creep stress

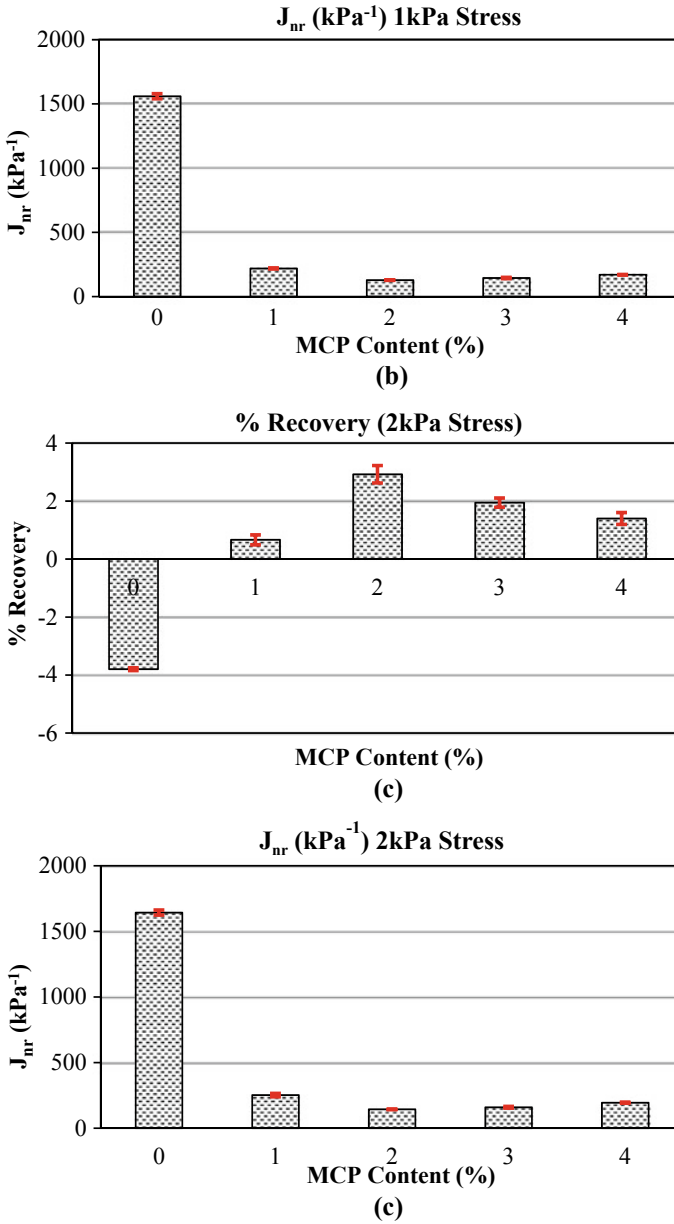


Fig. 9 (continued)

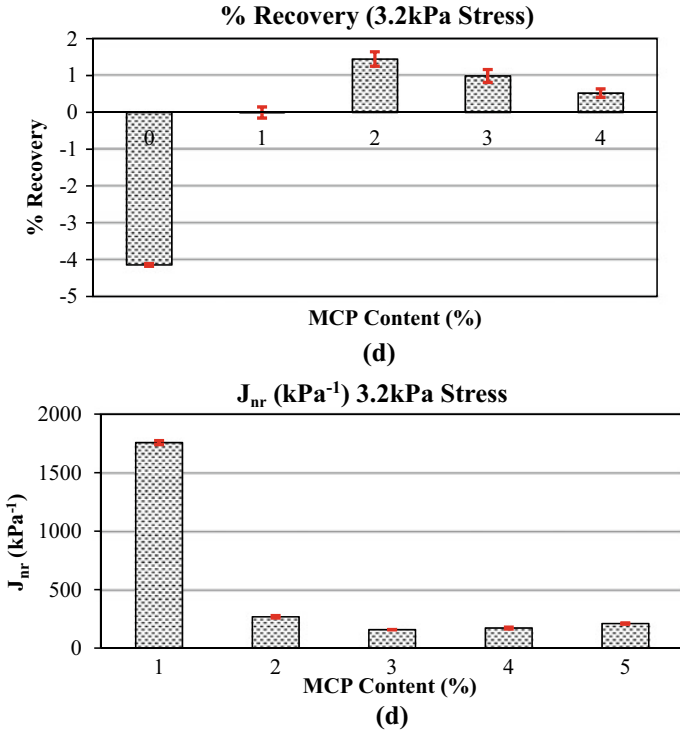


Fig. 9 (continued)

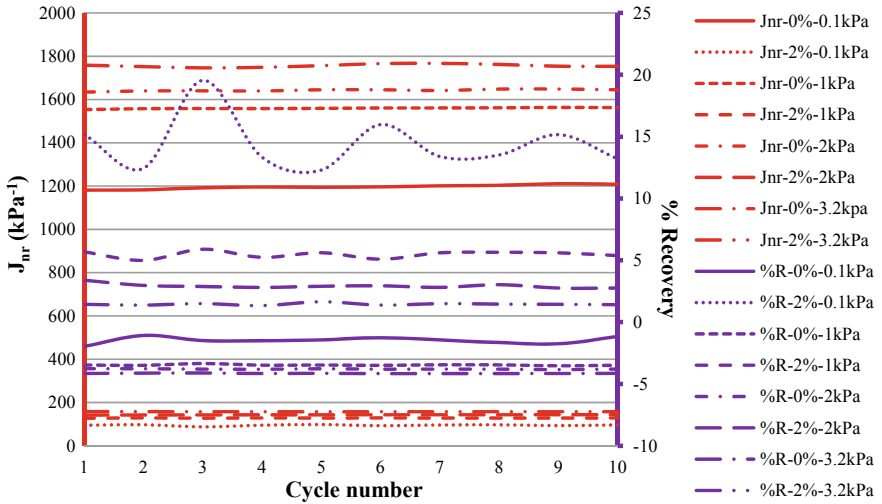


Fig. 10 Non-recoverable creep compliance and percent recovery for ten creep-recovery cycle of MSCR test at different stress level

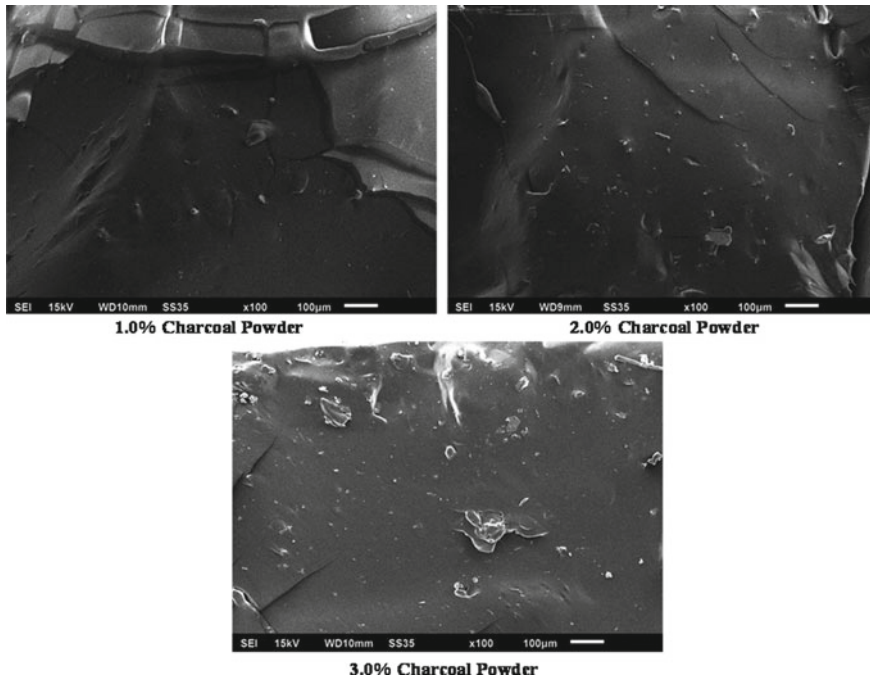


Fig. 11 SEM images of bitumen modified with coconut shell charcoal powder

1.0% charcoal powder seems to be dispersed scarcely as very few particles are seen on the fractured surface. However at 2.0%, the particles seem to be dispersed in a homogeneous matter. This type of dispersion helps in improving the permanent deformation characteristics as particles reinforce the bitumen to the maximum extent. But as the addition of particles increases, such as 3.0% in this case, particles start forming agglomerations (*shown as large spots in the image*) leading to heterogeneous dispersion reducing the reinforcing effect.

6 Conclusion

Modified bitumen is gaining attention due to increased loading of vehicles and climate change. This study attempted in understanding the physical and rheological behavior of bitumen modified with coconut shell charcoal, which is a bio-waste. The binder used was VG30, which is mostly used in pavements other than national and state highways. Based on the experimental study, the following conclusions can be made:

1. The addition of coconut shell charcoal was compatible with the bitumen as indicated by the storage stability tests. This gives provision to store the modified bitumen for longer duration without any significant changes in the properties.

2. The penetration of bitumen decreased, while the softening point increased with the addition of MCP to some extent. The improvement in softening point increases the usable temperature without any phase change. The rheological properties such as complex shear modulus showed an increasing and then decreasing trend with the addition of MCP, which was mainly due to stiffening effect. The elastic property was improved by addition of MCP as indicated by phase angle.
3. The MSCR test clearly signified the improvements in modification of bitumen using MCP. The percent recovery increased significantly, while the J_{nr} reduced indicating better permanent deformation resistance of the modified bitumen. Further, the modified binder was found to be significantly less stress sensitive in comparison to control binder.
4. The negative %recovery found in control binder was eliminated after addition of 1% MCP indicating the minimum improvements, which can be obtained with the addition of bio-materials in bitumen.
5. Overall, 2% addition by weight of bitumen was found to be optimum for the modification, which balanced all the physical and rheological properties.

References

1. Shrote Vinod K, Shukla M H.P Bitumen handbook. Hindustan Petroleum Corporation Limited, Mumbai
2. Chen M, Leng B, Wu S, Sang Y (2014) Physical, chemical and rheological properties of waste edible vegetable oil rejuvenated asphalt binders. *Constr Build Mater* 66:286–298
3. Moghaddam TB, Karim MR, Abdelaziz M (2011) A review on fatigue and rutting performance of asphalt mixes. *Sci Res Essays* 6(4):670–682
4. Hunter RN, Self A, Read J (2014) *The Shell Bitumen Handbook*, 6th edn. Institution of Civil Engineering (ICE), London
5. Yao Z, Zhang J, Gao F, Liu S, Yu T (2018) Integrated utilization of recycled crumb rubber and polyethylene for enhancing the performance of modified bitumen. *Constr Build Mater* 170:217–224
6. Rusbintardjo G, Hainin Mohd R, Yusoff Nur Izzu Md (2013) Fundamental and rheological properties of oil palm fruit as modified bitumen. *Constr Build Mater* 49:702–711
7. Hussin MW, Lim NHAS, Sam ARM, Ismail MA, Samadi M, Ariffin NF, Khalid NHA (2015) Long term studies on compressive strength of high volume ultrafine palm oil fuel ash mortar mixes. *Malaysia* 77:1–7
8. Jeffry SNA, Jaya RP, Hassan NA, Yaacob H, Mirza J, Drahrman SH (2018) Effects of nanocharcoal coconut-shell ash on the physical and rheological properties of bitumen. *Constr Build Mater* 158:1–10
9. Indoasianmoties, <https://www.indoasiancommodities.com/2018/06/05/coconut-production-india-high-growth-phase/>. 05 June 2018
10. Jeffry SNA, Jaya RP, Hassan NA, Yaacob HM, Satar M, Khairul I (2018) Mechanical performance of asphalt mixture containing nano-charcoal coconut shell ash. *Constr Build Mater* 173:4–48
11. Shafiq P, Mahmuda HB, Jumaat MZ, Zargar M (2014) Agricultural wastes as aggregate in concrete mixtures—a review. *Constr Build Mater* 53:110–117

12. Gunasekaran K, Kumar PS, Lakshmi pathy M (2011) Mechanical and bond properties of coconut shell concrete. *Constr Build Mater* 25:92–98
13. IS 1203 (1978) Indian standard methods for testing tar and bituminous materials: determination of penetration. 1st revision. Bureau of Indian Standards, New Delhi, India
14. IS 1205 (1978) Indian standard methods for testing tar and bituminous materials: determination of softening point. 1st revision. Bureau of Indian Standards, New Delhi, India
15. IS 15462 (2004) Indian standard polymer and rubber modified bitumen-specification: determination of separation. New Delhi, India
16. ASTM D5976 (2000) Standard specification for type 1 polymer modified asphalt cement for use in pavement construction. ASTM International, West Conshohocken, USA
17. AASHTO T315 (2010) Standard method of test for determining the rheological properties of asphalt binder using a dynamic shear rheometer (DSR). American of State Highway and Transportation Officials (2010).
18. AASHTO TP70 (2012) Standard method of test for multiple stress creep recovery (MSCR) test of asphalt binder using a dynamic shear rheometer (DSR). American of State Highway and Transportation Officials
19. FHWA-HIF-11-038 (2011) The multiple stress creep recovery (MSCR) procedure. Federal Highways Administration, US
20. Clyne TR, Marasteanu MO (2004) Inventory of properties of Minnesota certified asphalt binders. Report no.: MN/RC-2004-35, Minnesota Department of Transportation
21. Elkholy SA, El-Rahman Abd AMM, El-Shafie M, Abo-Shanab ZL (2018) Physical and rheological properties of modified sulfur Asphalt binder. *Int J Pavement Res Technol*
22. The Product of the SHRP Asphalt Research Program (1994) SHRP-A-370, binder characterization and evaluation, vol. 4: test methods. National Research Council, Washington, DC
23. De Visscher J, Paez-Duenas A, Cabanillas P, Carrera V, Cerny R, Durand G, Hagner T, Lancaster I (2016) European round robin tests for the multiple stress creep recovery test and contribution to the development of the European standard test method. *E&E Congress*
24. Laukkanen O-V, Soenen H, Pellinen T, Heyrman S, Lemoine G (2015) Creep-recovery behavior of Asphalt binders and its relation to Asphalt mixture rutting. *Mater Struct* 48:4039–4053

Planning for Demand Responsive Bus Service for Limited Area Using Simulation



Sharmeela Kale and Premjeet Das Gupta

1 Introduction

Rapid urbanization in India has increased the use of motorized vehicles as travel demand grows with increasing population of 4.6 times after post-independence [1], also which in turn has led to larger concentration of population in class 1 and million plus cities bringing with it the major challenges of urban transport [2]. Due to this there is increased number of registered motorized vehicles by 10.7% annually since 1950–2016 [2]. The growth rate of total registered vehicles during the period 2006–2016 were recorded by cars, jeeps & taxis and 2 wheelers 10.1% & buses was only 5.9% as per Ministry of Road Transport and Highway Annual report 2016 [2]. Increased travel demand has also caused a shift toward private vehicles from public modes, as it is observed, in number of registered motorized vehicular composition bus has reduced from 11 to 1.1% from 1950 till 2011 [2]. This shift from public transport to private transport is due to the quality of service offered by public transport. Bus ridership in major cities like Mumbai, Delhi, Chennai and Bangalore is decreasing since the past decade. Ridership of Mumbai public transport BEST is reduced from 16,000 lakh passengers to 12,000 lakh passengers from 2009 to 2015 as per KPMG Research analysis 2017 [3].

Based on the research conducted by KPMG share of public transport trips in India is only 7% whereas in Singapore is 86% and Brazil is 29% as per KPMG Research analysis 2017 [3]. Public transport also lack in required infrastructure and fleet size as Delhi has a net shortage of almost half the total number of required buses 2015. Public transport is also facing financial crises due to which transport operators are

S. Kale (✉) · P. Das Gupta
School of Planning and Architecture, Bhopal, India

P. Das Gupta
e-mail: premjeet@spabhupal.ac.in

unable to repair and maintain buses and provide the desired level of service to users which also is the reason why ridership is decreasing [3].

2 Need for Study

Existing Public Bus Services has many problems such as fixed route which leads longer commuting time, low ridership in non-peak hours, and low frequency of buses when demand is there, congested buses during peak hours, longer waiting time, non-availability of a seat, poor customer experience and, lack of use of technology [4]. Public transport is least preferred mode of travel, this is due to many reasons not only service provision and quality of services, but also people's perception toward service, social status and income, safety issues, ease of travel and time saving. In India existing public transport services are not well evolved to attract the potential customers, gradually reducing the modal share of public transport in cities. Public transport users face longer waiting time, unpredictable travel time and problematic travel circumstances which cause them to move away from private transport [5].

A demand of any service is based on user perception toward the service and which always changes with time and location, how the demand is perceived will not remain same in future. Demand for public transport is also dynamic in nature and depends on user behavior and choice whether to use service or not within a specific time window at a specific location. Thus, providing fixed service on static routes will not solve the problem of capturing user dynamic demand.

The shared economy in the Transport sector is a topic of discussion in recent years due to the success of emerging Uber, Ola, Lyft shared mobility providing service agencies (Ola, Uber, Lyft etc) which are the major contributor to the trend. There is a positive increasing trend toward this approach in urban areas as it has various benefits on the user side. As in the case of car sharing and ride sourcing, users may benefit due to timesaving, convenience, monetary savings and reliability [6]. Thus, application of technologies has become of prime importance for this transition toward sustainable transport in future.

Aim of the study is to assess the potential benefits of Demand Responsive Transport (DRT) under simulated conditions and explore the conditions required for its introduction.

2.1 *Demand Responsive Transport*

DRT is advance form of public transport based on flexible routing and scheduling of vehicles between pre-know pickup and drop off locations of passengers. The public transport services are operated as per the actual passengers travel demand and is flexible shared transport service that brings together people from the same area who are to be traveling at the same time and at nearby locations [7]. Demand Responsive

Transport is based on some of the essential concepts of Stopping point and Flexible route and built on which there are two types of DRT which are Door to Door service and Stop based service [8, 9].

Concepts of Demand Responsive Service

Stopping Points: Stopping points are locations where user can avail DRT services, which can be endpoints of service route, fixed intermediate stops at suitable locations, predefined stops not necessary fixed bus stops but can be convenient locations for passengers to board from their locality and non-predefined stops i.e. any location which can be preferred by user of service can be doorstep as well [9].

Route Flexibility: Routes can be partially or fully flexible based on network type. Semi fixed routes are those that are fixed for specific portion that could be main roads with fixed intermediate stops and flexible along internal roads with no predefined stops. Flexible routes are those where DRT service runs from fixed end stops, and Virtual flexible routes are where service runs with no fixed end or intermediate stop points and no fixed times. [9].

Technology-Based: Application of technology is crucial in operationalizing of DRT services. Pre-booking and reservation systems dynamically assign passengers to vehicles and optimize the routes are followed [8, 10].

Vehicle: Vehicle selection for DRT is vital in improving the efficiency of offered service, various vehicles mostly cars, buses, mini buses, vans can be used for DRT [9].

2.2 Case Studies

Previous studies on DRT was focused more on the appropriate type of vehicles used for pickup and delivery and routing and scheduling of services whereas less explored issues of DRT schemes is user-friendliness [10]. The success and failure of service at macro scale are based on various factors like political influences, economic influence, socio-cultural influence and technological influence and at micro level market demand is guided by flexibility, approach to booking vehicle, operator, eligible users, geographical coverage, pricing [10, 11].

Evaluation of DRT services in Europe [12, 13] proves that DRT is the more strategical way forward to implement in more regulated conditions without being in any conflict with other public transport modes. In Europe, government has relaxed all the norms against the development of flexible shared service like route registration to promote community-based shared service.

Hong Kong, China-Public Light Bus (PBS) [14, 15] is minibus service introduced in 1969, which covers 15% of public transport trips with minibus vehicles of a capacity, less than 16 seats. Public Light Bus provide two type of services one with green roofs (GMBs) and with a red roof (RMBs). RMBs provides non-scheduled service purely based on demand that will operate flexibly subjected to market demand and no control on routes and fare by transport authority. This service is permitted

in all existing service areas except for in new town housing development in Hong Kong. They have also introduced local stopping restriction on PLBs to prevent the congestion on the curb side and at a road junction. With the policy intervention, government introduced GMBs as scheduled feeder service for mass transport like rail and BRTs. In the case of Hong Kong with a high capacity for Rail and Bus public transport systems where private vehicle ownership is very less there is still market to be captured for Demand Responsive Transport Service.

Study of **fixed routes and demand responsive feeder transit** [16] in Atlanta city where comparison of passengers cost and operating cost of existing feeder routes and demand responsive routes is done. It proves DRT service outperforms fixed route service and performance can be improved by adjusting routing algorithm. Demand responsive flexible routes are more cost effective and efficient as demand for service which changes widely across metropolitan area with location due to population density and specific time of day. Also, the comparison can be done when DRT best meet the customer demand and minimize the operating cost.

Survey of Demand Responsive Transport [11] in **Great Britain states**. Since the 1970s, Demand Responsive Transport (DRT) has been promoted as a transport solution in circumstances where more traditional services are not economically viable. Mobility on demand can be designed in different ways with respect to the resolution of stops and timings, and the potential patronage. Without a commercially sustainable funding mechanism for DRT, long-term financial sustainability is always questionable.

Singapore: Study of dynamic bus routing service in Singapore, captures assessment of high capacity on demand mobility services efficiencies over conventional fixed route. Study focuses on dynamic routing of large capacity buses of 30 seaters to provide feeder service to mass transit in a specified highly dense travel demand area where existing fixed route 90 seater capacity buses run. In this paper [17], simulation is carried out in R language for small time interval morning peak 6:30–9 am. As a result of which various potential benefits of dynamic bus routing in terms of travel time reduction, fleet size reduction are achieved and have benefits of enhancing existing fixed routed public transport by integrating on demand mass transport mode with them [17].

Los Angeles County: A simulation study of demand responsive transit system. In this research [18] they have simulated DRT service based on two assumptions time window effect (time between calls for service and request of service) and second is zoning of a city for running service zone wise. As per the simulation results of DRT, (i) each minute increased in the time-window size of the bus service, saves approximately 2 vehicles, 260 miles driven and 750 min waiting time while satisfying the same demand; and (ii) adopting zoning policy (zoning direction wise N, S, E and W into 4 quadrants, clubbing of 2 zones NE, SW or SE, NW simultaneously)—centralized strategy or no zoning is able to satisfy the same demand as of zoning by employing 60 less vehicles and driving 10,000 less total miles with respect to a decentralized strategy.

Cottbus, Germany—Assessment study [19] of shared autonomous vehicles (SAV) by its introduction in market is capable of changing the existing transportation

scenario. Provision of Mobility as a Service (MaaS) has potential to replace existing feeder buses or tram lines in cities with more than 200,000 inhabitants. This study follows a simulation based approach to introduce Mobility as a Service in Cottbus, Germany with 100,000 inhabitants. Shared Autonomous vehicles are simulated using MATSim software for 21,000 trips conducted using public transport within a city for a day. Existing services include 5 tram lines and 17 city buses with frequency of 15–20 min each. So these existing services were replaced by feeder mini buses of 8 seater capacity on door to door and stopped based scheme bases. Walking distance to existing stops was reduced from 585 to 270 m. It was observed that fleet utilization was reduced from 400 in door to door scheme to 300 in stopped based scheme with same level of service provision. In case of travel time, in base case was 35 min which was reduced to 27 min using DRT services.

Cases of Failure of DRT in Various Cities

As studied by Dr. Marcus Enoch in 2006 [20], following are the reasons for failure of DRT services in various cities.

1. Dial-a-Bus- Milton, Keynes and Buckinghamshire, UK- due to hostile land use, service operated over low concentrated demand.
2. Dial-a-Bus, Adelaide, SA, Australia- due to unmetabled ‘many to many’ services in the low-density area.
3. Plus Bus, Truro, Cornwall, UK- Operated over a too large area
4. Other reasons for the failure of DRT-Technical Difficulties, lack of support from the public, lack of planning and market research.

3 Methodology

3.1 Simulation Technique Used in Research

An **agent-based model** is a technique to simulate several operations simultaneously by the interaction between multi-agents with an attempt to recreate the scenario for anticipating the appearance of a complex travel phenomenon. Agent-based models for simulating traffic follows has proven to be most beneficial in transportation modeling. It consists of an agent i.e. individual person which is considered an object in software which has a set of attributes that gives a detailed description of the population. An agent-based model consists of (i) agent (person or vehicle) dynamics, (ii) transport network (nodes and links), (iii) demand model, (iv) route choice strategies and (v) performance standards [21]. Multi-agent based modeling is one of the tools of Geosimulation that optimize the simulation with a large number of agents with their distinct specific characteristics [19]. Decision agents include Mode choice, Route choice, Location choice, Activity type choice (determining whether to go for some activity or to restrict), Activity chain choice (determining of sequence to do the

activity), Activity starting time choice, Activity duration choice, Group composition choice (choice of selecting group of people to do activity).

As represented in various studies in previous section, Demand Responsive Transport is an innovative approach over existing scheduled conventional public transport bus and taxi service with flexible demand service for customers on shared ride mode which is cost-effective for operators and fulfills mobility needs of authorities. Urban Mass Responsive Transport to capture dynamic spatiotemporal demand is currently absent in urban areas and its applicability in dense urban areas is least observed. Thus, testing its applicability in dense urban areas will be experimented to know whether this service can perform well under high demand situations. Concept of demand responsive services is adapting dynamically to demand by instant routing and scheduling of fleet vehicles and operating without any fixed routes or timetables. Also, such kind of services are successful when implementing in a specific part of the city rather than for an entire city [7].

3.2 Study Area Selection

Case study area selected is Pune city being least contributor to public transport usage among similar cities like Mumbai, Chennai, Bangalore and Ahmedabad [4, 22, 23]. Metro service is under implementation process in Pune city, so area for study purpose is one of the catchments of Metro Station area in Pune City. As per City Development Plan [24] of Pune, analyzing the growth of city it is evident that urban sprawl is significantly in the eastern, southern and south-western directions beyond the administrative boundaries. So, chosen metro station for research is last station of corridor 2 which is Ramwadi, as demand for feeder service is highest at end station of mass transit (Fig. 1).

Delineation

Study is based on building conceptual model for future scenario, for providing Demand Responsive Transport for future feeder demand. For the same purpose, area delineation is based on catchment area of Metro station where there is possibility of providing such DRT services considering trunk line, road widths, activity areas, neighboring land-use and distance from Metro station.

Study area population is 107,556 persons over an area 9.13 km² with density within area ranging from 35 to 350 persons/ha [25]. Study area is served by total of 15 routes for 5 destinations or end locations within study area i.e. 15% of total 371 routes in Pune city [26]. Study area has 15 bus routes that serves to 6 destinations i.e. Vadgaonsheri, Vimannagar, Kharadi Gaon, Anand Park, Ramwadi, Sainathnagar, within study area and these bus routes are overlapping with one another as each destination is served by more than 1 route so only 6 routes are visible in the map (Fig. 2.). For example, Vadgaonsheri area is served by 3 routes i.e. via Ramavadi, via Shubham society and via Anand Park. Buses routes connects study area with three major destinations Pune Station, Ma Na Pa and Swargate within the Pune city.

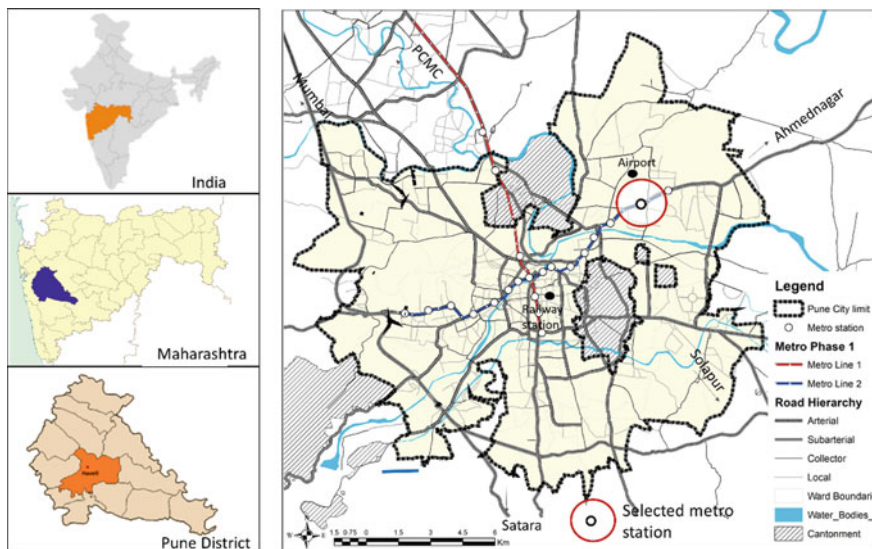


Fig. 1 Case study area

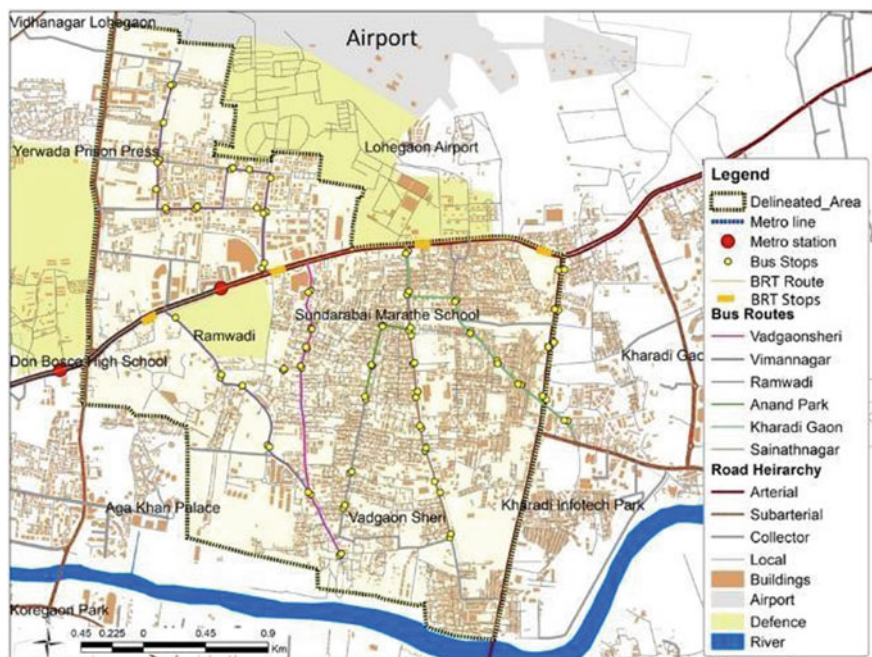


Fig. 2 Delineated area with existing bus routes

3.3 Sampling Techniques

The need for the study requires a wide variety of population samples to analyses and capture the spatio-temporal travel demand of the study area.

Using Yamane [27] sample size calculating formula as in equation below, Yamane formula is a simplified version to determine sample size for large population size to determine the sample size that will reflect a similar proportion of interests among datasets. The sample size is been estimated at 95% confidence level

$$n = \frac{N}{1 + N(e)^2}$$

where n is the sample size, N is the population size, and e is the level of precision i.e. 5%. So, 400 samples of data were collected.

Sampling approach used is systematic cluster sampling to pick up a sample of 10 people each from 40 different clusters formed based on distance factor summing up to a sample of 400 people. Each cluster formed is a small-scale representation of the total population which is mutually exclusive and collectively exhaustive. The survey questionnaire included detailed travel diary of passenger's trips with respect to departure and arrival timings and location and the second part encompasses stated preference survey for different mode users to estimate willingness to shift to demand responsive bus service in future.

3.4 Future Scenarios for Research

This research is based on travel mode which is not present at today's time, so to evaluate the performance of such service it is mandatory to estimate the demand that will be attracted by DRT service or the potential users of new feeder service based on various conditions.

Two scenarios are generated based on probable demand for DRT:

1. Future demand for DRT will be same as existing fixed route public bus service
2. Future demand for DRT is based on passengers willingness to shift from other modes (two wheeler, auto, taxi) to DRT.

Conceptual Model to Develop for Future Scenario Challenges

This study is based on future travel behavior of mode which is not available at present so it requires to set up some assumptions to understand, the nature of best suited DRT situation for the selected case study area. For the same, there are various major challenges in the process which are-

1. The assumption of the appropriate fleet size is on the trial and error method.

2. Estimating future demand for existing fixed route service and future demand for feeder trips.

4 Simulation Modeling

Agent-based model simulates the simultaneous operations and interaction of multi-agents to recreate the scenario and predict the appearance of complex traffic flows. It is capable of simulating private cars, two-wheeler traffic and public transport traffic with a large level of detailing and it also simulates pedestrians and cyclists’ traffic. Agent-based modeling can be done for a limited time window, in most of the cases is full one day and we can track any single agent in simulation. Agents involved in the simulation are each passenger with the planned trip and DRT vehicles [28, 29] (Fig. 3).

MATSim is available in a jar file format that works on java platform and to carry out simulations in MATSim software. Also, there is a need to have an understanding of programming languages like java, python and various file formats in the computer to work with MATSim[28]. To carry out simulations input data needs to be in XML file format which includes network file, populations or plans file, vehicle file, DRT stops file and configuration file, all these files need to be saved in .xml file format to use them in simulation. Java codes were operated on Eclipse, which is an integrated development environment or workspace for computer programming used widely as this is open source software [6, 29–31].

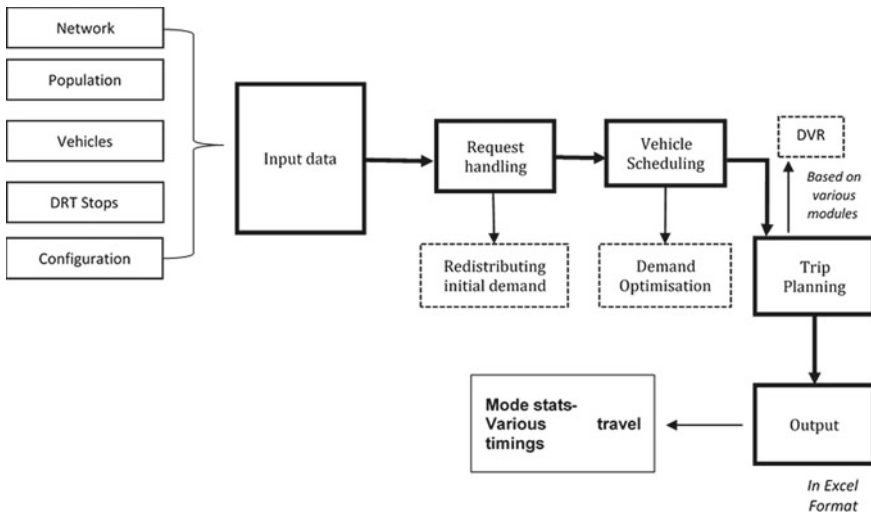


Fig. 3 Simulation process used for generating traffic flows

4.1 Input File Format

All the files used for running the simulations are listed below.

1. Network file: Network file includes all the nodes of the intersection, links that connect the nodes, width of the road, speed on-road and one-way and two-way details with UTM coordinates to make the network that resembles the real network on the ground.
2. Population file: Population or plans file is the estimated travel demand, i.e. the list of agents and their day plans or travel inventory of each individual passenger. Agent plans are different when they travel on a fixed route and different when they travel by flexible route. When they travel by fixed route then details of which link they will be traveling needs to be given and when they travel by flexible route only details of start and end location need to be given, and network of travel is auto assigned.
3. Vehicles file: Vehicular plans are mentioned with the number of DRT vehicles, the capacity of vehicle and location of start and point.
4. DRT stops file: DRT stops file comprises of locations of DRT stops for boarding and alighting of passengers into and from DRT vehicles given in UTM coordinates.
5. Configuration file: Configuration file is a most important file which runs the simulation and states all the conditions such as minimum waiting time of passenger, vehicle stopping time, type of scheme to be used, late arrival window of passengers, required statistical results. [6, 29, 30].

Definitions

To understand the scenario generations of two scenarios as stated before in section 3.4 and results obtained from simulations, we need to understand the various terminologies used in analysis further which are as follows:

1. **Time Window setting:** Time window setting is conditions of different timings that have been assumed and assigned to agents in simulations to enhance the accuracy of results obtained, to make simulations more realistic in nature.
 - (i) Vehicle stopping time window: It is the maximum time for which vehicle will stop at DRT stop when requested by the passenger or else there will be no stopping of the vehicle at all the stops.
 - (ii) Passenger Waiting time window: Passenger waiting time or passenger pickup time is the time for which passengers will have to wait for vehicle or time for which passenger is more likely to wait for vehicle and is assumed based on existing average waiting time.
 - (iii) Late arrival window: Late arrival window is passenger not arriving on time at DRT stop, it is introduced to capture the probable human behavior of traveling.

2. **Rejection Rate:** It is the percentage of total passenger trips or demand requests not served by DRT service in simulations. But in real-world scenario it will be ride requests not served on time or rides which will have more waiting time than expected due to abnormality in handling requests in software caused because of multiple requests occurring at same time or vehicle is taking too long to reach DRT stop due to many reasons like congestion, late arrival of passengers etc.
3. **Ride request:** This are number of requests made by passenger to book a DRT ride through IT application, phone call or through message.

4.2 DRT Stop Location in Study Area Based on Road Width

The proposed DRT type for the study area is stop based service as mini buses cannot access remote locations within a dense area. New DRT stops (Fig. 4.) are located such that all the areas are accessible within 300 m of walking distance or less than 7 min walking time which is an existing average walking time for public transport users. DRT stops are located based on existing public transport demand, therefore more number of stopping points are located in existing high demand areas by identifying high-frequency bus routes and daily ridership generated from the area. Considering

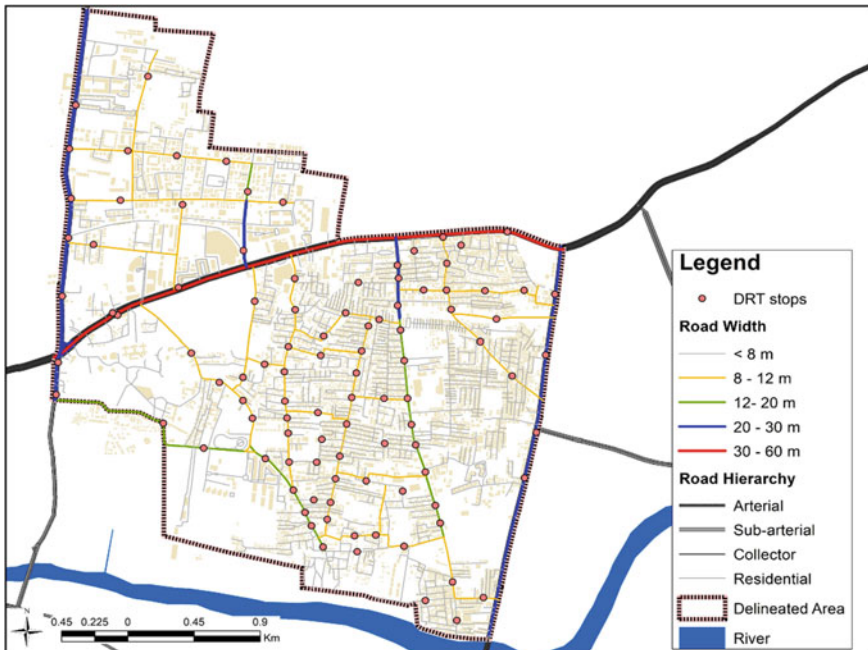


Fig. 4 New DRT stop locations

the widths of roads, it has been proposed that DRT stops for the mini buses are located on roads having a minimum width of 8 m or more.

5 Data Analysis

As per the primary survey conducted to collect information of travel diary inventory of study area it is observed, public transport users from study area is only 12.67% as per modal split of motorized trips and trip rate is 1.3. Therefore total 8858 passengers from study area travel daily by public transport service and 64 large capacity 45 seater bus is utilized for public transport service of study area. Existing total number of bus trips per day is 964 in the study area which constitutes to be 6% of total bus trips of the city.

Analyzing the temporal demand (Fig. 5.) for public transport based on collected samples and extrapolating it to total demand using programing tools on the eclipse platform, it is observed that peak demand requests per hour during the morning is between 8:30 to 10:30 and in the evening is between 18:00 to 20:00. Between the same time, demand for DRT is highest which is 2600 requests per hour in the morning and 2400 requests per hour in the evening.

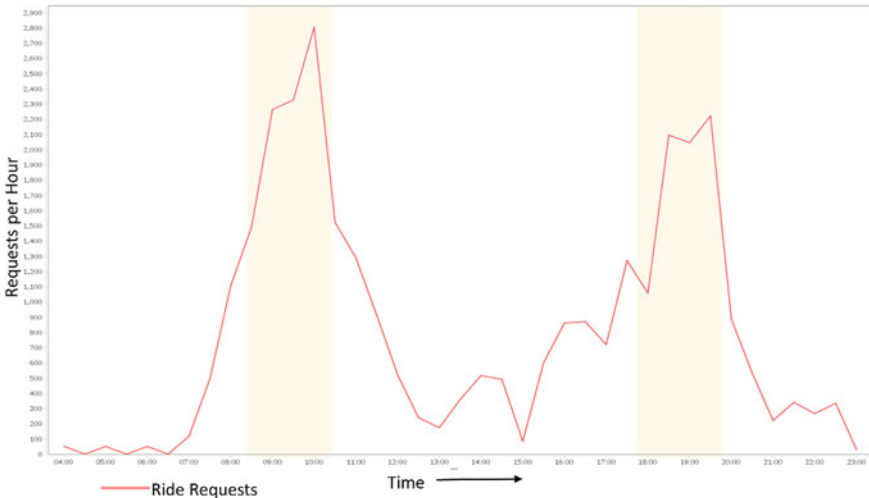


Fig. 5 DRT ride request per hour for temporal travel demand with the morning and evening peak demand for DRT highlighted in graph

5.1 Scenario 1: Demand for Demand Responsive Feeder Service is the Same as the Existing Demand for Public Transport

Various assumptions are made within Scenario 1 and further 6 different situations are generated based on permutations and combinations of indicators with certain changes in each sub scenario to optimize the results of the scenario and measure the efficiency of DRT under simulated conditions. Scenario 1 is based on the following assumptions.

Indicators for Generating Different Situations

1. Fleet size- 60, 65, 70, 72, 75 and 76
2. Vehicle capacity- 16 seater
3. Demand—Existing demand of PT 8,858 persons and 11,515 trips
4. Time Window setting–
 - (i) Passenger waiting time– 5 min, 8 min and 10 min
 - (ii) Vehicle stopping time– 30 sec, 45 sec and 60 sec

Scenario generation is based on assumptions of different fleet size of DRT vehicles, where fleet size number was derived from trial and error method. Each scenario is simulated with the different fleet size to fulfil the same passenger travel demand. The results obtained are average pickup time of passenger, rejection rate in simulation and travel demand fulfilled by simulation with each different fleet size (Table 1).

Time Window Setting

Time window setting in simulation is used for simulating data with real-life scenarios by configuring passenger waiting time restriction i.e. maximum time passenger is willing to wait for bus service and stopping time of vehicle on DRT stops to serve maximum demand by DRT.

Determining Stopping time for DRT vehicle at stopping points

To determine optimized stopping time for vehicle 18 simulations were run with 30, 45 and 60 sec stopping time. To determine stopping time window for DRT vehicles simulations were run for 6 different fleet size options. As per the simulation

Table 1 Scenario 1 based on assumptions of parameters

Parameters	Base case	Option 1	Option 2	Option 3	Option 4	Option 5	Option 6
Target demand	8858	8858	8858	8858	8858	8858	8858
Demand fulfilled	11,515	11,170	11,170	11,285	11,285	11,400	11,400
Fleet size utilization	64	60	65	70	72	75	76
Vehicle capacity	45	16	16	16	16	16	16
Rejection rate	–	3%	3%	2%	2%	1%	1%

results, efficiency of demand served by DRT increases with decreasing the stopping time of DRT vehicles at stopping points. It is evident from the simulation results in Fig. 6, 7 and 8, with increasing stopping time restriction window of passengers, rejection rate also increases, so the most desirable stopping time for vehicle obtained is 30 s with maximum travel demand fulfilled up to 99%. With every 30 sec decrease in stopping time of vehicles, there are an additional 760 passenger trips demand served.

Determining Passenger waiting time restriction

To determine optimized passenger waiting time restrictions or maximum passenger pickup time for bus, 18 simulations were carried out with 5, 8 and 10 min waiting time restriction (Figs. 9, 10 and 11).

To determine waiting time window for passengers simulations are run under 6 settings each with 3 different passengers waiting time restriction window of 5, 8, 10 min. The waiting time window is selected based on existing waiting time for the bus which is 5–15 min with average waiting time of 11 min. So the selected range is

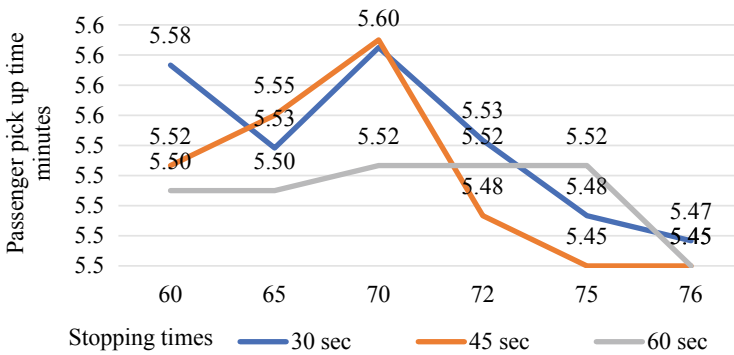


Fig. 6 DRT vehicle stopping time and average pickup time in minutes

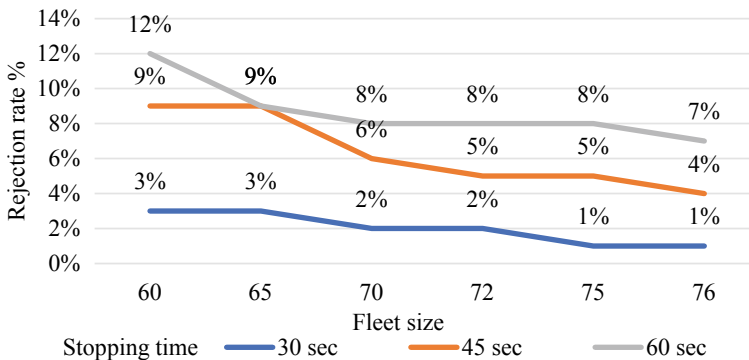


Fig. 7 DRT stopping time and rejection rate for scenarios

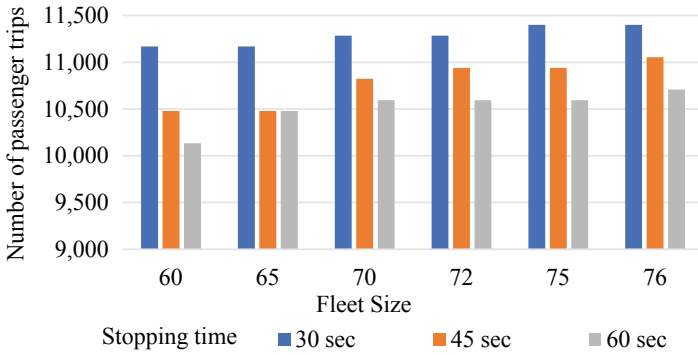


Fig. 8 Demand served by changing DRT vehicle stopping times—30 sec, 45 sec and 60 sec

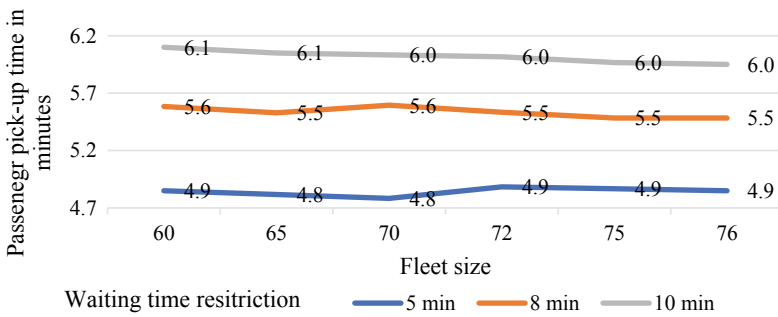


Fig. 9 Average pickup times obtained from waiting time restriction of 5, 8 and 10 min

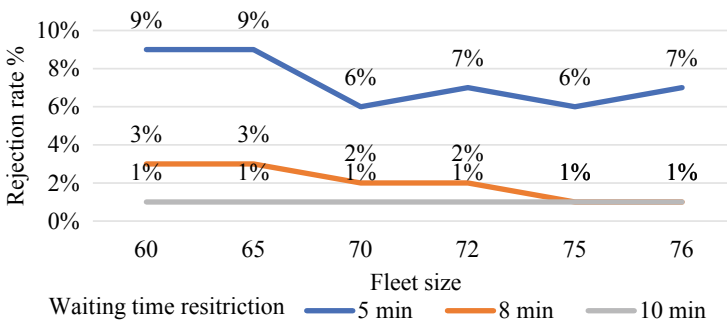


Fig. 10 Passenger waiting time restriction and rejection rate for scenario 1

such that the maximum time people are willing to wait for the bus is below the existing average waiting time window of 11 min. Based on the results of the simulation, time window for passenger waiting time selected is 8 min as it has the least trip rejection rate and its average waiting time for the passenger is 5.5 min, which is close to the

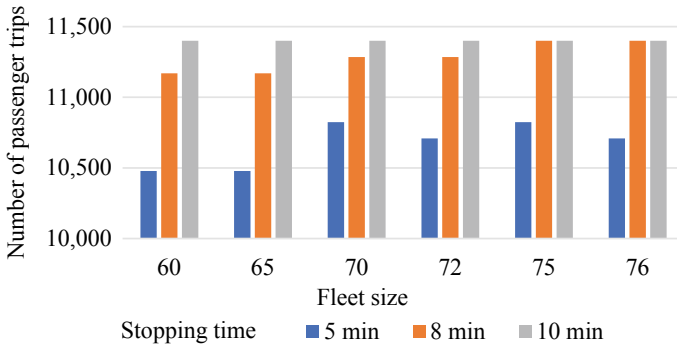


Fig. 11 Demand served by changing waiting time restrictions—5, 8 and 10 min

existing minimum waiting time for the bus in peak hour. Also, smaller pickup time creates difficulty in handling the ride requests and trip planning, as studied from case failure of DRT [7]. Also, it is observed with an additional 1 min of waiting time restriction from 5 to 8 min there is an additional 210 trips demand served and which remains constant while increasing 8 min window to 10 min (Fig. 12).

Selected time window settings for stop-based DRT service are stopping time of DRT vehicle of 30 sec and passenger waiting time restriction of 8 min. Six simulation were carried out with 6 different fleet sizes, with 30 sec vehicle stopping time window and 8 min passenger waiting time window. Travel demand served by DRT vehicles shows demand served increases with number of vehicles used and is maximum for 75 and 76 vehicles (Option 5 and 6). Rejection rate decreases with number of vehicles

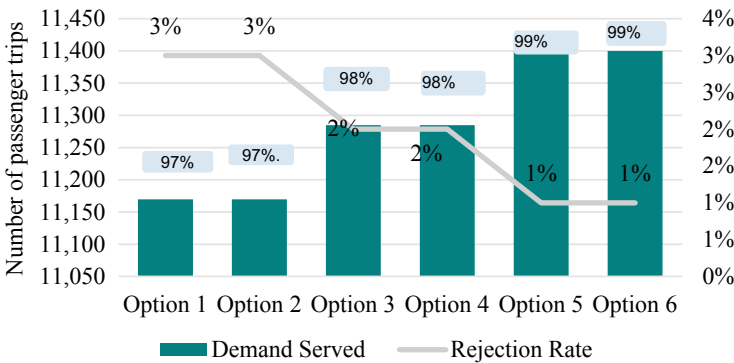


Fig. 12 Demand served by DRT under simulated conditions

Table 2 Passenger efficiency indicators

	Base case	Option 1	Option 2	Option 3	Option 4	Option 5	Option 6
Fleet size	64	60	65	70	72	75	76
1. Average walking time (mm:ss)	7:00	4:52	4:29	4:29	4:30	4:12	4:25
2. Average waiting time (mm:ss)	11:0	5:35	5:31	5:35	5:32	5:29	5:29
3. Average distance travel/person/day (km)	3.1	2.09	2.09	2.089	2.089	2.093	2.115
4. In-vehicle time (mm:ss)	7:00	6:47	6:53	6:51	6:55	7:00	7:02
5. Total journey time (mm:ss)	25:0	17:14	16:53	16:55	19:39	16:41	16:56

used and is lowest for in case of Option 5 and 6 which is 1%. So, from the above analysis quality of service provided remains same after fleet size of 75 mini buses.

Passenger—Efficiency Indicators

Passenger side efficiency indicators are measured by various travel timings of passenger while using public transport such as, average walking time, average waiting time, average in vehicle time and total travel time also average distance traveled per person. Table 2 shows the values of existing base case and 6 scenarios generated using simulation for efficiency indicator.

Travel times

Passenger waiting time: In the existing base case average waiting time of passengers for traveling in public transport is 11 min and which ranges from 5 min in peak hour to 15 min in the non-peak hour. Waiting time for public transport buses also shows spatio-temporal change throughout the area as per the frequency of bus trips in the area. The frequency of bus trips in Vadgaonsheri and Kharadi gaathan area is high as compared to the rest of the area. After simulating 6 different fleet sizes with different time window settings results obtained show average waiting time can be reduced to approximately 5 min and 30 sec by allowing passenger pickup time restriction to 8 min (Fig. 13).

In the next case average waiting time for passenger can be reduced to 4 min approximately by allowing passenger pickup window restriction to 10 min and it can be reduced to 6 min approximately by allowing passenger pickup time window to 5 min (Figs. 14 and 15).

Results

Time savings: Average waiting time for bus reduces by 0.5 times of existing waiting time. Average walking time to bus stop reduces by 0.43 times of existing walking time. Average in-vehicle time remains almost the same. Average total travel

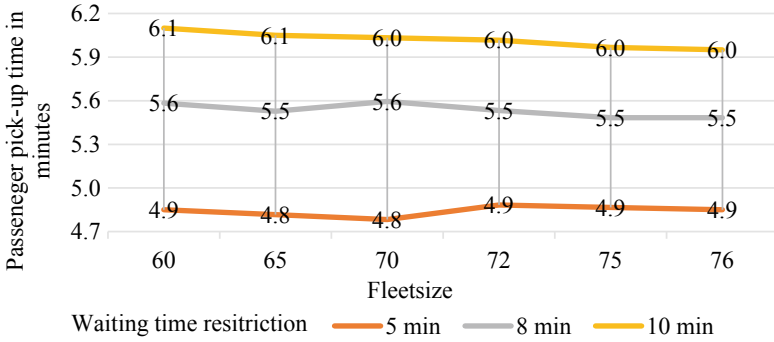


Fig. 13 Average waiting times obtained from a pickup time window of 5, 8 and 10 min

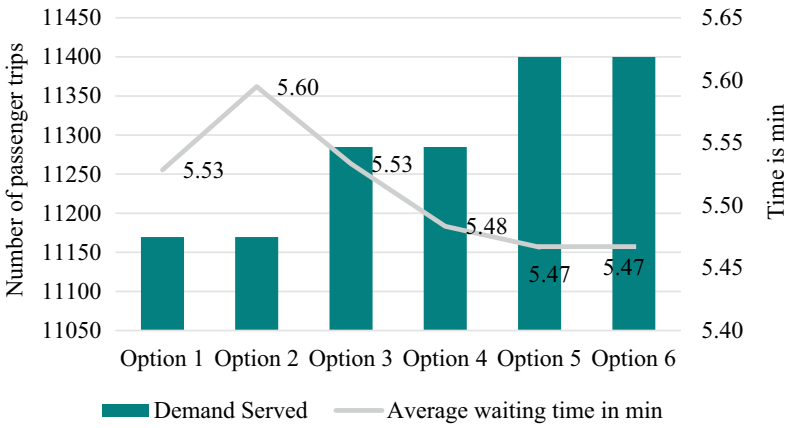


Fig. 14 Average waiting for demand served by DRT

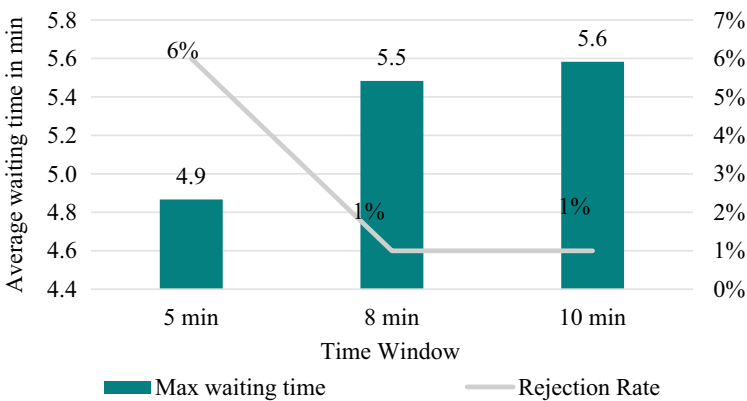


Fig. 15 Average waiting times for different time window restrictions-Fleet size 75

time reduces by 0.32 times and average per passenger distance traveled reduces by 0.35 times of existing average distance traveled.

Operators-Efficiency Indicators

Operator’s efficiency indicators include Demand served efficiently by DRT service, rejection rate of service, fleet utilization, total distance traveled, operating cost, and average distance driven. Table 3 shows the operator efficiency indicator values for base case and 6 scenarios based on assumption for DRT case.

Operating cost for minibus reduces by 0.35 times in comparison with existing 45 seater buses, as mini buses consume less fuel compared to large capacity buses. The fuel consumption of 45 seater buses is almost 3.25 times more than 16 seater mini buses. Existing PMPML buses has operating cost of 85 Rs per km, Operating cost of minibus considered is 1.45 Rs per seat per km as per WRI bus aggregator viability study [32] (Table 4).

Table 3 Operators efficiency indicators

Indicators	Base case	Option 1	Option 2	Option 3	Option 4	Option 5	Option 6
Target demand (persons)	8858	8858	8858	8858	8858	8858	8858
Demand fulfilled (trips)	11,515	11,170	11,170	11,285	11,285	11,400	11,400
Demand fulfilled (%)	100	97	97	98	98	99	99
1. Fleet size utilization	64	60	65	70	72	75	76
2. Vehicle capacity	45	16	16	16	16	16	16
3. Total distance Traveled	3987	8893	8693	8719	8798	8904	8648
4. Operating cost (Rs)	338,895	206,318	201,678	202,281	204,114	206,573	200,634
5. Average driven distance km	228	118	99	99	97	94	91
6. Rejection rate	0%	3%	3%	2%	2%	1%	1%

Table 4 Vehicular km per day by changing waiting time restriction

Waiting time restrictions (s)	Distance driven in km					
	Option 1	Option 2	Option 3	Option 4	Option 5	Option 6
5 min	7873	7921	7915	7947	8057	8055
8 min	8893	8693	8719	8798	8705	8648
10 min	9485	9430	9401	9421	9541	9399

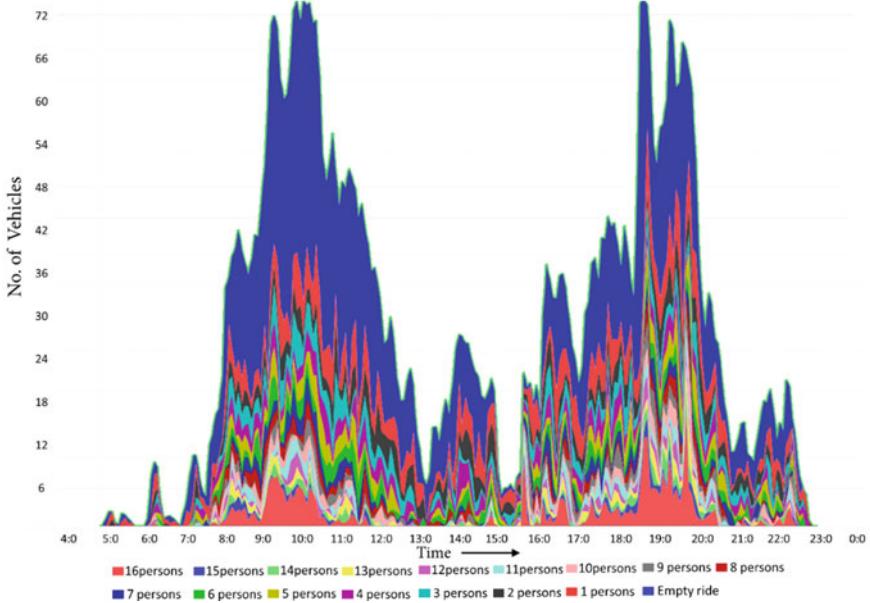


Fig. 16 Vehicle occupancy ratio for scenario 5 with fleet size 75

With every increasing minute waiting time restriction from 5 to 10 min distance traveled increases by 300 km per day. Thus, lower waiting time reduces distance traveled.

Vehicle occupancy

Vehicle occupancy at each time interval of 75 vehicles is plotted. In peak hours 9:00 to 10:00 in the morning and 6:30 to 7:30 in the evening, there is 100% utilization of vehicles. However the occupancy for only 11% fleet is observed to be 100% that is 16 persons (Fig. 16).

These results obtained from simulation can be used to identify the actual number of vehicles required at any point of time in a day instead of departing all fleet vehicles in the field, the rest of the vehicles can be put to other use. Also, similar occupancy data for each individual bus at each point of time is a data gap in the existing base case so comparison for the same was not possible.

5.2 Scenario 2: Demand for DRT Based on passenger’s Willingness to Shift from Other Modes (Public Transport, Two Wheeler, Auto, Taxi) to DRT

Stated Preference Options for DRT

To estimate probability of persons willingness to use DRT service if provided in future, stated preference survey was conducted for persons with existing mode as four wheeler, two wheeler, auto rickshaw, cab and public transport for set of 6 options where they were asked a choice whether they will use DRT or their existing mode under certain conditions of waiting time, walking time, travel time and travel cost.

Total of 400 samples were collected from individual households and each individual answered a set of 6 options in Yes or No to shift to DRT, so in total 2400 datasets were available to estimate the probability of shifting to new mode. As per the primary survey out of total samples 100 car users, 168 two-wheeler users, 50 bus users and 62 auto and cab users were surveyed. State preference questionnaire to conduct survey for future DRT users is mentioned in the Tables 5 and 6.

Willingness to shift to DRT

The conditional probability (Pr) measures the chances of occurring an event such that person will be choosing DRT mode over its existing mode. So the choices asked

Table 5 Stated preference survey options for car users

If car user						
Option	1	2	3	4	5	6
Waiting time	2 min	5 min	8 min	5 min	5 min	2 min
Walking time	8 min	12 min	12 min	3 min	8 min	12 min
Travel time	1.25 times	1 time	1 time	1.25 times	1 time	1.25 times
Travel cost	0.5 times	0.5 times	1 time	0.5 times	1.5 times	1 time
Choice						

Choice = 1 existing mode; 2 DRT

Table 6 Stated preference survey options for other users

2-wheeler, IPT, PT						
Option	1	2	3	4	5	6
Waiting time	5 min	8 min	5 min	2 min	5 min	2 min
Walking time	3 min	12 min	12 min	8 min	8 min	12 min
Travel time	1 time	0.5 times	1 time	1 time	0.5 times	1.5 times
Travel cost	1.25 times	1 time	1.25 times	1 time	1.5 times	1.5 times
Choice						

Choice = 1 existing mode; 2 DRT

Table 7 Goodness of fit test results (Hosmer and Lemeshow Test)

Modes	χ^2	df	p
Car	2.562	8	0.959
2-wheeler	5.604	8	0.691
Bus	6.428	8	0.599
AuAuto and cab	14.393	8	0.072

in stated preference survey whether to use existing mode or DRT is dependent variable which is dependent on four independent variable as in stated preference survey i.e. walking time, waiting time, travel cost and travel time. To measure the dependency of variables, logistic regression was necessary. Since the variable of choice was dichotomous in nature, binary logistic regression was performed to analyze willingness to shift to DRT. Model development was based on 2 choices to select among DRT or existing mode, so binary logic model is used which is of the following form (Table 7).

$Pr(DRT/EM)$ = Probability of shifting to DRT conditioned on existing mode(EM)

$$Pr(DRT/EM) = [e^{VDRT}]/[e^{VDRT} + e^{VEM}]$$

where,

- V_{DRT} - Deterministic component of utility of DRT,
- V_{EM} - Deterministic component of utility of Existing Mode.

$$\begin{aligned}
 V_{Car} &= 0.617 - 0.007 Tw - 0.020 Ti + 0.0001 Tt - 0.085 Tc \\
 V_{2w} &= 0.841 - 0.108 Tw - 0.126 Ti + 0.029 Tt - 0.05 Tc \\
 V_{Pt} &= 1.082 - 0.004 Tw - 0.011 Ti - -0.002 Tt - -0.158 Tc \\
 V_{IPT} &= 3.19 - 0.305 Tw - 0.215 Ti - 0.033 Tt - 0.020 Tc
 \end{aligned}$$

where,

- Tw- Waiting time
- Ti- Walking time
- Tt- Travel time
- Tc- Travel cost

As per the results, to evaluate goodness to fit of logistic model dataset against the actual outcomes suggests that, in above table p -value for all 4 modes as for Hosmer and Lemeshow Test is >0.05 which states the model is good fit (Table 8).

Table 8 Results for willingness to shift to DRT

Modes	Option 1	Option 2	Option 3	Option 4	Option 5	Option 6	Existing
Car	47%	44%	30%	49%	22%	32%	51%
2-wheeler	51%	17%	31%	47%	30%	38%	75%
Bus	63%	48%	60%	49%	37%	36%	48%
Auto and cab	58%	5%	12%	36%	19%	11%	25%

As per primary survey analysis trips outside study area with more than 3 km travel distance consists 74% of the total motorized trips, and out of these trips 40% of passengers trips are willing to use mass transit such as Metro or BRT in future. The people’s willingness to shift to DRT is estimated with binary logistic regression.

Thus, demand estimation in second scenario is based on willingness to shift, and is calculated as the results of state preference survey in table 8. The maximum number of people willing to shift to DRT to board mass transit (metro rail, BRTs) from every other mode under six stated preference option is 49% of Car users, 51% of two-wheeler users, 63% of public transport users, 58% of auto-rickshaw and cab users. The total demand of 11,444 persons and 14,876 trips are estimated to have probability to shift to DRT.

Passenger—Efficiency Indicators

In second scenario demand is based on number of existing car, two wheeler, public transport and IPT users willing to shift to DRT. In the base scenario, waiting and walking time for private vehicle users is zero, thus average waiting and walking time for only IPT, (Auto and Cab) and public transport users is considered in this scenario i.e. average 7 min walking time and average 7 min 30 sec waiting (Table 9).

Average waiting time for various passenger pickup time

Average waiting time predicted for different pickup time window is least in case of 5-min window which is average 4.4 min for all fleet sizes and in maximum for 11-min waiting window which is average 5.6 min for all fleet sizes. Similar approach to select time window setting as explained in Scenario 1 is adopted, such that waiting time window is less than the average waiting time for existing mode which in this case is also 8 min (Fig. 17).

As in existing case average waiting time in auto is 4.5 min and public transport is 11 min. It is observed with each 1 min increase in waiting time restriction from 5

Table 9 Passenger efficiency indicators for 2nd scenario

	Base case	Option 1	Option 2	Option 3	Option 4	Option 5	Option 6
Fleet size	–	75	80	85	90	95	96
1. Avg. walking time (mm:ss)	7	3:52	3:29	3:29	3.30	3:12	3:25
2. Avg. waiting time (mm:ss)	7:30	5:12	5:11	5:11	5:13	5:08	5:08

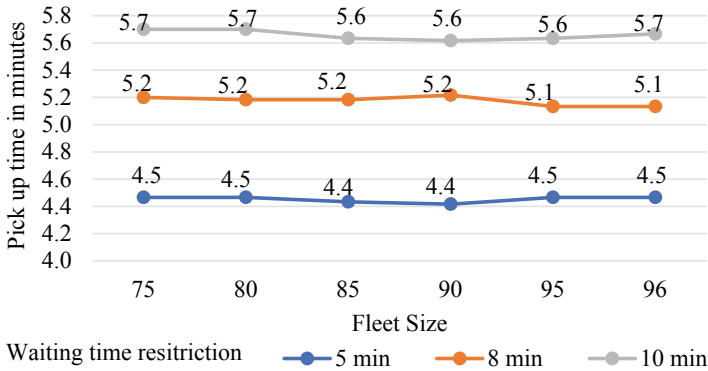


Fig. 17 Average pickup time window for waiting time window restriction for Scenario 2

to 8 min there are additional 264 trips demand served, and which remains constant after 8 min. Average pickup time obtained after simulation is 5.2 min (Fig. 18).

In this case, the rejection rate for 8 min window and 10 min window is almost the same and the number of trips served increases from 5 min window to 8 min window. The existing waiting time window is 7.30 min, it was necessary to select a close time window so that pickup time for passengers should not increase that will create inconvenience. Thus, 8 min window is adopted to fulfil the travel demand (Fig. 19).

Results are obtained by simulating travel demand of 11,444 persons, with different fleet size of bus 75, 80, 85, 90, 95 and 96, it is observed there is reduction in waiting time and walking time for IPT and public transport users but for private vehicle users there will be increase in travel time by DRT bus service. To simulate demand of 14,879 passengers 6 cases generation with fleet size from 75 to 96 were done. Fleet size of 95 is ideal to implement in this case as it has least rejection rate & average pickup waiting time (Table 10).

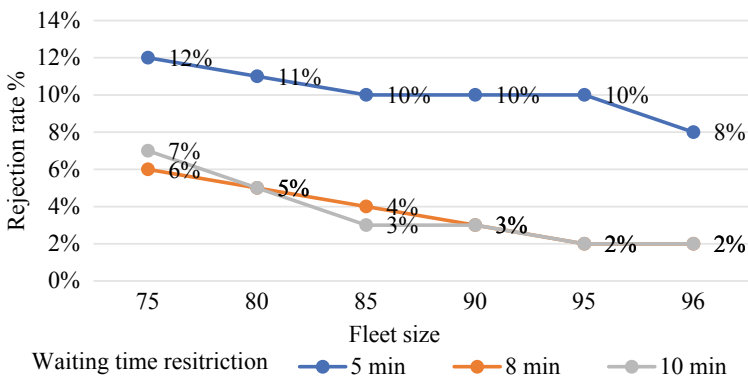


Fig. 18 Average waiting time window and rejection rates for scenario 2

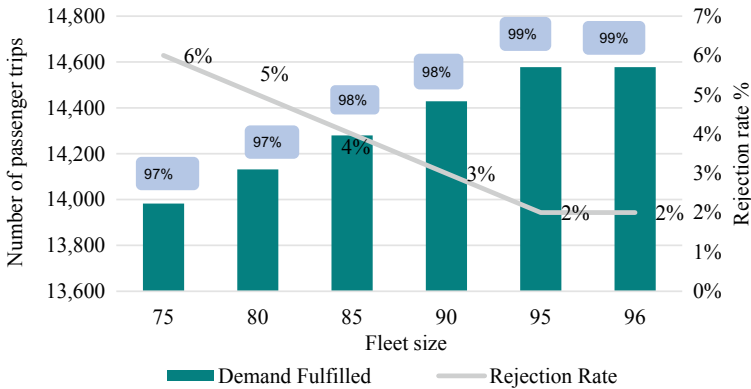


Fig. 19 Demand served by DRT in scenario 2

Table 10 Average travel time and travel cost for existing and DRT mode

	Car	2-Wheeler	Bus	Auto & cab	DRT
Average time min	14.58	12.37	25.05	18.45	17.12
Average cost Rs	16.466	7.893	6.876	34.54	10.368

Results

Travel time and Travel cost: Existing average travel time and travel cost to reach metro station using modes such as a car, two-wheeler, public transport, auto, cab, and DRT bus service are mentioned in Table 12. It is observed, DRT will be beneficial in reducing travel times for exiting public transport and IPT users by 0.32 times to 0.07 times of existing travel time whereas, of car and two-wheeler users travel time will increase slightly by 0.17 times to 0.41 times of existing travel time. So to fulfil future feeder demand of mass transport systems 95 fleet vehicles of 16 seater buses will be required. And since it is the hypothetical scenario, so existing bus fleet usage, distance traveled and investment cost is unknown so there is no scope for evaluating operator side efficiency indicators, but none the less the operating cost of mini bus as explained in scenario 1 will always be less than 45 seater capacity buses.

5.3 Conclusions

As per the results obtained from Scenario 1 and 2 by using DRT of 16 seater capacity mini buses as feeder to metro will be efficient in reducing travel time and increase convenience. Existing average waiting time of 11 min for bus service will be reduced to 5:30 min. Existing average walking time to bus stop is 8 min, with new stopping points of DRT accessible within 300 m walking distance time is reduced to 4 min 12 sec. Providing DRT within small area increases the efficiency of shared service

by making it feasible to operate for transport authority. The bus utilisation, within peak hour 9:00 to 10:00 and 18:30 to 19:30 DRT is 100% and 5 hours in day is more than 50% vehicle utilization.

In non-peak hour when vehicle utilization is low DRT vehicles can be used for alternate use i.e., intra area trips for work- IT industries, recreation-Shopping Mall, education- Private coaching classes. With increasing 1 min of passenger waiting time restriction there is additional 210 trips served and decreasing stopping time of vehicle by 30 sec increases additional 710 trips served per day.

Dynamic Pricing

Existing static price of public transport will not be financially viable for DRT. So, principle of dynamic pricing needs to be followed, where price changes with respect to demand and supply. Price for DRT will be maximum during peak hours when demand for DRT is high and minimum during non-peak hour when it is easy to get DRT when demand is low (Table 11).

In existing scenario of public transport bus service, earnings from bus service is lower than the spending's on operation of bus service, thus transport authorities procure huge losses that is why it is not possible for them to provide quality service. Also after introduction of DRT, it is not possible to achieve profit with the same public transport pricing (Fig. 20).

Moreover, people are willing to spend more when they are assured to get convenient and comfortable service. So, the dynamic pricing of DRT bus service is derived, considering the temporal demand variation of ride requested per hour throughout day as depicted in Fig. 5. Therefore, proposed dynamic pricing for DRT is estimated such

Table 11 Earnings from existing and DRT service

	Base case (fixed route bus service)	DRT Option 5 in scenario 1
Total passenger travel time hrs	9297	6352
Earnings from passenger in Rs	2,16,998	2,10,148
Operating cost	3,38,895	2,06,573
Benefit cost ratio	0.64	1.23

Table 12 Change in mode of travel

Mode	Before DRT		After DRT	
	%	Persons	Persons	%
2-wheeler	42.6	29,782	26,640	38.1
Car	25.3	17,687	12,398	17.7
Auto and cab	13.83	8858	8228	11.8
Public transport	12.67	9669	7284	10.4
DRT	0	0	11,444	16.4
Institutional buses	5.6	3915	3915	5.6



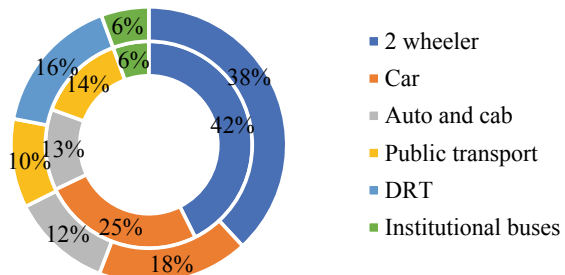
Fig. 20 Dynamic pricing for DRT bus service

as the price will be highest in morning and evening peak hours i.e. 1.5 times of existing price during peak hours, 4 hours per day and price will be 1.38 times of existing price during next 2 hours of peak demand i.e. 8 hours per day. Later price will be same during rest of the time during low demand in non-peak hour.

Change in Mode of Travel

After introduction of DRT bus services as a feeder there will be shift of passenger’s mode of travel from existing fixed route public bus users, private vehicle users, auto rickshaw and cab users to DRT service. Change in mode has been calculated based on the people’s willingness to shift to DRT from existing mode, as per the results of state preference survey conducted to estimate the probability of people willing to shift from each individual mode in Table 12. Modal share of public transport usage will increase from 12.67 to 26% and private vehicle usage will reduce for two wheeler and car users by 4 and 7% (Fig. 21; Table 13).

Fig. 21 Modal shift after introduction of DRT services in scenario 2



Inner circle shows modal split before DRT and outer circle shows after DRT

Table 13 Reduction in private vehicle usage

Shift to DRT	
Existing private vehicle users	47,469
Private vehicle users reduced after DRT	8431
Reduction %	18%

After introduction of DRT, 18% reduction in private personalized vehicle usage is anticipated which will improve road congestion situation in urban area. Out of total reduce private vehicles users, 60% are car users and 40% are two-wheeler users.

6 Recommendation

Demand responsive bus services has the potential to shift users from single occupancy vehicles to mass transit modes and help alleviate urban road congestion. Demand responsive services will be successful when operated over a small delineated area rather than of the whole city, as unshared ride distance increases beyond 4 km travel distance. Thus, increased unshared ride distance for the large capacity vehicle will not be financially beneficial for transport authority to operate. In this study, travel demand is estimated only for the passengers traveling outside the study area by mass transit like metro rail which will be coming in 2–3 years, existing BRTs and passengers using existing fixed route public bus service. As a result, of which the ride requests are maximum in morning and evening peak hours, also total fleet size of DRT vehicles is underutilized in non-peak hours. During this time intra area travel trips need to be targeted which are generated due to presence of IT industrial area and educational institutions which have flexible timings.

In case of Scenario 1 where demand for DRT is the same as that of existing public transport demand, option 5 with fleet size 75 and in Scenario 2 where demand for DRT is based on people willing to shift to DRT from existing mode, option 5 with fleet size 95 vehicles is the ideal situation for implementation of such project. Average waiting time for existing fixed route bus reduces by 0.5 times when operated as demand responsive bus service. Average walking time to bus stop reduces by 0.43 times of existing walking time. Average in-vehicle time remains almost the same. Average total travel time reduces by 0.32 times and average per passenger distance traveled reduces by 0.35 times of existing average distance traveled. This can prove to be lucrative options for users.

To make DRT service financially viable concept of dynamic pricing needs to be followed or else project will not be successful. The dynamic pricing, will increase the price of public transport by 1.5 times of existing price in peak hrs, and will be same in non-peak hrs. Also, increasing the DRT transport price by 0.3 times throughout the day will balance the cost. There is a potential of value addition to existing fixed route public bus service if integrated with the mass on demand ride sharing service or DRT feeder service as per the results obtained from research.

This research may help in giving insights of working of dynamic routing of bus and mass ridesharing service, but this research can be further continued to achieve more realistic results.

6.1 Way Forward in Research

Concept of minimum occupancy of vehicle is missing in research addition of which will give better results for operator's efficiency indicators.

Further research can be taken to make demand responsive service more realistic on ground for implementation by including–

- Changing the composition and combination of DRT stop locations,
- Combination of varied capacity bus service,
- Adjusting zoning effect with decentralization and centralization and
- More importantly working with realistic spatio-temporal data on daily basis,
- And identifying minimum allowable time between pre booking and scheduling of ride for trip planning can only be done post implementation.

References

1. Khan U (2011) Emerging trends of urbanization in India: an evaluation from environmental perspectives. Infibnet. Retrieved from <http://hdl.handle.net/10603/12949>
2. MoRTH (2013) Basic road statistics of India 2012–13. Ministry of Road Transport and Highways, Government of India, 13, 70
3. KPMG (2017) Reimagining public transport in India, (October)
4. Gupta N (2016). Urban bus sector in india-implementing efficient & sustainable city bus systems. In: Urban mobility India 2016
5. NUTP (2014) National urban transport policy, 2014. Retrieved from www.iutindia.org
6. Rieser M, Dobler C, Dubernet T, Grether D, Horni A, Gregor L, Nagel K (2014) MATSim user guide
7. Hall CH, Lundgren JT, Varbrand P (2008) Evaluation of an integrated public transport system: a simulation approach. Arch Transport 20(1–2):29–46. Retrieved from http://webstaff.itm.liu.se/~carha/Parallell_v_LITRES_paper.pdf
8. Ronald N, Navidi Z, Wang Y, Rigby M, Jain S, Kutadinata R, Thompson R (2017). Mobility patterns in shared, autonomous, and connected urban transport á ride sharing á, pp 275–290. <https://doi.org/10.1007/978-3-319-51602-8>
9. Westerlund Y, Stahl A, Nelson J, Mageean J (2000). Transport telematics for elderly users: successful use of automated booking and call-back for demand responsive transport services in Gothenburg
10. Davison L, Enoch M, Ryley T, Quddus M, Wang C (2012) Research in transportation business & management identifying potential market niches for demand responsive transport. RTBM 3:50–61. <https://doi.org/10.1016/j.rtbm.2012.04.007>
11. Davison L, Enoch M, Ryley T, Quddus M, Wang C (2014) A survey of demand responsive transport in Great Britain. Transp Policy 31:47–54. <https://doi.org/10.1016/j.tranpol.2013.11.004>
12. Mageean J, Nelson JD (2003) The evaluation of demand responsive transport services in Europe, 11(August 2002), pp 255–270. [https://doi.org/10.1016/S0966-6923\(03\)00026-7](https://doi.org/10.1016/S0966-6923(03)00026-7)
13. Brake J, Nelson JD, Wright S (2004) Demand responsive transport: towards the emergence of a new market segment. J Transp Geogr 12(4):323–337. <https://doi.org/10.1016/j.jtrangeo.2004.08.011>
14. Enoch MP (2005) Demand responsive transport: lessons to be learnt from less developed countries

15. Transport and Housing Bureau HK (2017) Public transport strategy study. Retrieved from https://www.td.gov.hk/filemanager/en/publication/ptss_final_report_eng.pdf
16. Edwards D, Watkins K, Edwards D (2016) Comparing fixed-route and demand responsive feeder transit systems in real-world settings, (December 2013). <https://doi.org/10.3141/2352-15>
17. Koh K, Ng C, Pan D, Mak KS (2018) Dynamic bus routing : a study on the viability of on-demand high-capacity ridesharing as an alternative to fixed-route buses in Singapore. In: 2018 21st international conference on intelligent transportation systems (ITSC), pp 34–40
18. Quadrifoglio L, Dessouky MM, Ordo F (2008) A simulation study of demand responsive transit system design, 42:718–737. <https://doi.org/10.1016/j.tra.2008.01.018>
19. Bischoff J, Führer K, Maciejewski M (2018) Impact assessment of autonomous demand responsive transport (DRT) systems
20. Enoch M, Potter S, Parkhurst G, Smith M (nd) Why do demand responsive transport systems fail? In: Transportation Research Board 85th annual meeting, 22–26 Jan 2006, Washington DC
21. Inturri G, Giuffrida N, Ignaccolo M, Le M, Pluchino A, Rapisarda A (nd) Testing demand responsive shared transport services via agent-based simulations
22. WRI and Embrac (2016) Chapter-1 Urban bus-transport India—status and trends. Retrieved from WRI cities hub: <https://wricitieshub.org/>
23. UNDP, IUT India, UTP, & Ministry of Urban Development, G. of I. (nd) Public transport scenario in India.
24. Pune Municipal Corporation (2012) Draft city development plan for Pune—2041 https://pmc.gov.in/sites/default/files/project-glimpses/Draft_City_Development_Plan_for_Pune_City_2041_Vol-1.pdf.
25. Pune Municipal Corporation, Datastore <http://opendata.punecorporation.org/Citizen/User>
26. Pune Mahanagar Parivahan Mahamandal Ltd. <https://www.pmpml.org/>
27. Israel GD (1992) Determining sample size 1(November):1–5
28. Ma Z (nd) MATMASSim : multi-agent transportation simulation using MASS. University of Washington, Bothell
29. Rieser M (2010) Adding transit to an agent-based transportation simulation. Doctor of Engineering). Technische Universität, Berlin. Retrieved from http://opus4.kobv.de/opus4-tuberlin/frontdoor/deliver/index/docId/2642/file/rieser_marcel.pdf
30. Axhausen KW, Rieser M, Horni A (2016) Generation of the initial MATSim input. The multi-agent transport simulation MATSim, pp 61–64. <https://doi.org/10.5334/baw.7>
31. Horni A, Nagel K, Axhausen KW (2016) The multi-agent transport simulation title of book : The multi-agent transport simulation MATSim.
32. WRI Ross Center for Sustainable Cities (nd) Role of bus aggregators in improving city bus services in India. Retrieved from <https://shaktifoundation.in/report/role-bus-aggregators-improving-city-bus-services-india/>
33. Häme L (2013) Demand-responsive transport: models and algorithms. Aalto University School of Science
http://hongkongextras.com/_minibus_public_light_bus.html
34. http://hongkongextras.com/_minibus_public_light_bus.html
35. Maciejewski M, Nagel K (2012) Towards multi-agent simulation of the dynamic vehicle routing problem in MATSim. In: Lecture notes in computer science (including subseries lecture notes in artificial intelligence and lecture notes in bioinformatics), 7204 LNCS (PART 2), pp. 551–560. https://doi.org/10.1007/978-3-642-31500-8_57

A Heuristic Method of Prioritizing Flexible Pavement Sections



V. S. Sanjay Kumar and Abin Joseph

1 Introduction

The state of Kerala in India has a good network of roads with efficient connectivity to all major and minor places in the state. The base of this road network is 11 National Highways passing across the length and breadth of the state and 72 State Highways spread within the state. Besides the National Highways and State Highways, the road network comprises of Major District Roads and village roads. The total length of Kerala's road network is about 2.19 lakh km. Out of this, only 1781.57 km is the length of National Highways. Kerala is a state with average annual rainfall of about 3000 mm and high vehicular traffic through almost all categories of roads. The state has 110.3 lakh registered motor vehicles as of March 2017. For the last two decades, it has experienced a compounded annual growth rate of above 10% in the number of motor vehicles. The number of vehicles per 1000 population in March 2017 is 330. According to World Development Indicators (2015), number of vehicles per 1000 population in India is 18, China is 47, and United States is 507. Due to the climatic conditions and high vehicular traffic, the road networks in Kerala is in great danger. Even though Kerala has a good road network, there is a lack of proper maintenance strategy. A prioritization strategy is to be developed considering the limited budget and striving toward good pavement performance. The paper discusses such a methodology for arriving at a suitable maintenance priority strategy using the data on pavement distress, traffic volume, and structural performance.

V. S. Sanjay Kumar (✉) · A. Joseph
National Transportation Planning and Research Centre, Thiruvananthapuram, India

© The Author(s), under exclusive license to Springer Nature Singapore Pte Ltd. 2022
D. Singh et al. (eds.), *Proceedings of the Fifth International Conference of Transportation Research Group of India*, Lecture Notes in Civil Engineering 218,
https://doi.org/10.1007/978-981-16-9921-4_3

1.1 Literature Review

Reddy and Veeraragavan developed a methodology of priority ranking of pavements [1]. This methodology involves assigning a priority index to different sections based on their overall distress index model and traffic adjustment factors. Narasimha et al. gives a procedure for prioritizing roads in a network for periodic maintenance based on the subjective rating technique as per the guidelines of Asphalt Institute, Lexington, Kentucky, USA [2]. Shah et al. used the subjective rating method for prioritizing the urban roads [3]. This method was based on maintenance priority index which is a function of Road Condition Index, Traffic Volume Factor, Special Factor, and Drainage Factor. Road Condition Index is a function of degree, extent, and weightage of pavement distresses. Weightage for Special Factor is provided based on the class of road. Ahmed et al. used the Road Condition Index (RCI) method for prioritizing the pavement sections [4]. RCI is a function of degree, extent, and weightage of pavement distresses. The value of RCI varies between 1 for a new pavement with no distress and 25 for failed pavements. Pavements with higher RCI should be given higher priority for maintenance. All the above works are based on the type, quantity, and severity of pavement distress. Structural performance of the pavements was not directly accounted for prioritization. In this work in addition to the pavement distress, structural performance of the pavement is also considered for the prioritization.

2 Study Network and Data Collection

2.1 Study Road Network

The road network for the study was selected through reconnaissance survey and consisted of a total of six roads in Thrissur district, comprising of one National Highway, three State Highways, and two Major District Roads (MDR). The NH section comprises of the portion of NH 66 passing through Thrissur district. The State Highways selected are SH 75 (Vadanapally–Thrissur, VT), SH 51 (Kodakara–Kodungalloor, KK), and SH 61 (Potta–Moonupeedika, PM). The MDRs selected are Cherpu–Thriprayar (CT) road and Peringotukara–Kaanjany–Chavakkadu (PKC) road. The selected roads are interconnected and form a good road network, with a total length of 165 km. Also the roads in the network are complementing to each other in cases where traffic diversion are required. Figure 1 shows the road network.



Fig. 1 Road network selected for the study

2.2 Data Collection

Pavement Condition Survey: Pavement condition refers to the condition of the pavement surface in terms of its general appearance. The type, quantity, and severity of all the distresses present on the pavement are noted, and the pavement condition survey was carried out at 100 m interval, each lane separately. The quantity of distresses

was measured based on visual inspections, and the distresses were classified based on their severity [5].

Unevenness Measurement: Roughness data was collected for the entire road network using fifth wheel bump integrator. The values obtained are converted to standard roughness value in terms of International Roughness Index (IRI).

Traffic Volume Survey: Mid-block classified traffic volume survey was carried out at selected points in the network. Locations were fixed in such a way that the data collected accounts for major deviations. The data was expressed as daily traffic in terms of Passenger Car Unit (PCU). For the purpose of prioritization, traffic in terms of msa was used.

Structural Performance Evaluation: Structural performance evaluation of the homogeneous sections was done by measuring the characteristic deflection of the pavement. Benkelman beam deflection technique, which is a non-destructive method of data collection, was used for the structural evaluation. The deflection measurements were taken as per the procedure laid down in IRC: 81 (1997).

Inventory Data Collection: Inventory data was collected for the entire road network, and it includes class of road, drainage condition, geometrics of the pavement section, etc.

3 Homogenization of Road Network and Demarcation of Control Sections

Homogenization of road network means splitting up the road network into sections in such a way that each section possesses similar characteristics. The study road network was divided into 29 homogeneous sections based on the Pavement Condition Index (PCI), International Roughness Index (IRI), and daily traffic. Homogenization was done in such a way that if consecutive 100 m interval sections have same rating based on Pavement Condition Index and International Roughness Index along with same daily traffic volume, then it is considered as a homogeneous section. If any one of the three parameter changes after a few sections, it was taken as next homogeneous section. If one or two 100 m interval sections have different ratings and the other sections before and after these sections have same ratings, then the ratings of these sections were neglected and entire section was considered as a single homogeneous section. In each of the homogeneous sections, control sections of length 1000 m each were demarcated. The control sections were selected in such a manner that the section is continuous, and there are no junctions within. Within the demarcated control sections, detailed pavement condition survey and structural performance evaluation were carried out [6]. The quantity and severity of each distress type was measured using a measuring tape. Table 1 shows the characteristic deflection of control sections.

Table 1 Characteristic deflection of control sections

Section	Characteristic deflection (mm)	Section	Characteristic deflection (mm)	Section	Characteristic deflection (mm)
NH 1	0.55	VT 1	0.89	KK 1	0.34
NH 2	0.98	VT 2	0.71	KK 2	0.31
NH 3	0.30	VT 3	0.38	KK 3	0.26
NH 4	0.33	PM 1	0.50	KK 4	0.61
NH 5	0.63	PM 2	0.56	KK 5	3.76
NH 6	0.57	PM 3	0.93	PKC 1	0.75
NH 7	0.19	PM 4	0.75	PKC 2	0.21
NH 8	0.35	CT 1	0.63	PKC 3	0.35
NH 9	0.46	CT 2	0.14	PKC 4	0.13
NH 10	0.50	CT 3	0.48		

4 Pavement Priority Index

The authors have arrived at a new index, Pavement Priority Index (PPI), which is a numerical value to define the overall priority to a road section for maintenance works. The index takes care of pavement distress, traffic volume, road category, drainage condition, and structural performance. Thus, it characterizes the functional as well as structural performance of the road section, with due consideration to traffic. PPI is given by Eq. (1), where RCI is the Road Condition Index, TVF is the Traffic Volume Factor, SF is the Special Factor, DF is the Drainage Factor, and CF is the Characteristic Deflection Factor.

$$PPI = RCI \times TVF \times SF \times DF \times CF \tag{1}$$

The equation adopted is an improvisation of Maintenance Priority Index (MPI) as per Shah et al. [3], which is given by Eq. (2).

$$MPI = RCI \times TVF \times SF \times DF \tag{2}$$

It may be noted that the calculation of PPI incorporates the effect of structural performance, taken as Characteristic Deflection Factor (CF). Higher value of PPI indicates poor condition of road section. Hence, road sections with higher PPI value should be given higher priority when formulating the maintenance strategy.

Road Condition Index (RCI) indicates the overall pavement condition of the road section and is calculated using Eq. (3), where, UI_i is the Urgency Index corresponding to distress type i , and W_i is the weight of the distress type i .

$$RCI = \frac{\sum(UI_i \times W_i)}{\sum W_i} \tag{3}$$

Urgency Index is calculated based on the severity and quantity of each distress type. The severity of distress is expressed as Degree and quantity is expressed as Extent. Hence UI is given as Eq. (4).

$$UI = \text{Degree} \times \text{Extent} \quad (4)$$

The value of degree and extent varies between 1 and 5. The values of degree and extent for various severity and quantity of distresses are given in Tables 2 and 3, respectively. As different distresses will have varying effect on pavement, a weightage factor is included. The weightage assigned to various distresses are given in Table 4.

An illustration for the calculation of RCI is given in Table 5.

Table 2 Severity of distress in terms of degree (*source* Shah et al.)

Degree (<i>D</i>)	Description
1	Very low severe: Minor importance or difficult to discern. No maintenance required
2	Low severe: Easy to discern, but of minor importance. No immediate maintenance required
3	Medium severe: Notable with respect to consequences, but still acceptable. Maintenance is, however, required
4	High severe: Of significant consequences, undesirable. Maintenance required fairly regularly
5	Very high severe: Of extreme consequences, unacceptable. Immediate maintenance required

Table 3 Quantity of distress in terms of extent (*source* Shah et al.)

Extent (<i>E</i>)	Description
1	5% of road affected
2	Between 5 and 15% of road affected
3	Between 15 and 30% of road affected
4	Between 30 and 60% of road affected
5	More than 60% of the road affected

Table 4 Weightage assigned to various distresses (*source* Shah et al.)

Distress type	Weight
Patching	1
Rutting	2
Raveling	3
Pot hole	4
Crack	5

Table 5 RCI calculation for control section KK1

KK 1	Patching			Rutting			Ravelling			Pot hole			Cracks		
	L	M	H	L	M	H	L	M	H	L	M	H	L	M	H
Distress (%)	0.21	0.021	0	0.098	0	0.005	0.82	0.0087	0.0036	0	0.00002	0.0014	0.16	0.014	0.018
Extent	1	1	0	1	0	1	1	1	1	0	1	1	1	1	1
Degree	1	2	3	1	2	3	1	2	3	1	2	3	1	2	3
UI	1	2	0	1	0	3	1	2	3	0	2	3	1	2	3
W	1	1	1	2	2	2	3	3	3	4	4	4	5	5	5
RCI	1.76														

L Low, *M* Medium, *H* High

Table 6 Traffic volume factor (*source* Shah et al.)

Traffic volume (msa)	TVF
<10	1
10–20	2
21–30	3
31–40	4
>40	5

Table 7 Special factor for class of road

Road class	SF
NH	5
SH	4
MDR	3
VR	2

4.1 Traffic Volume Factor

Traffic volume is an important factor when looking for prioritization and maintenance of road sections. Traffic volume is measured in terms of commercial vehicles per day (CVPD), and it is converted into cumulative number of million standard axles (msa). As per IRC 37-2012, the design life and annual growth rate are taken as 10 years and 5%, respectively. The Traffic Volume Factor (TVF) is dependent upon the traffic expressed in msa and the values are given in Table 6.

4.2 Special Factor

The class of roads has great importance on priority ranking for maintenance. National Highways have more importance than State Highways and Major District Roads. Hence, Special Factors are introduced to cater the importance of class of roads on priority ranking. Special Factors are weightages with low weightage for village roads and high weightage for NHs and are given in Table 7.

4.3 Drainage Factor

Absence of proper drainage facility damages the pavements very early. Hence, it is necessary to evaluate the condition of drainage facilities before working out the priority ranking. If the condition of the drainage facility is Poor, then the weightage given is 4 and if it is in good condition then weightage given is 1. The values for

Table 8 Drainage factor
(source Shah et al.)

Drainage condition	DF
Good	1
Fair	2
Satisfactory	3
Poor	4

Table 9 Characteristic deflection factor

Characteristic deflection (mm)	CF
0–0.5	1
0.5–1	2
1–2	3
2–3	4
>3	5

Drainage Factors are given in Table 8. For the study roads under consideration, the drainage condition is found to be satisfactory.

4.4 Characteristic Deflection Factor

Characteristic Deflection Factor incorporates the structural performance condition of the road section on priority ranking. Structural performance is measured in terms of deflection of the pavement. If the characteristic deflection has higher value, then it means that the pavement is structurally weak. Table 9 shows the characteristic deflection value ranges and corresponding factors.

4.5 Pavement Priority Index

Based on the collected data, the Pavement Priority Index for the various control sections is calculated using Eq. (1) and is given in Table 10. The table also includes the values of MPI as per Eq. (2), which is not taking account of the deflection parameter.

From Table 10, it can be seen that for control sections with characteristic deflections between zero and 0.5 mm, the MPI and PPI are same. For sections whose characteristic deflection is above 0.5 mm, the PPI value is higher than MPI. The PPI is double of MPI for 11 sections, and for one section (KK 5), PPI is five times MPI. (This is by virtue of the higher deflection value of 3.76 mm in KK 5). By considering Characteristic Deflection Factor, the priority for maintenance can be more specifically suggested.

Table 10 PPI and MPI of control sections

Section	RCI	TVF	SF	DF	CF	MPI	PPI
NH 1	0.18	2	5	3	2	5.33	10.67
NH 2	0.22	2	5	3	1	6.67	6.67
NH 3	0.87	5	5	3	1	65.00	65.00
NH 4	1.42	5	5	3	1	106.67	106.67
NH 5	1.42	5	5	3	2	106.67	213.33
NH 6	1.27	5	5	3	2	95.00	190.00
NH 7	1.22	5	5	3	1	91.67	91.67
NH 8	1.69	4	5	3	1	101.33	101.33
NH 9	1.84	5	5	3	1	138.33	138.33
NH 10	1.42	5	5	3	1	106.67	106.67
VT 1	1.62	3	4	3	2	58.40	116.80
VT 2	1.87	3	4	3	2	67.20	134.40
VT 3	1.31	4	4	3	1	62.93	62.93
PM 1	0.38	5	4	3	1	22.67	22.67
PM 2	0.33	5	4	3	2	20.00	40.00
PM 3	0.20	2	4	3	2	4.80	9.60
PM 4	0.20	2	4	3	2	4.80	9.60
KK 1	1.76	3	4	3	1	63.20	63.20
KK 2	0.36	5	4	3	1	21.33	22.00
KK 3	0.51	2	4	3	1	12.27	12.27
KK 4	1.29	2	4	3	2	30.93	61.87
KK 5	1.33	2	4	3	5	32.00	160.00
PKC 1	1.96	2	3	3	2	35.20	70.40
PKC 2	0.93	1	3	3	1	8.40	8.40
PKC 3	0.31	1	3	3	1	2.80	2.80
PKC 4	1.24	2	3	3	1	22.40	22.40
CT 1	1.42	2	3	3	2	25.60	51.20
CT 2	0.78	2	3	3	1	14.00	14.00
CT 3	1.71	2	3	3	1	30.80	30.80

5 Weighted Rating Value (As Per IRC 82-2015)

IRC 82-2015, Code of Practice for Maintenance of Bituminous Surface of Roads rates the pavement surface condition based on the type of distress as well as quantity of distress [7]. Higher rating indicates good condition of pavement, and accordingly sections with low rating should be given higher priority for maintenance work. The code also gives the maintenance strategies based on the distress types present on the pavement. IRC 82 emphasizes each distress type, their reason for occurrence,

Distress Type	Input (%)	RATING AS PER NORMS	Weightage	Weighted Rating Value
Cracking (%)	8.76	1.3	1.00	1.3
Ravelling (%)	1.01	2.0	0.75	1.5
Potholes (%)	0.00	3.0	0.50	1.5
Shoving (%)	0.00	3.0	1.00	3.0
Patching (%)	17.99	1.0	0.75	0.8
Settlements (%)	0.11	2.9	0.75	2.2
Rut Depth (%)	0.94	2.8	1.00	2.8
Final Rating				1.9
Condition				Fair

Fig. 2 Sample calculation of WRV (section NH 5)

location on the pavement where it occurs, how its severity varies, and treatment measures for the distress. Mainly three maintenance types are covered in this code: routine maintenance, preventive maintenance, and periodic maintenance. Pavement distress-based ratings for highways, MDRs, rural roads, and urban roads are given in this code. Serviceability indicators for highways and urban roads on the basis of roughness and skid resistance are also given in the code.

Based on the distress types present on the pavement surface, Weighted Rating Values (WRVs) are determined for the road sections under the purview, and various maintenance techniques are suggested. The density of each distress in percentage is provided as the input for the calculation of WRV. Figure 2 shows the calculation of WRV for the section NH 5. Table 11 shows the calculated WRV and corresponding pavement condition of all the control sections as per IRC 82-2015.

6 Prioritization Strategy

A prioritization strategy based on PPI and WRV is attempted. As explained, PPI is a composite index and represents pavement distress, traffic intensity, and structural performance. The road category and Drainage Factor are also accounted while calculating PPI.

The PPI of each of the control sections are determined based on the field investigation values obtained. The sections are then ranked based on the PPI value. The higher the PPI, more is the priority. On arriving at equal PPI for two or more sections, the RCI values are compared, and the section with higher RCI is given priority for maintenance option. If RCI value of two or more sections is also same, then the

Table 11 WRV and condition of homogeneous sections based on IRC-82-2015

Section	WRV	Condition
NH 1	2.4	Good
NH 2	2.4	Good
NH 3	2.2	Good
NH 4	2	Good
NH 5	1.9	Fair
NH 6	1.9	Fair
NH 7	2.1	Good
NH 8	1.9	Fair
NH 9	1.8	Fair
NH 10	1.8	Fair
VT 1	2	Good
VT 2	1.9	Fair
VT 3	2	Fair
PM 1	2	Good
PM 2	2.1	Good
PM 3	2.4	Good
PM 4	2.5	Good
KK 1	2.3	Good
KK 2	2.3	Good
KK 3	2.3	Good
KK 4	2.2	Good
KK 5	1.9	Fair
PKC 1	2.1	Good
PKC 2	2.2	Good
PKC 3	2.2	Good
PKC 4	2.2	Good
CT 1	2.1	Good
CT 2	2.2	Good
CT 3	2.2	Good

section with low WRV is given more priority. Table 12 shows the rank of control sections along with recommended maintenance strategy.

It can be seen from Table 12 that section NH 4 and NH 10 has PPI of 106.67 each. On comparing RCI, it can be seen that the RCI is also same (1.42 each). Then, WRV is checked, and the section with least WRV is given priority. This scenario is the same for sections PM 3 and PM 4.

The authors have selected suitable maintenance techniques from IRC 82-2015 based on the distress types observed on the pavement surface. The maintenance strategies considered are strengthening and rehabilitation (40 mm BC & 50 mm

Table 12 Prioritization of homogeneous sections and maintenance work recommended

Section	PPI	RCI	WRV	Rank	Maintenance work recommended (IRC 82:2015)
NH 5	213.33	1.42	1.9	1	Strengthening and rehabilitation (40 mm BC & 50 mm DBM)
NH 6	190.00	1.27	1.9	2	Strengthening and rehabilitation (40 mm BC & 50 mm DBM)
KK 5	160.00	1.33	1.9	3	Strengthening and rehabilitation (40 mm BC & 50 mm DBM)
NH 9	138.33	1.84	1.8	4	Strengthening and rehabilitation (40 mm BC & 50 mm DBM)
VT 2	134.40	1.87	1.9	5	Strengthening and rehabilitation (40 mm BC & 50 mm DBM)
VT 1	116.80	1.62	2	6	Strengthening and rehabilitation (40 mm BC & 50 mm DBM)
NH 10	106.67	1.42	1.8	7	Strengthening and rehabilitation (40 mm BC & 50 mm DBM)
NH 4	106.67	1.42	2	8	Strengthening and rehabilitation (40 mm BC & 50 mm DBM)
NH 8	101.33	1.69	1.9	9	Strengthening and rehabilitation (40 mm BC & 50 mm DBM)
NH 7	91.67	1.22	2.1	10	Thick overlay (40 mm BC)
PKC 1	70.40	1.96	2.1	11	20-25 mm SD/SDBC
NH 3	65.00	0.87	2.2	12	Thick overlay (40 mm BC)
KK 1	63.20	1.76	2.3	13	Microsurfacing
VT 3	62.93	1.31	2	14	Strengthening and rehabilitation (40 mm BC & 50 mm DBM)
KK 4	61.87	1.29	2.2	15	Thick overlay (40 mm BC)
CT 1	51.20	1.42	2.1	16	20–25 mm SD/SDBC
PM 2	40.00	0.33	2.1	17	Thick overlay (40 mm BC)
CT 3	30.80	1.71	2.2	18	Microsurfacing
PM 1	22.67	0.38	2	19	Thick overlay (40 mm BC)
PKC 4	22.40	1.24	2.2	20	Microsurfacing
KK 2	22.00	0.36	2.3	21	Microsurfacing
CT 2	14.00	0.78	2.2	22	Microsurfacing
KK 3	12.27	0.51	2.3	23	Microsurfacing
NH 1	10.67	0.18	2.4	24	Microsurfacing
PM 3	9.60	0.20	2.4	25	Microsurfacing
PM 4	9.60	0.20	2.5	26	Microsurfacing
PKC 2	8.40	0.93	2.2	27	Microsurfacing
NH 2	6.67	0.22	2.4	28	Microsurfacing
PKC 3	2.80	0.31	2.2	29	Microsurfacing

DBM), thick overlay (40 mm BC), and 20–25 mm SD/SDBC and microsurfacing. Road sections with WRV less than or equal to 2 are proposed to be provided with strengthening and rehabilitation, while sections in National Highways and State Highways whose WRV lies between 2 and 2.2 are proposed to be provided with thick overlays. Sections in MDRs whose WRV is above 2 and below 2.2 are proposed to be provided with 20–25 mm SD/SDBC. All other sections whose WRV is more than 2.2 are proposed to be provided with microsurfacing as they are observed to be in good condition.

7 Conclusion

Prioritization and maintenance of pavement sections are very important for providing the level of service demanded by the users. If a proper prioritization and maintenance strategy is absent, then it may lead to premature failure of pavements and cost of maintenance will be very high. A good pavement management system helps to provide good condition roads at minimum cost. For this purpose, an accurate prioritization method is required. In the proposed method pavement distresses, traffic volume, class of road, drainage condition, and structural performance of pavements were considered in determining the prioritization strategy. These factors were used to determine the Pavement Priority Index of sections, which is a composite index reflecting the structural and functional performance of the pavement. Weighted Rating Values of the road sections were also determined in accordance with IRC 82-2015. Prioritization strategy was determined as per the rankings based on PPI, RCI, and WRV. Control sections with high PPI value are given more priority for maintenance. If PPI values of two sections are equal, RCI values are compared and the section with higher RCI is given priority. If RCI also matches, then section with minimum WRV is given more priority. Suitable maintenance strategies as per IRC 82-2015 were also suggested. The method proposed is taking care of structural performance of the sections in addition to functional performance and traffic. The method can be utilized for prioritization of flexible pavements, as it requires minimum data.

References

1. Reddy BB, Veeraragavan A (2001) Priority ranking model for managing flexible pavements at network level. *J Indian Road Congress* 62(3):379–394
2. Narasimha VL, Sundararajan T, Raja M (2003) Subjective rating technique—a tool for prioritizing roads in a network for periodic maintenance. *Highway Res Bull Indian Road Congress* 69:1–14
3. Shah YU, Jain SS, Parida M (2012) Evaluation of prioritization methods for effective pavement maintenance of urban roads. *Int J Pavement Eng* 1–13 (Taylor and Francis)
4. Ahmed S, Vedagiri P, Krishna Rao KV (2017) Prioritization of pavement maintenance sections using objective based analytic hierarchy process. *Int J Pavement Res Technol* 10:158–170

5. ASTM D 6433:2007, Standard practice for roads and parking lots pavement condition index surveys. ASTM International, USA
6. IRC 81:1997, Guidelines for strengthening of flexible road pavements using Benkelman beam deflection technique. Indian Roads Congress, New Delhi
7. IRC 82:2015, Code of practice for maintenance of bituminous surface of roads. Indian Roads Congress, New Delhi

Effect of Compaction Levels on Moisture Susceptibility in Asphalt Mix



A. Jegan Bharath Kumar and Anoop. T. Vijayan

1 Introduction

Moisture susceptibility refers to the weakening of bituminous mixes due to an excess of moisture. Any bituminous mix is composed of asphalt, aggregate, and air voids. Moisture damage to the mix may occur in two ways. The first concern is that the binder's bonding to the aggregate may be reduced due to lower moisture content, and the second factor is that moisture may affect the rheological properties of binder, which can then impact the cohesion of the bituminous mix. If aggregate is porous, binder cannot able to bond with aggregate due to moisture, and if the mix is loaded again and again, the binder strips from the aggregate resulting in loss of adhesion. Pavement moisture damage results in distress, degradation, and further maintenance [1]. A major difficulty caused by water penetration within the asphalt aggregate interface is stripping, which is one of the most common problems. Water can be found in pores used for the preparation of a mixture or by filtering through asphalt cracks. The literature shows that there are approximately seven distinct stripping mechanisms, namely detachment, displacement, spontaneous emulsification, pore pressure, hydraulic scour, pH instability, and environmental impacts on asphalt aggregate structures. Since damage to moisture is the distress identified in HMA, considerable efforts produced to determine mechanisms of moisture susceptibility. Therefore, moisture damage is a significant concern as it diminishes the performance and service life of the pavement and hence results in a huge maintenance and rehabilitation cost to the agencies.

Without proper compaction, asphalt mixtures cannot be designed or produced correctly [2]. Compaction is the process of compacting an asphalt mixture by using outside pressures to reduce the volume of air. In this process, the mix occupies

A. Jegan Bharath Kumar (✉) · Anoop. T. Vijayan
National Transportation Planning & Research Centre (NATPAC), Thiruvananthapuram, Kerala
695011, India

a smaller space enabled by the air which driven out; hence, there is an increase in density of mix. Density of asphalt mix is better attained by using compaction conditions like compaction blows and compaction temperature. The volume of air in mix is crucial because it has a considerable impact on pavement performance. Each increase in air voids in 1% is around 10% of the life of the pavement [3]. Air voids should not go beyond 8% or drop below 3% in case of the dense-graded mix as pavement distress happens when the air voids deviate from the specified range [4]. The best defense against stripping is mixing, and construction of impermeable mat with adequate compaction depends on variables such as the aging of asphalt material, the disintegration of the aggregate, and the removal from the aggregate of the asphalt film [5]. Pavement durability is also connected with stripping. While some researchers and organizations believe the latter is better equipped to recognize stripping in numerous common testing procedures, including as boiling tests, indirect tensile tests, and Marshall testing, [6]. Examining the moisture behavior of asphalt mix under different compaction levels for static stability test and indirect tensile strength was done.

2 Materials Characteristics

2.1 Tests on Aggregates

The coarse aggregates chosen in this study were granite procured from a quarry located in Thiruvananthapuram, and the laboratory tests conducted to determine the aggregate engineering properties listed in Table 1. It found that aggregates collected from the quarry are of good quality and are suitable for roads. The combined and Flakiness elongation index of the selected aggregates is 10.58%, whereas the aggregate impact value is 21%. The water absorption of the aggregate observed to be 0.29%.

Table 1 Engineering properties of aggregates

Aggregate property	Test	Results	Limits
Particle shape	Combined flakiness & elongation index	10.58%	Max. 35%
Strength	Aggregate impact value	21.00%	Max. 24%
Water absorption	Water absorption	0.29%	Max. 2%
Abrasion test	Los Angeles abrasion test	25.00%	Max 40%
Specific gravity	Pyconometer	2.73%	2.5–3.2

Table 2 Physical parameters of asphalt as per IS: 73-2013

Parameter	Method of test	Specification IS 73:2013	Results
Penetration at 25 °C, 100 g, 5 s, 0.1 mm	IS 1203	Minimum 45	53.3
Softening point in °C	IS 1205	Minimum 47	49.0
Ductility at 25 °C, cm, after thin film oven test	IS 1208	Minimum 40	92.0
Specific gravity	IS 1202	Min 0.9	1.0

2.2 Tests on Asphalt

Kochi Refinery, BPCL, have guaranteed the quality of VG 30, but still, it examined for its various physical strength and the results of the asphalt given in Table 2. From the Brookfield viscosity test conducted, the mixing temperature was obtained at 160 °C and compaction temperature at 150 °C.

2.3 Aggregate Gradation

The combined grading of coarse aggregates and filler have selected within the limit specified as per MORTH specification 2013 and tested according to the IS 2386 Part I. Class I aggregate grading selected from MORTH specification with the nominal aggregate size of the aggregate is 19 mm, and the layer thickness is 50 mm. The

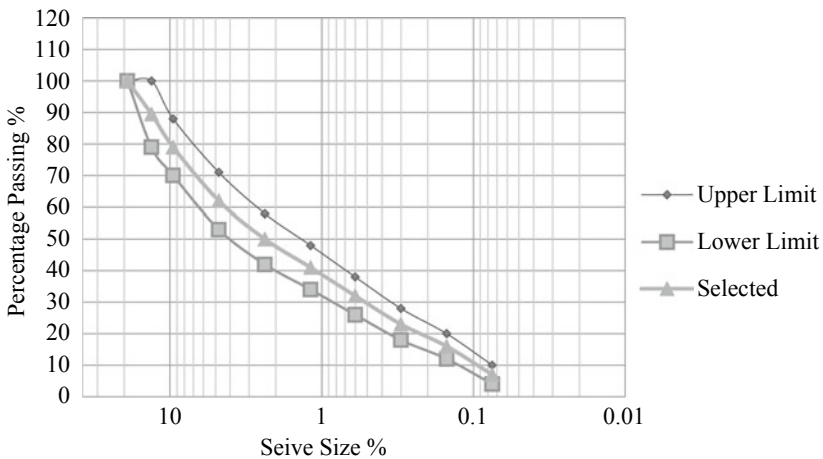


Fig. 1 Adopted aggregate gradation

selected aggregate gradation is displayed in figure (see Fig. 1). The mix design included the aggregates that were satisfied by the MORTH specifications.

3 Mix Design and Experimental Program

The material such as aggregate and asphalt was tested for various experiments and checked whether the selected aggregate or asphalt could be used for the road construction. The obtained test results compared with the standard results recommended by MORTH specification.

For designing of the mix by Marshall method, specimens were prepared with the selected aggregate gradation and the designed optimum binder content. The mixing temperature of the mix is 160 °C, and the specimens are compacted at the temperature of 150 °C. Bulk and maximum specific gravities of the entire specimen are to be determined. In order to adjust the air voids obtained from the mix configuration for the designed optimum binder content, the mix compliance with compaction blows is varied to test the mix's moisture sensitivity behavior. To examine the moisture susceptibility behavior of the mix, static immersion test and indirect tensile strength test were carried out following ASTM D 1075 and AASHTO T283-14. In static immersion test, the specimen was tested under two circumstances such as allowing the specimen to soak in water for 30–45 min and allowing the specimen to soak in water for 24 h, respectively. The specimen is kept at a temperature of 60 °C during both conditions. The tensile test strength of the specimen tested under two conditions, namely dry condition and wet condition. In dry condition, the specimen is allowed to soak in water for two hours and tested for indirect tensile test strength at 25 °C. The specimen may be freeze-dried in wet conditions for 16 h, then kept at 60 °C in the water bath for 24 h after which the specimen may be kept at a temperature of 25 °C for 2 h and then the specimen tested for indirect tensile resistance at 25 °C for 25 h. In this work, the impact of compaction on the stability and tensile strength of mixes on moisture susceptibility has been examined [7]. The asphalt behavior of mix at varying compaction levels such as 75 blows per face, 60 blows per face, 50 blows, and 40 blows per face is studied.

3.1 Mix Design

The asphalt mixture (BC-I) was designed by the Asphalt Institute, MS-2 for hot mixtures employing Marshall method. The optimum asphalt was obtained in the narrow range 5.3–5.5%, and hence, 5.3% was adopted as optimum binder content for design of mix. MORTH specification also specifies that the minimum asphalt content requirement is 5.3%. The volumetric properties of the design mixture are also evaluated using Marshall method as defined by IRC: SP: 101-2014, to determine whether a situation is amenable to compactibility of mix due to blows.

Table 3 Volumetric properties of mix

S. N	Property	Result	Specification (MORTH)
1	Optimum binder content (%)	5.3	Min 5.2
2	Marshall stability (kN)	20.09	9
3	Flow value (mm)	2.13	2–4
4	Air voids (%)	4.5	3–6
5	Voids in mineral aggregate (%)	13.70	12–14
6	Voids filled in asphalt (%)	69.23	65–75

3.2 Volumetric Properties

The volumetric properties of fabricated mix are examined and found that optimum binder content of the mix is 5.3. The property of the mix for the obtained OBC is given in Table 3 with the allowable limits as mentioned by MORTH specification. The stability of the mix is found to be 20.09 kN with the flow of 2.13 mm, and air voids of the mix are found to be 4.5%. About 13.7% voids in mineral aggregate is obtained with the voids filled in asphalt is 69.23%.

3.3 Bulk Specific Gravity

The density of mix has a great impact on the compaction levels. As the compaction levels increases, the bulk specific density decreases from 2.450 to 2.230 in the scenario of compaction blow ranging from 75 blows per face to 40 blows per face. The densities obtained are tabulated in Table 4, and the trend is shown in Fig. 2.

Table 4 Bulk specific gravity at different compaction levels

Compaction temperature	Compaction levels	Bulk density (g/cc)
150 °C	75 blows per face	2.450
	60 blows per face	2.400
	50 blows per face	2.250
	40 blows per face	2.230

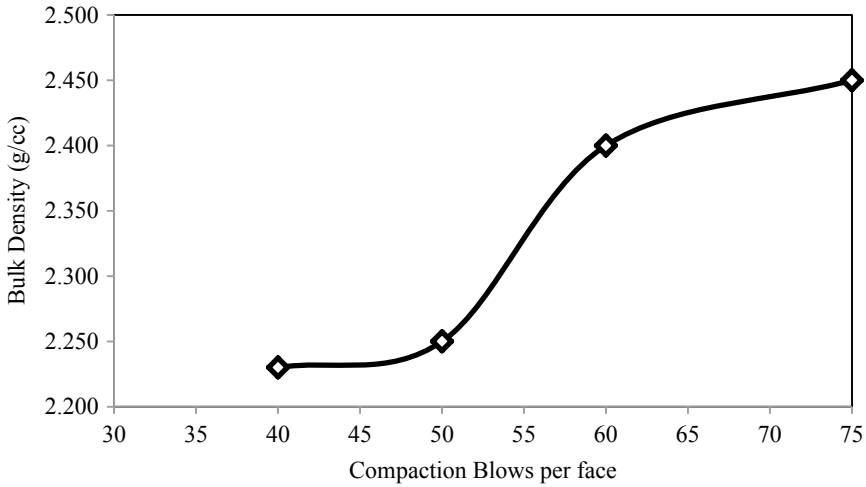


Fig. 2 Bulk specific gravity trend of mix

4 Results and Discussion

4.1 Static Immersion Test

The compacted mix is tested for static immersion test defined in ASTM D 1075. The compacted mix with different compaction levels such as 75 blows, 60 blows, 50 blows, and 40 blows undergone static immersion test under two conditions. The three sets of compacted specimens are conditioned around 60 °C maintained water bath for 40 min and tested for stability. The next three sets of compacted specimens are conditioned at 60 °C maintained water bath for 24 h and tested for stability. The performance of the mix tested is given in Table 5 and displayed in figure (see Fig. 5).

Table 5 Stability performance of mix

Compaction temperature	Compaction levels	Marshal stability dry (kN)	Marshal stability wet (kN)
150 °C	75 blows per face	20.09	19.1
	60 blows per face	16.84	15.21
	50 blows per face	15.88	12.66
	40 blows per face	14.92	10.01

Fig. 3 Compacted samples

Figures that illustrate the samples that were compacted and those that were set for the Marshall stability test are on display (see Figs. 3 & 4).

The stability of the mix decreases as the compaction level decreases in the event of two conditioning process dry and wet. The highest stability observed at the compaction level of 75 blows and the stability under dry condition and wet condition are recorded as 20.09 and 19.1 kN. It is to be noted that the same trend observed in case of different compaction blows as the compaction level increases the stability also increases.

4.2 Tensile Strength Ratio

The compacted mix specimens are monitored for their performance under indirect tensile strength in line with AASHTO T-283-14. The specimen subjected to undergo two series of testing one being the dry process and other being freeze–thaw conditioning cycle process. In dry process, three specimens of compacted samples are prepared, and its theoretical maximum specific gravity and bulk specific gravity are determined. Then, saturate the subset partly to be conditioned by distilled water using vacuum chamber at room temperature. Saturation is partially possible and a partial vacuum, such as 70 kPa is applied for a short period of five minutes. Following that the sampled is humidified by a soak for 1 h in the water bath, at 25 °C (77 °F) and tensile strength determined at 25 °C (77 °F). Each specimen should be wrapped

Fig. 4 Samples under stability test

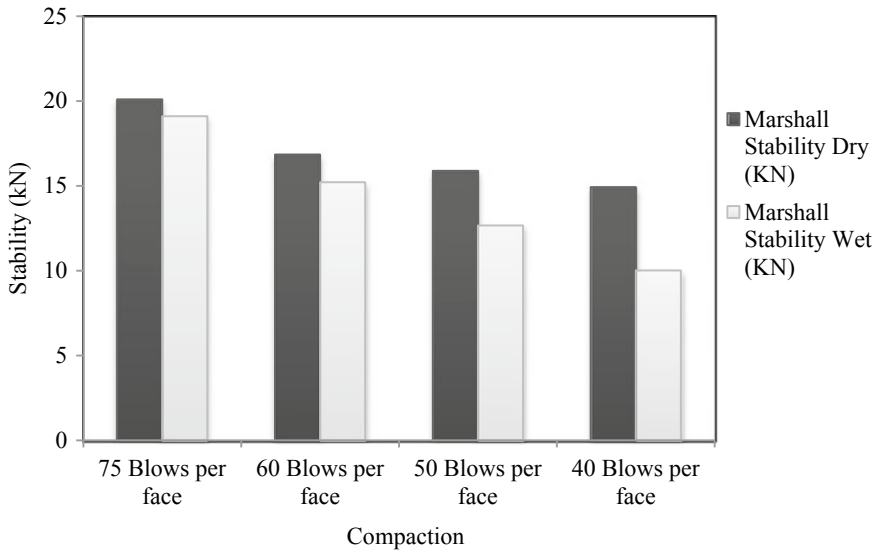


Fig. 5 Stability of mix at different compactibility

tightly with two layers of plastic film, using the masking band for wrapping if necessary. Wrap the specimen in a leak-proof plastic bag containing 3 ml distilled water and secure the bag with a tie or tape. The specimens should be kept at $-18\text{ }^{\circ}\text{C}$ for 16 h and then packaged and put in the freezer. Remove the specimens, dip them in water bath for 24 h at $60\text{ }^{\circ}\text{C}$. Once 3 min after surface thaw has taken place, the bag should be removed, and the specimens wrapped, and then the moisture-conditioned sample should be soaked in water for 1 h at $25\text{ }^{\circ}\text{C}$, then tensile strength should be determined.

The tensile strength computed in line with AASHTO T283 as follows:

$$\text{ITS} = \frac{2P}{\pi T D} \tag{1}$$

where P maximum load (kN), T thickness of specimen (mm), and D diameter (mm). Finally, asphalt mix resistance to effect of water is expressed as follows:

$$\text{TSR} = \frac{\text{ITS}_{\text{wet}}}{\text{ITS}_{\text{dry}}} \tag{2}$$

The above procedures are followed to determine indirect tensile strength of asphalt mix, and the values obtained are given in the below Table 6.

Figures shown below (see Figs. 7, 8, 9 and 10) display the process involved in the testing of samples for indirect tensile strength.

The indirect tensile strength of mix at four different compaction levels was tested under two conditioning, in dry condition and another under one freeze and thaw cycle. The results obtained are represented in Fig. 6. It shows that as the compaction levels decrease from 75 blows to indirect tensile strength at dry condition increase with the increases in compaction blows and the indirect tensile strength of the mix under one freeze cycle (wet condition) also increases with the increases in compaction blows.

From the experimental results (Fig. 6.), the tensile strength of asphalt sample is performed in the dry condition such that the compaction levels increased from 75 blows per face to 60 blows and then drops at 50 blows and then further drops in 40

Table 6 Stability ratio and TSR

Compaction temperature	Compaction levels	Stability ratio (%)	TSR (%)
150°C	75 blows per face	95	82
	60 blows per face	90	76
	50 blows per face	80	75
	40 blows per face	67	75

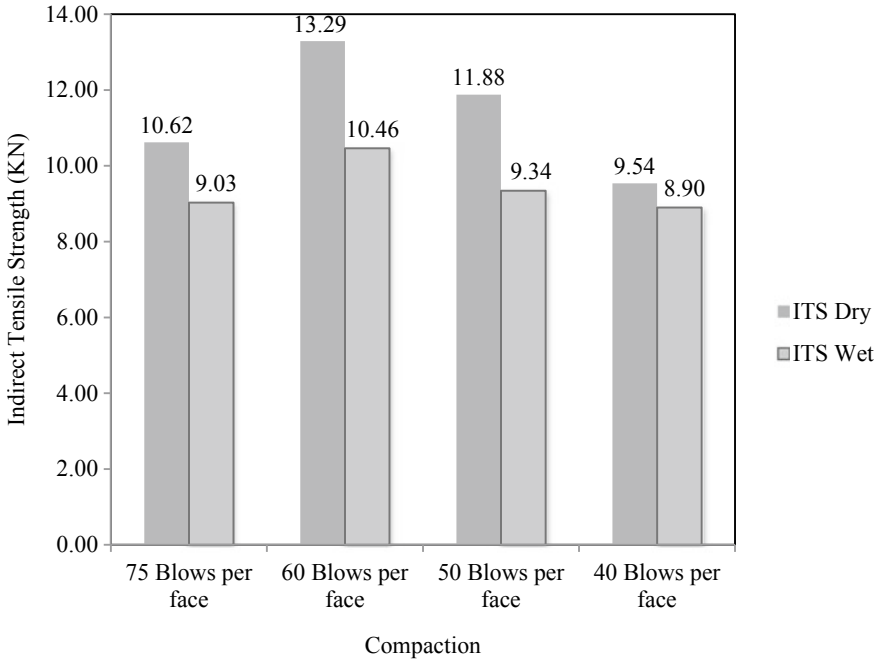


Fig. 6 Indirect tensile strength dry and wet

Fig. 7 Samples before conditioning



Fig. 8 Samples after freeze-thaw cycle in plastic bag



Fig. 9 Samples after freeze-thaw cycle



Fig. 10 Samples in water bath at 25 °C after removing from plastic bag



blows per face. It was examined that there was 25% change from 75 to 60 blows, 10% drop from 60 to 50 blows, and 19% drop from 50 to 40 blows.

After undergoing conditioning asphalt sample performed such that the compaction levels decreases from 75 blows per face to 50 blows, the tensile strength increases gradually there after it remains almost same. It observed that there is 5.21% increase from 75 to 60 blows and 8% increase from 60 to 50 blows (Fig. 11).

(See Fig. 11) displays relationship between the ratios (stability ratio and TSR) under multiple loads for twelve mixtures which were compacted at different compaction levels. In the figure, it is clearly seen that the asphalt samples for TSR and the stability ratio vary from 75 to 82% and 67% to 95%. The moisture performance of the compaction level 75 blows per face observed to be good as the TSR values are more than 80%.

5 Summary and Conclusion

Following this evidence, the following conclusions were made based on experimental data obtained from laboratory testing on asphalt mixes, and the density of the compacted mix was seen as it decreased compaction levels. The bulk density of mix has a great impact on the compaction levels. The maximum dry density of the loose aggregates from the designed mix seems to be unchanged. This is due to the fact

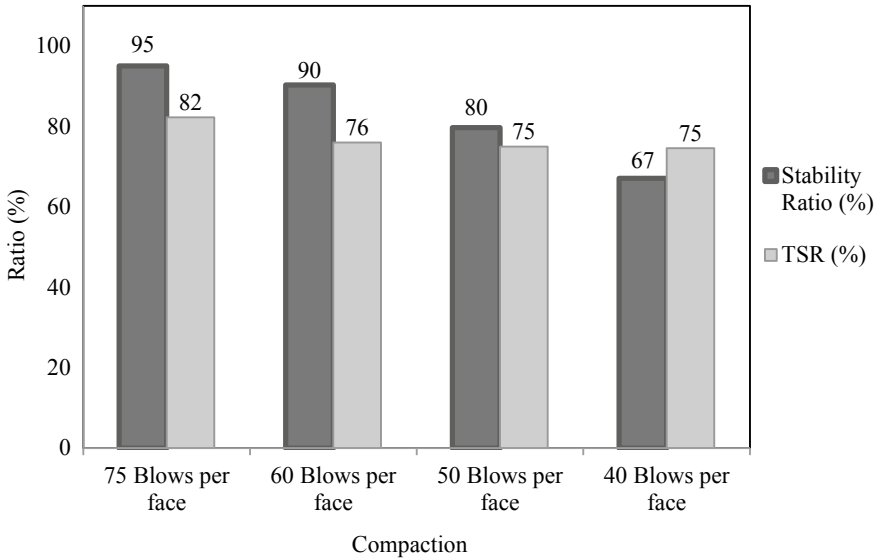


Fig. 11 Stability ratio and TSR at different compactibility

that the compactibility of asphalt mix does not have any cause on the maximum dry density. Stability of the design mix decreases as compaction level decreases in the case of two conditioning process. The maximum stability is observed for the sample compacted with the compaction blow of 75 numbers per face. All the asphalt mixes with the compaction blow of 75 on each face satisfy the minimum amount of 80% TSR rather the mix with low compaction level does not satisfy tensile strength ratio, and the stability ratio varies from 75 to 82%.

References

1. Xiao F, Jordan J, Amirghanian SN (2009) Laboratory investigation of moisture damage in warm-mix asphalt containing moist aggregate. *Transp Res Record J Transp Res Board*
2. Hot mix asphalt materials, mixture design and construction. National Center for Asphalt Technology (2006)
3. Linden RN, Mahoney JP, Jackson NC (1989) The effect of compaction on asphalt concrete performance. In: Annual meeting of the Transportation Research Board, Washington, DC
4. Roberts FL, Kandhal PS, Brown ER, Lee DY, Kennedy TW (1996) Hot mix asphalt materials, mixture design, and construction. National Asphalt Paving Association Education Foundation. Lanham, MD
5. Manual Series No. 02 (MS-2) Asphalt mix design methods (2014)
6. Khodaii A, Haghshenas HF, Kazemi Tehrani H (2012) Effect of grading and lime content on HMA stripping using statistical methodology. *Constr Build Mater* 34:131–135
7. AASHTO T283-14: Resistance of compacted bituminous mixture to moisture induced damage (2014)

Rutting Characterisation of EVA Modified Bitumen for High Modulus Asphalt Mixes (HiMA)



B. Anil Kumar, Gautam Gaurav, Kranthi Kuna, M. Amaranatha Reddy, and K. Sudhakar Reddy

1 Introduction

Overloading and high temperatures are the main challenging issues for the bituminous pavements in India as these often cause premature rutting failure in bituminous pavements. Among the approaches adopted worldwide for producing better rut resistant mixes, selection of suitable aggregate gradation and binder type, are considered as the key parameters. The French asphalt mix called enrobé à module élevé (EME) also called as high modulus asphalt (HiMA) mixes developed in the mid 1980s has been successfully used in countries like Australia [1] and South Africa [2] as high performing rut resistant mix to meet the requirements of the ever-increasing traffic volumes. These mixes are usually produced with hard grade (low penetration) bitumen [3].

Hard grade bitumens are usually produced in refineries by propane-deasphalting method or by air blowing method. Pavements laid with HiMA produced by air blown bitumen failed prematurely in fatigue [4]. Although the performance of the asphalt mixes produced with PDA bitumen is found to be satisfactory in most cases [4], very few refineries in India have this method of refining petroleum. Thus, different other high performing (hard grade) bitumens produced essentially by polymer modification of normal bitumen were used to produce high performing bituminous mixes having

B. Anil Kumar (✉) · G. Gaurav · K. Kuna · M. Amaranatha Reddy · K. Sudhakar Reddy
Department of Civil Engineering, Indian Institute of Technology Kharagpur, Kharagpur, West Bengal 721302, India

K. Kuna
e-mail: kranthi@iitkgp.ac.in

M. Amaranatha Reddy
e-mail: manreddy@iitkgp.ac.in

K. Sudhakar Reddy
e-mail: ksreddy@civil.iitkgp.ernet.in

significantly higher rut resistance than conventional mixes [5]. Use of polyethylene in the production of hard grade bitumen was found to result in very high rut resistance of mixes compared to standard road base mixes [5]. Modification of virgin binder using ethylene vinyl acetate (EVA) polymer for the production of hard grade bitumen showed improved rut resistance of HiMA at elevated temperatures [2]. The properties of EVA copolymers are mainly dependent on the vinyl acetate content.

This present study examines the feasibility of composite EVA polymer modification in the production of hard grade bitumen targeting mainly to achieve the rutting of the hard grade bitumen produced by the propane-deasphalting method as mixes prepared with hard grade bitumen were found to have satisfactory rutting resistance [4]. The composite modifiers used in the present study are ethylene vinyl acetate: EVA-18 and EVA-28 where 18 and 28 represent the percentages of vinyl acetate content in EVA. If the vinyl acetate content is low, the degree of crystallization is high resulting in the formation of a tough and rigid network imparting high resistance to deformation. On the other hand, high vinyl content produces a rubbery rich amorphous phase [6]. Therefore, the main objective of the study is to develop a hard grade bitumen using different combinations of EVA-18 and EVA-28 targeting to achieve the rutting properties of hard grade bitumen produced by propane-deasphalting method. It is expected that this composite polymer modification enables the production of a binder having rut resistance properties similar to those of the hard grade bitumen.

2 Materials and Experimental Work

2.1 Material Selection

The base bitumen used in the study for producing composite polymer modified bitumen is VG-40 viscosity grade bitumen. Two thermo-plastomeric polymers, EVA-18 and EVA-28, were used. The target bitumen considered in the study is the hard grade bitumen produced by propane-propane-deasphalting method. Both VG-40 and hard grade bitumen were procured from IOCL, Haldia refinery. Tables 1 and 2, respectively, present the physical properties of bitumen and EVA polymers used in the study.

The aggregates used for producing the asphalt mixes were procured from the construction site of Jharpokharia-Baripada-Baleashwar (Km 0+000 to Km 80+600)

Table 1 Physical properties of base bitumen and target bitumen

Properties	VG-40	Hard bitumen
Penetration at 25 °C	38	21
Softening Point, °C	52	58
Ductility @ 27 °C, cm	>100	>100
Viscosity @ 60 °C, Poise	4406	9850

Table 2 Physical properties of EVA polymers

Property	EVA-18	EVA-28
Vinyl acetate content	18	28
Density (g/cc)	0.941	0.944
Softening temperature, °C	62	<60
Elongation at break	820	900

Table 3 Physical properties of aggregates

Property	Value
Aggregate impact value (%)	15.5
Los Angeles abrasion value (%)	19
Combined flakiness and elongation index (%)	21

road project on national highway (NH)-18. The aggregate gradation considered in the study is dense bituminous macadam (DBM)-II as per MoRTH [7]. Table 3 presents the physical properties of the aggregates used in the study.

2.2 Methodology

The methodology adopted for the present study involves the evaluation of the properties of the hard binder and different modified binders, produced using different combinations of EVA-18 and EVA-28 polymers. The rheological characterisation (Temperature-frequency oscillation test and multiple stress and creep recovery) of the base bitumen, EVA modified bitumen and hard grade bitumen was carried out to select the polymer combinations that can be taken forward to asphalt mix testing. The asphalt mixes were prepared at optimum bitumen contents selected from mix design exercise. The rutting performance of the mixes was evaluated at 60 °C temperature using dry wheel tracker.

2.3 Preparation of EVA Modified Bitumen

The EVA modified blends were prepared by initially heating the base bitumen (VG-40) to a temperature of 170 °C after which EVA was added. The mix of VG-40 bitumen and EVA was blended in a blender with a stirrer arrangement. Different blends were prepared using different proportions of EVA polymer. The blending temperature was maintained between 170 °C and 175 °C and the blending was continued for a duration of 80–90 min with a shear rate of 1500–1700 rpm. The blending temperature and blending time were selected based on previous

research studies [8, 9]. The following blends were prepared in the present study. The designations used for different blends are given in the parentheses.

- VG-40 + 1% EVA-18 (V4E1)
- VG-40 + 2% EVA-18 (V4E2)
- VG-40 + 1% EVA-18 + 1% EVA-28 (V4E11)
- VG-40 + 1% EVA-18 + 2% EVA-28 (V4E12)
- VG-40 + 1% EVA-18 + 3% EVA-28 (V4E13)
- VG-40 + 1% EVA-18 + 4% EVA-28 (V4E14).

The initial trials involved the addition of EVA-18 (1% and 2%) to VG-40 base binder. Addition of 2% EVA-18 resulted in decrease in the ductility of the binder which may indicate excessive brittleness and greater cracking susceptibility of bitumen. Hence, EVA-28 is added further to improve the recovery properties.

2.4 Rheological Characterization of Bitumen

The visco-elastic rheological parameters such as complex shear modulus (G^*) and phase angle (δ) were determined for unaged and short-term aged bitumen as per AASHTO T-315 using a Kinexus dynamic shear rheometer (DSR). A 25 mm diameter parallel plate geometry with a 1 mm gap was used to characterize the rheological parameters. Temperature and frequency sweep tests were conducted on all the binders by varying the test temperature from 46 to 82 °C and frequency ranging from 10 to 0.1 Hz. The performance grading (PG) characterization of the bitumen was done by estimating the upper PG temperatures. The selection criterion for the upper PG temperature is the resistance offered by the binder to high-temperature pavement distress, rutting. AASHTO T-315 specifies minimum values for the superpave binder rutting parameter $G^*/\sin \delta$, tested in an oscillatory shear stress mode at 1.59 Hz. The minimum values for unaged and short-term aged binders are 1.0 kPa and 2.2 kPa, respectively. From the temperature sweep test carried out at 1.59 Hz, the bitumen upper PG temperature was determined for all unaged and short-term aged bitumen.

2.5 Multiple Stress Creep and Recovery (MSCR) Test

Rutting potential of short-term aged (RTFO) bitumen considered in the study was evaluated by multiple stress creep and recovery (MSCR) test as per AASTHO T-350 (2014). The test evaluates the rutting potential of base and modified bituminous binders in linear and nonlinear visco-elastic domains through a parameter called non-recoverable creep compliance (J_{nr}). It is the ratio of the non-recoverable strain to the applied peak shear stress. The bitumen sample of 1 mm thickness was sandwiched between two parallel plates of 25 mm diameter. The test was performed at stress levels of 0.1 kPa and 3.2 kPa and at 60 °C temperature.

2.6 Rutting Potential of Bituminous Mixes

Rutting potential of the selected bituminous mixes was measured in the laboratory using dry wheel tracker at 60 °C. Figure 1 shows the test set up used for the evaluation of the rutting potential of bituminous mixes. It consisted of an arrangement for application of a normal load of 700 ± 10 N on the specimens. The platform holding the specimens moves to-and-fro resulting in repeated tracking of a normally loaded wheel on the specimens. The entire test set up was housed in an environmental chamber, in which a constant test temperature can be maintained. The specimens of bituminous mixes were conditioned for 4 h before testing them at the test temperature of 60 °C. The deformation of the sample was measured using linear variable displacement transducers (LVDT). The least count of the displacement transducer was 0.001 mm. One to-and-fro motion of the wheel was considered as one cycle. The test was carried out for 5000 cycles at a frequency of 20 cycles per minute.

The specimens for the wheel tracking test were prepared to have an air void content of $7 \pm 0.5\%$. 100 mm diameter specimens of 63 mm height were prepared using Marshall compactor to achieve the target air void. The compacted specimens were sliced to have a height of 50 mm, and the vertical faces of the specimens were trimmed, to fit into the rigid mould.

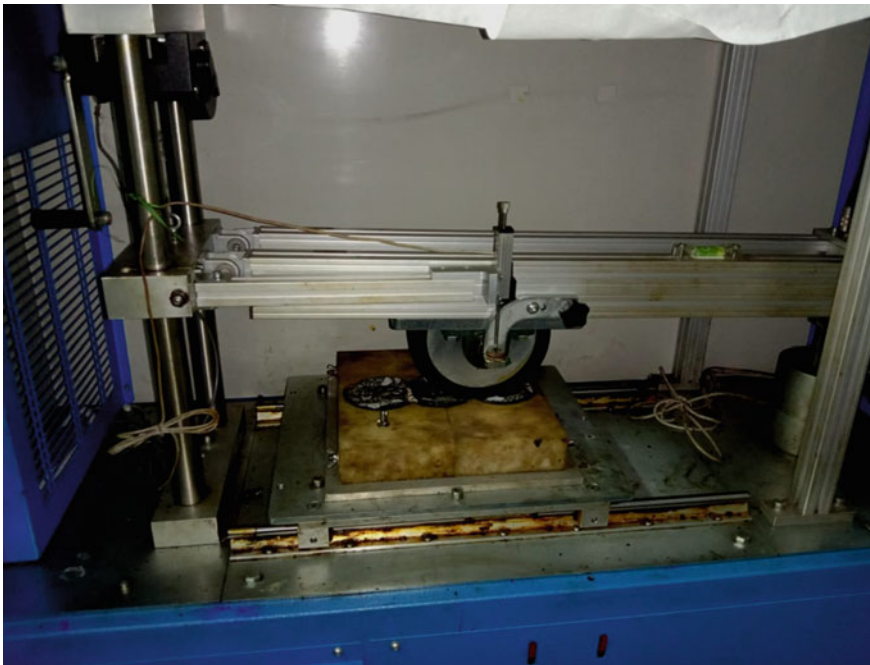


Fig. 1 Wheel tracker test set up

3 Results and Discussion

The physical properties of bitumen such as softening point and ductility of base bitumen, hard grade bitumen produced by PDA method and EVA modified bitumen are given in Table 4.

EVA modified bitumen has higher softening point values when compared to the base bitumen VG-40. It implies that the bitumen became stiffer with the addition of EVA. With the addition of 2% EVA-18, the ductility of bitumen decreased significantly as compared to VG-40 and V4E1 binders. This can be due to the high degree of crystallisation of EVA-18 at low vinyl acetate contents. Hence, further addition of EVA-18 was not considered, and a combination of EVA-18 and EVA-28 are studied further to improve the elastic properties of bitumen.

3.1 Evaluation of Rutting Resistance of Bitumen

Rutting resistance of base bitumen, hard grade bitumen and EVA modified bitumen are evaluated by using Superpave rutting parameter ($G^*/\sin \delta$), J_{nr} and percentage recovery indicators. Superpave rutting parameter was determined by conducting a temperature sweep test on unaged and short-term aged bitumen at 1.59 Hz frequency using DSR. Considering the minimum $G^*/\sin \delta$ 1.0 and 2.2 kPa for fresh (unaged) and rolling thin film oven (RTFO) aged binders, the continuous grading temperatures and upper performance grading temperatures have been selected. The values are given in Table 5.

The continuous PG upper temperatures of EVA modified bitumen samples are found to be higher than that of the base bitumen (VG-40) and smaller than that of the

Table 4 Physical properties of bitumen

Tests	Bitumen							
	VG-40	Hard bitumen	V4E1	V4E2	V4E11	V4E12	V4E13	V4E14
Softening point, °C	52	58	56	58	55	55.5	56	56
Ductility @ 27 °C, cm	>100	>100	82	26	75	69	56	50

Table 5 PG upper temperature of bitumen

Temperature (°C)	Bitumen							
	VG-40	Hard bitumen	V4E1	V4E2	V4E11	V4E12	V4E13	V4E14
Continuous PG	64.8	78.1	74.8	76.8	76.6	76.0	76.3	77.5
PG upper	64	76	70	76	76	76	76	76

PDA hard binder. However, the variation in the EVA content (either EVA-18 or EVA-18 in combination with EVA-28) did not has significant effect on the continuous upper PG temperature. This suggests that the superpave rutting parameter $G^*/\sin \delta$ does not appear to be able to distinguish the differences (if any) among the different modified binders investigated in this study. Hence, MSCR test was performed to see whether these binders can be distinguished more clearly in terms of their rutting resistance and to select an appropriate modifier percentage for preparation and evaluation of mixes for rutting resistance.

3.2 Master Curves

Master curves provide the relationship between the bitumen parameter (complex shear modulus, phase angle, viscosity, etc.) and reduced frequency applicable over a range of temperatures and frequencies. Master curves were constructed for unaged and short-term aged bitumen using the time–temperature superposition (TTS) principle. TTS is the technique of shifting the test data obtained at different temperatures to frequencies that correspond to a selected reference temperature so that different curves can be united to form a single master curve valid for a reference temperature. Complex shear modulus data obtained at different frequencies and temperatures were shifted to a reference temperature of 60 °C and various frequencies. Williams-Landel-Ferry (WLF) equation was used to determine the shift factors and curves are modelled with a sigmoidal function as follows:

$$\log G^* = \delta + \frac{\alpha}{e^{\beta + \gamma(\log f_r)}} \tag{1}$$

where

- G^* Complex shear modulus
- δ Minimum value of G^* , Pa
- $\alpha + \delta$ Maximum value of G^* , Pa
- β, γ Shape factors of the sigmoidal function
- f_r Reduced frequency, i.e. loading time at the reference temperature, Hz.

Master curves constructed for unaged and short-term aged bitumen are shown in Figs. 2 and 3.

For short-term aged bitumen, complex shear modulus of hard bitumen is 1.4 to 1.9 times higher than EVA modified bitumen at low frequencies and 1.1 to 1.9 times higher at higher frequencies.

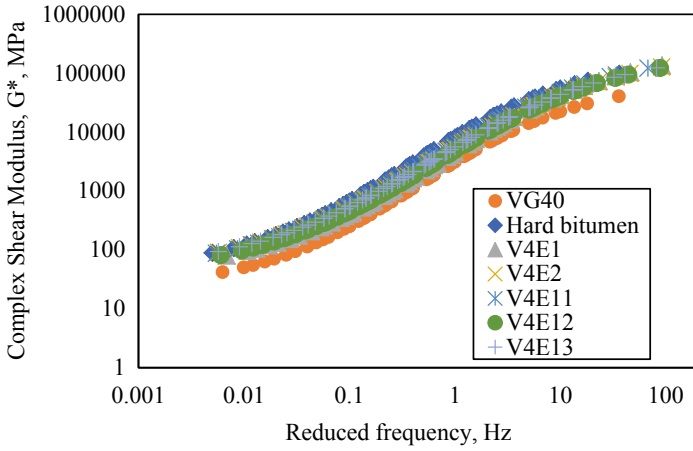


Fig. 2 Master curves of unaged bitumen

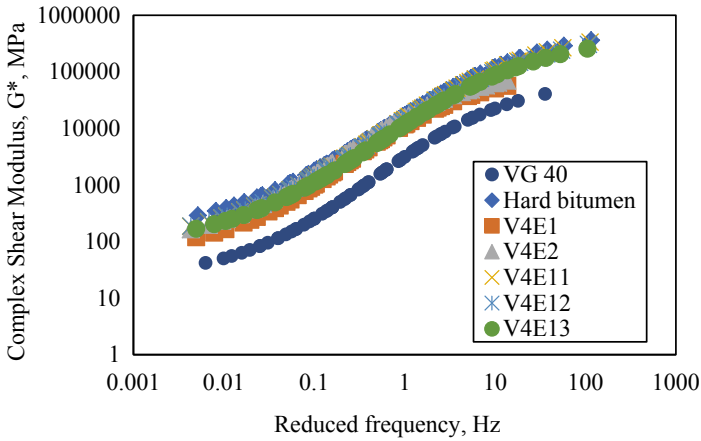


Fig. 3 Master curves of short-term aged bitumen

3.3 Multiple Stress Creep and Recovery

The rutting resistance of modified bitumen can be better explained by the non-recoverable compliance (J_{nr}) parameter, which is the ratio of the non-recoverable strain and the applied shear stress. Multiple stress creep recovery (MSCR) test was performed at 60 °C on short-term aged bitumen samples for two different stress levels of 0.1 kPa and 3.2 kPa. Short-term aged bitumen samples were subjected to a constant shear stress for 1.0 s and were allowed to recover during the rest period of 9 s as per AASTHO T-350 (2014). A lower J_{nr} value represents higher resistance to rutting. The

non-recoverable compliance (J_{nr}) and the percentage recovery properties of different short-term aged bitumen samples are presented in Figs. 4 and 5, respectively.

It is observed that PDA hard bitumen has significantly better rutting resistance characteristics (J_{nr} and percent recovery) compared to VG-40 binder. It can further be seen that modification of VG-40 binder using EVA has significantly improved the percent recovery value and also decreased the J_{nr} value. V4E12 and V4E13 modified binders out-performed other EVA modified binders and base bitumen with low J_{nr} and high percentage recovery values. The higher percentage recovery observed for V4E12 and V4E13 binders can be attributed to the presence of higher proportions of rubbery rich amorphous phase in bitumen-polymer matrix contributed by EVA-28.

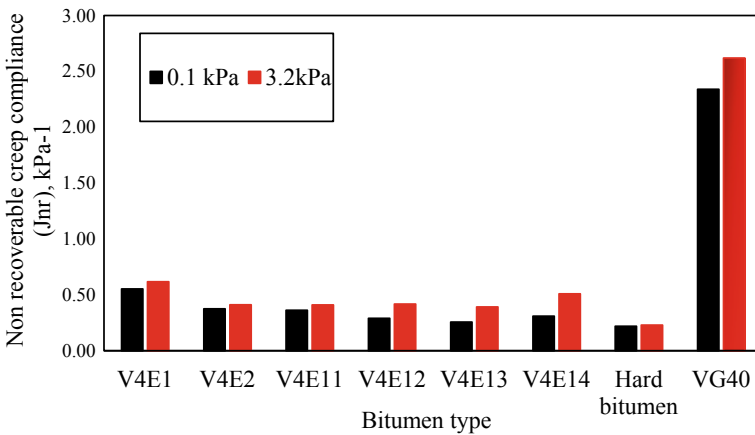


Fig. 4 Non recoverable compliance (J_{nr}) of different binders

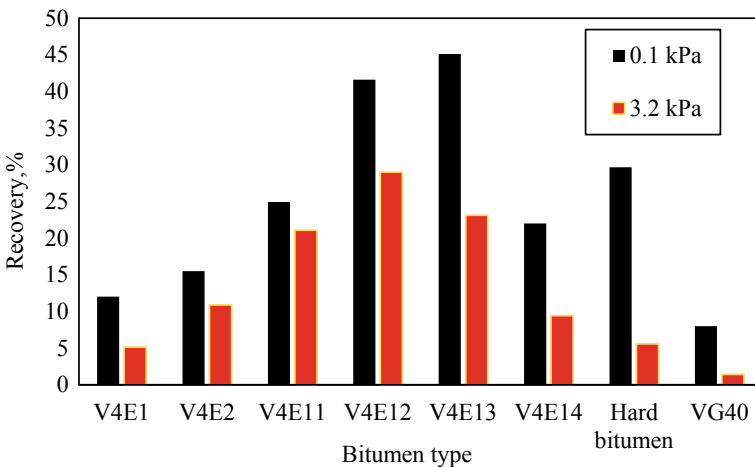


Fig. 5 Percentage recovery of different binders

The decrease in the percent recovery and increase in J_{nr} noted for V4E14 bitumen may due to possible instability of two-phase system. Generally, when the polymer content is about 5%, two-phase systems of continuous and interconnected micro structures are created. Controlling such type of system is difficult which causes instability in the bitumen matrix [10]. Based on these observations V4E12 and V4E13 binders were taken forward for asphalt mix rutting resistance evaluation.

3.4 Rutting Potential of Bituminous Mixes

The rutting potential of the mixes prepared using base bitumen and the modified binders V4E12 and V4E13 selected for preparing the mixes was measured in the laboratory using dry wheel tracker at a test temperature of 60 °C. 5000 load cycles (10,000 to-and-fro movements) were applied on the specimens at a rate of 20 rpm. The specimens for the wheel tracking test were prepared at optimum bitumen content and were compacted to have an air void content of $7 \pm 0.5\%$. The mixing temperatures for V4E12 and V4E13 binders were selected as 172 °C and 175 °C, respectively, from their viscosity-temperature relationships. The aggregate gradation used for preparing the mixes was the mid-point gradation of DBM-II mixes as specified by the ministry of road transport and highways [7]. Mix design was carried as per Marshall method of mix design and optimum bitumen contents of different bituminous mixes were selected corresponding to 3% air void content in the compacted specimens.

The 3% air void content was selected as per the recommendations of Indian roads congress [11] for rich bottom high fatigue resistant bituminous mixes with lower design air void contents. The optimum binder contents are given in Table 6. The final rut depth values measured for different bituminous mixes prepared using base bitumen, PDA hard bitumen, V4E12 and V4E13 are given in Table 7. It can

Table 6 Optimum bitumen content (OBC) of bituminous mixes

Mix type	Design binder content @ 3% air void (% by weight of mix)
Base bitumen—VG-40	5.2
Hard bitumen	5.15
V4E12	5.2
V4E13	5.4

Table 7 Rut depth of bituminous mixes

Mix type	Rut depth (mm)
Base bitumen—VG-40	5.22
Hard bitumen	2.10
V4E12	2.25
V4E13	2.22

be noted that the EVA modification of bituminous binders resulted in significant improvement in the rutting resistance of VG-40 binders as noted from the rutting resistance measured in wheel tracking test. The difference between the rut resistances of V4E12 and V4E13 mixes are marginal. The performance of these two modified mixes is comparable to that of the mix prepared using hard bitumen.

4 Conclusions

In this study, composite EVA modifiers were blended with VG-40 bitumen to produce binders having similar rutting resistance as that of the hard bitumen produced by the propane-deasphalting method. The optimum combination of the composite EVA modifiers was determined by considering the superpave rutting parameter ($G^*/\sin \delta$), non-recoverable compliance (J_{nr}), percentage recovery of bitumen and mix rut resistance.

With increase in the proportion of EVA-18 in the VG-40 base binder from 1 to 2%, while there is some increase in the stiffness of the binder, the ductility of the binder reduced significantly. Hence a combination of EVA-18 and EVA-28 (which is more amorphous in nature compared to the highly crystalline EVA-18) was considered to improve the elastic nature of the modified binder. The J_{nr} and percent recovery properties of V4E12 (i.e. 1% EVA-18 and 2% EVA-28) and V4E13 (i.e. 1% EVA-18 and 3% EVA-28) suggest better rut resistance of the binders which is comparable to that of hard grade bitumen. EVA modified bituminous mixes are observed to be superior in terms of their rut resistance as compared to conventional VG-40 bituminous mix. From the binder and mix rutting studies, V4E12 and V4E13 can be considered as suitable for producing high modulus mixes with higher rutting resistance and more ductile nature (which is conducive for better fatigue resistance). It is, however, necessary to evaluate the fatigue performance of the mixes to establish their satisfactory fatigue performance.

References

1. Petho L, Denneman E (2013) EME technology transfer to Australia: an explorative study. Austroads technical report
2. Komba JJ, Verhaeghe BMJ, O'Connell JS, Anochie-Boateng JK, Nortje W (2015) Evaluation of the use of polymer modified bitumen in the production of high modulus asphalt for heavily-trafficked roads. 7th Africa transportation technology transfer conference
3. Nunn ME, Smith T (1997) Road trials of high modulus base for heavily trafficked roads, vol 231. Thomas Telford
4. Corte JF (2001) Development and uses of hard-grade asphalt and of high-modulus asphalt mixes in France. Transportation Research Circular 503:12–31
5. Serfass JP, Bense P, Pellevoisin P (1997) Properties and new developments of high modulus asphalt concrete. Eighth international conference on Asphalt pavements, vol I

6. Zhu J, Birgisson B, Kringos N (2014) Polymer modification of bitumen: advances and challenges. *Eur Polymer J* 54:18–38
7. MoRTH: Ministry of Road Transport and Highways (2013) Specifications for road and bridge works, 5th Revision, Indian Roads Congress, New Delhi
8. Vachhani KK, Mishra CB (2014) Assessing the impact of VG30 grade bitumen with and without additive (EVA) on short term aging. *IOSR J Mech Civil Eng* 36–40
9. Kumar P, Khan T, Singh M (2013) Study on EVA modified bitumen. *Elixir Int J Chem Eng A* 54:12616–12618
10. Honarmand M, Tanzadeh J, Beiranvand M (2019) Bitumen and its modifier for use in pavement engineering. In: *Sustainable construction and building materials*. Intech open
11. IRC 37 (2018) Guidelines for the design of flexible pavements, 4th Revision, Indian Roads Congress, New Delhi, India

A Review on the Use of Alternative Materials as a Sustainable Approach in the Manufacture of Concrete Paver Blocks



Sumit Nandi  and G. D. R. N. Ransinchung 

1 Introduction

History embarks the fast-growing construction period after the Second World War as the reviving period of the concrete paver blocks [1]. These concrete blocks being cheaper and produced in mass replaced the kiln-fired paver bricks due to the shortage of coal during the 1950s in the Netherland. Paver blocks represent a system of metameric-shaped blocks or paving units cushioned over a layer of bedding sand and the joints being filled with jointing sand. The substructure beneath is analogous to that of a bituminous pavement system. Edge restraints in the form of edge blocks and kerbs counteract the tendency of the block to move sideways under the braking and manoeuvring action of the vehicles. Concrete block pavement (CBP) utilizing these paver blocks as a hard wearing surface refrains from using very costly technology or methods for its regular maintenance and provides an effective means of addressing the maintenance issues arising from recurrent damage. The manufacture of paver blocks utilizes a vibro-compaction technique emphasizing that simultaneous vibration and compaction are needed to get adequate compaction of the semi-dry mixes [2]. This methodology helps in achieving denser and stronger blocks serving as a durable paving surface.

The rapid growth of the construction industry has made a negative impact on the environment by excessive usage of concrete. This has led to an uncontrolled quarrying and mining activity of the aggregates and cement production [3]. Both

S. Nandi (✉)

PhD Research Scholar, Civil Engineering Department, Indian Institute of Technology Roorkee, Roorkee, Uttarakhand, India
e-mail: snandi@ce.iitr.ac.in

G. D. R. N. Ransinchung

Professor, Civil Engineering Department, Indian Institute of Technology Roorkee, Roorkee, Uttarakhand, India
e-mail: gdranf@iitr.ac.in

these activities have disturbed the ecological balance and resulted in the emission of greenhouse gases. On the other hand, a huge amount of waste generated every year needs to be properly recycled and reused to avert damage to the ecosystem and to prevent contamination of water, soil and air. So, there is a quenching thirst for the production of green concrete through the utilization of industrial waste and by-products as alternative materials.

The different attributes of the paver block like handy and quick construction averting the use of heavy construction equipment's, simple maintenance, ease of access to utilities, negligible expansion and contraction under temperature, resistance to spillage of oils, durability and eco-friendly technology along with the incorporation of the alternative materials will certainly have a socio-economic impact and address the sustainability issue. Therefore, this study performs a review of previous research on the usage of alternative materials for the production of paver blocks accompanying their comparative analysis on the basis of compaction and curing methods.

2 Literature Review

This section covers the studies on the use of alternative materials obtained as waste or by-product from different industries in the production of concrete paver blocks. Past research has shown that these alternative materials in lieu of their novel characteristics can have value-added sustainable applications adding to the profitability of the road sector.

2.1 *Waste from C&D Industry*

Poon et al. [4] presented a method for manufacturing concrete bricks and blocks incorporating recycled aggregates (RA). The recycled aggregates substituted the natural coarse and natural fine aggregates up to levels of 100% by weight, along with or without the use of fly ash. Laboratory results showed that when natural aggregates are substituted with recycled aggregates above 50%, significant reduction in compressive strength values occurs, but the transverse strength values are improved. Study concluded that using 100% recycled aggregate only, paver blocks having 28-day compressive strength of 49 MPa and above can be manufactured, while fly ash along with 100% recycled aggregate can be used to produce paving units for footway and masonry bricks requiring lower compressive strength. Satisfactory performance of the concrete products was seen for the skid resistance and shrinkage tests.

Poon and Chan [5] explored the feasibility of using recycled concrete aggregate (RCA) and crushed clay brick (CB) for paver block manufacturing. CB was used in replacing the control mix prepared using RCA in replacement ratios of 25, 50 and 75%. Test results of the study reported that the use of CB led to a reduction of the

density, compressive strength and splitting tensile strength of the blocks while significantly increasing its water absorption. Incorporation of fly ash helped in improving the compressive strength and water absorption properties though a negative effect which was seen in terms of skid resistance. Mix containing only fine fraction (less than 5 mm) had a positive effect on the water absorption and splitting tensile strength properties but led to a reduction of the density. Study recommended that paving units containing 50% CB and 50% RCA blend are feasible for pedestrian areas, while 25% CB meets the requirements in trafficked areas in Hong Kong.

Poon et al. [6] studied the properties of concrete blocks produced using low-grade recycled aggregates (RA) sorted from a construction and demolition (C&D) waste sorting site located in Hong Kong. The low-grade recycled aggregates were used to replace the natural coarse aggregate (100%) and natural fine aggregate (0, 25, 50, 75 and 100%). The study showed that incorporation of recycled fine aggregate led to a decrease in density and compressive strength, while the drying shrinkage increased. The reduction in compressive strength of the blocks after being exposed to a temperature of 800 °C decreased due to higher soil content in the recycled aggregates. The SEM images and XRD patterns indicated the presence of calcium aluminium silicate crystals (named as zeolite) after heating. Researchers suggested the use of these low-grade recycled aggregates as aggregates in precast concrete blocks for non-structural applications and recommended to replace natural fine aggregate by 50% recycled fines for optimal results.

Soutsos et al. [2] examined the potential of using recycled demolition aggregate in the production of precast concrete paver blocks. Researchers concluded that along with compression, simultaneous application of vibration is needed for proper replication of the industrial procedure of production of paver blocks (shown in Fig. 1). Recycled demolition aggregate was used to substitute both the coarse and fine fractions of natural aggregates at replacement levels of 25, 50, 75 and 100% varying the cement content in the range of 230–380 kg/m³. Study recommended the use of concrete-derived recycled demolition aggregate up to 60% replacement level for both the coarser and finer fractions which need to be conservatively brought down to 55% for coarser fraction and 25% for finer fraction so that the water absorption value is restricted to less than 6%. For the masonry-derived recycled demolition aggregate, the replacement level for coarse and fine fraction was recommended as 55% and 20% if the water absorption criteria need to be adhered to.

Serrano-Guzman and Perez-Ruiz [7] carried out a laboratory investigation to explore the potential of using recycled materials (coarse and fine fractions of concrete aggregates and brick debris) from construction and demolition (C&D) waste in paver blocks. The research aimed at identifying and characterizing the recycled aggregates from C&D debris from multiple project sites, establishment of a blended mix of alternative and natural material and finally determining the properties of the blended material keeping the mix design proper. Results showed that better performance can be achieved by the proper blending of recycled aggregates (40% natural fine aggregate, 50% natural coarse aggregate, 10% coarse recycled concrete aggregate), whereas incorporating the same in paver blocks resulted in an environmental friendly cost-effective product addressing the disposal issue.

Fig. 1 Clamped-on vibrator used along with an electric hammer to replicate the industrial procedure of paver block production (Source Soutsos et al. [2])



Table 1 presents a comparative study of the alternative materials from C&D industry used in paver block manufacturing.

2.2 Waste from Marble Industry

Gencel et al. [8] made an attempt to prepare concrete paver blocks of adequate quality replacing aggregates with marble waste at substitution levels of 10, 20, 30 and 40%. Results of the study showed that the mechanical properties like compressive strength, splitting tensile strength, density and modulus of elasticity decreased with higher aggregate replacement level. Further, a positive impact was seen in terms of abrasive resistance and freeze–thaw durability of the blocks. Study concluded that the cement type stands as an important parameter for the strength, freeze–thaw durability and elastic modulus of the paver blocks.

Uygunoğlu et al. [9] examined the feasibility of using marble waste and concrete waste as fine aggregate for the manufacture of precast concrete paver blocks using a dry-mixed method. Study included the effect of replacement of cement with fly ash (at replacement levels of 10, 20, 30 and 40% by weight) on the block properties. Comparison of the test results presented a decrease in the strength properties of

Table 1 Comparative study of the alternative materials from C&D industry used in the manufacture of paver blocks

Researchers	Alternative material	Compaction and curing method	Parameters and property tests
Poon et al. [4]	RA from C&D waste	Compressive force applied Steam bath curing followed by air curing at room temperature	Density, skid resistance, compressive strength, flexural strength, drying shrinkage
Poon and Chan [5]	RCA and CB	First two layers manually compacted followed by application of static compaction pressure twice Subjected to water curing	Density, compressive strength, water absorption (hot and cold), splitting tensile strength, skid resistance, abrasion resistance
Poon et al. [6]	Low-grade RA from C&D waste	Similar to Poon and Chan [5] Curing by hemp bags (RH > 90%) at room temperature	Density, compressive strength, transverse strength, drying shrinkage, high temperature exposure (800 °C), SEM, XRD
Soutsos et al. [2]	Recycled demolition aggregate (concrete-derived and masonry-derived)	Vibro-compaction method applied using an electric hammer and vibrating table	Compressive strength, water absorption, splitting tensile strength
Serrano-Guzman and Perez-Ruiz [7]	RCA and brick debris	Water cured till the day of testing	Flexural strength, compressive strength

the paver blocks prepared using concrete and marble waste. Use of concrete waste resulted in higher water absorption and porosity values, whereas the blocks showed somehow better resistance against abrasion. Researchers recommended fly ash to be incorporated at levels of 10–20% for better results and resistance against alkali-silica reaction (ASR). Marble waste somehow helped in achieving the required splitting tensile strength and freeze–thaw durability of the concrete paver blocks.

Mashaly et al. [10] studied the feasibility of using marble sludge replacing cement (10, 20, 30 and 40% by weight) in the fabrication of concrete paver blocks. Up to 20% replacement level, the 28-day compressive and flexural strength improved by 9.7% and 21.3%, respectively, in comparison with the control mix. Results showed that water absorption, bulk density and abrasion resistance properties improved by incorporating marble sludge.

A comparative study of the alternative materials from marble industry used in paver block manufacturing is presented in Table 2.

Table 2 Comparative study of the alternative materials from marble industry used in the manufacture of paver blocks

Researchers	Alternative material	Compaction and curing method	Parameters and property tests
Gencil et al. [8]	Crushed waste marble	Pressure and vibration applied Cured under a relative humidity of 65% and maintaining a constant temperature of 20 °C	Density, compressive strength, splitting tensile strength, NDT ^a tests (Schmidt hardness, UPV ^b), elastic modulus, water absorption, freeze–thaw resistance, abrasion resistance
Uygunoğlu et al. [9]	Marble waste, concrete waste	Pressure and vibration applied simultaneously First 7 days cured under water, then air-cured	Density, compressive strength, water absorption, splitting tensile strength, abrasion resistance, specific porosity, ASR expansion, freeze–thaw resistance
Mashaly et al. [10]	Marble sludge	Mechanical vibrator used Covered with plastic sheets for curing	Water absorption, bulk density, permeable voids, sorptivity, freeze–thaw resistance, compressive strength, flexural strength

^aNDT non-destructive tests

^bUPV ultrasonic pulse velocity

2.3 Waste from Ceramic and Tile Production Industry

Wattanasiriwech et al. [11] conducted a study to investigate the viability of using waste mud obtained from ceramic tile production for the fabrication of paver blocks. The range of cement binder in the mix (cement-mud) varied from 15 to 30% by weight. Study revealed the role played by different parameters like water content, curing water, compaction pressure and cement content. Results showed that incorporation of $\geq 20\%$ cement by weight helps in adequate strength gain just after 14 days curing, while much higher strength gain occurs when the blocks are subjected to a full 28-day curing.

Sadek and El Nouhy [12] examined the properties of concrete paver units produced using crushed ceramic. The facing and backing layers of the blocks had crushed ceramic replacing the natural coarse and natural fine aggregates at replacement levels of 50 and 100% by weight. Study revealed that incorporating finer fraction of crushed ceramic provides better results than its coarser fraction while maintaining a similar level of replacement of natural aggregates. Researches recommended to use 50 and 100% crushed ceramic as fine aggregate in the backing layer and facing layer,

Table 3 Comparative study of the alternative materials from ceramic and tile production industry used in the manufacture of paver blocks

Researchers	Alternative material	Compaction and curing method	Parameters and property tests
Wattanasiriwech et al. [11]	Waste mud from ceramic tile production	Compacted by a hydraulic press First set cured by damp cloth accompanied by spraying of water and second set was kept under water for 5 min every 24 h	Compressive strength, XRD, SEM
Sadek and El Nouhy [12]	Crushed ceramic	Pressure of 200 bars accompanied by vibration used Cured by spraying water twice a day daily	Compressive strength, skid resistance, water absorption, abrasion resistance, splitting tensile strength
Penteado et al. [13]	Ceramic tile polishing waste	Each layer compacted 30 s on a shaking table Cured in a moisture chamber	Compressive strength, water absorption, porosity

respectively, for an enhancement of the physicomechanical properties of the paver blocks.

Penteado et al. [13] investigated the potential of using ceramic tile polishing wastes (namely porcelain tile, stoneware tile and porous tile) from a ceramic tile industry in Brazil for the manufacture of concrete paver blocks. The tile wastes were used as a substitute of sand at replacement levels of 5, 10, 15, 20, 25 and 30%, whereas only porcelain tile waste was used to substitute cement at similar replacement levels due to its positive response to pozzolanic activity tests. Results from the study recommended substitution of 30% fine aggregate with ceramic tile polishing waste and 20% cement with porcelain tile waste for achieving the standard requirement (50 MPa) for heavy vehicle use.

A comparative study of the alternative materials from ceramic and tile production industry used in paver block manufacturing is presented in Table 3.

2.4 Waste from Plastic Industry

Ohemeng et al. [14] investigated the feasibility of utilizing waste low-density polyethylene (LDPE) for the production of concrete paver blocks. LDPE was used to replace natural sand at replacement levels of 10–60% by volume. Test results reported that although the addition of waste LDPE had a negative effect on the physicomechanical properties, incorporating the same at replacement levels of 10–50% achieves

Table 4 Comparative study of the alternative materials from plastic industry used in the manufacture of paver blocks

Researchers	Alternative material	Compaction and curing method	Parameters and property tests
Ohemeng et al. [14]	Waste LDPE	Mechanical compaction Cured by spraying water twice a day	Compressive strength, water absorption, flexural strength, splitting tensile strength
Vanitha et al. [15]	Waste plastic from daily use	Tamping and vibration used for compaction Demoulded and cured under water	Compressive strength

the strength requirement of paver blocks to be used for pedestrian, light and heavy traffic situations.

Vanitha et al. [15] studied the potential of using waste plastic from daily use in the manufacture of concrete paver blocks. The waste plastic was added as a substitution of coarse aggregates at different percentages (0, 2, 4, 6, 8 and 10%). Laboratory results reported a decrease in the compressive strength of the waste plastic-added concrete blocks. Study recommended the use of waste plastic at 4% replacement levels for paver blocks as optimum.

A comparative study of the alternative materials from plastic industry used in paver block manufacturing is presented in Table 4.

2.5 Waste from Rubber Industry

Sukontasukkul and Chaikaew [16] made an attempt to manufacture concrete pedestrian block using crumb rubber. Study used two particle sizes of crumb rubber partially substituting both the coarser and finer fractions of natural aggregates at an equal amount of 10 and 20% (by weight). Addition of crumb rubber showed a decrease of the flexural and compressive strength, while the toughness property improved. Test results reported that the inclusion of rubber particles had a positive impact on the skid resistance, while the abrasion resistance decreased. Blocks made with crumb rubber (up to 20%) exhibited lighter weight and more flexibility with better energy absorption.

Ling et al. [17] conducted a laboratory investigation to examine the feasibility of using crumb rubber as a partial replacement of natural sand (5, 10, 15, 20, 25, 30, 40 and 50% by volume) in the production of concrete paver blocks. Different parameters like effect of the crumb rubber size (1–3 mm, 3–5 mm and combined), variation of water-cement ratio (0.45, 0.50, 0.55) and inclusion of styrene-butadiene rubber (SBR) latex at percentages of 1, 2, 3 and 4% were included in the study. Addition of SBR latex up to 4% in the crumb rubber blocks improved the density, skid resistance, but SEM images showed no betterment of the strength and bonding.

The mechanical properties reduced with an increase in the rubber percentage, and better skid resistance can be achieved using smaller sizes of crumb rubber. Results indicated that inclusion of 15% crumb rubber at a water-cement ratio of 0.55 in paver blocks without any SBR latex attained 30 MPa compressive strength.

Ling et al. [18] studied the possibility of using shredded waste car tyre in the manufacture of paver blocks. Crumb rubber was used to substitute fine and coarse sand in the face and base layer of the paver block mix at replacement levels of 10, 20 and 30% volumetrically. Study recommended the crumb rubber substitution up to 20%, beyond which excessive deterioration of compressive strength occurs. Researchers suggested that crumb rubber may help in addressing the noise generation problems in paver blocks due to its higher sound absorption coefficient values.

Ling [19] made a comparative study of the plant-manufactured and manually manufactured paver blocks prepared using recycled tyre waste. The tyre waste was used to partially replace natural sand at levels of 10, 20 and 30% on a volume basis. Researchers found out from the study that when crumb rubber is incorporated in small proportions ($\leq 10\%$), the filling mechanism is dominant over the deformability property of the soft rubber particles resulting in improved strength of the blocks (shown in Fig. 2). The soft rubber particles presented the blocks with increased toughness and deformability property. The blocks demonstrated ductile behaviour combating the post-failure loads better and showing greater energy absorption properties. Study recommended paver blocks to be manufactured and compacted in the plant for better results including higher density.

Murugan et al. [20] studied the applicability of crumb rubber produced from shredded waste tyres as a sustainable material for CBP. Fine aggregate was substituted volumetrically by crumb rubber at levels of 5, 10, 15, 20 and 25% maintaining a water-cement ratio of 0.5 for the control mix. Slump, impact resistance and ductility index values increased with the subsequent addition of crumb rubber up to 25%. Laboratory test results showed an increase in flexural strength till 15% crumb rubber inclusion decreasing thereafter while a negative impact was seen in terms of compressive strength at all replacement levels.

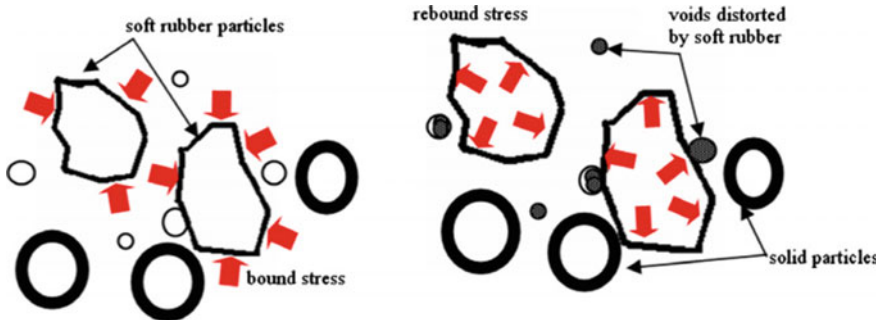


Fig. 2 Interaction behaviour between soft rubber particles and solids **a** When compaction force applied and **b** Once force released (Source Ling [19])

Table 5 Comparative study of the alternative materials from rubber industry used in the manufacture of paver blocks

Researchers	Alternative material	Compaction and curing method	Parameters and property tests
Sukontasukkul and Chaikaew [16]	Crumb rubber	Compacted under pressure Air-cured	Compressive strength, density, flexural strength, skid resistance, abrasion resistance
Ling et al. [17]	Crumb rubber and SBR latex	Manual compaction using a hammer Cured at a temperature of 30 °C and relative humidity of 65%	Density, skid resistance, compressive strength, SEM
Ling et al. [18]	Waste car tyre	Vibration and pressure applied Cured in curing chambers	Density, water absorption, voids, acoustic properties, compressive strength, abrasion resistance, skid resistance, impact resistance
Ling [19]	Recycled tyre waste	Plant-made: subjected to different levels of compaction and vibration Cured under controlled temperature and relative humidity Manually made: ramming by hand Cured under controlled temperature and relative humidity	Compressive strength, flexural strength, density, skid resistance, SEM
Murugan et al. [20]	Shredded waste tyre	Similar to that of wet mixes	Workability, compressive strength, modulus of elasticity, ductility index, flexural strength, impact energy

A comparative study of the alternative materials from rubber industry used in paver block manufacturing is presented in Table 5.

2.6 Waste from Glass Industry

Lam et al. [21] made an attempt to enhance the performance of concrete paver blocks produced from recycled crushed glass (RCG) considering the ASR expansion. Researchers recommended an addition of 10% pulverized fuel ash (PFA) by weight

of total aggregates in concrete mixtures containing more than 25% RCG to keep the ASR expansion within limits. RCG helped in decreasing the water absorption of paver blocks containing recycled aggregates. Results of the study suggested the fabrication of eco-friendly and good quality paver blocks using 100% recycled aggregate (50% recycled crushed glass and 50% recycled fine aggregate) along with the addition of 10% PFA.

Turgut and Yahlizade [22] conducted an experimental investigation for studying the feasibility of using different proportions of recycled waste glass as a replacement of fine aggregate (10, 20 and 30%) in concrete paver blocks. Study revealed that replacement of fine aggregate with fine glass (FG) showed better improvement in physicomaterial properties compared to coarse glass (CG). Experimental results showed that 20% FG replacement in paver blocks improved the compressive strength, splitting tensile strength, flexural strength and abrasion resistance values by 69, 47, 90 and 15%, respectively, over the control specimens.

Ling and Poon [23] examined the properties of concrete paver blocks produced using recycled cathode ray tube (CRT) funnel glass by a dry-mixed method. The recycled CRT glass was used at replacement levels of 50 and 100% by volume of the recycled concrete fine aggregates. The effect of recycled CRT glass on the photocatalytic reaction involving the removal of nitrogen oxide (NO) was studied by adding 5% titanium oxide (TiO_2) by weight of cementitious materials (cement and fly ash) to the surface layer of the concrete blocks. Results of the study showed that CRT glass helped in improving the water absorption, drying shrinkage and photocatalytic performance of the blocks. Using recycled CRT glass as 100% replacement of fine aggregate achieved required compressive strength greater than 45 MPa and ASR expansion levels below 0.1% as shown in Fig. 3. Researchers recommended restricted use of CRT glass below 25% due to the problem of lead leaching which could be overcome by adopting effective casting methods.

A comparative study of the alternative materials from glass industry used in paver block manufacturing is presented in Table 6.

2.7 Other Industrial Wastes and By-Products

Yüksel and Bilir [24] studied the properties of concrete paver blocks manufactured using granulated blast-furnace slag (GBFS) replacing fine aggregate (20, 30, 40 and 50%) by volume. Test results showed that till 30% GBFS replacement though negative impact can be seen in terms of water absorption ratio, compressive strength and freeze–thaw resistance, their losses were under limits. Further incorporation of GBFS beyond 30% increases the compressive strength and improves the abrasion resistance values.

Said et al. [25] examined the practicability of using dredged marine sediments as a replacement of sand in concrete paver blocks. The paver blocks manufactured in laboratory and factory had dredged sediment at replacement levels 12.5–100%. Inclusion of marine sediments made the blocks denser and improved the weathering

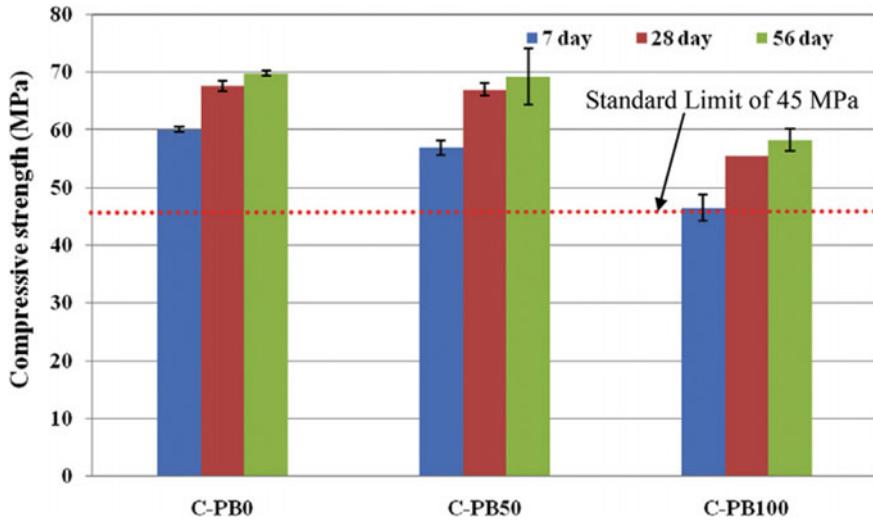


Fig. 3 Compressive strength development of paver blocks with RCA as coarse aggregate and CRT funnel glass replacing recycled fine aggregate at 0, 50 and 100% by volume (Source Ling and Poon [23])

Table 6 Comparative study of the alternative materials from glass industry used in the manufacture of paver blocks

Researchers	Alternative material	Compaction and curing method	Parameters and property tests
Lam et al. [21]	RCG, PFA, MK	Similar to Poon and Chan [5]	Compressive strength, density, splitting tensile strength, abrasion resistance, water absorption, skid resistance
Turgut and Yahlizade [22]	Waste glass	Pressure of 17 MPa for 1 min applied Water cured	Compressive strength, density, flexural strength, splitting tensile strength, UPV test, abrasion resistance
Ling and Poon [23]	Recycled CRT funnel glass	Similar to Poon and Chan [5]	Density, water absorption, compressive strength, drying shrinkage, ASR expansion, TCLP ^a test, photocatalytic removal of NO, SEM

^aTCLP: toxicity characteristic leaching procedure

Table 7 Comparative study of the alternative materials from other industrial waste and by-products used in the manufacture of paver blocks

Researchers	Alternative material	Compaction and curing method	Parameters and property tests
Yüksel and Bilir [24]	GBFS	Not mentioned	Freeze–thaw resistance, compressive strength, water absorption, abrasion resistance
Said et al. [25]	Dredged marine sediment	Simultaneous pressure (120 bars) and vibration used	Water absorption, abrasion resistance, TCLP test, splitting tensile strength
Wang et al. [26]	Contaminated dredged sediment	Pressure of 30 KN for 30 s applied Cured in a curing chamber	Compressive strength, TCLP test, GC-MS ^a , ICP-AES ^b , TGA ^c , SEM, XRD, MIP ^d test

^aGC–MS gas chromatography-mass spectrometry

^bICP–AES inductively coupled plasma-atomic emission spectrometry

^cTGA thermogravimetric analysis

^dMIP mercury intrusion porosimeter

resistance. Splitting tensile strength and water absorption values also met the standard requirements. Researchers suggested 12.5 and 19% as optimal replacement levels of dredged sediment for laboratory and factory manufactured blocks keeping the heavy metal concentration within regulatory limits.

Wang et al. [26] attempted to provide an innovative solution to contaminated dredged sediment disposal by incorporating the same in concrete paver blocks through solidification/stabilization technique. Dredged sediments possess contaminants preventing the hydrate formation, so proper selection of binders, design mix and fabrication procedures needs to be adopted to achieve desirable properties. Economic assessment of the study showed considerable cost benefits.

A comparative study of the alternative materials from other industrial waste and by-products used in paver block manufacturing is presented in Table 7.

3 Discussion

The present review study has shown that alternative waste materials from the industrial sector have found value-added application in the production of concrete paver blocks. This can be attributed to the novel characteristics of different types of waste materials. A comparative study of the different alternative materials used by researchers in the sustainable production of paver blocks with reference to their compaction and curing methods has been presented in tabular format from Tables 1, 2, 3, 4, 5, 6 and 7.

Study revealed that some wastes like recycled concrete, brick debris, waste glass, recycled CRT glass, crushed ceramic, plastic waste and GBFS can be used to replace natural aggregates in paver blocks at higher percentages ranging from 50 to 100% [2, 4–7, 11–15, 21–24]. Recycled concrete aggregate (RCA) due to its porous nature, low strengths and high water absorption properties leads to a decrease in the physico-mechanical properties of the paver blocks which can be improved with proper compaction techniques, optimal blended mix design [7] and CO₂ curing. Weaker bonding with the cement paste can be seen when RCA, marble waste and recycled glass are used as aggregates leading to a weaker interfacial transition zone (ITZ) [8]. Though the use of crushed brick aggregates had a negative impact on the compressive strength values due to its higher water absorption, lower strength and density values, combining the finer fractions of RCA and crushed brick debris demonstrated a filler effect and helped in reducing the porosity [5]. Supplementary cementitious materials (SCMs) like fly ash and pulverized fuel ash (PFA) help in resisting ASR expansion [9, 21]. Self-cleansing property is manifested by incorporating waste CRT glass as fine aggregate activating titanium oxide compounds by photocatalytic reaction [23]. The poor intrinsic properties shown by dredged marine sediments, waste marble and tyre waste limit their inclusion percentage below 30% in paver blocks [8–10, 16–20, 25, 26]. Using waste marble and plastic helps in enhancing the durability properties like freeze–thaw resistance and water absorption [8–10, 14, 15]. Crumb rubber (lightweight and soft) and waste plastic (lightweight) provide good insulation, ductility and shock absorption properties to paver blocks [16–20]. Solidification/stabilization technique can be used to prepare concrete paver blocks for some wastes like CRT funnel glass and dredged sediment. This serves as a more efficient method to keep the leaching of heavy metals within stipulated limits [23, 25].

4 Conclusions

The literature survey on the use of alternative materials in the production of concrete paver blocks manifests the beneficial aspect of lower natural resource consumption and highlights an economically viable solution to waste disposal. Following conclusions can be drawn from the literature review study of the use of alternative materials:

- Presence of some inherent inert properties, higher hardness and strength values allowed C&D wastes, recycled glass, ceramic and tile waste, recycled plastic waste and GBFS to be used in paver blocks at higher replacement ratios of 50–100%, whereas the use of crumb rubber, dredged marine sediment and marble waste as alternative materials is restricted to below 30% because of their lower intrinsic properties. Thus, the novel characteristics of the different alternative materials help in valorizing them as value-added products.
- The use of finer fractions of certain wastes like ceramic waste, crushed brick, recycled glass and dredged sediment helps in improving the compressive strength

of the paver blocks. This can be attributed to the filler effect and pozzolanic activity of the fines.

- Reduction of porosity and densification of the concrete matrix can be achieved with proper aggregate gradation, optimal blends of the different aggregates and proper compaction and curing techniques.
- Solidification/stabilization technique serves an effective means of incorporating some wastes (CRT funnel glass and marine sediment) in concrete paver blocks owing to the presence of heavy metals.
- Fly ash and PFA can be used as supplementary cementitious materials to restrict the ASR expansion. This can also be controlled by the finer fraction of waste glass demonstrating pozzolanic activity.
- Better insulation, shock absorption and ductility properties can be achieved by incorporating crumb rubber and waste plastic as aggregates.
- Use of CRT funnel glass fuels the photocatalytic activity in paver blocks and helps in the removal of nitrogen oxide from air.
- Resistance to freeze–thaw, abrasion and skid can be improved by using wastes like marble, plastic, GBFS and crumb rubber in paver blocks.

References

1. Shackel B (1980) The design of interlocking concrete block pavements for road traffic. In: Proceedings of 1st International Conference on Concrete Block Paving, pp. 23–32
2. Soutsos MN, Tang K, Millard SG (2011) Use of recycled demolition aggregate in precast products, phase II: concrete paving blocks. *Constr Build Mater* 25(7):3131–3143
3. Mo KH, Alengaram UJ, Jumaat MZ, Yap SP, Lee SC (2016) Green concrete partially comprised of farming waste residues: a review. *J Clean Prod* 117:122–138
4. Poon CS, Kou SC, Lam L (2002) Use of recycled aggregates in molded concrete bricks and blocks. *Constr Build Mater* 16(5):281–289
5. Poon CS, Chan D (2006) Paving blocks made with recycled concrete aggregate and crushed clay brick. *Constr Build Mater* 20(8):569–577
6. Poon CS, Kou SC, Wan HW, Etxeberria M (2009) Properties of concrete blocks prepared with low grade recycled aggregates. *Waste Manage* 29(8):2369–2377
7. Serrano-Guzman MF, Perez-Ruiz DD (2011) Use of recycled materials to build paver blocks for low-volume roads in developing countries. *Transp Res Rec* 2205(1):138–146
8. Gencel O, Ozel C, Koksall F, Erdogmus E, Martínez-Barrera G, Brostow W (2012) Properties of concrete paving blocks made with waste marble. *J Clean Prod* 21(1):62–70
9. Uygunoğlu T, Topcu IB, Gencel O, Brostow W (2012) The effect of fly ash content and types of aggregates on the properties of pre-fabricated concrete interlocking blocks (PCIBs). *Constr Build Mater* 30:180–187
10. Mashaly AO, El-Kaliouby BA, Shalaby BN, El-Gohary AM, Rashwan MA (2016) Effects of marble sludge incorporation on the properties of cement composites and concrete paving blocks. *J Clean Prod* 112:731–741
11. Wattanasiriwech D, Saiton A, Wattanasiriwech S (2009) Paving blocks from ceramic tile production waste. *J Clean Prod* 17(18):1663–1668
12. Sadek DM, El Nouhy HA (2014) Properties of paving units incorporating crushed ceramic. *HBRC J* 10(2):198–205

13. Penteado CS, de Carvalho EV, Lintz RC (2016) Reusing ceramic tile polishing waste in paving block manufacturing. *J Clean Prod* 112:514–520
14. Ohemeng EA, Yalley PP, Dadzie J, Djokoto SD (2014) Utilization of waste low density polyethylene in high strengths concrete pavement blocks production. *Civil Environ Res* 6(5):126–135
15. Vanitha S, Natarajan V, Praba M (2015) Utilisation of waste plastics as a partial replacement of coarse aggregate in concrete blocks. *Indian J Sci Technol* 8(12):1
16. Sukontasukkul P, Chaikaew C (2006) Properties of concrete pedestrian block mixed with crumb rubber. *Constr Build Mater* 20(7):450–457
17. Ling TC, Nor HM, Hainin MR (2009) Properties of crumb rubber concrete paving blocks with SBR latex. *Road Mater Pavement Des* 10(1):213–222
18. Ling TC, Nor HM, Lim SK (2010) Using recycled waste tyres in concrete paving blocks. In: *Proceeding of the institution of civil engineers*, pp 37–45
19. Ling TC (2012) Effects of compaction method and rubber content on the properties of concrete paving blocks. *Constr Build Mater* 28(1):164–175
20. Murugan RB, Natarajan C, Chen SE (2016) Material development for a sustainable precast concrete block pavement. *J. Traffic Transp Eng (English Edition)* 3(5):483–491
21. Lam CS, Poon CS, Chan D (2007) Enhancing the performance of pre-cast concrete blocks by incorporating waste glass—ASR consideration. *Cem Concr Compos* 29(8):616–625
22. Turgut P, Yahlizade ES (2009) Research into concrete blocks with waste glass. *Int J Civil Environ Eng* 1(4):203–209
23. Ling TC, Poon CS (2014) Use of recycled CRT funnel glass as fine aggregate in dry-mixed concrete paving blocks. *J Clean Prod* 68:209–215
24. Yüksel İ, Bilir T (2007) Usage of industrial by-products to produce plain concrete elements. *Constr Build Mater* 21(3):686–694
25. Said I, Missaoui A, Lafhaj Z (2015) Reuse of Tunisian marine sediments in paving blocks: factory scale experiment. *J Clean Prod* 102:66–77
26. Wang L, Chen L, Tsang DC, Li JS, Baek K, Hou D, Ding S, Poon CS (2018) Recycling dredged sediment into fill materials, partition blocks, and paving blocks: technical and economic assessment. *J Clean Prod* 199:69–76

Activity-Based Model: Requisite for a New Travel Demand Forecasting Approach for India



Suchismita Nayak and Debapratim Pandit

1 Introduction

Travel behavior in developing countries has been substantially varying in recent years with growing vehicle ownership and the introduction of new modes. Modeling commuters' travel pattern is important for planners and decision-makers for the selection and implementation of the right mix of policies toward the creation of a sustainable travel environment. The traditional aggregated methods fail to estimate travel demand accurately for developing countries particularly due to heterogeneity in terms of income, religion, nature of jobs, family structure and size, culture, travel modes, and traffic flows which result in varied and complex travel environment. Thus, there is a need for a disaggregated realistic travel demand model for efficient travel demand forecasts for developing countries within budget and time constraints. However, till date in India, the traditional four-stage modeling approach has been being used for the estimation of travel demand in most cases.

The progress in behavioral research has helped to identify several shortcomings in the traditional four-stage model such as lack of integrity among various sub-models, interdependency between the four steps, strong aggregate nature both in time and space and lack of behavioral realism. In addition, in the early 1990s, the introduction of the concept of “travel as derived demand” [1] has brought a paradigm shift in travel behavior analysis which has led to the growth of ABMs. During the last two decades, the research and application of ABMs in different developed countries have advanced significantly, whereas very little research has been taken up in developing countries. Additionally, a country like India, where population density and diversity are very high, requires a comprehensive framework to understand the travel pattern of

S. Nayak (✉) · D. Pandit

Department of Architecture and Regional Planning, Indian Institute of Technology Kharagpur,
Kharagpur 721302, India

e-mail: suchismita@iitkgp.ac.in

individuals for better travel demand management. This paper is an attempt to establish the need for the formulation of an integrated land use-transportation modeling framework for India through an intense conjectural study on existing travel demand models in India and different ABMs developed across the globe. The rest of the paper has been divided into four sections. The first section details the concept and evolution of activity-based models that have been adopted in other countries to identify limitations and applicability in the Indian context followed by the comparative analysis between the four-stage model and ABMs. The next phase involves critical analysis of earlier travel demand modeling studies in India to identify gaps and future direction of research followed by the description of the present Indian urban transportation scenario to establish the need for a new transport demand modeling approach. Finally, the paper has been concluded with a proposed activity-based modeling framework for India.

2 Appraisals of Different Activity-Based Models

In 1990, for the successful implementation of Clean Air Act Amendments in the USA, the application of traditional aggregate models was found to be inadequate for the accurate forecast of mobile emission. This led to the development of disaggregate ABMs to address the limitations of traditional models. In addition, strategies such as teleworking, congesting pricing, and ridesharing require a disaggregate travel demand model for precise assessment. Thus, since the last decade, ABMs are quite popular in many countries across the globe. The concept, component, and computational evolution of ABMs are narrated in detail in the subsequent sections.

2.1 *Concept of Activity-Based Model*

ABMs have been adopted with an aim to address the limitations of the four-stage models. In the early 1970s, Chapin has argued that instead of traveling aimlessly people travel to perform an activity [1, 2] and the choice of place to perform the activity is responsible for the creation of spatial patterns [3]. Hence, instead of relying on normative location theories, identification of activity patterns should be considered. As per Chapin, four reasons has been identified behind the willingness to take part in an activity such as propensity (people tend to deviate from their choices due to several factors such as lifecycle, health, etc.), opportunity (the favorable environment to perform an activity which is created by physical and spatial characteristics), situation (whether the state of the art of the surrounding environment is suitable for performance of an activity or not), and environmental context [1]. To perform the selected activities commuters choose travel options based on their socio-economic conditions, lifestyle and awareness of available options and constraints. Thus, the

aim of ABMs is to predict the sequence of trip chains and all the attributes associated with each trip such as where, when, for how long by individuals under several constraints imposed by the travel environment, institution, other household members, and limited resource (time and budget). The concept of constraints, which limits the choices of an individual, was detailed out by Hägerstrand (1970). In his research, the constraints are broadly divided into three categories such as.

- Capability constraints: for biological reasons, e.g., time requirement for eating, sleeping
- Coupling constraints: performance of a joint activity when, where, for how long, and with whom
- Authority constraints: control of an administrative authority or law on an individual or group [4].

2.2 *Activity-Based Model Components*

The ABMs are composed of two sub-models such as activity generation and activity scheduling [5]. The activity generation model predicts the aspiration of an individual to participate in activities (i.e., activity demand). Then, the travel, which is conducted to perform the activity, is scheduled considering all the constraints (i.e., activity scheduling). Even after intense research in this field, research on activity generation remains relatively neglected in comparison with activity scheduling. During the initial era of the ABMs, an econometric modeling approach has been adopted which is mostly based on the utility maximization principle. These models act on the basis of determination of the probability of a decision while different choice alternatives are available. It has been found that different logit models (i.e., multinomial logit (MNL) models, nested logit (NL) models) are popular for econometric modeling approaches [5–9]. Though this modeling technique is capable of analyzing the casual relationships among various hypotheses, due to unrealistic assumption of utility maximization behavior (i.e., all commuters are rational and have complete information regarding travel time, cost, and availability of all the available alternative modes), it often fails to capture the actual decision-making processes with adequate accuracy. Computational process models (CPMs) have been developed with an aim to address some behavioral assumptions of econometric models and are based on the condition-action rules (if-then) principle along with the ability to model the interdependent decisions [10]. Based on the modeling approaches, CPM can be further categorized as weak CPM and strong CPM. A weak CPM can be defined as the model consisting of heuristic decision rules with assumptions of unbounded rationality (e.g., utility maximization principle) at the individual level [11–14]. A strong CPM is based only on decision rules and there is no assumption related to unbounded rationality [15–19]. Though there is no comparative analysis has been conducted between econometric based and computational process-based ABMs, several comparative analysis has been conducted for mode choice analysis and it has been proved that decision rule-based algorithms such as decision tree,

random forest decision tree, and neural networks have been performed (i.e., level of prediction accuracy) better than logit models [20–22].

3 Comparison Between Activity-Based Models and Four-Stage Models

The activity-based modeling concept, in which activity participation is the focus point, has been developed with an aim to address the limitations of four-step models. Most of the ABMs have concentrated on the analysis of destination and mode choice, and very few models have included route choice [23]. However, like the four-stage models, ABMs also generate time-dependent OD matrices which can be further processed for the route choice model. In the overall travel demand modeling framework, there is hardly any difference between the four-stage model and ABMs. But, certain properties associated with ABMs such as integrity, allowance for complex dependencies, higher resolution, and disaggregate nature make ABMs more efficient and policy-sensitive than the traditional four-stage model. The disaggregated ABMs maintain both intra-person and inter-person integrity within a household. Intra-person integrity has been achieved by considering different constraints (institutional, temporal, spatial, and spatio-temporal) during the scheduling of activity sequences. Inter-person integrity within a household has been gained by including coordination among individuals' daily activity-travel patterns (DATPs) at the household level, joint travel to perform joint activities, drop-off and pick-up decisions, and allocation of household maintenance work. Besides, to improved integrity, ABMs have enhanced the interdependencies among different sub-models through checks on the interrelationship among various component of DATPs, consistency in modal choice during a tour, compatibility between activity-travel generation, the state of the travel environment and travel time, and interconnection between out-of-home activities and in-home activities [3]. A higher spatial and temporal resolution are also embedded within ABMs, which make these models more policy-sensitive and efficient tools for travel demand management.

In recent years, new technology platforms such as Google Maps, Google traffic, etc., have made it easier to get real-time information on the congestion status of urban roads. This influences travelers to shift their time of travel as per their convenience and most likely to non-peak-hours or to decide against joint tours if commuters have to pass through congested areas to pick-up or drop-off the second traveler. The emergence of telecommuters has also led to a change in travel patterns in urban areas. A study in California found that telecommuters distribute their trips, over the day and avoid peak-period travel (by 60%). In this way, telecommuters have also reduced the total distance traveled and freeway miles by 70%, and 90%, respectively [24]. The changing travel pattern requires us to analyze the travel demand for the whole day instead of peak hours only. As the rebound effect of teleworkers has not been included within the traditional travel demand modeling frameworks, these

frameworks are unable to estimate the impact of teleworking on the urban travel environment [25]. Thus, there is a need to develop a modeling framework based on what-if relationships that would determine the effect of change in activity schedule.

The increasing usage of smartphones, mobile computing, and other ICTs has also reduced the difference between activities and travel episodes and also encourages multitasking during travel [26, 27]. This is also changing the way people plan their activities. Thus, the impact of real-time travel data on the travel choice of the individual also needs to be incorporated into the travel demand forecast.

Next, the introduction of ridesourcing services (i.e., OLA/UBER) has also brought a remarkable change in the urban transportation system during the last decade. The concept of ridesourcing has evolved from the idea of shared mobility. Shared mobility encompasses a wide range of services from public transportation, shuttles, and taxis to real-time on-demand ride services [28]. The growing popularity of on-demand shared modes suggests the necessity to develop an efficient demand estimation model. The demand estimation through traditional four-stage models has led to disequilibrium conditions since demand is dependent on the temporal and spatial variation in the availability of these shared modes, i.e., people may change their mode choice if the waiting time for shared modes is more than a certain threshold value. In this regard, individuals' multi-modal multi-activity trip chains must be considered to help policymakers to reduce the demand–supply gap and the application of ABMs in this context is appropriate to deal with commuters daily multi-modal multi-activity trip chains [29].

During the last two decades, several ABMs have been developed in different countries and some of these models have been able to address all the major issues related to the traditional four-step models. However, there are several limitations and issues associated with existing ABMs that need to be addressed. To reduce the computational and data burden of ABMs, a synthetic population is used for simulation which is again developed based on sample population characteristics, which result in a fair amount of uncertainty in the prediction. Uncertainty also results from inappropriate inputs in the models and from several studies, it has been found that with an increase of sample size, uncertainty associated with the model is reduced. However, in most cases, computational run time increases at an exponential rate with an increase in sample size [30]. Thus, there is a need for a tradeoff between sample size and the number of model runs (computational time). Most of the current models simulate activity-travel patterns for a single day of the week (preferably any working day), which gives an unrealistic prediction of travel demand due to lack of integrity across all the days of the week (especially working days and holidays). Though recently, developed ABMs include the influence of travel attributes, socio-economic characteristics on the individuals, and households' choice, but the psychological factors and imperfect nonlinear perceptions are not considered. These attitudinal attributes are important components of behavioral models. In this context, hybrid choice models might be a solution to this, which demands further research before reaching to a conclusion. Though further research is required to address the limitations associated

with ABMs, it has been already established by the large number of literature that ABMs gives a more realistic and accurate prediction than the traditional four-stage model.

4 Changes in Travel Behavior of Indian Citizens: Progress in Travel Demand Modeling Approach

In India, 31.2% of the population (377 million) lives in urban areas [31] and the urban economy contributes almost 60% of the country's GDP. However, most of the cities (i.e., 78% of the 5 million-plus cities) suffer from the lack of organized transportation facilities and only a few cities have deployed mass rapid transit systems [32]. During the last two decades, the share of public transportation at the city-level has also declined (between 1994 to 2007 from 69 to 38% for 4 million-plus cities) [32]. Therefore, to cope with the poor public transportation facilities, the number of registered vehicles (mostly two-wheelers) has increased from 55 million in 2001 to 142 million by 2011 and is estimated to be 195.6 million in 2016. Urban road infrastructure has failed to keep pace with this increased demand leading to severe congestion, pollution, traffic accidents and fatalities, longer trip lengths, and a higher per-capita trip rate [33]. Various policies have been recommended to deal with these transportation externalities [34, 35] but a precise assessment of the impact of policy using the existing conventional modeling framework is an arduous task for transportation planners and decision-makers.

Urban transport-related issues are mostly addressed in National Urban Transportation Policies [36], Comprehensive Mobility Plans (CMP), and Master Plan of different cities, which usually focuses on a long-term vision to create a suitable travel environment for people and goods in a city and recommends the appropriate strategies and investment initiatives to meet the vision [36]. Understanding of travel behavior and prediction of future demand of citizens is inevitable to suggest appropriate strategy and policy control the aggregate phenomena such as congestion, land use patterns, and emissions. However, these policies instead of affecting the aggregate phenomena directly, affect them indirectly through the behavior of individuals. Moreover, the travel demand modeling technique is not mentioned in several cities' CMPs and in many cities, there is no CMP. Till date in India, all the CMPs have been based on four-stage transportation demand models (trip generation, trip distribution, mode choice, and network assignment) in which the effect of long-term choices (household and work location choice), vehicle ownership in future, and the effect of transportation on the environment is ignored [37–42]. The travel demand approach and software used for transportation demand prediction in the top 20 populous cities of India have been listed in Table 1 which shows that there is no complete integrated land use-transportation model that has been developed for India till date. In addition, freight and passenger demand are estimated separately, which creates further

Table 1 Transportation demand modeling approach in CMPs of different Indian cities

Sl. No	City	Travel demand model approach	Software used
1	Mumbai	Standard four-stage travel demand modeling approach	EMME
2	Delhi	Not mentioned	
3	Bangalore	Traditional four-stage integrated land use transport transportation model	CUBE
4	Hyderabad	Traditional four-stage model	Not mentioned
5	Ahmedabad	Not mentioned	
6	Chennai	A four-stage model with combined trip distribution and modal split phase using a conventional doubly constrained gravity model	CUBE
7	Kolkata	Not available	
8	Surat	Not mentioned	
9	Pune	Conventional 4-stage transport model	CUBE
10	Jaipur	Conventional 4-stage transport model	CUBE 5.0
11	Lucknow	A conventional 4-stage transport model	CUBE 5.0
12	Kanpur	Conventional 4-stage transport model	CUBE
13	Nagpur	Conventional 4-stage transport model	CUBE
14	Indore	Not mentioned	
15	Thane	Not mentioned	
16	Bhopal	Not available	
17	Visakhapatnam	Conventional 4-stage transport model	Not mentioned
18	Pimpri and Chinchwad	Conventional 4-stage transport model	Not mentioned
19	Patna	Conventional 4-stage transport model	Not mentioned
20	Vadodara	Not available	

incomprehension for network analysis. The existing models fail to reflect behavioral realism and do not consider any interrelationships among trips performed by an individual on the same day or even among the trips belonging from the same tour, dependencies among different household members, and different choice facets (e.g., trip choice and mode choice).

During the last decade, India has also witnessed the same changes arising out of new information communication technology (ICT) platforms similar to developed countries. Additionally, the introduction of ridesourcing services, telecommuting, and the government investments in “smart city program,” “National Electric Mobility Mission Plan 2020,” Make in India, “Automotive Mission Plan 2026,” etc., have been contributing toward the creation of a more dynamic and flexible travel environment which would be more challenging for the transport modeler. Thus, to cope

with the changing travel pattern of Indian citizens, there is a need for the development of a comprehensive framework (integrated land use-transportation modeling framework), which would be based on disaggregated activity-based modeling framework including the characteristics of land use and built environment, household and individual socio-economic characteristics, travel attributes, impacts of households interaction, joint tours, modal switching, and multiple activities in one tour [43].

In recent years, the formulation of ABMs has been studied in different Indian cities, which have been discussed here briefly to understand their scope and limitations. In Mumbai Metropolitan Region, trip chaining behavior has been analyzed with the help of activity-travel survey data [43, 44] using NL model based on the random utility theory. This has been used to classify the trip chains into three categories, namely simple (two trips and one activity in-between), complex (all trip chains with at least one activity), and open chains (missing information) for two trip purposes, i.e., work and non-work. This simple classification has limited ability to predict the complex travel pattern and behavioral mechanism of commuters and the subsequent impact of different policy interventions. In another recent study in Thiruvananthapuram urban area, an activity-based mode choice model has been developed by using a MNL, which has explored only single activity [45]. Out-of-home activity participation behavior of “*non-student-non-workers*” (retired, homemakers, and unemployed) in Bangalore was analyzed for maintenance and discretionary activities [46]. The outcome of this research was to determine the frequency of stops for two types of activities for different age groups and genders. An activity-based mode choice model was also developed for rural areas in Ernakulam district of Kerala, India [47]. To ensure the applicability of this model for urban areas in India demands further research. In short, till date, there is a lack of comprehensive activity-based demand modeling structure in India as either existing models suffer from assumptions associated with the estimation techniques or are limited to a specific group of commuters.

The main challenge in the formulation of ABM is its data-intensive nature. While no national travel survey is conducted by the government in India, the socio-economic heterogeneity of the population demands more sample size than developed countries. Therefore, the collection of this huge amount of data considering the limited budget and time at regular intervals is the biggest hindrance to the adoption of ABMs in India. But, in recent years, advancement in information and communications technologies (ICTs) has led to the increased use of intelligent transport system (ITS), mobile app-based transportation services, open-source databases, and Web services which could be accessed through custom APIs such as Google API for Google maps and traffic Web services which have provided the opportunities for transportation planners, urban planners, and decision-makers to access an enormous amount of data, which can bring down the cost of development and implementation of ABMs. Therefore, the hassles related to data collection are going to diminish in the near future. The analysis of travel behavior for a wide range of heterogeneous population is a big data analytics problem which could be solved more efficiently with shorter computational time using machine learning algorithms [20, 22, 48–52]. These algorithms for ABMs in the context of India are yet to be explored.

Due to socio-economic heterogeneity, context-specific policy adoption and differences in cultural values make the transferability of models developed in other countries to India uncertain. In India, the residential choice is a household-level decision rather than an individual's or earning member's decision. Thus, the residential choice is pre-decided, and in most cases, rental accommodation is preferred over a change in permanent accommodation. In addition, affordability, ethnicity, religion, and other social aspect play a major role in residential location choice, which is quite different than in developed countries. The recent trend also shows the younger generation to prefer on-demand services since it reduces the burden to pay for, maintain, and drive a car. This along with the adoption of electric vehicles necessitates the prediction of vehicle ownership and shared mobility demand. Finally, delivery systems for goods and services ordered online are instrumental in changing the activity and travel patterns of consumers. This necessitates the estimation of trips and modes used for last-mile delivery services within the activity-based travel demand modeling framework. As discussed earlier, real-time information regarding traffic conditions of route and cancelation of activity during travel also need to be considered. Another important component of the ABMs is population synthesis. The attributes used for Census data collection in India are different from other countries which demand the formulation of a fresh population synthesis model for India. Micro-simulation of activity patterns of a synthetic population with high resolution in regards to space and time can also be applied to establish a dynamic exposure assessment model for air pollution.

In Fig. 1, a comprehensive integrated land use modeling framework has been suggested which includes different sub-models that are required together to predict travel demand in the Indian context. The overall framework is an amalgamation of six major models such as population synthesis model, location choice model, vehicle ownership model, activity-based travel demand model, auxiliary model, and emission model. The activity-based travel demand model can be further divided into three components such as activity generation, activity scheduling, and traffic assignment. For the creation of a synthetic population, the household survey format must include the variables mentioned in the Census of India. The suitable activity-travel diary for India would be designed in such a way that it will be affordable and user-friendly. The booklet format which is common for space-time data collection is not encouraged in the Indian context due to budget constraints. In addition, survey methods used in developed countries will not work here due to low literacy rates and poor access to the internet. To predict the travel demand, the residential and work location of the synthesized population for the forecasted year must be known. The choice of new residence depends on the availability of housing, price, proximity to the workplace, and other infrastructures. To forecast the vehicle ownership status, stated preference survey will be conducted to know the willingness to purchase and what type of vehicle will be purchased (e.g., electric vehicle). Besides, a simulator would be part of the framework that will estimate the demand for services provided by various transportation network companies (i.e., Ola/Uber/Shuttle) at different times of the day across a city and the availability of supply for the same. This will help to establish a demand-supply equilibrium with fleet size optimization [28]. Also, the

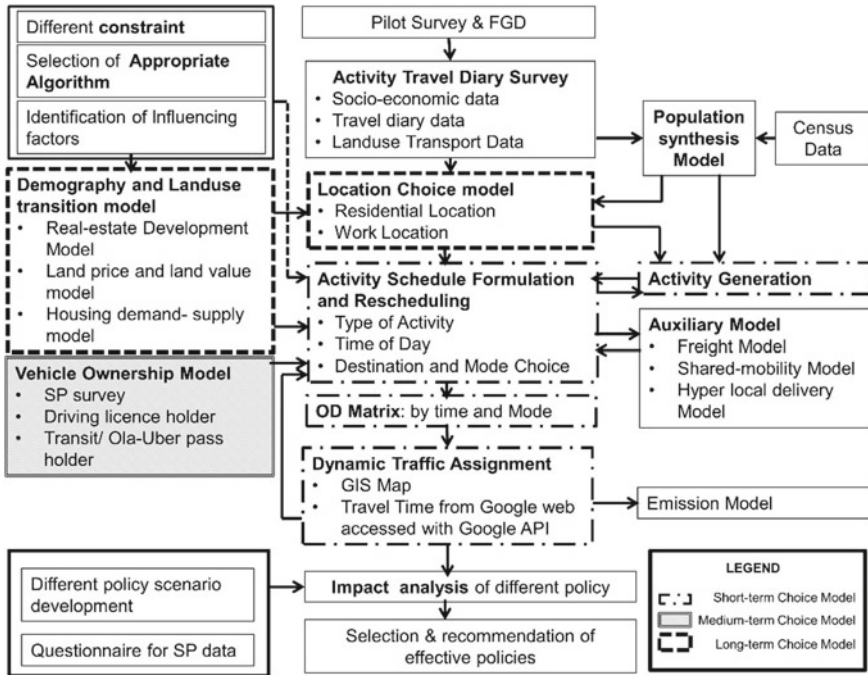


Fig. 1 Framework of integrated land use-transportation and activity-based demand model for India

demand generated for last-mile delivery services will be estimated. All the generated demand from the auxiliary models will be included in the network assignment to get the real network condition which will assist in determining the travel time more accurately. In addition, travel time between any two points within the study area for a particular time of a day will be collected from the Google Website accessed by using Google API. The output of this travel time will be used for the scheduling of activities generated by the synthetic population. The sampled households can be categorized into several “similar activities generating groups” by using unsupervised learning techniques. After that, each synthesized household can be labeled to any determined category based on their socio-economic characteristics (household size, number of job earners, income, type of jobs, number of students, age and gender of a household member, transit pass holder, and so on). After the generation of the activity list performed by the households, the activity schedule will be prepared for each person considering the household interaction effects, availability of different modes, travel time, cost of travel, and other constraints. This stage is the most critical and activity scheduling, network assignment, and auxiliary models are highly interconnected. After the allocation of travel routes and modes to a traveler to perform an activity, network load and auxiliary models will be updated. Thus, there will be continuous to and fro checks among activity scheduling, auxiliary model, and network assignment. After the allocation of activities for every synthesized household, the output from the

demand model can be utilized to estimate emission caused by every kind of activity and travel distinctly. In addition, it can assist to analyze the impact of any policy related to transportation demand management to reach the right mix of policies.

5 Conclusion

This paper presents a comparative analysis between four-stage and activity-based travel demand models and identifies the scope of future research on developing integrated land use-transportation models in the Indian context. This research is also helpful in understanding the need for ABMs in India and the formulation of a simple yet efficient ABM-based travel demand modeling framework considering the constraints related to cost, time, and availability of data. The discussion also touches upon the computational complexity of ABMs where a new modeling approach is proposed on what-if relationships to determine the effect of change in the activity schedule. This research also deliberated on the changing travel environment and how an ABM can reflect the travel behavior more accurately and efficiently than the traditional four-stage model. Since no activity-based travel demand modeling framework has been constructed for India due to difficulties in data collection and computational challenges, this research has also provided insights to make use of publicly shared databases and Web services. The need for integrating long-term choices such as residential location choice and car ownership has also been considered while developing the modeling framework. This new activity-based integrated land use-transportation modeling framework would be capable of assisting the policymakers to reach the right combination of policies toward the fulfillment of a particular vision.

Acknowledgements This study is part of an ongoing doctoral thesis funded by the Ministry of Education (MoE), Government of India. We are also thankful for the constructive comments of the anonymous reviewers and editor. The authors also report no conflict of interest.

References

1. Stuart Chapin F (1971) Free time activities and quality of urban life. *J Am Plan Assoc* 37:411–417
2. Stuart Chapin F, Hightower HC (1965) Household activity patterns and land use. *J Am Inst Plann* 31:222–231
3. Rasouli S, Timmermans H (2014) Activity-based models of travel demand: promises, progress and prospects. *Int J Urban Sci* 18:31–60
4. Hägerstrand T (1970) What about people in regional science? *Pap Reg Sci* 24:7–24
5. Bhat CR, Koppelman FS (1999) Activity-based modeling of travel demand. In: Hall RW (eds) *Handbook of transportation science. International series in operations research & management science, vol 23*. Springer, Boston, pp 35–61
6. Bowman JL (1995) Activity based travel demand model system with daily activity schedules. *J Bus Manag M.S* 92:1–94

7. Bowman JL, Ben-Akiva ME (2001) Activity-based disaggregate travel demand model system with activity schedules. *Transp Res Part A Policy Pract* 35:1–28
8. Vovsha P, Petensen E, Donnelly R (1898) Impact of intrahousehold interactions on individual daily activity-travel patterns. *Transp Res Rec J Transp Res Board* 2004:87–97
9. Yagi S, Mohammadian A (2010) An activity-based microsimulation model of travel demand in the Jakarta metropolitan area. *J Choice Model* 3:32–57
10. Gärling T, Kwan MP, Golledge RG (1994) Computational-process modelling of household activity scheduling. *Transp Res Part B* 28:355–364
11. Kitamura R, Fujii S (1998) Two computational process models of activity-travel behavior. In: Garling T, Laitila T, Westin K (eds) *Theoretical foundations of travel choice modeling*. Emerald Group Publishing, pp 251–279
12. Pendyala RM, Kitamura R, Prasuna Reddy DVG (1998) Application of an activity-based travel-demand model incorporating a rule-based algorithm. *Environ Plan B Plan Des* 25:753–772
13. Recker WW, McNally MG, Root GS (1986) A model of complex travel behavior: Part I-Theoretical development. *Transp Res Part A Gen* 20:307–318
14. Ettema D, Borgers A, Timmermans H (1993) Simulation model of activity scheduling behavior. *Transp Res Rec* 1413:1–11
15. de Palma A, Lindsey R, Quinet E, Vickerman R, Pinjari AR (2013) Activity-based travel demand analysis. In: de Palma A, Lindsey R, Quinet E, Vickerman R (ed) *A handbook of transport economics*. Edward Elgar Publishing, pp 213–248
16. Arentze T, Hofman F, Van Mourik H, Timmermans H (2000) ALBATROSS: multiagent, rule-based model of activity pattern decisions. *Transp Res Rec* 1706:136–144
17. Arentze TA, Timmermans HJP (2004) A learning-based transportation oriented simulation system. *Transp Res Part B Methodol* 38:613–633
18. Roorda MJ, Miller EJ, Nurul Habib KM (2008) Validation of TASHA: A 24-h activity scheduling microsimulation model. *Transp Res Part A Policy Pract* 42:360–375
19. Auld J, Mohammadian AK (2012) Activity planning processes in the agent-based dynamic activity planning and travel scheduling (ADAPTS) model. *Transp Res Part A Policy Pract* 46:1386–1403
20. Hagenauer J, Helbich M (2017) A comparative study of machine learning classifiers for modeling travel mode choice. *Expert Syst Appl* 78:273–282
21. Cantarella GE, De Luca S (2003) Modeling transportation mode choice through artificial neural networks. In: 4th International symposium on uncertainty modeling and analysis, ISUMA 2003, pp 84–90
22. Sekhar CR, Minal ME (2016) Mode choice analysis using random Forrest decision trees. *Transp Res Procedia* 17:644–652
23. Miller EJ, Roorda MJ (1831) Prototype model of household activity-travel scheduling. *Transp Res Rec J Transp Res Board* 2003:114–121
24. Pendyala RM, Goulias KG, Kitamura R (1991) Impact of telecommuting on spatial and temporal patterns of household travel. *Transportation (Amst)*. 18:383–409
25. Moeckel R (2017) Working from home: modeling the impact of telework on transportation and land use. *Transp Res Procedia* 26:207–214
26. Kenyon S, Lyons G (2007) Introducing multitasking to the study of travel and ICT: examining its extent and assessing its potential importance. *Transp Res Part A Policy Pract* 41:161–175
27. Zhang J, Timmermans H (2010) Scobit-based panel analysis of multitasking behavior of public transport users. *Transp Res Rec* 2157:46–53
28. Chakraborty J, Pandit D, Xia J (Cecilia), Chan F (2020) A protocol for simulation modeling of ridesourcing services: optimisation of fleet size in an urban environment. *Int J Intell Transp Syst Res* 18:267–276
29. Li Q, Liao F, Timmermans HJP, Huang H, Zhou J (2018) Incorporating free-floating car-sharing into an activity-based dynamic user equilibrium model: a demand-side model. *Transp Res Part B Methodol* 107:102–123
30. Kwak M-A, Arentze T, Romph E, De Rasouli S (2012) Activity-based dynamic traffic modeling: influence of population sampling fraction size on simulation error. *Int Conf Travel Behav Res* 1–17

31. Government of India (2011): National Portal of India
32. The World Bank (2011) Urbanization in India: integral part of economic growth 5–9
33. Singh J (2016) City public transportation developments in India. *Intell Transp*
34. Pucher J, Korattyswaropam N, Mittal N, Ittyerah N (2005) Urban transport crisis in India. *Transp Policy* 12:185–198
35. Sudhakara Reddy B, Balachandra P (2012) Urban mobility: a comparative analysis of megacities of India. *Transp Policy* 21:152–164
36. National Urban Transport Policy (2014) Ministry of Urban Development, Government of India
37. Comprehensive Mobility Plan (CMP) for Pimpri-Chinchwad Municipal Corporation (2008)
38. Comprehensive Mobility Plan (CMP) for Greater Mumbai (2016)
39. Comprehensive Mobility Plan for Jaipur (2010)
40. Comprehensive Mobility Plan for Bengaluru (2019)
41. Preparing a Comprehensive Mobility Plan (CMP) (2014) A Toolkit. Ministry of Urban Development, Government of India
42. Chennai Comprehensive Transportation Study (2010)
43. Subbarao SSV, Krishna Rao KV (2013) Analysis of household activity and travel characteristics in Mumbai metropolitan region (MMR). *Int J Emerg Technol Adv Eng* 3:98–109
44. Subbarao SSV, Krishna Rao KV (2013) Trip chaining behavior in developing countries: a study of Mumbai metropolitan region, India. *Eur. Transp. Trasp. Eur.* 53:1–7
45. Lekshmi GRA, Landge VS, Kumar VSS (2016) Activity based travel demand modeling of Thiruvananthapuram urban area. *Transp Res Procedia* 17:498–505
46. Malayath M, Verma A (2013) Activity based travel demand models as a tool for evaluating sustainable transportation policies. *Res Transp Econ* 38:45–66
47. Philip M, Sreelatha T, George S (2013) Activity based travel behavioural study and mode choice modelling. *Int J Innov Res Sci Eng Technol* 2:181–190
48. Al-Ahmadi HM (2007) Development of intercity work mode choice model for Saudi Arabia. *WIT Trans Built Environ* 96:677–685
49. Sekhar CR (2014) Mode choice analysis: the data, the models and future ahead. *Int J Traffic Transp Eng* 4:269–285
50. Juremalani J, Chauhan KA (2017) Comparison of different mode choice models for work trips using data mining process. *Indian J Sci Technol* 10:1–3
51. Omrani H (2015) Predicting travel mode of individuals by machine learning. *Transp Res Procedia* 10:840–849
52. Yasmin F, Morency C, Roorda MJ (2015) Assessment of spatial transferability of an activity-based model, TASHA. *Transp Res Part A Policy Pract* 78:200–213

Analysis of Falling Weight Deflectometer (FWD) Data of a Flexible Pavement Using Two Different Programs



Shubham Mishra, Rakesh Kumar Srivastava, Pradeep Kumar,
and Tanuj Chopra

1 Introduction

A highway pavement comprises of different layers above soil subgrade. It is used to disperse the vehicular load to subgrade. To decrease the stresses, which are transmitting due to wheel load and so that these stresses will not go beyond the strength of subgrade. There are mainly two types of pavement, specifically flexible rigid pavements. In flexible pavement, wheel loads are transferred by grain-to-grain contact of the aggregate through the coarse structure [1]. These types of pavements experience deformation under action of the loads because of negligible flexural strength.

The load from motor vehicle is firstly applied on the top surface of pavement which is surface course, and it is distributed from surface course to the base, subbase, and subgrade courses in form of a truncated cone. These stresses initiated by the loads carrying on the pavement are maximum at top, and wearing course has highest stiffness due to which pavement gets its most strength. The subgrade plays a significant role of transmitting load from layers present above to ground. Evaluation of in service roads is very important for keeping them in good serviceable condition. All pavements get deteriorated with time due to repetitive application of wheel loads and due to effect of atmospheric conditions. Various factors are responsible for the rate of deterioration. These factors are initial condition of pavement, magnitude of vehicular loading, atmospheric conditions, and various other factors. For the construction of expressways and highways, huge amount of money is being invested in India. There is a need to evaluate these facilities periodically in terms of functional and

S. Mishra (✉) · T. Chopra
Department of Civil Engineering, Thapar Institute of Engineering and Technology, Patiala,
Punjab, India

R. K. Srivastava · P. Kumar
Pavement Evaluation Division, CSIR—Central Road Research Institute (CRRI), New Delhi, India

structural performance to determine the requirement for maintenance and rehabilitation measures [2]. To calculate the need of rehabilitation measures, the highway infrastructure that has been constructed at a huge cost should be evaluated regularly.

FWD is a technique which, nowadays, is being used for structural evaluation of flexible pavements. The surface deflection bowls obtained by FWD tests are analyzed by using back-calculation process to estimate the effective moduli of different layers of pavement which are useful for determination of remaining life and overlay design of pavement. In the present paper, an effort has been made to broadly describe history and recent works done by various researchers for evaluating the falling weight deflectometer data by using different programs.

2 Structural Evaluation of Flexible Pavement

Structural evaluation is a condition that represents the load carrying ability of pavement. After construction due to traffic loading, the pavement's ability to carry loads reduces with time. To enhance the pavement, capacity to carry the increased loads overlay can be designed. Structural capacity is calculated in terms of reaction of pavement to the applied load which can be determined in terms of stresses, strains, and deflections. Most common parameter utilized in almost all the pavement evaluation systems is surface deflection because it is easy to measure.

The data attained after evaluating different studies are utilized for estimating the type of essential maintenance procedures, prioritization of maintenance works, and for creating a PMMS [3]. The pavements are structurally evaluated to determine the structural strength, to obtain the remaining life of road, to compute the thickness of overlay, and to establish a PMMS based on performance of the road.

Two types of testing (destructive and non-destructive) are used for the determination of structural strength of pavements. In destructive testing, laboratory tests can be used for detecting the structural deficiencies in various layers of pavement. In these tests, samples of materials are excavated from different layers and taken to laboratory for assessment. In this method, road gets heavily damaged due to the destruction at different levels and at regular intervals. To repair such damaged pavements, a large amount of money is required. Because of this, destructive testing (DT) methods have become unpopular practice. Therefore, various non-destructive techniques have become popular in recent years because of their speed, low-cost, and reliability. NDT testing includes use of static and dynamic loading equipment. Benkelman beam, the Lacroix deflectograph, light weight deflectometer, falling weight deflectometer, rolling weight deflectometer, traffic speed deflectometer, etc., are some of the non-destructive testing equipment which are used for evaluating flexible pavements.

2.1 Benkelman Beam Deflection (BBD) Method

In this method, the reaction of a pavement is measured in terms of surface rebound deflection under static loading. It is trouble-free, low-cost, and dependable apparatus used to compute the structural capability of pavement. BB method is adopted for routine structural assessment and to design the overlay thickness of pavement. The detailed method of structural assessment of bituminous pavement by employing BBD is given in IRC: 81–1997. BBD test equipment is depicts in Fig. 1.

Limitations of the BBD Method

1. In this technique, the load application on road surface is static which does not represent the loads which are applied on pavements by fast moving traffic.
2. It has very slow speed of operation which reduces its feasibility for routine evaluation.
3. More manual labor is required for BBD testing as compared to other NDT testing.
4. Only maximum surface deflection is determined by using this method. The profile of entire deflection bowl is not measured and also not considered in the design of overlay thickness as per IRC: 81-1997 guidelines. Two pavements with same maximum deflection can have different deflection bowls which indicate that strain in asphalt pavement depends on the stiffness of individual layers of



Fig. 1 BBD test equipment

the pavement. Therefore, to compute the strength properties of individual layers, measurement of entire deflection bowl is important.

5. The front leg of the BBD may fall in the region of deflected bowl if deflection bowl area is wide. The movement of beam support resting in the deflection bowl can result in erroneous deflection measurements.
6. A few Benkelman beams can be placed along the pavement deflection bowl to measure the entire deflection bowl but this method requires more time and labor [3].

Due to these limitations of BBD method, FWD method is preferred for the structural evaluation of pavements.

2.2 FWD Method

In this method, deflected shape of surface is measured by applying impulse force on the pavement surface. A typical falling weight deflectometer has an arrangement to drop a pre-determined magnitude of mass over a buffered circular loading plate which is placed on the surface of the pavement. Load is transmitted to pavement through a loading plate by load is falling on spring system [4].

It can transfer heavier loads on to the surface of the pavement as compared to any other NDT deflection testing device. The loading range varies depending on the model. Applied load can be varied by altering the magnitude of the falling load and fall height. Velocity transducers or sensors are installed at different radial locations from middle of plate which are utilized to assess the vertical surface deformations of pavement. Usually, about six to nine geophones are utilized to compute surface deformations. It gives deformation bowl whose features are analyzed and utilized for back-calculation of modulus values of pavement layers. The detailed guidelines for structural assessment of flexible pavements using FWD are given in IRC: 115-2014 [5]. Figure 2 depicts the working principle of FWD.

FWD is normally used for

- To measure deflections
- Finding in-situ layer moduli
- Structural capacity and remaining life estimates
- Load transfer efficiency of joints in concrete pavement
- Pavement analysis and design
- Overlay design/pavement rehabilitation
- Pavement management

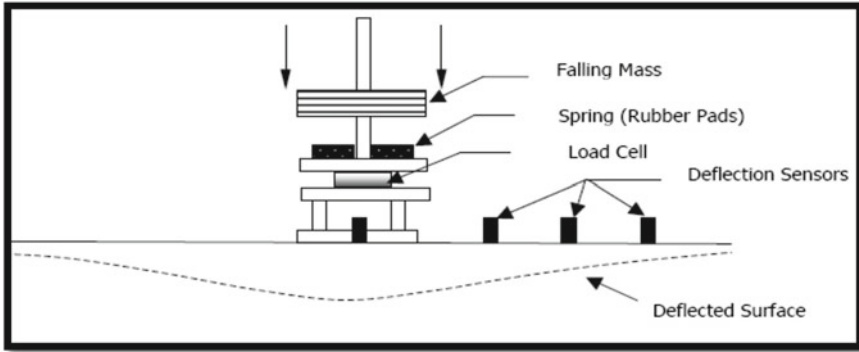


Fig. 2 Working principle of FWD [4]

3 Literature Review

Various national and international journals are reviewed so as to summarize the literature available on this topic and due to space restrictions, only significant studies are examined in this paper. Au and Paul [6] evaluated four programs for the analysis of deflection data with laboratory results. They used both destructive and non-destructive methods for evaluating material properties. Software evaluated was ELMOD, OAF, MODCOMP2, and VESYS. The researchers observed that back-calculated modulus values using VESYS model had the least variation from laboratory values. They concluded that VESYS and ELMOD were more suitable for prediction of pavement layer moduli. Rada et al. [7] carried out a relative study on four programs; specifically ISSEM4, MODCOMP3, MODULUS, and WESDEF for the purpose of developing a strategic highway research program (SHRP). Deflection data and other important information were used for evaluating selected software by the different evaluators, and at the end, their analysis was compared. Even though, grading of software different from one assessor to another but the MODCOMP3, MODULUS, and WESDEF were graded as top back-calculation software in decreasing order. Then, the program to program comparison of the back-calculated moduli was conducted. It was found, MODCOMP3 program be likely to calculate more subgrade modulus but less base and subbase modulus, when compared with WESDEF results. Van Deusen [8] compared the performance of several back-calculation programs for selection of flexible pavement back-calculation software for Minneosta road research project. Four programs were selected for this study such as EVERCALC v.3.3, MODCOMP3 v.3.6, WESDEF, and EVERCALC v.4.1. After evaluating different programs, it was found that the agreement between WESDEF and EVERCALC v.3.3 was the best among the programs investigated. Output of MODCOMP3 program frequently has become unstable during analysis of field data. The use of EVERCALC v.4.1 as a “standard” back-calculation program should be

implemented (at least for Mn/ROAD and research work). Sharma and Das [9] developed an artificial neural network (ANN) for back-calculation of pavement layer modulus. Authors compared performance of ANN back-calculation with performance of other standard programs which were EVERCALC and ExPaS. In this study, authors found that preparing of ANN took additional time and its performance depends on its training.

Ameri et al. [10] compared four programs which were MODULUS 6.0, ELMOD 5.0, EVERCALC 5.0, and dynamic back-calculation with system identification (DBSID). Elmod 5.0 overvalued the modulus of subgrade in a few cases. MODULUS 6.0 and EVERCALC 5.0 showed good reliability in outcomes of all three layers. Subgrade modulus value anticipated by DBSID changed into 2.5 instances more than subgrade modulus value forecasted by MODULUS 6.0. Base moduli calculated by MODULUS 6.0 had been almost 1.3 instances more than that of DBSID. Dynamic back-calculation is time consuming task. Overall, they found that MODULUS 6.0 is most appropriate program for this study. Priddy et al. [11] compared back-calculation results of selected programs by utilizing heavy weight deflectometer (HWD) data acquired during airfield pavement evaluations. In this study, authors used BAKFAA, ELMOD6, and WESDEF programs for back-calculating the moduli for airfield pavements. BAKFAA produced similar back-calculated moduli to those obtained with WESDEF. ELMOD6 did not produce similar back-calculated moduli results to those obtained using WESDEF and produced more unreasonable modulus values than the other programs. The ELMOD6 program anticipated higher moduli for the subgrades among the sections analyzed. The forward calculation subgrade moduli correlated nicely to the back-calculated subgrade moduli. It was suggested that the United States Air Force (USAF) continues utilizing WESDEF for back-calculation.

In this study, two programs, namely KGPBACK and KUAB, were used for analysis of FWD data. KGPBACK is specific version of BACKGA program. It is recommended in IRC: 115-2014 guidelines to use this software for back-calculation of pavement layer modulus values. It is based on genetic algorithm model. KUAB software is recommended by manufacturers of falling weight deflectometer. This program follows iterative approach and uses method of equivalent thickness approach in order to calculate pavement layer moduli.

4 Analysis of FWD Data for Flexible Pavement

A Jhatikra village road in Delhi was selected for present study. Deflection survey was conducted with KUAB FWD on twenty points. Other field data such as crust details, pavement temperature, and air temperature at different chainage were also collected during the survey. FWD which is used for this study is depicts in Fig. 3.

Thickness of bituminous layer was 150 mm, and for base layer, it was 260 mm. In this study, two software (KUAB and KGPBACK) were evaluated for analyzing falling weight deflectometer data and the modulus values of different layers of the pavement were compared.



Fig. 3 View of FWD used for structural evaluation of pavement

4.1 Comparison of Moduli Values of Different Layers Obtained from KGPBACK and KUAB Software

Surface Layer

Surface moduli values obtained from KUAB and KGPBACK software were plotted in Fig. 4. The correlation between surface moduli calculated from KGPBACK and KUAB software was determined (Fig. 5.)

$$y = 1.467x - 559.2 \quad (R^2 = 0.616) \tag{1}$$

Here,

- y Back-calculated surface moduli from KUAB software (MPa)
- x Back-calculated surface moduli from KGPBACK software (MPa)

Base Layer

Base moduli values obtained from KUAB and KGPBACK software were plotted in Fig. 6. The correlation between base moduli calculated from KGPBACK and KUAB software was determined (Fig. 7.)

$$y = 3.222x^2 - 974.3x + 73799 \quad (R^2 = 0.896) \tag{2}$$

Here,

- y Back-calculated base moduli from KUAB software (MPa)
- x Back-calculated base moduli from KGPBACK software (MPa)

Subgrade Layer

Subgrade moduli values obtained from KUAB and KGPBACK software were plotted in Fig. 8. The correlation between subgrade moduli calculated from KGPBACK and KUAB software was determined (Fig. 9.)

$$y = 0.862x - 13.98 \quad (R^2 = 0.892) \tag{3}$$

Here,

- y Back-calculated subgrade moduli from KUAB software (MPa)
- x Back-calculated subgrade moduli from KGPBACK software (MPa)

Comparison between surface moduli values obtained from KUAB and KGPBACK software

See Figs. 4 and 5.

Comparison between base moduli values obtained from KUAB and KGPBACK software

See Figs. 6 and 7.

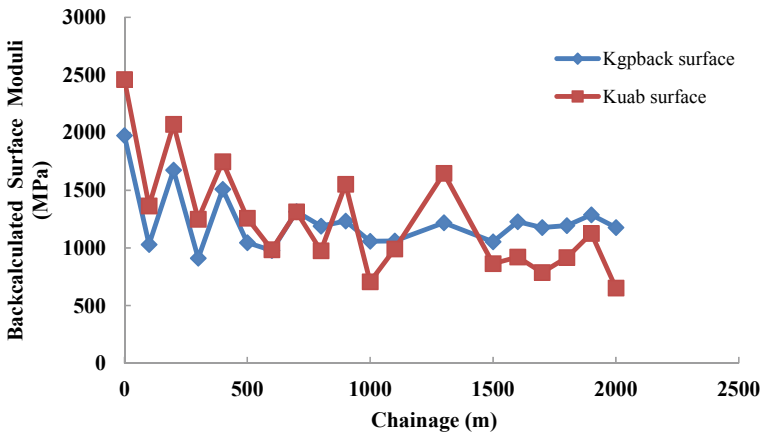


Fig. 4 Surface moduli values obtained from KUAB and KGPBACK software

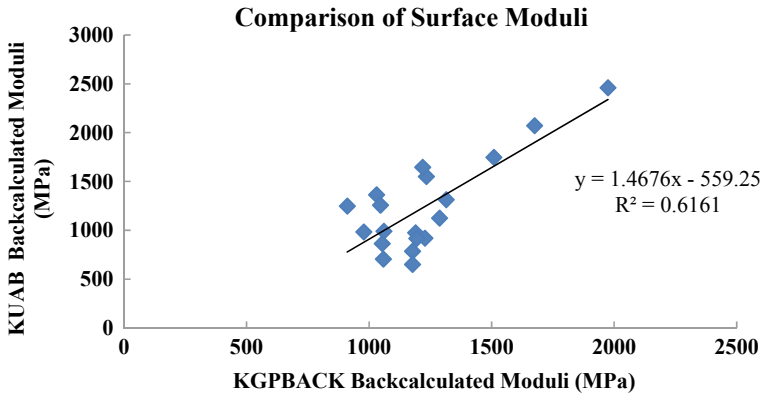


Fig. 5 Correlation between surface moduli values obtained from KGPBACK and KUAB software

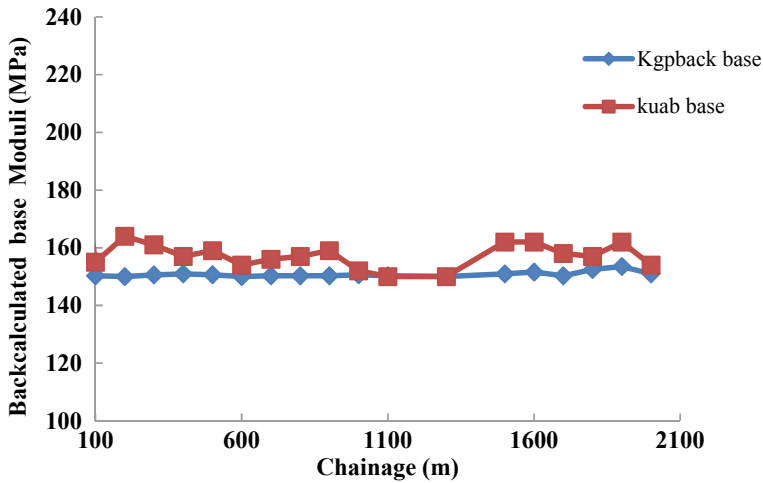


Fig. 6 Base moduli values obtained from KUAB and KGPBACK software

Comparison between subgrade moduli values obtained from KUAB and KGPBACK software

See Figs. 8 and 9.

5 Conclusion

- This paper gives an overview about back-calculation process used by different program for analyzing FWD data. As the use of FWD is increasing, a number

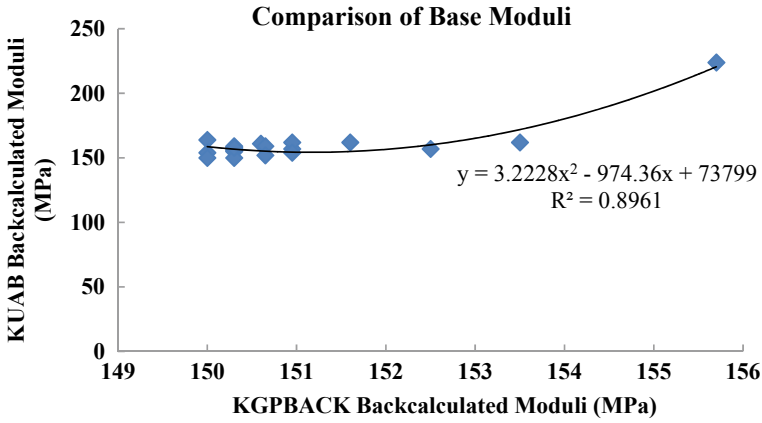


Fig. 7 Correlation between base moduli values obtained from KGPBACK and KUAB software

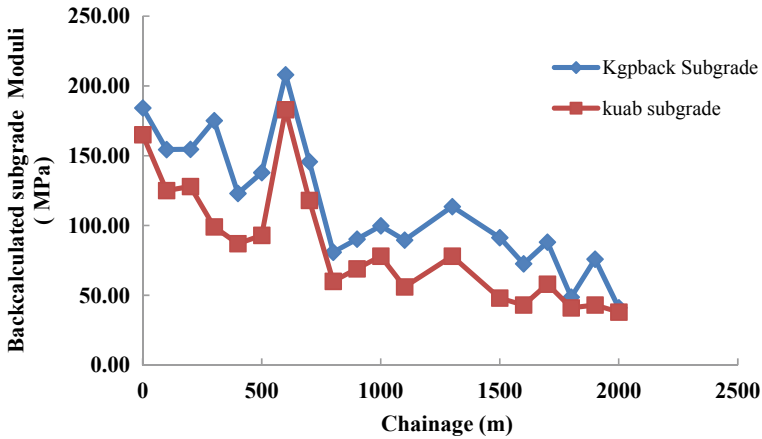


Fig. 8 Subgrade moduli values obtained from KUAB and KGPBACK software

of back-calculation techniques have been proposed. Different back-calculation programs use different algorithms due to which modulus values calculated from these programs usually differ from each other. That is why it is important to evaluate different programs in order to select the reliable back-calculation program for any study.

- Due to improper selection of software/algorithm, the modulus values for different layers, obtained from back-calculation process, may not be precise though, measured, and computed deflection basin may equivalent within reasonable limits.
- The back-calculated layer modulus plays very vital role in pavement evaluation because the modulus value is not only used for design but also to compute remaining life of the pavement.

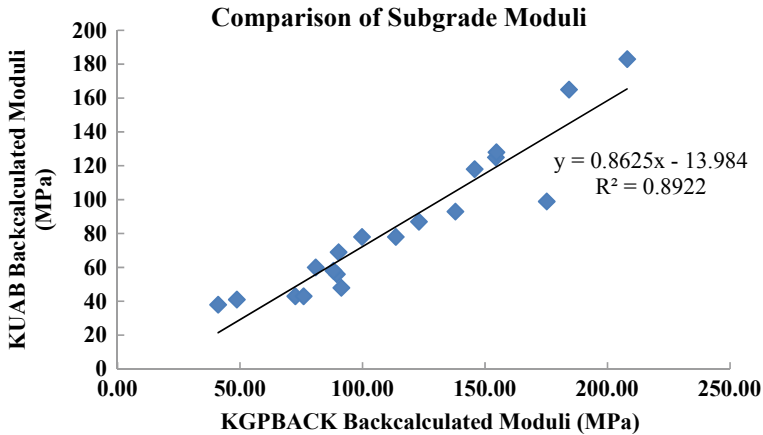


Fig. 9 Correlation between subgrade moduli values obtained from KGPBACK and KUAB software

- Lower value of back-calculated modulus can result in over design of pavement thickness. If back-calculated modulus is greater than actual modulus then it will predict remaining life greater than actual life. Therefore, it is important to examine the accuracy of back-calculated modulus to forecast the correct value of remaining life of pavement.
- Another problem with the back-calculation software is the lack of consistency of the results which means that back-calculated modulus computed using different loads are not having the same value or at least very close to each other. If difference between the back-calculated modulus from the software is significant then software can be considered to have a lack of consistency.
- In this present study for the FWD data, back-calculation analysis was performed using KGPBACK software and the results were compared with those obtained from KUAB FWD software.
- Based on comparison of KGPBACK and KUAB software, it was found that base modulus and subgrade modulus values obtained from them are more comparable with each other as compared to surface modulus values. R square value for surface modulus comparison was found to be 0.616, for base modulus, it was 0.896, and for subgrade modulus, it was found to be 0.892.

References

1. Mathew TV (2009) Introduction to pavement design. In: IIT Bombay website
2. Reddy PK (2008) Introduction to transportation engineering. Available: <http://www.nptel.ac.in>
3. Kumar RS (2014) Pavement evaluation & maintenance management system. Universities Press, Hyderabad

4. Reddy KS (2003) "Structural evaluation of pavements in Eastern Indian using falling weight deflectometer," Ministry of Road Transport and Highways (MORT&H). Indian Institute of Technology Kharagpur, India
5. IRC, "IRC:115 guidelines for structural evaluation and strengthening of flexible pavements using falling weight deflectometer technique," Indian Road Congress 2014
6. Au N, Paul N (1987) Determination of layer moduli using a falling weight deflectometer
7. Rada GR, Richter CA, Jordahl P (1994) SHRP's Layer moduli backcalculation procedure. In: Nondestructive testing of pavements and backcalculation of moduli; second volume. ASTM International
8. Van Deusen D (1996) Selection of flexible backcalculation software for the Minnesota road research project
9. Sharma S, Das A (2008) Backcalculation of pavement layer moduli from falling weight deflectometer data using an artificial neural network. *Can J Civ Eng* 35:57–66
10. Ameri M, Yavari N, Scullion T (2009) Comparison of static and dynamic back calculation of flexible pavement layers moduli, using four software programs. *Asian J Appl Sci* 2:197–210
11. Priddy LP, Bianchini A, Gonzalez CR, Dossett CS (2015) Evaluation of procedures for backcalculation of airfield pavement moduli. Engineer Research and Development Center Vicksburg MS Geotechnical and ...2015

Understanding the Preferences and Attitudes of App-Based Taxi Users Toward Existing Modes



Punyabeet Sarangi, M. Manoj, and Geetam Tiwari

1 Introduction

Recent years have seen an upward trend in demand for app-based, on-demand ride-sharing services. Based on the platform-based sharing economy concept introduced by Benkler [1], these ride-sharing services have been credited with providing a reliable, affordable transportation option in remote areas of the city and hailed for addressing the last mile connectivity issues and, to an extent, the growing unemployment problems [2]. The ride-sharing services thrive by leveraging the advances in technology to redistribute unused or under-utilized assets to people who are willing to pay for the services [3]. However, the rapid adoption of such services (both in the Indian context and globally) has posed serious questions regarding their market infiltration and their role in shaping an existing urban transportation system. Furthermore, very little is known about the user profile, travel behavior, and individual preferences for alternative modes in the absence of app-based taxis. Such details could provide information for designing appropriate regulations, guidelines, and public policy to shape transportation decisions and travel patterns [4].

In a developing economy like India, app-based taxis have gained a significant share of urban commuters since their inception in 2010 [5]. Apart from the digital marketplace created by such cabs in India, they are also expected to add another \$7 billion to their total industrial output by 2020 [6]. App-based taxis have been recognized in the National Urban Transport Policy (NUTP) of the Government of India [7]. According to the mobility as a service (MaaS) concept of NUTP, such taxis could be listed as paratransit and could cater to the travel demand of urban centers as well as towns nearby. App-based taxis could be considered an alternative to private vehicle ownership and a mode to improve last mile connectivity. It should also be

P. Sarangi · M. Manoj (✉) · G. Tiwari
Department of Civil Engineering, Indian Institute of Technology Delhi, New Delhi 110016, India
e-mail: manojm@civil.iitd.ac.in

highlighted that due to the informal and unorganized nature of the transportation sector and inadequate mass rapid transit (MRT) infrastructure in India, as noted in the NUTP 2014 (page 17) [7], these platform-based sharing economy services ply on Indian cities without many constraints. This has led to the decline in the demand for other existing modes of transport with whom these ride-hailing services compete directly or indirectly. The app-based sharing services also contribute to traffic congestion and environmental pollution in urban areas.

With the increasing urban population worldwide and especially in India, it is vital to understand the public's opinions toward app-based modes and how they evaluate this system compared to other existing modes of transport [8]. In particular, Delhi's Master Plan 2021 projects that travel demand in Delhi in 2021 is likely to increase to 27.9 million from 13.9 million passenger trips in 2001 [9]. However, as per the statistics of the Ministry of Road Transport and Highways, private vehicle ownership and the informal, unregulated modes of transport have seen rapid growth. In contrast, the number of registered public modes has seen very little growth [10].

The discussion until now indicates the need for investigating the passenger profile and their opinions and evaluations of an app-based taxi. Hence, the objectives of the present study are to explore the user profile and travel patterns of app-based taxi riders in the city of New Delhi. In particular, the present research aims as follows: (i) to understand the sociodemographic characteristics of app-based taxi riders, (ii) to explore the travel patterns of app-based taxi riders, (iii) to understand the user evaluation of app-based taxi concerning comfort, safety, satisfaction, etc., and (iv) their preference for alternative modes of transport when an app-based taxi was not available for the completed trip.

The remainder of this paper is structured as follows: Sect. 2 presents a brief literature review followed by Sect. 3 that discusses the methodology adopted in this study. Subsequently, Sect. 4 presents a descriptive summary of the data and introduces the explanatory variables. The penultimate section discusses the model estimation results and their behavioral interpretations. Finally, conclusions and scopes for future research are presented in Sect. 6.

2 Literature Review

Private companies that provide personalized or hired taxis are often called transportation network companies. However, with the advancement of information technology and the rapid use of smartphones, the last decade has seen the popularization of app-based taxis. These taxis rely on smartphones to provide services to passengers [11]. Even though these services have a rapidly growing, geographically dispersed market, they frame themselves as ride-sharing services in order to steer clear of the safety, labor, and supply regulations that have constrained the growth of the taxi industry in general [2].

Rayle et al. [11] observed that the overall impact of ride-hailing services on other modes of vehicular travel is still unclear. They observed that when an individual uses

ride-sourcing services to travel instead of using his/her vehicle, it is merely the case that one vehicle trip is being replaced with another chauffeur-driven vehicle trip. Due to the novelty of app-based taxi services and the lack of data openness from the major players, a majority of literature on this domain has focused mainly on the adoption and familiarity of such services among the millennial. Only, a handful of studies have investigated the competition of app-based taxis with other conventional modes.

Among the few existing studies, Light [12] observed that ride-sourcing is most noticeably competing with conventional taxis in an urban context. In this aspect, many studies have taken Uber as the case study and have compared it with the existing taxi services. These studies [13, 14] have found that dynamic pricing, and robust road network optimizing framework significantly reduce the overall travel cost and hold an advantage over conventional taxis. Moreover, as passengers can monitor the vehicle's real-time location, it reduces their anxiety and safety concerns [13]. Further, an experimental study conducted by Smart et al. [15] in Los Angeles city and by Contreras and Paz in Las Vegas, Nevada [16] indicated that ride-hailing services were cheaper and faster than taxis, and the waiting time was also less than that of taxis [15]. Even though the economic efficiency and improved transport connectivity have fueled a positive perception toward app-based taxis in areas with insufficient alternative mobility options, places like San Francisco have experienced worsened traffic congestions due to the sudden booming of these services [17]. These conclusions were in contrast to the findings of Nie [18], who estimated that ride-sourcing services had a mild impact on congestion issues in Shenzhen, China. Given the differences in the impacts of app-based taxis on transportation systems, it is important to consider the modal shift from public transit to ride-sourcing options, which is more likely to worsen congestions and lead to unsustainable transport developments.

The existing literature on ride-sourcing concludes that app-based services both complement and compete with public transit. In case of complementary services, it fills the role of public transit during late-night hours and weekends. Apart from these, it also serves as a feeder mode to public transit, alleviating the last mile connectivity issues [19]. For instance, Davidson et al. [20] accessed the data from a mobile app named 'TRANSIT' and fused it with the publicly available UBER data for New York city. After conducting various statistical tests on the fused dataset, they inferred that UBER filled the gap in public transit services rather than substituting public transit. However, the same is not always the case, as studies have found that ride-sourcing does compete with public transit. One such evidence is provided by Rayle et al. [3], who conducted an intercept survey in the San Francisco area and concluded that 33% of the ride-sourcing users would have taken public transit in the absence of ride-sourcing. The share (41%) was even higher for non-car owners. Studies by Henao [21], Clewlow, and Mishra [4] support these findings.

Even though cities deliberate over the need to prohibit or regulate app-based taxis, ride-sourcing services can complement both taxis and public transit if adequate policies are put in place. For public transit, they can serve as the last mile connectivity option, while they can complement the personal cars by increasing the shared rides

without flouting the economic constraints. However, the authors did not find any substantial literature in the Indian context to update the status of app-based taxi use.

3 Methodology

Based on the motive behind conducting this research, the present study utilizes a set of empirical approaches to achieve the study objectives. First, an exploratory factor analysis (EFA) is performed on the obtained data to examine the underlying latent factor structure that causes the 17 measurement variables (attitudinal questions) to covary. Next, a mixed multinomial logit (MMNL) is formulated and specified to study the impact of sociodemographic variables, random attributes, and factor scores as obtained from the latent factors on the propensity of choosing an alternative mode in the absence of app-based taxi by an individual. The theory behind both these statistical frameworks is presented in the following subsections.

3.1 *Exploratory Factor Analysis (EFA)*

EFA was performed on the 17 measurement items asked in the survey questionnaire. First, the validity of the EFA process on the data is checked from the Kaiser–Meyer–Olkin (KMO) value which should be 0.7 or higher [22]. Only then, the factor extraction method and the rotation technique are chosen. Principal component analysis method, along with promax (Oblique) rotation technique, was used for the present research work to derive the minimum number of factors [23]. After extraction, it was decided how many latent factors to retain as over-extraction or under-extraction can have deleterious effects on the results. Thus, factors with an eigenvalue greater than one and item loading greater than 0.4 with no cross-loadings were set as the cutoff criteria [24]. Finally, the factor scores are computed from the obtained factors using Bartlett’s approach that are used as explanatory variables in the MMNL model specification. The advantage of this approach over other refined methods of extracting factor scores is that the Bartlett factor scores only correlate with their own factor in an orthogonal solution. The procedure produces unbiased estimates of the true factor scores [25].

3.2 *Mixed Multinomial Logit*

This section presents the theory behind model formulation and specification. The model formulation follows the traditional mixed logit model, which is a highly flexible random utility model. Here, for ease of notation, the model will be referred to as mixed multinomial logit (MMNL). The MMNL model offers significant advantages

over the multinomial logit (MNL) model by allowing for flexibility that enables to specify the random taste variations across individuals [26]. Such specifications address the restrictive property of independence of irrelevant alternatives (IIA) of the MNL model, thus acknowledging differences in individual sensitivities across attributes. For the present study, attributes that have random coefficients are satisfaction, availability, health risk, safety, cost, reliability, and comfort. It is believed that these attributes vary across individuals over their choice of choosing a mode in the absence of app-based taxi—active mode, personal car, public bus, metro, and auto-rickshaw. Then, the choice probabilities of the MMNL model is the integral of the MNL's choice probability multiplied by the density function of the random parameters, as shown in Eq. (1).

$$P_{ni} = \int \frac{e^{V(\beta, X_{ni})}}{\sum_j e^{V(\beta, X_{nj})}} f(\beta/\theta) d\beta \quad (1)$$

where X_{ni} is the set of explanatory variables for alternative i , faced by the decision-maker n . The vector of random taste coefficients is represented by β , and the observed utility of alternative i is given by the function (β, X_{ni}) [27]. Besides these, the density function of the random taste coefficient vector β is represented as (β/θ) , where θ vector contains the list of all those parameters that define an assumed distribution, i.e., if the random parameters are assumed normal distributed, then estimating the mean and variance of the distribution. The maximum simulated likelihood estimation approach allows the estimation of the distributions for each of the random parameters, thus providing a rich array of preference information.

4 Data Collection

4.1 Study Area

The primary data collection was carried out in the city of New Delhi during February–March, 2018. The city has a population density of around 6000 persons per sq. km, and it accounts for more than 7% of all motorized vehicles in India [28]. Furthermore, the struggle of the capital city with ambient air quality, transport crisis, high fatality rate due to excessive penetration of personal motorized modes, etc., has been well documented [29, 30]. The addition of app-based taxis has further added to the capacity restriction of roads, congested traffic flows, and thus further worsening vehicular pollution. Another area of concern is the daily ridership on the metro and bus systems, where projections indicate a less bleak outlook [8, 31].

4.2 Survey Design

The final survey instrument was designed based on the experiences of a pilot survey. As high non-responses were experienced toward open-ended questions, mostly related to the individual attributes, close-ended questions with multiple suitable options were considered in the questionnaire [32]. The final version of the questionnaire consisted of three sections. Section 1 gathered information about the sociodemographic details of individuals. Section 2 collected their trip details and mode preferences if app-based taxis were not available for the last trip of the user, and Section 3 focused on the attributes of a mode that the respondents seek while commuting, and their perception toward other modes was evaluated on a three-point Likert scale. The questions in part 3 of the survey were mostly taken from past studies [8, 33]. The survey followed a face-to-face intercept interview approach, conducted in the month of February–March, 2018. A random sampling technique was followed, and the information related to the recently completed trip on the app-based taxi was captured from the respondents. It was ensured that the trip origins and destinations represented the entirety of the Delhi National Capital Region. A total of 295 samples were collected. After screening out the incomplete questionnaires, responses from 279 survey forms were analyzed. Using the widely accepted Cochran's formula of sample size estimation [34], assuming a level of precision, $p = 0.5$, level of confidence, $z = 1.645$ (for 90% CI), and degree of variability, $e = 0.05$, the estimated sample size was found to be 272, indicating the present study's sample size to be significant at 90% level.

4.3 Sociodemographic Characteristics

A summary of the sociodemographic characteristics of the sample is presented in Table 1. It is observed that the mean age of the respondents using app-based taxi services is nearly 30 years, indicating that relatively younger individuals have a higher preference toward ride-hailing services. In case of gender, the share of females using app-based taxi services is slightly higher than males. A majority of individuals are graduates. Employment background is captured using three levels, namely: a regular job, self-employed, and students. Here, regular jobs referred to the full-time government or private jobs, while self-employed referred to people in business, farmers, and homemakers. It can be seen that about 58.42% of app-based taxi users own a driving license. Furthermore, more than 50% of users who used these ride-hailing services in New Delhi belonged to the income group whose individual income is less than INR 300,000 per annum.

In case of personal car and two-wheeler ownership levels, the shares of individuals owning at least one car or one two-wheeler are found to be 25.81 and 32.62%, respectively. This sample share is nearly close to the car and two-wheeler shares reported by the Ministry of Road Transport and Highways (MoRTH), indicating

Table 1 Sample characteristics

Characteristics	Share in %	Characteristics	Share in %
Age (in years)	28.65 (8.74)*	Two-wheeler ownership	
Gender		No TW [#]	67.38
Male	49.82	At least 1 TW	32.62
Female [#]	50.18	Bi-cycle ownership	
Education		No bi-cycle [#]	86.02
Up to intermediate	17.56	At least 1 bi-cycle	13.98
Graduate	60.93	No. of smartphones	
Post-graduate [#]	21.51	One [#]	78.31
Employment		Two or more	21.69
Regular job	42.29	Trip purpose	
Self-employed [#]	14.34	Work	23.30
Students	43.01	Airport	11.83
Owned a driving license		School/college	10.04
Yes	58.42	Recreation	46.59
No [#]	41.58	Others [#]	8.23
Annual income (in INR)		Type of app-based taxi used	
Less than 300,000	53.05	Uber	53.52
300,000–600,000	21.86	Ola	43.87
600,000–900,000	14.34	Others	2.61
More than 900,000 [#]	10.75	Trip distance (in km)	14.71 (9.81)*
Car ownership		Wait time (in min)	7.02 (4.47)*
No car [#]	74.19	Travel time (in min)	40.95 (21.75)*
At least 1 car	25.81	No of passengers	2.39 (1.19)*

* Represents the mean (std dev.) for that variable. Rest all are in %

[#] Represents the explanatory variables taken as reference levels in model estimation

16% of people owning cars and 30% owning two-wheelers in the Delhi NCR region [35]. However, bicycle ownership among the app-based users is relatively low as compared to cars and two-wheelers. About 80% of individuals who participated in the survey had at least one smartphone.

4.4 Travel Characteristics

Trip Characteristics. The characteristics of the last trip on an app-based taxi are explored in this section. The findings in Table 1 indicate that close to half of the total trips are for recreational purposes, followed by work trips that hold one-fourth of

the total proportion of trips made using app-based taxis in New Delhi. This may be due to the hassle-free and last mile connectivity services app-based services provide. The travel distance, wait time, and total travel time were calculated from the person's last trip details, as shown in the mobile app. By taking the mean travel distance and travel time ratio, we obtain an average speed of around 22 km/h for the Delhi region, which is on the lower side of the global average speed for app-based taxis [36].

Further, the origin (O) and destination (D) locations of the trips taken by respondents using an app-based taxi are represented in Fig. 1. From the map shown in Fig. 1, it can be concluded that the majority of trips taken using app-based taxis were short-distance trips and mainly concentrated in the southeast and east of Delhi.

Trip Time Characteristics. The time of the day (in 24-h format) versus the frequency of trips undertaken was plotted and is represented in Fig. 2. Figure 2 shows two major peaks: one during the morning between 9:00 and 10:00 AM and the other around afternoon, between 1:00 and 2:00 PM. The first peak is quite intuitive and is often termed as the 'rush hours'. The second peak period may be due to the large share of

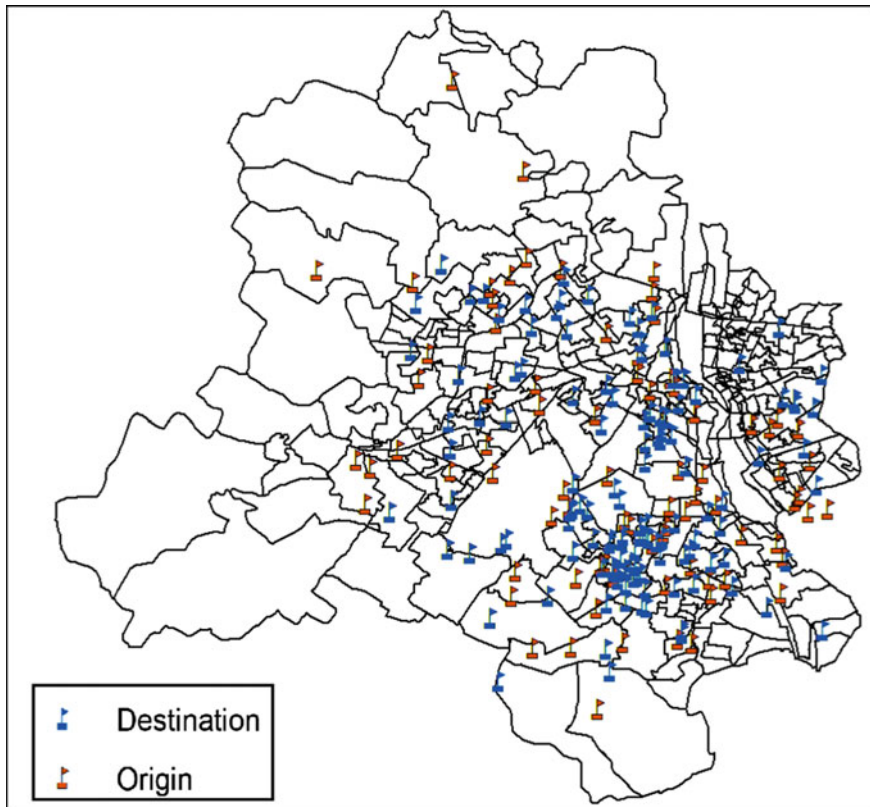


Fig. 1 Origin and destination locations of the trips made using an app-based taxi

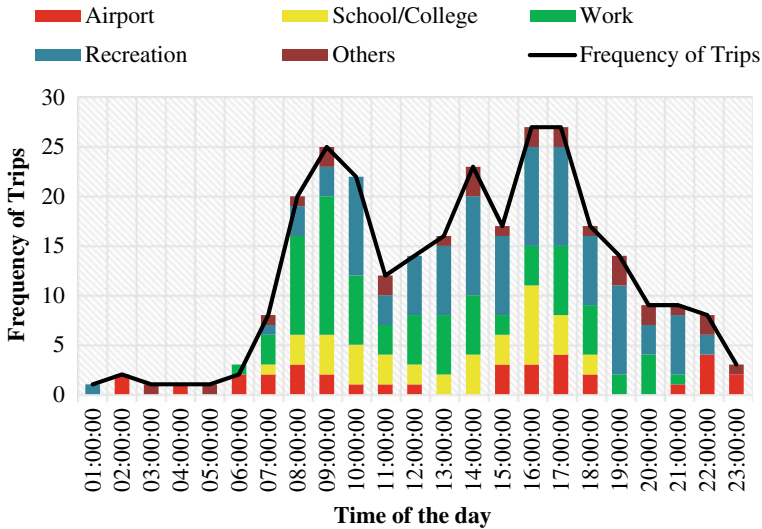


Fig. 2 Trip demand by time-of-day

recreation trips, which has no time constraints, unlike the work trips or educational trips (school/college). However, these findings are in contrast with the observations made by Habib KN, in his study of mode choice modeling of ride-hailing services in greater Toronto and Hamilton area of Canada, where the author found that app-based taxi trips are more likely to be made in the late afternoon, evening, and night than in the morning peak period and mid-day [37]. The flat line for the early morning hours maybe because most of the app-based services taxis do not provide service, or there is very little demand for travel.

Mode Choice Characteristics. To understand the preferences of app-based users toward other modes, the respondents were requested to reveal what mode they would have chosen had the app-based taxi were not available for their last trip. It was a closed-ended question with five alternatives: auto-rickshaw, public bus, metro, personal car, and active mode (walking/cycling). The sample share for auto-rickshaw, public bus, metro, personal car, and active mode is 36.92%, 10.04%, 35.48%, 10.04%, and 7.53%, respectively. The sample shares indicate that auto-rickshaw is the most preferred mode followed by metro. This may be attributed to the fact that both auto-rickshaw services and metro networks have extensive coverage in and around New Delhi. As expected, the active mode has the lowest share as with an increase in travel distance, the propensity to walk or cycle substantially decreases. The preference for public bus service or personal cars is similar; however, the overall share represents only 10% of the entire sample.

4.5 Attitudes and Perceptions of App-Based Taxi Users

Based on the past studies [8, 33, 38, 39], several mode-related attributes were included in the questionnaire to ascertain the riders' attitudes toward 'Other' modes (auto-rickshaw, metro, public bus, personal car, active mode) as compared to an app-based taxi. The paper also collected information on the perception behind choosing app-based taxis from respondents.

Attitude Toward Other Modes. Among the mode-related attributes (Table 2), barring health risks, all others are very commonly used in past studies. The health risk was included since New Delhi has been severely affected due to air pollution. The respondents were then asked to evaluate each of these attributes across all the modes with respect to app-based taxis. A three-scale rating pattern was followed with '-1' being worst, '0' as comparable, and '1' being better. The ratings of attributes for each mode in % are presented in Table 2. It can be concluded that metro and personal car are preferable and perceived better than app-based taxis, while auto-rickshaws, public bus, and active modes are rated to be worse than ride-hailing services across all attributes in general. Further, health risk has the maximum negative rating among all the attributes for an auto-rickshaw mode, which may be due to exposure to pollutants. A similar trend is also observed for safety attribute for auto-rickshaws, which is negatively maximum across all the modes. As expected, satisfaction and comfort are found to have the highest rating for a personal car, while high reliability is associated with the metro mode. Cost has a high negative rating between auto-rickshaw and personal car, and a high positive rating with public bus indicating buses are cheaper than personal cars or auto to commute in New Delhi as compared to app-based taxis.

Perception Toward App-Based Taxi. The questionnaire contained a list of 17 perception-based questions on why the respondents preferred the use of app-based taxi services. They were requested to respond on a three-point Likert scale ranging from 1 (Strongly disagree) to 3 (Strongly agree). These 17 items are presented in Table 3, along with their mean and standard deviation and % of responses. Among all measurement items, item 1 has the maximum number of 'strongly agree' responses, which is 92.47%, hence the highest mean score. A reverse pattern is observed in item 10, which has the lowest mean value signaling the maximum number of strongly disagree responses that are slightly above 48%. An exploratory factor analysis (EFA) was performed on these 17 measurement items, whose results are explained in detail in the next section.

5 Results and Discussion

This section highlights the findings of the modeling exercises undertaken in this study. Section 5.1 summarizes the results of the exploratory factor analysis. Section 5.2

Table 2 Attribute rating of ‘other modes’ as compared to app-based taxi ($n = 279$)

Mode attributes	Scale rating	Attribute share in % for ‘other’ modes as compared to app-based taxi				
		Auto-rickshaw	Metro	Public bus	Personal car	Active mode
Comfort	Worst (-1)	54.84	19.00	75.99	11.11	41.58
	Comparable (0)	24.37	25.09	13.98	12.90	12.90
	Better (1)	20.79	55.91	10.04	75.99	45.52
Reliability	Worst (-1)	48.75	4.66	44.44	6.09	66.67
	Comparable (0)	32.26	18.28	27.60	14.34	10.39
	Better (1)	19.00	77.06	27.96	79.57	22.94
Cost	Worst (-1)	32.97	14.34	8.24	34.41	82.44
	Comparable (0)	34.41	27.60	9.32	24.37	7.53
	Better (1)	32.62	58.06	82.44	41.22	10.04
Safety	Worst (-1)	58.06	6.81	42.65	6.81	46.24
	Comparable (0)	28.67	18.64	27.24	19.35	20.07
	Better (1)	13.26	74.55	30.11	73.84	33.69
Health risk	Worst (-1)	60.93	22.22	63.44	8.60	45.52
	Comparable (0)	27.96	19.00	24.73	24.73	18.64
	Better (1)	11.11	58.78	11.83	66.67	35.84
Availability	Worst (-1)	26.88	12.19	48.39	9.32	77.06
	Comparable (0)	30.47	21.15	26.52	12.90	8.96
	Better (1)	42.65	66.67	25.09	77.78	13.98
Satisfaction	Worst (-1)	44.80	3.58	41.94	6.45	52.33
	Comparable (0)	38.71	31.54	44.44	19.00	24.37
	Better (1)	16.49	64.87	13.62	74.55	23.30

presents the estimation results of the mixed multinomial logit model to understand the mode preferences of riders when an app-based taxi is not available.

Table 3 Perception-based Likert scale questions

Serial no	Perception-based measurement items	Item score mean (SD)	Share in %		
			Strongly agree	Neutral	Strongly disagree
Item 1	Comfort	2.91 (0.32)	92.47	6.45	1.08
Item 2	Availability in large numbers	2.63 (0.55)	66.31	30.11	3.58
Item 3	Less pollution exposure	2.37 (0.73)	52.33	32.62	15.05
Item 4	On time at destination	2.54 (0.59)	59.14	36.20	4.66
Item 5	No driving needed	2.76 (0.47)	77.78	20.43	1.79
Item 6	No bicycle infrastructure	2.22 (0.79)	44.09	33.69	22.22
Item 7	Ease of payment	2.74 (0.53)	78.14	17.56	4.30
Item 8	Short waiting time	2.43 (0.66)	52.69	37.99	9.32
Item 9	Safety	2.62 (0.58)	66.67	28.32	5.02
Item 10	Cheaper than other mode	1.73 (0.79)	21.51	30.11	48.39
Item 11	Fastest way to go there	2.22 (0.72)	38.71	44.09	17.20
Item 12	Avoids drunken drive	2.38 (0.76)	54.48	28.67	16.85
Item 13	No parking access	2.56 (0.65)	64.16	27.24	8.60
Item 14	Reliable	2.65 (0.55)	68.46	27.96	3.58
Item 15	No public transport available	2.01 (0.79)	31.54	38.35	30.11
Item 16	Unreliable public transport	2.15 (0.75)	36.56	41.58	21.86
Item 17	No bargaining	2.69 (0.57)	74.19	20.43	5.38

5.1 Exploratory Factor Analysis (EFA) Results

EFA was performed on the 17 measurement items shown in Table 3. The structured pattern matrix of measurement items is reported in Table 4. The obtained results indicated 13 items out of the 17 loaded significantly on five factors. The five factors obtained are accounted for a cumulative variance of 57.40% of the data, which is within the acceptable limit of 50% or higher [23]. The Cronbach's alpha for all the first-order factors was above the allowable limit of 0.5 [40]; hence, all the factors

Table 4 EFA results

Factors	Items	Item loadings	Eigen value	Cumulative variance	Cronbach's alpha
Factor 1 (reliable and safe)	Item 4	0.83	2.04	15.69	0.63
	Item 8	0.72			
	Item 9	0.61			
	Item 14	0.49			
Factor 2 (perceived benefits)	Item 2	0.78	1.71	28.81	0.51
	Item 5	0.67			
	Item 6	0.65			
Factor 3 (secure)	Item 12	0.75	1.29	38.72	0.56
	Item 13	0.65			
Factor 4 (poor public transit)	Item 15	0.69	1.26	48.37	0.55
	Item 16	0.65			
Factor 5 (level of service)	Item 10	0.62	1.17	57.40	0.53
	Item 11	0.52			

were considered for further analysis rather than being dropped. Finally, as discussed in Sect. 3.1, the factor scores were extracted from the five factors and were used as input in the logit model framework.

5.2 Mixed Multinomial Logit Model Results

Model Fit Measures and Model Comparison. The study initially estimated a multinomial logit model (MNL) to evaluate the mode choice preferences of app-based users if app-based taxis were unavailable. However, due to the assumption that the seven alternate specific attributes (shown in Table 2 and discussed in Sect. 4.5) varying randomly across the population; a pair of mixed logit models (with and without correlation) were introduced. The statistical measures, namely final log-likelihood (LL), number of estimated parameters (DF), adjusted *R* square, etc., are reported for each of these three models in Table 5. Further, the likelihood ratio test (LRT) was conducted to choose the best-fit model for the empirical data. From the LRT results, it is concluded that both versions of the random parameter models (with and without correlation) are better than the MNL model; however, it was found that there is no significant difference in the mixed logit uncorrelated model (MMNL) and the random parameter correlated model (MCMNL). Hence, the mixed multinomial logit model without any correlation between the random parameters was considered for the interpretation of significant estimates in the next sub-section. The entire procedure was carried out in R software version 3.6.0 using the ‘mlogit’ package [41].

Table 5 Mixed multinomial model (MMNL) estimation results ($n = 279$)

Explanatory variables	Alternatives			
	Auto-rickshaw	Metro	Public bus	Personal car
<i>Intercept</i>	7.27***	7.49***	5.89*	6.42**
<i>Age</i>	–	–0.09**	–	–0.14***
<i>Gender (ref female)</i>				
Male	1.49*	–	2.15**	–1.56*
<i>Annual income (ref more than 900,000)</i>				
Less than 300,000	–	–2.66***	3.66*	–
INR 300,000–600,000	–	–	–2.38**	–
INR 600,000–900,000	–	–	–2.64**	–
<i>Trip purpose (ref others)</i>				
School/college	–1.97*	–	–	–
Recreational	–	–0.93*	–	–
<i>Car ownership (ref no car)</i>				
At least one car	–	–	2.20*	1.56**
<i>Trip distance</i>	–0.08**	–	–	–
<i>Latent factors</i>				
Factor 1—reliable and safe	0.51*	–	0.71*	1.15***
Factor 5—level of service	–	0.44**	–	1.07***
Model fit parameters	Multinomial model		Mixed multinomial model	
Final log-likelihood (LL)	–321.09		–300.46	
Estimated parameters (DF)	27		31	
Adjusted <i>R</i> -square	0.177		0.183	

Note *, ** and *** represents significant at 90, 95 and 99% confidence level, respectively

Interpretation of Explanatory Variables. The list of explanatory variables summarized in Table 1 was given as input during the estimation of the MMNL model. Only, the estimated coefficients that were found to be statistically significant at 90% CI or higher are reported in Table 5. Here, active mode is taken as the reference category among the alternatives.

Table 5 indicates that the intercepts for all modes are positive and significant. However, as such, they do not have any behavioral interpretation. Age is found to have a negative impact on the use of the metro and personal cars. This indicates that individuals are less likely to prefer metro or personal cars with an increase in age in the absence of an app-based taxi. Regarding gender, it is observed that males have a higher preference for auto-rickshaws and public buses as compared to females. On the contrary, males are less likely to use a personal car if the app-based taxi service is not available. The effect of annual income levels of individuals on choosing any one of the five alternative modes is studied by including dummy variables for less than

or equal to 300,000; 300,001–600,000; 600,001–900,000 levels with above 900,000 serving as the reference level. It is noticed that low-income groups (less than or equal to 300,000 INR) have a higher probability of using public buses than availing metro service. However, the same cannot be said about the middle (300,001–600,000 INR), and higher-income groups (600,001–900,000) as the income coefficient was found to be negatively correlated with public bus use. This can be explained from the general observation that individuals of low-income households find it cheaper to commute in a public bus as compared to using app-based taxis due to income constraints. In contrast, middle and high-income individuals may be able to afford such services. College-goers are found to have lower preferences toward auto-rickshaws in the absence of an app-based taxi. In addition, individuals who undertake recreational trips on app-based taxis are less likely to use metro services. Furthermore, individuals of families with at least one car exhibit a higher likelihood of taking a ride in a personal car. However, the positive impact of car ownership levels on public bus is counter-intuitive and needs to be explored further. As expected, individuals traveling longer distances for activity participation are less likely to hire auto-rickshaws in the absence of an app-based taxi.

Finally, a set of five latent factor variables as obtained from the EFA process were given as input during the MMNL model estimation process. Only, two of them (factors 1 and 5) were found to have a notable influence on the mode choice alternatives. Examining the coefficients in Table 5, it can be concluded that individuals who look for reliability, and safety attributes in a mode, are most likely to choose personal car followed by public bus and auto-rickshaw. A similar trend is also observed for factor 5, which can be interpreted as individuals who perceive the level of service (LOS) as of utmost importance to them have a higher probability of choosing either a personal car or metro for their trip if app-based taxi services were unavailable.

Interpretation of Random Parameters. The MMNL model estimated seven random parameters across the five alternatives. The variables attached to the random parameters followed a three-scale rating pattern. As discussed previously (discrete and are bounded at the ends), they are assumed to be continuous and follow a standard normal distribution. The evidence behind this is based on the series of parametric tests conducted on ordinal and Likert scales by Geoff Norman, who concluded that parametric statistics could be used with ordinal/Likert data, with small sample sizes, unequal variances, and with non-normal distributions [42].

Among the seven attributes (Table 2), the estimates of three attributes, namely comfort, health risk, and availability, were found to be insignificant at 90% CI and hence dropped from the final model estimation. Estimated means and standard deviations (SD) provide information on the population share of each significant random attribute, which is presented in Table 6. From Table 6, it can be seen that the cost attribute obtains an estimated mean of 0.108 and SD of 0.398, such that about 61% of the distribution is above zero and 39% below it. This implies that about 61% of the total share of app-based users find the ‘cost’ attribute of ‘other’ modes to be more attractive and efficient than an app-based taxi. A similar interpretation can also be given for the ‘reliability’ attribute. Further, looking at the shares of ‘safety’, it

Table 6 Measures of random parameters

Attributes	Mean	SD	Share in %
Cost	0.11	0.40	60.69
Reliability	0.18	0.29	73.36
Safety	-0.09	0.23	65.23
Satisfaction	-0.19	0.69	61.09

can be said that about 65% of the population that uses app-based taxis is estimated to dislike the safety services available for ‘other’ modes with respect to app-based taxi. Similarly, around 61% of respondents is found to nurture a distaste with the ‘satisfaction’ they get while traveling in ‘other’ modes as compared to an app-based taxi.

6 Conclusion

The present study explores the user profile and travel patterns of app-based taxi riders in the city of New Delhi. The data were gathered through a primary survey. Along with sociodemographic details and trip characteristics, the respondents were asked to evaluate a set of seven attributes that compared ‘other’ modes with app-based taxi. In addition, the respondents were also requested to indicate their level of agreement/disagreement with a list of 17 perception-based questions to ascertain the reasons to choose ride-hailing services. An exploratory analysis of the attributes indicated that metro and personal cars are preferable and better-perceived modes than app-based taxis, while auto-rickshaws, public buses, and active modes are rated to be worse than the ride-hailing services, across all attributes in general. Moreover, an exploratory factor analysis (EFA) was performed on these 17 measurement items, and the iterative process yielded five latent factors, which, taken together, explained approximately 58% of the variance in the data. These factors provide meaningful insights into the understanding of preferences and attitudes of such users toward existing modes of travel.

To understand the preference of modes when an app-based taxi is unavailable, the present study used a mixed multinomial logit model. Five mode types, namely public bus, metro, auto-rickshaw, personal car, and active modes (commuting by walking or bicycling), were the dependent variables in the logit framework. The key findings of the model include—

- (i) with an increase in age, individuals are less likely to prefer metro or personal car in the absence of app-based taxi;
- (ii) males have a higher preference to use auto-rickshaws and public bus as compared to females;
- (iii) college-goers are found to have a lower affinity toward using auto-rickshaws for their commute in the absence of an app-based taxi;

- (iv) individuals who value reliability, safety, and punctuality in a mode are more likely to choose personal cars followed by public buses and auto-rickshaws.

The study findings provide vital inputs regarding the effect of sociodemographic features, perceptions, and mode attributes on the preference of alternative modes in a metropolitan city like Delhi. The study is the first of a kind in an Indian setting that offers plausible explanations from a planning and policy perspective. However, the study comes with certain limitations. MMNL model suffers from the choice of distribution to be used for random taste coefficients. Moreover, rather than providing a set of qualitative attributes for mode, stated preference choices could have been provided. A comparison between the mixed logit and latent class choice model for this set of data can be a scope of future research.

Acknowledgements The authors would like to acknowledge the efforts of Kautilya Mishra in assisting us in both data collection and data entry. The authors also acknowledge the opportunity to submit the research work at the 5th Conference of the Transportation Research Group of India held at Bhopal (India) from December 18–21, 2019, which forms the basis of this article.

References

1. Benkler Y (2002) Coase's Penguin, or, Linux and "The nature of the firm." *Yale Law J* 112:369–446
2. Shaheen S, Cohen A, Zohdy I (2016) Shared mobility: current practices and guiding principles
3. Rayle L, Shaheen SA, Chan N, Dai D, Cervero R (2014) App-based, on-demand ride services: comparing taxi and ridesourcing trips and user characteristics in San Francisco. *Univ Calif Transp Cent* 94720:1–20. <https://doi.org/10.1007/s13398-014-0173-7.2>
4. Clewlow RR, Mishra GS (2017) Disruptive transportation: the adoption, utilization, and impacts of ride-hailing in the United States. http://usa.streetsblog.org/wp-content/uploads/sites/5/2017/10/2017_UCD-ITS-RR-17-07.pdf
5. Muralidhar SH (2016) How Ola disrupted taxi services in India? *Rev Manag* 6:5–17
6. Surie A, Koduganti J (2016) The emerging nature of work in platform economy companies in Bengaluru, India: the case of Uber and Ola cab drivers. *E J Int Comp Labour Stud* 5:36. Issn 2280-4056
7. NUTP: National Urban Transport Policy (2014) *Minist Urban Dev Gov India* 2:1–39
8. Suman HK, Bolia NB, Tiwari G (2016) Analysis of the factors influencing the use of public buses in Delhi. *J Urban Plan Dev* 142:04016003. [https://doi.org/10.1061/\(ASCE\)up.1943-5444.0000316](https://doi.org/10.1061/(ASCE)up.1943-5444.0000316)
9. Alam MA, Ahmed F (2013) Urban transport systems and congestion: a case study of Indian cities. *Transp Commun Bull Asia Pac* 33–43
10. Davis N, Joseph HR, Raina G, Jagannathan K (2017) Congestion costs incurred on Indian roads: a case study for New Delhi
11. Rayle L, Dai D, Chan N, Cervero R, Shaheen S (2017) Just a better taxi? A survey-based comparison of taxis, transit, and ridesourcing services in San Francisco. *Transp Policy* 45:168–178. <https://doi.org/10.1016/j.tranpol.2015.10.004>
12. Light SE (2017) Precautionary federalism and the sharing economy
13. Edelman BG, Geradin D (2015) Efficiencies and regulatory shortcuts: how should we regulate companies like Airbnb and Uber? <https://doi.org/10.2139/ssrn.2658603>
14. Rogers B (2015) The social costs of Uber. <https://doi.org/10.2139/ssrn.2608017>

15. Smart R, Rowe B, Hawken A et al (2015) Faster and cheaper: how ride-sourcing fills a gap in low-income Los Angeles neighborhoods. BOTEC Analysis Corp
16. Contreras SD, Paz A (2018) The effects of ride-hailing companies on the taxicab industry in Las Vegas, Nevada. *Transp Res Part A Policy Pract* 115:63–70. <https://doi.org/10.1016/j.tra.2017.11.008>
17. Anderson DN (2014) “Not just a taxi”? For-profit ridesharing, driver strategies, and VMT. *Transportation (Amst)* 41:1099–1117. <https://doi.org/10.1007/s11116-014-9531-8>
18. Nie Y (Marco) (2017) How can the taxi industry survive the tide of ridesourcing? Evidence from Shenzhen, China. *Transp Res Part C Emerg Technol* 79:242–256. <https://doi.org/10.1016/j.trc.2017.03.017>
19. Jin ST, Kong H, Wu R, Sui DZ (2018) Ridesourcing, the sharing economy, and the future of cities. *Cities* 76:96–104. <https://doi.org/10.1016/j.cities.2018.01.012>
20. Davidson A, Peters J, Brakewood C (2017) Interactive travel modes: Uber, transit and mobility in New York City
21. Henao A (2017) Impacts of ridesourcing—LYFT and UBER—on transportation including VMT, mode replacement, parking, and travel behavior. http://digital.auraria.edu/content/AA/00/00/60/55/00001/Henao_ucdenver_0765D_10823.pdf
22. Cerny CA, Kaiser HF (1977) A study of a measure of sampling adequacy for factor-analytic correlation matrices. *Multivar Behav Res* 12:43–47. https://doi.org/10.1207/s15327906mbr1201_3
23. Hair JF, Black WC, Babin BJ, Anderson RE (2013) *Multivariate data analysis*, vol 7. Pearson Prentice Hall, Upper Saddle River, NJ
24. Tabachnick BG, Fidell LS (2007) *Multivariate analysis of variance and covariance*. Using *Multivar Stat* 3:402–407
25. Distefano C, Zhu M, Mîndrilă D (2009) Understanding and using factor scores: considerations for the applied researcher—practical assessment, research & evaluation. *Pract Assess Res Eval* 14:1–11
26. McFadden D, Train K (2000) Mixed MNL models for discrete response. *J Appl Econom* 15:447–470. [https://doi.org/10.1002/1099-1255\(200009/10\)15:5%3c447::AID-JAE570%3e3.0.CO;2-1](https://doi.org/10.1002/1099-1255(200009/10)15:5%3c447::AID-JAE570%3e3.0.CO;2-1)
27. Train KE (2009) *Discrete choice methods with simulation*, second edition. Cambridge University Press. <https://doi.org/10.1017/CBO9780511753930>
28. National Transport Development Policy Committee on Railways (2013)
29. Thynell M, Mohan D, Tiwari G (2010) Sustainable transport and the modernisation of urban transport in Delhi and Stockholm. *Cities* 27:421–429. <https://doi.org/10.1016/J.CITIES.2010.04.002>
30. Pucher J, Peng ZR, Mittal N, Zhu Y, Korattyswaroopam N (2007) Urban transport trends and policies in China and India: impacts of rapid economic growth. <https://doi.org/10.1080/01441640601089988>
31. Mohan D (2008) Mythologies, metro rail systems and future urban transport. <https://doi.org/10.2307/40277079>
32. Stopher PR (2012) *Collecting, managing, and assessing data using sample surveys*. Cambridge University Press
33. Tarabay R, Abou-Zeid M (2019) Modeling the choice to switch from traditional modes to ridesourcing services for social/recreational trips in Lebanon. *Transportation (Amst)* 1–31. <https://doi.org/10.1007/s11116-019-09973-x>
34. Cochran WG (1977) *Sampling techniques*. Wiley. <https://doi.org/10.1080/00401706.1978.10489623>
35. Motor Vehicles—Statistical Year Book India 2016|Ministry of Statistics and Program Implementation|Government of India. <http://www.mospi.gov.in/statistical-year-book-india/2016/189> (2017)
36. Improving Road Safety in Cincinnati’s Northside neighborhood. <https://medium.com/uber-movement/oki-8b77c95bb368>. Last accessed 04 June 2019

37. Nurul Habib K (2019) Mode choice modelling for hailable rides: an investigation of the competition of Uber with other modes by using an integrated non-compensatory choice model with probabilistic choice set formation. In: 98th annual meeting of TRB, Washington DC, January 13–17 (2019)
38. Cheng X, Fu S, de Vreede GJ (2018) A mixed method investigation of sharing economy driven car-hailing services: online and offline perspectives. *Int J Inf Manag* 41:57–64. <https://doi.org/10.1016/j.ijinfomgt.2018.03.005>
39. Hawlitschek F, Teubner T, Gimpel H (2016) Understanding the sharing economy—drivers and impediments for participation in peer-to-peer rental. In: Proceedings of the annual Hawaii international conference on system sciences. IEEE, pp 4782–4791. <https://doi.org/10.1109/HICSS.2016.593>
40. Lance CE, Butts MM, Michels LC (2006) The sources of four commonly reported cutoff criteria. *Organ Res Methods* 9:202–220. <https://doi.org/10.1177/1094428105284919>
41. Croissant Y (2006) mlogit: multinomial logit models. <https://cran.r-project.org/package=mlogit>. <https://CRAN.R-project.org/package=mlogit>
42. Norman G (2010) Likert scales, levels of measurement and the “laws” of statistics. *Adv Heal Sci Educ* 15:625–632. <https://doi.org/10.1007/s10459-010-9222-y>

Estimation of Trip Generation Rates for Different Landuses for an Indian City



Ashish Verma and Shubhayan Ukil

1 Introduction

Traffic impact analysis is done to estimate the impact of the site-generated traffic volumes on the public street system and identify the on-site and off-site improvements that might be needed as a result of the development. Traditionally, traffic impact assessment needs to be performed in the early stages of a site development as building location, on-site circulation, multi-modal access to the development, and parking space are all inter-related [1]. Preliminary traffic study would help identify the potential traffic problems and eliminate them. Ignoring the traffic issues generated from site development would restrict the financial success of the development, lead to economic loss, and also impact the environment, especially in contemporary times of global environmental crisis.

Cities in India have witnessed rampant growth in the previous decade. The urban population percentage grew from 28.6% in 2001 to 37.7% in 2011 [2]. India is projected to add 416 million dwellers to urban areas by 2050 [3]. Also, the cities are experiencing economic growth. According to a report by Oxford Economics [4], the top 10 fastest growing cities by Gross Domestic Product in the world by 2035 will be in India. This growth is physically manifested in the form of increasing employment centers and associated housing and retail development. The report by Knight Frank [5] shows that in the year 2018, there was a 13% increase in the millions of sq. ft. of office space development in India and a 12% increase in the transaction of

A. Verma (✉)

Transportation Systems Engineering, Department of Civil Engineering, Indian Institute of Science (IISc), Bengaluru, Karnataka 560012, India
e-mail: ashishv@iisc.ac.in

S. Ukil

Taubman College of Architecture and Urban Planning, University of Michigan, 2223C Art and Architecture Building, 2000 Bonisteel Blvd., Ann Arbor, MI 48109-2069, USA

office space sq. ft.. Also, the housing market saw an increase of 76% in the number of housing units launched in 2018 with an increase of 6% increase in the sale of housing units in the same year.

The increasing urban population and accompanied societal changes have led to a greater need for travel. This has created a burden on existing road infrastructure. In times of road infrastructure crisis, a new commercial or residential development in the wake of the growing economy can increase the burden on existing road infrastructure, leading to congestion with widespread ramifications, impacting economy, environment, and health. Hence, it is essential to understand the impact of a proposed development on surrounding public street system and take adequate measures to mitigate the negative impact.

2 Methods for Estimating Future Traffic

Traffic impact analysis of a proposed development can be done by forecasting the future traffic generated from proposed development. The future traffic in the study area is a summation of the background traffic, development traffic, and the generated additional off-site development traffic. It is essential to accurately project the future traffic as the accuracy of the traffic analysis is dependent upon the accuracy of the traffic projections [6].

The amount of traffic generated from a development is majorly influenced by the development's size and landuse types. The volume of new traffic produced by the development is impacted significantly by the type of landuse (e.g., residential, retail, industrial, office, etc.) as well as the time of day in which the new traffic will be added [6].

The methods for calculating forecasted trips at proposed developments are based on the following [7]:

- A graphical plot of trip ends and size of the study area
- A regression equation based on the above graphical plot, and
- Weighted trip generation rate (number of weighted trip ends per unit of study area).

The three methods are:

- **Graphic Plot:** This method displays a plot of trip ends versus area of each individual study. The area for a proposed development is plotted on the graph, and number of trip ends is estimated based on the existing data points. The reliability of the method is based on the number of data points to define a relationship between the two variables, especially in the area of the graph where the proposed development fits. If the number of data points is not sufficient, interpreting and interpolating between data points results are not accurate.
- **Equation:** In this method, a mathematical relation is defined between trip ends and the area of the study. Regression analysis is a tool to develop an equation,

which “best fits” through the data points and defines the trend line. The equation allows a direct calculation of forecasted trip ends based on the area of proposed development, reducing the inaccuracy in calculation based on interpolation of a plot of individual data points.

- **Weighted Average Rate:** This method forecasts trips by estimating a weighted average trip generation rate, i.e., number of trip ends per unit of area for a landuse type multiplied by the number of units of the area associated with the landuse type in the proposed development. The standard deviation gives a measure of the dispersion of the data points around the calculated average. The weighted average rate assumes a linear relationship between trip ends and the independent variable in the graph, with the straight line passing through the origin and having a slope equal to the rate.

Both, equation and weighted average rate are reliable methods to be used for forecasting traffic as compared to the scatter graph. Further, with good sample, size and their distribution within a range of typical values of the study area lead to a regression equation that describes the best fit line in the data points. Also, it is important to note that statistically there are confidence intervals associated with both the regression line and the rate line.

Performing survey for estimating trips generated to perform traffic impact analysis every time a new development is proposed which is financially burdensome. Hence, the trips generated are usually estimated using the trip rate analysis, which is a process of determining average trip production and trip attraction rates associated with the trip generators (landuse types) within a study area. The trip rates usually represent person trips in contrast to vehicle trips, per thousand square feet of each landuse. Typically for the retail, non-retail, and office landuse type, trip attraction rate is expressed as the number of trips attracted per employee [8–10].

Several countries across the world have developed standard trip generation rates by landuse type, time of the day, as well as the location of development within the urban area. In the USA, standard trip generation rates are developed by the Institute of Transportation Engineers, providing person-based trip rates for different categories of landuse type by time period and urban/rural location setting [11]. Trip generation rates for the United Kingdom and the Northern Ireland region can be calculated through the TRICS system, which includes trip rates for 110 landuse types. The trip rates can be calculated on a case to case basis or from a group of selected survey counts. The TRICS system is designed to take users through step by step stages of data filtering, beginning with the entire database for a whole development type until all compatibility requirements have been met, leading to a smaller, compatible dataset ready for trip rate calculation at the end by the users [12]. The trip generation rates for different landuse types by the time of day for the USA and the United Kingdom are given in Table 1.

For the Indian Scenario, some studies have tried to establish standard trip rates for specific landuse types, mostly retail. The study by Bali and Zala [13] established a regression model to predict the number of trips attracted to a Shopping Mall for Vadodara city. The trips are predicted based on available two-wheeler parking space

Table 1 Standard trip generation rates for different countries

Landuse	AM peak				PM peak			
	Entry		Exit		Entry		Exit	
	ITE (trips per 1000 sq. ft.)	TRICS (trips per 1000 sq. ft.)	ITE (trips per 1000 sq. ft.)	TRICS (trips per 1000 sq. ft.)	ITE (trips per 1000 sq. ft.)	TRICS (trips per 1000 sq. ft.)	ITE (trips per 1000 sq. ft.)	TRICS (trips per 1000 sq. ft.)
Office (SEZ)	1.52	0.51	0.19	0.13	0.21	0.07	1.27	0.47
Office (non-SEZ)	1.29	1.60	0.18	0.19	0.26	0.19	1.16	1.31
Retail—weekday	1.62	0.67	1.38	0.35	2.10	1.28	2.10	1.37
Residential	0.09	0.07	0.23	0.21	0.25	0.19	0.16	0.08
Theater	6.20	0.00	0.00	0.00	6.20	2.03	6.20	2.01

and floor area of the mall. Another study by Karuturi et al. [14] established trip rates for different typologies of commercial centers, during peak hour for weekdays and weekend. The typologies are based on physical features of the study area (sq. ft.), parking spaces, number of employees, number of stores, number of people attracting, etc. [14]. Despite efforts made toward defining trip rates for prominent landuse types, there are no established trip rates, which can be used for calculating traffic impact analysis efficiently and accurately. Understanding the vital importance of pre-construction traffic impact analysis, it is important to establish standard trip rates for Indian scenario.

3 Case Study—Bengaluru

Several Indian cities have experienced tremendous growth economically in the previous three decades post-economic liberalization of India in 1991 [15]. Bengaluru is one of the cities that has seen immense economic and population growth in the past two decades. The city along with other southern Indian cities like Chennai has attracted a significant amount of foreign and Indian investment since 1991, especially post its comprehensive State Industrial Policy, 1996, which was aimed to attract large-scale domestic and foreign investment through the provision of concessions and incentives. The city has risen to the status of IT hub in the country and is also known as the ‘Silicon Valley of India’ [16]. Bengaluru has branch offices for some of the biggest multinational technology companies and developmental centers. The city has also attracted foreign investment in automobiles and textile sectors [16].

The Special Economic Zone (SEZ) policy was enacted in 2000, which has the objective of enhancing foreign direct investment by providing them tax breaks to investors and having economic laws different from the usual economic laws in the country. After it, foreign direct investment increased tremendously in Bengaluru. The

city at present has maximum share of multi-tenanted SEZ office space, accounting to 39% [17]. The presence of large IT industry in Bengaluru makes it a lucrative place for new IT companies to open up and big multinational companies to invest. Therefore, Bengaluru is currently experiencing a boom in retail and residential development. Hence, it has been selected as the study area. Cities with similar developments like Hyderabad, Chennai, and Northern Capital Region can also use the trip rates for the purpose of traffic impact assessment.

4 Estimating Trip Generation Rate

The trip rates are estimated for main landuse types in Bengaluru that is currently being developed in the city by analyzing the number of trips attracted to/produced from the development, using cases comparable in area and function to the landuse in Bengaluru city.

The main landuse types considered are:

- Special Economic Zone (SEZ)
- Non-Special Economic Zone (SEZ)
- Retail
- Residential—Apartments.

It should be noted that the data used for obtaining trip generation rates are largely obtained from secondary sources.

4.1 *Special Economic Zone (SEZ) and Non-special Economic Zone (Non-SEZ)*

The comparable cases considered for SEZ landuse type are given below:

- Manyata Tech Park, Bengaluru (Area—8,300,000 sq. ft.).
- WIPRO SEZ, Electronic City, Bengaluru (Area—2,980,094 sq. ft.).
- Global Tech Park, Bengaluru (Area—1,000,000 sq. ft.).

The comparable cases considered for non-SEZ landuse type are given below:

- Manyata Tech Park, Bengaluru (Area—4,800,000 sq. ft.).
- World Trade Center (WTC), Bengaluru (Area—1,100,000 sq. ft.).
- Electronic City, Bengaluru (Area—1,127,168 sq. ft.).

The average number of daily trips per 1000 sq. ft. area for the comparable cases of SEZ and non-SEZ office is shown in Fig. 1.

The hourly distribution of office trips produced from and attracted to World Trade Center is provided in Fig. 2.

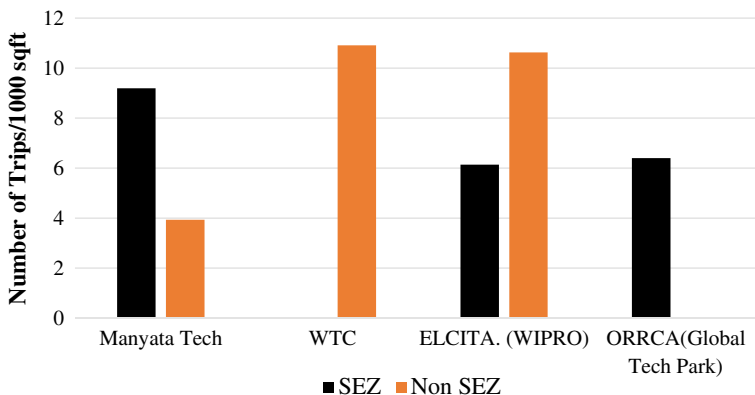


Fig. 1 Trip rates—comparable cases

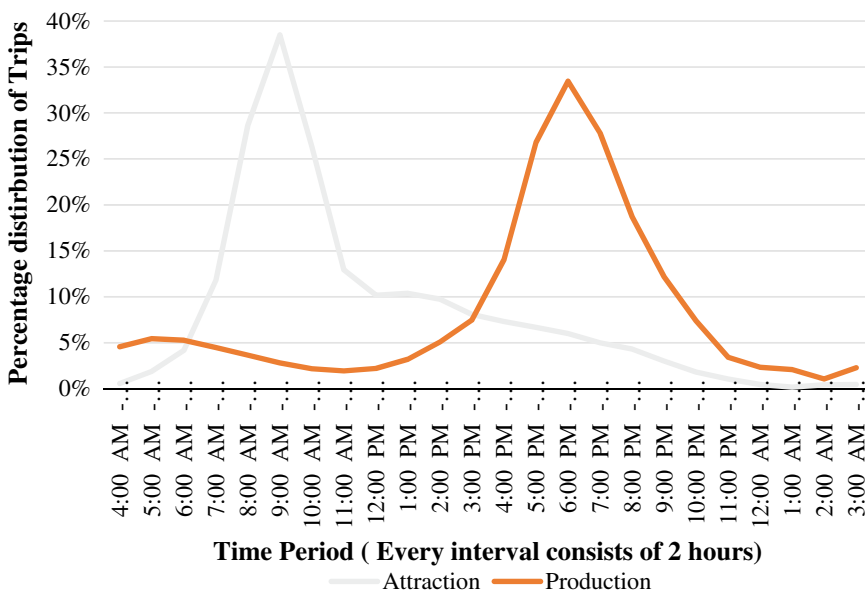


Fig. 2 Trip distribution by time of day for comparable case of World Trade Center

The hourly distribution clearly shows that the morning peak period is between 9 and 11 AM (38.5% of total trips in the day are attracted during this time) and the evening peak period is between 6 and 8 PM (33.5% of total trips in the day are produced during this time). The daily trip rate for SEZ office space is 9.2 trips/1000 sq. ft.. The average number of trips per 1000 sq. ft. based on the daily trip rate and hourly trip distribution is attracted to and produced from SEZ office during the morning peak period are 3.54 and 0.25, respectively. The average trip rate per 1000

sq. ft. for trips attracted to and produced from SEZ office during the evening peak period is 0.55 and 3.08, respectively.

For the non-SEZ office space, the daily trip rate is 6.4 trips/1000 sq. ft.. The average number of trips per 1000 sq. ft. based on the daily trip rate and hourly trip distribution the average trip rate per 1000 sq. ft. for trips attracted and produced during the morning peak period are 2.46 and 0.17, respectively. The average trip rate per 1000 sq. ft. for trips attracted to and produced from non-SEZ office during the evening peak period is 0.4 and 2.1, respectively.

4.2 Residential

For residential development, the average daily trip rates per household were calculated based on the data for the Comprehensive Traffic and Transportation Study (CTTS) [18]. The main trips for residential development are the work-related trips, which are mostly generated during the morning and produced during the evening peak period. As a result, the trips attracted during morning peak hour and generated during evening peak hour from/to residential landuse are negligible. For the residential space, 1.35 trips per household are produced during the AM peak period, and the trips per household attracted during the evening peak period are 2.25.

Also, the households with children experience conjoined trips, where parents leave for work along with their children to drop them to school. These conjoined trips are usually observed to occur during the pre-AM peak. However, in the evening peak period, the children come back home from school early, i.e., during the pre-PM peak. This is the reason for the trip rate during the AM peak period being lower than the PM peak period. The trips rate for trips produced during the pre-AM peak is 1.4 trips per household, and the trips attracted during the pre-PM peak is 0.5 trips per household.

4.3 Retail

For the retail trips, weekday trip rate is calculated based on primary and secondary data collected for Orion Mall, Bengaluru. The daily trip rate is used to calculate peak period trips, based on hourly trip distribution from another study for malls in Vadodara, Gujarat, as shown in Fig. 3 [13].

During AM peak, the trips are assumed to be attracted from 10 AM; hence, the AM peak for retail trips is only for 1 h. Also, it is assumed that the customers spend on an average more than an hour in the mall. Hence, there are no trips produced during AM peak.

The average trip rate for trips attracted during the morning peak period is 1.81 per 1000 sq. ft.. During the PM peak, the number of trips attracted to the retail spaces is 14.73 per 1000 sq. ft.. However, during PM peak period, it is assumed that the

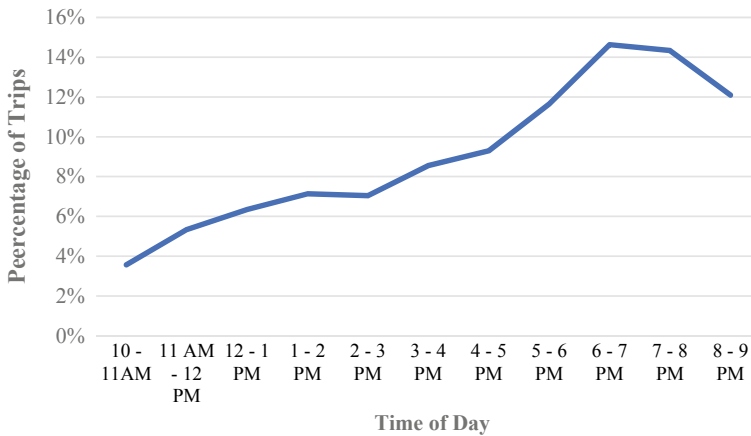


Fig. 3 Retail trips distribution by time of day for malls in Vadodara, Gujarat [13]

number of trips attracted is equal to the number of trips produced from the retail landuse, so as to avoid underestimation of trips generated from retail spaces. Further, during weekends, retail trips will be attracted and produced during the peak period, which is mostly between 12 and 4 PM. The average trip rate for trips attracted during the hours of peak period is 22.10 per 1000 sq. ft.. Similar to a weekday, it is assumed that the number of trips attracted is equal to the number of trips produced from the retail landuse so as to avoid underestimation of trips generated from retail spaces. Table 2 gives the estimated standard trip rates by landuse type and time of day for the case study: Bengaluru.

Traffic impact analysis using these estimated trip rates has several planning implications. It will help the developer’s to be pro-active so as to mitigate the negative impacts of generated traffic and eliminate hurdles in the path of getting approval for the development. It will also help the local authorities giving approval for developments to make more informed decision. As per the [19], dated September 14, 2006, as amended 2009, and in 2016 issued under Environment (Protection) Act, 1986, it

Table 2 Estimated trip rate for Indian scenario

Landuse	AM peak		PM peak	
	Entry	Exit	Entry	Exit
	Calculated (trips/1000 sq. ft.)	Calculated (trips/1000 sq. ft.)	Calculated (trips/1000 sq. ft.)	Calculated (trips/1000 sq. ft.)
Office (SEZ)	3.54	0.13	0.55	3.08
Office (non-SEZ)	2.46	0.19	0.38	2.14
Retail—weekday	1.81	0.35	14.74	14.74
Residential	0.00	0.21	2.25	0.00

is mandatory to obtain environmental clearance for specified categories of developmental projects. A part of environment impact assessment is to assess the impact of increased traffic generated as a result of the proposed constructions and its environmental ramifications. Hence, these trip rates can be used to accurately perform traffic impact assessment without being cost intensive.

5 Summary and Conclusion

The rampant development in the major urban centers in India definitely needs to be regulated so as to minimize its negative externalities. Several checks are done before a development is approved to ensure it has a minimum negative impact. Traffic impact assessment is one of the measures done to prevent any negative traffic and environmental impact. However, the lack of standard trip rates prevents an accurate assessment of traffic impact on the surrounding transport system of a proposed development. Through this study, we have tried to establish standard trip rates for the main landuse types in an urban setting for the Indian cities. Though the trip rates are calculated for the city of Bengaluru, they can be applied to other cities, provided that the city is comparable to Bengaluru in size and functioning. In present times, when traffic congestion is a big issue, accurate traffic impact assessment is necessary to tackle any potential traffic issues due to proposed development and reduce its impact on the environment.

- The study concludes that SEZ office space attracts more trips per 1000 sq. ft. of area as compared to non-SEZ office space.
- The retail trips on a typical weekday are more during the evening peak hour as compared to the morning hour.
- The residential trips generated during morning peak hour are lower than those attracted during evening peak hour as few of the trips generated during morning hour are conjoined trips, occurring during pre-AM peak hour.

6 Future Scope

The results of the study are severely restricted due to limited data availability. However, the accuracy of trip rates can be improved by considering several other case studies, not just in Bengaluru city, but across the country. This would help to establish national trip rates. Further, the list of landuse categories needs to be expanded for which standard trip rates are estimated so as to ease out the traffic impact assessment process. Also, each landuse category needs to be detailed out to include possible subcategories within main landuse types.

References

1. Ohio LTAP Center (2015) What is a traffic impact study, and when is one needed? The Ohio LTAP Center
2. Census of India (2019) Urban growth, 29 April 2019 (Online). Available: http://censusindia.gov.in/2011-prov-results/paper2/data_files/india/Rural_Urban_2011.pdf
3. United Nations (2018) 2018 revision of world urbanization prospects
4. Oxford Economics (2018) Global cities: which cities will be leading the global economy in 2035? Oxford Economics, Oxford, UK
5. Knight Frank (2019) India real estate—residential and office (July–December 2018). Knight Frank
6. Bureau of Traffic Operations (2017) Wisconsin department of transportation. Traffic impact analysis guidelines
7. ITE Technical Council Committee 6A-32 (1990) Guidelines for using trip generation rates or equations. ITE J
8. Papacostas CS, Prevedouros PD (2001) Transportation engineering and planning. Prentice-Hall of India Private Limited, New Delhi
9. ACT Government-Transport Canberra and City Services (2016) Guidelines for transport impact assessment
10. MHRD (n.d.) Details of trip generation (Online). Available: <https://nptel.ac.in/courses/105107067/module5/lecture2/lecture2.pdf>
11. Institute of Transportation Engineers (2019) Trip generation, 10th edition formats, 5 May 2019 (Online). Available: <https://www.ite.org/technical-resources/topics/trip-and-parking-generation/trip-generation-10th-edition-formats/>
12. TRICS (2019) Trip rate calculations, 6 May 2019 (Online). Available: http://www.trics.org/trip_rate_calc.aspx
13. Bali NP, Zala LP (2017) Trip attraction models for shopping malls: a case study. Int J Res Appl Sci Eng Technol (IJRASET) 5(IV)
14. Karuturi S, Yeluri VV, Subbarao SSV (2016) Trip attraction rates of commercial land use: a case study. Indian J Sci Technol 9(30)
15. Banga R, Das A (2012) Twenty years of India's liberalization experiences and lessons. United Nation Publication, Geneva
16. Shaw A (2007) Metropolitan restructuring in post-liberalized India: separating the global and the local. Cities 24(2):148–163
17. Bandyopadhyay N (2018) Karnataka slow on SEZ creation, Bengaluru
18. Karnataka Urban Infrastructure Development and Finance Corporation (2011) Comprehensive traffic & transportation study
19. Ministry of Environment and Forests (2006) Notification S.O. 1533(E). Gazette of India, no. 2, September 14 2006

Economic and Environmental Analysis of Adaptation Strategies to Mitigate Impact of Climate Change on Pavements



Megha Sharma, Sundeep Inti, and Vivek Tandon

1 Introduction

The projected climate of the earth is continuing to change over and beyond this century, as is the climate of Texas. The temperature for most of the region in Texas has increased between 1.0 and 1.5 °F in the past century [1]. The rainstorms and floods are becoming more severe and intense, and average rainfall is increasing in Texas. Climate models projected an increase in hurricane intensity and storm surge, sea-level rise, and heavy precipitation between long dry spells for Texas. As per the United States Geological Survey (USGS) in Texas, the severity and frequency of extreme events are expected to occur with rising temperatures and changing precipitation patterns [2]. Past trends have shown the impact of weather events on the highway infrastructure. The flooding of 2015 in Texas costs \$3 billion in damage to the road and other public infrastructure [3]. The infrastructure damage due to Hurricane Harvey, 2017 in Houston adds to \$5–\$10 billion [4]. These climate change intensities will increase in future years. All the fluctuations in weather will increase the damage and deterioration of the pavement structure, like, more cracks and potholes, buckling, and bleeding in the pavements. Thus, making highway infrastructure more vulnerable to the change in climate and weather patterns.

Climate affects the selection of pavement structure, including materials used in the individual layers such that pavement can withstand the environmental burden and provide intended service life [5]. A change in precipitation pattern influences

M. Sharma (✉) · V. Tandon
The University of Texas at El Paso, El Paso, TX 79902, USA

V. Tandon
e-mail: vivek@utep.edu

S. Inti
Purdue University Northwest, Westville, IN 46391, USA
e-mail: inti@pnw.edu

the slope stability of infrastructure, reduces the strength of subgrade, and damages the asphalt concrete layer due to stripping, among others. Similarly, extremely hot and cold days affect pavements with softening and rutting, buckling in concrete pavements, and bleeding of the asphalt surface. These unexpected levels of change in climate adversely jeopardize the service life of transportation infrastructure. Climate change vulnerability and risk assessment studies are required to assess the influence of climate change on transportation assets and develop a cost-optimized solution. A well-planned adaptation strategy provides a sound and robust base for decision-making when met with climate uncertainties. For instance, rerouting, mode change, and modified designs are some approaches that can alleviate the impact of climate change to a certain extent [6].

The selection of pavement materials, thickness, and construction practices rely mostly on historical weather data. Typically, pavement design and analysis are conducted using Pavement ME Design software, which uses a climate database from 1979 to 2003, and the updated data is for 2015 [7]. Therefore, the new design method should include the projected future climate to ensure the pavements can endure the likely changes [8].

Although the impact of changing climate on the transportation infrastructure has been studied, the influence of the adaptation strategies on economic and environmental impact has not been studied and focuses on in this study. Thus, the objectives of this paper are to: (a) identify models providing future climates compatible with pavement design software, (b) understand the consequences of the predicted change in climate stressors (such as precipitation and temperature) on pavement performance, (c) developing alternative pavement designs to mitigate the influence of climate stressors, and (d) economic and environmental impact of alternative pavement designs.

1.1 Methodology

To achieve objectives, a three-step approach was selected and is presented below:

- I. The first section presents information regarding climate models available that can be modified and used in pavement design software. In total, eleven different climate models were identified to be compatible with pavement design software. Since pavement design software has its weather data, a total of twelve climate models were evaluated. In addition, the variation of different climate parameters (precipitation, temperature, etc.) from historical weather data was also evaluated.
- II. In the second section, the performance of the selected roadway section for twenty years is estimated using the twelve climate models in terms of the International Roughness Index (IRI) and the historical weather data available in Pavement ME software.

III. In the end, alternative pavement designs to mitigate the impact of climate changes were proposed. Out of the twelve climate models, only one model that represents an average of twelve models was chosen for further analysis. The higher cost of constructing a resilient pavement structure was evaluated along with the long-term benefits derived from the enhanced service life of the pavement.

Climate Models. The climate model uses various emission scenarios proposed by the Intergovernmental Panel on Climate Change (IPCC) special report on emission scenarios (SRES) [9]. The climate data source used in this study is from the North American Regional Climate Change Assessment Program (NARCCAP) [10]. The future projections are for SRES A2 emission scenarios. The climate data are downscaled for the local resolution, as per the process proposed by Mearns et al. [10]. Dynamic downscaling is done by using high-resolution regional climate models (RCMs), which are driven by boundary conditions from general circulation models (GCMs) [11]. NARCCAP database includes six RCMs and four GCMs and having twelve climate model projections (a combination of RCMs and GCMs). The climate variables available from NARCCAP use projected coordinate systems (x_c , y_c) referred to as grid points, and data are in ‘NetCDF’ format. So, using the latitude and longitude of the station and grid cell maps for the RCM, the grid points for each RCM can be identified. The outputs from the climate models were three-hourly temperature, precipitation, humidity, and wind speed for each grid point location.

Pavement Section. The roadway (Fig. 1) of a frontage road of Fort Worth (TX) is considered in this study. The individual layer thickness, material properties, and traffic details are also included in Fig. 1. A traffic growth rate of 0.75% is considered for 20 years of performance analysis using AASHTO software for pavement design.

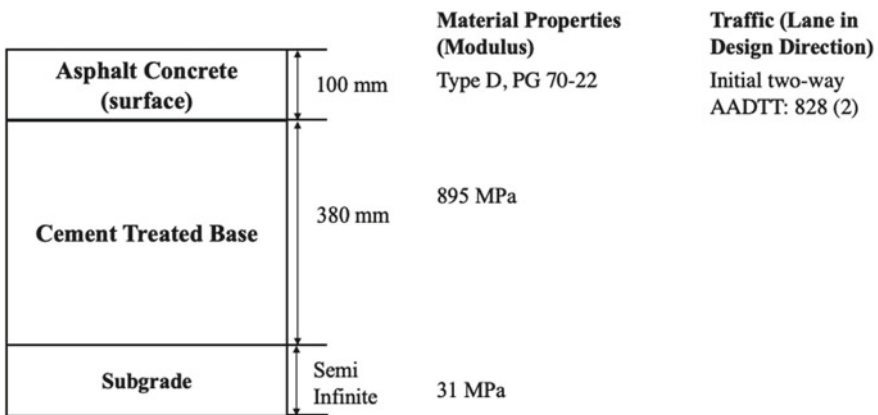


Fig. 1 IH30 (Tarrant County, Fort Worth) frontage road roadway section

2 Results and Discussion

2.1 Climate Data

The climate parameters required as input in the design software were obtained from twelve climate models. If the climate parameters were not available in the climate model databases, the historical weather data provided in the Pavement ME Design software were used.

Figure 2 shows the monthly mean temperature predicted for Fort Worth, Texas, corresponding to eleven climate prediction models and Pavement ME historical climate. It is evident from the plots that except for GCM-HADCM3 other climate models are predicting hotter summer and colder winter for Texas.

Figure 3 shows the summary of mean precipitation of climate prediction models; every model predicts either an increase or decrease in precipitation. Of all the climate models, GFDL and CCSM precipitation predictions are maximum and minimum among the selected climate models for Fort Worth, TX.

Similarly, Fig. 3 shows the annual mean wind speed and relative humidity. Future predicted mean annual wind speed is increased with the ECP2-GFDL climate model predicting lower wind speed. Wind speed climate predictions are maximum and minimum for CGCM3 and HadCM3 climate models among the selected models. Similarly, simulations for relative humidity are maximum for HadCM3 and GFDL climate models, while they are minimum for CCSM climate models.

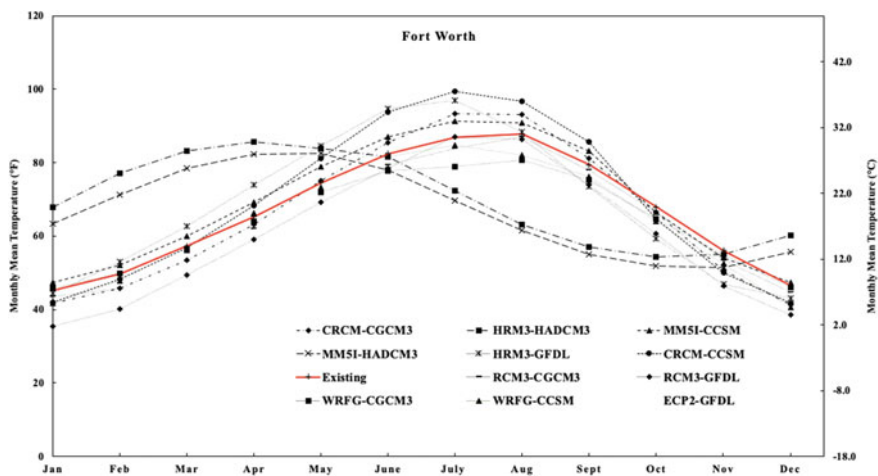


Fig. 2 Fort Worth monthly mean temperature predicted by all climate prediction models (2030–2050)

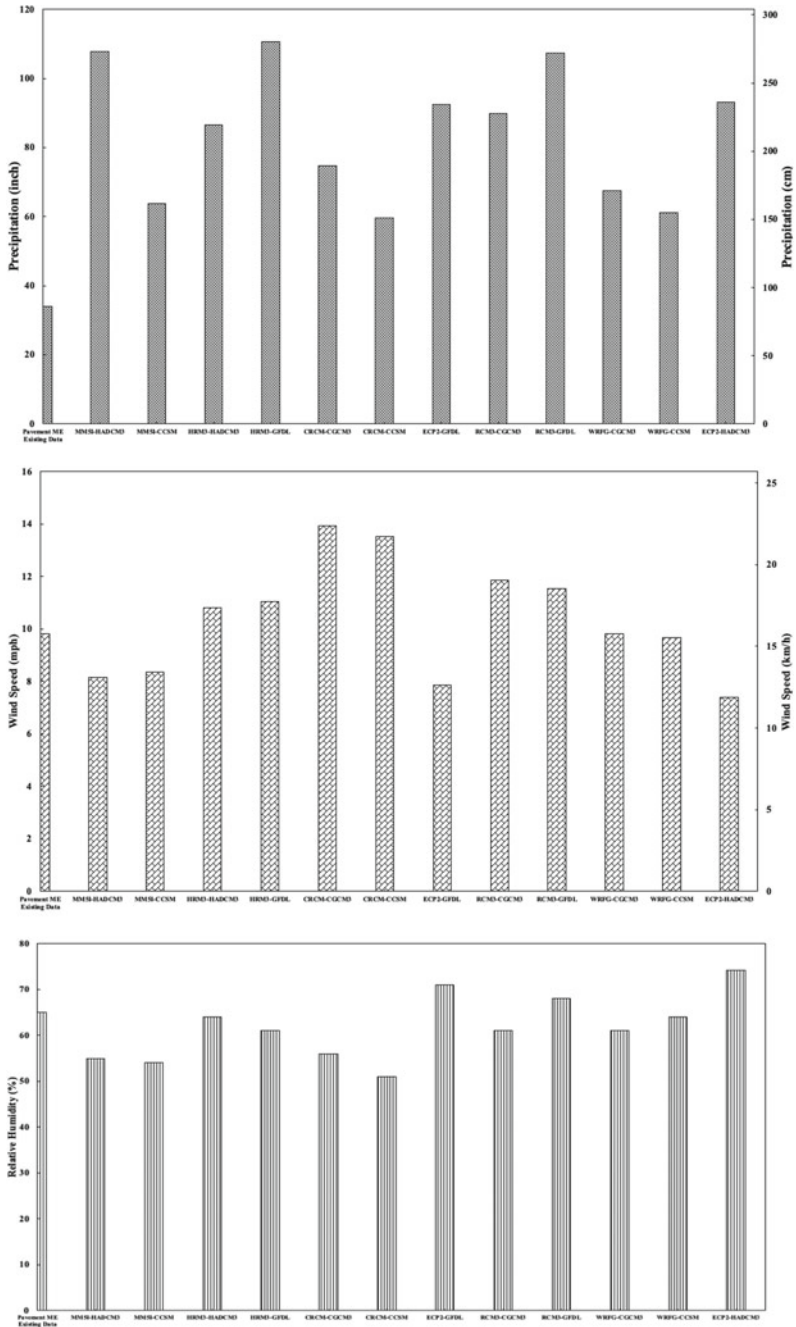


Fig. 3 Comparison of climate prediction models for Fort Worth area

2.2 Pavement Performance Analysis

The pavement performance is evaluated for all the selected cities using climate data from all climate models. The results obtained from the ME Design software are shown in Fig. 4. Based on the 1.6 m/km (100 in/mile) IRI criterion, the pavement maintenance schedule varies between 8.5 and 10 years, depending on the climate model selected. The historical data suggest maintenance after 9.5 years of service. On the other hand, maintenance will be required within 8.5 years if the roadway section experiences CRCM-CCSM (average of all climate models) predicted climate. Thus, earlier maintenance may be required.

Adaptation Methods. A mitigation approach is required to enhance resiliency by mitigating the influence of future climate. To counteract the influence of climate, it is proposed to enhance the performance by changing the AC layer thickness from 100 to 125.4 mm. The evaluation results are summarized in Fig. 5, where CC refers to climate prediction models CRCM-CCSM. The maintenance schedule varies between 8.3 and 9.4 years. Climate change (CC) will require maintenance 0.8 years earlier than the historical climate. However, the maintenance requirement will be delayed by 0.3 years if climate change is considered in the design phase.

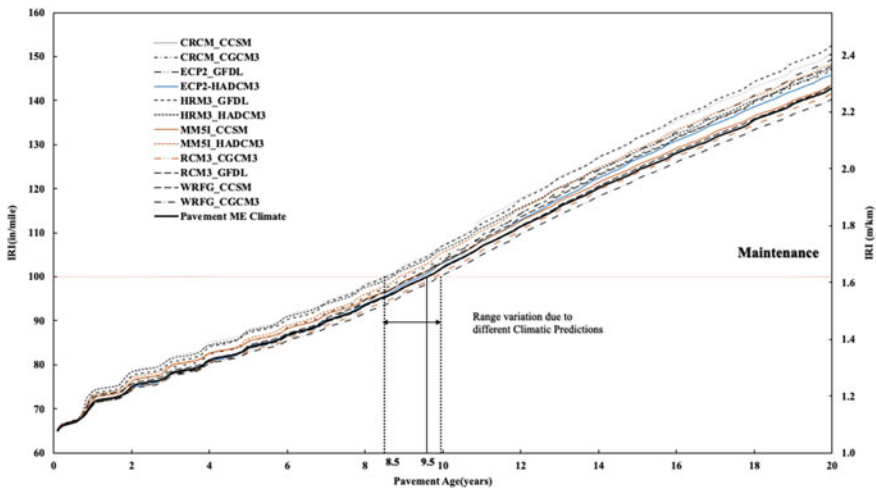


Fig. 4 Climate change influence on IRI (Fort Worth, Texas)

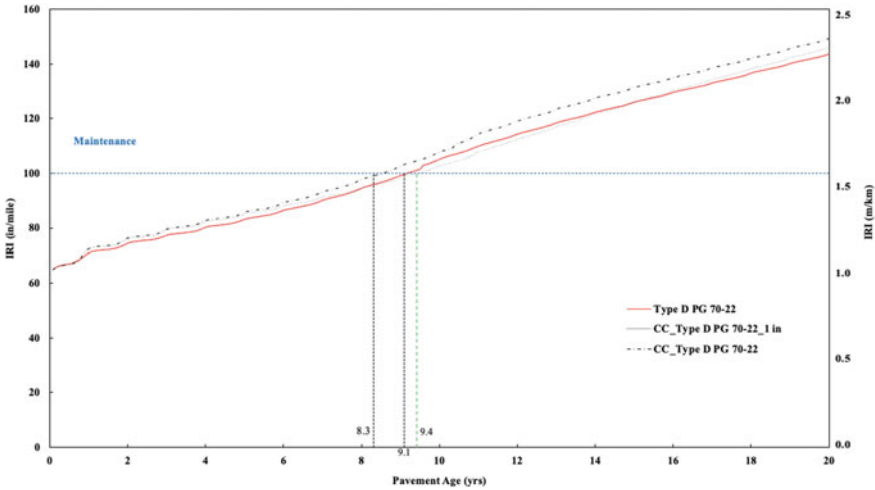


Fig. 5 Observed performance change with change in layer thickness

2.3 Economic and Environmental Analysis

In case a pavement deteriorates at a faster rate, there will be numerous consequences like frequent maintenance, traffic delays during maintenance, traffic congestion, increase in wear and tear of vehicles, and reduced life of tires.

This study suggests developing a resilient pavement structure by increasing the layer thickness; however, the increase in thickness increases construction costs. Thus, a transformation of pavement performance data into decision input is required for assessing the adaptation strategies and benefits derived from enhancing the resilience of pavement. This study employed both environmental and economic analysis for evaluating the derived benefits of the modified design. The analysis is demonstrated using a section for Fort Worth (Fig. 1). The following steps were followed to achieve the same:

- Pavement performance is analyzed using future climate data.
- If the performance deteriorates, an alternate design is proposed to provide similar levels of performance.
- Evaluate the derived benefits (both costs and emissions) by design modification.
- Also, assess the scenario where climate change did not occur.

The analysis performed for the section is shown in Fig. 6. Climate change induces an increased rate of deterioration requiring early maintenance for the pavement section (Design A). As a result, the reduction in pavement service life is close to a year (Fig. 6b). Therefore, an alternate design, Design B (Fig. 6c), was proposed and evaluated that considers an average change in climate (CRCM-CCSM). For this analysis, all other inputs remained constant as Design A except climate data. The main difference between the two designs is the surface layer thicknesses, which was increased

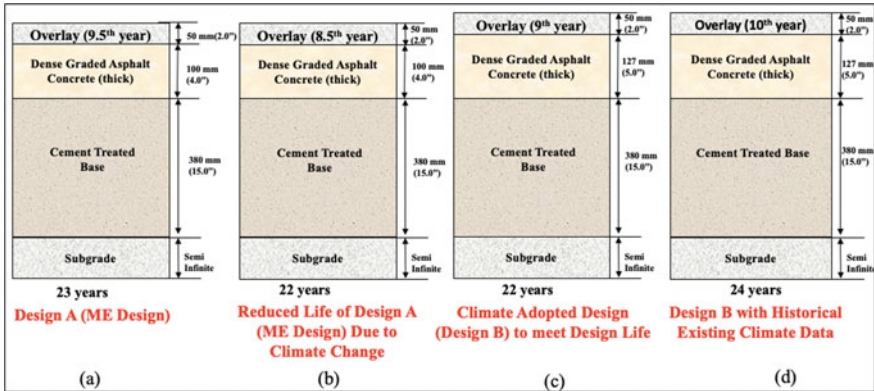


Fig. 6 Influence of design adaptation on cost-benefit analysis

by 25 mm. The increase in surface thickness enhances the pavement service life to levels similar if historical weather data are used. Thus, an increase in layer thickness is an alternative to minimize the loss in performance. However, the agency costs increase with additional surface layer thickness. Therefore, a cost-benefit analysis was performed to identify long-term benefits in terms of emissions.

In this study, the economic analysis was performed by using the life cycle cost analysis (LCCA) tool, while the environmental impact was evaluated using the life cycle assessment (LCA) tool to compare benefits derived from adaptation strategies. The LCA and LCCA evaluation process is included in Fig. 7 [12].

Cost Analysis. Primarily, there are two costs associated with highways: (1) the costs incurred by a highway agency during construction and maintenance phases (mainly referred to as agency costs), (2) the additional costs incurred by the user of highways in terms of additional repairs to their vehicles (commonly referred to as user costs). The agency costs for construction and maintenance of the designs shown in Fig. 6 were calculated and converted to net present worth (NPW).

The three user costs (fuel consumption, reduced life of tire, and additional vehicle maintenance) were estimated in this study. Table 1 shows the estimated costs for all

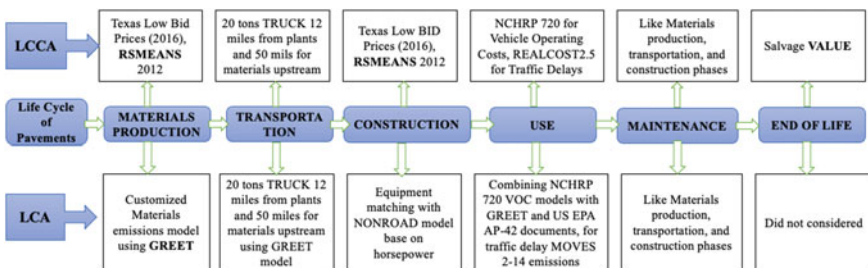


Fig. 7 Phases in life cycle of pavements, models used for LCCA and LCA

Table 1 Life cycle costs for agency and user

Design	Units	Agency costs	Fuel consumption costs	Tire wear costs	M&R costs	Total user costs
Design A	Costs in million dollars	\$9.52	\$569.98	\$46.35	\$141.75	\$758.08
Reduced life design A		\$9.71	\$571.09	\$46.40	\$142.55	\$760.04
Design B		\$9.79	\$570.52	\$46.37	\$141.94	\$758.83
Design B with existing climate		\$9.53	\$567.35	\$46.32	\$141.14	\$754.81

the alternatives included in Fig. 6. The current design and assessment are performed for an AADT of 22,990. In this assessment, a daily trip of 8 kilometer per day is assumed. However, the average kilometers traveled by a passenger car in the US are 18,089 kilometer per year [13], and the average kilometers traveled per day are around 56 km in a personal vehicle [14].

The first row of Table 1 shows the agency and user costs for Design A as \$9.52 and \$758.08 million, respectively. Due to climate change, the user and agency costs increase to \$9.71 and \$ 760.04 million, respectively. Therefore, the change in climate will require agencies and users to additionally incur \$190,000 and \$1,960,000, respectively. For Design B, the agency and user costs are \$9.79 and \$758.83 million, respectively. By comparing both the design, the agency spends \$270,000 (cost) more for constructing the road, and the user's cost is reduced by \$750,000 (benefit). Even if climate change didn't occur and adopted design (fourth row in Table 1) is considered, the agency is spending only \$10,000 more, but users will incur less (a benefit of \$3,270,000) because of the improved performance the climate change adopted design.

The impact of an increase in traffic on the benefits is illustrated by considering AADT from 20,000 to 100,000 (Fig. 8). Climate change adaptation has benefits even at lower traffic (20,000), but the magnitude of benefits is higher for heavier traffic (100,000).

Some earlier studies [15] considered user costs for passenger cars for 19,312 km traveled per year while estimated agency costs for 1.6 km length. This means each passenger car is going 33 trips per day on 1.6 km, which yields a very high user cost–benefit. Therefore, agency cost is estimated for 1.6 km of stretch, and variation of the benefit–cost ratio is demonstrated in Fig. 9 with changing the km traveled by the passenger cars per day for 1.6 km length. However, the AADT of 22,990 and 1.6 km traveled by trucks as 8 km per day for 1.6 km length were kept constant.

Estimation. The global warming potential (GWP) was estimated using the life cycle assessment (LCA) tool throughout the life of a highway was utilized. LCA was performed according to the guidance of the International Organization of Standardization (ISO) documents 14,040 (2006) [16] and 14,044 (2006) [17]. Table 2 shows

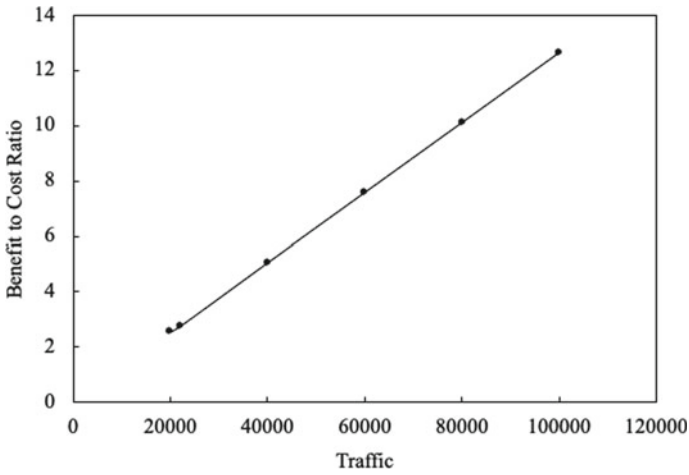


Fig. 8 Influence of increasing traffic on benefit to cost ratio

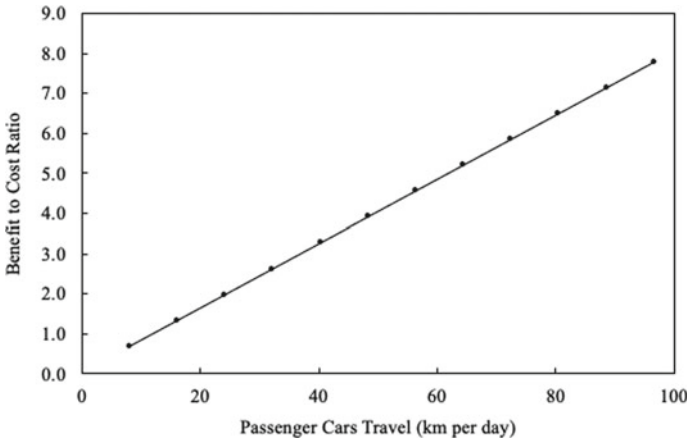


Fig. 9 Influence of kilometers traveled on benefit to cost ratio

Table 2 User emission

Design	Units	Fuel consumption emissions	Tire wear emissions	Emissions during use phase
Design A	Global warming potential (GWP) CO ₂ e in Mg	2,258,485	28,356	2,286,841
Reduced life design A		2,262,960	28,387	2,291,347
Design B		2,260,333	28,369	2,288,702
Design B with existing climate		2,255,091	28,333	2,283,424

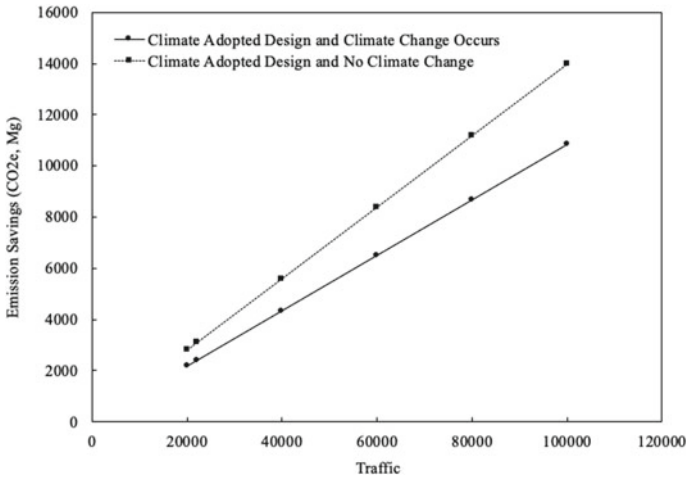


Fig. 10 Emission savings with increase in traffic

emissions generated by the user for all the designs of Fig. 6. The rows of Table 2 are organized for designs similar to the ones presented in Table 1.

The user emissions for Design A (Designed and performance predicted using historical climate data) are 2,286,641 Mg of CO₂e, while reduced performance predicted with CRCM-CCSM climate model generates 2,291,347 Mg of CO₂e. So, if climate change occurs and the design is not modified, the emissions will go up by 4506 Mg of CO₂e. On the other hand, the selection of Design B (with increased layer thickness) reduces the emissions by 3417 Mg of CO₂e even if climate change doesn't occur as predicted.

The impact of an increase in traffic on the benefits is illustrated (Fig. 10) by considering the AADT increase from 20,000 to 100,000. The projected increase in CO₂e is more than five times with an increase in AADT. Similarly, the benefit of passenger car traveled per day on emission savings is shown in Fig. 11. For analysis shown in Fig. 11, AADT of 22,990 was considered, and 8 km traveled by trucks is considered to be constant. In the event of passenger cars traveling more distance in a day, the saving in GWP is going up from 1000 to 7000 CO₂e of Mg for 1.6 km in length.

3 Closure

The influence of climate change on roadway performance was evaluated in this study. First, the influence was evaluated by obtaining future climate data, modifying the data format as per the pavement design software, and analyzing pavement performance

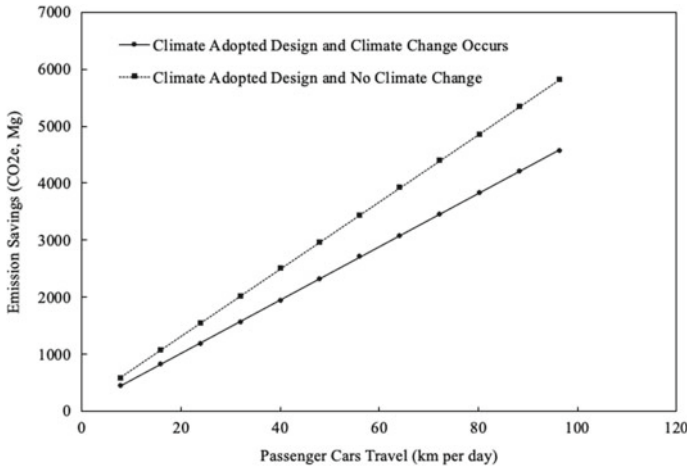


Fig. 11 Emission savings with increase in km traveled

using future climate data. Then, based on the evaluation, alternative roadway structures were proposed and analyzed to mitigate climate change. Also, a cost–benefit analysis was performed that included environmental as economical analysis.

A frontage pavement section from Fort Worth (Texas) was selected to perform an evaluation and document the benefits of the alternative pavement structure. Based on performance analysis, an early strengthening of pavements (by modifying the current design practice) will significantly minimize economic and environmental impact in the event of climate changes as predicted. The benefit is also evident with growth in traffic or km traveled. However, the following issues need to be further addressed:

- This study used various climate models for predicting future climate. However, several models exist, and there is a need for guidance on selecting the appropriate climate model.
- There is inherent uncertainty in the climate prediction models, benefit–cost analysis, life cycle assessments, etc. Thus, a future study is needed that quantifies risk and includes it in the decision-making.

References

1. The United States Environmental Protection Agency (2016) What climate change means for Texas, EPA 430-F-16-045 (August 2016)
2. Southern Climate Impacts Planning Program (SCIIPP) Climate change in Texas. <http://www.southernclimate.org/>. Last accessed 06 June 2019
3. Chron Homepage. <https://www.chron.com/news/houston-texas/texas/article/texas-flood-damage-cost-climate-change-el-ni-o-6594008.php>. Last accessed 06 June 2019

4. Government Technology Homepage. <https://www.govtech.com/fs/Harvey-Could-Blast-10-Billion-Hole-In-Texas-Infrastructure.html>. Last accessed 06 June 2019
5. Li BQ, Mills L, McNeil S (2011) The implications of climate change on pavement performance and design. University of Delaware University Transportation Center
6. Melillo JM (2014) Climate change impacts in the United States, highlights: US national climate assessment. Government Printing Office
7. Guide for mechanistic-empirical design of new and rehabilitated pavement structures. NCHRP Project 1-37A (2004)
8. Daniel JS, Jacobs JM, Douglas E, Mallick RB, Hayhoe K (2014) Impact of climate change on pavement performance: preliminary lessons learned through the infrastructure and climate network (ICNet). In: International symposium of climatic effects on pavement and geotechnical infrastructure 2013
9. Intergovernmental Panel on Climate Change (2000) Working Group III. Emissions scenarios: summary for policymakers. A special report of IPCC Working Group III. Intergovernmental panel on climate change
10. Mearns LO, Gutowski WJ, Jones R, Leung L-Y, McGinnis S, Nunes AMB, Qian Y (2007) The North American regional climate change assessment program dataset. National Center for Atmospheric Research Earth System Grid data portal, Boulder, CO, 2007, updated 2014, Data downloaded 2015–10–23
11. Trzaska S, Schnarr E (2014) A review of downscaling methods for climate change projections United States Agency for International Development by Tetra Tech ARD, pp 1–42
12. Sharma M (2018) Understanding the consequences and costs of climate change on Texas pavements. The University of Texas at El Paso, Ph.D. Dissertation, August 2018
13. Alternative Fuels Data Center. Maps and data. <http://www.afdc.energy.gov/data/>. Accessed 26 July 2017
14. Bureau of Transportation Statistics. US States Department of Transportation. http://www.rita.dot.gov/bts/sites/rita.dot.gov/bts/files/publications/highlights_of_the_2001_national_household_travel_survey/html/section_02.html. Accessed 26 July 2017
15. Buttlar WG, Paulino GH (2015) Integration of pavement cracking prediction model with asset management and vehicle-infrastructure interaction models. NEXTRANS Project No. 0731Y03
16. International Organization for Standardization (2006) ISO 14040:2006 environmental management-life cycle assessment-principles and framework
17. International Organization for Standardization (2006) Environmental management: life cycle assessment; requirements and guidelines. ISO 14044

Performance Analysis of Black Cotton Soil Treated with Dimensional Limestone (Kota Stone) Slurry Waste



Pradeep Kumar Gautam, Pravesh Saini, Pawan Kalla, Ajay Singh Jethoo,
and Harshwardhan Singh Chouhan

Nomenclature

A specific nomenclature was used to identify each mix, and neat soil sample, taken as control sample, is denoted as BCs. For samples containing slurry as additive, the numerical value in between letter B and L indicates the percentage replacement of DLS in BCS; i.e., mixes B2.5L, B5L, B7.5L, B10L, B12.5L, B15L, B17.5L, B19L and B20L are black cotton soil sample containing 2.5%, 5%, 7.5%, 10%, 12.5%, 15%, 17.5%, 19% and 20% DLS slurry as replacement additive, respectively.

1 Introduction

The black cotton soil is expansive inorganic clayey soil belonging to smectite group, meaning, it is a fine-grained soil which undergoes abrupt volumetric change when introduced to moisture condition [1, 2]. Because of this property, this soil becomes unfit to be used for construction purposes, as it causes distress and damage to structures constructed over them [3]. Utilizing this soil as subgrade leads to rutting,

P. K. Gautam (✉)

National Institute of Technology, Shillong, Meghalaya, India
e-mail: pradeepkrgautam@nitm.ac.in

P. Saini

Government Engineering College, Ajmer, India
e-mail: pravesh.saini@ecajmer.ac.in

P. Kalla · A. S. Jethoo

National Institute of Technology Jaipur, Jaipur, India
e-mail: pkalla.ce@nit.ac.in

H. S. Chouhan

Poornima College of Engineering, Jaipur, India

raveling and ultimately failure of a road. Hence, stabilization becomes an essential step to improve its properties and making it fit for construction purpose [4].

Stabilization, in general, is a resultant composite material produced by combining and optimizing individual materials [5]. Conventional stabilization material includes hydrated lime, Portland cement, fly ash and chemicals like sulfonated oil, potassium compounds, enzymes, polymer [6]. However, studies are available where locally generated waste has proved to be successful in modifying properties of soil. Okagbue and Yakubu, 2000, studied the effect of limestone ash waste on geotechnical properties of native soil. The residue was added in different weight replacement of soil sample, i.e., 2, 4, 6, 8 and 10%. To study changes in compaction characteristics of the soil, standard and modified British compaction effort was incorporated; the difference in bearing capacity of soil was evaluated using CBR test. The test results showed a decrease in dry density and increase in optimum water content of soil, which was attributed to increase in lime content and high affinity of lime with water. The CBR value was improved till 6% addition of limestone ash waste, after which value was observed to follow a decrement trend. Based on test results, it was established that 6% addition of limestone dust by weight of soil sample improves its geotechnical properties [7]. Soosan et al., 2005, used quarry dust to enhance geotechnical properties of three type of soils, namely red earth, kaolinite and coaching marine clay soil, which were to be used for highway construction. Quarry dust was added as percentage weight replacement of soil, starting from 20% and going up to 80% at an interval of 20, i.e., 20, 40, 60 and 80%. Each sample was analyzed on the change in liquid limit, compaction characteristics and CBR value. Test result indicated a consistent decrease in liquid limit of all soil samples. Standard Proctor test was used to find maximum dry density and optimum moisture content of the soil, and it was observed that with the increase in quarry waste, optimum moisture content decreased while increasing the maximum dry density, indicating an improvement in compaction characteristics of soil samples. Similar was the observation in CBR test, where quarry dust-soil combination gave higher CBR values [8]. Another study by Sivrikaya et al., 2014, used three varieties of stone waste, namely calcite marble, dolomitic marble and granite powder, to stabilize three types of artificial clayey soil samples which were made by mixing two variants of soil, namely low-plasticity kaolinite and high-plasticity bentonite. The artificial soil samples were designated as Clay samples A, B and C prepared by adding 95% kaolinite and 5% bentonite, 90% kaolinite and 10% bentonite and 80% kaolinite and 20% bentonite, respectively; the waste was added in 5, 10, 20, 30 and 50% by weight. The performance was judged based on change in index properties and compaction parameters, where it was found that inclusion of waste material reduced liquid limit, increased plastic limit and improved compaction properties of all variants of clay samples. The most significant decrease in liquid limit was found by samples containing dolomite marble waste followed by calcite marble and granite marble. Increase in maximum dry density and reduction of optimum moisture content were observed best with the addition of dolomite marble samples. The study successfully demonstrated that dimensional stone waste has potential to be used as an alternative to conventional material [9]. Similarly, Prasad and Prasada Raju, 2015, used quarry dust to improve geotechnical properties of black cotton soil

available in significant part of Andhra Pradesh, India. The dust was added as weight replacement proportion of 5, 10 and 15% of the neat soil sample. Each mix was tested for CBR test, free swell test and direct shear test. The results showed a decrease in swelling characteristics and improved CBR value with addition of quarry dust. The study also included a cyclic load test on a laboratory-mode flexible pavement where samples were subjected to an incremental load. Result expressed in the form of cyclic pressure deformation curve indicated an increased load-carrying capacity of black cotton soil with 10% quarry dust as an additive [10].

1.1 Objective of This Study

The primary aim of this study is to use slurry waste generated from the quarrying and polishing of dimensional limestone (locally called Kota stone) to improve the characteristics of black cotton soil. A stone that satisfies high-quality geological and non-geological parameters is classified as dimensional stones [11]. They are hard, durable rocks with vibrant color and texture. Because of these properties, they are used as ornament, flooring and decorative purpose around the world. India, China, Turkey, Italy are among the topmost producer, consumer and exporter of these type of stones [12].

Manufacturing of these stone is highly unsustainable process. Around 20–40% of the quarried mineral is discarded as waste, which was reported to be about 21.2 million tons in the United Kingdom, 18 million ton in Greece, and in Turkey, it was about 30 million ton for year 2007 worldwide. With rapid increase in demand, mining of these stone has also seen a surge, and with it, the waste generation has also increased. It is estimated that for past two decades, the rate of waste generation has increased at an exponential rate of 7%. This huge amount of waste generated is dumped in open air dumpsite which results in air water and soil pollution.

Studies are available where dimensional quarry waste was recycled into aggregates and was successfully used in concrete; however, use of slurry waste as soil stabilization has been limited. This study is an attempt to reuse this slurry waste as an adhesive to stabilize black cotton soil.

2 Material and Methods

2.1 Black Cotton Soil

Black cotton soil used in this study was procured from Kota city, situated in south-eastern part of the North Indian state of Rajasthan, India. The sample was taken from 20 m below surface. Physical and geotechnical properties of soil are summarized in Table 1.

Table 1 Physical and geotechnical properties of black cotton soil

Parameters	Value	Code
Soil type	CI	IS: 1498 [22]
Liquid limit (%)	47.5	IS: 2720 Part V [18]
Plastic limit (%)	27.78	IS: 2720 Part V [18]
Optimum moisture content (%)	20.5	IS: 2720 Part VII [19]
Maximum dry density (gm/cc)	1.524 gm/cc	IS: 2720 Part VII [19]
Specific gravity	2.62	IS: 2720 Part III [17]

Table 2 Physical and mechanical properties of slurry

Parameters	Value	Code
Specific gravity	2.7	IS: 2720 Part III [17]
Liquid limit	23.90%	IS: 2720 Part V [18]
Plastic limit	Non-plastic	IS: 2720 Part V [18]
Optimum moisture content (%)	21.9	IS: 2720 Part VII [19]
Maximum dry density (gm/cc)	1.604	IS: 2720 Part VII [19]

2.2 Dimensional Limestone Slurry

The slurry used for this study was obtained from mining and polishing dumping ground located at outskirts of Kota and Jhalawar districts of Rajasthan, India. Table 2 summarizes the physical properties slurry used.

2.3 Chemical Test

The chemical composition of black cotton soil and slurry was determined at Center for Development of Stone, Jaipur, Rajasthan. The test result is shown in Table 3. The major composition of dimensional limestone slurry is CaO and SiO₂, while in black cotton soil, the dominant compound is SiO₂.

Table 3 Chemical composition of black cotton soil and slurry

Chemical composition (in %)	CaO	SiO ₂	MgO	Fe ₂ O ₃	Al ₂ O ₃	LOI
Black cotton soil	6.15	65.45	2.01	4.98	Traces	Nil
Dimensional limestone slurry	37.15	23.14	7.02	Traces	Nil	31.89

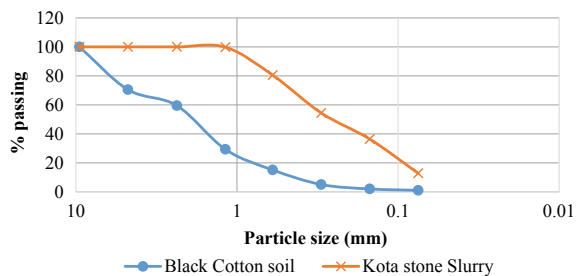
2.4 Sample Preparation

In this study, oven-dried dimensional limestone slurry waste (DLS) was added to black cotton soil sample in percentage weight replacement, starting from 2.5% and proceeding in interval of 2.5% till further addition of DLS had no positive effect on compaction, bearing resistance and durability properties of soil. The proportion interval was decided based upon the review of literatures and initial trials. It was observed that properties variation was clearly visible at 2.5% replacement interval; less than this replacement proportion showed little to no change among samples. Change in soil properties with the addition of DLS was compared with control soil sample containing 0% additive and 100% black cotton soil, referred as BCs. The addition of waste was done by sandwiching in between the layers of black cotton soil and then mixing via shovel till sample was free from any white streak or nodule of slurry, and uniform blend was obtained.

2.5 Particle Size Analysis

Gradation of black cotton soil and limestone slurry is shown in Fig. 1. To analyze the particle size distribution finer than 75 microns in BCS and DLS, samples passing this sieve were analyzed using particle size analyzer device. The results obtained using particle size analyzer are shown in Figs. 2 and 3. From the figures, in BCS, the majority of particle size lie between 10 and 100 microns; in DLS, the particle size distribution is comparably wider, with particles ranging from 0.5 to 100 microns. This further supports the use of DLS as a stabilizer as its use in BCS will give a well-graded mix at the micron level.

Fig. 1 Gradation of BCS and DLS



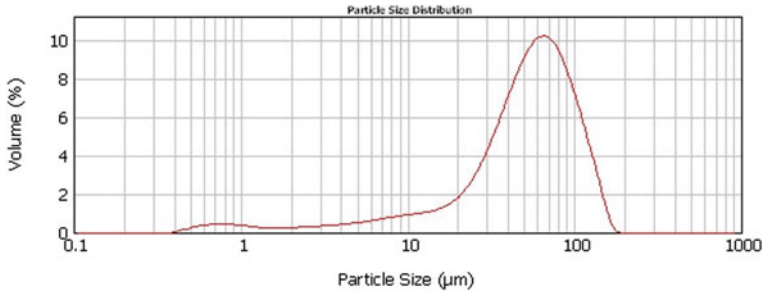


Fig. 2 Particle size distribution (finer than 75 micron) of BCS

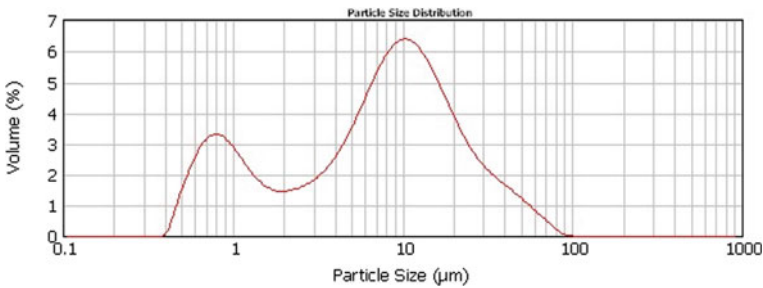


Fig. 3 Particle size distribution (finer than 75 micron) of DLS

2.6 Soil Properties Test

Atterberg limit. Index properties of soil were determined as per IS: 2720 Part V [18]; each sample was tested for liquid limit, plastic limit and plasticity index. In each mix, first, the material in its original form was mixed and then passed through 425-micron sieve, which was later used to study index properties.

Optimum moisture content and maximum dry density. To determine optimum water content (OMC) and maximum dry density (MDD), standard Proctor test was performed as per IS: 2720 Part VII [19]. Each sample was casted in the mold with detachable collar and detachable base plate; in three layers, each layer subjected to 25 blows by hammer weighing 2.5 kg forms free fall height of 30 cm.

Bearing capacity. Soaked CBR test was used to assess the strength of each sample as per IS: 2720 Part XVI [20]. Samples were casted at their respective OMC and then submerged in water at room temperature for 96 h, under a surcharge load of 2.5 kg. At the end of the soaking period, samples were taken out of curing tank, and excess water was allowed to drain out under the action of gravity and then sample was tested.

Free swell index. Change in swelling behavior of BCS on the addition of DLS was assessed by free swell index test, performed as per IS: 2720 Part XL [21]. Ten grams of oven-dried sample passing 425-micron sieve was used for this study. Each specimen was poured in two glass graduated cylinder of 100 ml capacity. One cylinder was filled with kerosene oil and other with distilled water up to 100 ml. After removal of entrapped air, samples were left for 24 h and then final volume change was noted, and free swell index was calculated using formula

$$\text{Free swell index} = \frac{Vd - Vk}{Vd} \times 100 \quad (1)$$

where

- Vd* soil specimen volume read (in cm) from graduated cylinder after 24 h, read from cylinder containing distilled water
- Vk* soil specimen volume read (in cm) from graduated cylinder after 24 h, read from cylinder containing distilled kerosene

Durability. Unconfined compressive strength was used to assess the durability of mixes as per IS: 2720 Part X. The samples were tested for dry and moist conditions both. In dry condition, UCS samples, prepared at respective OMC, were tested immediately, while in wet-UCS, samples were cured by wrapping in airtight polythene and submerging in water for seven days prior to testing.

Microanalysis. Morphology analysis was conducted for each sample by scanning electron microscopy. UCS sample was analyzed from its broken surface, by first coating thin gold coating layer and then scanning in high-resolution scanning electron microscope.

3 Result and Discussion

3.1 Index Properties

Figure 4 shows the result of liquid limit, plastic limit and plasticity index obtained by replacing BCS with DLS. With the addition of DLS to the soil, the liquid limit decreased, plasticity limit of soil increased which in turn lead to an overall decrease in plasticity index of soil, indicating improved workability of the mixture. This was also experienced during sample preparation for Proctor test and CBR test, where with an increase in DLS, the mixing, casting and extraction of material from the mold for mixes with higher proportion of slurry required less effort as compared to control BCS sample. The reason for decreased plasticity index can be attributed to cation exchange reaction taking place between clay particle and calcium ion of DLS, leading to flocculation of particles which in turn behave like silt particles [13]. Depending on liquid limit value and plasticity index obtained, the classification of

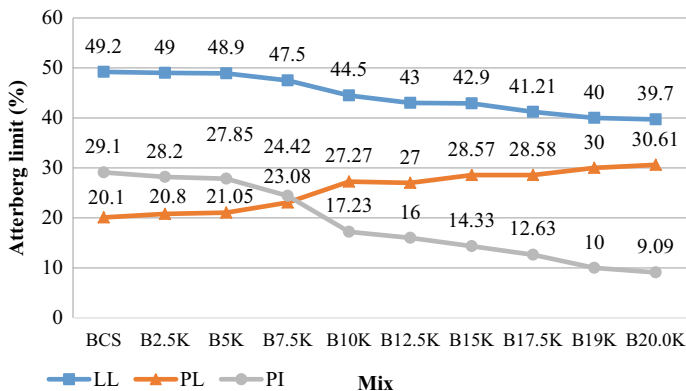


Fig. 4 Effect of additive on Atterberg limit of black cotton soil

soil as per IS: 498 (1970) changed from lean clay to mild silt upon addition of 20% slurry to soil.

3.2 Optimum Moisture Content and Maximum Dry Density

Figure 5 shows OMC and MDD of samples obtained with the addition of DLS. An overall observation of OMC data summarizes that with the addition of slurry, water requirement and maximum dry density of soil samples followed an incremental trend. The increase in water requirement can be attributed to fine gradation and higher specific gravity of slurry particles, requiring higher moisture for lubrication [14]. Addition of slurry resulted in formation of hard cementitious matrix resulting in

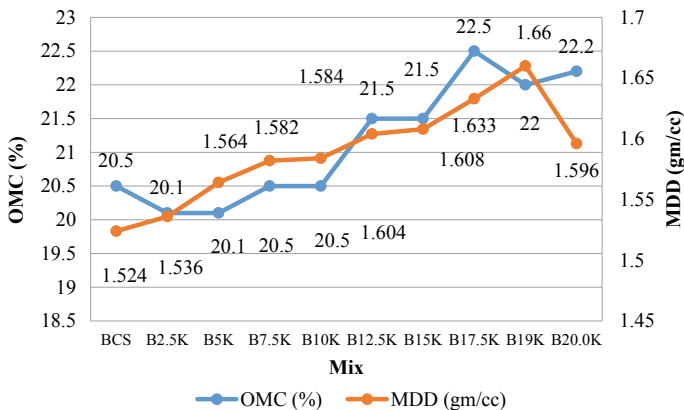


Fig. 5 Effect of slurry on optimum moisture content and maximum dry density of soil samples

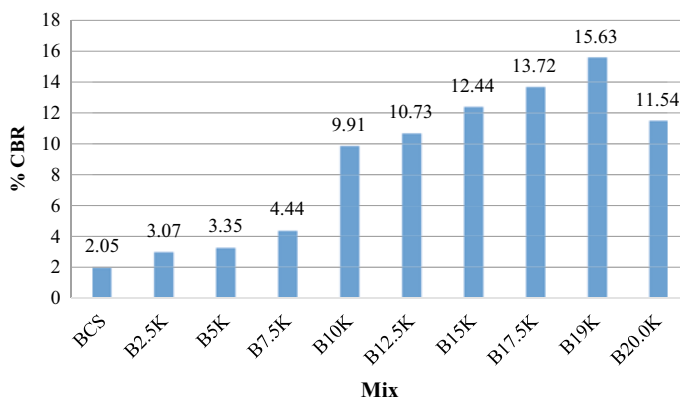


Fig. 6 Effect of slurry on soaked CBR of soil

reduced compactability and improved maximum dry density. MDD of soil changed from 1.524 to 1.66 gm/cc on 19% by weight replacement, after which an increase in the volume of voids created due to flocculation and agglomeration of soil and slurry particles leads to decrease in MDD of the mix.

3.3 Bearing Capacity

Figure 6 illustrates the test results of soaked CBR test for soil samples. The CBR value increased from 2.05% of neat soil sample to 15.26% with 19% addition of slurry after which it decreased. The increment in strength of clay soil sample depends upon the quantity of pozzolanic elements present in additive [13]. Addition of slurry to soil sample leads to pozzolanic activity under submerged water condition, forming calcium silicate hydrate gel leading to improved strength properties. IRC 37:2012 suggest a minimum CBR value of subgrade to be 8% for traffic of 450 commercial vehicle per day or higher. Based on test results, it can be established that slurry modified black cotton soil can be used as subgrade for medium to low volume roads in flexible pavements.

3.4 Unconfined Compression Test

The result of dry-UCS and wet-UCS is presented in Fig. 7. The peak UCS value increased with the inclusion of DLS in soil sample till 17.5% replacement after which it decreased. This increment was due to a well-graded structure and flocculation and agglomeration reaction between soil and slurry particles. As for wet-UCS, it was observed that inclusion of DLS improved strength; however, strength was less

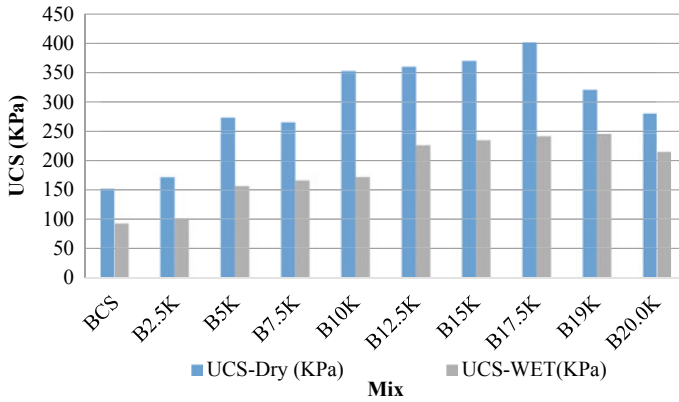


Fig. 7 Effect of slurry on UCS for dry and saturated conditions

compared to their respective dry-UCS sample. This was because the sample preparation for UCS requires material passing 425-micron sieve size. The material obtained through this majorly consists of slurry particles, which are smooth and have less cohesion as observed in plasticity analysis in Table 2, leading to comparatively less strength. However, each wet-UCS mix satisfied the conventional criteria of maximum allowable strength loss of 20% of dry-UCS value [15].

From stress–strain graph presented in Fig. 8 for the dry-UCS test, it is observed that with the inclusion of slurry, resistance to strain value increased consistently. Samples B10L, B12.5L, B15L and B17.5L are giving almost similar initial resistance value; however, for mixes B19L and B20L, resistance to deformation decreased, and this can be attributed to a higher proportion of slurry particles in the mix, which lacks

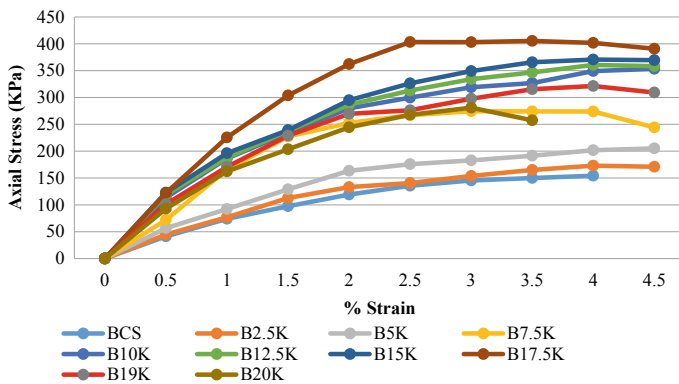


Fig. 8 Variation of stress–strain at replacement interval in dry-UCS

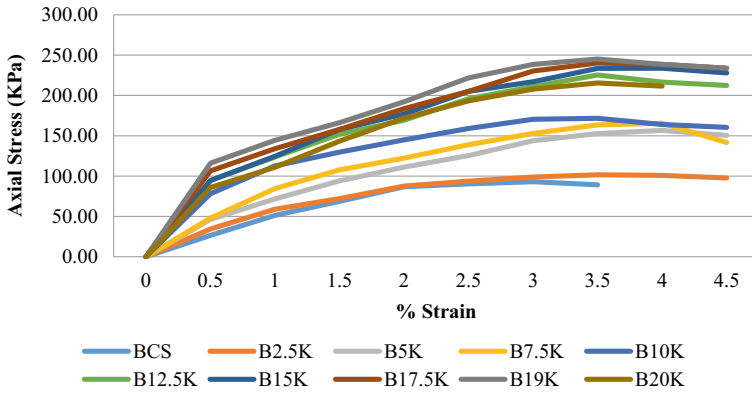


Fig. 9 Variation of stress–strain at replacement interval in wet-UCS

considerable friction and cohesion leading to comparably weaker resistance. In wet-UCS, similar results was obtained (Fig. 9), and it was also observed that resistance to deformation of Sample B19L is improved.

3.5 Free Swell Index

The results of the free swell index of treated and untreated soil sample are presented in Fig. 10. Swelling decreased with increase in DLS in mix. This behavior was attributed to DLS particles acting as filler material [16] and cation exchange reaction taking place between clay ions and calcium ion of slurry resulting in reducing swelling [13]. The swelling decreased from 45.6% of sample BCs to 34.4% with inclusion of 20% slurry as replacement of BCS. Slurry was not able to control swelling property

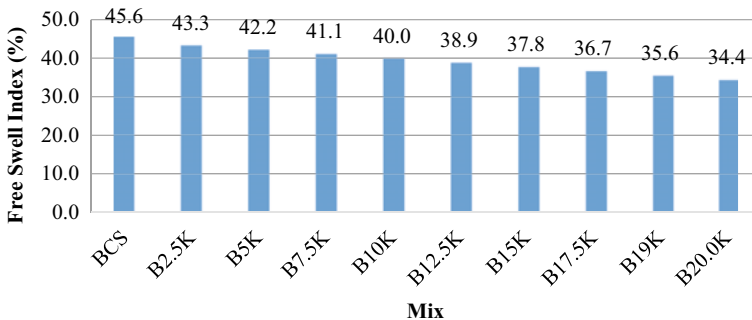


Fig. 10 Change in free swell index on addition of slurry

completely. The reason for this may be due to less proportion of CaO in DLS because of which less calcium ions are available for cation exchange process.

3.6 Scanning Microscope Analysis

Figure 11a shows SEM image of sample BCS, where an irregular, discontinued structure containing void is visible. Figure 11b is a microscopic image of sample B19L which clearly shows change in structure attributed to pozzolanic reaction between soil and slurry particles forming calcium silica hydrate (CSH) gel. A more uniform, well-packed structure resulted in improved MDD, CBR and UCS value of soil sample containing slurry.

4 Conclusion

In the present study, an attempt was made to utilize the DLS as a stabilizing agent in BCS. The test result indicates that inclusion of slurry improved the workability and improved compaction characteristics of the soil sample. Bearing property was found to improve till 19% replacement of soil sample with DLS, and similar was the performance in dry- and wet-UCS studies, where it was observed that with the inclusion of DLS, it gave peak strength of 321.09 kPa for dry-UCS and 245 kPa for wet-UCS samples, respectively. This was about 80% increase in durability in dry-UCS case and almost 130% increase in wet-UCS test. Overall, the test result supports that the use of 17–19% of dimensional limestone polishing waste as weight replacement of black cotton soil will provide durable, stable and sustainable pavement system. Using this waste will provide disposal solution for accumulated waste, reclaim the degraded land and will also conserve hauling energy and dumping cost attached to it.

5 Limitation and Further Scope

Based upon the laboratory investigation, it is established that use of DLS has positive impact on BCS, and its use will promote sustainable development. The scope of the present study is limited to laboratory investigation. For a more detailed understanding of the effect and behavior of dimensional limestone slurry on black cotton soil, a practical field investigation is required.

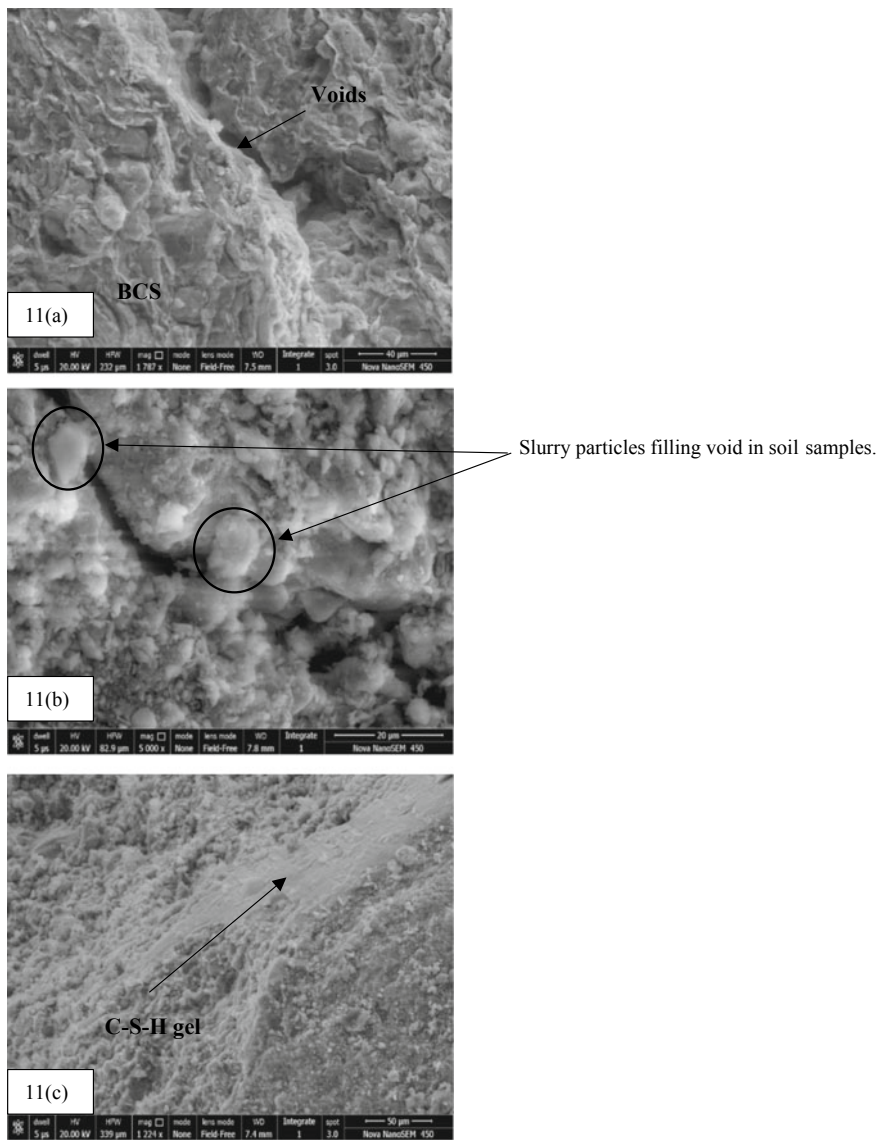


Fig. 11 a-c Showing difference in morphology between neat soil sample and BCS containing 19% slurry

References

1. Zhang P, Huang J, Shen Z, Wang X, Luo F, Zhang P, Wang J, Miao S (2017) Fired hollow clay bricks manufactured from black cotton soils and natural pozzolans in Kenya. *Constr Build Mater* 141:435–441. <https://doi.org/10.1016/j.conbuildmat.2017.03.018>

2. Dalal SP, Patel R, Dalal PD (2017) Effect on engineering properties of black cotton soil treated with agricultural and industrial waste. *Mater Today Proc* 4:9640–9644. <https://doi.org/10.1016/j.matpr.2017.06.240>
3. Al-Rawas AA, Hago AW, Al-Sarmi H (2005) Effect of lime, cement and Sarooj (artificial pozzolan) on the swelling potential of an expansive soil from Oman. *Build Environ* 40:681–687. <https://doi.org/10.1016/j.buildenv.2004.08.028>
4. Osinubi KJ (2006) Influence of compactive efforts on lime-slag treated tropical black clay. *J Mater Civ Eng* 18:175–181. [https://doi.org/10.1061/\(ASCE\)0899-1561\(2006\)18:2\(175\)](https://doi.org/10.1061/(ASCE)0899-1561(2006)18:2(175))
5. Basha EA, Hashim R, Mahmud HB, Muntohar AS (2005) Stabilization of residual soil with rice husk ash and cement. *Constr Build Mater* 19:448–453. <https://doi.org/10.1016/j.conbuildmat.2004.08.001>
6. Petry TM, Little DN (2002) Review of stabilization of clays and expansive soils in pavements and lightly loaded structures—history, practice, and future. *J Mater Civ Eng* 14:447–460. [https://doi.org/10.1061/\(ASCE\)0899-1561\(2002\)14:6\(447\)](https://doi.org/10.1061/(ASCE)0899-1561(2002)14:6(447))
7. Okagbue CO, Yakubu JA (2000) Limestone ash waste as a substitute for lime in soil improvement for engineering construction. *Bull Eng Geol Environ* 58:107–113. <https://doi.org/10.1007/s100640050004>
8. Soosan TG, Sridharan A, Jose BT, Abraham BM (2005) Utilization of quarry dust to improve the geotechnical properties of soils in highway construction. *Geotech Test J* 28:391–400. <https://doi.org/10.1520/GTJ11768>
9. Sivrikaya O, Kiyildi KR, Karaca Z (2014) Recycling waste from natural stone processing plants to stabilise clayey soil. *Environ Earth Sci* 71:4397–4407. <https://doi.org/10.1007/s12665-013-2833-x>
10. Prasad D, Prasada Raju D (2015) Study on geotechnical properties of stabilized expansive soil-quarry dust mixes. *IOSR J Mech Civ Eng* 12:2278–1684. <https://doi.org/10.9790/1684-1265104110>
11. Selonen O, Luodes H, Ehlers C (2000) Exploration for dimensional stone-implications and examples from the Precambrian of southern Finland. *Eng Geol* 56:275–291. [https://doi.org/10.1016/S0013-7952\(99\)00091-5](https://doi.org/10.1016/S0013-7952(99)00091-5)
12. Rana A, Kalla P, Verma HK, Mohnot JK (2016) Recycling of dimensional stone waste in concrete: a review. *J Clean Prod* 135:312–331. <https://doi.org/10.1016/j.jclepro.2016.06.126>
13. Bell FG (1996) Lime stabilization of clay minerals and soils. *Eng Geol* 42:223–237. [https://doi.org/10.1016/0013-7952\(96\)00028-2](https://doi.org/10.1016/0013-7952(96)00028-2)
14. Modarres A, Nosoudy YM (2015) Clay stabilization using coal waste and lime—technical and environmental impacts. *Appl Clay Sci* 116–117:281–288. <https://doi.org/10.1016/j.clay.2015.03.026>
15. Eze-Uzomaka O, Johnson A (2010) Daniel, suitability of quarry dust as improvement to cement stabilized- laterite for road bases. *Electron J Geotech Eng* 15:1053–1066
16. Aldaood A, Bouasker M, Al-Mukhtar M (2014) Free swell potential of lime-treated gypseous soil. *Appl Clay Sci* 102:93–103. <https://doi.org/10.1016/j.clay.2014.10.015>
17. IS 2720 Part III: method of test for soils-determination of specific gravity of soils
18. IS 2720 Part V: method of test for soils-determination of liquid limit and plastic limit of soils
19. IS 2720 Part VII: method of test for soils-determination of water content-dry density relation using light compaction.
20. IS 2720 Part XVI: Method of test for soils-laboratory determination of CBR
21. IS 2720 Part XL: Method of test for soil-determination of free swell index of soils
22. IS 1498: Classification and identification of soils for general engineering purposes

Experimental Investigation on the Feasibility of Using Construction Demolition Waste Materials for Subbase Layer in Flexible Pavement



R. Chandra Prathap and U. Salini

1 Introduction

Pavement performance depends on various factors such as strength of the subgrade, quality of materials used for pavement construction, thickness of pavement layers, axle load, climatic, and other environmental conditions. Among these, the quality of materials used for pavement construction is more significant as it incurs greater costs. The pavement comprises of bituminous layers resting on strong foundation layers such as base, subbase, and subgrade. The base and subbase layer comprise of natural resources such as crushed rock, aggregate, and gravel. As there is a shortage of good quality natural resources, it is necessary to find feasible alternate materials that can substitute these in the base and subbase layer. Construction demolition (CD) waste is one such alternative material that can lead to sustainable road construction. A lot of research has been carried out to understand the characteristics of CD waste such as recycled concrete aggregate and brick waste, so as to utilize them in subbase and base course of pavement layer. Chini et al. [1], Nataatmadja and Tan [2], Molenaar and van Niekerk [3], Park [4], Taha et al. [5], Poon and Chan [6] have brought out the feasibility of using recycled concrete and masonry rubble in base and subbase layer as they showed comparable strength and water absorption to that of natural aggregate. Taherkhani [7], Brooks and Cetin [8], and Jayakody et al. [9] brought out that the degree of compaction of the mix containing different percentages of the natural aggregate and construction demolition waste affects the mechanical characteristics, CBR strength, and resilient modulus of the subbase material. On the whole, these research findings encourage the use of CD waste as a viable option for base and subbase construction but not much is studied on the effect of the type of CD waste on the behavior of granular subbase (GSB) layer. This paper presents the feasibility

R. Chandra Prathap (✉) · U. Salini
National Transportation Planning and Research Center, Thiruvananthapuram, Kerala 695011, India

of using construction demolition (CD) waste for improving the performance of granular subbase (GSB) layer of the pavement structure. The study is highly significant because the CD waste is currently disposed as waste material without any further use and this is creating lot of environmental issues in the State of Kerala, India. The reuse of CD waste as subbase material will eliminate the waste disposal issue as well as reduce the consumption of natural resources. Also, the type of CD waste used affects the strength and permeability of the GSB layer. Hence, the paper also brings out the adverse effect of using brick waste in GSB layer.

2 Material Characterization

2.1 Materials

The materials used for the study include the construction demolition waste obtained from different demolition sites in Trivandrum and virgin aggregates from a quarry site. Construction demolition (CD) waste used in the present study includes concrete aggregate waste (CAW), concrete hollow block waste (CHBW), and clay brick waste (CBW) as shown in Fig. 1. All the CD wastes were crushed manually to obtain aggregates of size ranging from 26 mm to less than 75 μ in size. It was also ensured that the age of the concrete aggregate waste, concrete hollow block waste, and clay brick waste were more than 20 years. The properties of the CD waste and virgin aggregates are given in Table 1.

Fig. 1 Construction demolition waste



Table 1 Material properties

Test	CD waste			Virgin aggregate	IS code	Limiting values
	CAW	CHBW	CBW			
Aggregate impact value	28.1	29.4	–	21.4	IS 2386 (P-4) and IS 5640	Max. 30%
Los Angeles abrasion	33.8	35.3	–	28.4	IS 2386 (P-4)	Max. 40%
Water absorption	5.51	5.93	8.53	0.324	IS 2386 (P-3)	<2%
specific gravity	3.1	2.7	0.66	2.71	IS 2386 (P-3)	2.5–3.2
Flakiness index	10.8	–	–	5.81	IS 2386 (P-1)	Max. 15%
Elongation index	16.1			13.02	IS 2386 (P-1)	Max. 15%
Liquid limit (LL) and plasticity index (PI)	Nonplastic				IS 2720 (P-5)	Max. 25% and 6%

2.2 Mix Proportioning and GSB Grading

The three CD wastes were blended together in known ratios to form different samples of S1, S2, and S3 as shown in Table 2. A control mix was also prepared with fresh aggregates. All the mixes were prepared conforming to Grading VI for granular subbase material [10] as shown in Table 3. The blended mixes were tested for their engineering properties, and the test results are reported in Table 4.

3 Experimental Program

The suitability of the CD waste mixes as GSB material was assessed by conducting California bearing ratio (CBR) test and permeability test on the proportioned GSB mixes. CBR and permeability tests were carried out on GSB mixes compacted to maximum dry density (MDD) and optimum moisture content (OMC). Modified proctor compaction test was carried out to determine the OMC and MDD as per IS

Table 2 Proportioning of samples

Samples	CAW	CHBW	CBW
S0	Control mix with fresh aggregates		
S1	100	0	0
S2	80	10	10
S3	60	20	20

Table 3 Grading for granular subbase materials [10]

IS sieve (mm)	Percent by weight passing IS sieve
	Grading VI
75.0	–
53.0	100
26.5	75–100
9.50	55–75
4.75	30–55
2.36	10–25
0.85	–
0.425	0–8
0.075	0–3

Table 4 Engineering properties of different mixes proportioned mix

Test	S0 (Control mix)	S1 (100:0:0)	S2 (80:10:10)	S3 (60:20:20)	IS code	Limiting values
Aggregate impact value	21.4	25.3	27.5	27.9	IS 2386 (P-4) and IS 5640	Max. 30%
Los Angeles abrasion	28.4		35.3	33.8	IS 2386 (P-4)	Max. 40%
Water absorption	0.324	3.26	4.64	7.29	IS 2386 (P-3)	<4%
Specific gravity	2.71	2.45	2.34	2.21	IS 2386 (P-3)	2.5–3.2
LL and PI		Nonplastic			IS 2720 (P-5)	Max. 25% and 6%

2720—Part8 [11]. California bearing ratio test was performed as per IS: 2720—Part 16 [12] on the compacted specimens after soaking them for 4 days. The average value of three trials is reported as the CBR value. Vertical permeability test was carried out in laboratory in constant head permeameter as per IS: 2720 (Part 17) [13] and *ASTM D 2434–68* [14] in a cylindrical mold of 10 cm diameter and height 15 cm as shown in Fig. 2. It was ensured that the setup did not have any kind of leakage. The compacted GSB mix was kept for saturation for 24 h, and the permeability readings were taken once steady state of flow was attained. The results of the above tests are presented in the following section.



Fig. 2 Experimental setup of constant head permeability test

4 Results and Discussion

4.1 Compaction Test

The compaction curve gives an indication of sensitivity of dry density with respect to changes in water content [6]. The sharper the curve the higher the sensitivity, i.e., a small change in water content causes large variation in density. Therefore, the identification of the exact OMC plays a significant role. Figure 3 plots the compaction curves for the three CD waste mixes (S1, S2, and S3) and the control mix (S0). Their

Fig. 3 Compaction curve (modified proctor compaction test)

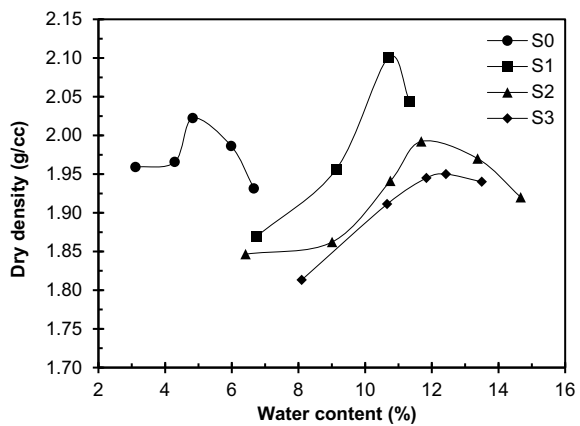


Table 5 Results of modified proctor compaction test

Property	S0 Control mix	S1 100:0:0	S2 80:10:100	S3 60:20:20
MDD	2.02	2.1	1.99	1.95
OMC	4.9	10.8	11.7	12.4

OMC and MDD values are summarized in Table 5. It can be seen from the figure that the S1 mix having only CAW has highest MDD and the MDD value decreased with the reduction of CAW and increase in CBW in the mix (S2 and S3). Also, the OMC increased with an increase in CBW in the mix. As all the mixes have same grading, this reduction in MDD and increase in OMC is due to the porous CBW which has a high-water absorption tendency. The S1 mix has a higher MDD compared even to the control mix due to the higher particle density and lower voids within the material. But the OMC of S1 mix is higher compared to the control mix due to the presence of cement mortar around the aggregate. The figure also shows that S1 mix has sharper compaction curve and hence is more sensitive to changes in moisture content compared to S2 and S3 mixes.

4.2 California Bearing Ratio Test

Figure 4 compares the CBR values of the CD waste mixes with the control mix. It can be seen that, all the mixes with CD waste had higher CBR values compared to the control mix. Also, among the CD waste mixes, the S1 mix (having only CAW) had highest CBR value compared to S2 and S3 mixes. The CBR value decreased with increase in clay brick waste content as the clay brick waste has lower density

Fig. 4 Average CBR values of four days soaked samples

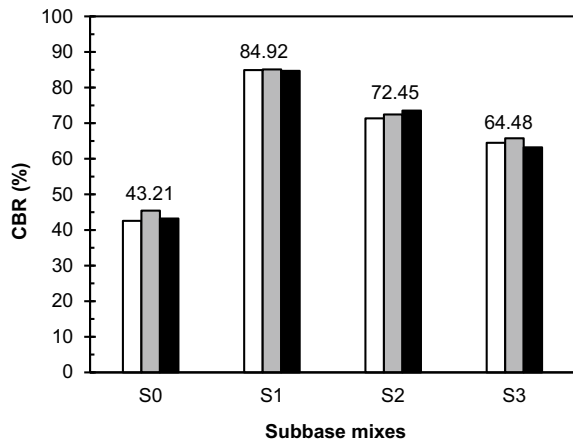


Table 6 Permeability of different mix proportions

Sample designation	Mix types	Permeability (m/day)
S0	Control mix	22
S1	100:0:0	19
S2	80:10:10	16
S3	60:20:20	12

and is susceptible to greater crushing compared to concrete. Poon and Chan [6] and Jayakody et al. [9] also obtained similar trend in CBR value when clay brick waste was used in the subbase layer. They inferred that the reduction in CBR is due to poor interlocking among the materials in the mix.

4.3 Vertical Permeability Test

The vertical permeability obtained for the GSB mixes is shown in Table 6. Using the permeability setup shown in Fig. 2, the control mix had a permeability of 22 m/day. The permeability of GSB mix, S1 (having only CAW) had permeability of 19 m/day which is comparable to that of control mix. In the case of S2 and S3 mixes, the permeability reduced comparatively due to the increase in fines which filled the voids and reduced the flow path.

5 Conclusions

In order to reduce the consumption of natural resources and to solve the problem of construction waste disposal, this present study was carried out. This study presents an experimental investigation on the use of different CD wastes such as concrete aggregate wastes, concrete hollow block wastes, and clay brick wastes in GSB layer. The following conclusions were made based on the results obtained from the experimental investigations.

- The characterization of different construction demolition waste obtained showed that concrete aggregate waste is superior to concrete hollow block waste and clay brick waste
- The subbase layer with only concrete aggregate waste (100%) had higher maximum dry density compared to the subbase layer prepared with natural aggregates.
- The use of clay brick waste and concrete hollow block waste along with concrete aggregate waste caused reduction in MDD even lower than GSB layer with natural aggregates and increase in OMC due to higher water absorption

- The strength of different GSB mixes evaluated in terms of soaked CBR values showed that even though the use of crushed brick lowered the CBR value, the CBR value was higher for all the mixes prepared using CD waste compared to control mix. Hence, it is feasible to blend recycled concrete aggregate and crushed brick to produce a subbase with a soaked CBR value more than 30%.
- The vertical permeability values obtained for all the three CD waste mixes were comparable to that of control mix samples.

The mix proportion 100:0:0 with only concrete aggregate waste was found most suitable as GSB material than the other two proportions which have clay brick waste content. Therefore, while using the CD waste as GSB material, care should be taken to remove clay brick waste as they reduce the strength and permeability of the GSB layer.

References

1. Chini AR, Kuo SS, Armaghani JM, Duxbury JP (2001) Test of recycled concrete aggregate in accelerated test track. *J Transp Eng* 127(6):486–492
2. Nataatmadja A, Tan YL (2001) Resilient response of recycled concrete road aggregates. *J Transp Eng* 127(5):450–453
3. Molenaar AAA, van Niekerk AA (2002) Effects of gradation, composition, and degree of compaction on the mechanical characteristics of recycled unbound materials. *Transp Res Rec* 1787:73–82
4. Park T (2003) Application of construction and building debris as base and subbase materials in rigid pavement. *J Transp Eng* 129(5):558–563
5. Taha R, Al-Rawas A, Al-Jabri K, Al-Harthy A, Hassan H, Al-Oraimi S (2004) An overview of waste materials recycling in the Sultanate of Oman. *Resour Conserv Recycl* 41(4):293–306
6. Poon CS, Chan D (2006) Feasible use of recycled concrete aggregates and crushed clay brick as unbound road sub-base. *Constr Build Mater* 20:578–585
7. Taherkhani H (2015) Evaluation of the physical properties of unbound base layer containing recycled aggregates. *Int J Environ Sci Dev* 6(4):279
8. Brooks RM, Cetin M (2012) Application of construction demolition waste for improving performance of subgrade and subbase layers. *Int J Res Rev Appl Sci* 12(3):375
9. Jayakody S, Gallage C, Kumar A (2012) Assessment of recycled concrete aggregates for road base and sub-base. In: Proceedings of the second international conference on geotechnique, construction materials and environment, pp 575–579
10. MoRTH (2013) Specifications for road and bridge works (5th revision). Ministry of road transport and highways, in Indian road congress, New Delhi, India
11. IS 2720-Part 8 (1983) Methods of test for soils: determination of water content-dry density relation using heavy compaction. Reaffirmed 2006. Bureau of Indian Standards, New Delhi, India
12. IS 2720-Part 16 (1987) Methods of test for soils: laboratory determination of CBR. Bureau of Indian Standards, New Delhi, India
13. IS 2720-Part 17 (1986) Methods of test for soils: laboratory determination of permeability. Bureau of Indian Standards, New Delhi, India
14. ASTM D 2434-68 (2006) Test method for permeability of granular soils (Constant Head). Philadelphia, PA

Condition Assessment of Reinforced Concrete Bridge Deck Using Infrared Thermography



Vidhi Vyas, Ajit Pratap Singh, and Anshuman Srivastava

1 Introduction

Road infrastructure including highways and bridges of any country necessitates its timely performance monitoring, in order to avert mishaps and ensure safety of its citizens. Many cases of sudden collapse of bridges have been already observed in recent past, possibly due to lack of proper inspection and the use of substandard construction materials [1, 2]. Ministry of Road Transport and Highways, Government of India, have performed a safety audit of 1.6 lakh bridges and have found that more than one hundred structures are in unsound condition and require immediate attention [3].

Bridge deck is one of the major components of bridge superstructure. It is highly prone to rapid deterioration and has lesser service life, than any other component since it carries moving traffic [4]. In order to estimate its repair costs and allocate fund for maintenance, their current condition assessment and monitoring are essential. One of the major challenges in the direction of bridge deck condition evaluation is the identification of hidden internal defects. The most prevalent practice to examine the present state of bridge deck condition is through visual survey. Subjective opinion could also be provided based on sounding or chain drag operations, when a dull or hollow sound represents the delaminated areas [5]. Destructive method of coring, do provide reliable information. Nevertheless, none of these methods have been found to be very trustworthy and quick in providing information. Visual survey would provide evidence only when the internal defect has sufficiently progressed up to the surface so as to be visible through naked eyes. Subjective judgment is limited to experience of

V. Vyas (✉)

Central Road Research Institute (CSIR-CRRI), New Delhi 110025, India

e-mail: vidhivyas.ccri@nic.in

A. P. Singh · A. Srivastava

Birla Institute of Technology and Science, Pilani 333031, India

professional inspectors and the conditions prevailing during the examination. Cores do not ensure that the condition of remaining part of the structure is similar, also it is time-consuming, cannot be performed everywhere, and only a limited number of cores can be extracted.

NDT methods overcome these limitations and provide the opportunity to engineers for rapid inspection of bridge structures without causing any alternation in their physical and chemical properties. Large areas can be tested quickly and with reasonable accuracy. They also provide an easy approach to regularly monitor the structure at various stages from its construction to aging. Various NDT methods widely used for bridge deck flaw detection are ground-penetrating radar, impact echo, IRT, half-cell potential, ultrasonic pulse echo, ultrasonic surface waves, chain dragging, etc. The detailed principle of operation, theory, advantages, and limitations of these methods can be found elsewhere [6].

Infrared thermography is based on capturing the radiations emitted by any object/structure with the wavelength proportional to their temperature and lying in the infrared portion (wavelength 0.75 μm and 1000 μm) of the electromagnetic spectrum [7]. Radiations are emitted by all bodies whose temperature is over 0 K and these radiations lie in infrared portion of the electromagnetic spectrum [8]. Any subsurface flaw creates hindrance to the flow of heat through it and this results in localized temperature differences. These can be captured by a thermal imaging camera which transforms the captured radiations and visible images are produced [9, 10].

This work is an attempt to explore the potential of infrared thermography for detection of internal flaws in reinforced concrete bridge decks. The test is performed extensively on an in-situ reinforced concrete bridge deck induced with various artificial defects. The results are presented in the form of thermal images. Estimation of delamination detection time zone for Indian conditions is performed by finding the interchange time durations between nighttime cooling and daytime heating cycles.

2 Literature Review

Several NDT techniques have been considered for bridge deck condition examination. Researchers have discussed the applicability and potential of different techniques to detect the subsurface flaws. These flaws can be of varying dimensions and located at different depths. It has been found from laboratory and field measurements that each one of the testing techniques has fair to good accuracy in detecting different flaws commonly occurring in concrete bridge decks. These include rebar corrosion, delamination, voids, vertical cracks, honeycombing, etc.

IRT has been reported to detect shallow and large delaminations in bridge decks and asphalt pavements [7, 11]. Other studies have also reported that the deeper defects have less chances to be detected, particularly the ones deeper than 51 mm [6, 12, 13]. Ideally, area with delamination shows a hot spot during daylight and cool spot at nighttime. However, appropriate weather conditions and collection of data at the

right time of day and night cycle are found to largely govern the detection of flaws in passive thermography [13]. Different authors have made different recommendations regarding the time of data collection, when the defect is detectable. According to Washer et al. [14], subsurface delaminations were detectable 5–9 h after sunrise based on their depth from surface. Gucunski et al. [6] concluded that delaminations captured 40 min after sunrise provided better results. The night cooling cycle has been observed to provide better clarity results when compared to daytime heating cycle, with clear sky being a favorable condition [13, 15, 16]. Also, delaminations go undetected during the interchange durations of nighttime cooling and daytime heating. This duration is about 1 to 2 h, for morning and evening, respectively [15]. Vaghefi et al. [17] have made an attempt to calculate the percentage of delaminated area using thermal infrared images. Nevertheless, it has been concluded that area of delamination is a key factor affecting temperature difference rather than thickness or volume and thus making it detectable [15]. Washer et al. [14] have concluded that in absence of solar loading, a positive or negative ambient temperature change of at least 8.3 °C (15 °F) could be used as a standard practice to assess subsurface defects. The soffit area of a bridge has been evaluated based on this guideline with reasonable accuracy and ensures the inspection of areas subjected to spalling [14]. Maser [18] has recommended the use of active infrared thermography by employing high intensity pavement heaters to briefly heat the entire concrete bridge deck. The cost and time of testing are reported to get highly reduced as compared to chain dragging testing operations. However, the technique has not found capable to detect corrosion or cracks and does not provide the depth of flaws [19]. Vaghefi et al. [17] have suggested three-dimensional optical bridge evaluation system and thermal infrared imagery along with the use of ArcGIS, to identify and quantify the bridge deck data.

Based on the above studies, it can be concluded that the detection time of subsurface delaminations highly varies and before using IRT for defect detection in field, it should be first proven for simulated flaws and approximate detection time zone should be estimated for that area. Moreover, since the detection is performed through passive infrared thermography, it is highly dependent on the amount of solar load available during a day at any location. Such study has not been performed for Indian conditions. Therefore, in this study, the potential of IRT for delamination detection in concrete bridge decks is explored particularly for Indian conditions. Extensive IRT testing is conducted on an in-situ concrete bridge deck artificially induced with delaminations of various dimensions, located at different depths.

3 Study Objectives

The objectives of the present study are firstly to simulate concrete bridge deck for Indian conditions, secondly to assess IRT for its potential to detect bridge deck delamination, and finally, to evaluate the time zone during the entire day for successfully

inspecting field decks by IRT. In addition to this, limitations and advantages of IRT are discussed in this reference.

4 Experimental Investigation

The experimental investigation is performed on a fabricated bridge deck using IRT. The technique is based on detection of thermal differentials over delaminated and sound areas of bridge deck using an infrared camera. A visual delamination image is produced which provides good accuracy regarding the location of defect. However, its detection ability is subjected to depth limitations and amount of solar radiation in case of passive infrared thermography approach.

IRT has been performed using a FLIR T250 camera in this study, in accordance with ASTM D4788-88 standards [20]. The thermal camera captures and stores images of 320×240 pixels resolution. Some of the main technical specifications of the thermal camera are summarized in Table 1. The temperature differentials over the test slab have occurred due to sunlight (passive approach). Environmental conditions such as ambient air temperature, relative humidity and wind speed, test slab surface temperature, and emissivity of concrete have been considered. It is important to note that there was no effect of clouds or rainy conditions during the period of testing.

Detailed investigation and data collection have been performed over a period of one month in order to capture the best results. Infrared images at all the locations where delaminations were induced have been taken regularly over one hour time interval (from 00:00 h to 23:00 h). To ensure reproducibility in measurements, the

Table 1 Technical specifications of FLIR T250 thermal camera

Particulars	Specifications	Unit
Measurement object temperature range	-20 to +350	°C
Accuracy	2% of reading or ± 2	°C
Thermal sensitivity at 30 °C	80	mK
IR resolution	320×240	pixel
Minimum focus distance	0.4	m
Spatial resolution	2.18	mrad
Field of view	25×19	°
Imaging frequency	30	Hz
Spectral range	7.5–13	μm
Focal plane array	Uncooled microbolometer	–
Digital zoom	1–2 \times	–

images are captured from same height, measurement angle and direction every time. Due to brevity reasons, the results of a typical sunny summer day have been presented.

4.1 Fabrication of Concrete Bridge Deck Slab

A concrete bridge deck slab of lateral dimensions 3 m × 2 m and 0.2 m nominal thickness was designed and fabricated. The design requirements have been performed per IRC specifications and guidelines. M30 concrete mix was adopted for deck construction. The slab was simulated with delaminations of dimensions commonly occurring in actual bridge decks. One-third area of the slab (2 m × 1 m) was kept free from any defect in order to compare the conditions of sound and defected area. Two mats of steel reinforcement bars consisted of 12 mm diameter and spaced 200 mm center-to-center in both longitudinal and transverse direction were provided. The clear cover of 40 mm was taken for both top and bottom. Since there is no analysis of loading and unloading behavior, therefore the provision of reinforcement is considered on the basis of minimum reinforcement criteria with two mats provided, as given in IRC code.

Delaminations were simulated using foam of different sizes. This is because the value of thermal conductivity for foam is $0.033 \text{ W (mK)}^{-1}$ which is very close to that of air ($0.024 \text{ W (mK)}^{-1}$). Commonly, delaminations occurring in decks have thickness of 1–2 mm. The four different dimensions of foam are taken which are placed at three depths. This helps to discover the minimum dimension and maximum depth at which the delamination is detectable using thermal camera. The defect distribution in the fabricated slab is as given in Table 2. The delaminations were placed over the two levels of reinforcement mat (40 and 136 mm deep from surface) and at 25 mm depth.

5 Results

Infrared thermal images of fabricated slab were taken on different days and at different times to study the impact of variation in temperature on detectability through thermal camera. All the tests were performed on sunny days when ambient temperature ranged from 28 to 40 °C. Most accurate results were obtained during the time periods of maximum heating. Figure 1a–h presents the images of different delaminations at various times of the day in which delaminated area is marked with dashed lines. It is important to note that not all the delaminations were apparently visible through the thermal images. Therefore, only those which were clearly visible at various times of a day are presented here. The delamination areas are spotted as hot spots (marked with dashed lines) in the thermal images with higher temperature around the center. This is evident from the fact that the area above delamination hinders the heat flow through it and heats up faster than the surrounding area.

Table 2 Details of artificially induced defects in fabricated slab

Code	Size (mm)	Thickness (mm)	Depth (mm)
DL-1/5/A	5 × 5	1	25
DL-2/5/A	5 × 5	2	25
DL-1/10/A	10 × 10	1	25
DL-2/10/A	10 × 10	2	25
DL-1/15/B	15 × 15	1	40
DL-2/15/B	15 × 15	2	40
DL-1/15/C	15 × 15	1	136
DL-2/15/C	15 × 15	2	136
DL-1/5/C	5 × 5	1	136
DL-2/5/C	5 × 5	2	136
DL-1/5/B	5 × 5	1	40
DL-2/5/B	5 × 5	2	40
DL-1/10/B	10 × 10	1	40
DL-2/10/B	10 × 10	2	40
DL-1/10/C	10 × 10	1	136
DL-2/10/C	10 × 10	2	136
DL-1/20/B	20 × 20	1	40
DL-2/20/B	20 × 20	2	40
DL-1/20/C	20 × 20	1	136
DL-2/20/C	20 × 20	2	136

Table 3 presents the summary of results of delamination detectability during different time slots in a day using IRT stating if a particular delamination was detected, partially detected or not detected. It can be seen clearly that IRT is able to detect shallow delaminations up to 50 mm depth in this study. This is evident from the table since the delaminations located at 136 mm below surface are either partially detected or not detected. Thus, this technique is not suitable for delaminations located at greater depths.

In addition to this, important conclusions have been obtained regarding the time duration of delamination detectability in a day. It can be clearly seen from the table that 4–5 h after the sunrise is the best time zone during which the delaminations can be detected since majority of delaminations are detectable from 11:00 am to around 3:00 pm. It has been noted that the delamination detectability through IRT is very low 3:00 pm onwards until the next morning. Therefore, the best time frame to inspect real field conditions would be from 11:00 am to 3:00 pm. With reference to the thickness of delaminations, it can be observed that the 2 mm thick delaminations are more prominently visible than 1 mm thick delaminations because they hinder the heat flow to a larger extent. This concludes that as the delamination progresses or its thickness of increases, there are higher chances of its detection through IRT. This

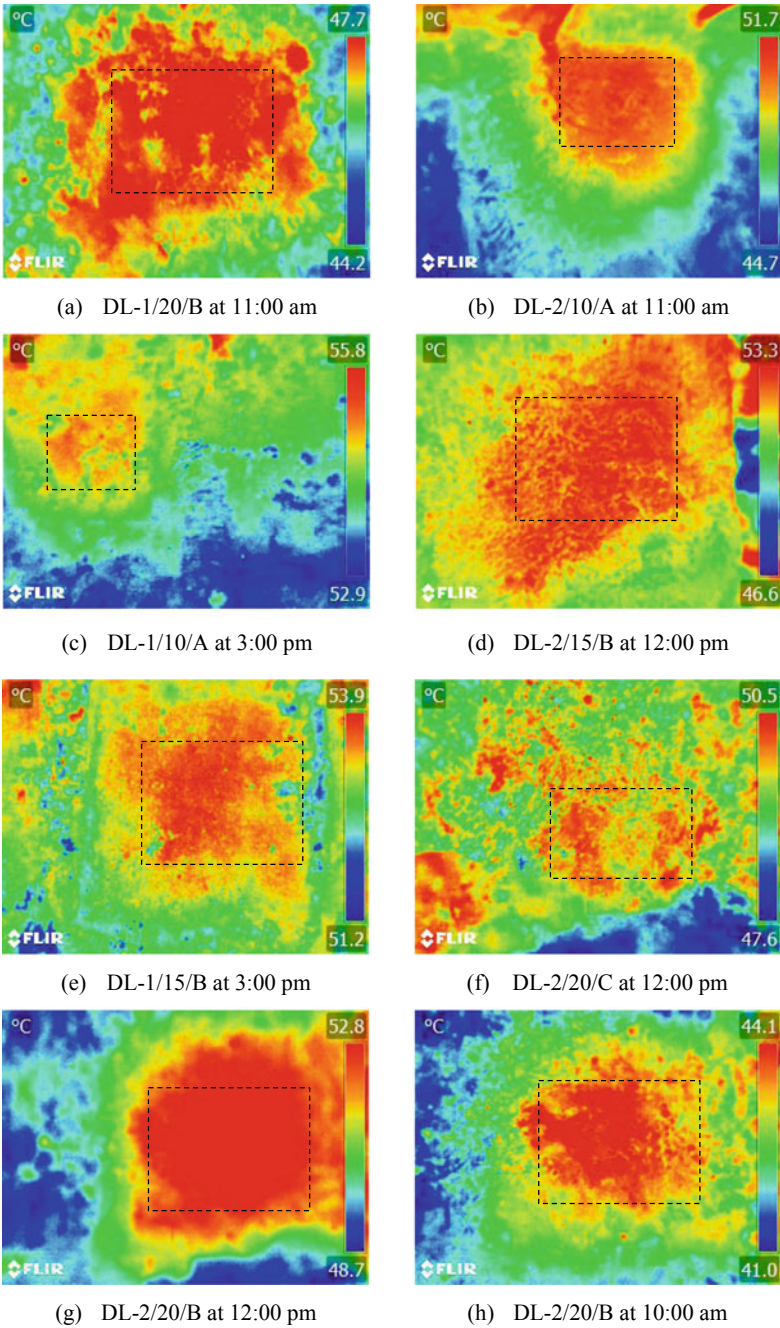


Fig. 1 Thermal images of various delaminations captured at different times of the day

Table 3 Summary of IRT results for delamination detectability

Code	Time			
	6:00 am to 11:00 am	11:00 am to 3:00 pm	3:00 pm to midnight	Midnight to 6:00 am
DL-1/5/A	ND	ND	ND	ND
DL-2/5/A	ND	ND	ND	ND
DL-1/10/A	ND	PD	ND	ND
DL-2/10/A	D	D	PD	PD
DL-1/5/B	ND	ND	ND	PD
DL-2/5/B	ND	ND	ND	ND
DL-1/10/B	ND	ND	ND	PD
DL-2/10/B	ND	PD	ND	ND
DL-1/15/B	PD	D	ND	ND
DL-2/15/B	PD	D	ND	ND
DL-1/20/B	PD	D	PD	ND
DL-2/20/B	D	D	PD	PD
DL-1/5/C	ND	ND	ND	ND
DL-2/5/C	ND	ND	ND	ND
DL-1/10/C	ND	ND	ND	PD
DL-2/10/C	ND	ND	ND	ND
DL-1/15/C	ND	ND	ND	ND
DL-2/15/C	ND	ND	ND	PD
DL-1/20/C	ND	ND	ND	ND
DL-2/20/C	PD	PD	ND	ND

Note D = detected, PD = partially detected and ND = not detected

also infers that delaminations at their very early stages are difficult to be captured in thermal images.

In the present study, delamination detection could be successfully performed through visual observation of thermal images. However, a few inconsistencies may arise out of visual examination in real field condition, such as a hotspot may occur due to some foreign object which may be wrongly interpreted as delamination. Therefore, to enhance reliability of delamination detection, post-processing of these thermal images and verification using another NDT method such as impact echo would be highly beneficial.

6 Conclusion

The study draws interesting conclusions by conducting extensive IRT testing on an in-situ concrete bridge deck. Delaminations of various dimensions are induced at different depths in the bridge deck to assess the potential of IRT for detecting these defects. The study also intends to identify the time zone of delamination detection during a day for carrying out actual field inspections.

From the thermal images, it can be observed that the delaminated areas appear as hot spots since they hinder the heat flow through them and heat up faster than the surrounding areas. The results conclude that IRT is able to clearly detect shallow delaminations up to 50 mm depth in this study. The delaminations located at greater depths are either partially detected or undetected. Also, the ideal time for field testing is estimated to be 4–5 h after the sunrise since majority of delaminations were detectable from 11:00 am to around 3:00 pm. The study also concludes that IRT being an area-based testing technique can quickly scan large areas and identify potential locations of defects, particularly those located at shallow depths. Therefore, it can be highly useful for field inspections of bridges. It is fairly successful in detecting the internal flaws located at shallow depths. However, for delaminations located at greater depths, IRT should be suitably used along with other NDT techniques and their combination would yield better results.

It should be noted that in this study, the delaminations were readily visible in the thermal images. Therefore, the need for post-processing of images was not felt necessary. However, if it is difficult to identify delaminations visually or in case of real defects, post-processing of images such as noise removal would be necessary to enhance the reliability of defect detection.

7 Future Work

The future work comprises of application of other NDT techniques in addition to IRT which would increase the accuracy of defect detection in concrete bridge decks. In addition to this, post-processing of thermal images would be done to facilitate increased reliability of defect detection.

References

1. <http://www.bbc.com/news/world-asia-india-35933452>. Last Accessed on 13 June 2021
2. <https://www.hindustantimes.com/india-news/six-injured-as-bridge-collapses-in-himachal-pradesh/story-4YLhaTTsMK7yzi3jL2AreP.html>. Last Accessed on 13 June 2021
3. <https://timesofindia.indiatimes.com/india/100-bridges-across-the-country-can-collapse-any-time-transport-minister-nitin-gadkari/articleshow/59899965.cms>. Last Accessed on 13 June 2021

4. Azizinamini A et al (2014) Design guide for bridges for service life. SHRP 2 Report S2–R19A–RW-2, Transportation Research Board, Washington DC
5. Oh T, Kee SH, Arndt RW, Popovics JS, Zhu J (2012) Comparison of NDT methods for assessment of a concrete bridge deck. *J Eng Mech* 139(3):305–314
6. Gucunski N et al (2013) Nondestructive testing to identify concrete bridge deck deterioration. SHRP 2 Report S2–R06A–RR-1, Transportation Research Board, Washington DC
7. Vyas V, Patil VJ, Singh AP, Srivastava A (2019) Application of infrared thermography for debonding detection in asphalt pavements. *J Civ Struct Health Monit* 9(3):325–337
8. Solla M, Lagüela S, González-Jorge H, Arias P (2014) Approach to identify cracking in asphalt pavement using GPR and infrared thermographic methods: preliminary findings. *NDT E Int* 62:55–65
9. Malhotra VM, Carino NJ (2003) Handbook on non-destructive testing of concrete, 2nd edn. CRC Press, Florida
10. Wolfe WL, Zissis GJ (1978) The infrared handbook. The Office, Washington
11. Vyas V, Patil VJ, Singh AP, Srivastava A (2020) Debonding detection in asphalt pavements using infrared thermography. *Transp Res Procedia* 48:3850–3859
12. Yehia S, Abudayyeh O, Nabulsi S, Abdelqader I (2007) Detection of common defects in concrete bridge decks using nondestructive evaluation techniques. *J Bridge Eng* 12(2):215–225
13. Kee SH, Oh T, Popovics JS, Arndt RW, Zhu J (2011) Nondestructive bridge deck testing with air-coupled impact-echo and infrared thermography. *J Bridge Eng* 17(6):928–939
14. Washer G, Bolleni N, Fenwick R (2010) Thermographic imaging of subsurface deterioration in concrete bridges. *Transp Res Rec* 2201(1):27–33
15. Hiasa S (2016) Investigation of infrared thermography for subsurface damage detection of concrete structures. Ph.D. Thesis, University of Central Florida
16. Hiasa S, Birgul R, Matsumoto M, Catbas FN (2018) Experimental and numerical studies for suitable infrared thermography implementation on concrete bridge decks. *Measurement* 121:144–159
17. Vaghefi K, Melo e Silva H, Harris D, Ahlborn R (2011) Application of thermal IR imagery for concrete bridge inspection. In: PCI national bridge conference, PCI/NBC, Salt Lake City: UT, pp 1–12
18. Maser K (2004) Active heating infrared thermography for detection of subsurface bridge deck deterioration. Final report for highway IDEA Project 101, Transportation Research Board, Washington DC
19. White J, Hurlbaeus S, Wimsatt A (2015) Concrete bridge deck condition assessment using multi-method nondestructive testing techniques. In: International symposium on non-destructive testing in civil engineering, Berlin, Germany, pp 400–403
20. ASTM D4788–03: Standard test method for detecting delaminations in bridge decks using infrared thermography. ASTM International, West Conshohocken

A Purpose Based Trip Distribution Gravity Model for an Indian City



V. S. Sanjay Kumar and M. V. L. R. Anjaneyulu

1 Introduction

The process of Urban Transportation Planning includes four stages or models, viz. trip generation, trip distribution, mode choice and trip assignment. A model is defined as a simplified representation of part of the real world which concentrates on certain elements considered important for the analysis from a particular point of view [1]. Trip generation models aim at predicting the total number of trips produced in a given origin and the number of trips attracted to a particular destination. Trip distribution models predict the pattern of trips that occur between various zones in the region under study. Mode choice models are meant for predicting mode-wise distribution of trips whereas trip assignment models predict route-wise distribution of trips between a given pair of Origin and Destination.

Trip distribution methods can be broadly divided into Growth factor based and Synthetic method based. Growth factor methods are based on the assumption that the present travel patterns can be projected to the design year in the future by using expansion factors. Synthetic models utilize the existing data to discern a relationship between trip making, the resistance to travel between zones and the relative attractiveness of the zones. Synthetic models have an advantage that they can be used not only to predict future trip distributions but also to synthesize the base year flows.

One of the well-known synthetic models is the Gravity model, which is based on the Newton's concept of gravity. It assumes that the interchange of trips between zones in an area is dependent upon the relative attraction between the zones and the spatial separation between them as measured by an appropriate function of distance.

V. S. Sanjay Kumar (✉)

National Transportation Planning and Research Centre (NATPAC), Thiruvananthapuram, India

M. V. L. R. Anjaneyulu

National Institute of Technology Calicut, Thiruvananthapuram, India

In the original Newtonian formulation, the attraction F , between two bodies of respective masses M_1 and M_2 are separated by a distance D , will be equal to

$$F = g \frac{M_1 M_2}{D^2} \quad (1)$$

where, g is the gravitational constant in the Newtonian formula and is a constant or scaling factor which ensures that the equation is balanced in terms of the measurement units. The numerator of the function is the *attraction* term (or, alternatively, the attraction of M_2 for M_1) while the denominator of the equation, D^2 , indicates that the attraction between the two bodies falls off as a function of their squared distance.

1.1 Literature Review

Abdel-Aal [1] calibrated gravity model of trip distribution for various trip purposes for the City of Alexandria and purpose-based dispersion parameters were estimated based on the weighted sample. Chaeranita et al. [2] developed a gravity model using Tanner Barrier function for Mataram City, Indonesia. Herijanto and Thorpe [3] developed a singly constrained gravity model for Surabaya, Indonesia and used trip attraction factor for each zone based on the amount of trading and industrial activity. Duanmu et al. [4] did freight distribution analysis with Gravity Model and Genetic Algorithm and concluded that travel times were more appropriate for friction factor calculations and also that gamma function was more suitable than the exponential function for friction factor calculations. Xiao-Qiang [5] made use of maximum entropy principle and deduced doubly restraint gravity model with the parameters of mixed land-use entropy. Murat [6] developed a trip distribution model for Istanbul using small sample size and concluded that, a sample size around 1000 for each trip purpose would produce approximately the same parameter estimate as the gravity model with larger sample sizes. Kim et al. [7] developed a trip distribution model for Seoul City using Interzonal Relative Attractiveness and concluded that the interzonal relative attractiveness is non-linear and explained it using variables of zonal spatial properties and interzonal spatial association. The diversity of land use of zones was taken care of in this.

In the Indian context, Shukla and Vyas [8] calibrated a gravity model for trip distribution for Morbi city of Gujarat, India using TransCAD. Impedance factors were developed for travel distance, travel time and travel cost. Salini et al. developed a fuzzy rule based urban trip distribution model on income criteria basis at zonal level for the city of Surat, India. The outcome of their model was frequency of the trips within the zone itself with reference to various income group, with deterrence factor ' α ' of gravity model to vary from 1.74 to 1.60 for varied income groups [9]. Kartik et al. [10] calibrated gravity model for the Anand district, India and used Gravity Model Calibration tool from TransCAD matrix using distance, time and cost attributes.

2 Study Area

The study area selected is Thiruvananthapuram, the capital of Kerala. The City houses several Central and State Government offices and organizations. Apart from being the political nerve center of Kerala, it is also a major academic hub and is home to several institutions. Located strategically nearer to the international sea-route, it is acting as a leading tourist destination and as an administrative center for a long time. With added feathers to its hat like Technopark, one of Asia's largest and first IT hub, new proposed investments like Technocity, proposed International Deep-sea Container Transshipment Terminal, a mass transit system—along the arterial road of the city and studded with the richest temple in the world, Thiruvananthapuram is striding ahead with firm steps to redefine its role in the global systems of cities. As per 2011 census, the total population of Thiruvananthapuram Corporation is 9,86,578 and that of Thiruvananthapuram district is 33,07,284. The population size is more in coastal wards, and the size is less in wards located toward city core.

The map of Thiruvananthapuram Corporation showing the corporation wards is given in Fig. 1.

3 Data Collection and Analysis

Household data collected by the authors for another research study is used for the development of trip distribution models. The travel data of individuals were collected from a sample number of houses in the study area. Table 1 shows the general character of data set obtained from the survey.

4 Trip Distribution Model

Trip distribution was done with gravity model. As implemented for planning models, the Newtonian analogy has been replaced with the hypothesis that the trips between zones i and j is a function of trips originating in zone i and the relative attractiveness and/or accessibility of zone j with respect to all zones. This relative attractiveness and/or accessibility are modeled as an impedance function. Many different measures of impedance can be used, such as travel distance, travel time or travel cost. In this work, the impedance function used is the travel time. For this the zone to zone distance between various zones was calculated. Based on the results from the questionnaire survey, the travel time matrix for zone to zone travel was found. For missing values, the travel time was determined based on the distance and travel time of nearby zones. The adopted Gravity model is as

$$T_{ij} = \alpha O_i D_j f(C_{ij}) \quad (2)$$

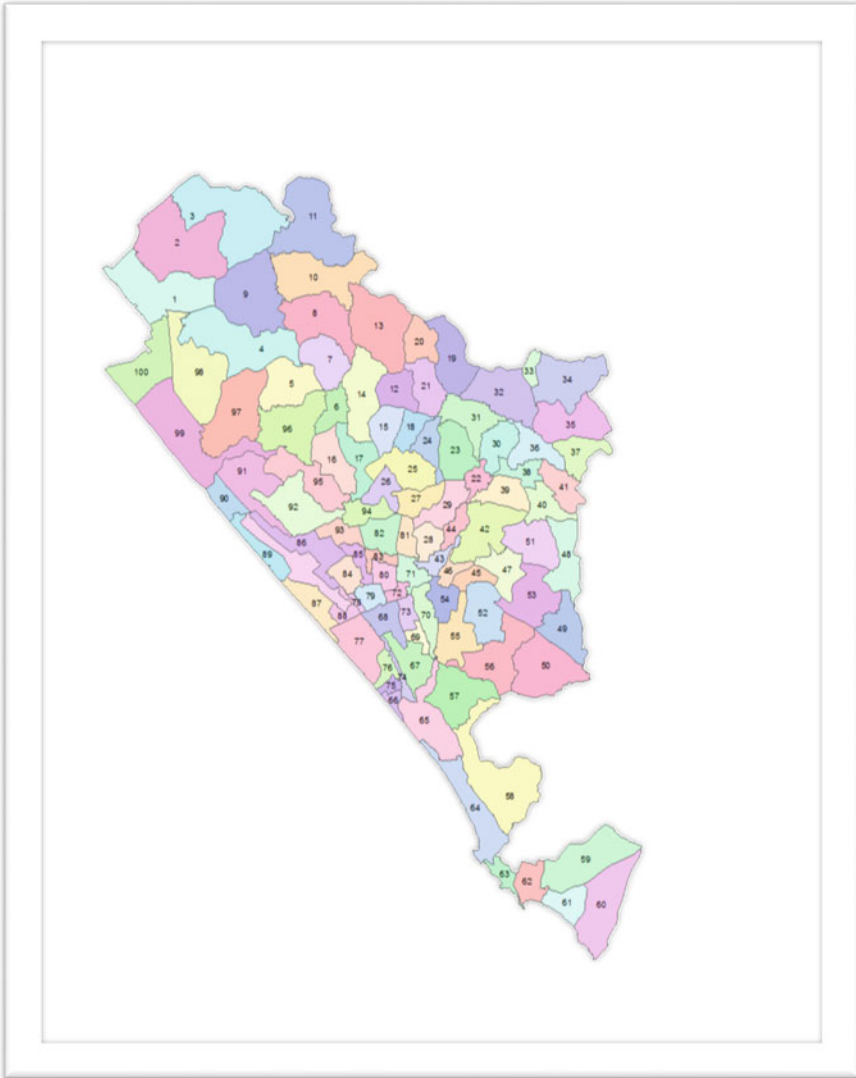


Fig. 1 Ward map of Thiruvananthapuram corporation

where, T_{ij} is the number of trips produced in zone i and attracted to zone j , O_i, D_j the total trip ends produced at i and attracted at j , $f(C_{ij})$ is the generalized travel cost function between any pair of zones i and α is the proportionality factor. The sum of the trips produced between any origin zone i and all destination zones should be equal to the total trip ends produced at the origin zone. Similar statement can be made for any destination zone. These are known as the flow conservation constraints and are given as follows:

Table 1 Characteristics of data set

Variable	Classification	Percentage
Age	<5	4.65
	5–15	10.42
	15–25	16.27
	25–40	26.61
	40–60	29.57
	>60	12.48
Gender	Male	51.18
	Female	48.82
Occupation	Full time	22.15
	Part time	1.61
	Self-employed	9.09
	Student	22.80
	Retired	8.96
	Housewife	27.71
	Unemployed	2.56
	Others	5.13
Income	<1500	1.11
	1501–3000	1.04
	3001–5000	2.72
	5001–10,000	16.57
	10,001–20,000	32.59
	20,001–30,000	19.14
	30,001–40,000	10.91
	40,001–50,000	6.19
	>50,000	9.74
Vehicle ownership	Cycle	0.07
	Two wheeler	0.78
	Car	0.39
	Auto rickshaw	0.04

$$\sum_j T_{ij} = O_i \tag{3}$$

$$\sum_i T_{ij} = D_j \tag{4}$$

To ensure the flow conservation constraints given in Eqs. (3) and (4), the single proportionality factor α should be replaced by two sets of balancing factors A_i and B_j . Introducing these balancing factors in Eq. (2) results in the classical version of

the doubly constrained gravity model which is given as follows:

$$T_{ij} = A_i O_i B_j D_j f(C_{ij}) \quad (5)$$

where

$$A_i = \frac{1}{\sum_j B_j D_j f(C_{ij})} \quad (6)$$

$$B_j = \frac{1}{\sum_i A_i O_i f(C_{ij})} \quad (7)$$

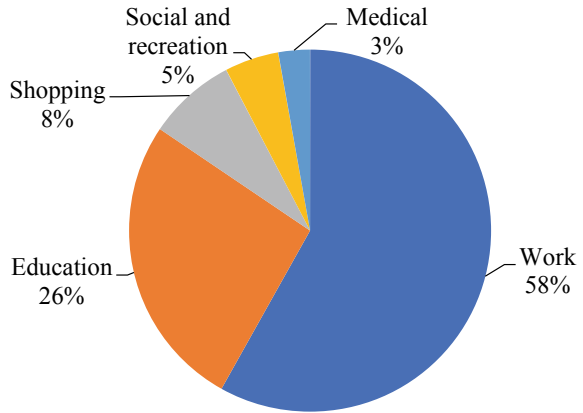
The balancing factors are, clearly, interdependent which suggests that the calculation of one set of the balancing factors requires the values of the other set. This indicates an iterative process.

4.1 Trip Purposes

The present paper is an attempt to model the trip distribution on a purpose-wise manner. It has been assumed that trip distribution is a function of travel time (impedance) and is negatively or inversely proportional, the more the impedance, the lesser will be the number of trips between a given pair of origin and destination. For a given zone, most of the produced trips will get attracted to the nearby zones (destinations itself), with some getting attracted to distant zones, depending on the purpose. For instance, work trips will be destined to the zone where the particular person works and may be at a distance from the home zone. The location of residence will also play a major role in destination selection. Thus, it can be seen that the trip distribution is a function of trip purpose as well, as deterrence function has more relevance in non-work trips than work and education trips, which are mostly of mandatory nature. This necessitates including trip purpose as a variable in the trip distribution model, and in turn resulting in purpose-wise trip distribution models. The trip purposes considered are, W: work trips, E: educational trips (inclusive of both school and college/university trips), S: Shopping trips, SnR: Social and Recreation trips, M: Medical trips.

The distribution of trips by various purposes as per the household survey is given in Fig. 2.

Fig. 2 Purpose wise distribution of trips



4.2 Zone System

The study area for the work, Thiruvananthapuram Corporation is divided into 100 municipal wards. Each of these wards is considered as an internal zone. Along with this, 11 external zones are identified. For the purpose of developing trip distribution model, the trips performed within the study area (with both origin and destination as internal zones) are considered.

4.3 Development of Origin–Destination Matrix

As per the zoning pattern adopted, the total trips generated from the study area were coded and the corresponding Origin–Destination table (O–D) has been obtained. A total of 10,73,958 trips were found to be performed by the city population on a reference day. Of this, proportion of trips having origin and destination outside the study boundary was obtained to be 4.79% and 5.04% respectively. As the O–D matrix is of size 100×100 , the same is not included in the paper.

4.4 Development of Travel Time Matrix

The travel time between each of the O–D pair is determined based on the travel data revealed by the respondents in the questionnaire survey. Corresponding matrix is also generated, which is also of size 100×100 .

4.5 Model Formulation

Trip distribution models were developed in a purpose-wise manner as per Eq. (5). Models were formulated for the following purposes:

- All trips
- Work trips
- Education trips
- Shopping trips
- Social trips
- Medical trips

4.6 Calibration of Gravity Model

Before the gravity model can be used for prediction of future travel demand, it must be calibrated. Calibration for trip distribution is the determination of the values of travel time factors (F_{ij}) and zone-to-zone adjustment factors (K_{ij}) which will produce the zone-to-zone trip tables of the base year from the trip ends (productions and attractions) which are observed in the base year. These factors, F_{ij} and K_{ij} are then assumed constant over time, and by applying them to the trip ends computed for the forecasted year, the future trip-interchanges from zone-to-zone can be computed. To create initial friction factors, the productions and attractions trip table and a network skims matrix are needed. The trip length frequencies from the initial friction factors are compared to observed trip frequencies from the survey for reasonability. Calibrating a gravity model involves adjusting the friction factors until the model adequately reproduces the productions and attractions trip table and matches the observed average trip length and frequencies from the survey. It is suggested that the gravity model simulated and observed trip length frequency distributions should exhibit the following two characteristics:

- (1) The shape and position of both curves should be relatively close to one another when compared visually.
- (2) The differences between the average trip lengths should be within $\pm 3\%$.

4.7 Functions for Friction Factors

In the present work, two types of functions were attempted to determine the friction factor for trip distribution model. They are:

$$f(C_{ij}) = e^{-\beta \times TT} \quad (8)$$

$$f(C_{ij}) = 1/TT^\beta \quad (9)$$

where, β is the dispersion parameter and TT is the travel time which is considered as offering exponential resistance to the trip distribution pattern in Eq. (8). In Eq. (9), the travel time and trip distribution are assumed to be inversely proportional.

4.8 Cumulative Trip Length Frequency Distribution

For different values α , iterations were made to arrive at the best fit between observed and actual trip distribution, complying with the doubly constrained gravity model. Corresponding to the best value of α , Cumulative Trip length frequency distribution plots were obtained for all the trip purposes under consideration using the two types of friction functions and are given from Figs. 3 and 4.

Table 2 summarizes the values of α for each purpose type and function type along with observed and model estimated average trip length, in minutes. The goodness of fit, in terms of χ^2 is also given in the table. As per the observed data, the average trip lengths of different purposes in the study region were almost same. The best fit functions for friction factors and thereby for trip distributions can be inferred from the table.

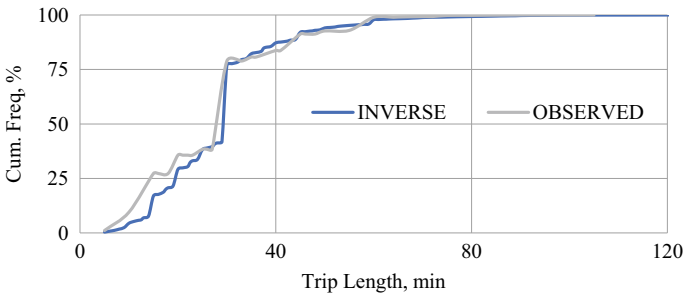


Fig. 3 Cumulative trip length frequency distribution for all trips using inverse function

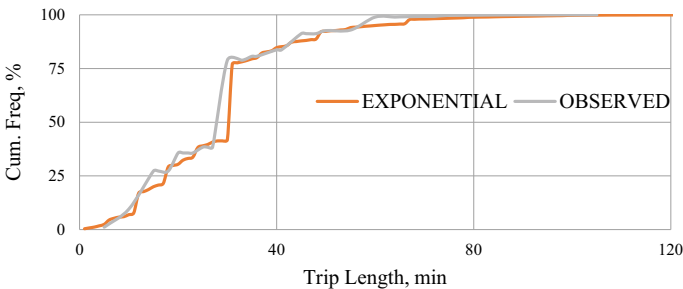


Fig. 4 Cumulative trip length frequency distribution for all trips using exponential function

Table 2 Comparison of friction factors

Trip purpose	Function	Co-efficient	Avg trip length, min		χ^2
			Observed	Estimated	
All trips	Inverse	0.440	28.9378	28.9470	3E-06
	Exponential	0.010		28.8483	3E-04
Work trips	Inverse	0.420	28.2313	28.2203	4E-06
	Exponential	0.013		28.2196	5E-06
Education trips	Inverse	0.425	28.5696	28.5569	6E-06
	Exponential	0.014		28.6082	5E-05
Shopping trips	Inverse	0.425	28.5696	28.6889	5E-04
	Exponential	0.014		28.5569	6E-06
Social trips	Inverse	0.735	25.7611	25.7414	2E-05
	Exponential	0.028		25.7614	3E-09
Medical trips	Inverse	0.240	27.8518	27.8305	2E-05
	Exponential	0.008		27.8561	7E-07

It can be seen that inverse function holds good for all trips, work trips and shopping trips, with the friction factor co-efficient being 0.440, 0.420 and 0.425 respectively. The work trips and education trips are of mandatory in nature. For the non-mandatory trips viz shopping trips, social trips and medical trips, exponential function seemed to fit well with β values as 0.014, 0.028 and 0.008 respectively.

4.9 Formulated Gravity Models

The gravity models formulated in a purpose-wise mode, for the study area under consideration are tabulated in Table 3.

Table 3 Purpose wise trip distribution models

Purpose	Model
All trips	$T_{ij} = A_i O_i B_j D_j \times TT^{-0.44}$
Work trips	$T_{ij} = A_i O_i B_j D_j \times TT^{-0.42}$
Educational trips	$T_{ij} = A_i O_i B_j D_j \times TT^{-0.425}$
Shopping trips	$T_{ij} = A_i O_i B_j D_j \times e^{-0.014 \times TT}$
Social trips	$T_{ij} = A_i O_i B_j D_j \times e^{-0.028 \times TT}$
Medical trips	$T_{ij} = A_i O_i B_j D_j \times e^{-0.008 \times TT}$

5 Conclusion

The paper is an elaboration of development of framework for calibrating and developing a doubly constrained gravity model for an Indian city. Purpose-wise calibration parameters has been determined considering that some of the trip purposes are mandatory and are to be destined to the place of attraction barring the impedance factor whereas some trip types like shopping and social trips are non-mandatory, where impedance effect is more. The whole procedure was based on the household survey carried out in the study region. The travel time between the zone centroids has been taken as the impedance for developing trip distribution functions. The calibration was done through an iterative process. Two types of functions viz inverse and exponential functions were attempted. The results obtained were used to determine the average trip length (which was taken as travel time in minutes). The function which approximated the estimated average trip length with the observed trip length is taken as most suited. It was observed that inverse function holds good for all trips, work trips and shopping trips whereas for the non-mandatory trips viz shopping trips, social trips and medical trips, exponential function fitted well. The developed model is observed to match with the realistic data and can determine the trip distribution pattern for the city.

References

1. Abdel-Aal MMA (2014) Calibrating a trip distribution gravity model stratified by the trip purposes for the city of Alexandria. *Alex Eng J* 53:677–689
2. Chaeranita HF, Abusini S, Marjono MT (2017) Analysis of gravity model with tanner barrier function influenced by entropy of land use integrated. *Am J Eng Res*
3. Herijanto W, Thorpe N (2005) Developing the singly constrained gravity model for application in developing countries. *J Eastern Asia Soc Trans Stud*
4. Duanmu J, Foytik P, Khattak A, Robinson RM (2012) Distribution analysis of freight transportation with gravity model and genetic algorithm. *Transp Res Record*
5. Xiao-Qiang L (2015) The proof of gravity model with negative exponential land-mixed entropy and similar to the method of Hyman calibration technology. *Open Civil Eng J*
6. Murat CH (2010) Sample size needed for calibrating trip distribution and behavior of the gravity model. *J Transp Geography* 18
7. Kim TG, Rho JH, Kim G (2010) Developing a trip distribution model using the interzonal relative attractiveness for the Seoul metropolitan city. *J Eastern Asia Soc Transp Stud*
8. Shukla RN, Vyas T (2018) Calibration of gravity model with impedance factors for medium town in India. *Global Res Dev J Eng*
9. Salini PS, Katti BK, Silpa PP, Krishna J (2016) Developing a fuzzy rule based urban trip distribution model on income criteria basis at zonal level: a case study. *IOSR J Mech Civil Eng*
10. Kartik SZ, Zala RLB, Vankar AA (2013) Gravity model calibration and use in trip distribution. *J Int Acad Res Multidisciplinary*

Effect of Jarosite as Partial Replacement of Fine Aggregate in Pavement Quality Concrete Mixes



Dinesh Ganvir and Binod Kumar

1 Introduction

Solid waste management is a major challenge around the world due to ever-increasing quantities of waste materials and industrial by-products. Because of the scarcity of land-filling area and the rising expense of disposal, the use of industrial by-products and waste materials has become a more appealing option. Industrial trash and by-products come in a variety of forms. The use of such components in concrete not only makes it more cost-effective, but it also helps to alleviate disposal worries. Jarosite waste is one such industrial by-product. Jarosite is a waste product created during the hydrometallurgy process of extracting zinc ore concentrate. Zinc ore concentrate contains about 50% zinc. This concentration is roasted at 900 °C and subjected to leaching where jarosite is formed as a waste material. This material is mixed with 2–3% lime and is pumped to jarosite pond in slurry form having around 55% waste. The accumulated jarosite material from Hindustan Zinc Ltd. at Chittorgarh, Rajasthan, India, is around 10 lac metric tonnes. The amount of collected material that has not been used is estimated to be around 1.5 million metric tonnes. [1].

Various types of industries produce large volumes of industrial waste by-products, such as foundry sand, copper slag, zinc slag, and steel slag [2]. These materials were regarded as waste for many years and discarded near the industrial plant. Research investigations are being conducted to see if this trash can be used in different layers of pavement and concrete. The feasibility of jarosite as a concrete addition has been investigated through research.

Chen and Dutrizac [3] Jarosite material has been stabilized using portland cement for safe disposal. Vsevolod [4] has advocated for the use of jarosite mixed with

D. Ganvir (✉) · B. Kumar
Rigid Pavement Division, CSIR-CRRI, NewDelhi 110025, India

B. Kumar
e-mail: binod.ccri@nic.in

a small percentage of cement and lime to increase strength in a variety of applications, including road subbase and base layer, air field pavement, dams, and the replacement of natural crushed stone/gravel/sand in the production of tiles, bricks and other building materials. Pappu [5, 6] conducted research on utilization of jarosite in making of composite bricks. Aggrawal et al. [7] studies the beneficial use of jarosite with ordinary portland cement in aggressive environment. Jarofix's potential as a fine aggregate substitute in embankment and sub-base construction has been demonstrated [8]. The quantity of jarosite as a cement replacement in concrete pavement were investigated, and it was suggested that 15% of jarosite may be employed as a cement replacement in concrete pavement [9]. Mehra et al. [10] studied the effect of jarosite on mechanical and durability properties of concrete and recommended that jarosite can be used as partial replacement of sand upto 25% when used with mineral admixture and 15% as a replacement of sand for road and building construction purpose. Due to limited literature available on the use of jarosite in civil engineering applications, the current study was conducted to investigate the possible use of jarosite as a fine aggregate replacement in pavement quality concrete.

The goal of the research is to investigate jarosite as a partial replacement for fine aggregate in rigid pavement construction and to test its strength and durability properties in pavement concrete mixtures (PQC). Initially, PQC mixtures were proportioned by replacing the fine aggregate with jarosite of varying concentrations. For PQC mixes, the effect of jarosite on concrete workability, compressive strength, flexural strength, drying shrinkage and abrasion resistance was investigated.

2 Material

In the present study, OPC 43 grade cement conforming to IS:8112 was used. The cement's compressive strength was 35.3 and 49.0 MPa at 7 and 28 days, respectively. Coarse aggregate used was crushed stones with maximum nominal sizes of 20 mm and 10 mm. The coarse aggregate's density and water absorption were 2.72 g/cm³ and 0.54%, respectively. Fine aggregate used was double washed filter sand and density, water absorption and fineness modulus (FM) 2.71 g/cm³, 1.20% and 2.02 respectively. The jarosite used in the study was supplied by Hindustan Zinc Limited. The specific gravity of jarosite was 3.0. Composition of the jarosite used in the study contain 27–35% iron oxide, 23–29% sulfur trioxide, 9–12% silicon oxide, 7–9% calcium oxide and 6–8% aluminum oxide. A polycarboxylic ether based superplasticizer was used in the study to achieve the desired workability in the concrete.

3 Methodology

The proportions of the mixture were calculated based on the absolute volume of the wet mixture with 2% entrapped air. Fine and coarse aggregates each accounted for

Table 1 Mix proportioning for pavement quality concrete (PQC)

Ingredients	Proportions (Kg/m ³)			
	J0	J10	J20	J30
Cement	400	400	400	400
Water	156	156	156	156
Jarosite	Nil	84.12	168	252
Fine aggregate	737	664	590	516
Crushed stone	1144	1144	1144	1144
Superplasticizer	3.2	3.2	3.2	3.2

40% and 60% of the total coarse aggregates, respectively. The effect of jarosite on the characteristics of green and hardened concrete was investigated using mixtures containing varying amounts of jarosite. For controlled mixtures, the cement content and water cement (w-c) ratio were 400 kg/m³ and 0.39, respectively. For optimal workability with jarosite, the amount of superplasticizer was found to be 0.8% by weight of the cementitious material. Concrete mixtures containing 0%, 10%, 20% and 30% jarosite as replacement of fine aggregate were prepared. Concrete mix proportions for pavement quality concrete are given in Table 1. J0, J10, J20 and J30 denotes the mixture containing 0, 10, 20 and 30% jarosite respectively.

For each mixture, six cubes (100 mm) for compressive strength, six beams (100 × 100 × 500 mm) for flexural strength, 3 prism (75 × 75 × 275 mm) for drying shrinkage and three slabs (500 × 500 × 100 mm) for conducting the abrasion resistance of concrete were prepared.

4 Result and Discussion

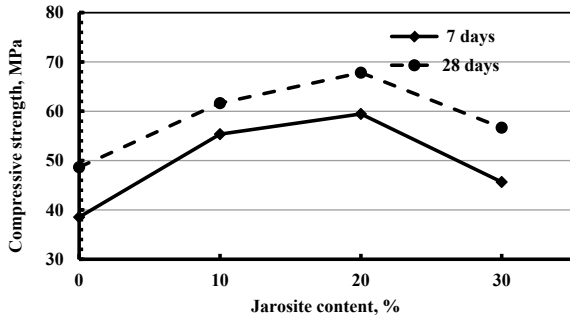
4.1 Workability

The compaction factor, which is defined as the ratio of the weight of partially compacted concrete to the weight of fully compacted concrete when the test is completed according to Indian Standard IS 1199, was used to assess the workability of the PQC mixes (BIS 2004). The values of the compacting factor are given in Table 2. The concrete's compacting factor decreased as the amount of jarosite in the mix increased. When jarosite was replaced with fine aggregate, the mix's water requirement increased, lowering the compaction factor for the same amount of water and superplasticizer. The decrease in compacting values were due finer gradation of jarosite compared to fine aggregate used in the study. In the mixes containing jarosite, however, there was no segregation or separation of cement slurry was observed.

Table 2 Compacting factor values

Mix designation	Compacting factor
J0	0.92
J10	0.90
J20	0.89
J30	0.86

Fig. 1 Jarosite content versus compressive strength



4.2 Compressive Strength

All PQC mixes, concrete cube specimens were tested for compressive strength at 7 and 28 days after being removed from the water curing tank. Figure 1 depicts the compressive strength of all of the blends containing varying percentage of jarosite.

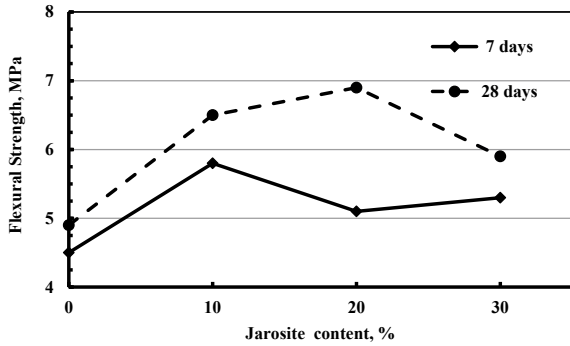
The results of compressive strength of the mixtures ranged between 38 and 59 MPa after 7 days and 48.8 MPa and 67.83 MPa after 28 days. It can be seen from the Fig. 1 that replacement of jarosite with fine aggregate showed a significant increase in 7 and 28 days compressive strength upto 20% replacement. Further replacement led to the decrease in strength at all 7 and 28 days. The strength development of the mixes with jarosite up to 20% substitution of fine aggregate showed a definite pattern.

The compressive strength of the concrete was influenced by the content of jarosite. As a result, it was determined that up to 20% jarosite fine aggregate had no negative impact on the compressive strength of concrete.

4.3 Flexural Strength

The flexural strength of concrete is important in the design of concrete pavement which is based on the flexural stresses of concrete. The flexural strength of all the concrete mixtures was determined by testing concrete beam specimens with dimensions of 100 mm × 100 mm × 500 mm under a third-point loading system shortly after their removal from the water tank after curing. Figure 2 depicts the flexural strength development of all concrete combinations.

Fig. 2 Jarosite content versus flexural strength



The results show an increase in flexural strength in 7 and 28 days with an increase in jarosite content of up to 20%, with greater replacement lowering the strength. At 7 and 28 days, the flexural strength of concrete increased by up to 20% when jarosite was replaced with fine aggregate.

4.4 Drying Shrinkage

A length measurement frame with a digital dial gauge capable of measuring up to 0.001 mm was used to calculate the drying shrinkage of the concrete or the change in length owing to a change in moisture content, as per the Indian standard IS 1199. Before testing, concrete samples were allowed to cure for 28 days. The initial length of a specimen was measured immediately after it was removed from the water. During the test, cycles of drying for 44 h and cooling for 4 h were repeated until a constant specimen length was attained. Figure 3 shows the variation in drying shrinkage values of concrete mixtures including various amounts of jarosite.

The drying shrinkage of the concrete decreased as the percentage of jarosite concentration increased, as seen in Fig. 3. It reduced from 675 microstrains in the

Fig. 3 Effect of Jarosite content on drying shrinkage

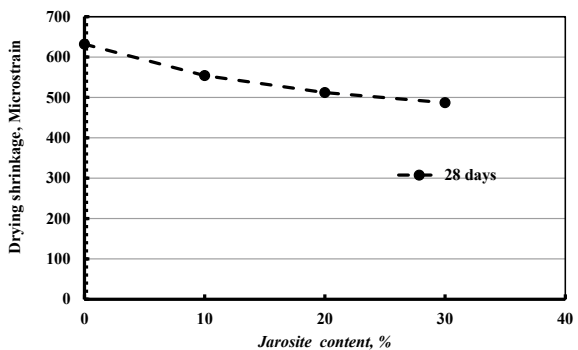
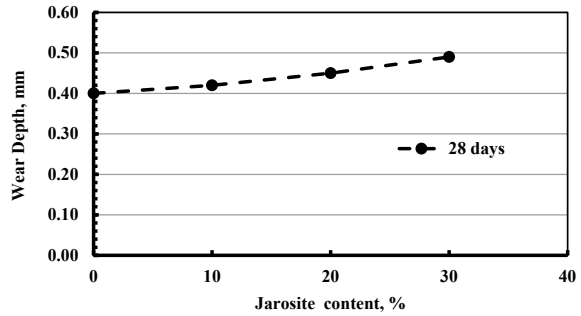


Fig. 4 Effect of Jarosite content on abrasion resistance of concrete



control mix J0 to 475 microstrains in the mix J30. When fine aggregate is replaced with jarosite in the concrete mix, the drying shrinkage of the concrete is reduced.

4.5 Abrasion Resistance of Concrete

Relative abrasion resistance of concrete mixes containing different amount of jarosite was determined in terms of wear depth produced on the concrete surface due to revolving discs of the machine in conjunction with abrasive grit as per procedure of ASTM standard C779 (ASTM 2000). In order to conduct the test, a concrete specimen measuring 500 mm × 500 mm × 100 mm was produced in the laboratory. After 28 days of water curing, the specimens were tested (Fig. 4).

After 60 min, the wear depth on the slab was measured, and it increased as the amount of jarosite in the mix increased. The wear depth of slab after 60 min, increased from 0.40 mm for the control mix to 0.49 mm for the J30 mix. As a result, when compared to the control mix, the abrasion resistance of the concrete containing jarosite reduced marginally.

5 Conclusion

Based on the laboratory investigation, the following conclusions were drawn.

- Replacement of fine aggregate with jarosite significantly reduces the workability of the concrete mixes.
- By substituting jarosite for cement up to 20%, the concrete mix's compressive and flexural strength increased.
- Drying shrinkage of the concrete reduce significantly with increase in jarosite content.
- Abrasion resistance of concrete decreased with increase in jarosite content.

- In pavement quality concrete mixes, jarosite can be used as a partial replacement for fine aggregate up to a percentage of 20%.

Acknowledgements Prof. Satish Chandra, Director, CSIR-Central Road Research Institute, granted permission to publish the research article to the authors. The project was funded under the 12th five-year plan project sponsored by CSIR, New Delhi. The help provided by Ms. Aashia, Technician during laboratory work is thankfully acknowledged.

References

1. CRRRI Report (2010) Feasibility study of Jarofix waste material for embankment and sub grade. Published by Central Road Research Institute under Council of Scientific and Industrial Research (CSIR), New Delhi, India
2. Collins RJ, Ciesielski SK (1994) Recycling and use of waste materials and by-products in highway construction. NCHRP synthesis of highway practice No. 199, Transportation Research Board, Washington, DC
3. Chen TT, Dutrizac JE (2000) A mineralogical study of Jarofix products for the stabilization of Jarosite residues for disposal. TMS, pp 917–933
4. Vsevolod AM, Haroldo AP, Patricio RI (2005) Potential application of acid Jarosite wastes as the main component of construction materials. *J Constr Build Mater* 19:141–146
5. Pappu A, Saxena M, Shyam R (2006) Hazardous jarosite use in developing non-hazardous product of engineering application. *J Hazardous Mater* 137(3):1589–1591
6. Pappu A, Saxena M, Asolekar SR (2006) Jarosite characteristics and utilization potentials. *Sci Total Environ* 359:1–3.232–243
7. Aggrawal SK, Ali M, Pahuja A, Singh BK, Duggal S (2014) Mineralizing effect of jarosite: a zinc industry by-product in the manufacturing of cement. *Adv Cement Res* 27(5):248–258
8. Sinha AK, Havanagi VG, Arora VK, Mathur S (2012) Design, construction and Evaluation of jarofix embankment and subgrade layers. *Int J Environ Eng Res* I(3):97–103
9. Gupta T, Sachdeva SN (2019) Investigations of Jarosite mixed cement concrete pavements. *Arabian J Sci Eng*. <https://doi.org/10.1007/s13369-019-03801-1>
10. Mehra P, Gupta RC, Thomas BS (2016) Properties of concrete containing jarosite as partial substitute for fine aggregate. *J Clean Prod* 120:241–248

Comparison of Various Approaches for Evaluation and Overlay Design of a Concrete Pavement



Shubham Mishra, Rakesh Kumar Srivastava, Pradeep Kumar, and Tanuj Chopra

1 Introduction

Portland cement concrete pavement slab may be constructed with or without steel reinforcement. Under wheel load, top and bottom fibres of slab experience compressive as well as tensile stresses, respectively. The stresses developed are resisted by beam action or flexural strength of cement concrete slab. Concrete pavement has slab action and through a broader area it will transfer the wheel load stress [1]. Components of cement concrete pavement are depicted in Fig. 1.

In rigid pavement, the critical condition of stress is highest flexural tension taking place in slab because of wheel load and temperature alterations where as in bituminous pavement it is due to allocation of compressive stresses. Comparison between flexible and rigid pavement is shown in Fig. 2.

2 General Methodologies for Design of Overlay

The method for overlay design is analogous to design of latest road expects that during overlay, remaining life of active road is considered. By considering pavement as a new, the overlay design technique is also utilised for design of new combined pavement [4].

There are primarily three approaches which can be utilised for design of overlay:

1. Effective—thickness approach

S. Mishra (✉) · T. Chopra
Department of Civil Engineering, Thapar Institute of Engineering and Technology, Patiala,
Punjab, India

R. K. Srivastava · P. Kumar
Pavement Evaluation Division, CSIR—Central Road Research Institute (CRRI), New Delhi, India

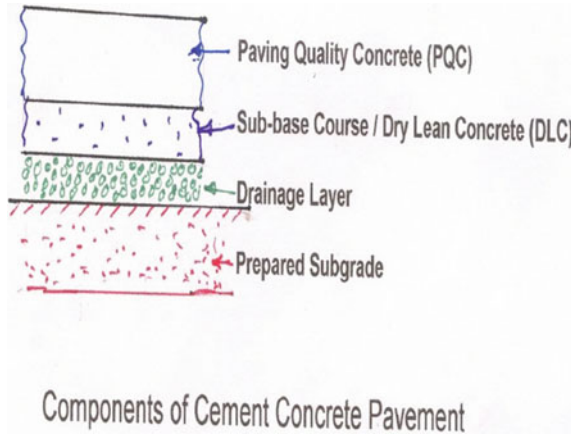


Fig. 1 Components of cement concrete pavement [2]

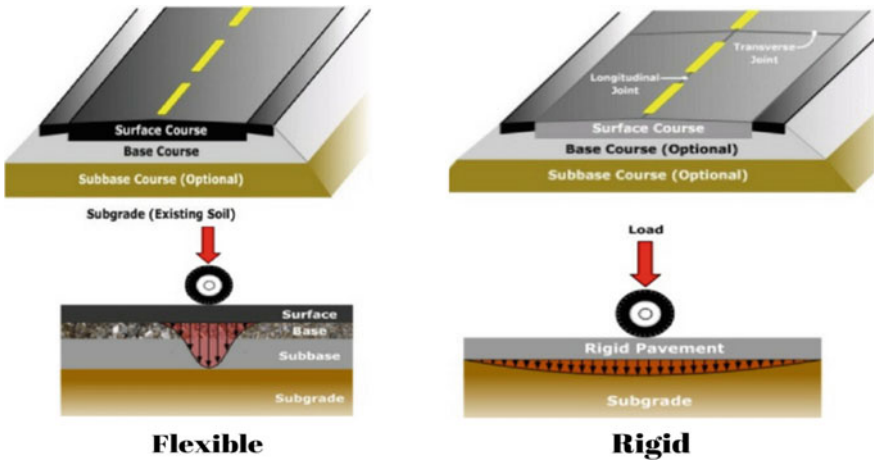


Fig. 2 Comparison of flexible and rigid pavement [3]

- 2. Deflection approach
- 3. Mechanistic empirical approach.

2.1 Effective-Thickness Approach

The fundamental idea of this approach is that the deviation among thickness requisite for latest road and effective thickness of active road gives the requisite overlay thickness. This approach has been used by AASTHO method.

$$D_{ol} = D_f - D_{eff} \quad (1)$$

D_{ol} = Required thickness of overlay

D_f = Thickness of new pavement

D_{eff} = Effective thickness of existing pavement.

2.2 Deflection Approach

The fundamental idea of this approach is that the very weak road and subgrade which are signified by greater the value of road surface deformations requires thick overlays. Thickness of the overlay is so that deformations reduce to adequate quantity. Only larger deformation below the load is computed in this approach.

2.3 Mechanistic Empirical Approach

This approach is analogous to design of latest roads. Critical stress, strain and deformation are computed in the road by utilising this approach. The consequential harm to the road can be calculated by utilising mechanistic techniques. Firstly, the present situation of residual life of active road is computed. Then on the basis of that residual life and thickness of overlay is then determined [1].

3 American Association of State Highway and Transportation Officials Method (AASTHO Method)

3.1 PCC Overlays on PCC Pavements

PCC overlays on PCC pavements are primarily categorised in three:

1. Un-bonded
2. Bonded
3. Partially bonded

Un-bonded Overlay

It is mainly a thick Portland cement concrete sheet over an existing concrete pavement. Its thickness relatively varies from 125 to 305 mm (5 –12 in.). These overlays are typically placed on badly cracked pavements. To prevent the reflection cracking in between new overlay and the existing pavement, a division layer generally comprising of sand asphalt is placed in between them (Fig. 3).

Fig. 3 Un-bonded overlay [5]

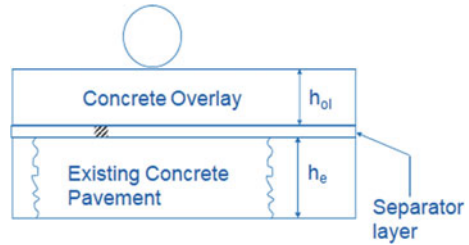
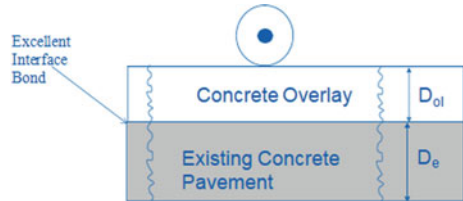


Fig. 4 Bonded overlay [5]



Partially Bonded Overlay

In this overlay, on the existing dirt-free slab a concrete is spread directly over it. This overlay is designed less thick than above mentioned overlay so that stress which is reduced can be utilised.

Bonded Overlay

It is mainly a thin PCC sheet over an existing concrete pavement. Its thickness is typically less than 100 mm (4 in.). This type of overlay is utilised when severe distresses have restored and active road is in better situation. Slurry or grout is used to make a bond between active road and new overlay (Fig. 4).

In this study, existing pavement was found to be in good condition therefore, **bonded PCC overlay** was adopted.

4 Design of Thickness

If overlay is provided for functional enhancement of the pavement such as to improve roughness properties of road then a least thickness of overlay may be adopted. But if it is to be provided to structurally enhance the pavement (Fig. 5) then it should meet the upcoming traffic demand [4].

In this study, overlay thickness was determined by using effective thickness approach.

There are mainly two methods to calculate the effective thickness of active slab:

1. D_{eff} (By utilising condition survey for PCC pavements)
2. D_{eff} (By utilising remaining life for PCC pavements)

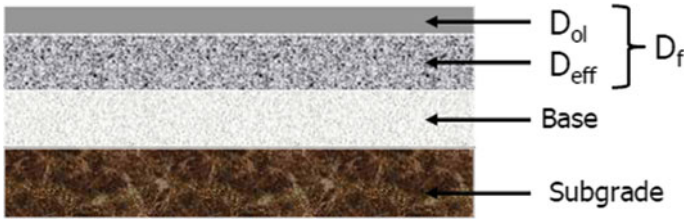


Fig. 5 Bonded overlay thickness design [5]

In this study, the effective thickness was calculated from condition survey for PCC pavements.

4.1 D_{eff} (by Utilising Condition Survey)

Effective thickness of active slab is computed by using subsequent equation:

$$D_{eff} = F_J \times F_D \times F_F \times D \tag{2}$$

Here,

- D = Thickness of active PCC slab, inches
- F_J = Joints and cracks modification factor
- F_D = Durability modification factor
- F_F = Fatigue damage modification.

As all the weaken joints and cracks in the active slab were repaired before overlay hence the joints and cracks adjustment factor was taken to be $F_J = 1$. Since, in the existing section only durability cracking was found and there was no sign of spalling, therefore, durability adjustment factor for existing road was taken to be $F_D = 0.96$. Most of the cracks were repaired before the overlay so there were only few transverse cracks left. Hence, fatigue damage adjustment factor was taken to be $F_F = 0.97$.

Effective thickness of existing slab was calculated using Eq. (2)

where

$$F_J = 1, F_D = 0.96, F_F = 0.97, D = 340 \text{ mm}$$

Therefore, using Eq. (2) $D_{eff} = 316.6 \text{ mm} = 12.5 \text{ in.}$

4.2 Computation of Requisite Slab Thickness for Upcoming Traffic (D_f)

Thickness of slab requires for upcoming traffic was calculated using design equation of concrete pavement (which is given in AASHTO 1993). The rigid pavement design equation is given below:

$$\begin{aligned} \text{Log}_{10}(W_{18}) = & Z_R S_O + 7.35 \text{Log}_{10}(D_f + 1) - 0.06 \\ & + \left(\text{Log}_{10} \left(\frac{\left\{ \frac{\Delta \text{PSI}}{(4.5-1.5)} \right\}}{1 + \frac{1.624 \times 10^7}{(D_f + 1)^{3.46}}} \right) \right) \\ & + (4.22 - 0.32 P_t) \times \text{Log}_{10} \left(\frac{S_c \times C (D_f^{0.75} - 1.132)}{215.63 \times J \left(D_f^{0.75} - \frac{18.42}{\left(\frac{E}{k} \right)^{0.25}} \right)} \right) \end{aligned} \quad (3)$$

where in this case,

D_f = Thickness of slab (inches)

W_{18} = 30 million standard axles (MSA)

P_t = Serviceability at time $t = 2.5$

Z_R = Standard normal deviate = 1.282 (for 90% reliability)

J = Load transfer coefficient = 4.1 (for tied PCC shoulder with no load transfer device)

S_O = Common standard error = $S_o = 0.39$ (If traffic projection error is considered)

P_i = Serviceability at time $t = 2.5$

ΔPSI = Drop in present serviceability index = $P_i - P_t = 4.2 - 2.5 = 1.7$

C = Drainage coefficient = 1.14

E = Elastic modulus (psi)

S_c = Modulus of rupture of concrete (psi)

k = Modulus of subgrade reaction (pci)

To calculate E , S_c and k structural evaluation of rigid pavement was performed. In this study, deflection values were measured by **falling weight deflectometer** with sensor located at 0, 200, 300, 450, 600, 900, and 1200 mm (0, 8, 12, 18, 24, 36, 48 in.).

Structural Evaluation Using FWD

FWD simulates a moving wheel load and measure the deflection of pavement surface. Load is created by dropping weights on top of a loading plate from specified height on to a sequence of springs. The maximum load and maximum vertical deflection of surface are measured at altered radial locations. Working of FWD is shown in Fig. 6 [6].

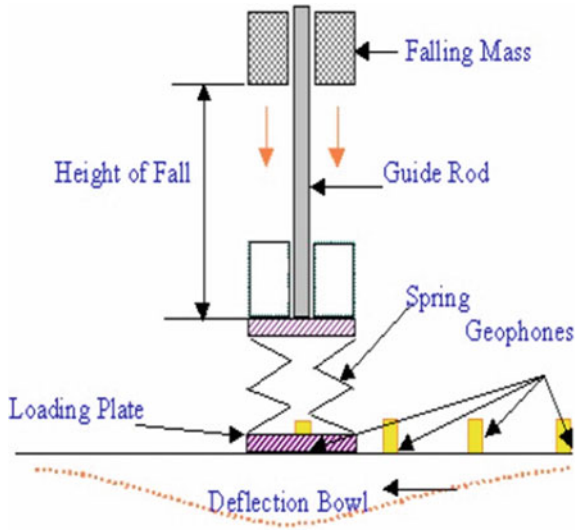


Fig. 6 Working of FWD [6]

According to IRC-117, 300 mm diameter load plate is suggested for evaluation of rigid pavements. Figure 7 is showing the deflection profile recorded by FWD at different sensor locations.

Deflection profile is a key output. Temperature and load data are used with deflections for back-calculation of pavement structure characteristics. Effective k-value

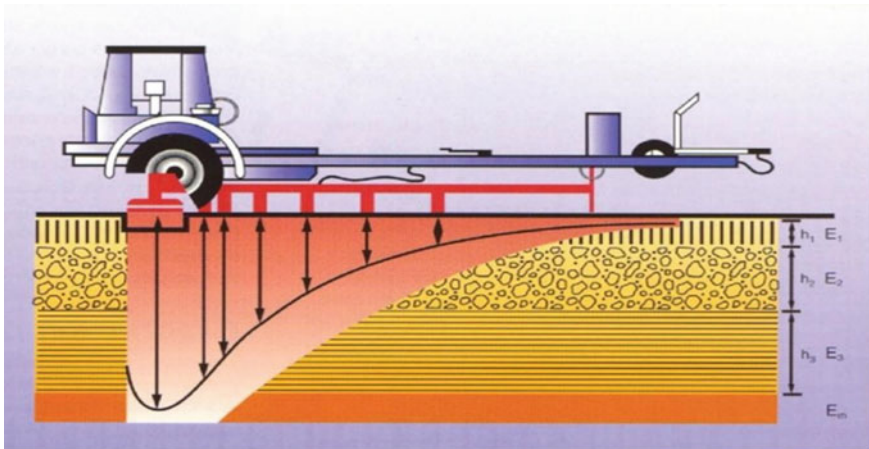


Fig. 7 FWD trailer showing deflection profile recorded at different sensor locations. Source Road Infrastructure Management Support New-Zealand

Table 1 Various parameter calculated as per IRC-117 guidelines [8]

Serial No.	Area parameter (mm)	Radius of relative stiffness (mm)	Dynamic modulus of subgrade reaction (MPa/m)	Effective modulus of subgrade reaction (MPa/m)	Modulus of elasticity (E_c) (MPa)	Flexural strength of concrete (MPa)
1	742.384	747.062	196.236	98.118	18,265.521	2.56
2	758.921	813.875	169.413	84.7065	22,212.908	3.11
3	760.325	820.09	177.92	88.96	24,049.074	3.37
4	780.151	918.673	138.27	69.135	29,430.67	4.12
5	771.832	874.695	151.15	75.575	26,439.906	3.7
6	753.035	788.79	146.407	73.2035	16,936.906	2.37
7	755.073	797.301	192.795	96.3975	23,281.474	3.26
8	730.25	704.569	228.114	114.057	16,798.618	2.35
9	807.904	1099.951	106.854	53.427	46,742.566	6.54
10	812.8	1138.68	105.637	52.8185	53,069.63	7.43
11	769.471	862.928	139.063	69.5315	23,042.853	3.23
12	778.79	911.197	111.695	55.8475	23,009.661	3.22
13	719.75	671.523	230.008	115.004	13,977.028	1.96
14	766.618	849.113	146.936	73.468	22,825.293	3.2
15	779.282	913.89	132.398	66.199	27,598.474	3.86
16	814.251	1150.62	74.867	37.4335	39,214.316	5.49
17	801.816	1054.93	88.112	44.056	32,610.609	4.57
Average				74.58	27,029.73571	3.78

and modulus of elasticity of slab were calculated by means of excel sheet provided by IRC-117 and presented in Table 1.

FWD deflection data was composed at interiors, corners, transverse and longitudinal joints on external lane at a distance of 500 m because heavy loads travel mostly on outer lanes. Pavement and air temperatures were also recorded during FWD testing. Load position for corner, interior, transverse and longitudinal shoulder joints is shown in Fig. 8 [6].

Evaluation of Subgrade Modulus, Elastic Modulus of Concrete and Strength of Pavement Concrete

In this study, deflections were calculated at 17 points by using FWD.

Thickness PQC = 340 mm.

DLC Thickness = 150 mm.

Radius of loading plate = 150 mm.

Elastic modulus of concrete (E_c) = 27,029.74 MPa.

Since, 1 MPa = 144.93 psi

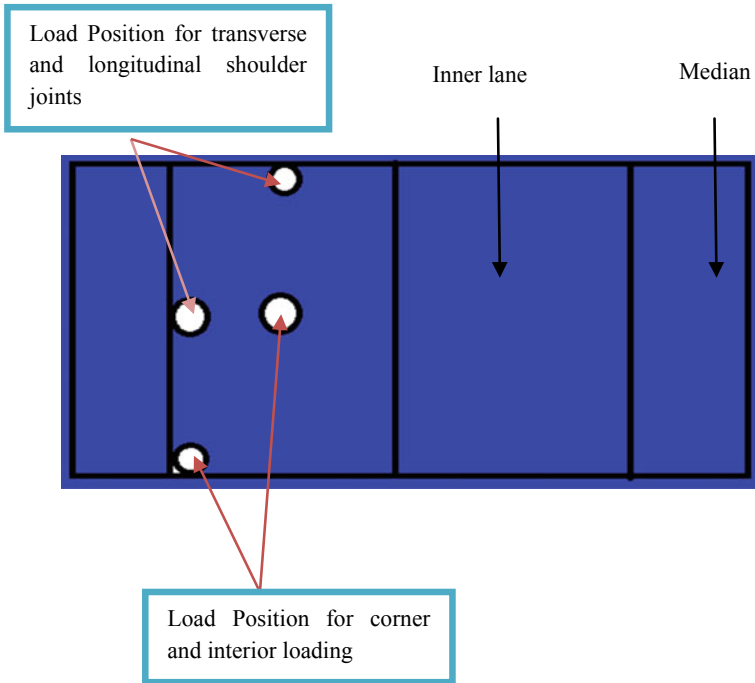


Fig. 8 Load position for corner, interior, transverse and longitudinal shoulder joints

$$E_c = 3917353.62 \text{ psi}$$

Flexural strength of concrete (S_c) = 3.78 MPa.

$$S_c = 547.83 \text{ psi}$$

Modulus of subgrade reaction (k) = 74.58 MPa/m.

Since, 1 MPa/m = 3.69 pci.

$$k = 275.2 \text{ pci}$$

Values of above parameters were substituted in design equation and the value of requisite thickness of slab was calculated (D_f) = 13.93 in. = 353.82 mm.

Required thickness of bonded PCC overlay (D_{ol}) was calculated as per Eq. (1).
where

D_f = Thickness of slab = 13.93 in. = 353.82 mm.

D_{eff} = Effective thickness of active slab = 12.5 in. = 316.6 mm.

Therefore, $D_{ol} = 1.43 \text{ in.} = \mathbf{38 \text{ mm.}}$

4.3 Evaluation of Subgrade Modulus, Elastic Modulus of Concrete and Strength of Pavement Concrete Using Different Approaches

Serial No.4 from Table 1. was selected for evaluation of subgrade modulus, elastic modulus of concrete and strength of pavement concrete using different approaches. Deflection values at 0, 200, 300, 450, 600, 900 and 1200 mm sensor locations were 93.2, 87.1, 83.1, 79, 73.9, 69.9 and 58.8 μm .

FHWA Procedure [7]

Area Parameter

It is computed utilising following formulae [8]

$$A = 6 \left[1 + 2 \left(\frac{D_1}{D_0} \right) + 2 \left(\frac{D_2}{D_0} \right) + \frac{D_3}{D_0} \right] \quad (4)$$

Here

A = Area parameter of deflection basin.

D_0 = Deflection at centre of loading plate in mm = 0.0932 mm.

D_1 = Deflection in mm at 300 mm from middle of plate = 0.0831 mm.

D_2 = Deflection in mm at 600 mm from middle of plate = 0.0739 mm.

D_3 = Deflection in mm at 900 mm from middle of plate = 0.0699 mm.

Therefore, area of deflection basin using Eq. (4) = 30.71 in.

Radius of Relative Stiffness [8]

Area and radius of relative stiffness are correlated to each other as shown in Eq. (5) and the values of regression coefficients k_1 k_2 k_3 and k_4 were taken from FHWA guidelines.

$$1 = \left[\frac{\ln \left(\frac{k_1 - A}{k_2} \right)}{-k_3} \right]^{\frac{1}{k_4}} \quad (5)$$

$k_1 = 36$, $k_2 = 1812.597$, $k_3 = 2.559$, $1/k_4 = 4.387$ [6]

$A = 30.71$ in.

Therefore using Eq. (5) $l = 37.24$ in. = 945.81 mm.

Calculation of Normalised Deflection Values [8, 9]

Normalised deflections are calculated by using following equation

$$dr'' = a * e - b * e^{(-c * l)} \quad (6)$$

where

d_r'' = non-dimensional deflection coefficient (Normalised deflections) at a distance r from load

a, b, c are coefficients of regression

l = Radius of relative stiffness in inches

Using Eq. (6)

$$d_0' = 0.123$$

$$d_{12}' = 0.115$$

$$d_{24}' = 0.100$$

$$d_{36}' = 0.082$$

Modulus of Subgrade Reaction [8]

It was calculated by using following equation

$$k_i = \frac{P * d_r''}{l * l * Di} \quad (7)$$

where

$$i = 1, 2, 3, 4$$

k_i = Modulus of subgrade reaction MPa/mm

c = Subgrade constant MPa

P = Load in KN

Di = Measured deflections in mm at various radial distance (inches)

d_r'' = Normalised deflections in mm at various radial distances

Using Eq. (7) $k = 131.477$ MPa/m.

Elastic Modulus of Concrete [10]

It was calculated by using following equation

$$E_c = \frac{12(1 - \mu_c * \mu_c)k * l^4}{1000 * h^3} \quad (8)$$

where

$$\mu_c = 0.15$$

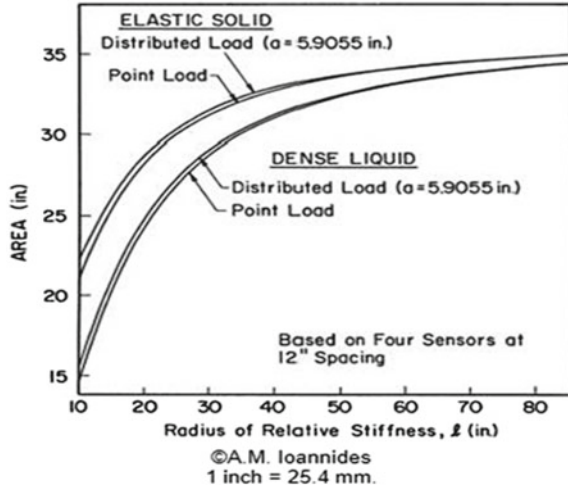
$$h = 340 \text{ mm}$$

$$l = 919.067 \text{ mm}$$

$$k = 138.27 \text{ MPa/m}$$

E_c = Elastic modulus of concrete in MPa

Fig. 9 Variation in area with radius of relative stiffness [4]



Using Eq. (8)

$$E_c = 31452.18 \text{ MPa}$$

Ioannides, Barenberg and Lary Approach [11]

They establish a sole connection between radius of relative stiffness and AREA, as depicted in Fig. 9. From Fig. 9 for area of 30.71 in., radius of relative stiffness = 40.1 in. = 1018.54 mm.

Effective Dynamic k -Value

It was determined using Fig. 10, which shows the relationship between highest deformation and deformation basin area.

In this case maximum deflection = 0.093 mm.

Since, 1 mm = 39.37 mils.

Therefore, maximum deflection = $d_0 = 3.669$ mils.

From the graph (Fig. 10.)

$$k = 380 \text{ pci}$$

Therefore, $k = 103.09 \text{ MPa/m}$ (since, 1 pci = 0. 2713 MPa/m).

The k -value which was obtained from chart was dynamic k -value, whereas the k -value to be utilised by AASTHO design equation is Static k -value. The following equation was used for conversion:

$$\text{Static } k - \text{value} = \frac{\text{Dynamic } k - \text{value}}{2} \tag{9}$$

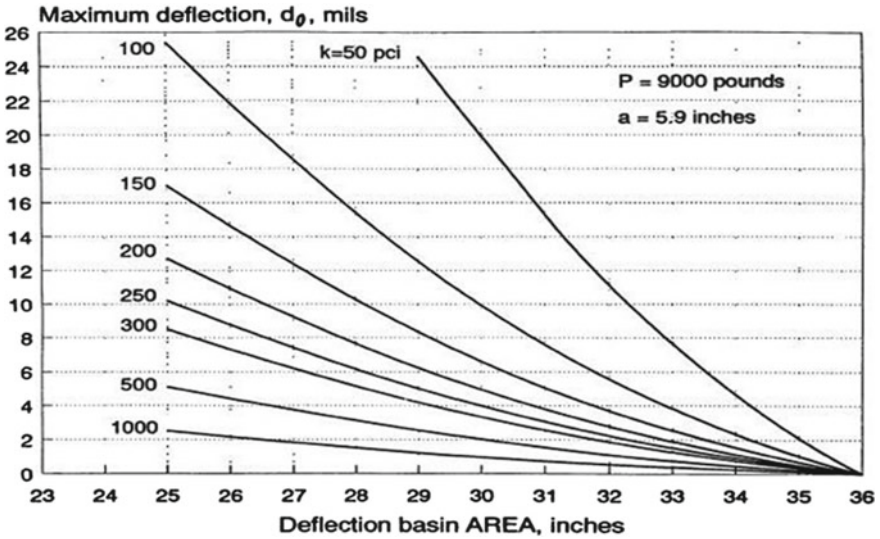


Fig. 10 Effective k -value computation from d_0 and deformation basin area [4]

Therefore, static k -value using Eq. (9) = 51.55 MPa/m.

Elastic Modulus of concrete [12]

It was computed from k -value, area and slab thickness by using Fig. 11. From Fig. 11 for $A = 30.71$ in. and $k = 380$ pci

$$ED^3 = 10^{9.91}$$

Since, D = slab thickness in inches, $D = 340$ mm = 13.39 in. Therefore,

$$E = 3385776.36 \text{ psi} = 23361.86 \text{ MPa} (1 \text{ psi} = 0.0069 \text{ MPa})$$

The results obtained from three approaches are presented in Table 2.

5 Conclusion

In this study, Falling weight deflectometer was used for measuring the deflection values of the project road. These deflection values were utilised for computation of area parameter, radius of relative stiffness, modulus of subgrade reaction and elastic modulus of concrete as per IRC-117 code guidelines. These parameters were also calculated using graphs given by Ioannides and Barenberg and FHWA procedure. A comparison was made and percentage variability was computed. It was found that

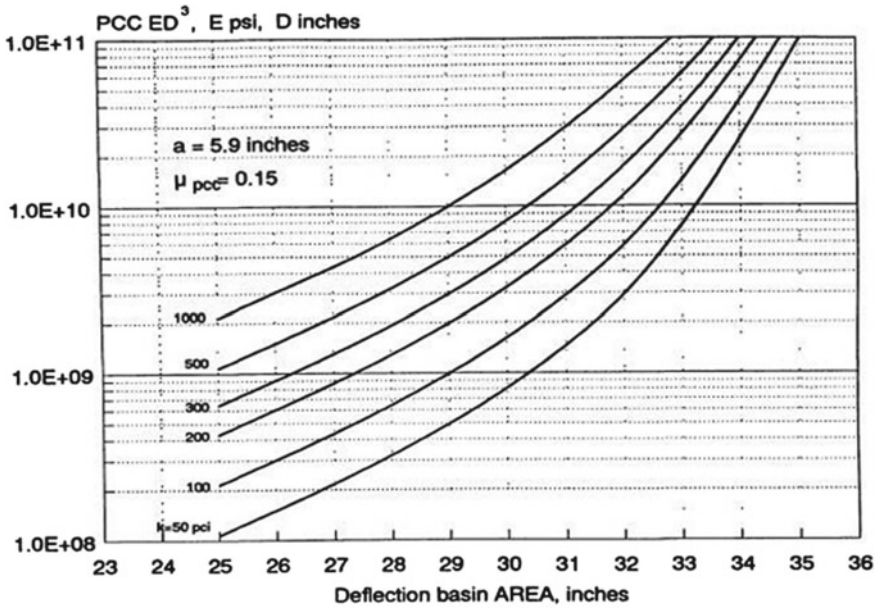


Fig. 11 Computation of elastic modulus of concrete [4]

Table 2 Comparison of results obtained from three approaches

Methods	Area parameter (A) (inches)	Radius of relative stiffness (l) (mm)	Modulus of subgrade reaction (k) (MPa/m)	Elastic modulus of concrete (E _c) (MPa)	Difference of E _c from IRC-117 guidelines (%)
IRC-117 guidelines	30.71	918.67	69.08	29,430.67	
FHWA Procedure	30.71	945.81	65.74	31,452.18	6.87
Ioannides, Barenberg and Lary Approach	30.71	1018.54	51.55	23,361.86	20.62

elastic modulus of concrete, calculated using Ioannides and Barenberg graphs varied substantially with the IRC-117 guidelines in comparison with the FHWA procedure. Percentage difference for elastic modulus of concrete between IRC-117 guidelines and Ioannides and Barenberg approach was found to be 20.62%, whereas for FHWA procedure it was only 6.87%. PCC bonded overlay thickness was also designed for the rigid pavement using AASHTO method and it was determined to be 38 mm.

References

1. AASHTO guide for design of pavement structures. American Association of State Highway and Transportation Officials, Washington, DC (1993)
2. Bombay I (n.d.) Pavement types and design factors. Retrieved from IIT Bombay Web site: <https://www.civil.iitb.ac.in>
3. Comparison of Flexible and Rigid Pavement (n.d.) Retrieved from Engineering Discoveries Web site: <https://engineeringdiscoveries.com/>
4. Huang YH (1993) Pavement analysis and design
5. Roesler J (2015) Concrete pavement overlay design. University of Illinois Urbana, Champaign
6. IRC-117 (2015) Guidelines for the Structural Evaluation of Rigid Pavement by Falling Weight deflectometer. Indian Road Congress, Delhi
7. Using Falling Weight Deflectometer data with Mechanistic-Empirical Design and Analysis Volume I: Final Report. (2018). Retrieved from fhwa.dot.gov: <http://www.fhwa.dot.gov>
8. Nokes WA (1993) Evaluation of backcalculation methods to predict pavement layer moduli
9. Flintsch GW, Al-Qadi IL, Loulizi A, Lahouar S, McGhee KK, Clark T (2005) Field investigation of high performance pavements in Virginia. Virginia Center for Transportation Innovation and Research
10. Hall KT (1992) Backcalculation solutions for concrete pavements. A paper prepared for long-term pavement performance data analysis
11. Barenberg EJ, Petros KA (1991) Evaluation of Concrete Pavements Using NDT Results. Final Summary Report. No. FHWA/IL/UI 233
12. Ioannides AM (1990) Dimensional analysis in NDT rigid pavement evaluation. J Transp Eng 116(1):23–36

Investigating the Intention to Use Metro Services: A Behavioral Approach



Anshamol N. Rahim, Jomy Thomas, and Vishnu Baburajan

1 Introduction

India faces severe traffic congestion, environmental pollution and other urban problems. To address the issues related to urban transportation, the Government of India and various state governments have initiated projects that aim at encouraging the use of public transport and reducing the use of personal vehicles [1]. Several megacities have developed metro rail systems as an efficient and environment-friendly mass rapid transportation mode.

Kochi (aka Cochin) is one of India's important ports and a major naval base. The population of Greater Cochin area is growing at a rate of 1.4% per annum. The absence of an efficient and reliable mass transport system has contributed to a steep increase in the number of personalized motor vehicles in Greater Cochin Development Authority (GCDA) area. From a modest number of 68,271 in 1987, the number of vehicles has surged to a whopping 446,959 vehicles by the year 2003 of which 64% are motorized two-wheelers [2]. The increasing vehicular population has contributed to a steep increase in air pollution, road accidents and travel time in the city. Kochi metro rail project was aimed to be a sustainable and comfortable transportation solution that will shift travelers toward public transport.

Shifting from personal vehicles to public transport depends largely on how attractive the service is to the travelers. Studies investigating the attitudes and shifts toward metro can be categorized into two studies carried out prior to the implementation

A. N. Rahim (✉) · J. Thomas

Department of Civil Engineering, Rajiv Gandhi Institute of Technology, Kottayam, India

J. Thomas

e-mail: jomy@rit.ac.in

V. Baburajan

MIT-Portugal Program, Instituto Superior Técnico, Universidade de Lisboa, Lisboa, Portugal

e-mail: vishnu.baburajan@tecnico.ulisboa.pt

and after the implementation of the project. Past studies have aimed at understanding the commuter's perception of various transfer facility attributes in and around metro stations in Kolkata [1]. The results indicate that commuters give importance to the qualitative attributes of transfer facility and contradict the common belief that the metro fare is the major concern for commuters in emerging countries such as India. Another study investigated the commuter's willingness to pay (WTP) for improvement to the transfer facilities in Kolkata and the findings indicate high WTP of metro commuters as compared to the average metro fare for improvement of various qualitative attributes of transfer facilities in the station [3]. Other factors influencing the willingness to use were the location of metro stations, metro station's features, metro's features, gender, the number of daily trips, the purpose of trips and the average travel [4]. Furthermore, mode shift behavior of auto, taxi, bus, electric bicycle and bicycle users after the implementation of metro service was studied based on Stated Preference (SP) survey data in Xi'an, China [5]. The results indicate that auto travelers located in suburban regions are more willing to shift to metro for work trips. Female taxi and auto users are more likely to shift to metro than males and long-distance travelers using taxi and electric bicycles prefer to choose the new metro mode. Mode shifting behavior toward a newly operational metro rail in Mumbai was studied to understand the factors considered most important by user. A Revealed Preference (RP) survey on commuters using newly operational metro rail line and a SP survey on commuters living in the catchment of proposed additional metro rail line were conducted [6]. The results show that all the parameters of waiting time, travel time, travel cost and discomfort are highly significant.

The decision to use a new mode of transport is guided by the socio-demographic and travel characteristics of the individual. However, unobserved factors such as attitudinal factors also play a very important role in this decision-making. This makes it important to analyze the role of attitudes influencing the intention to use the new mode (metro)—which has not received much attention in India, to our best knowledge. The present work aims to bridge this gap by investigating the intention to use the second phase of Kochi metro for commute using a behavioral approach. We use the theory of planned behavior (TPB) proposed by Ajzen [7]. In developing countries such as India, where the financial resources are scarce, undertaking such studies will help to understand the factors that need to be given due consideration, prior to the implementation of the new transportation infrastructure.

In this regard, this study pursues the following two objectives:

- To investigate the intention to use the second phase of Kochi metro for commute
- To analyze the role of attitudes of the individual, friends and family and a conducive environment in the intention to use the proposed service

A paper-based survey instrument was designed for the study, and responses were collected from commuters in the study area. The behavioral framework linked the intention to use Kochi Metro to the attitudes toward that behavior, subjective norms and perceived behavioral control. Exploratory factor analysis was applied to the TPB construct items to extract the factors which were later used as explanatory variables to model the intention to use the metro. In addition to these, the socio-demographic

characteristics and current trip characteristics were included in the specification. An ordered probit model was used to estimate the intention to use the metro service for commute along the proposed extension, considering the ordinal nature of the dependent variable.

The travel demand generated in Kochi includes trips for various purposes such as work, shopping, leisure, education, business and goods transport. This study includes only commuter trips to offices, commercial establishments and educational institutions within the study area. This is because travel for these activities is the major contributor to the congestion during peak hours. The survey was conducted among commuters residing, working or studying in areas within one km on either side of proposed alignment of Phase II of Kochi metro from Jawahar Lal Nehru (JLN) International Stadium located at Kaloor to Infopark via Kakkanad.

The remainder of the paper is structured as follows. The next section describes the data collection methodology. The third section presents the analysis and model estimation results. The very last section gives a summarized discussion of the results. The limitations of this study and the scope for further research are also discussed in this section.

2 Data

2.1 Study Area

Kochi Metro Rail started operating along the 18 km stretch between Aluva, a suburb of Kochi, and the city center near Maharaja's College with 16 stations along the route. The extension of this first phase connecting Maharaja's College to Pettah is also currently operational. The proposed Phase II is an 11.2 km extension connecting JLN Stadium to Infopark via Kakkanad with 11 stations on the line. The State Cabinet approved Phase II of the Kochi Metro in May 2017 which is expected to cost Rs. 2500 crore. Our study area includes the regions along the proposed Phase II extension of Kochi metro.

2.2 Description of the Study Area

The JLN Stadium-Kakkanad route is one of the busiest routes in Kochi. As per the revised DPR, it is likely to attract about 1.04 lakh passengers by 2023. We intend to figure out the underlying factors that are of importance to the users—prior to the implementation of the project. The study will help to understand commuter's behavior and identify factors that motivate or discourage people to use the proposed extension of Kochi metro. Employees from Infopark, Kakkanad Civil Station, other state and

central government establishments at Kakkanad, and many private and government educational institutions and business establishments along the route were included in the study.

2.3 Behavioral Framework

The framework is based on the theory of planned behavior (TPB), a theory used to predict and explain human behavior in specific contexts. The theory links behavioral intentions to attitudes, subjective norms and perceived behavioral control. According to TPB, the more favorable the attitude toward the behavior and subjective norms and the greater the perceived behavioral control, the stronger will be an individual's intention to perform the behavior under consideration [7]. Interested readers may refer to [7] for further information on TPB. It has been used extensively in travel behavior research—in analyzing intention to use public transport [8], mass rapid transit system [9], urban bike-sharing systems [10], shared autonomous vehicles [11] and to study the relationship between young people's transit use and their perceptions of equity concepts in transit service provision [12]—to name a few.

The behavioral framework adopted in the current study to explain the commuter's intention to use the new metro mode is shown in Fig. 1. This framework served as the basis for the design of the survey for data collection and the quantitative analysis described in the following sections.

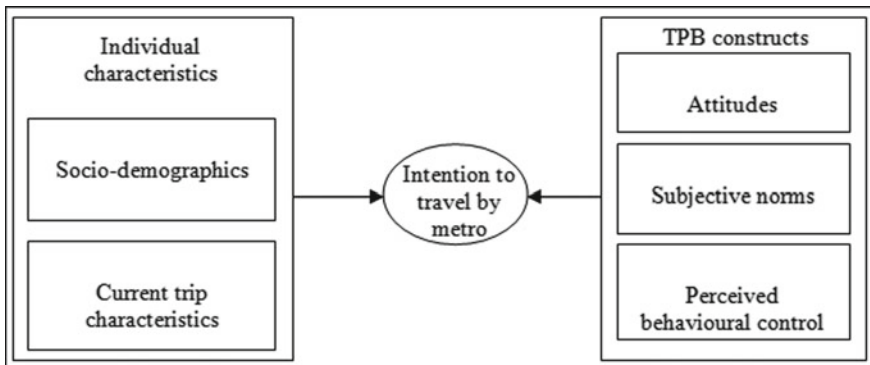


Fig. 1 Behavioral framework

2.4 Survey Design

The questionnaire designed in accordance with the theory of planned behavior was based upon a review of the related literature. The questionnaire consists of 50 questions grouped into six sections. The responses to the attitudinal questions were collected using a five-point Likert scale anchored between the two extremes “strongly disagree” and “strongly agree.” A detailed discussion on each of the six sections is presented below:

Part I: Socio-demographic variables: These variables depict the characteristics of the individuals surveyed. They include measures such as gender, age group, education, occupation, monthly income and vehicle ownership.

Part II: Attitude toward metro—Attitude means the degree to which a person has a favorable or unfavorable appraisal of behavior. In order to obtain in-depth qualitative information about traveler attitudes toward Kochi metro, a series of attitudinal statements are presented in this section. Examples of such statements include “I am interested in using public transit services such as metro,” “I think metro is affordable,” “I think the metro makes travel faster,” etc. All the items in this section pertain to the construct “attitude” of TPB.

Part III: Subjective norms: This section captures the perceived social pressure to perform or not to perform the behavior. A series of statements regarding what the friends and family think are presented in this section. Examples of such statements include “Most of my friends and family would encourage me using Kochi metro,” “Most of my friends and family consider metro affordable,” “Most of my friends and family think metro makes travel faster,” etc. All the items in this section pertain to the construct “subjective norms” of TPB.

Part IV: Perceived behavioral control: It includes questions to understand how difficult or easy it may be for them to take metro while traveling to work. The respondents indicate the extent to which they agree or disagree with the statements given in the section on a five-point Likert scale. Examples of such statements include “I have concerns regarding the frequency of service of Kochi metro,” “I have concerns regarding parking facilities at metro station,” “I think metro is a comfortable mode of travel,” etc. All the items in this section constitute the construct “perceived behavioral control” of TPB.

Part V: Intention to use: We asked commuters to indicate their intention of choosing the second phase of Kochi Metro for their daily commute on a five-point scale ranging from extremely unlikely to extremely likely.

Part VI: Trip characteristics information: This portion of the survey collected detailed information about the daily trip made by the respondent. They include work location, mode used for commute, average trip duration (per side) in minutes, daily travel expenses for the current trip, distance from home to the nearest bus stop/metro station and that from the bus stop/metro station to final destination, mode of transport to travel from home to nearest bus stop/metro station and that from bus stop/metro station to final destination. The respondents were also asked whether they have a penalty for late arrival at the workplace.

The survey instrument was revised and finalized according to feedback from the pilot survey carried out on 18 commuters (taken as a convenience sample) in the study area. This helped to find out the time taken to administer the questionnaire and to remove any ambiguity in questions. The time taken for a single response was around 4–5 min when the respondents filled in the questionnaire by themselves and about 12–15 min if the questionnaire was administered personally to the respondents. To prevent respondents from answering the questionnaire without reading the questions, it was decided that the survey will be administered by enumerators to all the respondents in the main survey. Cronbach alpha scores were determined for analyzing the reliability or internal consistency of items in the questionnaire and was found to be above 0.7 (acceptable) [13].

2.5 Survey Administration

An on-site survey was conducted among commuters working or studying in the areas within 1 km on either side of proposed metro line alignment of Phase II of Kochi metro. The convenience sampling technique was employed as the population of commuters in the area was not available [9]. The survey was conducted at workplaces and educational institutions during working days with prior consent. The questionnaire was designed in English. It was administered personally to the respondents. Some respondents were unable to take the full survey and left midway citing reasons like lack of time or accidental distractions. After removing records with incomplete responses, the final sample size comprised of 326 responses.

3 Data Analysis and Model Development

3.1 Sample Characteristics

The collected data were entered in MS Excel and the descriptive analysis of the data was done. The socio-demographic characteristics of respondents' gender, age, level of education, occupation, monthly income and mode used for the trip are shown in Fig. 2. There were respondents falling under all categories of age group, education and monthly income. The sample had a slight over-representation of women, individuals aged between 26 and 35, highly educated (graduates and postgraduates) and professionals.

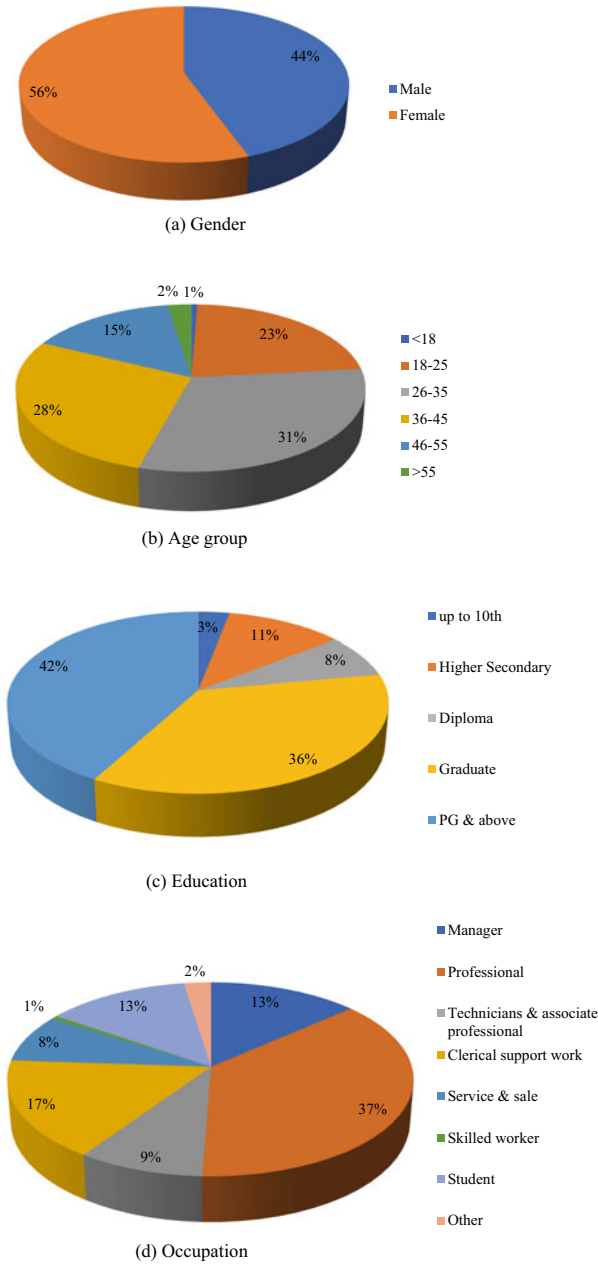
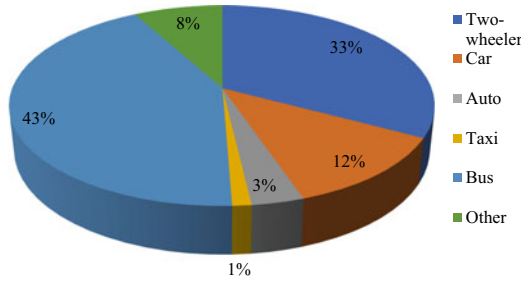
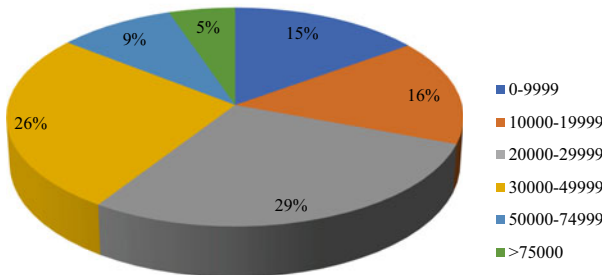


Fig. 2 Socio-demographic characteristics of the respondents



(e) Mode of travel used for commute



(f) Monthly income

Fig. 2 (continued)

3.2 Exploratory Factor Analysis

The factors under attitudes, subjective norms and perceived behavioral control related to intention to use metro were obtained by means of exploratory factor analysis (EFA) using SPSS software. Cronbach alpha coefficients were calculated to check for the internal consistency of all TPB constructs prior to obtaining meaningful factors. Alpha values range between 0 and 1. The closer Cronbach’s alpha coefficient is to 1.0, the greater the internal consistency of the items in the scale. The Cronbach alpha coefficient for attitude, subjective norms and perceived behavioral control were obtained as 0.722, 0.824, and 0.720, respectively. Hence, all the alpha values obtained were greater than the minimum acceptable value (0.7) indicating that internal consistency is acceptable [13].

Exploratory factor analysis using the principal component with varimax rotation technique was applied to TPB construct items [14]. This helps to reduce the number of variables tested in the models and also minimize potential collinearity problems. The Kaiser–Meyer–Olkin (KMO) measure was used to check the sampling adequacy and its value ranges from 0 to 1. In this study, the KMO value obtained for each construct (0.718, 0.827 and 0.709) suggests that the data are well suited for factor analysis. Factors with an eigenvalue (the amount of variance accounted for a factor) greater than 1.0 were only retained. The items under each factor were retained only if they had

value of loadings greater than 0.5. Six items were removed due to low communalities and low factor loadings. The estimation results of the principal component factor analysis with the factor loadings are presented in Table 1. The resulting factors were then added to the data set and used as explanatory variables in the model.

The various factors extracted from EFA are explained below:

- “F_A_Safe” reflects the role of the metro as a fast mode and more importantly as a safe mode for women as well as a mode of transport safe from accidents. It also captures attitude toward cleanliness in metro train and stations.
- “F_A_Enviro” captures the role of the metro as an environment-friendly mode that reduces pollution while addressing the issue of congestion.
- “F_A_PubTra” reflects the interest of people toward public transit such as metro and their comfortability in sharing travel with others.
- “F_A_Conv” depicts the perception of the metro as a convenient mode of transport that enhances the mobility of women, aged and differently abled while enabling individuals to pursue other activities such as browsing, newspaper reading, music listening and interacting with people during travel.
- “F_S_Use” depicts the perception toward the use of metro (currently operational) among friends and family and their encouragement to use the metro. It also reflects the intention of the respondents’ friends and family to use the second phase of Kochi metro.
- “F_S_Att” captures the positive attitude of friends and family toward the metro as a fast, safe, environment-friendly and congestion-free mode of transport.
- “F_P_Comf” reflects people’s perception of the metro as a comfortable and secure mode of travel.
- “F_P_Manag” represents people’s perception of the management of metro train and station (frequency of service, formalities at station such as ticketing and baggage checking).
- “F_P_Con” represents people’s perception on the first and last-mile connectivity to and from metro station as well as the flexibility of combining travel for shopping, recreation etc. with work trip while using metro mode.
- “F_P_Oper” reflects people’s perception of operating hours of Kochi metro.

3.3 Ordered Probit Model

Since the intention to use the second phase of Kochi metro for daily commute was measured on a five-point Likert scale, an ordered probit model was used in this study for the estimation of the model for predicting the intention to use Kochi Metro [15]. To gain more insights into the underlying principle and the estimation procedure, readers could refer to [16, 17]. Ordered probit models have been used extensively in travel behavior research to study the willingness to use a public bicycle system in Nanjing City [18], for the analysis of work-zone crashes in Egypt [19], for the analysis of life satisfaction in Albania [20], to study the intention to use shared autonomous vehicles [11], to name a few.

Table 1 Estimation results of factor analysis

Variable	Factor_1	Factor_2	Factor_3	Factor_4
Latent factors for attitude	F_A_Safe	F_A_Enviro	F_A_PubTra	F_A_Conv
Interest in using public transit services such as metro			0.807	
Comfortable sharing travel with others			0.813	
Metro helps to reduce pollution from transportation		0.884		
Metro reduces transport problems such as congestion		0.860		
Metro offers safe travel by reducing accidents	0.642			
Metro makes travel faster	0.681			
Metro ensures safety for women	0.790			
Cleanliness is given importance in metro stations and trains	0.621			
Browsing, listening to music, newspaper reading and interacting with people is possible during metro travel				0.864
Metro enhance mobility to women, aged and differently abled				0.537
KMO statistic	0.718			
Latent factors for subjective norms	F_S_Att	F_S_Use		
Friends and family use Kochi metro		0.897		
Friends and family encourage me using Kochi metro		0.871		
Friends and family intend to use the second phase of Kochi metro		0.698		
Friends and family consider metro environment-friendly	0.818			
Friends and family think metro makes travel faster	0.874			
Friends and family think metro offers safe travel	0.889			
Friends and family think metro reduces congestion	0.834			
Friends and family think metro is safe for women	0.726			
KMO Statistic	0.827			
Latent factors for perceived behavioral control	F_P_Comf	F_P_Manag	F_P_Con	F_P_Oper

(continued)

Table 1 (continued)

Variable	Factor_1	Factor_2	Factor_3	Factor_4
Metro is a comfortable mode of travel	0.909			
Metro offers secure travel	0.919			
Operating hours of Kochi metro is a concern				0.862
The flexibility of combining travel for shopping, recreation, etc. with work trip			0.773	
First and last-mile connectivity to and from metro station			0.863	
Frequency of service of Kochi metro		0.577		
Frequency of service should be adjusted to reduce crowding		0.700		
Formalities at the metro station (baggage checking, ticketing) need to be simpler		0.731		
KMO statistic	0.709			

The model assumes a latent parameter and the different levels are chosen based on the values of this latent parameter. For every level of the ordered dependent variable, there exists a threshold value for the latent parameter. Based on this, the probability of choice is determined. The objective of the research is to estimate a model for this latent parameter. The functional forms for latent variable for each of the three models (explained in the following paragraphs) are given below:

Constants only model

$$\text{latent parameter}(\mu) = \beta_0 \tag{1}$$

Model 1

$$\begin{aligned} \text{latent parameter}(\mu) = & 0.072 * FA_{\text{Safe}} + 0.152 * FA_{\text{Enviro}} + 0.125 * FA_{\text{PubTra}} \\ & + 0.107 * FA_{\text{Conv}} + 0.060 * FS_{\text{Att}} + 0.202 * FS_{\text{Use}} \\ & + 0.225 * FP_{\text{Manag}} + 0.111 * FP_{\text{Oper}} \end{aligned} \tag{2}$$

Model 2

$$\begin{aligned} \text{latent parameter}(\mu) = & 0.182 * FA_{\text{Safe}} + 0.162 * FA_{\text{Enviro}} + 0.137 * FA_{\text{PubTra}} \\ & + 0.042 * FA_{\text{Conv}} + 0.000 * FS_{\text{Att}} + 0.168 * FS_{\text{Use}} \\ & + 0.216 * FP_{\text{Manag}} + 0.194 * FP_{\text{Oper}} - 0.361 * \text{Non} - \text{Graduates} \\ & + 0.541 * \text{No} - \text{vehicles} - \text{owned} + 0.259 * \text{Trip} - \text{duration}_{0-15} \\ & + 0.347 * \text{Trip} - \text{duration}_{15-30} + 0.197 * \text{Trip} - \text{duration}_{30-60} \\ & + 0.914 * \text{Trip} - \text{duration}_{60-120} - 0.747 * \text{Trip} - \text{cost}_{0-25} \end{aligned}$$

$$\begin{aligned}
 & - 0.314 * \text{Trip} - \text{cost}_{25-50} - 0.207 * \text{Trip} - \text{cost}_{50-100} \\
 & - 0.836 * \text{Trip} - \text{cost}_{100-120}
 \end{aligned}
 \tag{3}$$

Firstly, a model (Model 1) was estimated by including only the TPB factors as explanatory variables. A second model (Model 2) was estimated by adding the socio-demographics and current trip characteristics in the specification, in addition to TPB factors. The results of the ordered probit model and the goodness-of-fit measures for both the models are presented in Table 2. Wald testing was used to test the coefficient significance of the model [18]. For both models, the relationship between significant independent variables and intention to use the metro services was analyzed. It must, however, be noted that some variables, whose coefficients are meaningful but are not statistically significant, have also been retained to avoid the risk of Type II error [11].

The performances of models were assessed based on the goodness-of-fit measures (See Table 2). From an initial log-likelihood (constants only) value of -503.32 , the inclusion of the factors of TPB (Model 1) improved the log-likelihood value to -470.9 (ρ^2 value of 0.064). For Model 2, log-likelihood (constants only) value of -451.62 improved to a value of -394.23 (ρ^2 value of 0.127). Thus, the improvement over the constants only model is higher for Model 2. The “% correctly predicted” also showed improvement in adding the socioeconomic characteristics and current trip characteristics to the TPB factors. Akaike Information Criterion (AIC) was first developed by Akaike (1973) to compare different models on a given outcome. AIC score for Model 1 and Model 2 was obtained as 965.806 and 886.459. The best model is the one with the lowest AIC score [21]. Thus, considering all goodness-of-fit measures, Model 2 shows better model fit.

In Table 2, two TPB factors “F_P_Comf” and “F_P_Con,” without meaningful coefficients and statistical significance, were removed retaining eight TPB factors. The sign of coefficients is positive for all the TPB variables—indicating that an improvement in these variables positively influences the probability of using the metro services. Out of the four factors measuring attitude toward the metro, “F_A_Enviro” and “F_A_Safe” were found to be statistically significant at 5% level in Model 2 indicating the importance of attitudes in influencing the intention to use metro services. Individuals considering the metro as an environment-friendly and congestion-free mode (F_A_Enviro) are more likely to use the second phase of Kochi metro. The environmental consciousness of the individual and the notion that metro might facilitate congestion-free travel could be the influencing factors. Individuals considering metro as a fast and safe mode as well as a mode that reduces accidents while ensuring safety for women (F_A_Safe) are more likely to use the proposed service. Individuals who have an interest in using public transit services and are comfortable sharing travel with others (F_A_PubTra) are more likely to use the new metro service. Presence of friends and family members who use metro currently and encourage the use of metro (F_S_Use) are likely to motivate the individual to use the proposed metro service. This indicates the importance of subjective norms in an individual’s intention to perform a particular behavior as hypothesized in TPB.

Table 2 Ordered probit model estimation results

Variables		Coefficients	
		Model 1	Model 2
F_A_Safe		0.072	0.182**
F_A_Enviro		0.152**	0.162**
F_A_PubTra		0.125**	0.137*
F_A_Conv		0.107	0.042
F_S_Att		0.060	0.000
F_S_Use		0.202***	0.168**
F_P_Manag		0.225***	0.216***
F_P_Oper		0.111*	0.194***
Education	Non-graduates		-0.361**
	Graduates		(Reference)
Vehicle ownership	No		0.541
	Yes		(Reference)
Current trip duration (minutes)	0–15		0.259*
	15–30		0.347
	30–60		0.197
	60–120		0.914
	> 120		(Reference)
Current trip expense (INR)	0–25		-0.747**
	25–50		-0.314
	50–100		-0.207
	100–120		-0.836
	> 120		(Reference)
Threshold	Intention = 1	-1.095***	0.430
	Intention = 2	-0.633***	0.866
	Intention = 3	-0.140*	1.411
	Intention = 4	0.778***	2.398*
Number of observations		326	291
Goodness-of-fit parameters			
Log-likelihood (constants only)		-503.32	-451.62
Log-likelihood (Final)		-470.9	-394.23
Akaike's Information Criterion (AIC)		965.806	886.459
ρ^2 (McFadden)		0.064	0.127
% Correctly predicted		40.18	43.64

Note ***, **, * indicate significance at 1%, 5% and 10% level, respectively

Similarly, individuals with a positive perception toward ease of using metro services (operating hours, frequency of service, formalities at station) are more likely to use the proposed service as can be observed from the coefficients of “F_P_Manag” and “F_P_Oper.” The results indicate the suitability of TPB in predicting the intentions related to the use of metro services.

It can be seen from Table 2 that only a few socioeconomic characteristics and current trip characteristics were observed to influence the intention to use the proposed metro service. Education does influence the intention to use the metro. Compared to the graduates (reference category), non-graduates are less likely to use metro services. Individuals spending less for their current daily travel (less than INR 200) are less likely to use the proposed service—this could be related to the current fares of Kochi metro. Respondents traveling more than two hours for their daily commute are less likely to use metro services. This is expected as these people might be traveling long distance and they might find it comfortable to commute by a long-distance bus or train and not by metro. Travel time and travel cost were earlier also identified as significant factors in a similar study investigating mode shifting behavior toward the newly operational metro rail in Mumbai [6]. “Vehicle ownership” being an important factor was retained even though it was found to be statistically insignificant. People who own their own vehicles are less likely to use the proposed service, compared to those without vehicles. This might be because people prefer the comfort and convenience of their personal vehicles.

4 Conclusions

New transport infrastructures such as metro play an important role in sustainable transportation development. As discussed previously, the study had two objectives. This paper contributes by studying the intention to use the proposed second phase of metro services in Kochi. We have relied on one of the most frequently used social-psychological theories, theory of planned behavior, to measure the intention to use the proposed extension of Kochi Metro. For the estimation of the models, factor analysis was used to extract the factors, which were later used in the estimation of the ordered probit model.

Based on the review of literature, we hypothesized the intention to use the proposed extension of Kochi Metro to be influenced by the socio-demographic and current travel characteristics of the individual. In addition to these, the role of attitudes toward the behavior, subjective norms and perceived behavioral control variables were hypothesized to influence the intention to use the proposed extension of Kochi metro. Among the different attitudes analyzed, the role of the metro as an environment-friendly, congestion-free rapid transit, safe from accidents was found to be important. Another significant factor identified was safety for women. The perceived social pressure was also found to be significant in affecting people’s intention to use metro. The operating hours of Kochi metro, frequency of service and the functioning of metro stations were important factors which influenced people’s

perception of the ease of travel in Kochi metro. Apart from the TPB factors, education and current trip expenses were found to be significant among the socioeconomic and trip characteristic variables.

The second objective was to analyze the role of attitudes of the individual, friends and family and a conducive environment in the intention to use the proposed service. The discussion presented in the paragraph above indicates the importance of these variables in measuring the intention to use the proposed service. This indicates the potential of the use of TPB and its suitability in predicting the intentions related to the use of metro services. The results emphasize the need to develop strategies that influence the various perceptions of individuals. The study also indicates the need for improving the satisfaction levels of the current users as they could leverage on the same to influence potential users considering the importance of subjective norms. The results indicate the need for further studies that emphasizes on the attitudes of individuals—to better design strategies to shift more individuals toward sustainable modes. Projecting the environment-friendly nature of metro service is a strategy that can indirectly influence behavior to attract patronage. That metro is a women-friendly safe and secure mode suitable for congestion-free and reliable travel need to be publicized.

This study has limitations that need to be addressed in future studies. It should be noted that despite most of the variables being statistically significant, few variables measuring the TPB constructs were found to be insignificant. This could possibly be not the case if the questionnaire is further refined. More stratified socioeconomic variables (such as age, education, income levels) were not considered while collecting data. The sample size was another issue associated with the study. In addition to this, advanced modeling techniques could also be used for the estimation of the models.

References

1. Sadhukhan S, Banerjee UK, Maitra B (2014) Commuters' perception towards transfer facility attributes in and around metro stations: experience in Kolkata. *J Urban Plan Dev* 141(4):04014038-1-8
2. D. M. R. C. Ltd. (2011) Detailed project report-Kochi Metro Project
3. Sadhukhan S, Banerjee UK, Maitra B (2016) Commuters' willingness-to-pay for improvement of transfer facilities in and around metro stations—a case study in Kolkata. *Transp Res Part A Policy Pract* 92:43–58
4. Shaaban K, Hassan HM (2014) Modeling significant factors affecting commuters' perspectives and propensity to use the new proposed metro service in Doha. *Can J Civ Eng* 41(12):1054–1064
5. Wang Y, Li L, Wang Z, Lv T, Wang L (2013) Mode shift behavior impacts from the introduction of metro service: case study mode shift behavior impacts from the introduction of metro service : case study of Xi'an China. *J Urban Plan Dev* 139(3):216–225
6. Sohoni AV, Thomas M, Rao KVK (2017) Mode shift behaviour of commuters due to the introduction of new rail transit mode. *Transp Res Procedia* 25:2603–2618
7. Ajzen I (1991) The theory of planned behaviour. *Organ Behav Hum Decis Process* 50(2):179–211

8. Ambak K, Kasvar KK, Daniel BD, Prasetijo J, Abd Ghani AR (2016) Behavioral intention to use public transport based on theory of planned behavior. In: MATEC Web Conf., vol 47, p 03008-1-7
9. Lai WT, Chen CF (2011) Behavioral intentions of public transit passengers—the roles of service quality, perceived value, satisfaction and involvement. *Transp Policy* 18(2):318–325
10. Kaplan S, Manca F, Nielsen TAS, Prato CG (2015) Intentions to use bike-sharing for holiday cycling: an application of the theory of planned behavior. *Tour Manag* 47:34–46
11. Baburajan V, de Abreu e Silva J, Pereira FC (2018) Opening up the conversation: topic modeling for automated text analysis in travel surveys. In: 2018 21st international conference on intelligent transportation systems (ITSC), pp 3657–3661
12. Kaplan S, de Abreu e Silva J, di Ciommo F (2014) The relationship between young people’s transit use and their perceptions of equity concepts in transit service provision. *Transp Policy* 36:79–87
13. Gliem JA, Gliem RR (2003) Calculating, interpreting, and reporting Cronbach’s alpha reliability coefficient for likert-type scales. In: 2003 Midwest Res. to Pract. Conf. Adult, Contin. Community Educ., pp 82–88
14. Kaiser HF (1958) The varimax criterion for analytic rotation in factor analysis. *Psychometrika* 23(3):187–200
15. Mckelvey RD, Zavoina W (1975) A statistical model for the analysis of ordinal level dependent variables. *J Math Sociol* 4(1):103–120 (August 2013)
16. Greene WH, Hensher DA (2010) *Modelling ordered choices: a primer*, 1st edn. Cambridge University Press, New York
17. Train KE (2009) “Probit,” in *discrete choice methods with simulation*, Second., no. 1960. Cambridge University Press, pp 97–133
18. Feng P, Li W (2016) Willingness to use a public bicycle system: an example in Nanjing City. *J Public Transp* 19(1):84–96
19. Zhang K, Hassan M, Yahaya M, Yang S (2018) Analysis of work-zone crashes using the ordered probit model with factor analysis in Egypt. *J Adv Transp* 2018:1–10
20. Litchfield J, Reilly B, Veneziani M (2012) An analysis of life satisfaction in Albania: an heteroscedastic ordered probit model approach. *J Econ Behav Organ* 81(3):731–741
21. Snipes M, Taylor DC (2014) Model selection and Akaike information criteria: an example from wine ratings and prices. *Wine Econ Policy* 3(1):3–9

Determining Optimum Antistripping Additive Content in Asphalt Mixtures Using Boil Test



Shivpal Yadav, Abhilash Kusam, Zahra M. Tayebali,
and Akhtarhusein A. Tayebali

1 Introduction

Moisture sensitivity of asphalt mixtures is a major problem affecting the performance of pavements, as moisture damage is one of the primary causes of premature failure of asphalt pavements [1]. Two main mechanisms of moisture damage are identified as—adhesive failure between asphalt and aggregate (stripping) and cohesive failure (loss of adhesion between asphalt particles) [2–7]. To improve adhesion between asphalt and aggregate in the asphalt mixture and thus improve the resistance of the asphalt mixtures to moisture damage, various antistrip additives are used in asphalt mixtures. Therefore, it is important to determine the compatibility of an antistrip additive and its optimum additive content for a particular asphalt mixture.

Wasiuddin et al. used surface free energy concept to evaluate the effect of antistrip additive on asphalt binder. It was observed that the total surface free energy of asphalt binder increased with the increase in additive content, and the increase in surface energy enhanced the adhesion between aggregate and asphalt binder [8]. Zhu et al. studied the effect of antistrip agents on rheological properties of asphalt binder at

S. Yadav (✉) · A. A. Tayebali
Department of Civil, Construction, and Environmental Engineering, North Carolina State
University, Raleigh, USA
e-mail: syadav2@ncsu.edu

A. A. Tayebali
e-mail: tayebali@ncsu.edu

A. Kusam
Materials Engineer, Trimat Materials Testing Inc, Concord, USA
e-mail: akusam@trimattesting.com

Z. M. Tayebali
North Carolina State University, Raleigh, USA

high temperature [9]. The results show that rheological properties like rotational viscosity, G^* , δ , and $G^*/\sin\delta$ depend on antistrip agents and their dosage.

Currently, tensile strength ratio (TSR) with a modified AASHTO T 283 conditioning procedure is the most commonly used test to evaluate the moisture sensitivity of asphalt mixtures [1, 5, 7, 10]. Tunncliffe et al. also recommended the use of tensile strength ratio (TSR) test to evaluate moisture sensitivity and the effect of antistrip additives [11]. The current test method uses the ratio of the indirect tensile strength of the conditioned and unconditioned specimens (TSR). Modified AASHTO T 283 procedure takes 24-h to condition the specimens in addition to the time required to bring the specimen to saturation level and perform the indirect tensile testing. Hence, TSR test is a time-consuming test which takes anywhere between three days to a week to complete the test. The variability involved in TSR test results is also observed to be high [10]. There is a need for a quicker test method(s) that is quantitative, has less variability, and simple enough to be used as a quality control test method for moisture sensitivity of plant-produced asphalt mixtures.

A simple and commonly used test method to evaluate moisture sensitivity is the boil test (ASTM D3625). This is a quick and easy test to determine the loss of adhesion (or stripping) in asphalt mixtures. The drawback of this test method is that it was a visual subjective test method. However, Tayebali et al. have successfully used a color-measuring device, spectrophotometer, to quantify the boil test [1]. They used the spectrophotometer—a color-measuring device to determine the percentage stripping in asphalt mixtures due to the boil test.

2 Research Objective

The study presents the use of a color-measuring device in boil test to determine the optimum antistrip additive content for all asphalt mixtures. This method is more helpful in selecting a more cost-effective and compatible antistrip additive for a given asphalt mixture. Additionally, this methodology can be used as a quality control test method for plant-produced asphalt mixtures in the field.

3 Experimental Plan

The mixtures used in this study had a wide range of moisture sensitivity with and without antistrip additive. Asphalt mixtures are prepared with varying antistrip additive content. Boil test (ASTM D3625) was conducted on all the mixtures. A spectrophotometer device was used after the boil test to evaluate stripping in asphalt mixtures. The percent stripping determined using spectrophotometer device was plotted against the antistrip additive content, and optimum antistrip additive content was determined.

3.1 Materials and Specimen Preparation

In this study, two different types of aggregates were used to prepare the asphalt mixtures—limestone aggregate and granite aggregate. Limestone aggregate was obtained from Tulsa, OK. Two different sources of granite aggregate were used—Crabtree Quarry, Raleigh, NC and Garner Quarry, NC. Six different asphalt mixtures were prepared from each aggregate source by varying the amount of antistrip additive content ranging from 0 to 1% by weight of asphalt binder. Three different kinds of antistrip additives were used in this study. PG 64-22 binder was used to prepare all mixtures. The asphalt binder content (by weight of asphalt mix) used in preparing asphalt mixtures are 6% for Garner quarry, 6.4% for Crabtree Quarry, and 5.1% for Tulsa, OK. In total, fifty-four asphalt mixtures were prepared. For each asphalt mixture, four different specimens were prepared to do the boil test. The testing plan carried out in this study is shown in Table 1.

4 Testing Procedures

The boil test was conducted on loose mixtures only. Each loose mixture specimen weighed 450 g. One specimen remained un-boiled, and rest three specimens were boiled. Boil test was done on all asphalt mixtures. A spectrophotometer device was used on specimens before and after the boil test to calculate percentage stripping for all the asphalt mixtures. In this study, the loose mixture was boiled for 30 min instead of 10 min to reduce operator variability. The spectrophotometer device gives an L^* reading that measures the color index based on a grayscale. The L^* value obtained was then used to determine the percent stripping or stripping potential (LD_{RB}^*) using Eq. 1.

$$LD_{RB}^* = \frac{(\text{Boiled } L^* - \text{Unboiled } L^*)}{\text{Aggregate } L^* - \text{Unboiled } L^*} \tag{1}$$

Table 1 List of asphalt mixtures used in this study

Aggregate source	Aggregate type	Antistrip additive	Antistrip additive content (%) (% by weight of asphalt content)
Garner Quarry, Raleigh, NC	Granite	LOF 65-00	0, 0.15, 0.25, 0.50, 0.75 & 1.0
		Evotherm U3	0, 0.15, 0.25, 0.50, 0.75 & 1.0
		Morelife 5000	0, 0.15, 0.25, 0.50, 0.75 & 1.0
Crabtree Quarry, Raleigh, NC	Granite	LOF 65-00	0, 0.15, 0.25, 0.50, 0.75 & 1.0
		Evotherm U3	0, 0.15, 0.25, 0.50, 0.75 & 1.0
		Morelife 5000	0, 0.15, 0.25, 0.50, 0.75 & 1.0
Tulsa, Ok	Limestone	LOF 65-00	0, 0.15, 0.25, 0.50, 0.75 & 1.0
		Evotherm U3	0, 0.15, 0.25, 0.50, 0.75 & 1.0
		Morelife 5000	0, 0.15, 0.25, 0.50, 0.75 & 1.0



Fig. 1 Boil test setup

The percentage stripping or LD_{RB}^* is calculated for the asphalt mixtures and plotted against antistripping additive content to determine the optimum antistripping additive content.

4.1 Boil Test (ASTM D3625)

Boil test method (ASTM D3625 and Tex-530-C) is a standard test to determine the moisture sensitivity of asphalt mixtures. Stripping or loss of adhesion between aggregate materials and asphalt binder is determined to evaluate moisture sensitivity of the asphalt mixtures. It is a simple and quick test method that requires less effort and material; however, it is visually subjective test method. The boil test results can be quantified using the spectrophotometer device [1]. As per the ASTM standard, the loose asphalt mixture is boiled in distilled water for 10 min. The boiling of asphalt mixtures will lead to the stripping of asphalt from the aggregate material if there is poor adhesion between the asphalt and aggregate hence leading to adhesive failure. The stripping in the mixture will lead to exposed aggregates and result in a noticeable color change compared to the un-boiled mixture. This change in color can be used as a basis to estimate the amount of stripping. In this study, the loose asphalt mixture was boiled for 30 min instead of the standard recommendation of 10 min to reduce user variability. Figure 1 shows the boil test setup.

4.2 Spectrophotometer Device

A spectrophotometer is a device that can be used to measure the color of an object. In this study, Chroma Meter CR400 manufactured by Konica Minolta was used to

measure the color of the loose asphalt mixture specimens before and after the boil test as shown in Fig. 2. Similar spectrophotometer devices manufactured and sold by other companies can also be used effectively. Tayebali et al. used this device to quantify the stripping in asphalt mixtures using boil test, and TSR test using the modified AASHTO T 283 conditioning [1]. The device emits a standard light source on the target object, and the reflection from the material is used to measure the color of the object. The light emitting outlet is placed on the specimen such that there is no interference from the background light sources. Color index specified by ASTM E284-17 is used to analyze the color as per the standard terminology of appearance. This study uses the widely used L^* , a^* , and b^* method to measure color [12]. In this study, the L^* reading was used to measure stripping as L^* reading measures the lightness or darkness of an object.

The spectrophotometer device was also used on virgin aggregates to take measurements to get the L^* values. The L^* value of virgin aggregate is used as a reference value to calculate the amount of stripping in asphalt mixtures. L^* values for all asphalt mixtures were measured in two different states—30 min boiled and un-boiled. The

Fig. 2 Chroma meter CR 400. Source Konica Minolta Web site



L^* values measured before and after boiling are then used to calculate the stripping in asphalt mixtures using Eq. 1.

5 Results

5.1 Boil Test Results

L^* readings were obtained before and after boil test using spectrophotometer device. The L^* values were used to calculate percentage stripping (LD_{RB}^*) using Eq. 1. Table 2 shows the average percentage stripping (LD_{RB}^*) values of asphalt mixtures prepared from Crabtree aggregate source. Table 2 shows the average percentage stripping for each antistrip additive with their varying additive content from 0 to 1% (% by weight of asphalt binder).

Figure 3 shows the plot of percentage stripping (LD_{RB}^*) against (%) antistrip additive content for all three antistrip additives used in this study for Crabtree aggregate source.

Figure 3 shows that all three antistrip additives follow the same trend for varying additive content. There is a good logarithmic correlation for all three antistrip additives with $R^2 > 0.95$. In addition, it can be observed from the figure that there is a significant decrease in percentage stripping value for asphalt mixture with no dosage to 0.25% dosage of antistrip additive.

A similar procedure was repeated for asphalt mixtures prepared from Garner aggregate source and limestone aggregate. Table 3 shows the average percentage stripping (LD_{RB}^*) values of asphalt mixtures prepared from Garner aggregate source with varying antistrip additive content.

Figure 4 shows the plot of percentage stripping (LD_{RB}^*) against antistrip additive content for all three antistrip additives used in this study for Garner aggregate source. The plot shows a similar trend as observed in asphalt mixtures prepared from Crabtree aggregate source. A good logarithmic correlation also exists in this case too for all three antistrip additives with $R^2 > 0.95$.

Table 2 Average LD_{RB}^* (%) values for Crabtree aggregates

Antistrip additive content (%) (% by weight of asphalt content)	LD_{RB}^* (%)		
	LOF 65-00	Evotherm U3	Morelife 5000
0	9.12	8.16	8.97
0.15	1.95	1.26	2.11
0.25	1.58	0.81	1.75
0.50	1.45	0.80	1.62
0.75	0.92	0.44	1.01
1.0	0.33	0.15	0.77

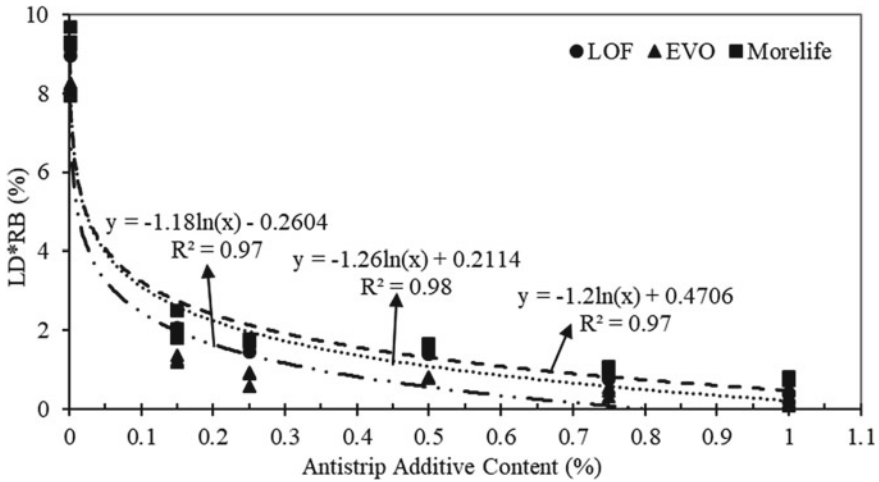


Fig. 3 Chroma meter CR 400. *Source* Konica Minolta Website

Table 3 Average LD^*_{RB} (%) values for Garner aggregates

Antistrip additive content (%) (% by weight of asphalt content)	LD^*_{RB} (%)		
	LOF 65-00	Evotherm U3	Morelife 5000
0	13.64	9.88	8.22
0.15	1.94	1.68	2.62
0.25	1.21	1.58	1.05
0.50	0.93	1.19	0.82
0.75	0.60	0.68	0.79
1.0	0.03	0.46	0.69

Table 4 shows the average percentage stripping values for each asphalt mixture prepared from limestone aggregate, and the plot of percentage stripping (LD^*_{RB}) against antistrip additive content is shown in Fig. 5.

In this case, a good linear correlation between percentage stripping and additive content is observed for limestone aggregate source compared to good logarithmic correlation observe for Crabtree and Garner aggregate source. However, there is a significant behavioral difference in percentage stripping values for LOF 65-00 antistrip additive compared to the other two additives (see Fig. 5).

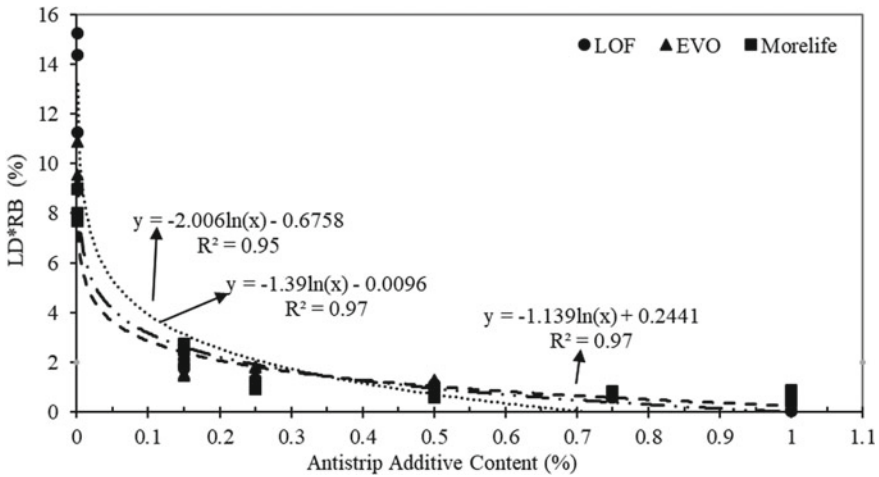


Fig. 4 Combined plot of LD^*_{RB} (%) versus antistrip additive content (%) for three different additive type used with Garner aggregate

Table 4 Average LD^*_{RB} (%) values for limestone aggregates

Antistrip additive content (%) (% by weight of asphalt content)	LD^*_{RB} (%)		
	LOF 65-00	Evotherm U3	Morelife 5000
0	8.32	7.77	7.62
0.15	6.95	5.6	6.17
0.25	6.36	4.34	5.52
0.50	5.91	3.77	4.13
0.75	5.82	3.37	3.32
1.0	4.83	2.28	2.71

5.2 Optimum Antistrip Additive Content for Crabtree Aggregates

After performing the boil test using spectrophotometer device on different asphalt mixtures prepared with varying antistrip additives, optimum antistrip additive content for all asphalt mixtures can be determined. To determine the optimum additive content (%) for an antistrip additive, the percent reduction in stripping or loss in adhesion was calculated. The percentage stripping determined for mixture with 0% antistrip additive content was considered as 100% loss in adhesion. Three different percent reductions (95, 90, and 85%) in stripping or loss in adhesion (5, 10, and 15%) were calculated and corresponding to that the % additive content was determined using correlation obtained in Fig. 3. The % additive content value calculated for Crabtree aggregates asphalt mixtures is shown in Table 5.

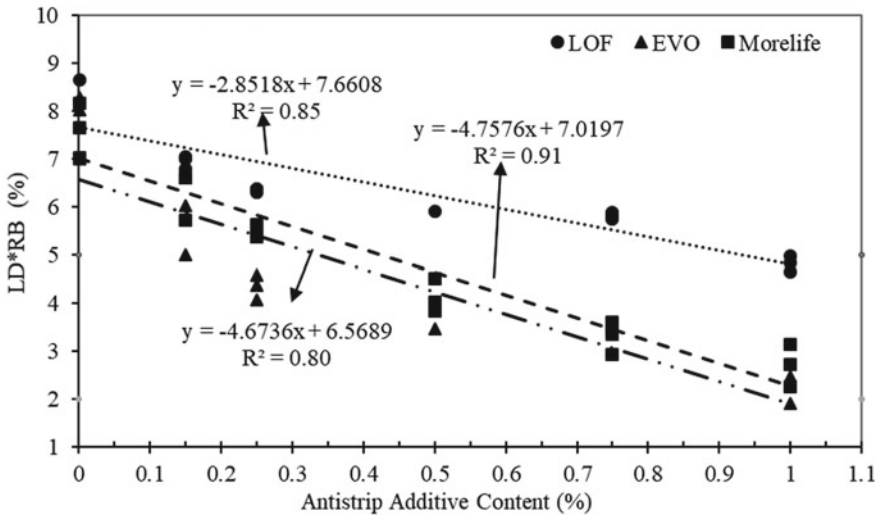


Fig. 5 Combined plot of LD*RB (%) against antistrip additive content (%) for three different additive types used with limestone aggregate

Table 5 Optimum antistrip additive content for Crabtree aggregates based on loss in adhesion

Loss in adhesion in asphalt mixtures prepared from Crabtree aggregates	5%	10%	15%
LOF additive content (%)	0.74	0.52	0.36
EVO additive content (%)	0.59	0.42	0.30
Morelife additive content (%)	0.96	0.67	0.47

The antistrip additive content at 10% loss in adhesion of asphalt mixture is recommended to select an optimum antistrip additive content. The reason for selecting 10% loss in adhesion was that from prior experiences with asphalt mixtures based on tensile strength test (TSR) value of 85% plus, and its corresponding percentage of antistrip percentages used [1].

5.3 Tensile Strength Ratio (TSR) Test Results

North Carolina Department of Transportation (NCDOT) currently uses TSR test with modified AASHTO T 283 conditioning procedure to test moisture sensitivity. Therefore, the TSR test was performed on asphalt mixture prepared from Crabtree aggregate source using this recommended optimum additive content. To calculate TSR, indirect tensile strength (ITS) values are needed. For indirect tensile (IDT) strength test, 95.0 mm tall and 150.0 mm diameter specimens were prepared using

Table 6 TSR test results on asphalt mixtures prepared from Crabtree aggregates

Asphalt mixtures (Crabtree aggregate)	TSR (%)	NCDOT 85% Criteria
LOF @ 0.5%	94.6	PASS
EVO @ 0.4%	96.7	PASS
Morelife @ 0.7%	99.5	PASS

a superpave gyratory compactor. The modified AASHTO T 283 test procedure was followed to determine ITS value, and using these values, TSR values are calculated. The TSR limiting value or pass/fail criteria for NCDOT for moisture sensitivity of asphalt mixtures are 85%.

The antistripping additive content based on the methodology above, 0.5% for LOF 65-00, 0.4% for Evotherm U3, and 0.7% for Morelife 5000 are recommended, respectively. TSR test was performed on these mixtures with the recommended respective antistripping dosages for the Crabtree valley granite aggregate as this aggregate is the most moisture sensitive. TSR results are shown in Table 6.

The TSR test results show that all three asphalt mixtures prepared using optimum antistripping additive content determined using methodology used in this study pass the NCDOT 85% TSR criteria. It may be noted that current practices use a much higher percentage of antistripping additives. The optimum antistripping additive content determined is significantly less compared to the manufacturer's recommendations. The manufacturer recommends 0.75% LOF content (% by weight of asphalt binder), while this method shows 0.5% LOF as the optimum content to be used, and it passes the TSR criteria too. There is a decrease of 33% additive content to be used, which significantly affect the cost of construction. Similarly, for Evotherm U3, the manufacturer recommends 0.5%, while an optimum content determined in this study is 0.4%, which also passes the TSR criteria. Using this method, the optimum antistripping additive content will result in significant economic benefits for the agency, as it is one of the expensive components used in asphalt mixture preparation.

Additionally, the percent reduction in stripping, or loss in adhesion can be very useful in quality control test for field asphalt mixtures. Once charts similar to one in Fig. 3 are prepared for a particular asphalt mixture, the optimum antistripping additive content can be recommended for that mixtures.

6 Conclusions

Stripping of asphalt binder from the aggregates is one of the major distress caused by the presence of moisture which leads to premature failure of asphalt pavements. The use of antistripping additives can significantly reduce the stripping in asphalt mixtures. Boil test (ASTM D3625) along with spectrophotometer device was used in this study to determine optimum antistripping additive content to be used to reduce stripping in asphalt mixtures. Boil test was conducted on a total of fifty-four loose asphalt

mixture specimens. TSR test was also done only on the asphalt mixtures prepared from Crabtree aggregates with optimum antistripping additive content determined from this method. The conclusion based on the results in this study is as follows:

1. A good correlation exists between percent stripping (LD_{RB}^*) and antistripping additive content for all asphalt mixtures.
2. For asphalt mixtures prepared from Crabtree and Garner aggregate source, a significant decrease in percentage stripping value for asphalt mixture with no dosage to 0.25% dosage of antistripping additive is observed.
3. For asphalt mixtures prepared from limestone aggregate source—antistripping additive LOF 65-00 has lesser effect as compared to the other two additives used in this study.
4. Asphalt mixture prepared from Crabtree aggregate source with optimum antistripping additives content determined in this study passes the NCDOT 85% TSR criteria.
5. There is a decrease of 33% LOF 65-00 additive content to be used relative to what is recommended by manufacturers, which significantly affect the cost of construction.
6. The suggested test method can help in selecting a more cost-effective and compatible antistripping additive for all asphalt mixtures.

6.1 Recommendations

The test methodology presented in this study should be used to determine the optimum antistripping additive content for all asphalt mixtures. This test procedure can also be used as a more effective and efficient quality control test for stripping in plant-produced asphalt mixtures.

Disclaimer. The conclusions, views, and methodology presented in this paper reflect the views of the authors only, and not necessarily the views of the North Carolina Department of Transportation or North Carolina State University.

Acknowledgements The authors acknowledge the financial support received from the North Carolina Department of Transportation.

References

1. Tayebali AA, Kusam A, Bacchi C (2018) An innovative method for interpretation of asphalt boil test. *J Test Eval*. <https://doi.org/10.1520/JTE20160383>. ISSN0090-3973
2. Hicks RG (1991) Moisture damage in asphalt concrete. Number 175 in NCHRP Synthesis of Highway Practice. Transportation Research Board
3. Cheng D, Little DN, Lytton RL, Holste JC (2003) Moisture damage evaluation of asphalt mixture by considering both moisture diffusion and repeated-load conditions. *Transp Res Rec J Transp Res Board* No. 1832 (paper no. 03-2730)

4. Little DN, Jones IV DR (2003) Chemical and mechanical processes of moisture damage in hot-mix asphalt pavements. Transportation Research Board National Seminar, San Diego, Calif., 2003, pp 37–74
5. Hicks RG, Santucci L, Ashchenbrener T (2003) Introduction and Seminar Objectives on Moisture Sensitivity of Asphalt Pavements. Transportation Research Board National Seminar, San Diego, Calif., pp 3–19
6. Doyle JD, Howard IL (2013) Rutting and moisture damage resistance of high RAP warm mixed asphalt: loaded wheel tracking vs conventional methods. Road Mater Pavement Des 14(Supplemental 2):148–172
7. Solaimanian M, Harvey, J, Tahmoressi M, Tandon V (2003) Test methods to predict moisture sensitivity of hot-mix asphalt pavements. Presented at moisture sensitivity of asphalt pavements: a national seminar, San Diego, CA, February 4–6, 2003, Transportation Research Board, Washington, DC, pp 77–110
8. Nazimuddin W, Chris F, Musharraf Z, Edgar A (2006) Effect of antistripping additives on surface free energy characteristics of asphalt binders for moisture-induced damage potential. J Testing Eval 35(1) (Paper ID JTE100290, July 2006)
9. Chongzheng Z, Guoqing X, Henglong Z, Feipeng X, Serji A, Chaofan W (2018) Influence of different anti-stripping agents on the rheological properties of asphalt binder at high temperature. Constr Build Mater 164:317–325
10. LaCroix A, Regimand A, James L (2016) Proposed approach for evaluation of cohesive and adhesive properties of asphalt mixtures for determination of moisture sensitivity. Transp Res Rec J Transp Res Board 2575:61–69
11. Tunncliffe DG, Root RE (1984) NCHRP report 274: use of antistripping additives in asphalt concrete mixtures-laboratory phase. TRB, National Research Council, Washington, D.C.
12. ASTM E284-17 (2017) Standard terminology of appearance (Superseded). ASTM International, West Conshohocken, PA. www.astm.org

Characterization of Nano-Alumina Modified Asphalt Binders and Mixtures



Pubali Nazir, Rajan Choudhary, Abhinay Kumar, and Ankush Kumar

1 Introduction

Asphalt binder modification is a popular technique to enhance the structural capacity and functional life of asphalt pavements. Several types of modifiers have been introduced in the realm of bituminous pavements aiming to combat premature deterioration and distress that occur on account of heavier traffic loads, high tire pressures, and severe climatic conditions. The materials that are used as asphalt modifiers include polymers, fibers, chemical agents, natural asphalt, tire rubber, and a more recently introduced class of modifiers, the nano-materials.

Nanotechnology is an emerging technology with the size of the material (at least one dimension) in the nano-size range (10^{-9} m). Although major nano-technological developments have taken place in the field of electronics, physics, and chemistry, the field has taken a recent stride toward construction engineering [1]. The behavior of nano-materials at the nano-range facilitates the improvement in the properties of construction materials, including pavement materials. Although asphalt binders and asphalt mixtures are used in bulk quantities for the construction and maintenance of pavements, their behavior on a macro-scale is influenced by their properties at micro- and nano-scales [2]. In recent times, various research efforts have been put into the application of nanotechnology to pavement engineering [3–5]. Several nano-materials that have been employed for this purpose are carbon nano-tubes (CNTs) [6, 7], nano-silica [8, 9], nano-clays [10], etc.

P. Nazir · R. Choudhary (✉) · A. Kumar · A. Kumar
Department of Civil Engineering, Indian Institute of Technology Guwahati, Assam, India
e-mail: rajandce@iitg.ac.in

A. Kumar
e-mail: abhinay.kumar@iitg.ac.in

A. Kumar
e-mail: ankus174104035@iitg.ac.in

Table 1 Properties of nano-alumina (nano- Al_2O_3)

Property	Unit	Value
Specific gravity	–	3.340
Specific surface area	m^2/g	100 + 15
Average primary particle size	nm	13
Tamped density	g/l	Approx. 50
Moisture	wt. %	<5.0
Ignition loss	wt. %	<3.0
pH (in 4% dispersion state)	–	4.5–5.5
Al_2O_3 content	wt. %	>99.8
Sieve residue	wt. %	<0.050

This study seeks to assess the influence of alumina nano-particles as a modifier to asphalt binders by analyzing the physical and rheological characteristics of the modified as well as neat (control) asphalt binders. Physical tests included in the study are specific gravity, softening point, and viscosity. Rheological tests conducted on binders include multiple stress creep and recovery (MSCR), temperature sweep, and frequency sweep. Further, the study included the performance characteristics of asphalt mixtures fabricated with nano-alumina modified binders.

2 Experimental Methods

2.1 Materials

The base binder used was a viscosity grade 30 (VG-30) binder meeting the requirements of IS 73 [11]. Nano-alumina (nano- Al_2O_3) was obtained from NU Patel & Company, Ahmedabad (India). Table 1 presents the properties of nano- Al_2O_3 particles. Figure 1 shows a naked eye view of nano- Al_2O_3 . Energy-dispersive X-ray (EDX) results shown in Fig. 2 indicate that aluminum (36.5%) and oxygen (63.5%) are the two elements present in nano- Al_2O_3 .

2.2 Preparation of Modified Asphalt Binders

The modified asphalt binder blends were prepared using dosages of nano- Al_2O_3 varying between 0 and 8% (by weight of base binder) at an increment of 2%. The neat binder was heated on a temperature-controlled hotplate to 160 °C. Then, the desired quantity of nano- Al_2O_3 was introduced and a high shear mixer was employed for blending under a speed of 14,000 rpm for 30 min. For uniform dispersion and homogeneity, the blends were then stored at –15 °C in metallic containers for further use.



Fig. 1 Naked eye view of nano-Al₂O₃

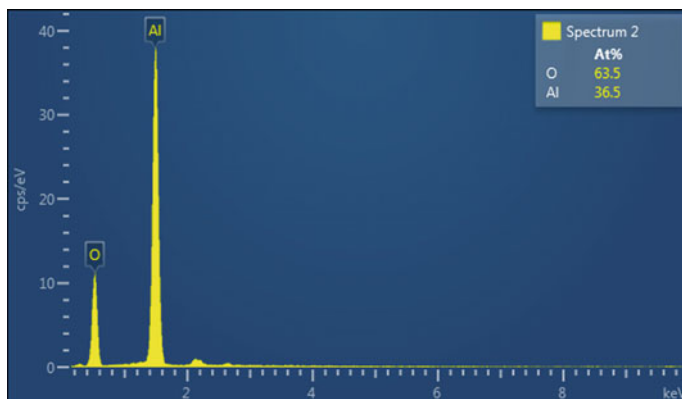


Fig. 2 EDX results of nano-Al₂O₃

2.3 Conventional Properties

The conventional properties including specific gravity, viscosity, and softening point were measured. The specific gravity of the binders was measured as per IS 1202 [12]. The softening point test was completed in line with IS 1205 with the ring and ball apparatus [13]. The viscosity of binders was computed at 135 °C through a Brookfield rotational viscometer with spindle #21, according to ASTM D4402 [14].



Fig. 3 Aluminum tubes used in the storage stability test

2.4 Storage Stability Test

The control binder and nano- Al_2O_3 modified binders were submitted to thermal storage stability test according to ASTM D7173 [15]. For this test, a 50-g bitumen sample was heated and poured in an aluminum tube of 14 cm height and 2.5 cm diameter. The sealed tube was kept at 163 °C in an oven for 48 h before being transferred to a freezer at -10 °C for 4 h. Thereafter, the difference in softening point of binder residues from the top and bottom third sections was checked for a limit of 3 °C, as per the requirements of IS 15462 [16]. Figure 3 shows the tubes used in the test along with a cut tube.

2.5 Rheological Tests and Modeling

Rheological characterization was conducted on short-term aged binders using a dynamic shear rheometer (DSR). As per ASTM D2872, the binders were aged in a rolling thin film oven (RTFO) for 85 min at 163 °C [17]. Rheological tests were conducted with a parallel plate geometry using a 1-mm-gap with a 25-mm-diameter plate. The two main rheological parameters, such as complex shear modulus (G^*) and phase angle (δ), were determined using a temperature sweep test. The range of temperatures considered was 25–80 °C at 10 rad/s (1.59 Hz) frequency. A frequency sweep test was conducted to assess the elastic modulus (G') and viscous modulus (G'') at frequencies varying between 0.1 and 100 rad/s. The MSCR test was also conducted on short-term aged control and nano- Al_2O_3 modified binders at 60 °C, a temperature representing the typical high-service pavement temperature. The MSCR test was performed in line with ASTM D7405 [18], with ten creep-recovery cycles (1 s creep and 9 s recovery for each cycle) at each 0.1 and 3.2 kPa stress level. The strain undergone by the binder was recorded as a function of time and was employed to calculate percent recovery (R) and non-recoverable creep compliance (J_{nr}) corresponding to each creep-recovery cycle and stress level. Equations 1 and 2 present

the expressions to determine R and J_{nr} , respectively.

$$R = \frac{\epsilon_t - \epsilon_r}{\epsilon_t} \times 100 \tag{1}$$

$$J_{nr} = \frac{\epsilon_r}{\sigma} \tag{2}$$

Here, ϵ_t = total strain, ϵ_r = residual strain, and σ = applied stress.

2.6 Design and Evaluation of Bituminous Concrete Mixtures

Bituminous mixtures were prepared using a bituminous concrete (BC) grading II (aggregate gradation shown in Fig. 4) with 13.2-mm nominal maximum aggregate size (NMAS). BC-II gradation is commonly used for the design of dense-graded bituminous mixtures for wearing courses of highways in India. Three mix specimens were produced at binder content between 4.5 and 6.5% at an increment of 0.5% by weight of mix during the design of the BC mix. The optimum binder content (OBC) in bituminous mix design was determined using the Marshall method, which is presently used in India. The OBC was found to be 5.5%, and the mix design parameters acquired at the OBC fulfilled the criteria outlined in MoRTH [19] guidelines. The OBC obtained with a neat binder was also used for the preparation of mixes with nano- Al_2O_3 modified binders. This technique enabled for an assessment of all mixes' efficacy without including the binder content as a separate variable.

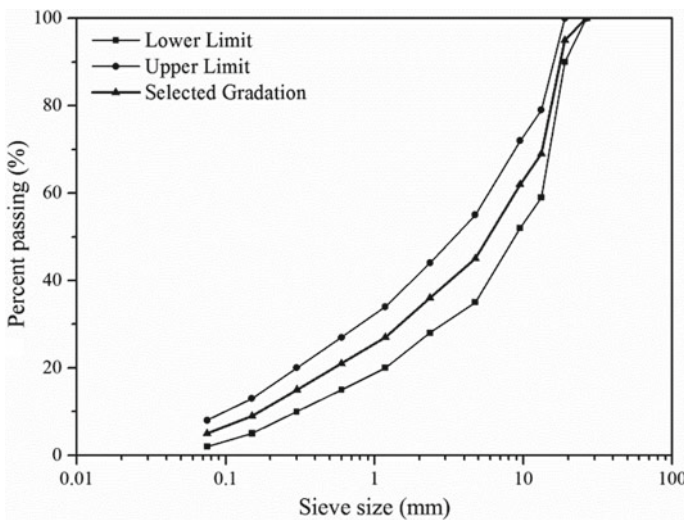
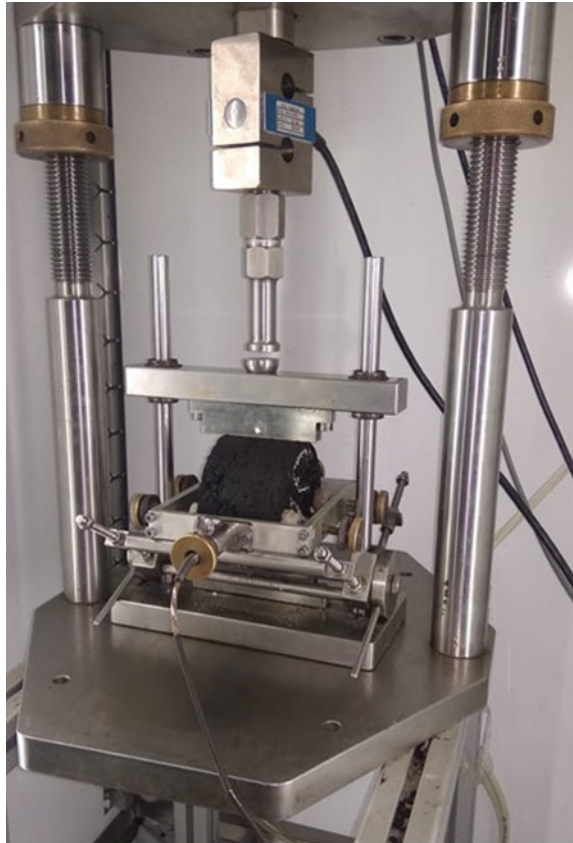


Fig. 4 Bituminous concrete (BC-II) gradation with specification limits

The performance of BC mixes containing control and nano- Al_2O_3 modified binders was assessed using the indirect tensile stiffness modulus (ITSM) test at two temperatures of 25 and 40 °C. The specimens were produced at $4 \pm 0.5\%$ air voids. The ITSM test evaluates the stiffness properties of asphalt mixtures and was analyzed in accordance with EN 12697-26 [20] protocol. A 14-kN universal testing machine was used for the test (Fig. 5). The test consisted of applying a haversine waveform load to reach a rise time of 124 ms (the time it takes for the load pulse to reach its maximum value). The specimen deformation was recorded in a horizontal plane. In the first ten load pulses, the stress magnitude was automatically adjusted for a transitory deformation of 0.005% of the diameter. The stiffness modulus was then calculated using the next five load pulses. After turning the specimen by 90 degrees, the test was repeated. Equation 3 was used for the modulus:

$$S_m = \frac{F \times (\mu + 0.27)}{z \times h} \quad (3)$$

Fig. 5 ITSM test assembly



Here, F = peak vertical load, N; h = sample height, mm; z = amplitude of the horizontal deformation, mm; μ = Poisson’s ratio (assumed 0.35); S_m = stiffness modulus, MPa.

3 Results and Discussion

3.1 Results on Nano-modified Asphalt Binders

Conventional Properties. The outcomes of conventional parameters (softening point, viscosity, and specific gravity) of control and nano- Al_2O_3 modified asphalt binders are shown in Fig. 6. As nano- Al_2O_3 particles had a high specific gravity of 3.340, their addition caused an increase in the specific gravity of the asphalt binder. The increase in binder stiffness with the addition of nano- Al_2O_3 is seen from an increase in softening point and viscosity measured at 135 °C. Further at 135 °C, both control and nano- Al_2O_3 modified binders fulfilled the viscosity threshold of 3.0 Pa s, which indicates that these binders would not pose a hindrance in pumping and mixing.

Storage Stability. The storage stability is computed as the difference in softening point between the top and bottom sections of the aluminum tube containing nano- Al_2O_3 modified binders. Figure 7 depicts a difference of less than 3 °C in softening point of the top and bottom sections for all nano- Al_2O_3 modified binders, indicating adequate storage stability. The results show that nano- Al_2O_3 modified binders had good compatibility and homogeneity at elevated temperatures. The very small particle volume of nano- Al_2O_3 is likely the reason for the good dispersion and compatibility of the modified binders.

Temperature Sweep. The temperature sweep test results for the control and nano- Al_2O_3 modified binders are shown in Fig. 8. After adding nano- Al_2O_3 to

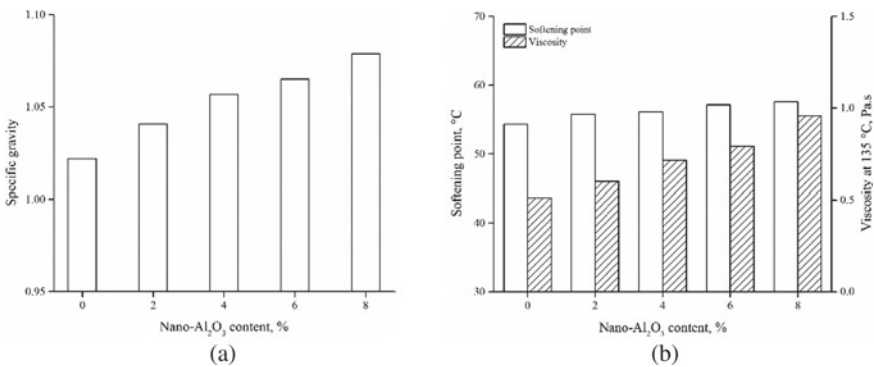


Fig. 6 a Specific gravity results. b Softening point and viscosity results

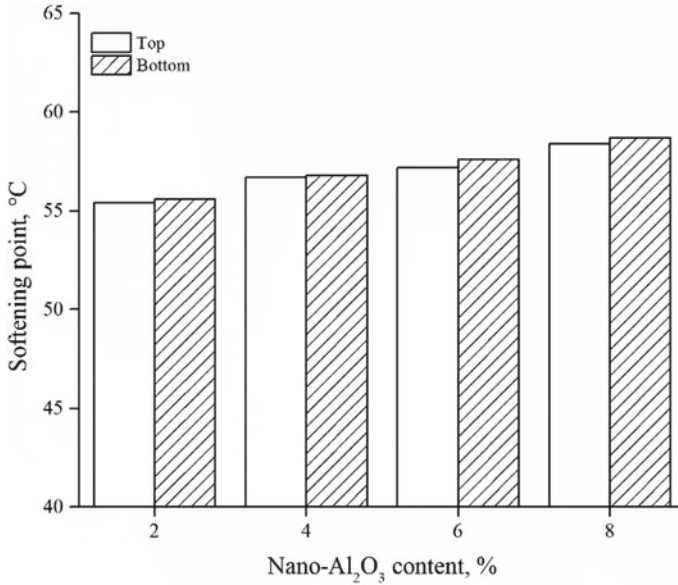


Fig. 7 Storage stability results

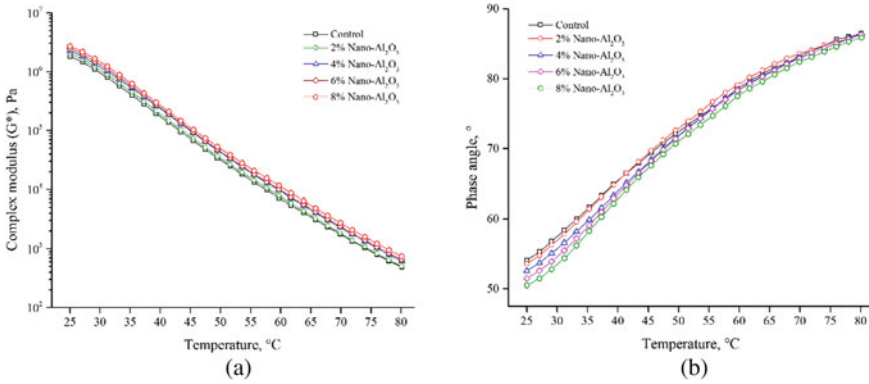


Fig. 8 Temperature sweep results: a G*, b δ

the base binder, G* increased and δ decreased at all temperatures, indicating that the binder's stiffness and elasticity improved. Additionally, when the nano-Al₂O₃ dosage increased, the G* increased and the δ lowered across the temperature domain considered in the test. Percent increase of 8%, 31%, 39%, and 55% was found for G* with 2, 4, 6, and 8% nano-Al₂O₃ contents, respectively, as compared to the control binder. For a greater ability of asphalt binder against deformation, a larger G* and a reduced δ are preferable [21, 22]; hence, the effects of nano-Al₂O₃ are beneficial toward a better deformation resistance.

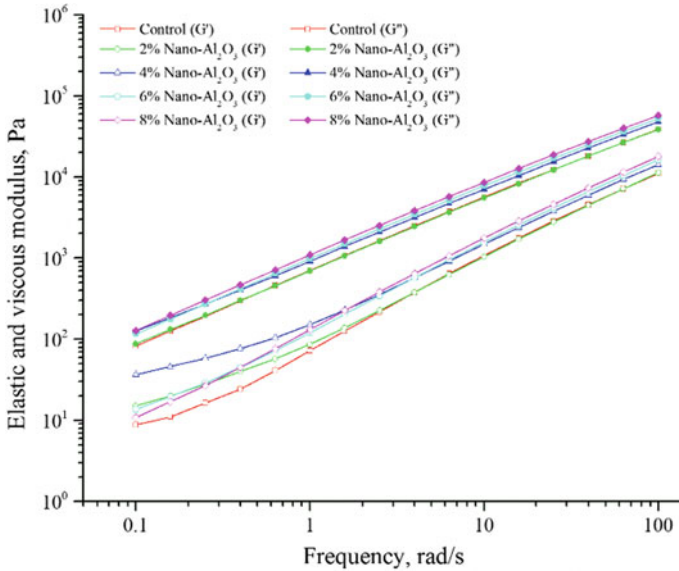


Fig. 9 Frequency sweep results at 60 °C

Frequency Sweep. The frequency sweep test was evaluated to assess the influence of nano-Al₂O₃ on rheological variables under varying frequencies at 60 °C temperature. The results over frequencies ranging from 0.1 to 100 rad/s are expressed as storage modulus (G') and loss modulus (G''). Figure 9 shows the trends of the frequency sweep test for different dosages of nano-Al₂O₃. The addition of nano-Al₂O₃ enhanced the G' and G'' of the binders at all frequencies, which shows that the viscoelastic characteristics of the binder improved. The highest moduli are observed for the binder with 8% nano-Al₂O₃.

MSCR. The MSRCR test was performed to assess the creep and recovery response of binders at 60 °C to study the resistance of binder against rutting. The plot of accumulated strain against time in the MSRCR test at both 0.1 and 3.2 kPa stress levels is shown in Fig. 10. Results from 0 to 100 s (Fig. 10a) and those from 100 to 200 s (Fig. 10b), respectively, represent the stress levels of 0.1 kPa and 3.2 kPa. When compared to the control binder at 0.1 kPa stress levels, the inclusion of nano-Al₂O₃ decreased the total strain by 13, 26, 34, and 45%. Corresponding reductions were 12, 23, 32, and 43% at 3.2 kPa stress level.

Figure 11a shows the variation of MSRCR creep compliance (J_{nr}) for different binders measured at both stress levels. A binder with lower J_{nr} is preferable for an improved potential against rutting. J_{nr} for the control binder was as 1.2 and 1.4 kPa⁻¹ at 0.1 kPa and 3.2 kPa stress levels, respectively. Further addition of nano-Al₂O₃ resulted in a significant reduction in J_{nr} at both stress levels, which is highly favorable for a better rutting performance. The results of MSRCR recovery are presented in Fig. 11b. Recovery results corroborate the results of J_{nr} . Since J_{nr} is related to the

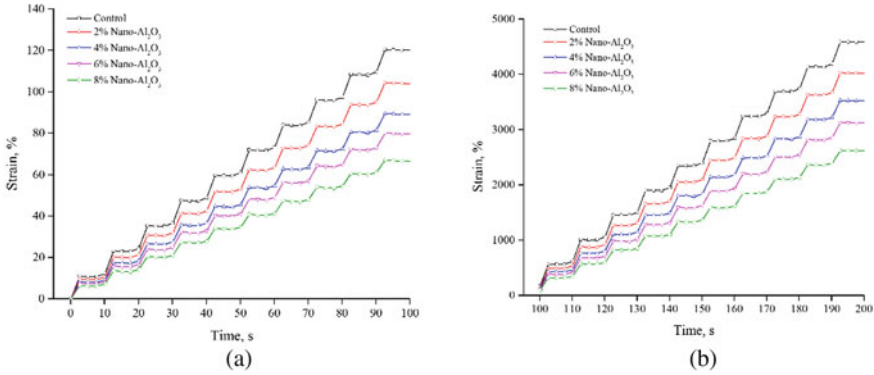


Fig. 10 MSCR accumulated strain versus time curves at stress levels of: a) 0.1 kPa; b) 3.2 kPa

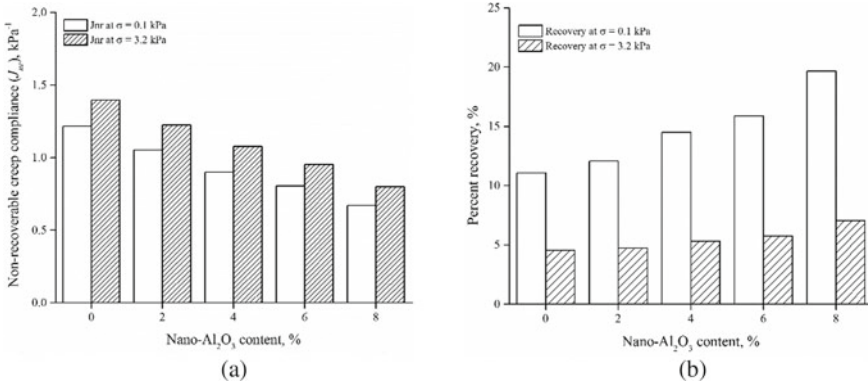


Fig. 11 MSCR results of a) J_{nr} ; b) recovery

amount of non-recovered strain in the creep-recovery cycle, a binder with a lower J_{nr} is expected to demonstrate a relatively higher recovery. Nano- Al_2O_3 particles enhance the rutting performance of the binder and thus can be highly beneficial to countries/regions with hot/tropical climatic conditions, e.g., India.

3.2 Characteristics of Asphalt Mixtures with Nano-modified Asphalt Binders

The ITSM test compares the stiffness of bituminous mixes with and without nano- Al_2O_3 . Results of the ITSM tests performed at 25 and 40 °C temperatures are presented in Fig. 12. As expected, the ITSM at 40 °C was lower than that at 25 °C as the binder’s stiffness reduces at higher temperatures. At 25 °C, the ITSM of mixtures

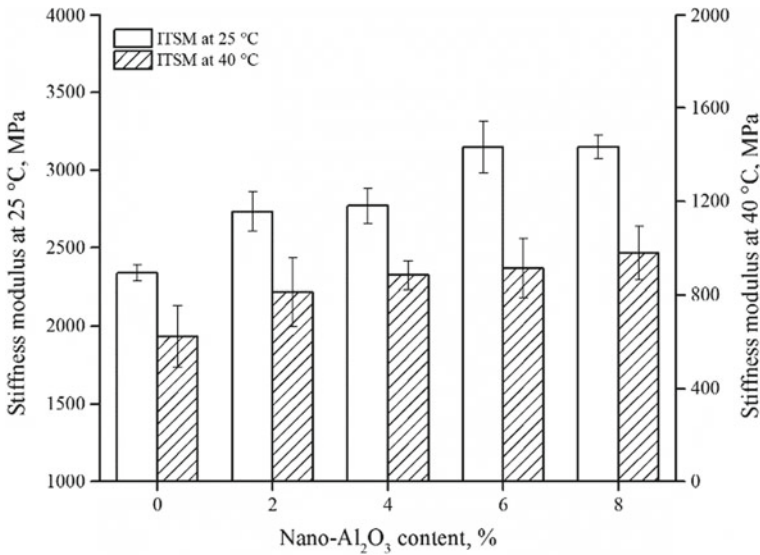


Fig. 12 ITSM results at 25 and 40 °C

with 2, 4, 6, and 8% nano-Al₂O₃ were 17, 19, 35, and 36% higher than the ITSM of the control mix. Corresponding improvements at 40 °C were 30, 42, 47, and 57%. The improvements at the high-service pavement temperature of 40 °C were more prominent than those at 25 °C. This finding indicated that the nano-Al₂O₃ modified mixtures demonstrated better stiffness properties than the control mixture, and the improvements increased with an increase in nano-Al₂O₃ content. The results of temperature sweep and MSCR testing also revealed that the nano-Al₂O₃ modified binder had a higher stiffness than the control binder.

4 Conclusions

In this study, the characteristics of asphalt binders and mixes modified with various dosages of nano-Al₂O₃ particles were examined. The following conclusions are formed based on the outcomes:

- Blends prepared with nano-Al₂O₃ were found to be storage stable. In comparison with the control binder, adding nano-Al₂O₃ enhanced the viscosity and softening point.
- The results of temperature and frequency sweep tests revealed that nano-Al₂O₃ improved the stiffness and elastic characteristics of the binders, resulting in improved rutting resistance.

- The MSCR J_{nr} values decreased when the nano- Al_2O_3 dosage was increased, indicating that the binders were more resistant to permanent deformation.
- The addition of nano- Al_2O_3 to the asphalt mixtures enhanced the indirect tensile stiffness modulus, showing that the asphalt mixes with nano- Al_2O_3 modified asphalt binders had improved stiffness characteristics.

Findings of the study indicate that nano- Al_2O_3 fares favorably as an asphalt binder modifier. Further, characterization of asphalt mixes incorporating the nano- Al_2O_3 modified binder needs to be done to arrive at understanding of fatigue and moisture damage resistance benefits of using the nano- Al_2O_3 in asphalt binder and mixes.

References

1. Steyn WJ (2009) Potential applications of nanotechnology in pavement engineering. *J Transp Eng ASCE* 135(10):764–772
2. Yang J, Tighe S (2013) A review of advances of nanotechnology in asphalt mixtures. *Procedia Soc Behav Sci* 96:1269–1276
3. Amirghanian AN, Xiao F, Amirghanian SN (2011) Evaluation of high temperature rheological characteristics of asphalt binders with carbon nano particles. *J Test Eval* 39(4):1–9
4. Bai JB, Allaoui A (2003) Effect of the length and the aggregate size of MWNTs on the improvement efficiency of the mechanical and electrical properties of nanocomposites—experimental investigation. *Compos A* 34(8):689–694
5. Mubarak M, Ali SIA, Ismail A, Yusoff NIM (2016) Rheological evaluation of asphalt cements modified With ASA Polymer and Al_2O_3 nanoparticles. *Procedia Eng* 143:1276–1284
6. Aqel A, El-Nour KMA, Ammar RA, Al-Warthan A (2012) Carbon nanotubes, science and technology part (I) structure, synthesis and characterisation. *Arab J Chem* 5(1):1–23
7. Amirghanian AN, Xiao F, Amirghanian SN (2010) Evaluation of high temperature rheological characteristics of asphalt binder with carbon nano particles. *J Test Eval* 39(4):583–591
8. Yao H, You Z, Li L, Lee CH, Wingard D, Yap YK, Goh SW (2013) Rheological properties and chemical bonding of asphalt modified with nanosilica. *J Mater Civ Eng* 25(11):1619–1630
9. Rahman IA, Padavettan V (2012) Synthesis of silica nanoparticles by sol-gel: size-dependent properties, surface modification, and applications in silica-polymer nanocomposites—a review. *J Nanomater* 2012:1–15
10. Ashish PK, Singh D, Bohm S (2016) Evaluation of rutting, fatigue and moisture damage performance of nanoclay modified asphalt binder. *Constr Build Mater* 113:341–350
11. IS 73 (2013) Paving Bitumen—specification. Bureau of Indian Standards, New Delhi
12. IS 1202 (1978) Methods for Testing Tar and Bituminous Materials, Determination of Specific Gravity, Bureau of Indian Standards, New Delhi
13. IS 1205 (1978) Methods for Testing Tar and Bituminous Materials, Softening Point Test. Bureau of Indian Standards, New Delhi
14. ASTM D4402 (2015) Standard test method for viscosity determination of asphalt at elevated temperatures using a rotational viscometer. ASTM International, West Conshohocken, PA
15. ASTM D7173 (2014) Standard practice for determining the separation tendency of polymer from polymer modified asphalt. ASTM International, West Conshohocken, PA
16. IS 15462 (2004) Polymer and rubber modified Bitumen—specification. Bureau of Indian Standards, New Delhi
17. ASTM D2872 (2012) Standard test method for effect of heat and air on a moving film of asphalt (Rolling Thin-Film Oven Test). ASTM International, West Conshohocken, PA

18. ASTM D7405 (2015) Standard test method for multiple stress creep and recovery (MSCR) of asphalt binder using a dynamic shear rheometer. ASTM International, West Conshohocken, PA
19. MoRTH (2013) Specifications for road and bridge works (Fifth Revision). Indian Roads Congress, Govt. of India, Ministry of Road Transport and Highways, New Delhi
20. British Standard Institution. BS EN 12697-26 (2004) Bituminous mixtures-test methods for hot mix asphalt-Part 26 stiffness, London, UK
21. Julaganti A, Choudhary R, Kumar A (2017) Rheology of modified binders under varying doses of WMA additive–Sasobit. *Pet Sci Technol* 35(10):975–982
22. Kumar A, Choudhary R, Kandhal PS, Julaganti A, Behera OP, Singh A, Kumar R (2018) Fatigue characterisation of modified asphalt binders containing warm mix asphalt additives. *Road Mater Pavement Des.* <https://doi.org/10.1080/14680629.2018.1507921>

Soil Stabilization Using Waste Plastic



Aiswarya Govind and Anjan Patel

1 Introduction

In present day, large quantities of plastic wastes are being generated worldwide [1]. India itself produces plastic waste of around 40 million tons per year [2]. This is mainly because of the growing population and rapid urbanization. Plastic waste is non-biodegradable and a threat to different forms of life on the earth. It is really a challenging task to handle the non-biodegradable plastic waste by following the procedure used for conventional solid waste management. Plastic wastes can be generally managed by recycling or re-using. However, all the plastics are not easily recyclable [3], and considering this, the best way to handle this waste is its bulk utilization in construction industries [4].

In construction industry and especially in roadways and site development projects, soil stabilization is widely used for improving soil properties [5, 6]. This process can be used to treat a wide range of soils having different physical, chemical, and mineralogical properties. However, some of the additives (viz lime, fly ash, gypsum and Portland cement, different chemicals, resins, enzymes, etc.) used for the stabilization process are many times not cost effective or are soil- and site-specific. Moreover, some of the additives are not environmental-friendly. Therefore, there is a need to explore other kinds of soil additives as well. With this in view, soil stabilization using plastic wastes is considered to be a good option that will reduce its amount in the environment.

In the past, several researchers have presented their works on soil stabilization using conventional as well as non-conventional methods. However, it is seen that most of available literature targets a particular type of soil. Keeping this in view,

A. Govind · A. Patel (✉)

Visvesvaraya National Institute of Technology, Nagpur 440010, India

e-mail: anjanpatel@civ.vnit.ac.in

behaviors of different types of soils (as per USCS classification) have been analyzed simultaneously by adding different percentages of plastic wastes in the present study.

2 Materials and Methodology

The soils used in the present study are classified as CH, CL, MH, and ML. Plastic wastes collected for mixing is basically composed of low-density polyethylene. The basic soil properties are presented in Table 1.

The plastic waste selected for this study is wrappers of snacks packets which were collected from college hostel premises of VNIT campus, Nagpur. These were cut into strips with width and length of 10 mm using a scissor and measuring ruler as shown in Fig. 1. For reference, mechanical properties of the polythene are presented in Table 2.

The optimum moisture content (OMC) and Maximum dry density (MDD) were obtained by performing standard proctor compaction test as per IS:2720(Part VIII)-1983. Compaction test was repeated for 0, 0.25, 0.5, 0.75, and 1% of mixed plastic in different soils.

Table 1 Basic soil properties

Properties	CH	CL	MH	ML
Specific gravity	2.54	2.53	2.62	2.61
Fines passing 75 μ sieve (%)	84.8	54.26	61	73
Liquid limit (%)	59	34	65	49
Plastic limit (%)	30	23	44	40
Plasticity index (%)	29	11	21	09

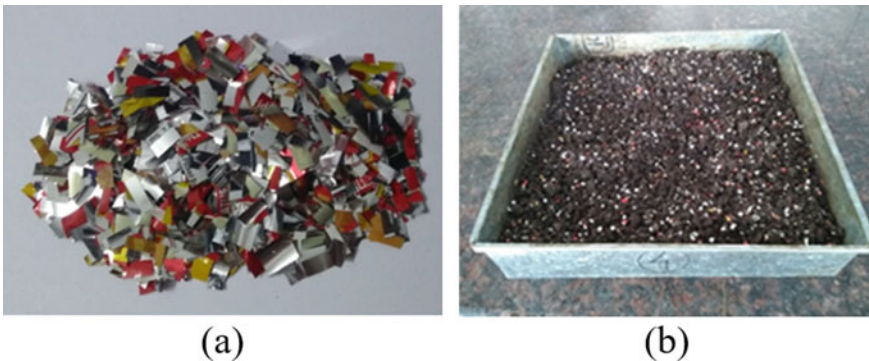


Fig. 1 a Polythene wrappers cut into strips of 10 mm wide and b plastic mixed soil

Table 2 Properties of polythene

Properties	Values
Tensile strength (MPa)	50.6
Elongation at break (%)	60.9
Young's modulus (MPa)	971.1

Corresponding to these OMC and MDD thus obtained, soaked CBR and direct shear test were carried out in the laboratory. All these tests were repeated with plastic waste mixed in different proportion as mentioned above.

3 Results and Discussions

OMC, MDD, CBR value, cohesion value (c), and angle of internal friction (ϕ) obtained from the tests are summarized in Tables 3, 4, 5 and 6. Load penetration curves of CBR tests which were conducted for all soil samples are presented in Fig. 2. The % change in CBR value by the addition of polythene was calculated for all soil samples and included in Table 7.

The variation in CBR value, c , and ϕ with different plastic contents are represented in Figs. 3, 4, and 5, respectively. The shear strengths of various soil samples were further calculated using the formula: $S = c + \sigma' \tan \phi$, where S and σ' are shear strength and effective stress, respectively. The results are presented in Fig. 6. For demonstration purpose, different σ' values (i.e., 100, 200, 300, and 400 kPa) were

Table 3 Test results of CH soil

Sample description	MDD (g/cc)	OMC (%)	CBR (%)	c (N/cm ²)	ϕ (°)
CH	1.58	23	3.35	10.3	18
CH with 0.25% polythene	1.52	21.07	3.82	9.02	19.23
CH with 0.5% polythene	1.46	17.25	3.48	8.29	25.68
CH with 0.75% polythene	1.45	22.3	2.54	7.63	33.97
CH with 1% polythene	1.46	20.82	2.27	6.54	41.5

Table 4 Test results of CL soil

Sample description	MDD (g/cc)	OMC (%)	CBR (%)	c (N/cm ²)	ϕ (°)
CL	1.68	21	7.04	9.21	31.05
CL with 0.25% polythene	1.62	20.5	8.18	8.1	34.45
CL with 0.5% polythene	1.58	24	8.24	7.3	41.5
CL with 0.75% polythene	1.56	22.5	7.6	6.58	45.31
CL with 1% polythene	1.55	20	7.2	5.79	49.26

Table 5 Test results of ML soil

Sample description	MDD (g/cc)	OMC (%)	CBR (%)	c (N/cm ²)	ϕ (°)
ML	1.64	17	10.45	6.23	32.3
ML with 0.25% polythene	1.62	19.04	10.79	4.61	35.6
ML with 0.5% polythene	1.58	20.23	10.92	3.98	41.08
ML with 0.75% polythene	1.57	21.03	11.26	3.57	45.99
ML with 1% polythene	1.53	20.87	11.59	2.95	47.59

Table 6 Test results of MH soil

Sample description	MDD (g/cc)	OMC (%)	CBR (%)	c (N/cm ²)	ϕ (°)
MH	1.67	20	2.61	7.62	27.33
MH with 0.25% polythene	1.64	22.54	2.74	7.15	29.51
MH with 0.5% polythene	1.61	19	2.88	6.25	38.9
MH with 0.75% polythene	1.59	18.62	3.28	5.75	42.64
MH with 1% polythene	1.55	21.03	3.42	5.14	45.5

considered. The shear failure patterns of four different soils are also depicted in Fig. 7.

Most of the previous researchers have observed an increase in CBR with the inclusion of plastic contents in soils up to a certain limit, and thereafter, it goes on decreasing. The optimum percentage of plastic contents which gives maximum improvement in CBR value of clayey soil is reported as 0.6% [7], 4% [8, 9], 2% [10], 0.5% [5, 11, 12], and 0.3% [6] depending upon the types and dimensions of the plastic strips. Naeini and Rahmani [13] have found that by increasing the plastic waste chips content, the value of cohesion and internal friction angle of reinforced silty soil increases. Kumar and Vageesh [14] have observed a significant improvement in soil strength due to increase in angle of internal friction, but not large variation in cohesion. It is reported that increase in MDD of soils with 1% replacement is due to the decrease in the number of voids in some cases with the addition of plastic which leads to effective compaction [15]. As reported by other researchers [16], an increase of plastic wastes results a reduction in c value of soil and increase in the ϕ value.

Based on present work, it can be observed that the polythene strips induce a reduction in MDD of the soils due to its low specific gravity. This point can be beneficial in the construction of embankments using lightweight materials. Also, it can be noticed that the addition of polythene strips decreases the OMC. It can be seen from Table 3 that CBR value for CH soil increases with increase of 0.25% of polythene strips. As the plastic content further increases, CBR goes on decreasing. In case of CL soil, CBR increases with the addition of polythene up to a certain limit (i.e., up to 0.5%) and beyond that it starts decreasing. Table 7 shows percentage change in CBR with various polythene contents. It gives a clear idea about optimum content that gives maximum possible value of CBR. For CH soil, 0.25% polythene

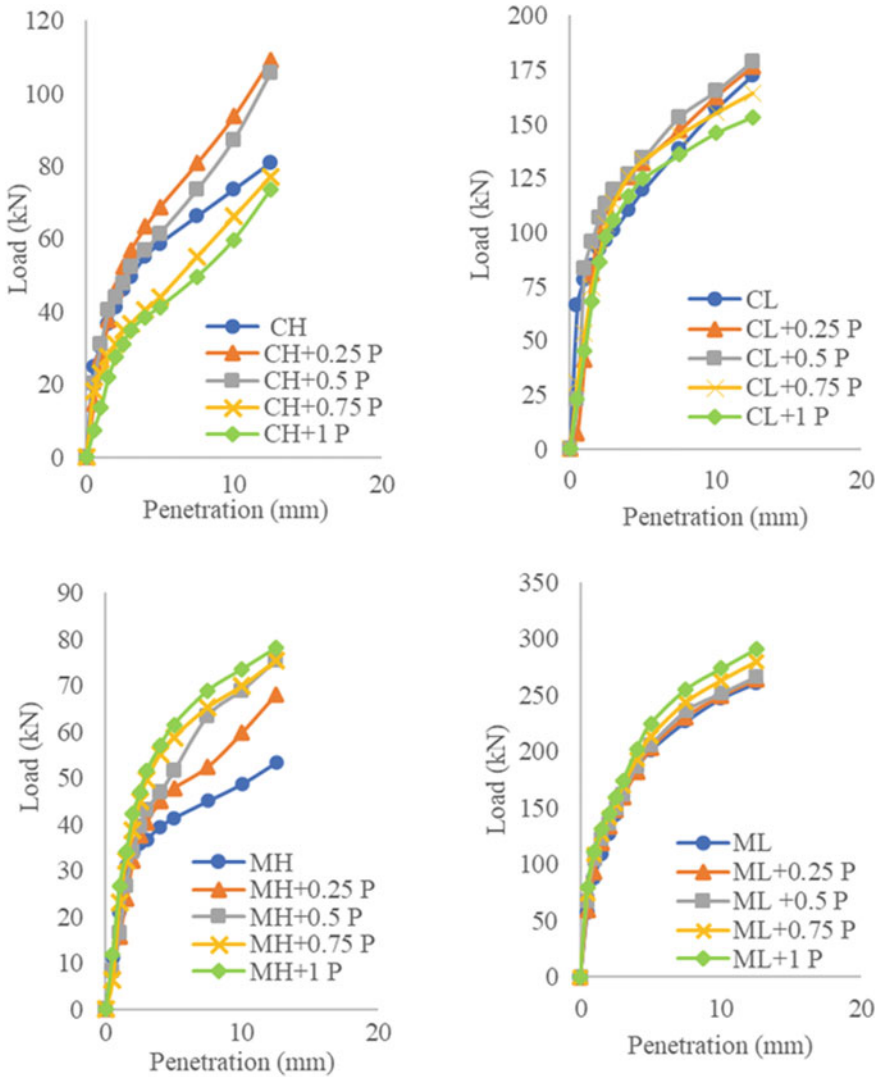


Fig. 2 Load penetration curve for different types of soils (* P indicates Polythene added in %)

Table 7 Percentage increase or decrease in CBR value with different % of polythene

Soil sample	% Polythene content			
	0.25%	0.50%	0.75%	1%
CH	14.03	3.88	-24.18	-32.24
CL	16.19	17.05	7.95	2.27
MH	4.98	10.34	25.67	31.03
ML	3.25	4.5	7.75	10.91

Fig. 3 Variation of CBR value with different % of polythene

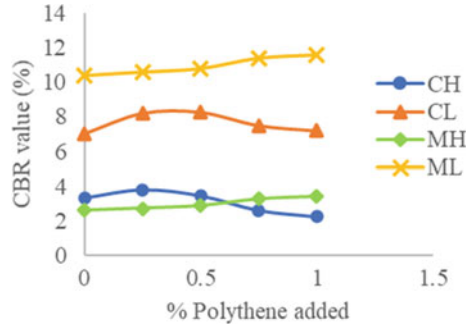


Fig. 4 Variation of c value with different % of polythene

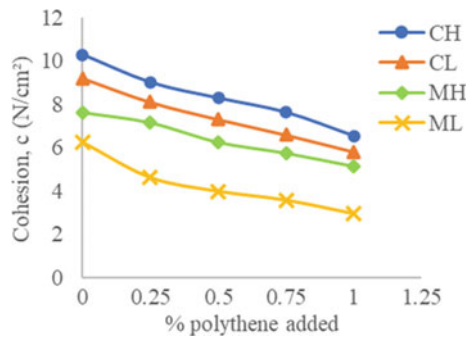
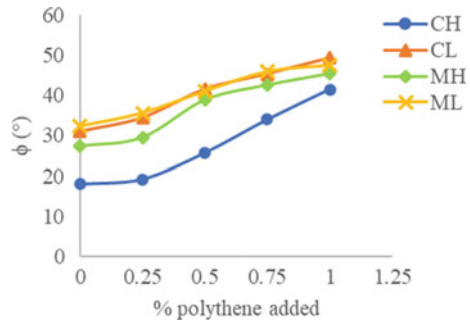


Fig. 5 Variation of ϕ value with different % of polythene



strip content is the observed limit where the CBR has an improvement of up to 14%. For CL soil, 0.5% of polythene strips gives 17% increment in CBR. Further higher percentages also cause increment, but the variation is not much significant. From Table 7, it can be seen that there is a similar variation in CBR for MH and ML soils, i.e., CBR goes on increasing by the addition of polythene. In case of ML soil, there is a slight increase in CBR, i.e., 10% with 1% polythene. However, for MH soil, there is a significant change in CBR. After 1% of polythene added, CBR increased by 31%. The value of cohesion decreases by increasing the percentages of polythene strips. This is due to the separation of soil particles by plastic pieces and reduction

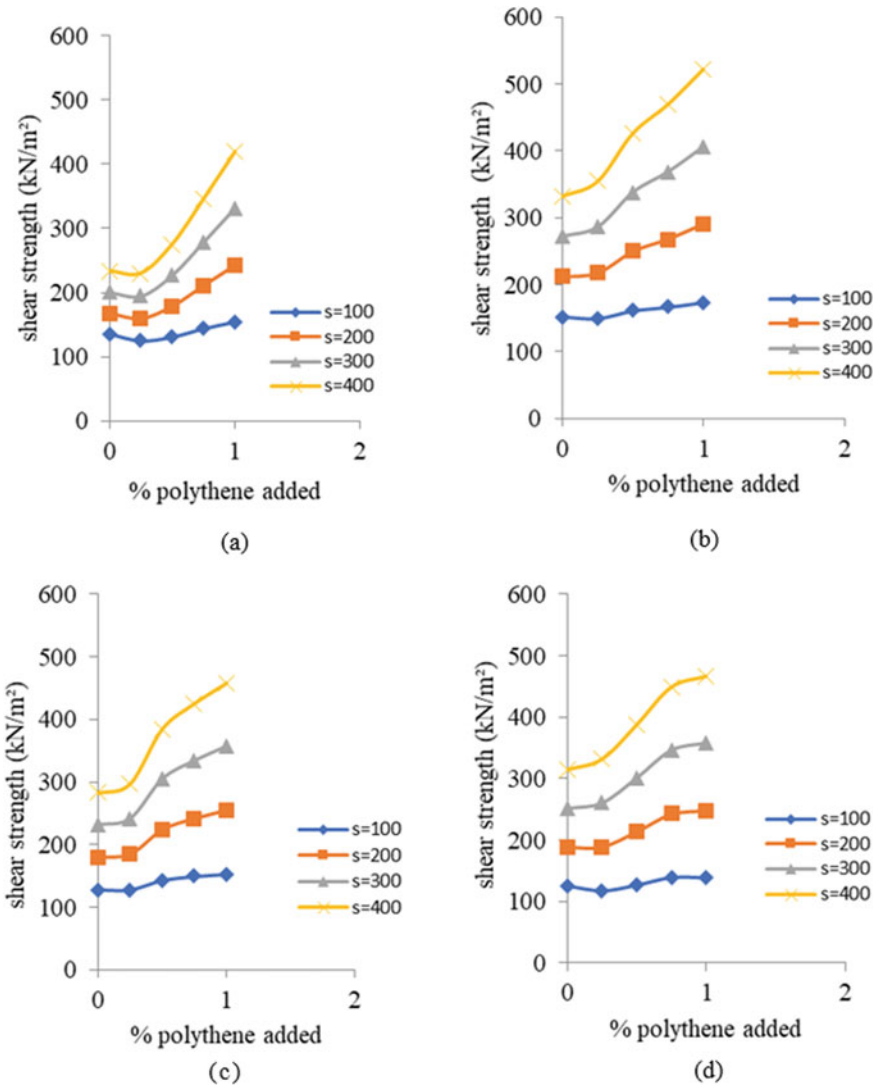


Fig. 6 Shear strength versus % polythene added for a CH, b CL, c MH, d ML types of soils

in MDD. The variation of ϕ value is shown in Fig. 5. It increases for all soils with addition of polythene strips which is due to increase in frictional resistance. Thus, there is a net increase in shear strength of soils by the addition of polythene strips. Among all type of soils, CH soil shows more increment in shear strength after adding the polythene strips. The results show that addition of plastic wastes improves soil properties and thereby stabilizing the weak soil which become further useful.

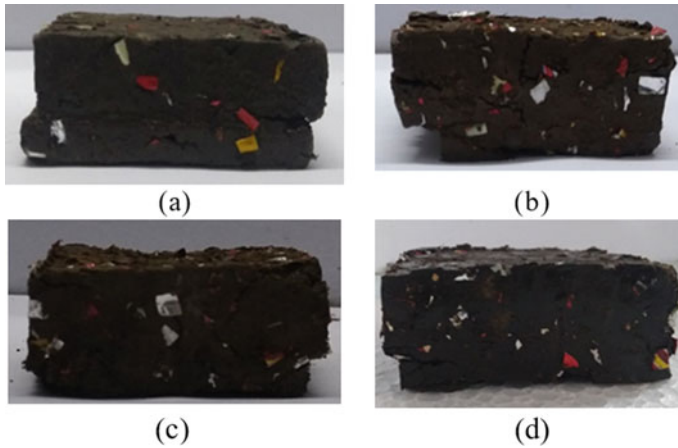


Fig. 7 Shear failure patterns for **a** ML, **b** MH, **c** CL, **d** CH soils

4 Conclusions

With addition of plastic waste, the c value decreases and ϕ value increases irrespective of the soil types. However, the overall change in shear strength may vary from soil to soil. There was a marginal increase in CBR value of some soils after adding the plastic waste. However, in some soils, the CBR value was found to decrease beyond certain extent of plastic waste added. It is recommended to evaluate the overall gain or loss of soil strength w.r.t. soil types as well as composition of plastic wastes used at the site.

References

1. Choudhary AK, Jha JN, Gill KS (2010) A study on CBR behaviour of waste plastic strip reinforced soil. *Emirates J Eng Res* 15:51–57
2. Anzar H (2017) Use of waste plastics for the enhancement of soil properties: a recent advancement in geotechnical engineering. *Int J Eng Res Technol* 6(7):102–111
3. Consoli NC, Montardo JP, Prietto PDM, Pasa GS (2002) Engineering behaviour of sand reinforced with plastic waste. *J Geotech Geoenviron Eng* 128(6):462–472
4. Biradar SV, Moniuddin MK (2015) Soil stabilization using waste pet fiber material. *Int J Sci Res Dev* 3(3):3578–3583
5. Harish C, Ashwini HM (2016) Stabilization of soil by using plastic bottle strips as a stabilizer. *Int Res J Eng Technol* 3(8):1874–1877
6. Dikkar H, Narkhede R, Dhande B, Avhad S, Shewale R, More V (2017) Improvement of soil properties by using waste plastic. *Int Res J Eng Technol* 4(4):3383–3388
7. Ashraf A, Sunil A, Dhanya J, Mariamma J, Varghese M, Veena M (2011) Soil stabilisation using raw plastic bottles. *Indian Geotech Conf* 9(4):812–815
8. Mallikarjuna V, Mani B (2016) Soil stabilization using plastic waste. *Int J Res Eng Technol* 5(5):391–394

9. Jha JN, Choudhary AK, Gill KS, Shukla SK (2014) Behaviour of plastic waste fiber-reinforced industrial wastes in pavement applications. *Int J Geotech Eng* 8(3):277–286
10. Bala RP, Prasad A, Chandra SA (2013) A study on CBR behaviour of waste plastic (PET) on stabilised red mud and fly ash. *Int J Struct Civil Eng Res* 2(3):231–240
11. Bhattarai P, Kumar B, Santosh K, Manikanta TC, Tejeswini K (2013) Engineering behaviour of soil reinforced with plastic strips. *Int J Civil Struct Environ Infrastruct Eng Res Dev (IJCSSEIRD)* 3(2):83–88
12. Das R, Majhi K, Khatun C, Maiti A (2017) Soil stabilization using plastic strips of varied sizes by enhancing the bearing capacity. *Int J Sci Eng Res* 8(3)
13. Naeini SA, Rahmani H (2017) Effect of waste bottle chips on strength parameters of silty soil. *Int J Civil Environ Eng* 11(1):6–10
14. Kumar ABG, Vageesh HP (2017) Effect of discarded plastic waste as stabilizer on engineering properties of cohesive soil. *Int J Eng Technol Sci Res* 4(12):779–786
15. Kalliyath VJ, Joy JT, Paul JM, Vadakkal AM (2016) Soil stabilization using plastic fibers. *Int J Sci Technol Eng* 2(2):484–487
16. Okoro CC, Vogtman J, Yousif A, Agnaou M, Khoury N (2011) Consolidation characteristics of soils stabilized with lime, coal combustion product, and plastic waste. In: *GEO-FRONTIERS 2011*. March 13-16, 2011 | Dallas, Texas, United States. [https://doi.org/10.1061/41165\(397\)123](https://doi.org/10.1061/41165(397)123)

Utilization of E-waste Plastic as Aggregate Replacement in Bituminous Concrete Mixes



Abhitesh Sachdeva and Umesh Sharma

1 Introduction

E-waste comprises of discarded or defective computers, laptops and various other devices of utility and entertainment. E-waste constitutes of 50% metallic residues, 21% plastic and the remaining percentage accounts for other materials and non-ferrous metals [1]. The major polymeric constituents of E-waste plastic are high impact polystyrene (HIPS) and acrylonitrile-butadiene styrene (ABS) [2]. Modern electronic items are designed for excellent thermal degradation and therefore these polymers have very high melting temperatures. The engineering properties of ABS and HIPS polymers are tabulated in Table 1.

Globally, it is estimated that 50 million metric tons (MMT) of E-waste is generated per year and therefore it has become a major concern for various waste management agencies. In India, its accumulation has increased tremendously at a rate of 18.5 lakh (MT) per year [3]. Lack of organized E-waste management and disposal mechanisms in our country necessitates its handling by unorganized sector comprising of unskilled labour and crude mechanisms. Traditional methods of E-waste plastic disposal such as incineration and land filling have proved to be a catastrophe for the environment and human health. There is an urgent need to develop methodologies having strategic approach to ensure efficient and sustainable disposal of E-waste plastic. It is evident from the past research works that conventional bituminous mixes can be effectively modified by replacing aggregates with waste plastic materials. Various test results have shown that such modifications enhance the load bearing capacity and strength of the bituminous mixes. Hence, plastic pavements are supposed to have much higher life depending upon the extent of modification and processes used for

A. Sachdeva (✉) · U. Sharma
Punjab Engineering College (PEC), Deemed to be University, Chandigarh 160012, India

Table 1 Engineering properties of ABS and HIPS polymers

S.No.	Properties	ABS	HIPS
1	Flexural strength (MPa)	75.84	±2126
2	Tensile strength(MPa)	44.81	22
3	Melting temperature (°C)	200	180–260
4	Density (g/cc)	1.01–1.21	1.04

modification. The present work was carried out to analyse the effect of incorporation of E-waste plastic as an aggregate replacement for both fine as well as coarse aggregates individually, which shall help to tackle the problems of E-waste plastic disposal.

2 Literature Review

Colbert [4] investigated the effect of incorporating E-waste plastic powder in varying percentages of 2.5, 5 and 15% in conventional asphalt binder. The improvement of modified binders was estimated in terms of binder viscosity, rutting susceptibility and mixing and blending temperatures. Specimens were subjected to various test procedures such as the rotational viscosity test, dynamic shear rheometer characterization, asphalt binder artificial ageing characterization and bending beam rheometer characterization. The modified binders were observed to be stiffer in comparison to controlled asphalt binders while having slightly lower m-values. Optimum low temperature performance was observed at 5% concentration for both HIPS and ABS modified asphalt binders. Modified binders were found to be less susceptible towards rutting in comparison to the virgin asphalt binders. At 5% ABS polymer concentration, the modified asphalt binder exceeded low temperature performance of virgin asphalt binder while having a creep stiffness of 298 MPa.

Giri [5] studied the performance of bituminous mixes prepared with recycled concrete aggregates and modified waste polyethylene binder in terms of various parameters like the Marshall stability, indirect tensile strength test, flow values, resilient modulus and the rutting susceptibility. Aggregates procured from construction and demolition waste were treated with different chemicals prior to mixing with binder and shredded polyethylene in varying percentages of 0% to 3% were used for preparation of the mixes. The OBC for different mixes was determined using Marshall test and thereafter various other properties for the mixes were evaluated at their respective OBCs. It was concluded that the mix prepared with pretreated recycled concrete aggregate and polyethylene gave the highest stability value compared to other mixes. These mixes fared better than other combinations in terms of indirect tensile strength, flow number, resilient modulus and the rutting susceptibility.

Murugan [6] conducted a research work on utilization of E-waste plastic as an aggregate replacement for coarse aggregates in bituminous mixes. Modified mixes were prepared by varying replacement percentages of E-waste plastic (0–4%) for

Table 2 Bitumen characterization

Bitumen property	Sample 1	Sample 2	Average	IS 73:2013	Test procedure
Penetration at 25 °C, 100 g, 5 s, 0.1 mm	63.4	67.5	65.4	50-70	IS 1203-1978
Softening point, °C, minimum	45.5	47.6	46.1	45-75	IS 1205-1978
Specific gravity	1.01	1.01	1.01	Min 0.99	IS 1202-1978
Ductility value @ 27 °C (cm)	84	85	84.5	Min 75	IS 1208-1978
Flash point (°C)	276	284	280	Min 220	IS1209-1978
Fire point (°C)	314	324	319	Min 220	IS1209-1978

coarse aggregates of size 6.7 mm, while percentages for size 11.2 mm and quarry dust were kept constant as 10 and 20% by the weight of total mix, respectively. An increasing trend was observed in MSV and Marshall quotient (MQ) with increasing replacement percentages. Maximum MSV was observed at 12% replacement of aggregates with E-waste plastic.

3 Materials

3.1 Bitumen (VG-30)

Neat VG-30 bitumen was procured from VARDHMAN STEELS, Rajpura Road, Patiala, Punjab. Various engineering properties of bitumen are tabulated in Table 2. The test results satisfy the requirements as per specifications of IS 73:2013.

3.2 Aggregates

Fresh aggregates were procured from Saraswati stone crusher, Derabassi, Mohali, Punjab. The procured aggregates were tested for various physical properties and the test's results obtained were compared with allowable values as per Ministry of Road Transport and Highways (MoRT and H) Vth revision specification as shown in Table 3.

Table 3 Aggregates characterization

Aggregate property	Sample 1	Sample 2	Average	MoRT and H (Vth revision)	Test procedure
Aggregate crushing value (%)	21.4	22.3	21.9	Max 30	IS 2386 (Part 4)-1963
Aggregate impact value (%)	12.3	11.9	21.1	Max 24	IS 2386 (Part 4)-1963
Los Angeles abrasion value (%)	19.8	20.0	19.9	Max 30	IS 2386 (Part 4)-1963
Absolute specific gravity	2.62	2.64	2.63	Min 2.5	IS 2386 (Part 3)-1963
Apparent specific gravity	2.70	2.72	2.71	Min 2.5	IS 2386 (Part 3)-1963
Total water absorption (%)	1.01	1.03	1.02	Max 2	IS 2386 (Part 3)-1963
Flakiness and elongation index	–	–	21.8	Max 30	IS 2386 (Part 1)-1963

3.3 E-waste Plastic

E-waste plastic was procured from D M RECYCLERS, Hapur Road, Meerut (U.P.). It constituted the plastic scrap of obsolete electronic gadgets such as computers and laptops. Shredded E-waste plastic was subjected to various laboratory experiments. The results are tabulated in Table 4 and were found to be in agreement with some previous research works involving E-waste plastic characterization [6].

Table 4 E-waste plastic characterization

Properties	E-waste plastic	Test procedure
Specific gravity	1.15	IS 2386 (Part 3)-1963
Water Absorption (%)	0	IS 2386 (Part 3)-1963
Colour	White and Grey	As Observed
Shape	Angular	IS 383-1970
Crushing value (%)	1.32	IS 2386 (Part 4)-1963
Impact value (%)	1.17	IS 2386 (Part 4)-1963
Flakiness and elongation index (%)	73	IS 2386 (Part 1)-1963

4 Methodology

Aggregate gradation for bituminous concrete mix was adopted in accordance with the specifications of MoRT and H (Vth) revision as shown in Table 5. The adopted gradation lies well within MoRT and H upper and lower cumulative passing percentage limits as shown in Fig. 1. E-waste plastic was shredded with the help of the marble cutter and the wire cutter. The procured waste material was first shredded into long strips by using the marble cutter and then the shredded material was cut into desired sizes with the help of a vernier calliper and wire cutter as shown in Fig. 2. Plastic granules passing IS sieve size 4.75 mm and retained on IS sieve size of 2.36 mm were used for fine aggregate replacement. Similarly, plastic granules passing IS sieve size 19 mm and retained 13.2 mm were used for coarse aggregate replacement as shown in Fig. 3. From the selected aggregate gradation it was observed that maximum proportion of aggregates retained on these sieve sizes. Therefore, these aggregate sizes have been selected for replacements in order to achieve maximum percentage replacement of aggregates by E-waste plastic.

Table 5 The composition of bituminous concrete pavement layer

Grading	1
Nominal aggregate size	19 mm
Layer thickness	50 mm
IS sieve (mm)	Cumulative percent by the weight of total aggregate passing
45	–
37.5	–
26.5	100
19	90–100
13.2	59–79
9.5	52–72
4.75	35–55
2.36	28–44
1.18	20–34
0.6	15–27
0.3	10–20
0.15	5–13
0.075	2–8
Bitumen content % by the mass of total mix	Min 5.2

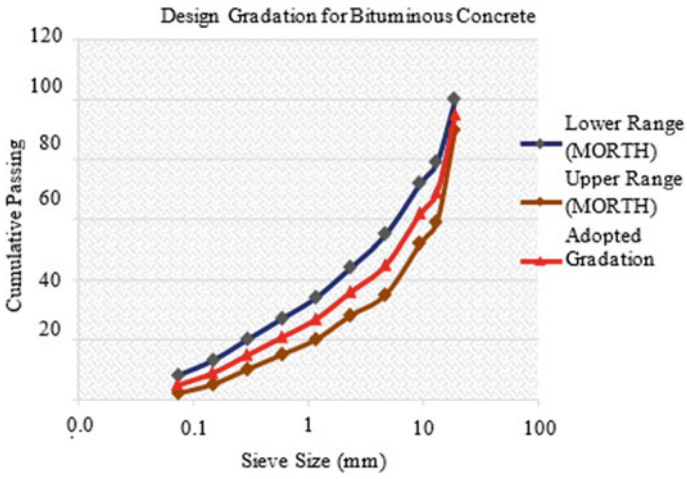


Fig. 1 Designed gradation for bituminous concrete

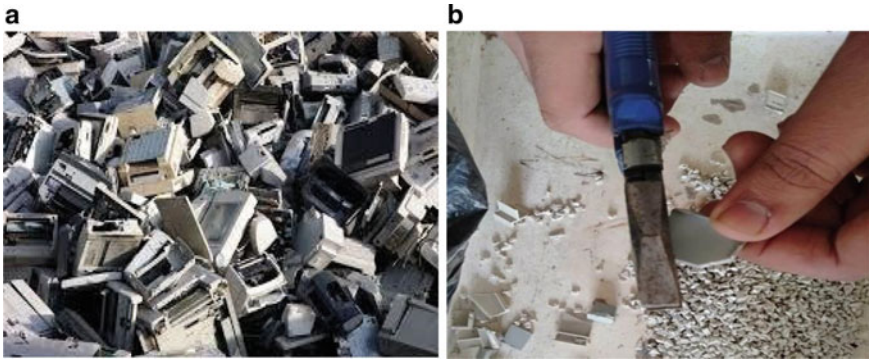


Fig. 2 E-waste plastic a before shredding, b E-waste plastic after shredding



Fig. 3 Shredded E-waste plastic of size 2.36 mm and 13.2 mm (retained IS sieve)

5 Preparation of Specimens

5.1 Marshall Stability Test

The control and modified mixes were prepared as per Marshall testing procedures. Bitumen heated up to 160 °C was added to heated aggregates (150–160) °C by total weight of the mix. Both the materials were thoroughly mixed at a blending temperature of about 150 °C. The prepared mix was then placed into Marshall mould assembly and compacted by giving 75 blows on each face. In case of modified mixes, E-waste plastic was added to heated aggregates just prior to the addition of bitumen. The aggregates were mixed with E-waste plastic for enough time to ensure homogeneity of the modified BC mixes.

E-waste plastic modified mixes were prepared with various replacement percentages for both the sizes. For fine aggregate replacement, the modified mixes were prepared with an initial replacement percentage of 1.0% by the total weight of aggregates retained on the IS sieve size of 2.36 mm with an incremental rate of 1.0% until test results show a declining trend after achieving a maximum MSV. Similarly, for coarse aggregate replacement the modified mixes were prepared with an initial percentage replacement of 0.5% by the total weight of aggregates retained on IS sieve size of 13.2 mm with an incremental rate of 0.5%. For all control and modified mixes, bitumen was added in varying binder percentages of 4.0, 5.0, 6.0 and 7.0%. The OBC was determined corresponding to the median of designed limits of percent air voids in the total mix (i.e. 4%) as per specifications of MoRT and H Vth revision.

5.2 Retained Marshall Stability Test

Moisture susceptibility of both control and modified mixes was evaluated in terms of retained Marshall stability (RMS) value in order to estimate the durability characteristics of these mixes. The test specimens were prepared for each type of the mix as per standard procedures of the Marshall stability test. The prepared specimens were conditioned in a thermostatic controlled water bath maintained at about 60 °C for a duration of about 24 h. RMS value was estimated as the ratio of the stability value of conditioned specimen to that of the unconditioned specimens, expressed as percentage.

5.3 Stripping Value Test

Stripping phenomenon for both controlled and modified mixes was estimated by conducting the stripping value test in accordance to IS: 6241-1971. Sample mixes

were prepared using 200 gm of aggregates passing IS sieve size 20 mm and retained on IS sieve size 12.5 mm. Bitumen heated up to 160 °C was added to heated aggregates (150–160) °C by the total weight of mix. Both the materials were thoroughly mixed at a blending temperature of about 150 °C. The uncompact mix was transferred to a glass beaker and allowed to cool for about two hours. The covered beaker was kept in water for a duration of 24 h at a temperature of about 40 °C. Stripping value, expressed as percentage, is defined as the ratio of the uncovered area (as observed visually) to the total area of aggregates. Table 7 shows the comparison between stripping values of the control mix and modified mixes.

Table 6 The Comparison between various strength parameters of control mix, modified mixes and MoRT and H (Vth Revision) specifications

Parameters	BC	2.36 mm modified BC mix	13.2 mm modified BC mix	MoRT and H
OBC (%)	5.66	5.36	5.26	≥5.2%
E-waste plastic (%)	0	9	3.5	–
Stability (at 60 °C KG)	1790.5	3247.5	2789.2	Min 900
Flow (0.25mm)	3.78	3.51	2.14	2–4
Air Void (%)	4	4	4	3–6
Voids in Mineral Aggregates (%)	15.75	16.73	16.36	–
Voids Filled with bitumen (%)	76.8	68.4	68.7	65–75
Bulk density (g/cc)	2.378	2.362	2.363	–
Stability (Conditioned, at 60 °C KG)	1569.9	2927.6	2375.5	Min 900
Flow (Conditioned, 0.25 mm)	3.91	3.62	2.33	2–4
Retained stability (%)	87.67	90.15	85.17	Min 75

Table 7 Comparison between stripping values of control mix and modified mixes

Mix type	Percent retained coating (%)	MoRT and H
Natural aggregates	96	Minimum retained coating 95%
E-plastic granules	98	

6 Analysis of Results

6.1 Determination of Optimum Bitumen Content

Marshall samples for both control and modified mixes were prepared with VG-30 bitumen as per Marshall method of mix design to obtain their respective OBCs. The variation of various volumetric properties of modified mixes at varying E-waste percentages is shown in Figs. 4 and 5. Maximum MSV for control mix was achieved at OBC of 5.66%. For modified mixes, it was observed that MSV increases with increasing percentages of E-waste plastic, achieves a peak value and then decreases. In case of 2.36 mm modified BC mix maximum MSV was achieved with 9% E-waste plastic at an OBC of 5.36%. Similarly, for 13.2 mm modified BC mix maximum MSV was achieved with 3.50% E-waste plastic at an OBC of 5.26%. Modified mixes were found to have lesser bulk densities in comparison to control mixes probably due to lower specific gravity of E-waste plastic as compared to natural aggregates. A decrease was observed in percentage voids filled with bitumen which might be because the quantity of bitumen used for modified mixes was lesser as compared to

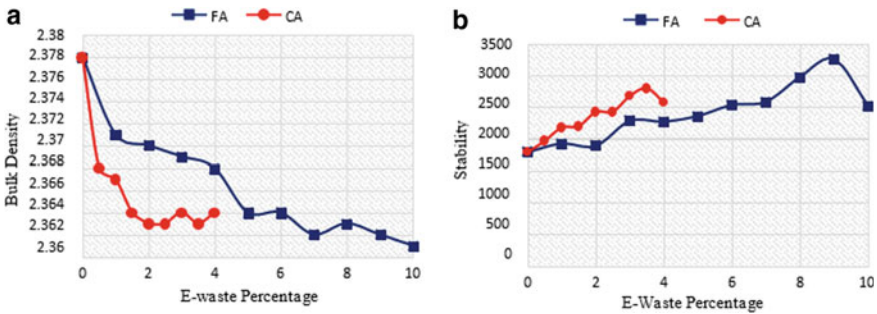


Fig. 4 Comparison of a Bulk density versus E-waste. b Stability versus E-waste

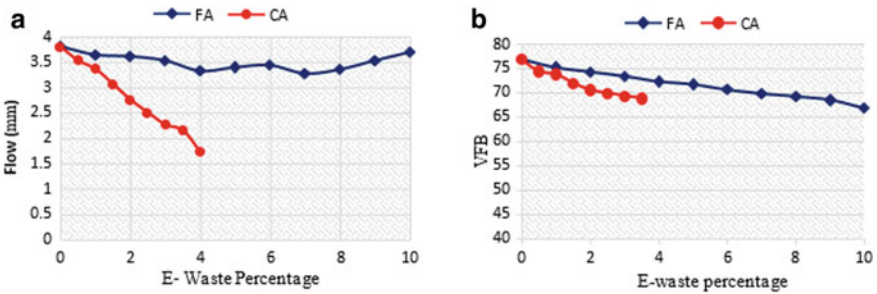


Fig. 5 Comparison of a Flow versus E-waste, b VFB versus E-waste

that of control mixes. The comparison between various strength parameters of control mix, modified mixes and MoRT and H (Vth Revision) specifications is tabulated in Table 6.

7 Cost Benefit and Material Saving

Taking into consideration the economic aspects of all construction projects, it is very important to compare the modified and control mixes in terms of material saving.

7.1 Aggregate

Aggregates of size 2.36 mm were replaced with E-waste plastic by the total weight of aggregates retained on IS sieve size of 2.36 mm. Maximum MSV was achieved at 9% aggregate replacement. Similarly, in case of 13.2 mm aggregate replacement, maximum MSV was obtained at 3.5% aggregate replacement. The MSV achieved with these modified BC mixes was relatively high in comparison to that of the control BC mix. Therefore, the adopted methodology effectively contributes in conservation of natural aggregate reserve.

7.2 Bitumen

For conventional bituminous mix, maximum MSV was obtained at an OBC of 5.66 % by the weight of total mix. In case of 2.36 mm modified BC mix and 13.2 mm modified BC mix, maximum MSV was obtained at OBCs of 5.36% and 5.26 %, respectively. Hence, it was observed that E-waste plastic modified mixes required a lesser quantity of bitumen to provide much higher stability values in comparison to neat bituminous mixes. 9% aggregate replacement with E-waste plastic resulted in a bitumen saving of 5.30% in 2.36 mm modified BC mix. Similarly, 3.5% aggregate replacement with E-waste plastic resulted in a bitumen saving of 7.06% in 13.2 mm modified BC mix as shown in Table 8.

8 Conclusions and Recommendations

The present study is found to be effective in providing a partial solution to E-waste plastic disposal problems. Incorporation of E-waste plastic significantly enhances the load bearing characteristics of conventional bituminous mixes as it provides comparatively very high values for Marshall stability. It is observed that modified mixes were

Table 8. Bitumen saving in modified mixes

S.No.	Type of mix	Optimum Bitumen content (%)	Marshall stability value (kg)	Material saving
1	Control mix	5.66	1790.5	–
2	Fine aggregate modified mix	5.36	3247.5	5.30%
3	Coarse aggregate modified mix	5.26	2789.2	7.06%

less susceptible to rutting and therefore are capable for improving pavement durability and performance. The conclusions derived from analysis of work carried in this study have been summarized below:

- MSV of modified mixes increases with increasing percentages of E-waste plastic up to 9% in case 2.36 mm modified BC mix and 3.5% for 13.2 mm modified BC mix and then decreases. In comparison to control mix, MSV increased by 44.86% for 2.36 mm modified BC mix and 35.80% for 13.2 mm modified BC mix. For both modified mixes, values of flow and MQ were within the permissible limits. The high impact and crushing resistance of E-waste plastic must have been responsible for the increased stability values.
- Bulk density of modified mixes was found to decrease with the increasing percentage of E-waste plastic. This might be due to lower specific gravity of E-waste plastic in comparison to natural aggregates. Decreased bulk density of the modified mix will certainly affect the haulage cost of material and therefore can effectively contribute to project savings.
- A decrease in percentage voids filled with bitumen was observed for modified mixes with incorporation of E-waste plastic probably because the quantity of bitumen required for modified mixes was lesser in comparison to control mix.
- All volumetric properties for control and modified mixes corresponding to their respective OBCs were found to within the specified limits.
- Based on various test results, it was found that E- plastic granules can be effectively used for fine aggregate replacement. In case of coarse aggregate replacement, the modified mixes performed better in comparison to the control mix under Marshall stability test. However, in this case, it was found that the 13.2 mm E- plastic granules had high flakiness index, and therefore these granules were weak and could not provide enough interlocking between the aggregates. This might have been a reason for decreased strength and stability values in comparison to that of 2.36 mm modified BC mix.
- Both control and modified mixes performed satisfactory under moisture sensitivity tests. The RMS value of conditioned specimens were found to decrease in comparison to the unconditioned specimens as they were exposed to the worst field conditions of high temperature and water immersion. Based on the stripping value test results, the loss of adhesion between the binder and aggregates was lesser in case of the E-plastic mix in comparison to that of natural aggregate mix.

- Research work can further be carried on developing suitable methodology by which E-waste plastic can be first melted and then reshaped in a form of 13.2 mm size coarse aggregates so that the issue of high flakiness index is eliminated. This will enable us to evaluate the practicality of utilizing reshaped 13.2 mm E-plastic granules as a coarse aggregate replacement in bituminous mixes for flexible road construction.
- The modified BC mix with 9% of E-waste plastic performed better in terms of various properties as compared to control BC mix. The OBC for the modified mixes were found to be lesser in comparison to that of the control mix. Therefore, the modified mixes effectively contribute in the bitumen saving and conservation of natural aggregate reserve.
- Keeping all these benefits in mind, utilization of E-waste plastic in bituminous mixes and road construction can surely motivate organized E-waste management. However, on-field application requires one time capital investment for the installation of suitable commercial shredders at nearby batching plants. Shredded E-plastic granules can be fed to the pug mill in the conventional manner for mixing and preparation of modified mixes. This innovative methodology can certainly curb the problems of E-waste plastic disposal and therefore will contribute to environmental conservation and provide sustainability in road infrastructure.
- Utilization of E-waste plastic and preparation of modified mixes was done as per standard procedures of Marshall mix design and requires no alterations.

References

1. Awasthi AK (2018) E-waste management in India: a mini-review. *Waste Manag Res* 36(5):408–414
2. Brunori C (2015) Innovative technologies for metals recovery and plastic valorization from electric and electronic waste: an integrated approach. *Environ Eng Manag J* 14(7):1553–1562
3. Janardhanan T (2017) Improvements in the microstructural and mechanical properties of geopolymer concrete containing NMF's of E-wastes as partial replacement of aggregates. *Eur J Environ Civil Eng* 10(4):373–379
4. Colbert BW (2012) Properties of modified asphalt binders blended with electronic waste powders. *J Mater Civil Eng ASCE* 24(10):1261–1267
5. Giri JP (2018) Performance of bituminous mixes containing emulsion-treated recycled concrete aggregates. *J Mater Civil Eng ASCE* 30(4):1–10
6. Murugan L (2018) Use of e-plastic waste in bituminous pavements. *Gradevinar* 70(7):607–615

Investigation of Physical and Chemical Properties in RAP Materials



Kajugaran Santhirasegaram, Wasantha Kumara Mampearachchi,
and Dharamveer Singh

1 Introduction

Reclaimed asphalt usage in pavement construction has been rapidly increased at world range due to environmental and economic benefits [1]. Aging of asphalt pavement depend on temperature, traffic loading, weather, and UV solar radiation. Bitumen aging oxidation process can be categorized into two aspect as such photo-oxidative and thermal oxidative depend on constituents and diversity of bitumen [2–4].

Marshall test method is used to find suitable optimum binder content for asphalt mixture which would not be adequate to investigate aged properties of asphalt, and it can be used to measure volumetric properties of asphalt mixture. Fourier transform infrared (FTIR) spectroscopy can be used to identify the functional groups and their concentration in bitumen by reflection and absorption energy of molecules. However, the carbonyls and sulfoxides functional groups would be analyzed as a research tool to identify the aging behavior of bitumen [5, 6]. At FTIR spectrum analysis, peaks of carbonyl (C=O) and sulfoxide (S=O) are obtained at 1700 and 1030 cm^{-1} wave-numbers which is shown at Fig. 1 [7].

In the laboratory, bitumen aging can be conducted by pressurized aging vessel (PAV) and rolling thin film oven (RTFO). Index of the carbonyl and sulfoxides functional groups in long-term aged bitumen and short-term aged bitumen can be analyzed using FTIR test with PAV and RTFO test sample. The physical properties such as “viscosity and brittleness of bitumen” are increased on aged bitumen which can be investigated through the conventional tests such as penetration, softening point, and ductility test.

K. Santhirasegaram (✉) · W. K. Mampearachchi
University of Moratuwa, Moratuwa, Sri Lanka

D. Singh
Indian Institute of Technology, Bombay, India

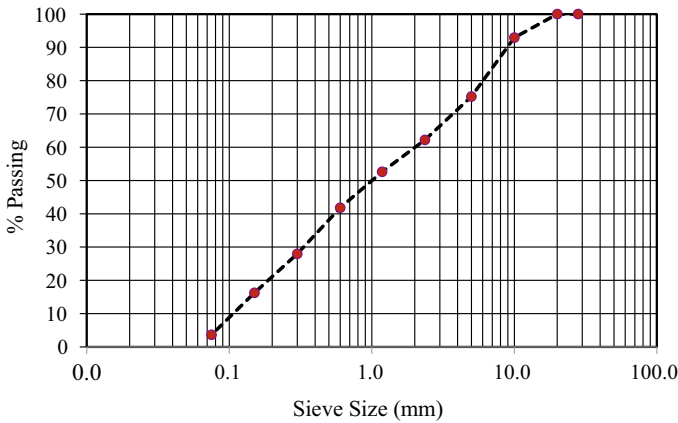


Fig. 1 Combine gradation of mineral aggregates with RAP

2 Experimental

2.1 Materials and Methods

The 60/70 penetration grade bitumen was used with 20%, 30%, and 40% of RAP in total weight of aggregates to conduct the Marshall mix design. The physical test properties such as penetration (ASTM D5), softening point (ASTM D36)m and ductility (ASTM D113-07) of 60/70 penetration grade bitumen and RAP are given in Table 1 [8–10]. The gradation of aggregates for asphalt mix design was adjusted according to the results of RAP aggregates. The designed gradation and specification limits are shown in Fig. 2. The different proportions of RAP such as 20, 30, and 40% of RAP in total weight of aggregates were mixed with virgin bitumen to conduct the Marshall mix design. Physical properties of asphalt mixture were measured, and the optimum binder asphalt mixture was prepared for extraction, recovery, and FTIR test. Recovered binder samples from extraction solution were subjected under PAV test. Finally, FTIR test was conducted to analyze the functional groups of aged bitumen.

Table 1 Conventional test results of binder

Types of binder	Softening point (°C)	Penetration (mm)	Ductility (cm)
RAP recovered binder	74	42	78
Neat bitumen (Penetration grade 60/70)	52	67	

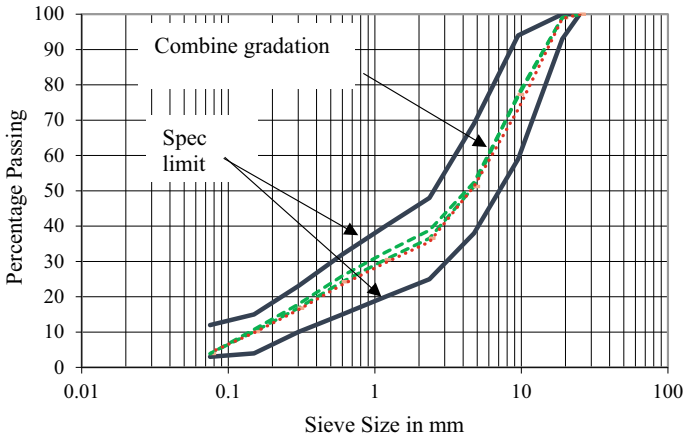


Fig. 2 Combine gradation of mineral aggregates with RAP

2.2 Marshall Test

The Marshall design was carried out with 0, 20, 30, and 40% of RAP materials in total weight of aggregates. The series of test specimens were prepared with binder content intervals from 3.5 to 5.5%. The virgin binder content was adjusted according aged binder content of RAP and total binder content of each specimen increased by 0.5% in total weight of aggregates. The Marshall test was conducted for each specimen to investigate the physical properties of asphalt mixture such as air voids, voids in mineral aggregates, stability, and flow. The optimum binder content was chosen, and series of asphalt mixture specimens with 0, 20, 30, and 40% of RAP materials were prepared to conduct the FTIR test.

2.3 Extraction and Recovery Test

The RAP mixture was extracted using the centrifuge extraction method (ASTM D2172) with trichloro ethylene (TCE), and 0, 20, 30, and 40% of RAP in total aggregates weight of asphalt mixture were also extracted, and RAP binders were recovered by the rotary evaporator (ASTM D5404) [11, 12].

2.4 Aging Process

The recovered binders for varied RAP asphalt mixtures were aged using pressure aging vessel (PAV) (ASTM D6521) to clearly observe and analyze the carbonyl and sulfoxide functional groups in aged recovered binder [13].

2.5 Fourier Transform Infrared Spectroscopy (FTIR) Test

The recovered and aged binders were prepared for FTIR test using the solution of trichloro ethylene which had a concentration of 75 g/l [8]. The index of carbonyl (ICO) and sulfoxide (ISO) functional groups was calculated at 1700 cm^{-1} peak and 1030 cm^{-1} peak using equations [14].

$$\text{ICO} = \text{Area at } 1700 \text{ cm}^{-1} / \text{Area at } 1460 \text{ cm}^{-1} \text{ and Area at } 1375 \text{ cm}^{-1} \quad (1)$$

$$\text{ISO} = \text{Area at } 1030 \text{ cm}^{-1} / \text{Area at } 1460 \text{ cm}^{-1} \text{ and Area at } 1375 \text{ cm}^{-1} \quad (2)$$

3 Results and Discussion

3.1 Results of Conventional Tests and Mechanical Sieve Analysis

The results of the conventional test for recovered RAP binder such as penetration, softening point, and ductility are given in Table 1. The binder content of RAP alone mixture was observed as 4.2%. The penetration and ductility of RAP binder were decreased, and softening point was increased due to the thermal oxidation and photo-oxidation of bitumen. The mechanical sieve analysis for RAP and mineral aggregates was done to find the predetermine gradation for asphalt mixture. The milling process produced a major portion of crushed aggregates in RAP materials, resulting in higher fines in the RAP mixture.

3.2 Results of Marshall Test

The Marshall design was carried out to find the optimum binder content of asphalt mixture for 0, 20, 30, and 40% RAP in total aggregates weight. The optimum binder content was chosen based on lower point of voids in mineral aggregates at minimum

Table 2 Results of marshall test

RAP%	Optimum binder content%	VMA	Voids	Stability (kN)	Flow (mm)
0	5	17.8	4.5	17.4	10.2
20	5	16.5	4.6	20.1	9.5
30	4.9	16	4.5	19.2	9.0
40	4.8	15.7	4.1	18.1	8.0
Spec limit in Sri Lanka		>13	3–5	>8	8–16

binder content. The physical properties of asphalt mixture such as air voids, voids in mineral aggregates, stability, and flow are given in Table 2. Marshall stability was increased up to 20% of RAP, and it was decreased with increase in RAP content. Therefore, significant changes were not obtained at Marshall test results. However, the flow was reduced with the increment of RAP content due to the aged binder which would not act as well coated materials and lubricants. Because of black rock effect and reduction of oil, part of bitumen can be involved on properties of aged RAP binder.

3.3 Results of Fourier Transform Infrared Spectroscopy (FTIR)

The RAP materials and different proportions of RAP mixture were extracted using centrifuge extraction method (ASTM D2172) with trichloro ethylene (TCE), and extracted solutions were recovered using rotary evaporator (ASTM D5404). The recovered binders were subjected in PAV for aging, and finally, samples were investigated under FTIR. The spectrum results of FTIR were illustrated in Fig. 3, carbonyl groups (C=O) were indicated by the peak at wavenumber of 1700 cm^{-1} , and sulfoxide groups (S=O) were shown by the peak at wavenumber of 1030 cm^{-1} . Further, the main elements' peak values of the spectrum were identified as hydrocarbons and aromatics. Index of carbonyl and sulfoxide was calculated, and they were increased with the increment of RAP content. The degree of oxidation was increased with RAP content and correlation between specified functional groups and RAP percentage which was shown in Figs. 4 and 5.

4 Conclusion

The objective of this research was the evaluation and investigation of physical and chemical characterization of RAP materials with volumetric test parameters and

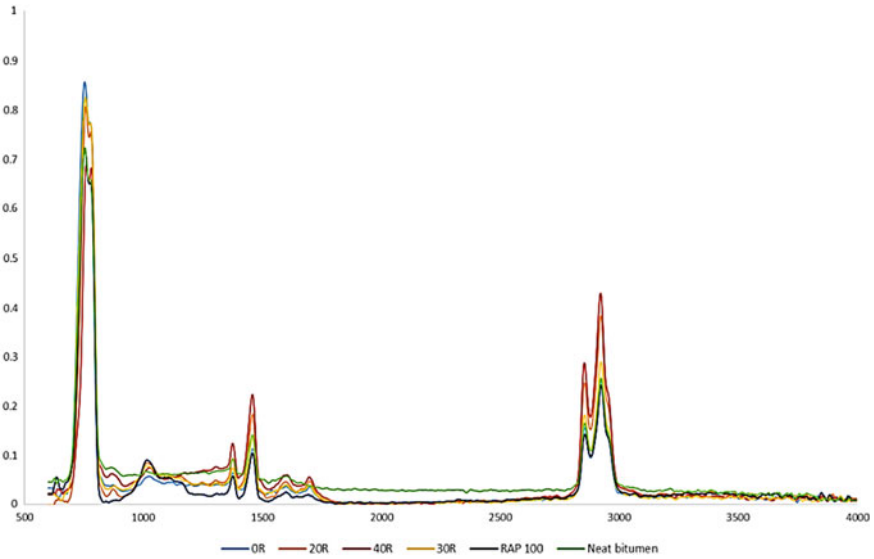


Fig. 3 FTIR spectrum results of binder

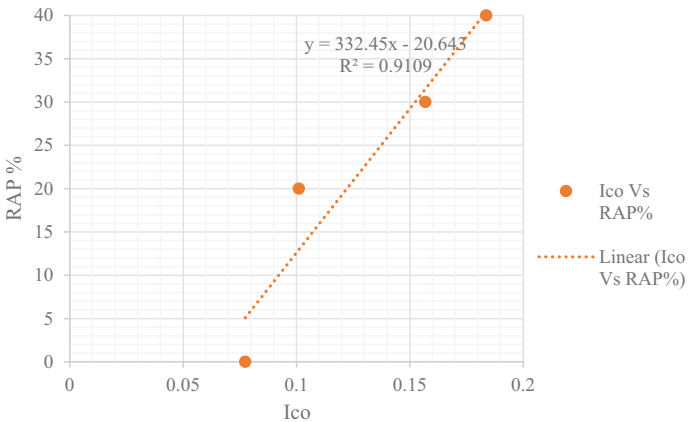


Fig. 4 ICO results versus RAP content

Fourier transform infrared (FTIR) spectroscopy results. The following conclusions were made from this experimental study.

- There are no significant changes in the volumetric properties with change in RAP content. However, physical and chemical properties can only be changed with RAP percentage. The flow value was reduced, and stability was increased with the increment of RAP content due to involvement of black rock effect. The 20%

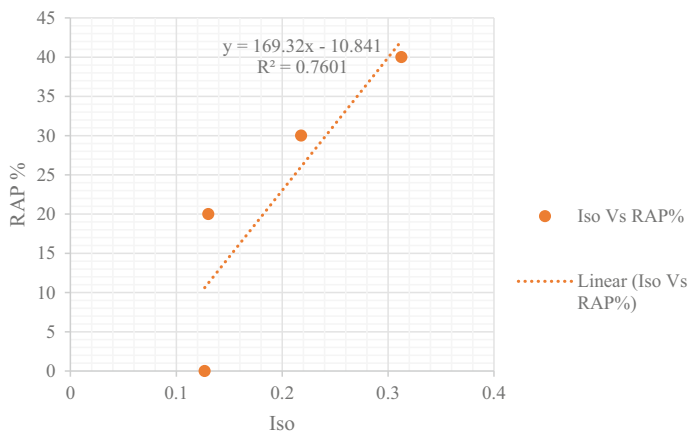


Fig. 5 ISO results versus RAP content

of RAP mixture without using rejuvenating agent would be recommended for flexible pavement construction.

- The spectrum of FTIR results can be used to identify the energy concentration level of carbonyl and sulfoxide which would be used to investigate the aged behavior of RAP materials.
- The correlations between RAP content and index of carbonyl and sulfoxide group can be drawn using equations which would be shown the degree of oxidation in bituminous materials.

Acknowledgements “The authors acknowledge the opportunity to submit the research work at the 5th conference of the Transportation Research Group of India held at Bhopal (India) from December 18–21, 2019, that forms the basis of this article.”

References

1. Al-qadi I, Elsefi M, Carpenter S (2007) Reclaimed asphalt pavement, a literature review. Illinois Center for Transportation, USA
2. Morian N, Hajj EY, Glover CJ, Sebaaly PE (2011) Oxidative aging of asphalt binders in hot mix asphalt mixtures. *Transp Res Record J Transp Res Board*, pp 107–116
3. Dehouche N, Kaci M, Mokhtar KA (2012) Influence of thermo-oxidative aging on chemical composition and physical properties of polymer modified bitumens. *Constr Build Mater* 26(1):350–356
4. Zeng WB, Wu SP, Wen J, Chen ZW (2015) The temperature effects in aging index of asphalt during UV aging. *Constr Build Mater* 93:1125–1131
5. Lu X, Isacson (2002) Effect of aging on bitumen chemistry and rheology. *Constr Build Mater* 16:15–22
6. Feng Z, Bian H, Li X, Yu J (2016) FTIR analysis of UV aging bitumen and its fraction. *Mater Struct* 49:1381–1389

7. Be Ze LE (2008) Recyclage a chaud des agregats d enrobes bitumenx Indentification de traceurs d homogeneite du melange entre bitume vieilli et bitume neuf d apport
8. ASTM International ASTM D5 (2013) Standard test method for penetration of bituminous material. USA: American Society for Testing and Materials
9. ASTM International ASTM D36 (2012) Standard test method for softening pint of bitumen (Ring and Ball Apparatus). USA: American Society for Testing and Materials
10. ASTM International ASTM D113-07 (2007) Standard test method for ductility of bituminous materials. USA: American Society for Testing and Materials
11. ASTM International ASTM D2172 (2011) Standard test method for quantitative extraction of bitumen from bituminous paving mixtures. USA: American Society for Testing and Materials
12. ASTM International ASTM D5404 (2011) Standard practice for recovery of asphalt from solution using the rotary evaporator. USA: American Society for Testing and Materials
13. ASTM International ASTM D6521 (2007) Standard test method for accelerated aging of asphalt binder using a pressurized aging vessel (PAV). USA: American Society for Testing and Materials
14. Liu G, Nielsen E, Komacka J, Leegwaer G, Ven M (2015) Influence of the soft bitumen on the chemical and rheological properties of reclaimed polymer modified binders from “old” surface-layer asphalt. *Constr Build Mater* 79:129–135

Application of New-fangled Tools and Techniques in Data Collection for Asset Management System for Urban Road Network in India



Bhaves Jain, Manoranjan Parida, Devesh Tiwari,
and Ramesh Anbanandam

1 Introduction

An urban road network plays a vital role in inter-city connectivity to ensure people and goods' smooth and timely movement. Availability of efficient, safe, and economical transportation to society is critical and necessary in meeting its objectives toward economic progress, social welfare, and domestic security. The structural and operational conditions of transportation facilities are crucial factors in the overall system's performance and the satisfaction of customers with the service provided. Thus, with the budget constraints and environmental issues, reconstruction of these roads cannot be the ultimate solution. Hence, it is the pressing need to overhaul the conventional practice, i.e., worst first and opt for asset management practices that believe in the proper maintenance and management of pavements and all their assets immediately after its construction.

In India, there have been several studies piloted for pavement management systems (PMS). However, most of them were conducted for the highways [1, 2] and low-volume rural roads [3–6], which required fewer attributes to be collected and related to

B. Jain (✉) · M. Parida · R. Anbanandam
Centre for Transportation Systems, Indian Institute of Technology Roorkee, Roorkee, Uttarakhand
247667, India
e-mail: bjain@ct.iitr.ac.in

M. Parida
Department of Civil Engineering, Indian Institute of Technology Roorkee, Roorkee, Uttarakhand
247667, India

D. Tiwari
CSIR—Central Road Research Institute, New Delhi 110025, India

R. Anbanandam
Department of Management Studies, Indian Institute of Technology Roorkee, Roorkee,
Uttarakhand 247667, India

functional and structural parameters of the pavement. There was also some research in urban roads [7–10], but these were limited to maintenance management of pavements. But, there are many other roadside assets in urban areas such as footpaths, cycle tracks, median, street lights, signage and signals, street furniture, guard rails, trees, on-street parking. These are also equally needed to be inventoried and maintained for better serviceability to the users.

These problems can be addressed through the institution of a more systematic tool like asset management system (AMS) for the road assets under a local municipal agency. As known, AMS is a data-driven process, and the outcomes of this system are as good and as reliable as the data fed into the system. But, the road inventory data available with any local body is also of scattered nature and is not useful in any statistical analysis or decision-making process. Not only data collection is one of the costliest aspects of asset management, but also the quality of data is also very critical to make informed decisions [11]. Hence, for effective implementation of AMS for any urban road network in India, first of all, extensive city-wide data collection is necessary to be carried out to cover various road assets and their characteristics under the jurisdiction of the local road agency. Conventional data collection practices involve manual methods using handheld devices that prove to be labor-intensive, potentially unsafe for personnel, and time-consuming [12]. Thus, to overcome these challenges, newfangled technologies and techniques in the data collection process must be considered. For automated data collection, specialized vehicles can be used, which are stocked with GPS (spatial data), photograph and video cameras (inventory and distress data), and several sensors such as laser scanners, profilers, and accelerometers [13–15].

This study utilizes the data collected for ‘Development of Road AMS for Pune City’, an initiative taken by Pune Smart City Development Corporation Limited (PSCDCL) and Pune Municipal Corporation (PMC) under the Smart City Mission by the Government of India. Ministry of Housing and Urban Affairs, Government of India, elaborates Smart City’s concept on their Web site (www.smartcities.gov.in) that the cities should provide necessary infrastructure and better quality of life to their citizens with the applications of ‘smart’ solutions. This mission focuses on promoting sustainable and inclusive development, keeping an idea in mind to replicate these solutions to other cities of the country [16].

This paper explicitly covers the data collection process of this study and the application of newfangled tools and technology. In this, the majority of the roadside assets, their attributes, road distress data, and road geometry data were collected using an automated data collection vehicle—Network Survey Vehicle (NSV). The inaccessible areas such as bridges and culverts were covered using GPS-enabled tablet devices and in-house developed mobile application. The application of these innovative tools proved to be fruitful as the time taken for the first cycle of data was around three months for the entire road network of about 1400 km, and the vehicle alone covered more than 100 attributes of various road assets which otherwise seemed unfeasible in the given timeframe. The vehicle’s output files presented the

road inventory and road distress data at every 10 m interval and road geometry data at every 100 m interval. These data points were provided with their respective latitudes and longitudes.

2 Background

For effective AMS for an urban road network, the database is the backbone of the whole process, which requires consistent and continuous information for pavements and other roadside assets [17]. Thus, the first step would be data collection, irrespective of the methods. A report from the USA discussed the data collection practices for AMS in its various states to define the link between the decision-making processes, data collection practices, policies, and standards. This study identified three extensive data collection methods, i.e., manual (using pen and paper, GIS-enabled tablets), automatic (using advanced survey vehicles), and remote (using aerial photography). It was observed that the manual method was dominant for the assets which were inaccessible by automated vehicles like drainage facilities and some roadside assets [18]. One study demonstrated the integration of GPS, navigation system, and high-resolution cameras mounted on a mapping vehicle for more accurate and reliable data collection road infrastructure. It also combined this data along with that of from aerial survey for a better understanding of the users [19].

The NCHRP 334 report discussed the process and image processing technology to compute distress values from the image data in detail (fig. 1) [20, 21].

Many previous studies were reviewed on different data collection methods of various road assets. They classified them based on the type of data into vision data, spatial data, and sensor data-based methods. It was pointed out that many were concentrated on one or two types of assets or distress and thus suggested to bring on-board a fully automatic low-cost data collection vehicle equipped with the sensors and tools to capture all the three types of data [13].

Many studies were conducted to check the reliability, accuracy, and efficiency of newfangled tools and techniques by comparing them with the conventional manual methods [22–26]. One of them evaluated the condition of traffic signs using the ‘stationary image-based method’ and manual methods to measure retroreflectivity as well. The former had several advantages over the others in terms of usability, accessibility, and safety [25]. Another carried out a study using two different methodologies of data collection techniques for managing the road assets: one using mobile inventory data collection vehicles, and the other was manual techniques to compare the feasibility of the former over the latter [24]. A similar study was conducted in which a total of six vendors with automatic survey vehicles participated [22]. The results of the statistical analysis conducted in this study displayed that mobile data collection was at par compared to the manual data. However, data collected for quantitative elements (like no. of markings, driveways, drop inlets) was more closely correlated between mobile and manual mode as compared to that of qualitative elements (like here for curb type) [22].

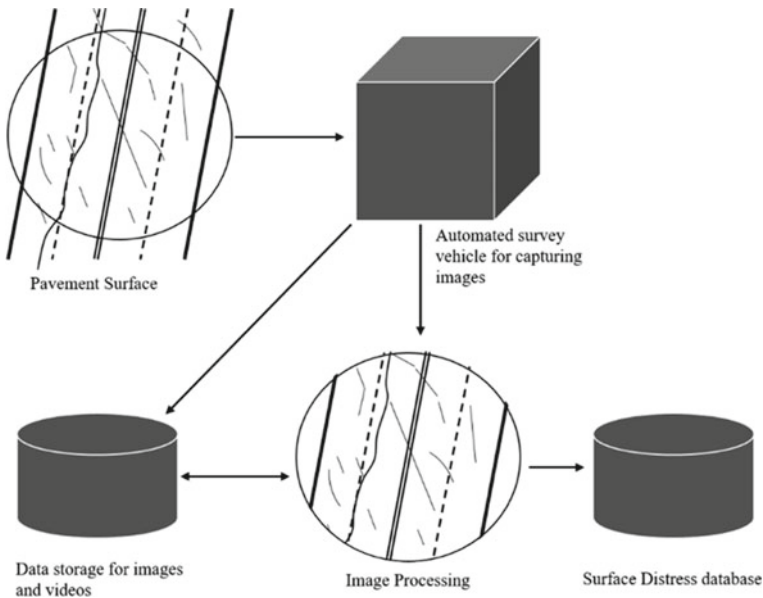


Fig. 1 Schematic diagram for the process of condition survey [21]

From these two studies conducted over the same study area, one of the significant bottlenecks identified with mobile vehicle vendors was the absence of some sort of two-way communication system to set standards and specifications for road elements. This issue was considered in the subsequent study by introducing the feedback mechanism between the vendor and the client, along with a pilot study prior to actual data collection [24]. With the incorporation of a feedback mechanism into the study, significant improvement in the data quality from automatic vehicles was observed. The automated methods and manual methods for distresses are like rut depth and cracking. PCR values were compared in one more study, and the results displayed higher variability in manual data. Even in the automated data, PCR values were inclined toward the upper set of values [23].

Various studies have been conducted to showcase the state-of-the-art techniques available for the data collection of multiple assets [26–30]. A study from the USA reviewed the tools available for various types of surface cracks. Regression analysis was applied to find the correlation between the data collected manually and automated vehicles [26]. Another deployed a sensing vehicle embedded with 3D laser technology, lidar system, and video logging system in the study area to monitor the pavements' performance against the development of the cracks. This technology was based on laser triangulation principles and had huge advantages over in-field manual methods for crack detection [27]. Machine learning techniques were also used to identify the roadside ancillary assets, such as traffic signs and signals, guardrails, and markings, from the video data collected using 2D video cameras mounted on survey vehicles [28]. One study showcased the application of fisheye/wide-angle lens

cameras mounted on a regular commuting vehicle. This method could be fruitful to identify and manage roadside assets such as traffic signs at a lower cost. This study also demonstrated the use of super-resolution technology (SR) to post-process lower quality images for better results [31]. Application of mobile applications (Android and iOS) and tablet devices provided a modern way of in situ data collection of transportation assets using mobile devices. In this study, Transportation Asset Management System (TAMS) was developed as a multiplatform asset management tool that utilizes a mobile application to collect, manage, and update asset data. It also acknowledged how mobile technology advancement and their integration with GPS sensors, accelerometer, and cameras provided an opportunity to develop tools and apps to address issues regarding data collection and its management. Otherwise, it could be very complicated, hectic, and costly proposition for the concerned authorities [29]. For the road assets other than pavements, like culverts and underground stormwater drainages, which are generally inaccessible to the modern data collection vehicles, innovative approaches are needed such as development of mobile applications [29]. Another study developed a framework for the assessment of culverts' condition and their management using analytic hierarchy process (AHP) [32]. It also incorporated the application of GIS into the framework for better decision-making [32, 33]. A total of 564 culverts were mapped throughout the region that showed the need for repair. Implementation of GIS in the study for information processing and database creation made decision-making more efficient [33]. For the condition assessment of pavement markings, a study developed an algorithm to extract the various attributes, including the retroreflectivity from mobile laser scanning (MLS) systems [34].

Based on the previous studies' learnings and the implementation of emerging technologies over the years, the data collection process has evolved to provide quality data for AMS, which is cost-effective and time-saving without compromising personnel safety. This has been possible with the incorporation of newfangled tools like automated survey vehicles, mobile-based applications to capture and manage data, implementation of remote sensing to survey using aerial photography, 3D video asset recognition using machine learning, and lidar and 3D laser technology for the mapping of cracks.

3 Methodology

3.1 General

This paper's basic framework is to compile and describe the newfangled tools and techniques implemented for the data collection for the development of RAMS for Pune city (fig. 2). This section describes the study area, fundamental approach, identified assets and their attributes, Network Survey Vehicle, and other data collection

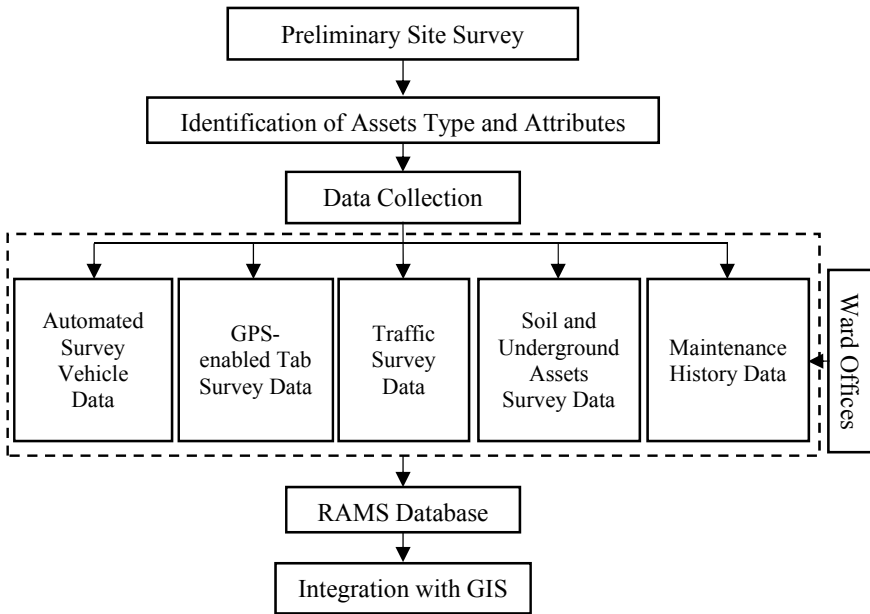


Fig. 2 Basic framework for the data collection for RAMS, Pune

tools. The application of GIS for data integration and interpretation is also briefly discussed.

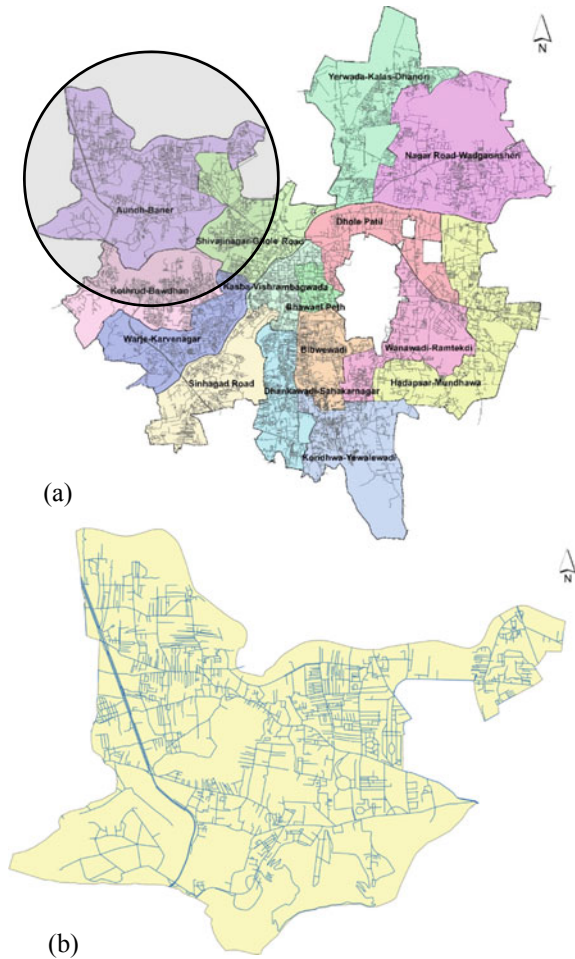
3.2 Study Area

The study for the development of RAMS for a smart city is conducted on the entire Pune road network (around 1400 km) (fig. 3a), covering different types of road class (arterial, sub-arterial, collector, and local) and surface types (bituminous, concrete, TWT, unsealed, paver's block, etc.). For this paper, the scope is limited to one ward of Pune, i.e., Aundh-Baner ward (fig. 3b), to describe the application of tools used for data collection for the entire city's road network. The total length of roads of this ward is 174 km.

3.3 Identification of Assets and Their Attributes

In general, an asset can be anything tangible or intangible, owned by a person or a company that has specific value and needs. Similarly, for an urban road network, a road asset is more than just pavement. It includes others such as footpaths, amenities,

Fig. 3 **a** Map of Pune with ward boundaries. **b** Road network of Aundh-Baner ward, Pune



signage, street lights in between the right of way of a road section [26]. It is owned, monitored, and managed by the local agency to improve the road users' experience.

For Pune's road network, a preliminary site survey was conducted (fig. 2). Officials from the local road agency were interviewed as well to list out the different types of assets that fall under the jurisdiction of the agency with the purpose of developing an integrated AMS for the city. Table 1 displays the various categories of data under which identified assets could be classified. The source or technique for obtaining the data is also mentioned in the table.

Inventory data listed down around 25 different asset types such as shoulder, median, footpath, cycle track, kerb, utility poles, signage, on-street parking, bus shelters, street furniture, pavement markings along with their respective attributes like location (latitude-longitude), type, material type, dimensions (width, length, thickness/height), or numbers.

Table 1 Classification of data for RAMS and their source

S. no	Classification of data	Source or method for data collection
1	Road inventory data	Using network survey vehicle
2	Road geometry data	Using network survey vehicle
3	Bridge and culvert inventory data	Using mobile app and GPS-enabled tablet
4	Pavement distress data	Using network survey vehicle
5	Pavement strength data	Benkelman beam deflection method
6	Pavement crust data	Manual inspection at locations across the area
7	Drainage data	Using mobile app and GPS-enabled tablet
8	Maintenance records data	Secondary data (from ward offices)
9	Traffic data	Videography and video processing

Geometry data covered grade (%), cross slope (%), horizontal and vertical curvature (1/km), rise and fall (m/km and no./km), and altitude.

Bridge and culvert data comprised of the attributes of bridges such as their type, width, span (no. and width), wing wall type, superstructure type, bearing type, sub-structure, pier (thickness and height), foundation type and similarly for culverts too, their type, slab thickness, wearing coat type and thickness, headwall. Pavement distress dataset managed to cover different types of distresses with respect to their surface type, their severity, and extent (%) along with potholes (no. and extent), mean rut depth (mm/km), and roughness (IRI, m/km).

Deflection (mm) was calculated using the Benkelman Beam deflection method at various locations to compute the strength of flexible pavements. For crust data, multiple layers' thickness was recorded manually at various construction sites across the study area.

The number of pipes, type, and diameter for the underground drainage was recorded using the mobile application. Traffic volume count for each vehicle type, ADT, and CVPD was computed at various locations.

From this classification of data, inventory, geometry, distress, and drainage data have been obtained with the application of innovative techniques. The attributes were defined, keeping the best interest and needs of the local agency in mind. Proper communication was maintained with the vehicle operator during the preliminary survey, pilot survey, and actual survey to maintain the integrity of the data.

Road inventory data comprised major roadside assets such as shoulder, median, footpath, arboriculture, pavement markings, and point data like utility poles, utility box, speed breaker, signage, street furniture, and bus shelters. The main attribute of these assets covered in the process was their geolocation (latitude and longitude), dimensions, material type, qualitative assessment of condition, and some asset-specific information. Geometry data included horizontal and vertical curvature, grade, cross slope, rise and fall, and altitude. Pavement distress data covered potholes, roughness, rut depth, severity, as well as extent (%) of different types of cracks on the

bituminous surface, and for concrete and thin white topping surface, distresses like spalling, faulting, depression, cracked slabs, and failures were considered as well.

The different elements of the superstructure and substructure of the bridge and the roadway's parameters were also identified, which were collected along with the culvert data, which majorly included the type, headwall, and wearing coat using the handheld tablet devices.

3.4 Data Collection

The road assets and their attributes were finalized after the preliminary site survey and conforming to the scope of tools used for the data collection process. As shown in the framework of the study (fig. 2), the data collection can be divided into five broad classifications based on the source of data and the methods used (table 1).

This paper's main objective is to showcase the innovative tools exercised to ease out the whole process of acquiring the data in a minimum timeframe while ensuring the reliability of data and personnel safety. The subsequent sections discussed the automated data collection vehicle, known as Network Survey Vehicle, and the handheld GPS-enabled tablet devices pre-installed with an in-house developed mobile application. The former covered the majority of pavement and roadside assets. The latter was used for inaccessible areas like under the bridge, culverts, and underground stormwater drainage (SWD).

Network Survey Vehicle. NSV is equipped with several sensors such as laser scanners, road profilers, accelerometers, global positioning system (GPS), and four cameras (three in front and one in back facing toward the pavement) mounted over the top of the vehicle [35]. The NSV was of Hawkeye 2000 series. Pavement roughness data is one of the most crucial parameters for pavement management as it directly impacts the riding quality. The laser sensors equipped in this vehicle for the roughness measurement have been classified in Class I category as compared to the conventional bump integrator which is placed in Class III category [36]. The vehicle covered the whole road network under the jurisdiction of PMC. It provided the information related to roughness, rut depth, transverse and longitudinal profile, curvature, pavement distress data, and inventory data at average traffic speed. The Aundh-Baner ward data was collected in December 2017, and the first round of data collection for the entire city was done within three months (December 2017–February 2018). Figure 4a shows the NSV used for this study, and fig. 4b is the display interface inside the vehicle for the personnel to operate the vehicle. The images from the three front cameras are synchronized, covering the whole row to extract the information as shown in fig. 5a, b is the sample image from center camera, along with the details extracted from that image. The data collected from NSV was provided in MS Excel format, along with the photographs georeferenced to the location. The output data acquired from the NSV survey can be classified into three sets, as shown in the flowchart (fig. 6).

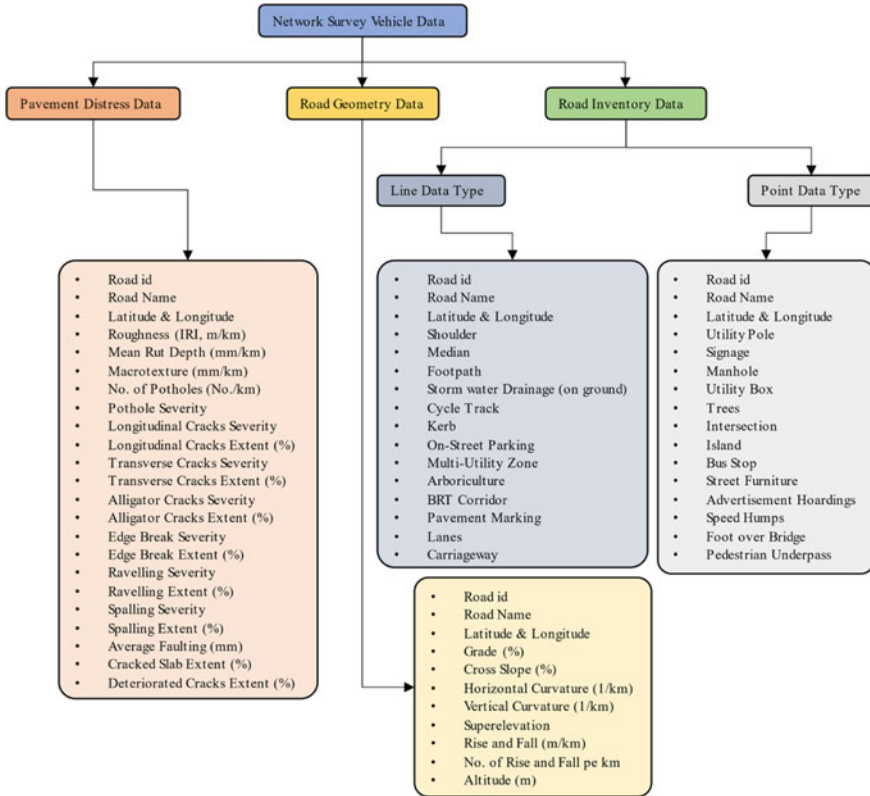


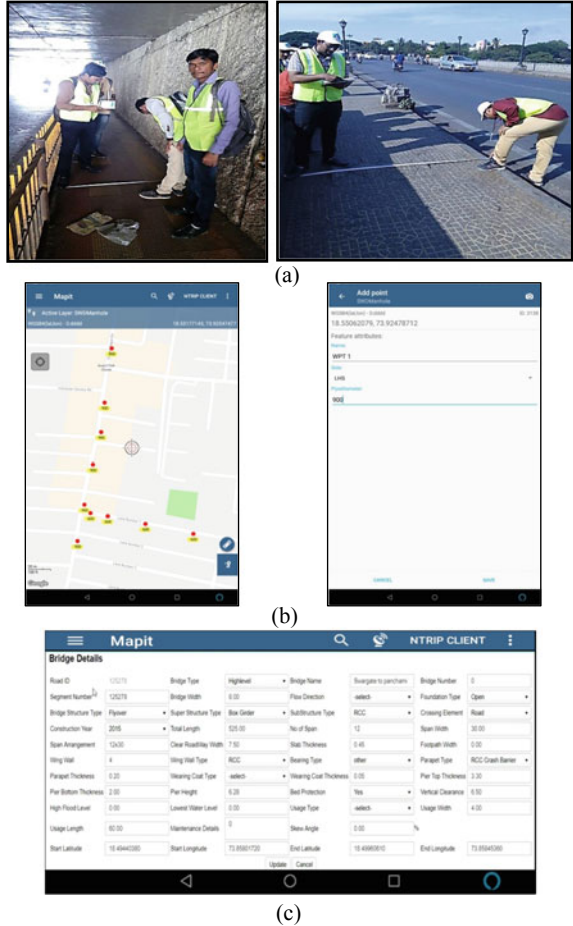
Fig. 6 Flowchart showing various road assets and attributes collected using NSV

Pavement distress data includes the various distress parameters for both rigid and flexible pavements. This set of data is crucial for pavement management tool such as HDM-4 road geometry data.

In conventional practices, road assets other than pavements or carriageway are generally sidelined. With the proposed framework, development of RAMS initially answers the two major questions for other assets: What do the agency own? And where is it located? Adhering to this, the road inventory data, third dataset from NSV, identifies total of different 26 assets, classified into line data and point data based on their geometry type in GIS.

GPS-enabled Tablet Devices. The assets like bridges, culverts, and underground stormwater drainage (SWD) were unreachable for the NSV. Hence, their data was needed to be acquired manually, so a mobile application was developed. It was used with GPS-enabled tablet devices to record the details digitally along with their latitudes and longitudes. As a result, the aggregate data could be exported to ArcGIS and on the RAMS interface directly. Otherwise, manual data collection using pen and paper would have made the entire exercise a very tedious and time-consuming

Fig. 7 a Data collection using tablets for the bridge sub-assets. **b** UI of the app for SWD data entry. **c** UI of the app for bridge data entry



job. The user interface (UI) of the application for SWD data entry is shown in fig. 7b. Data collection practice for bridges and culverts is shown in fig. 7c. The data could be extracted into ArcGIS and MS Excel directly for RAMS portal.

4 Results

Upon completing the survey for the Aundh-Baner ward, the data was brought from NSV and the tablet devices into the MS Excel format. Later, it was also pinned on the base map of Pune using the geolocations on ArcGIS. Some of the inferences that can be extracted from the data related to road inventory and pavement distresses are as follows:

- The total length of the road of Aundh-Baner ward is 174.69 km. Out of which around 97 km were local streets, 18 km collector, 35 km sub-arterial, and 24 km were arterial roads.
- Approximately 108 km length of pavement sections have bituminous surface, 38.5 km are concrete, 15 km have thin white topping (TWT), and remaining have other surface types such as pavers block, unsealed, and mastic (fig. 8).
- About 134 km of road sections were two lane in Aundh-Baner on one side of the road. About 25.2 km was single lane, 10.43 km was three lane, and 5 km was a four-lane road (fig. 9).
- Then, 76% of total road length has no footpath on either side of the carriageway.
- Approximately 30% of road sections have no shoulder, and only 37.75% have paved shoulders, and the remaining have earthen/grass ones (fig. 10).

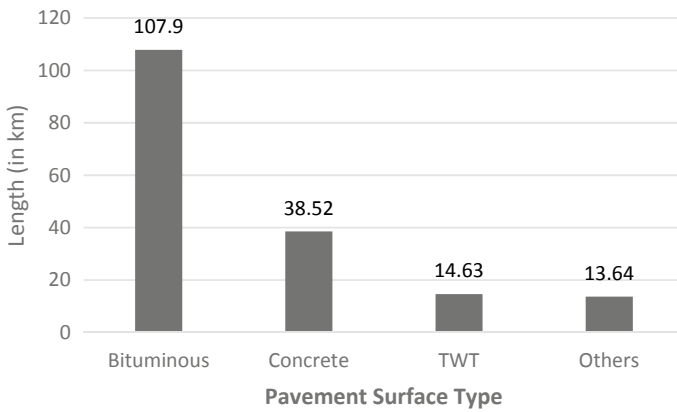


Fig. 8 Classification of road sections based on surface type for Aundh-Baner ward

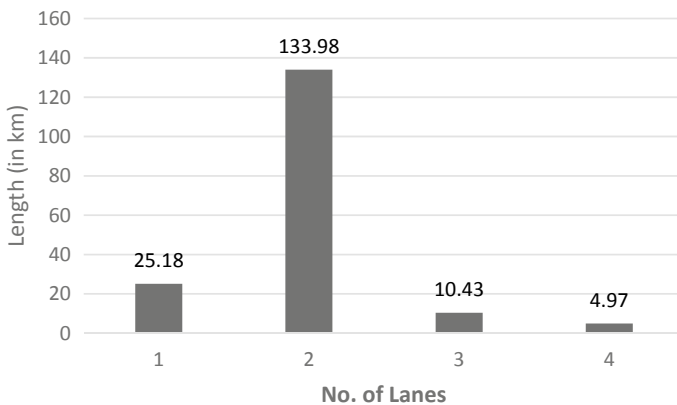


Fig. 9 Classification of road sections based on number of lanes for Aundh-Baner ward

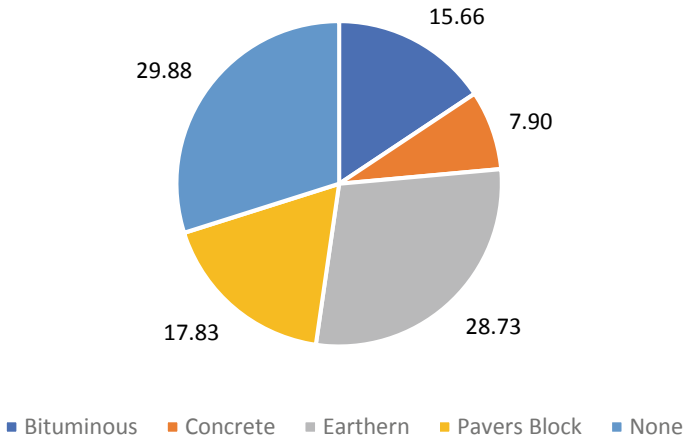


Fig. 10 Types of material for shoulder in Aundh-Baner

- The average IRI value for bituminous roads in the Aundh-Baner area is 3.333 m/km, whereas the same for concrete and TWT surface combined is 4.137 m/km.
- For bituminous roads, 77% of total length were free from raveling, and only 125 road sections of 10 m length were identified with one or more potholes.
- For bituminous roads, the three primary types of cracks—longitudinal, transverse, and alligator—were identified from the image data from the fourth camera of NSV (mounted on the back facing down toward the pavement). Each image was scaled and then processed to identify cracks, their severity, and extent using the Hawkeye toolkit software calibrated with NSV data and is plotted in fig. 10 in terms of percentage of total surface area (fig. 11).
- For bituminous roads, out of 10,790 sections of 10 m length, 126 units had at least one pothole. Only 182 sections had 20% or more raveled surface, and 2262 had 0–20% raveled surface, which collectively accounted for 22.65% of road sections of the study area.
- Figure 12a displays the data collected using tablet devices for a bridge (Bhopodi Bridge, Aundh) and its attributes imported directly into ArcGIS.
- Through tablet survey, 24 bridges and 43 culverts were identified and inspected in the Aundh-Baner ward alone. These bridges included river bridge, flyover, and rail-over bridge.
- The data was then imported into ArcGIS and was mapped on the Aundh-Baner ward map, as shown in fig. 12b.

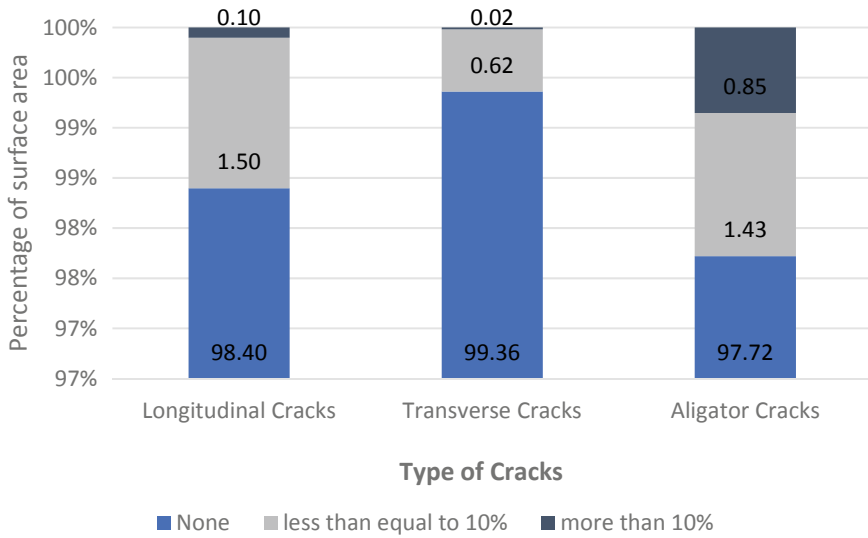


Fig. 11 Extent of different types of cracks for bituminous surface in Aundh-Baner

5 Summary and Future Scope

This paper’s primary purpose was to present the newfangled tools and techniques implemented in this study of developing a RAMS for an urban road network in an Indian scenario. About 30 road assets and a number of their respective attributes were identified. The deductions for some of the elements are discussed in the previous section (figs. 8, 9, 10, 11 and 12). For a local agency, in order to manage and preserve their assets, the foremost step is to know what they own and where it is located. With the application of modern tools, this study intended the same to inventory the various assets in spatial and tabular form of data. Thus, it can be concluded that these tools have the potential to ease out the entire process of data collection while ensuring the safety of personnel and delivering within the minimum timeframe possible. The cost and accuracy of inventory and distress data have always been the two major bottlenecks associated with the application of NSV. The cost for the use of NSV may be high compared to the manual methods, but it justifies its value for money in terms of time saved, safety, and widening of scope, i.e., collecting data for multiple assets at the same time. Many previous studies have been conducted by various authors, as discussed in the preceding section, where the manual data and vehicle data for the same stretch were compared to check the reliability of the automated vehicle data. Most of them have concluded that the data from the latter was at par with the minimum standards of the local authority. Even some studies found the discrepancy in the manual data. For this study, the data from NSV was validated by manually checking the values for randomly selected sections. As the data collected by NSV was at 10 m intervals, 5% of these 10 m length sections were randomly

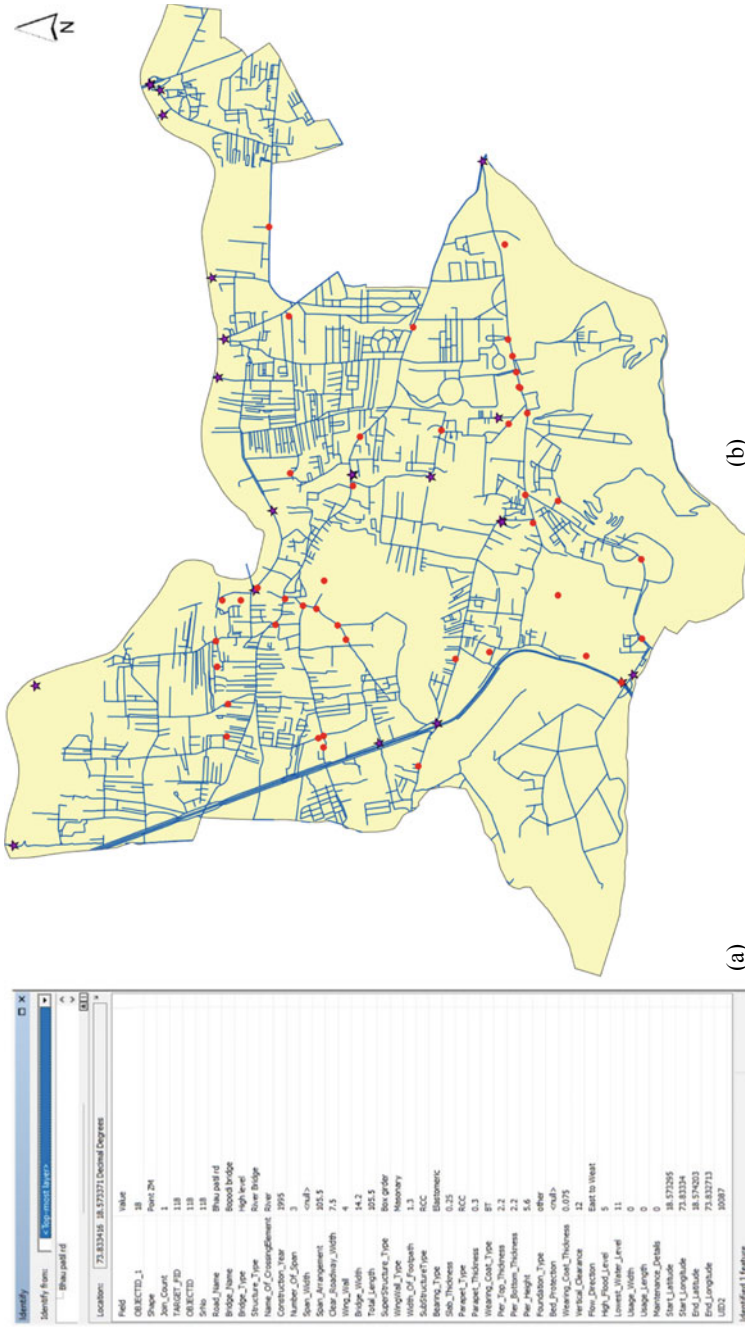


Fig. 12 a Snip from ArcGIS showing various attributes and their details for Bhopodi Bridge, Aundh b Bridge and culvert locations for Aundh-Baner ward imported into GIS map from tablet survey

selected, and the inventory data was manually verified. It was also approved by the local authority. Additionally, as suggested by (Cunningham et al. 2016) [24], proper two-way feedback communication was maintained with the operators and experts of NSV at every stage of the data collection process to improve the data quality further.

The future scope for this study is to take this from one ward to the whole city. It is also hoped to take the entire system on a web portal integrated with GIS to present the inventory and distress data on the maps and the graphical representation since this would make the decision-making process for the officials from a local agency more efficient and transparent. It is also desired to introduce the pavement management tool to optimize RAMS's budget for pavement maintenance as pavements have a significant share of maintenance costs compared to other ancillary assets. Additionally, it can be concluded that this study has paved the way toward developing a system for the management of urban roads and their assets, which can be brought out to other smart cities in the future as well.

Acknowledgements This study would not have been possible without the support of Pavetech Consultants, Pune, Pune Municipal Corporation (PMC), and Pune Smart City Development Corporation Limited (PSCDCL). The thoughts expressed and the conclusions drawn are solely of the authors and do not necessarily represent the opinions of PMC and PSCDCL. The authors wish their sincere gratitude toward PMC and PSCDCL to encourage this study under the Smart City Mission, an initiative by Indian government. We also want to extend our regards to IIT Roorkee and Ministry of Education, Government of India to provide computational and financial support.

The authors also acknowledge the opportunity to submit the research work at the 5th Conference of the Transportation Research Group of India held at Bhopal (India) from December 18–21, 2019, that forms the basis of this article.

References

1. Jain SS, Aggarwal S, Parida M (2005) HDM-4 pavement deterioration models for Indian national highway network. *J Transp Eng* 131:623–631. [https://doi.org/10.1061/\(ASCE\)0733-947X\(2005\)131:8\(623\)](https://doi.org/10.1061/(ASCE)0733-947X(2005)131:8(623))
2. Parida M, Aggarwal S, Jain SS (2005) Enhancing pavement management systems using GIS. *Proc Inst Civ Eng Transp* 158:107–113. <https://doi.org/10.1680/tran.2005.158.2.107>
3. Sunitha V, Veeraragavan A, Srinivasan KK, Mathew S (2012) Cluster-based pavement deterioration models for low-volume rural roads. *ISRN Civ Eng* 2012
4. Sunitha V, Veeraragavan A, Srinivasan KK, Mathew S (2013) Application of factor analysis in maintenance management of low volume roads. *Int J Pavement Res Technol* 6:130–135
5. Mathew BS, Rose S, Isaac KP, Chandrasekhar BP (2010) Pavement performance modelling and calibration of HDM-4 deterioration models for rural roads in India. *J Inst Eng* 91:29–35
6. Thube DT, Jain SS, Parida M (2007) Development of PCI based composite pavement deterioration curves for low volume roads in India. In: *Highway Research Bulletin, Indian Roads Congress*, pp 55–69
7. Shah YU, Jain SS, Tiwari D, Jain MK (2013) Development of overall pavement condition index for urban road network. *Procedia Soc Behav Sci* 104:332–341. <https://doi.org/10.1016/j.sbspro.2013.11.126>
8. Shah YU, Jain SS, Parida M (2014) Evaluation of prioritization methods for effective pavement maintenance of urban roads. *Int J Pavement Eng* 15:238–250. <https://doi.org/10.1080/10298436.2012.657798>

9. Prakasan AC, Tiwari D, Shah YU, Parida M (2015) Pavement maintenance prioritization of urban roads using analytical hierarchy process. *Int J Pavement Res Technol* 8:112–122. [https://doi.org/10.6135/IJPRT.ORG.TW/2015.8\(2\).112](https://doi.org/10.6135/IJPRT.ORG.TW/2015.8(2).112)
10. Chopra T, Parida M, Kwatra N, Chopra P (2018) Development of pavement distress deterioration prediction models for urban road network using genetic programming. *Adv Civ Eng* 2018:1–15. <https://doi.org/10.1155/2018/1253108>
11. Flintsch GW, McGhee KK (2009) Quality management of pavement condition data collection. National Academies Press, Washington DC. <https://doi.org/10.17226/14325>
12. Preston H, Atkins KC, Lebens M, Jensen M (2014) Traffic sign life expectancy
13. Radopoulou SC, Brilakis I (2016) Improving road asset condition monitoring. *Transp Res Procedia* 14:3004–3012. <https://doi.org/10.1016/j.trpro.2016.05.436>
14. DFT D (2011) SCANNER user guide and specification
15. Sairam N, Nagarajan S, Ornitz S (2016) Development of mobile mapping system for 3D road asset inventory. *Sensors* 16:367. <https://doi.org/10.3390/s16030367>
16. What is Smart City : SMART CITIES MISSION, Government of India, <http://smartcities.gov.in/content/innerpage/what-is-smart-city.php>. Last accessed 7 May 2019
17. Haas R, Hudson WR, Falls LC (2015) Pavement asset management. John Wiley & Sons, Inc., Hoboken, NJ, USA. <https://doi.org/10.1002/9781119038849>
18. Flintsch GW, Bryant JW (2006) Asset management data collection for supporting decision processes
19. He G, Orvets G (2000) Capturing road network data using mobile mapping technology. *Int Arch Photogramm Remote Sens* 33:272–277
20. Board TR, National Academies of Sciences and Medicine E (2004) Automated pavement distress collection techniques. The National Academies Press, Washington DC. <https://doi.org/10.17226/23348>
21. Board TR, National Academies of Sciences and Medicine E (2011) Automated imaging technologies for pavement distress surveys. Transportation Research Board, Washington DC. <https://doi.org/10.17226/22866>
22. Findley DJ, Cunningham CM, Hummer JE (2011) Comparison of mobile and manual data collection for roadway components. *Transp Res Part C Emerg Technol* 19:521–540. <https://doi.org/10.1016/j.trc.2010.08.002>
23. Underwood BS, Kim YR, Corley-Lay J (2011) Assessment of use of automated distress survey methods for network-level pavement management. *J Perform Constr Facil* 25:250–258. [https://doi.org/10.1061/\(ASCE\)CF.1943-5509.0000158](https://doi.org/10.1061/(ASCE)CF.1943-5509.0000158)
24. Cunningham CM, Findley DJ, Hovey K, Foley PB, Smith J, Fowler T, Chang J, Arnold J, Hummer JE (2016) Improved asset management and inventory development through sample analysis and vendor–client communication. *J Infrastruct Syst* 22:04015013. [https://doi.org/10.1061/\(ASCE\)IS.1943-555X.0000260](https://doi.org/10.1061/(ASCE)IS.1943-555X.0000260)
25. Khalilikhah M, Balali V, Heaslip K (2016) Using stationary image based data collection method for evaluation of traffic sign condition. *Int J Transp Sci Technol* 5:248–256. <https://doi.org/10.1016/j.ijst.2017.03.001>
26. Qiu X, Wang F (2014) Use of automated survey for surface cracking distress condition in a pavement management system. In: Pavement materials, structures, and performance, pp 351–363. American Society of Civil Engineers, Reston, VA. <https://doi.org/10.1061/9780784413418.035>
27. Wang Z, Tsai Y (James), Ding M (2017) Use of crack characteristics in crack sealing performance modeling and network-level project selection. *Transp Res Rec J Transp Res Board* 2612:11–19. <https://doi.org/10.3141/2612-02>
28. Balali V, Golparvar-Fard M (2015) Segmentation and recognition of roadway assets from car-mounted camera video streams using a scalable non-parametric image parsing method. *Autom Constr* 49:27–39
29. Khan G, Bueff A, Mihov I, Tessema N, Garrido J, Russel C, Parnia A (2016) Development of transportation asset management and data collection system (TAMS) using mobile applications. *Procedia Eng* 161:1180–1186. <https://doi.org/10.1016/j.proeng.2016.08.536>

30. Landa J, Prochazka D (2014) Automatic road inventory using LiDAR. *Procedia Econ Financ* 12:363–370. [https://doi.org/10.1016/S2212-5671\(14\)00356-6](https://doi.org/10.1016/S2212-5671(14)00356-6)
31. Takano T, Ono S, Kawasaki H, Ikeuchi K (2021) High-resolution image data collection scheme for road sensing using wide-angle cameras on general-use vehicle criteria to include/exclude collected images for super resolution. *Int J Intell Transp Syst Res*. <https://doi.org/10.1007/s13177-020-00243-0>
32. Najafi M, Bhattachar DV (2011) Development of a culvert inventory and inspection framework for asset management of road structures. *J King Saud Univ Sci* 23:243–254. <https://doi.org/10.1016/j.jksus.2010.11.001>
33. Delgado-Ramos F, Sanchez-Ladron-de-Guevara MS, Diez-Contreras A, Perez-Diaz M (2014) A methodology for the inventory of road culverts pathologies applied to the Province of Jaen (Andalusia, Spain). *Procedia Soc Behav Sci* 160:597–606. <https://doi.org/10.1016/j.sbspro.2014.12.173>
34. Kumar P, McElhinney CP, Lewis P, McCarthy T (2014) Automated road markings extraction from mobile laser scanning data. *Int J Appl Earth Obs Geoinf* 32:125–137. <https://doi.org/10.1016/j.jag.2014.03.023>
35. Hawkeye 2000 Series—ARRB Group, <http://arrbgroup.net/products/hawkeye-2000-series/>. Last accessed 23 Jan 2021
36. Bennett CR, De Solminihac H, Chamorro A (2006) Data collection technologies for road management. World Bank, Washington DC

Structural Design of the Pervious Concrete Pavements: A Computational Mechanics Approach



Avishreshth Singh, M. Nithyadharan, Prasanna Venkatesh Sampath, and Krishna Prapoorna Biligiri

1 Introduction

The development of a holistic approach that ameliorates the impacts of stormwater runoff on urban habitats is a matter of global concern. Out of the many strategies formulated to manage the stormwater, the use and construction of the pervious concrete pavements (PCPs) have been recognized and documented as a technically sound practice [1]. PCP is a structural concrete pavement characterized by its interconnected pore structure. The pervious concrete (PC) differs from traditional concrete as it allows infiltration of water through a lattice of aggregates held together with cement paste [2, 3]. PC offers multitude of benefits in terms of its hydrological performance. However, due to its macroporous structure, the strength characteristics are compromised, thus limiting its application to low-volume roads, parking lots, walkways, residential streets, medians, and shoulders [2, 4]. Several laboratory studies investigated the mechanical properties such as compressive strength, which varied between 3 and 28 MPa, and flexural strength that was in the realm of 1–3 MPa [2, 5, 6]. Besides laboratory investigations, field investigations have been performed in the past to analyze the structural behavior of PC using falling weight deflectometer

A. Singh (✉) · M. Nithyadharan · P. V. Sampath · K. P. Biligiri
Department of Civil and Environmental Engineering, Indian Institute of Technology, Tirupati,
Andhra Pradesh 517506, India
e-mail: ce18d001@iittp.ac.in

M. Nithyadharan
e-mail: nithyadharan@iittp.ac.in

P. V. Sampath
e-mail: prasvenk@iittp.ac.in

K. P. Biligiri
e-mail: bkp@iittp.ac.in

(FWD). FWD gives the load–deflection response of pavements by applying impulsive loads, and back calculation is performed to obtain the modulus of subgrade reaction (k) and modulus of elasticity (E) of the pavement system [7–9].

Much of the studies have focused on evaluating the structural response of an existing PCP system using FWD test, while computation of the structural thickness has received very less attention. The fatigue equations proposed in different design guidelines such as Portland Cement Association [10] and American Association of State Highway and Transportation Officials [11] for concrete pavements have been adopted by researchers in the past to assess the fatigue behavior of PC. However, PC being fundamentally different than traditional concrete pavements requires further investigation to establish methods for estimation of fatigue life. Additionally, the behavior of PC slab has been historically analyzed using different computer programs based on the principle of finite element for critical load positions such as edge, interior, and corner at tire pressure of 0.8 MPa [12]. Albeit the assessment of the structural behavior of a PC slab resting over a spring foundation system when subjected to a standard vehicular load of 200 kN (80 kN front axle load and 120 kN rear wheel load) is still a conjecture. With these research gaps, the objectives of the current study were twofold:

- development of an algorithm for computation of structural thickness of PC slab and
- analysis of the deflection response of PC slab when subjected to a moving load, which was later compared to that of a conventional concrete pavement slab.

To accomplish the proposed set of objectives, an MS Excel[®] program was developed that could be used for the structural thickness design of PC slab. The final PC slab was later analyzed for deflection using STAAD Pro[®] software.

2 Research Methodology

2.1 Computation of Fatigue Life

In the absence of a standard fatigue equation for computation of fatigue life of PC, the fatigue equation proposed in the Indian Roads Congress Guideline for Design of Low-Volume Roads [13] was utilized, which is as follows:

$$\log_{10} N_f = \frac{SR^{-2.222}}{0.523} \quad (1)$$

where

N_f = fatigue life of a pavement subjected to stresses caused by the combined effect of a wheel load of 50 kN and temperature differential,

SR = stress ratio, which is defined as the ratio of flexural stress due to wheel load and temperature to that of the flexural strength of concrete.

The equation considers a reliability of 60% (i.e., 40% of the pavement slabs are expected to crack at the end of design period) as compared to other fatigue equations that are based on 90% reliability. The use of this equation seems to be a logical assumption as the applicability of PC is limited to low-volume roads, where the average daily traffic does not exceed 450 commercial vehicles per day (CVPD). Further, heavy vehicular loads are not expected very frequently on low-volume roads. For traffic lower than 50 CVPD, computation of stresses generated due to wheel load of 50 kN is considered for thickness evaluation. This approximation is based on the assumption that there is very low probability of the occurrence of stresses due to maximum wheel load and temperature differential, simultaneously. For traffic falling in the realm of 50–150 CVPD, the thickness is estimated on the basis of total stresses generated due to combined effect of wheel load of 50 kN and temperature gradient. However, analysis for fatigue becomes essential when traffic exceeds 150 CVPD.

In order to create a programmed MS Excel[®] spreadsheet for estimation of structural thickness of PC slab, certain assumptions were made, which are summarized in Table 1. The input parameters can be changed based on the design requirements. IRC:SP:62–2014 permits a maximum transverse joint spacing of 4000 mm. However, for this particular study, the joint spacing was kept as 6000 mm, because controlled (frequented) cracking is not a concern in PC.

Although there was no experimental data for the computation of flexural stress, it was computed by the following Eq. (2) [15]:

Table 1 Design parameters for estimation of structural thickness of PC slab

S. No	Parameter	Assumption
1	Grade of concrete	M25
2	Design period	10 years
3	CBR of subgrade	10%
4	Traffic growth rate	4%
5	Tire pressure	0.8 MPa
6	Load on one wheel of dual set	30,000 N
7	Poisson's ratio	0.25 [14]
8	Modulus of elasticity of the pervious concrete	19,000 MPa [14]
9	Coefficient of thermal expansion	$10 \times 10^{-6}/^{\circ}\text{C}$
10	Modulus of subgrade reaction	0.06 kN/m ² per m
11	Spacing between centers of dual wheels	310 mm
12	Temperature differential	13.1 °C
13	Transverse joint spacing	6000 mm
14	Width of slab, B	4000 mm
15	Initial commercial vehicles per day	40

$$f_{cr} = 0.7 \times \sqrt{f_{ck}} \quad (2)$$

where

f_{cr} = 28-day flexural strength of the pervious concrete in MPa,
 f_{ck} = 28-day compressive strength of the pervious concrete in MPa.

The 90-day flexural strength was considered for fatigue analysis, which was taken as 1.1 times the 28-day flexural strength. The cumulative fatigue damage is generally very small in the first few months due to low number of vehicles traversing the pavement section during the initial period; therefore, it becomes logical to use the 90-day flexural strength (PCA, 1984). Westergaard's equation [16] was utilized for computation of edge stress caused by wheel loads:

$$\sigma_e = \frac{0.803P}{h^2} \left[4 \log \frac{I}{a} + 0.666 \frac{a}{I} - 0.034 \right] \quad (3)$$

where

σ_e = edge stress, MPa
 P = single wheel load, N
 I = radius of relative stiffness, mm
 a = radius of equivalent surface area, mm.

Bradbury's equation [16] was used to express the temperature stresses at edge:

$$\sigma_o = \frac{E\alpha t}{2} C \quad (4)$$

where

σ_o = temperature stress at edge, MPa
 E = modulus of elasticity of concrete, MPa
 α = coefficient of thermal expansion, /°C
 t = temperature differential, °C
 C = Bradbury's coefficient.

Corner load stress [16] was computed using the Eq. 5:

$$\sigma_c = \frac{3P}{h^2} \left(1 - \left(\frac{a\sqrt{2}}{I} \right)^{1.2} \right) \quad (5)$$

where

σ_c = corner load stress, MPa
 h = thickness of PC layer, mm

P , a , and I are the same as explained in above equations.

Expected repetitions were taken as 10% of the total number of cumulative vehicles at the end of design period, and cumulative fatigue damage (CFD) was expressed as the ratio of expected repetitions to the allowable repetitions [13]. For safe design, CFD must be less than 1.

2.2 Modeling of Pavement Using STAAD Pro[®] Software

The pavement slab was analyzed using STAAD Pro[®] software because of its flexible modeling environment and ability to accurately resemble the actual modeled system. The PC and traditional concrete slabs were modeled as a medium-thick rectangular plate of size $6000 \times 4000 \times 235$ mm resting on soil medium represented by elastic spring foundation. The rectangular plate was further sub-divided into a mesh of 10,000 small plate elements of size 60×40 mm and 235 mm thickness. The advantage of discretizing the slab into finer plate elements was that it helped capture the response of pavement slab with high levels of accuracy. However, the fine plate meshes increased the computational period and resulted in higher memory consumption of the computer hard drive. Two beams were modeled with equivalent stiffness properties as that of pavement slabs such that they served as a platform for the generation of moving loads on plates.

Two load cases were defined for analysis. In the first case, the load was applied at an equivalent distance of 800 mm from the two opposite ends of the pavement slab. In second case, the moving vehicular load was applied at a distance of 1560 mm from the left end of pavement slabs to ensure that the tires rolled near the edge of the pavement system. The wheel load arrangement along with tire footprint, loading conditions, and slab configuration is depicted in Fig. 1.

The material properties assigned to the plate elements are given in Table 2.

As the materials were assumed to be isotropic for full depth in each plate element, the Poisson's ratio and modulus of elasticity were similar in all directions for the entire slab. The k -value was defined as 60 MPa/m for both types of pavement systems. The vehicle characteristics are shown in Table 3.

3 Results and Analysis

3.1 Structural Thickness Based on Fatigue Life

For the design case presented in this study, though the initial CVPD was restricted to 40, the PC facility was still analyzed for fatigue to have an additional margin of safety. The computations involved in the structural design are shown in Table 4. The iterations began with a trial thickness of 150 mm and were stopped at 235 mm, which

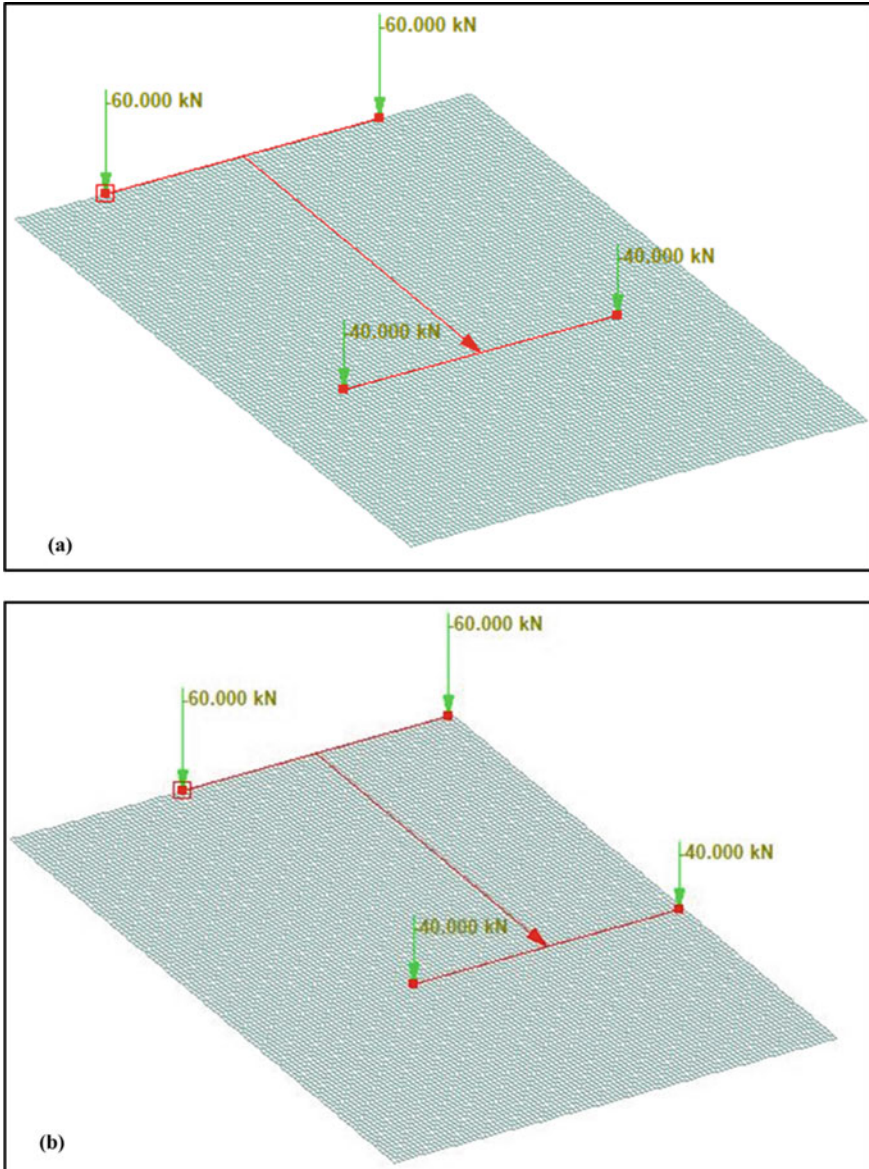


Fig. 1 Wheel load arrangement for vehicle placed: **a** at equal distance from opposite ends of slab and **b** neat the edge of pavement

Table 2 Material properties assigned to plate elements for analysis of the pervious concrete and traditional concrete slabs using STAAD Pro® software

S. No	Material	Element	Property
1	Pervious concrete	Rectangular plates—60 × 40 mm and 235 mm thick	Young’s modulus—19,000 MPa
			Poisson’s ratio—0.25
			Density— 1.8×10^{-5} MPa
			Thermal coefficient— $1 \times 10^{-5}/^{\circ}\text{C}$
2	Traditional concrete	Rectangular plates—60 × 40 mm and 235 mm thick	Young’s modulus—25,000 MPa
			Poisson’s ratio—0.15
			Density— 2.4×10^{-5} MPa
			Thermal coefficient— $1 \times 10^{-5}/^{\circ}\text{C}$

Table 3 Vehicle characteristics

S. No	Vehicle parameters	Input
1	Front axle load	80 kN
2	Rear axle load	120 kN
3	Axle width	2400 mm
4	Wheel base	3600 mm

Table 4 Computations involved for safe structural thickness design of 235 mm for the pervious concrete

S. No	Parameter	Results
1	28-day compressive strength	25 MPa
2	28-day flexural strength	3.5 MPa
3	90-day flexural strength	3.85 MPa
4	CVPD at the end of design period	175,289
5	Radius of relative stiffness	777.434 mm
6	Radius of equivalent surface area	141.587 mm
7	Edge stress due to wheel load	1.329 MPa < 3.85 MPa (safe)
8	Temperature stress at edge	1.318 MPa < 3.85 MPa (safe)
9	Total edge stress due to wheel load and temperature	2.646 MPa < 3.85 MPa (safe)
10	Corner load stress	1.310 MPa < 3.85 MPa (safe)
11	Stress ratio	0.687
12	Allowable number of repetitions	24,965
13	Expected number of repetitions	17,529
14	Cumulative fatigue damage	0.702 < 1 (safe)

Table 5 Summary of maximum slab deflection, major and minor principal stresses, and maximum base pressure for the pervious and conventional concrete slabs

Load case	Material	Maximum slab deflection (mm)	Major principal stress (Max top) (MPa)	Minor principal stress (Max top) (MPa)	Maximum base pressure (MPa)
I	Pervious concrete	1.007	1.210	2.983	0.060
	Conventional concrete	0.910	1.291	2.874	0.055
II	Pervious concrete	1.974	2.542	3.060	0.118
	Conventional concrete	1.753	2.566	2.966	0.105

was accorded as the safe structural thickness of PC surface course when fatigue was considered.

Further, it was observed that the stresses generated in the PC slab due to temperature and wheel loads were lower than normal concrete slab, which can be attributed to the fact that the modulus of elasticity of PC was lower, hence resulted in slightly lower stress values.

3.2 Output Generated from STAAD Pro[®]

The analysis was performed for the given wheel load configurations at an increment of every 60 mm in the direction of traffic over the pavement slabs. The results for deflection, major and minor principal stresses, and base pressure for PC slabs and conventional concrete were obtained for their behavioral comparison, and the peak magnitudes are reported in Table 5.

As observed from Table 5, the maximum slab deflection in PC was higher than that of conventional concrete slabs for either load conditions. It can be attributed to the fact that stiffness of traditional concrete slab is higher than PC slab, which resulted in reduced deflection of the system. The maximum principal stress at the top and bottom phase of the both the pavements are shown in Figs. 2 and 3, respectively. The maximum intensity of stress in the pavement occurs near the edges in load case I and edges and corners in load case II. The maximum stress magnitudes were well below the limiting compressive and tensile stress magnitudes assumed for analysis and design in this study. It was further established that there was no significant difference in the deflections and the actual compressive and tensile stresses were well below the allowable limiting stresses for both types of pavement systems. This dictates that for low-volume roads, PC can be an alternative to PCC pavement systems, specifically in regions where expensive stormwater management tools cannot be used.

Fig. 2 Summary of maximum major principal stress for vehicle placed at center of two pavement slabs: **a** PC (bottom); **b** PC (top); **c** PCC (bottom); **d** PCC (top)

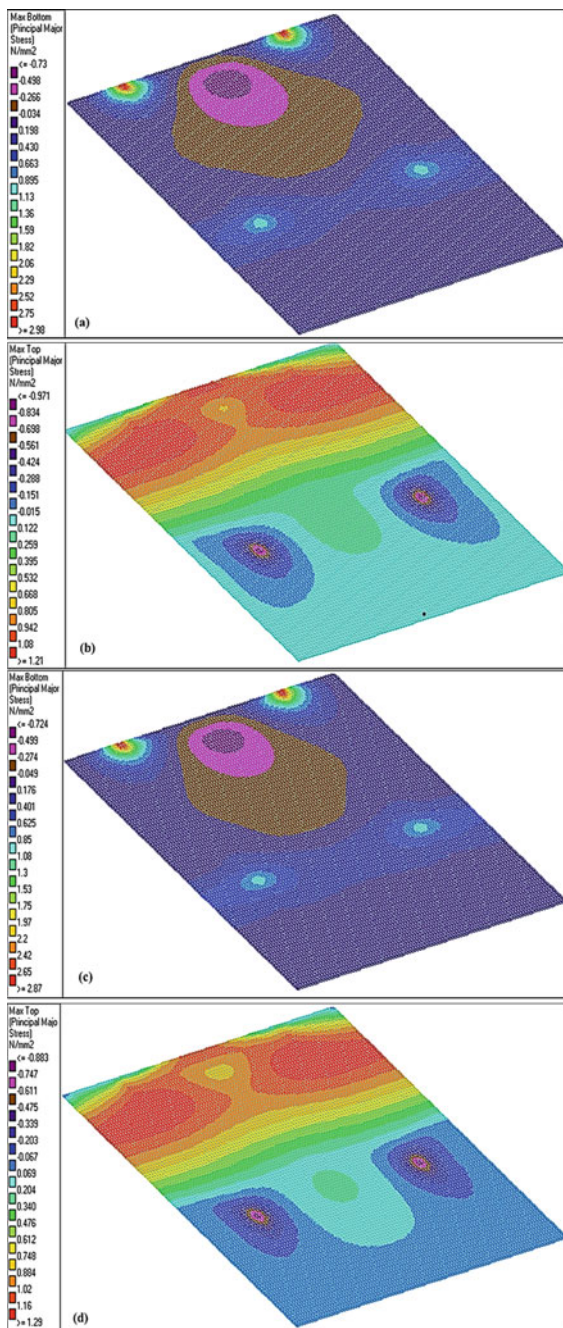
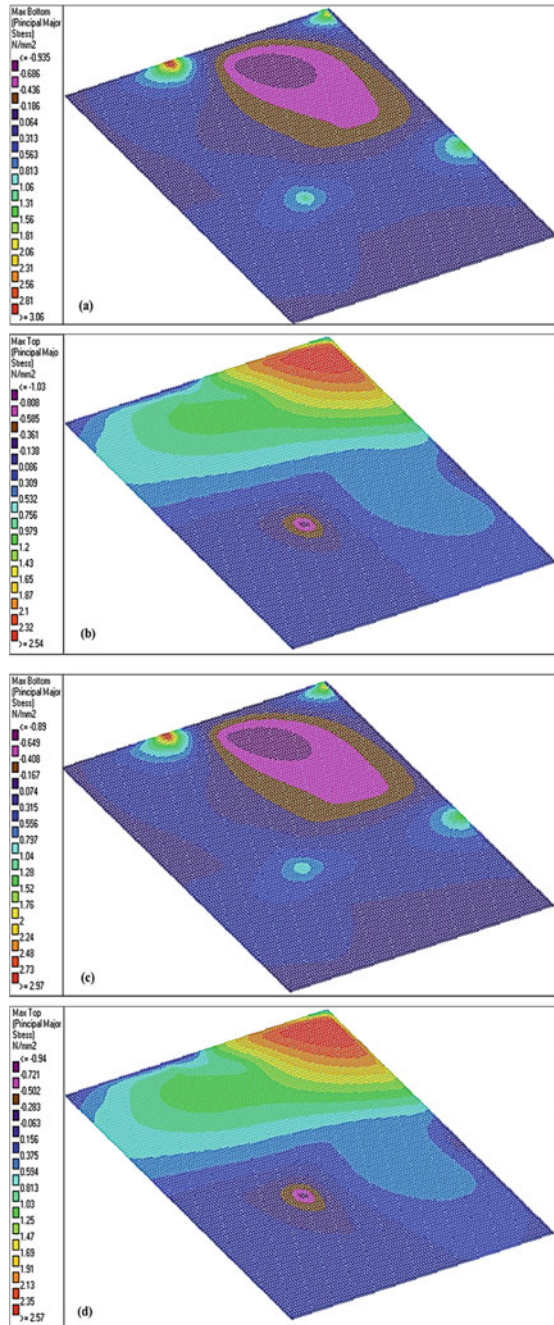


Fig. 3 Summary of maximum major principal stress for vehicle placed near edge of two pavement slabs: **a** PC (bottom); **b** PC (top); **c** PCC (bottom); **d** PCC (top)



4 Research Significance

Historically, several attempts have been made to design PCPs using fatigue equations that are based on high reliability (90%). As observed in this study, the pavement performance primarily depends on structural characteristics (strength), loading configuration and magnitude, support conditions, and material characteristics, which necessitate development of a mechanistic design methodology for PCP. In this direction, this study outlined a generic framework that can be adopted for structural analysis and design of PCP systems by engineers and practitioners for routine office design. Further, the proposed approach could be extended to develop design guidelines for PCP systems, albeit appropriate modifications. Additionally, this research highlighted the need for a more refined analysis with techniques such as discrete element method (DEM) consisting of constitutive law capable of modeling the damage behavior, including, but not limited to soil structure interaction of the PCP system as a whole.

5 Conclusions and Recommendation

The objective of this research was to establish a rational method for computation of structural thickness of PC material. The proposed thickness of 235 mm was attained using a fatigue equation given in IRC: SP:62–2014, which is based on 60% reliability. This approach was logical as PC is typically employed in low-volume traffic roads running at lower frequencies, so the conventional equations based on high reliability may lead to overestimation of PC thickness. This would not only incur higher cost of materials but demand greater quality control and precision during construction. Further, the application of STAAD Pro[®] software to analyze the PC for vehicle loads was a new and first-of-its-kind approach. It was observed that the structural behavior of PC was like that of conventional cement concrete pavement systems. PC followed comparable deflection and stress magnitudes as observed for conventional concrete pavement slab resting directly over the subgrade with equivalent modulus of subgrade reaction.

As PC is characteristically different from conventional concrete, it is essential to develop globally accepted performance-predictive fatigue models for structural design of PC. The effect of different mix proportions, pore characteristics, friction between underlying layers, environmental conditions (hydro-static pressure), stress levels, and frequencies of loading should be incorporated to improve accuracy of the models. Validation of the analysis carried out using STAAD Pro[®] is essential to quantify the relationship between practical and analytical techniques. Once validated, prototype models can be created for analysis using STAAD Pro[®] or similar software platform without the need for construction of physical models. Additionally, the future models should include multiple PC slabs for quantification of pavement's response when wheel load passes from one slab to the other. Raveling is another mode

of failure in PCP, thus future models should include both stress-related parameters and durability considerations to develop tools for more comprehensive and rigorous analysis of the special PC mixture.

Acknowledgements The authors are thankful to the CTRG 2019 organizers for their constant support during the submission process. Also, the authors would like to thank the scientific committee for their valuable contribution in reviewing this manuscript.

References

1. ACI 522R-10 (2010) Report on pervious concrete. ACI Committee 522, American Concrete Institute, Farmington Hills, USA
2. Tennis PD, Leming ML, Akers DJ (2004) Pervious concrete pavements. Portland Cement Association, Skokie, IL
3. Chandrappa A, Biligiri K (2016) Comprehensive investigation of permeability characteristics of pervious concrete: a hydrodynamic approach. *Constr Build Mater* 123:627–637
4. Rodden R, Voigt G, Smith T (2011) Structural and hydrological design of sustainable pervious concrete pavements. In: Annual conference on transportation successes: let's build on them, TAC, Edmonton, Alberta
5. Huang B, Wu H, Shu X, Burdette GE (2010) Laboratory evaluation of permeability and strength of polymer-modified pervious concrete. *Constr Build Mater* 24:818–823
6. Deo O, Neithalath N (2010) Compressive behavior of pervious concretes and a quantification of the influence of random pore structure features. *Mater Sci Eng A* 528(1):402–412
7. Vancura M, MacDonald K, Khazanovich L (2011) Structural analysis of pervious concrete pavement. *Transp Res Record J Transp Res Board* 2226:11–20
8. Gogo-Abite I, Chopra M, Uju I (2014) Evaluation of mechanical properties and structural integrity for pervious concrete pavement systems. *J Mater Civ Eng* 26(6):1–6
9. Nassiri S, AlShareedah O (2017) Preliminary procedure for structural design of pervious concrete pavements. Research report for Washington State Department of Transportation
10. PCA (1984) Thickness design of concrete highways and street pavements. Portland cement association, New York, USA
11. AASHTO (1993) Guide for design of pavement structures. American Association of State Highway Transportation Officials, Washington, DC
12. Alam A, Haselbach L, Cofer W (2011) Finite element evaluation of pervious concrete pavement for roadway shoulders. Research report for transportation Northwest TransNow and Washington State Department of Transportation
13. IRC:SP:62 (2014) Guidelines for design and construction of cement concrete pavements for low volume roads. Indian Roads Congress. First Revision, New Delhi, India
14. Chandrappa AK, Biligiri KP (2016) Influence of mix parameters on pore properties and modulus of pervious concrete: an application of ultrasonic pulse velocity. *Mater Struct* 49(12):5255–5271
15. IS:456 (2000) Plain and reinforced concrete—code of practice. Indian Standard, Fourth Revision, New Delhi, India
16. Huang YH (2004) Pavement analysis and design, 2nd ed. Pearson, Prentice Hall, Upper Saddle River, New Jersey, USA

PG Grading of Bitumen Using Capillary and Brookfield Viscometers



Akanksha Pandey, Sham S. Ravindranath, and Sridhar Raju

1 Introduction

Conventionally, the grading of bitumen has been carried out by measuring the penetration values at 25 °C, and later, viscosity grading came into existence by measuring the viscosity at 60 and 135 °C. Since measurements are performed at discrete temperatures, these conventional methods sometimes fail to effectively characterize bitumen samples over a wide range of temperatures [1].

Bitumen is a highly temperature-sensitive material and is exposed to a wide range of temperatures during pavement construction and service. During pavement construction, the bituminous mixture is exposed to nearly 150 °C, whereas during service, temperature varies widely between 60 °C and –30 °C. Many pavement distress like rutting, fatigue cracking, and thermal cracking occur over widely different pavement service temperatures. To predict pavement performance over a wide temperature range, Strategic Highway Research Program (SHRP) developed a new grading methodology, i.e., performance grading (PG) of bitumen. PG grading system proposes a criterion each for rutting, fatigue cracking, and thermal cracking that bitumen samples have to fulfill at temperatures dependent upon the area of use [2–7].

Bituminous roads are prone to rutting during their early life cycle and at higher service temperatures. Rutting is a permanent deformation in flexible pavements

A. Pandey · S. S. Ravindranath (✉)
Department of Polymer and Process Engineering, Indian Institute of Technology, Roorkee,
Uttarakhand, India
e-mail: shamrfps@iitr.ac.in; sham.ravindranath@pe.iitr.ac.in

S. Raju
Department of Civil Engineering, Birla Institute of Technology and Science, Pilani, Hyderabad,
India

caused by the consolidation and shear flow of the mixture at higher service temperature [8]. To measure the rutting resistance in pavement, SHRP proposed the criterion of $|G^*|/\sin\delta$. In SHRP studies, a good correlation was reported between the loss compliance ($1/J'' = |G^*|/\sin\delta$) measured in linear viscoelastic (LVE) region and rutting in pavements. To ensure that rutting in pavement is within the acceptable limits, a lower limiting value to $|G^*|/\sin\delta$ of the bitumen was fixed at the maximum 7-day average pavement service temperature. For convenience, the temperature at which rheological measurements are carried out is categorized in 6 °C intervals (example, 46, 52, 58, 64, 70, 76 °C, etc.). The loss compliance ($1/J'' = |G^*|/\sin\delta$) measured in the linear viscoelastic (LVE) region (angular frequency $\omega = 10$ rad/s, strain $\gamma_A = 10\%$) is adopted as grading criterion for rutting. Here, the angular frequency of 10 rad/s mimics the loading time on pavement applied by the vehicle traveling at a speed of 80 km/h.

The PG rutting criterion, which was a substitute for empirical grading methods, is currently an area of concern. Several publications have highlighted the lack of a good correlation between the rutting criterion of SHRP and the rutting performance of the pavement [9–20]. Due to the limitations in the rutting criterion, alternative methods were suggested, i.e., modification to $|G^*|/\sin\delta$ equation, variation in testing parameters, or use of zero shear viscosity method [10–12, 21–23].

In this study, through comprehensive rheological analysis, we clearly show that the limitation of the PG rutting criterion is that it can be simplified to the viscosity of bitumen sample. Apart from the dynamic shear rheometer, the viscosity of bitumen samples can also be determined using basic instruments, such as capillary and Brookfield viscometers. Hence, in light of the limitation of PG grading system, the objective of this study is to explore the possibility of PG grading of bitumen samples using capillary and Brookfield viscometers.

2 Materials and Methods

Source, continuous PG temperature, PG grade, and conventional properties of the four bitumen samples used to accomplish the objective of this study are given in Tables 1 and 2, respectively. The penetration and softening point of the four bitumens ranged

Table 1 Source, continuous PG upper limiting temperature (Tu), and PG grade of the four bitumen samples

Bitumen	Source	Continuous PG Temp (°C)		PG Grade
		Unaged	RTFO aged	
A-85	Juno Bitumen	62	61	PG-58
B-65	Tiki Tar Industries	64	63	
C-60	Juno Bitumen	65	64	PG-64
D-40	Tiki Tar Industries	72	71	PG-70

Table 2 Conventional properties of the four bitumen samples

Bitumen	Penetration @ 25 °C (dmm)	Softening point (°C)	Absolute viscosity at 60 °C (Poise)	Brookfield viscosity at 135 °C (Pa.s)	RTFO	
					Retained pen (%)	Viscosity ratio at 60 °C
A-85	85	46.6	1280	0.34	52	2.75
B-65	65	51.4	2167	0.42	54	3.33
C-60	60	52.8	2230	0.43	58	3.11
D-40	40	54.4	4190	0.63	58	2.61

Table 3 Tests, instruments, and corresponding standards

Test	Instrument	Standard
Penetration at 25 °C, (dmm)	Aimil 512	ASTM D5
Softening point, (°C)	Aimil 561	ASTM D36
PG grading	Anton Paar—Physica MCR102	ASTM D6373
Absolute viscosity	Capillary viscometer	IS1206 (part 2)
Brookfield viscosity	DV-E viscometer	ASTMD4402
Rolling thin film oven	Aimil Ltd	ASTM D2872

between 85 to 40 dmm and 46.6 to 54.4 °C, respectively. Additionally, mass loss after RTFO, solubility in trichloroethylene were also measured according to ASTM standard. Mass loss and solubility in trichloroethylene of the four bitumen samples were >230 °C, <1%, and >99%, respectively.

The purpose of selecting bitumen samples with different properties was to evaluate samples covering a wide range of properties that could be used for road construction. Penetration at 25 °C, softening point, performance grading (PG), viscosity using capillary, and Brookfield viscometers were measured in accordance to ASTM D5, ASTM D36, ASTM D6373, IS 1206 (part 2), and ASTMD4402, respectively. Aging of the samples was carried out by rolling thin film oven (RTFO) according to ASTM D2872. Table 3 provides information about the tests, instruments utilized, and respective standards employed. Rheological studies were carried out on Anton Paar's MCR 102 dynamic shear rheometer in accordance with ASTM standards.

3 Results and Discussion

3.1 Rutting Criterion

The rutting criterion was set as the temperature at which $|G^*|/\sin\delta \geq 1000/2200$ Pa (unaged/RTFO aged). Though bitumen is graded in 6 °C intervals, measurements were carried out at the temperature where $|G^*|/\sin\delta \simeq 1000/2200$ Pa (unaged/RTFO aged), and named as continuous PG upper limiting temperature (T_u). The $|G^*|/\sin\delta$ versus T_u of the four bitumen samples is presented in Fig. 1a, b. It can be seen from Fig. 1a, b that $|G^*|/\sin\delta$ is just above 1000 Pa and 2200 Pa at the corresponding T_u temperatures for unaged and RTFO aged bitumens, respectively. The plot of phase angle (δ) versus time also showed an interesting result, as shown in Fig. 2. When we carry out PG grading, it is actually the determination $G^*/\sin\delta$ with respect to time sweep. Hence, the phase angle values are plotted as a function of time. It can be seen from Fig. 2a, b that at T_u , the phase angle values of all the bitumen samples were above 83° (for both unaged and RTFO aged).

For $\delta = 83^\circ$, $\sin 83^\circ = 0.993 \approx 1$.

And from basic rheology, the complex viscosity $|\eta^*|$ and complex modulus $|G^*|$ are correlated as

$$|G^*| = |\eta^*| \cdot \omega \tag{1}$$

At angular frequency (ω) of 10 rad/s, Eq. (1) will be

$$|\eta^*| = |G^*|/10 \tag{2}$$

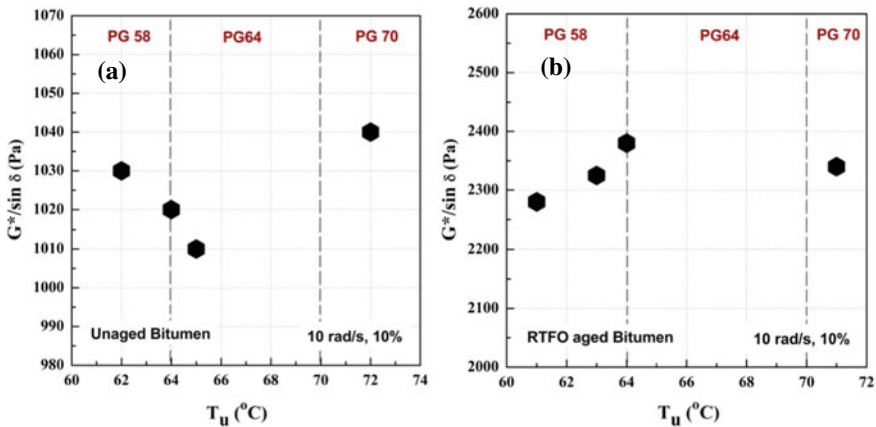


Fig. 1 Rutting criteria $|G^*|/\sin\delta$ versus continuous PG upper limiting temperatures (T_u) for the four **a** unaged **b** RTFO-aged bitumen samples

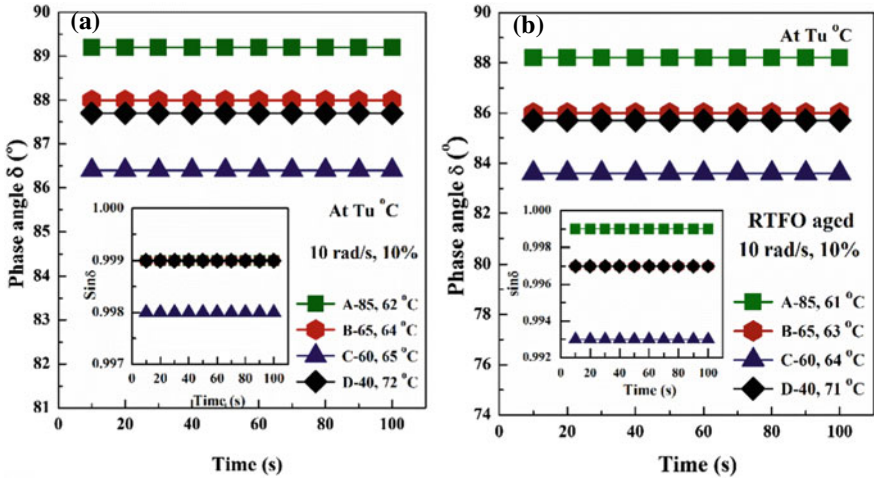


Fig. 2 Phase angle δ versus time at continuous PG upper limiting temperatures (T_u) for the four **a** unaged **b** RTFO aged bitumen samples. $\text{Sin}\delta$ values are shown in the inset

The verification of Eq. (2) is carried out by plotting $|l\eta^*|$ versus time at T_u for the four bitumen samples, as given in Fig. 3. It can be seen from Fig. 3a, b that the complex viscosity $|l\eta^*|$ at T_u of the four bitumen samples is nearly 100 Pa.s and 220 Pa.s for unaged and RTFO aged, respectively.

Further, validation of the above result is carried out through an equation provided by Witczak model [24]. According to the equation, phase angle, complex modulus, and complex viscosity are related as

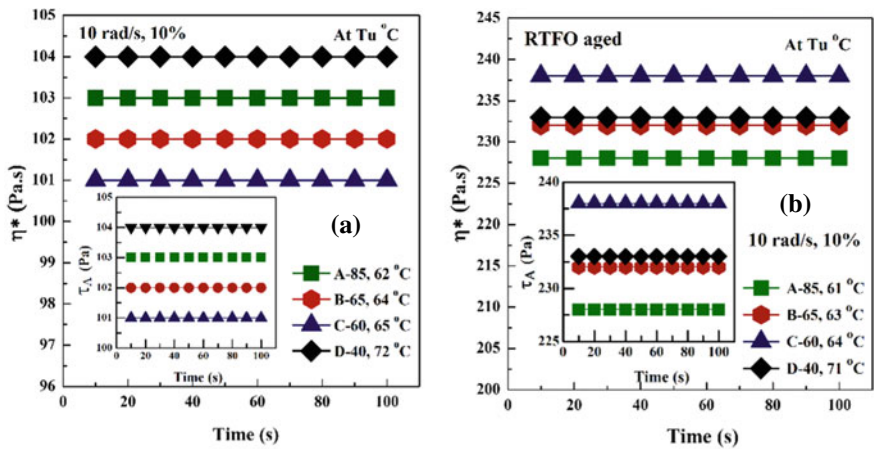


Fig. 3 Complex viscosity $|l\eta^*|$ versus time at continuous PG upper limiting temperatures T_u for the four **a** unaged **b** RTFO-aged bitumen samples. Shear stress amplitude τ_A values are shown in the inset

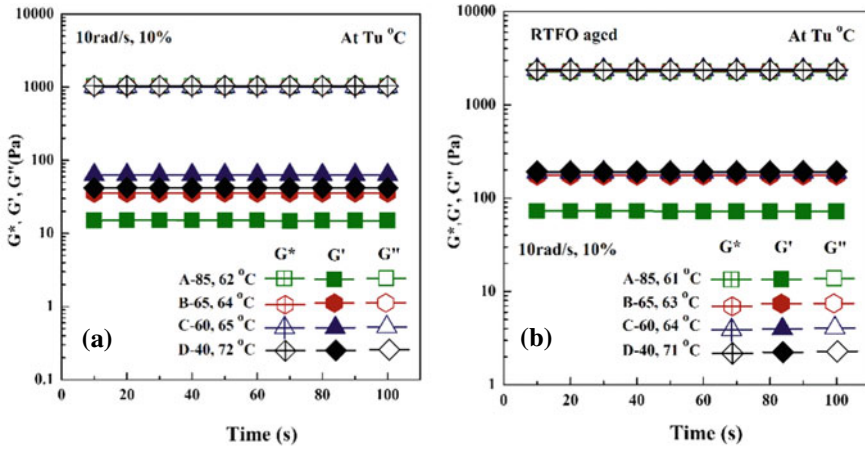


Fig. 4 $|G^*|$, G' , and G'' versus time at continuous PG upper limiting temperatures T_u for the four **a** unaged **b** RTFO-aged bitumen samples

$$|\eta^*| = \frac{|G^*|}{10} \left(\frac{1}{\sin \delta} \right)^{4.8628} \tag{3}$$

Since the phase angle (δ) is $>83^\circ$, $\sin 83^\circ = 0.993 \approx 1$. So, Eq. (3) also simplifies to

$$|\eta^*| = |G^*|/10 \tag{4}$$

Thus, for unaged and RTFO aged bitumen at continuous PG temperature T_u , at $\omega = 10$ rad/s and strain = 10%

$$\text{Rutting criteria : } |G^*|/\sin \delta = |\eta^*| \geq 100/ \text{ and } 220 \text{ Pa.s} \tag{5}$$

Since the phase angle values are nearly 90° , elastic modulus $G' = (\tau_A/\gamma_A) \cos \delta$ values will be negligible compared to loss modulus values $G'' = (\tau_A/\gamma_A) \sin \delta$. The contribution to the complex modulus $(|G^*|)^2 = \tau_A/\gamma_A = (G')^2 + (G'')^2$ will be mainly from the loss modulus G'' as shown in Fig. 4. Thus, at T_u the complex modulus $|G^*| \approx$ loss modulus G'' for the four bitumen samples, which again illustrates the viscous behavior of the bitumen at T_u .

3.2 Frequency Sweep

Frequency sweep measurements were carried out to understand the rheological behavior of both unaged and RTFO-aged bitumen. Frequency sweep was performed

from 50 to 0.5 rad/s at three different temperatures T_u , $T_u - 10$, and $T_u - 20$ °C. It can be seen from Fig. 5a, b that even below 20 °C from continuous PG upper limiting temperature (T_u), the minimum value of phase angle δ was 83° and 80° for unaged and RTFO aged A-85 bitumen. The corresponding $\sin\delta$ values will be 0.99 and 0.98, respectively. The result of remaining three bitumen samples is presented in the appendix section (Figs. 8 and 9). The insignificant change in $\sin\delta$ even at $T_u - 20$ °C results in simplifying the PG rutting criterion to complex modulus G^* as shown in Fig. 6. This further demonstrates that the term $\sin\delta$ in the rutting criterion for unmodified bitumens has no benefit.

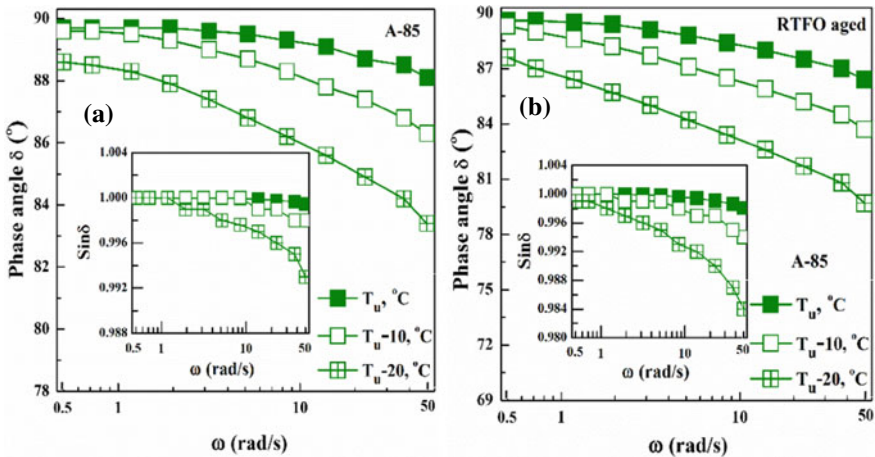


Fig. 5 Phase angle δ versus ω at T_u , $T_u - 10$, and $T_u - 20$ °C for a unaged and b RTFO-aged A-85 bitumen. $\sin\delta$ values are shown in the inset

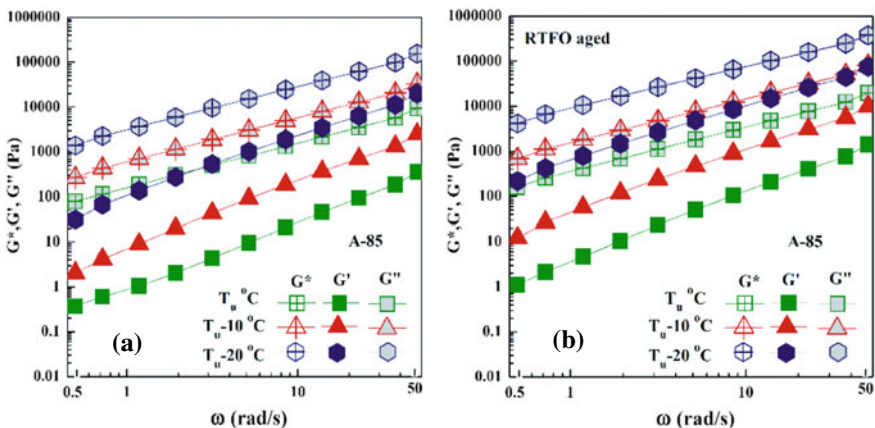


Fig. 6 $|G^*|$, G' , and G'' versus ω at T_u , $T_u - 10$, and $T_u - 20$ °C for a unaged and b RTFO-aged A-85 bitumen

3.3 Viscosity Measurements in a Rotational Mode

The results from Sects. 1 and 2 showed that at T_u phase angle values (δ) are close to 90° , and complex viscosity is nearly 100 and 220 Pa.s for unaged and RTFO aged bitumen, respectively. For liquids that exhibit $\delta \approx 90^\circ$ over a wide frequency range, complex viscosity $| \eta_c^* |$ determined through oscillatory shear in the linear viscoelastic region will be close to viscosity determined through rotational shear. Hence, further measurements were made in the continuous rotational mode as a function of shear rate. The rate ramp experiment from 0.1 to 10 s^{-1} in rotational mode was carried out at T_u using cone-plate geometry (diameter 25 mm, 2° angle). The response of the rotational shear mode experiment is shown in Fig. 7a, b. It can be seen from the figure that the shear viscosity η of the four bitumen samples is nearly 100 and 220 Pa.s over the applied shear rate of $0.1\text{--}10 \text{ s}^{-1}$. The shear stress ($\tau = \text{shear viscosity} \times \text{strain rate}$) values are shown in the inset of figure. Since the viscosity is nearly same throughout the strain rate ramp, shear stress varies linearly with the applied strain rate. Further, increment in shear rate causes edge instability; hence, experiments were not carried out.

The result shows that bitumen at T_u within the shear rate of $0.1\text{--}10 \text{ s}^{-1}$ is

$$|G^*| / \sin \delta \geq 1000/2200 \text{ Pa} = \text{shear viscosity } \eta \geq 100/220 \text{ Pa.s}$$

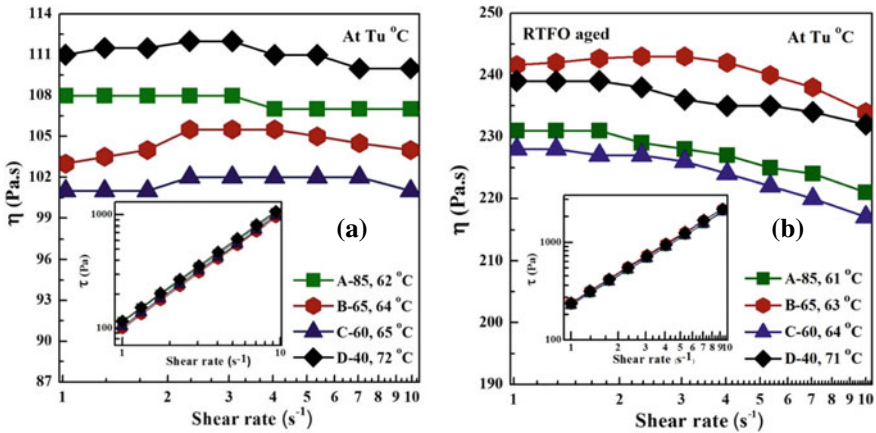


Fig. 7 Shear viscosity η versus shear rate at continuous PG upper limiting temperatures T_u for the four **a** unaged **b** RTFO-aged bitumen samples in a cone-plate geometry in rotational mode. Shear stress values are in inset

3.4 Viscosity Measurements in Capillary and Brookfield Viscometer

The results of Sect. 3 showed that even in rotational mode, the viscosity is close to 100 and 220 Pa.s for the four bitumen samples. Viscosity of bitumen samples can be measured using simple viscometer such as capillary and Brookfield viscometers. Hence, further measurement of viscosity for bitumen samples is carried out using capillary and Brookfield viscometers. Unlike the dynamic shear rheometers (DSR), these viscometers are inexpensive, very easy to operate, and have been used to find the viscosity of bitumen from long. In capillary viscometer, it is difficult to quantify the effect of shear rate on fluids; hence, measurements were also carried out using Brookfield viscometer. Table 4 summarizes the viscosity values of the four bitumen samples measured at T_u using capillary and Brookfield viscometers. The Brookfield viscometer measurements were made using spindle 21 and at 0.3 rpm. It can be seen from the table that even in simple measuring systems, the viscosity of the four bitumen samples were close to 100 and 220 Pa.s at T_u . Thus, PG grading of bitumen can be performed on inexpensive capillary and Brookfield viscometers instead of the expensive DSR's. Here, due to Brookfield viscometer limitations, the viscosity for RTFO aged was not measured. It can be seen in Table 5 that the PG grade of the four bitumen samples as determined through DSR, capillary, and Brookfield viscometers were similar.

Table 4 Measurements in capillary and Brookfield viscometers at T_u

Bitumen	Capillary viscometer (Absolute viscosity), (Pa.s)	Brookfield viscometer spindle 21, 0.3 rpm, (Pa.s)	RTFO
			Capillary viscometer (Absolute viscosity), (Pa.s)
A-85	92	118	244
B-65	97	113	252
C-60	89	124	267
D-40	104	121	280

Table 5 PG grade of four bitumen samples using DSR, capillary, and Brookfield viscometers

Bitumen	PG grade (DSR)	PG grade (Capillary viscometer)	PG grade (Brookfield viscometer)
A-85	PG-58	PG-58	PG-58
B-65	PG-58	PG-58	PG-58
C-60	PG-64	PG-64	PG-64
D-40	PG-70	PG-70	PG-70

4 Conclusions

- A thorough examination of rutting criterion for bitumen samples was carried out in a dynamic shear rheometer (DSR).
- The measurements in the DSR showed that the phase angle δ values of unaged/RTFO-aged bitumen samples at continuous PG upper limiting temperatures (T_u) were above 80° , and the corresponding $\sin\delta$ values will be ≈ 1 .

Therefore,

PG rutting criterion: $|G^*|/\sin\delta \geq 1000/2200$ Pa can also be expressed as $|\eta^*| \geq 100$ and 220 Pa.s (unaged/RTFO aged)

- In the rotational mode, the viscosity of bitumen samples was close to 100 and 220 Pa.s at T_u (unaged and RTFO aged)

Hence, rutting criterion can also be expressed as shear viscosity $\eta \geq 100$ and 220 Pa.s (unaged and RTFO aged)

- At continuous PG upper limiting temperature in capillary and Brookfield viscometers, the viscosity of bitumen was also close to 100 and 220 Pa.s (unaged/RTFO aged).
- In each case, oscillatory/rotational, capillary, and Brookfield viscometers, viscosity was 100 and 220 Pa.s at T_u for unaged and RTFO-aged bitumen, respectively.
- The PG grade of the four bitumen samples as determined through DSR, capillary, and Brookfield viscometers were similar.

Acknowledgements The authors acknowledge the 5th Conference of the Transportation Research Group (CTRG-2019) of India, held at Bhopal (India) from 18–21 December, to provide this opportunity. This work is supported by the ‘*Faculty Initiation grant*’ provided by the Indian Institute of Technology, Roorkee. Authors also thank Ministry of Human Resource Development, Government of India for providing student scholarship.

Appendix

See Figs. 8 and 9.

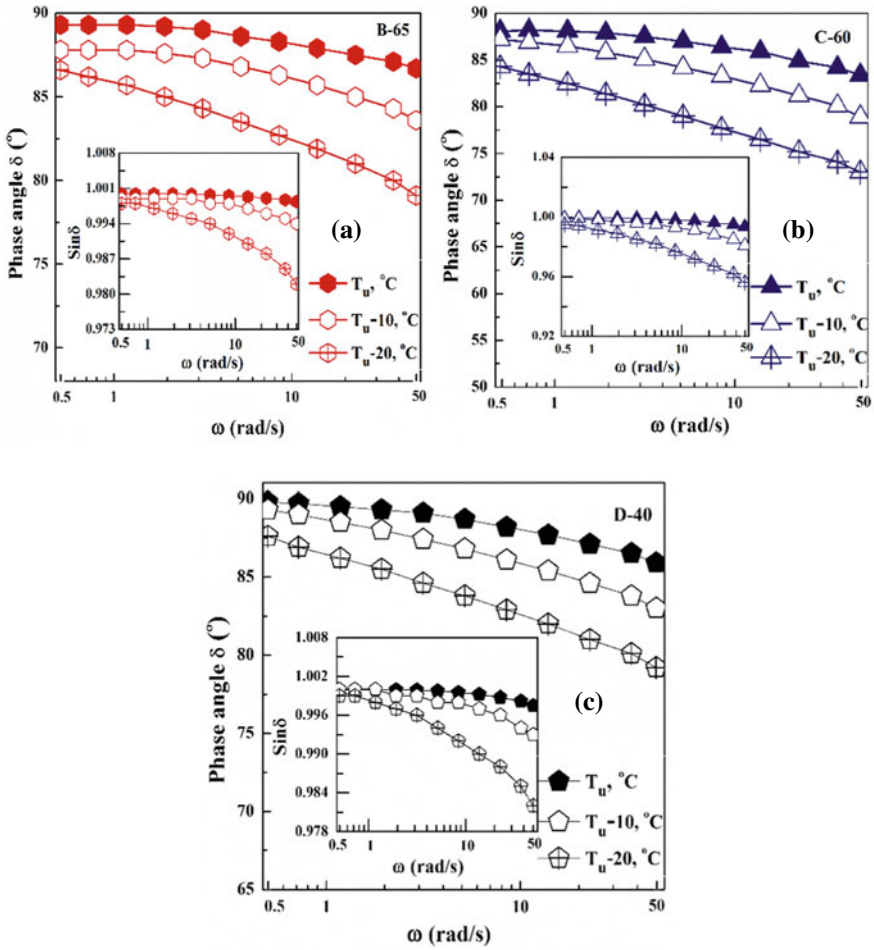


Fig. 8 Phase angle δ versus ω at T_u , $T_u - 10$, and $T_u - 20$ $^{\circ}\text{C}$ for **a** B-65 **b** C-60, and **c** D-40 remaining three bitumen samples. $\text{Sin} \delta$ values are shown in the inset

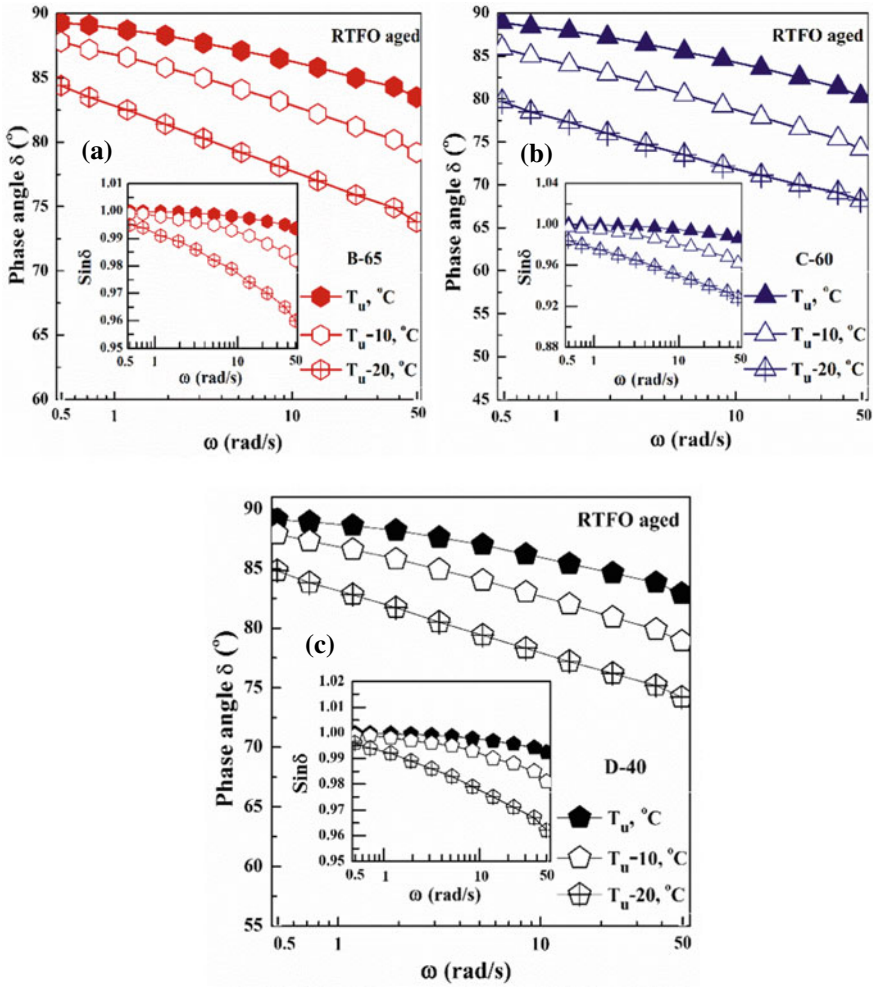


Fig. 9 Phase angle δ versus ω at T_u , $T_u - 10$, and $T_u - 20$ °C for **a** B-65 **b** C-60, and **c** D-40 remaining three RTFO aged bitumen samples. $\text{Sin}\delta$ values are shown in the inset

References

1. Nattaporn C, Kunnawee K (2012) Performance graded bitumen specifications. *Asian Transp Stud* 2(2):121–138
2. Petersen JC, Robertson RE, Branthaver JF, Harnsberger PM, Duvall JJ, Kim SS (1994) Binder characterization and evaluation, vol 1. Strategic Highway Research Program. National Research Council, Washington DC, Report: SHRP-A-367
3. Thomas WK, Gerald AH, Edward TH, Ronald JC, Charles SH, Harold VQ, James SM (1994) Superior performing asphalt pavements (Superpave): The product of the SHRP asphalt research program. Strategic Highway Research Program, National Research Council, Washington DC, Report: SHRP-A-410
4. McGennis RB, Shuler S, Bahia HU (1994) Background of Superpave asphalt binder test methods. National Asphalt Training Center, Demonstration Project 101, Federal Highway Research Administration
5. Mansour S (1994) Development of SHRP asphalt research program climatic databases. Strategic Highway Research Program, National Research Council, Washington DC, Report: SHRP-A-685
6. Khalid AG, Ghazi GAK (2013) Selection and verification of performance grading for asphalt binders produced in Jordan. *Int J Pavement Eng* 14:116–124
7. Mohseni A, Carpenter S, John AD (2005) Development of SUPERPAVE high-temperature performance grade (PG) based on rutting damage (with discussion and closure). *J Assoc Asphalt Paving Technol* 74
8. Shahbaz K, Nagabhushana MN, Devesh T, Jain PK (2013) Rutting in flexible pavement: an approach of evaluation with accelerated pavement testing facility. In: 2nd conference of transportation research group of India (2nd CTRG), *Procedia-social and behavioural science*, vol 104, pp 149–157
9. Chen JS, Tsai CJ (1999) How good are linear viscoelastic properties of asphalt binder to predict rutting and fatigue cracking? *J Mater Eng Perform* 8:443–449
10. Bahia HU, Zhai H, Zeng M, Hu Y, Turner P (2001) Development of binder specification parameters based on characterization of damage behaviour. *J Assoc Asphalt Paving Technol* 70:442–470
11. Shenoy A (2004) High temperature performance grading of asphalts through a specification criterion that could capture field performance. *J Transp Eng* 130
12. Morea F, Agnusdei JO, Zerbino R (2011) The use of low shear viscosity to predict permanent deformation performance of asphalt concrete. *Mater Struct* 44:1241–1248
13. Domingos MDI, Faxina AL (2016) Susceptibility of asphalt binders to rutting: literature review. *J Mater Civ Eng* 2(28):04015134
14. Subhy AS (2017) Advanced analytical techniques in fatigue and rutting related characterisations of modified bitumen: literature review. *Constr Build Mater* 156:28–45
15. Delgadillo R, Kitae N, Bahia HU (2006) Why do we need to change $|G^*|/\sin\delta$ and how? *Road Mater Pavement Des* 7:7–27
16. Morea F, Agnusdei JO, Zerbino R (2010) Comparison of methods for measuring zero shear viscosity in asphalts. *Mater Struct* 43:499–507
17. Radhakrishnan V, Ramya SM, Reddy KS (2018) Evaluation of asphalt binder rutting parameters. *Constr Build Mater* 173:298–307
18. Wasage TLJ, Stastna J, Zanzotto L (2011) Rheological analysis of multi-stress creep recovery (MSCR) test. *Int J Pavement Eng* 12(6):561–568
19. Behnood A, Ayesha S, Rebecca SM, Jan O (2016) Analysis of the multiple stress creep recovery asphalt binder test and specifications for use in Indiana. Joint Transportation Research Program, FHWA/IN/JTRP-2016/07
20. Soenen H, Blomberg T, Pellinen T, Laukkanen OV (2013) The multiple stress creep-recovery test: a detailed analysis of repeatability and reproducibility. *Road Mater Pavement Des* 14:2–11

21. Morea F, Zerbino R, Agnusdei J (2014) Wheel tracking rutting performance estimation based on bitumen low shear viscosity (LSV), loading and temperature conditions. *Mater Struct* 47(4):683–692
22. Wang C, Jhang J (2014) Evaluation of rutting parameters of asphalt binder based on rheological test. *IACSIT Int J Eng Technol* 6(1)
23. Mazurek G, Iwanski M (2016) Estimation of zero shear viscosity versus rutting resistance parameters of asphalt concrete. *Procedia Eng* 161:30–35
24. Ahmed MK, Sherif MB, Abbas AH, Mahmoud E (2014) Evaluation of Witczak E^* predictive models for the implementation of AASHTOW are-Pavement ME design in the kingdom of Saudi Arabia. *Constr Build Mater* 64:360–369

Studies on Temperature Differential for Different Types of Overlay Over Cement Concrete Pavement



M. Varuna, Deepak Raikar, and S. Sunil

1 Introduction

Temperature differential is an important factor in design of the concrete pavement. This kind of thermal fluctuations induces slab expansion and bending action which in turn induce thermal stresses. The maximum stresses induced in the slab will be directly related to concrete stiffness, concrete panel size and inversely related to concrete thickness and base stiffness [1–5].

In design consideration, temperature variation is assumed to be linear, but according to research, it is proved to be non-linear [1]. The non-linearity tends to increase with increase in thickness of slab. It is reported not taking into account the effect of non-linear temperature differential and partial sub-grade support results in early stage deterioration, i.e. slab cracking at centre, corner and edge. Coefficient of thermal expansion (CTE) is directly related to material properties, aggregates used in construction and prevailing temperature. CTE values were determined for mixes with fly ash, granulated blast furnace slag and varying aggregates proportion in mix design. Slag tends to increase CTE compared to fly ash. Sand type is an important parameter which determines CTE. The range of CTE is 7–11 micro-strains/Celsius. Below 8 micro-strains/Celsius, no transverse cracking and the rate of cracking started increasing as the CTE was increased. At 10.8 micro-strains/Celsius, 20% transverse cracking was observed. Increased CTE resulted in increased slab cracking, top-down and bottom-up cracking and increased IRI [6–8].

Temperature differential can be reduced by overlaying asphalt course. Asphalt concrete is a layer, which can be used as a thermal and permeable blanket, and this

M. Varuna (✉) · D. Raikar · S. Sunil
Department of Civil Engineering, RV College of Engineering, Bengaluru 560059, India
e-mail: varunam@rvce.edu.in

S. Sunil
e-mail: sunils@rvce.edu.in

helps in reduction of curling stresses [9–11]. Use of reclaimed concrete aggregate (RCA) will not affect durability of pavement, and also, changes in volume due to variation in temperature and moisture are less [12].

White topping is a successful rehabilitation method, used in major part of the country for development and maintenance of highways and airports. Reduction of tensile stresses due to temperature variation would increase the performance and provide longer life to the pavements. Hence, in the present study, an attempt is made to determine the temperature variation for CC slab casted as per IRC 44(2008) [13] with different material combinations and overlaid with bituminous mixes.

1.1 Scope and Objective

The study is aimed to determine the least variation in temperature for different slab thickness comparing with conventional and alternative materials.

- (i) To determine temperature variation in concrete slab by use of alternate materials, i.e. fly ash, ground granulated blast furnace slag (GGBS), silica fume and recycled concrete aggregates (RCAs)
- (ii) To determine temperature variation in concrete slab when bituminous mixes overlay is provided, i.e. bituminous concrete, stone matrix asphalt, open-graded friction course
- (iii) To determine thermal stresses by finite element modelling (FEM) using ANSYS.

2 Materials

2.1 Aggregates

Crushed aggregate of granite origin was procured from nearby crusher site, and basic physical properties tests of aggregates were conducted according to IS: 2386-1963—Part VI (Mechanical properties of aggregate) and IS: 2386-1963—Part I (Particle size and shape) as per MORTH V revision [14]. The test results of coarse and fine aggregates are presented in Tables 1 and 2.

2.2 Bitumen

For the present study, VG30 grade was used, and basic properties were tested as per IS 73: 2013 [15]. The test result of bitumen is presented in Table 3.

Table 1 Coarse aggregate test results

S. No	Test	Test results	MORTH specifications	IS Codes	Remarks
1	Specific gravity	2.68	2.6–2.9	IS 2386—Part 3	Permissible
2	Water absorption (%)	0.80	Max 2%	IS 2386—Part 3	Permissible
3	Sieve analysis	4%	Max 5%	IS 2386—Part 1	Permissible
4	Combined index (%)	28	Max 35	IS 2386—Part 1	Permissible
5	Angularity number	9	0–11	IS 2386—Part 1	Permissible
5	Aggregate impact (%)	18.2	Max 24	IS 2386—Part 4	Permissible
6	LAA (%)	24	Max 30	IS 2386—Part 4	Permissible
7	Crushing value (%)	28.7	Max 30	IS 2386—Part 4	Permissible

Table 2 Fine aggregate test results

S. No	Properties	Test results	MORTH specifications	IS Codes	Remarks
1	Specific gravity	2.74	2.6–2.9	IS 2386—Part 3	Permissible
2	Water absorption test	0.46%	Max 2%	IS 2386—Part 3	Permissible
3	Sieve analysis	Zone II	Zone I–IV	IS 2386—Part 1	Permissible

Table 3 Bitumen test results

S. No	Test	Test results	As per specifications	Remarks
1	Penetration, mm	62	60–70	Permissible
2	Softening point, °C	51	45–55	Permissible
3	Ductility, cm	79	>75 cm	Permissible
6	Viscosity, cp	541	Min 350	Permissible
7	Specific gravity	1.01	0.99–1.01	Permissible

2.3 Cement

Ordinary Portland cement of grade 53 was used which confirms the specifications of IS: 12,269-2013, and test results are presented in Table 4.

Table 4 Cement test results

S. No	Properties	Test results	MORTH specifications	IS Codes	Remarks
1	Specific gravity	3.15	3.0–3.25	IS 12269–2013	Permissible
2	Fineness test	Zone II	Zone I–IV	IS 2386—Part 1	Permissible
3	Initial and final setting time	>30 & <600 minutes	Min 30 and Max 600 min	IS: 4031—Part 1	Permissible

Table 5 Fly ash test results

S. No	Properties	Test results
1	Specific gravity	2.28

Table 6 GGBS test results

S. No	Properties	Test results
1	Specific gravity	2.84
2	Moisture content	5%
3	Standard consistency	34%

2.4 Fly Ash

Specific gravity of fly ash was determined, and results are presented in Table 5

2.5 Ground Granulated Blast Furnace Slag (GGBS)

GGBS samples were tested as per IS 12089: 1987, and results are presented in Table 6.

2.6 Micro-Silica Fume

The silica fume used is tested as per standards specified by ASTM C 1240 and AASHTO M 307. The test results are presented in Table 7.

Table 7 Micro-silica fume test results

S. No	Properties	Test results
1	Specific gravity	2.2
2	Fineness modulus	20000 m ² /kg
3	Bulk modulus	240 kg/m ³

2.7 Recycled Concrete Aggregates (RCA)

PCC blocks were broken down to smaller size with the help of crusher and were sieved. The RCA passing 4.75-mm sieve is designated to be RCA fines, and retained portion is designated as recycled concrete aggregates. Tests results are presented in Table 8.

3 Experimental Work

The study involves determination of temperature differential for following slab combinations.

Cement concrete slabs

- (i) PCC of M 40 grade
- (ii) 60% OPC + 40% fly ash concrete slab
- (iii) 80% OPC + 20% GGBS concrete slab
- (iv) 90% OPC + 10% silica fume concrete slab
- (v) 60% OPC + 40% silica fume concrete slab

Cement concrete slabs with bituminous overlay

- (vi) PCC slab + bituminous concrete overlay of 40 mm thickness
- (vii) PCC slab + stone matrix asphalt overlay of 40 mm thickness
- (viii) PCC slab + open-graded friction course overlay of 40 mm thickness
- (ix) Two-lift concrete slab

To determine temperature differential, slabs of dimension 0.5 × 0.5 × 0.1 m (ultra-thin) and 0.5 × 0.5 × 0.2 m were casted by adopting M40 grade. Total nine slabs were casted for above-mentioned dimension.

Sensors were inserted at 5, 10, 15 and 20 cm from top, and temperature variation in concrete slabs was determined. Subsequently, bituminous overlay of bituminous concrete, stone matrix asphalt, and open-graded friction course of 40 mm thickness

Table 8 RCA test results

S. No	Properties	Test results	IS Codes
1	Specific gravity	2.57	IS 2386—Part 3
2	Water absorption test	3.8%	IS 2386—Part 3

was laid over existing concrete slabs. Again, temperature variation was recorded for every 3-h interval. Later, obtained values were analysed by finite element method for determining stresses induced due to temperature.

3.1 Mix Design

Mix design was carried out as per IRC 44-2008: Guidelines for Cement Concrete Mix Design for Pavement (Second Revision) and IS 10262-2013 recommendations. For present study, SMA binder course, bituminous concrete grade-2 prescribed as per MoRTH (2013) is adopted. Gradation for OGFC is considered from MS II. Marshall mix design was carried out as per asphalt institute MS 2 (Seventh Edition).

3.2 Two-Lift Procedure

Concrete cubes were broken into pieces and were further crushed with the help jaw crusher. The recycled material was sieved and separated. The recycled constituents were proportioned and cast for M40 grade. Lower lift with 50 mm and 100 mm was cast with RCA for ultra-thin and thin white topping, respectively.

4 Data Collection

Temperature differential is measured for different slab combinations and shown in Fig. 1a, b.

4.1 Determination of Temperature at Different Depths for CC Slabs

Temperature readings were determined using thermocouple at top, 50 and 100 mm for 100-mm-thick concrete slab, and for 20-cm concrete slab, temperature was determined at top, 50, 100, 150 and 200 mm.

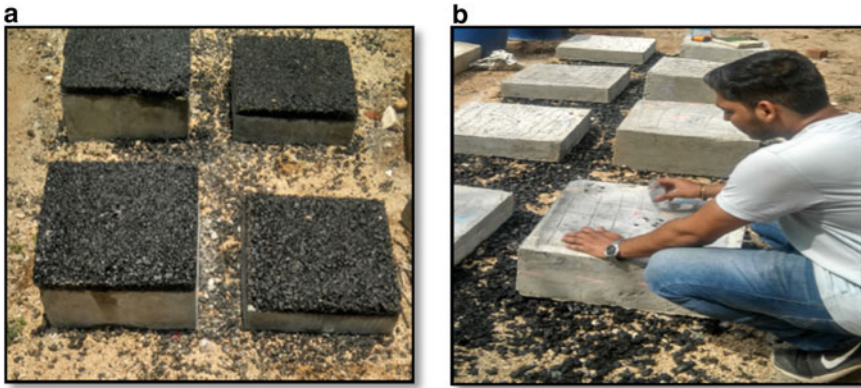


Fig. 1 a Temperature difference for different bituminous mixes. b Temperature difference different for different PCC mix

4.2 Determination of Temperature at Different Depths for CC Slabs with Bituminous Overlay

Temperature was measured at surface, interface, 90, 140 mm (depth considered from top of overlay) for ultra-thin white topping and at surface, interface, 40, 90, 140, 190 and 240 mm for thin white topping.

5 Results and Discussion

The basic physical properties of materials used for the study are presented in the following tables.

5.1 Compressive Strength

The cubes were tested using compression testing machine as per IS: 516(1959). The failure loads were noted, and results are shown in Fig. 2.

5.2 Flexural Strength

Beams of dimension 100 × 100 × 500mm were tested using flexure testing machine as per IS: 516(1959). Placement and loading of specimen in machine are done as per

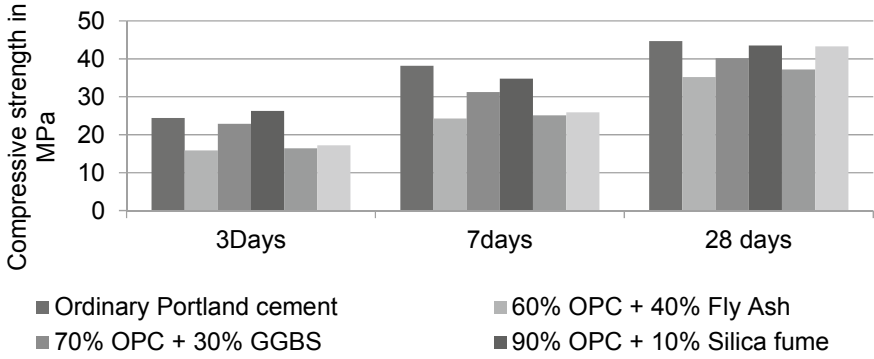


Fig. 2 Compressive strength of different mix designs at 3, 7 and 28 days

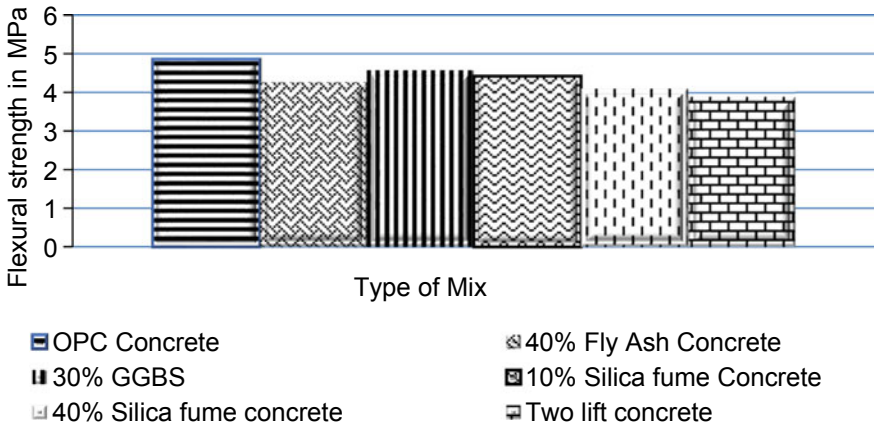


Fig. 3 Flexural strength of different mix design at 28 days

IS: 516-1959 in the clause no 8.3.1. The failure loads were noted and are shown in Fig. 3.

5.3 Temperature Differential in Slabs

Algebraic sum of temperature at surface and bottom of PCC slab is termed to be temperature differential. The temperature differential during day time and night time are termed as positive and negative temperature differential, respectively. Temperature differential determined is presented in Table 9.

Table 9 Temperature differential for slabs of thickness 100 and 200 mm with different mix design in corner region

Slab Number	Slab	Temperature differential for slab thickness of			
		100 mm		200 mm	
		Positive	Negative	Positive	Negative
1	PCC slab	12.3	7.4	14.6	9.6
2	40% fly ash concrete slab	7.8	5.4	11.3	6.1
3	20% GGBS concrete slab	6.9	4.9	13.2	6.5
4	10% silica fume concrete slab	7.5	5.1	13.3	7
5	40% silica fume concrete slab	4.8	4.6	10.6	5.8
6	With bituminous concrete overlay (40 mm)	11.2	6.1	12.3	7
7	With stone matrix asphalt overlay(40 mm)	9.7	3.1	9.6	9.6
8	With open-graded friction course overlay (40 mm)	11.6	4.4	15.5	4.7
9	Two-lift concrete slab	8.1	4.4	9.7	5.5

6 Stress Analysis

Finite element method (FEM) was used to determine thermal stresses for 100-mm and 200-mm PCC slab with different bituminous overlays of thickness 40 mm. Non-linear thermal loading is added with fine meshing to get accurate results. The base and sides of the slab are considered to be fixed during calculation of stresses and deflection. The results determined will be dependent on material properties as listed in Table 10. Figures 4 and 5 depict the thermal stresses generated for varying PCC slab thickness with bituminous overlay.

Table 10 Material properties used in ANSYS

Material	Properties	Values
Concrete	Density	2350 kg/m ³
	Young’s modulus	30000Mpa
	Poisson’s ratio	0.2
	Coefficient of thermal expansion	10E-6
	Compressive strength	41Mpa
	Flexural strength	4.8Mpa

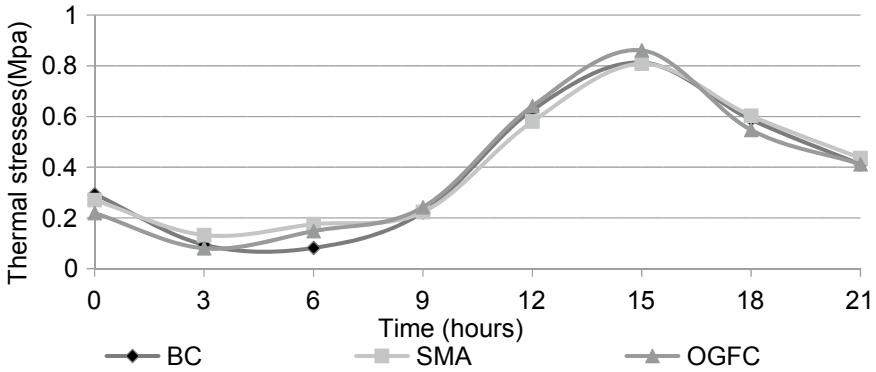


Fig. 4 Thermal stresses in 100-mm PCC slab and 40-mm bituminous overlay

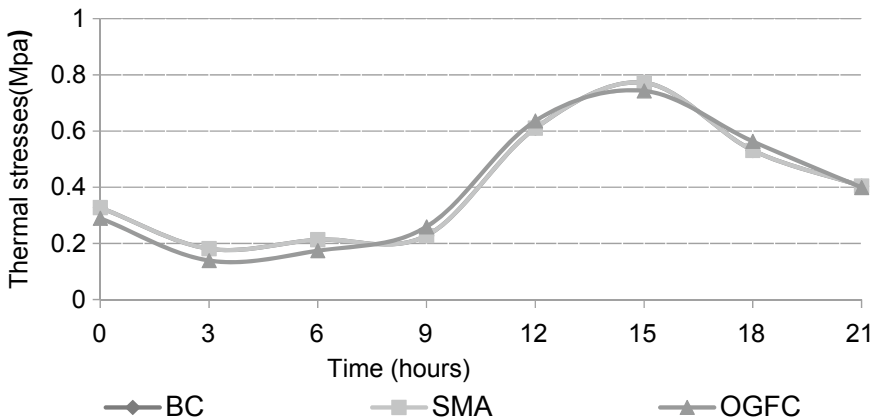


Fig. 5 Thermal stresses in 200-mm PCC slab and 40-mm bituminous overlay

7 Conclusions

- (i) It was observed that maximum positive and negative temperature differential was observed in PCC slab for 100 and 200 mm thickness. The maximum and minimum temperature differential occurred at 12 P.M and 3 A.M. for concrete slab casted with alternative materials. Temperature differential was found to be maximum for bituminous concrete overlay having maximum positive temperature differential of 11.2° and minimum negative temperature differential of 6.1° in corner region for 100-mm concrete overlay which occurred at 12 P.M and 3 A.M., respectively. Similarly, the minimum temperature differential was found to be for RCA slab having maximum positive temperature differential of 2.1 at corner and minimum negative temperature differential of 4.4 in edge

region in 100-mm concrete overlay which occurred at 9 A.M and 9 P.M., respectively.

From FEM, it was observed that thermal stress varied from 8.1Mpa to 1.2Mpa for concrete slab with bituminous overlay in 100-mm and 200-mm slab. Similarly, thermal stress varied from 6.1 to 0.8 Mpa for concrete slab casted with alternative materials.

- (ii) For 100-mm slab, with the addition of 40% fly ash, 20% GGBS, 10% silica fume and 40% silica fume, there was decrease in positive temperature differential by 36, 44, 35 and 44%, respectively, in corner region. Similarly, decrease in negative temperature differential was 27, 33, 31 and 36%, respectively, in corner region.
- (iii) For 200-mm slab, with the addition of 40% fly ash, 20% GGBS, 10% silica fume and 40% silica fume, there was decrease in positive temperature differential by 22, 9, 9 and 27%, respectively, in corner region. Similarly, decrease in negative temperature differential was 36, 32, 27 and 40%, respectively, in corner region.
- (iv) For bituminous concrete overlay, maximum positive and negative temperature differential was found to be less when compared with PCC slab casted with alternative materials.
- (v) 100-mm-thickness slab (Ultra-thin topping) found to have lesser temperature variation when casted with alternative materials and overlaid with bituminous overlay when compared with 200-mm-thickness slab.

From the study, temperature differential was found to be maximum for bituminous concrete overlay, and minimum temperature differential was found to be for RCA slab at corner regions. However, it was observed that there was no appreciable temperature differential (<2 °C change) for SMA, OGFC mixes when compared to BC mix at corner, edge and middle regions.

8 Scope and Limitations for Further Study

The experimental study conducted to determine temperature differentials in CC slabs was done in laboratory where it was exposed in all directions. However, in actual field conditions, concrete slabs are confined by slabs, support from base layers and shoulders. The semi-field studies may be conducted by casting concrete similar to actual field conditions to determine variation in temperature across the depth for different conditions. These conditions will help in building mechanistic-empirical design approach.

References

1. Choubane B, Tia M (1992) Nonlinear temperature differential effect on maximum warping stresses in rigid pavements. Transportation research record no. 1370, transportation research board, Washington DC
2. Mohamed AR, Hansen W (1997) Effect of non-linear temperature differential on curling stress in concrete pavements. Transportation research record 1568, transportation research board, Washington DC
3. William GW, Shoukry SN (2001) 3D finite element analysis of temperature-induced stresses in dowel jointed concrete pavements. *Int J Geomech* 1(3):291–307
4. Lin D-F, Wang H-Y (2005) Forensic investigation of ultrathin whitetopping failures in Taiwan. *J Perform Constr Facil* 19(2):165–171
5. Siddique Z, Hossain M, Meggers D (2006) Curling and curling stresses of new concrete pavements. In: *Airfield and highway pavements*, pp 671–682
6. Mallela J, Abbas A, Harman T, Rao C, Liu R, Darter MI (2005) Measurement and significance of the coefficient of thermal expansion of concrete in rigid pavement design. In: *Journal of transportation research board, transportation research record no. 1919*, transportation research board of the national academies, Washington DC, pp 38–46
7. Yang J, Kim S-H (2014) Factorial effects of mix design variables on the coefficient of thermal expansion of concrete mixtures. *Road Mater Pavement Des* 15(4):942–952 (Taylor and Francis)
8. Khazanovich L, Balbo JT, Lederle R, Marasteanu M, Saxena P, Tompkins D, Vancura M, Watson M, Johanneck L, Harvey J, Santero NJ, Signore J (2013) Design and construction guidelines for thermally insulated concrete pavements, research report MnDOT
9. Nishizawa T, Shimeno S, Komatsubara A, Koyanagawa M (2000) Temperature differential of concrete pavement slab overlaid with asphalt surface course. *Journal of the transportation research board, transportation research record: no. 1730*, transportation research board of the national academies, Washington DC, pp 25–33
10. Belshe M, Mamlouk MS, Kaloush KE, Rodezn M (2011) Temperature differential and curling stresses in concrete pavement with and without open-graded friction course. *J Transp Eng* 137(10):723–729
11. Kim S-H, Yang J, Nam BH, Jeong J-H (2015) Effect of materials and age on the coefficient of thermal expansion of concrete paving mixture. *Road Mater Pavement Des* 16(2):445–458 (Taylor and Francis)
12. Vancura M, Khazanovich L, Tompkins D (2009) Reappraisal of recycled concrete aggregate as coarse aggregate in concretes for rigid pavements. In: *Journal of the transportation research board, transportation research record: no 2113*, transportation research board of the national academies, Washington DC, pp 149–155
13. Indian Road Congress IRC 44 (2008) Guidelines for cement concrete mix design for pavement, New Delhi, India
14. MoRT&H (2013) Specification for Road and Bridge Works. 5th revision, Ministry of Road Transport and Highways, Govt. of India, New Delhi, India
15. IS 73 (2013) Paving bitumen specifications. Fourth Revision, Indian Standards Institution, New Delhi, India

Utilization of Waste Materials for Productions of Sustainable Roller-Compacted Concrete Pavements—A Review



Solomon Debbarma, G. D. Ransinchung R.N., Surender Singh,
and Surya Kant Sahdeo

1 Introduction

Roller-compacted concrete pavement (RCCP) is an emerging pavement technology and is gaining recent attention by academicians and highway agencies across the globe [1–7]. RCCP gets its name from the heavy asphalt vibratory drum/rubber-tired rollers used for compaction of the mixture [8–14]. Typically, RCCP has the same materials constituents and exhibits similar/nearly equivalent strength properties to that of Portland cement concrete (PCC) mixes, however, adopt the mixture proportions and construction practices of asphalt pavements [10–12]. The major difference is that the percentage of fine aggregates in RCCP is comparatively higher than in PCC mixes, and this allows for tight packing and consolidation of the mixture. Also, RCCP is fast to construct, requires less labor and machinery, and can be constructed without formworks, dowel bars or reinforcing steel members [12]. Furthermore, the initial construction costs of RCCP mixes were found to be ~10–20% lower than PCC mixes and ~30% lower to that of asphalt mixes indicating its effective potential over PCC and asphalt pavements [8]. RCCP is a no-slump concrete mixture and is stiff enough to be compacted by the help of vibrating rollers without leading to segregation of the mixture [8–14]. RCCP has been traditionally used as a base layer of pavements [10–12, 14]. However, with recent advances in the road sector industry,

S. Debbarma · G. D. Ransinchung R.N. (✉) · S. K. Sahdeo
Department of Civil Engineering, Indian Institute of Technology Roorkee, Roorkee 247667, India
e-mail: gdranfce@iitr.ac.in

S. K. Sahdeo
e-mail: ssahdeo@ce.iitr.ac.in

S. Singh
Transportation Engineering Division, Department of Civil Engineering, Indian Institute of
Technology Madras, Chennai 600036, India
e-mail: surender@iitm.ac.in

RCCP has been implemented to be used as surface layers too and provided it meets the requisite minimum compressive and flexural strength benchmark of 27.6 MPa and 3.67 MPa at 28 days [10, 11]. But, the main issue pertaining to the usage of RCCP as the surface layer is the riding quality [10, 11]. Generally, a 50 mm thin bituminous topping is laid over the RCCP surface so as to provide a good riding quality [10, 11]. Alternatively, diamond grinding may be also provided for smoothness and quietness of RCC pavements so as to serve high-speed traffic [12]. A few other applications of RCCP include access roads, parking lots, shipping yards and ports, aircraft parking lanes, and heavy-duty low volume roads [12].

With the rapid growth in road sector industry, the consumption of virgin materials has also seen a significant increase in the past few decades [6] and as result requiring for immediate measures and precautions to be taken for minimal consumption of the same so as to safe keep for future demand. This showed the way for the concept of sustainability, i.e., a type of pavement that will not only meet the economic demands but will also be environmentally friendly in nature. Thus, several government agencies worldwide are compelled to switch over to alternative road aggregates than the conventional virgin ones [15]. Not only this, but shortage of virgin aggregates owing to the ban on quarrying activities imposed by government agencies also led to further utilization of alternative road aggregates [16–23]. Recycled concrete aggregates (RCA) and reclaimed asphalt pavement (RAP) aggregates are one such of a kind that has shown potential in re-utilization for new pavement applications [5]. RAP is the precious material obtained after an existing flexible pavement that is milled/demolished for re-construction or maintenance activities of the same [16, 17, 22–32]. After milling/demolition, RAP is usually dumped in open dumps/landfills creating huge stockpiles and as a result leading to road esthetic issues, disposal problems, and greenhouse gases emission, etc. [18, 33, 34]. In the USA itself, around 85 million tons of RAP has been reported to remain unused even after its effective utilization in asphalt pavements in the year 2015 [27], whereas in India, a higher amount of RAP is generated after every monsoon season which is discarded as wastes owing to lack of confidence among Indian highway engineers.

On the other hand, RAP has been successfully and extensively re-used in the construction of new asphalt pavements, but its utilization in cement concrete pavements is of meager [35]. Owing to the superiority of concrete pavements over asphalt, the Ministry of Road Transport & Highways (MoRTH), Govt. of India, has decided to switch over to concrete pavements as the default mode of transportation across the nation [17]. Furthermore, the implementation of RCCP over PCC and replacing virgin aggregates by RAP seems to be a viable approach in developing countries like India. Therefore, the overall objective of the present study is to bring out the issues related to the effective utilization of RAP in RCCP mixes. In the same line, the efficacy of various pozzolanic-rich waste materials alongside RAP on the fresh and hardened properties RCCP will also be addressed.

2 Literature Review

2.1 Background

The first RCCP was constructed in Sweden in the early 1930s, and in the early 1940s, an airport runway in Yakima, Washington, the USA received its first RCCP pavement [10, 12, 14]. In the 1970s, RCC pavements became quite a common practice for use in timber manufacturing site in Canada [12]. Since then, RCC pavements have been extensively used for military facilities, ports, intermodal facilities, and low-to-moderate traffic streets and secondary highways in the USA [11]. Figure 1 shows the application of RCC pavements since the early 1930s. While in Europe, RCCP was initially reported in Spain and used as low volume roads only, and several kilometers of asphalt pavements were replaced by RCCP owing to the oil crisis and higher construction costs of asphalt pavements during the 1970s [10].

The first full-scale RCCP was constructed in Texas in the year 1984 by the US Corps of Engineers [10]. The project covered a total area of 15,175 m² and has been provided with a 254 mm thick RCCP slab and achieved a field flexural strength of 5.5 MPa. Since then, the idea of RCCP has been widely acknowledged and implemented extensively. In another project, a 216 mm thick RCCP covering an area of around 21,750 m² was constructed in Washington by the US Corps of Engineers again [10]. The largest RCCP project in the late 1980s covered a total area of 543,400 m² having a ~200–250 mm thick RCCP slab and was constructed in an automobile

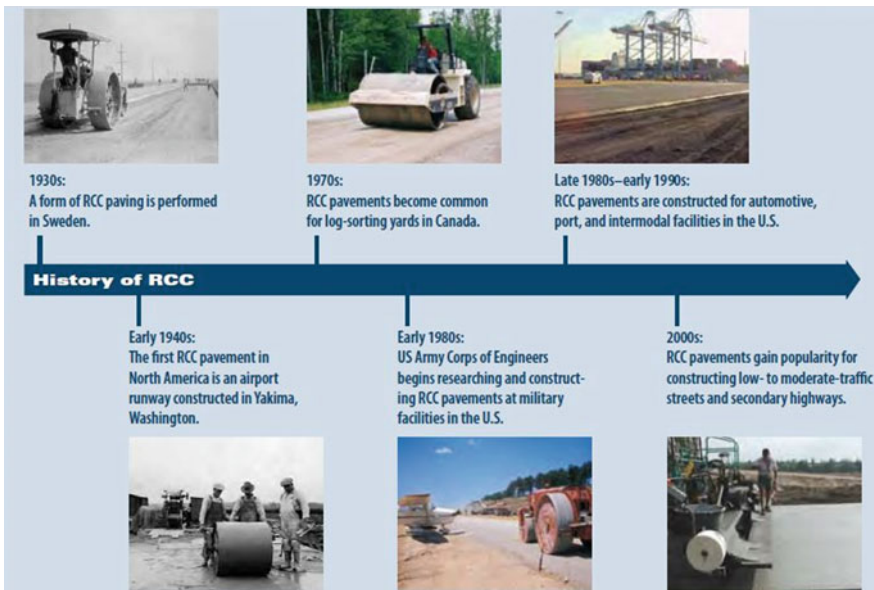


Fig. 1 History of RCCP applications [12]



Fig. 2 RCCP trial length being constructed under Pilot Project Package No. MP-0511 [36]

plant in Tennessee, USA [10]. Since then, academicians and highway engineers have started growing keen interest in the effective utilization of RCCP mixes for low to high volume roads, whereas in India, the implementation of RCCP is scanty. One such project carried out in India was constructed by the Madhya Pradesh Rural Road Development Authority (MPRRDA), Project Implementation Unit, Bhopal, under Pilot Project, Package No. MP-0511, Bhopal, MP (Fig. 2) [36]. A trial length of 40 m was laid out from Nipaniya to Kanera, Bhopal, MP, India. Portland pozzolana cement (PPC) content of 360 kg/m^3 , coarse aggregate (1129 kg/m^3), fine aggregate (662 kg/m^3), and water content of 6.17% by weight of total mixture were adopted in the above-mentioned pilot project, and compaction was carried out by vibratory roller of 80–100 kN static weight. An average cylindrical core compressive strength at 7 days of moist curing was achieved at 190.5 kg/cm^2 against the target strength of 180.2 kg/cm^2 and has been passed and recommended by the MPRRDA.

2.2 Effect of RAP on Fresh Properties

Modarres and Hosseini [8] investigated the effect of RAP of the fresh properties [i.e., optimum moisture content (OMC) and maximum dry density (MDD)] of RCCP mixes. Natural coarse and fine aggregates were replaced by 100% RAP individually as well as combinedly. In their study, the fresh properties were determined by heavy compaction method (modified Proctor method) as per ASTM D1557 [37]. As can be seen in Fig. 3, based on the study conducted by Modarres and Hosseini [8], incorporation of RAP aggregates reduced the OMC of the RCCP mixes, and this was attributed to the lower water absorption value of RAP aggregates. For instances, a percentage reduction of about 8.4%, 6.8%, and 11.8% was noted when natural aggregates were replaced by 100% coarse RAP, 100% fine RAP, and 100% total RAP, respectively. Contrary to the findings of Modarres and Hosseini [8], incorporation of RAP aggregates increased the OMC of the fresh RCCP mixes [9, 15]. Debbarma et al. [15] found that the highest increase in OMC was noted in the total RAP mixes

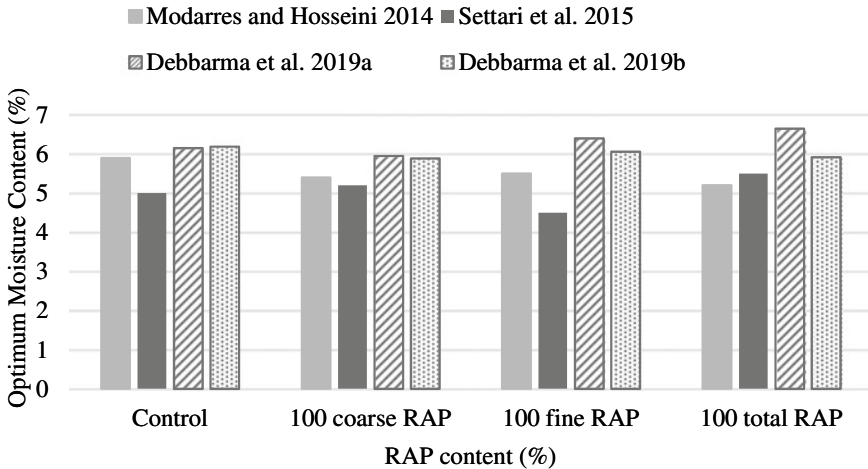


Fig. 3 Effect of RAP on the OMC of RCCP mixes [8, 9, 15, 38, 39]

followed by fine RAP and coarse RAP mixes. The increase in the OMC values was primarily due to the presence of dust contaminants in the considered RAP in the authors' study [15]. But in another study conducted by the same authors [38], incorporation of RAP aggregates reduced the OMC values of the fresh RCCP mixes, and this was attributed to the low water absorption values of the soft asphaltic film RAP aggregates. Additionally, the hydrophobic nature in the stated RAP may also be held responsible for lower OMC values.

As far as the maximum dry density (MDD) of the fresh RCCP mixes is concerned, incorporation of RAP aggregates was noted to cause a reduction in the MDD values. However, the percentage reduction is quite negligible since the associated difference w.r.t. control mix was around 5% only [15, 38]. Similar observations were also made by Ferrebee et al. [39] wherein the RCCP mix containing virgin aggregates had MDD 2347 kg/m^3 , whereas mix containing fractionated RAP had MDD of 2342 kg/m^3 , i.e., a negligible difference of <1%, however, increased the OMC by ~10%. This finding indicates that RAP aggregates would have a negative impact on the OMC of the RCCP mixes but would be profound in terms of its MDDs.

2.3 Effect of RAP on Compressive Strength

The influence of RAP aggregates on the compressive strength of the RCCP mixes (study conducted by several authors) is being illustrated in Table 1. Modarres and Hosseini [8] were the first to investigate the effect of RAP on the compressive strength of RCCP mixes. Virgin aggregates (VAs) were replaced by 100% coarse RAP, 100% fine RAP, and 100% total RAP, respectively. At 28 days of normal curing, only 100% coarse RAP mix achieved the stipulated compressive strength of 27.6 MPa as per

Table 1 Influence of RAP on the compressive strength of RCCP mixes

	Control	50 coarse RAP	100 coarse RAP	50 fine RAP	100 fine RAP	25 total RAP	50 total RAP	100 total RAP
Compressive strength (MPa)								
Modarres and Hosseini [8]								
7 days	33	-	22	-	17	-	-	11
28 days	40	-	30	-	23	-	-	16
120 days	45	-	33	-	27	-	-	19
Settari et al. [9]								
7 days	8.7	-	7.5	-	6.3	-	10	7.5
28 days	16.8	-	7.5	-	10	-	10	7.5
90 days	18.6	-	8.7	-	9	-	10	6.3
Fakhri and Amolsoltani [40]								
250 kg/m ³ cement	40	-	-	-	-	31	23	13
300 kg/m ³ cement	40	-	-	-	-	36	25.5	14
350 kg/m ³ cement	41	-	-	-	-	38	27.6	18
450 kg/m ³ cement	47	-	-	-	-	43	34.5	20
Debbarma et al. [15]								
7 days	21	18	20	23	27	-	24	23
28 days	38	29	25	34	32	-	30	24
91 days	42	39	31	43	38	-	33	29
Debbarma et al. [38]								

(continued)

Table 1 (continued)

	Control	50 coarse RAP	100 coarse RAP	50 fine RAP	100 fine RAP	25 total RAP	50 total RAP	100 total RAP
7 days	21	16	14	24	19	-	17	11
28 days	28	25	15	28	24	-	20	12
91 days	42	26	17	35	29	-	21	12
Ferrebee et al. [39]								
Virgin RCC (14 days)			38.3					
FRAP RCC (14 days)			28.1					

ACI [10, 11], whereas the total RAP mix had the lowest strength decrease followed by the fine RAP mixes, and this in line with finding of available literature reporting the potential of coarse RAP than fine/total RAP mixes [19, 20, 29].

In another study conducted by Ferrebee et al. [39], VA was replaced by 16% fractionated RAP (FRAP) wherein the decrease in compressive strength after 14 days was found to be 27%. The experimental results were also found to be statistically significant between VA and FRAP mixes with a 95% confidence level.

Settari et al. [9] carried out a study on RAP-RCCP mixes wherein VA was replaced by RAP in proportions of 100% coarse, 100% fine, 50% total, and 100% total RAP, respectively (Table 1). Based on their study, the percentage decrease was about 55%, 32%, 50%, and 48% when VA was replaced by 100% coarse RAP, 100% fine RAP, 50% total RAP, and 100% total RAP, respectively, and this in contradiction to the findings of Modarres and Hosseini [8] reporting coarse RAP as a better potential than fine RAP. This decrease in the compressive strength may be attributed to the amount of asphalt present in the RAP aggregates.

Similar observations were noted by Debbarma et al. [15] wherein fine RAP mixes were found to perform better than the coarse RAP mixes, and this was primarily attributed to the presence of dust contaminants in the fine RAP particles (Table 1). Generally, pavement milling in India is carried out employing uncontrolled milling technique (i.e., using a backhoe or bulldozer) wherein dust contaminants from the underlying layers get intermixed with the RAP aggregates and produce a well-graded fine RAP. This aforementioned reason along with the presence of stiffened asphalt coating of RAP aggregates may be held responsible for higher compressive strength of fine RAP than coarse/total RAP mixes. In another study by the same authors [38], the effect of soft asphaltic-coated RAP aggregates was investigated wherein a significant decrease in compressive strength of ~50% at 28 days upon replacing 100% VA by RAP was noted as compared to the RAP aggregates having a stiffened asphalt coating (Table 1). Similar findings to the authors' previous study were also noted wherein fine RAP mixes were found to perform better than coarse RAP mixes, but in the present case, the better performance of fine RAP mixes was attributed to the fact that the stated fine RAP (being gap graded owing to controlled milling technique) was filled by natural fine aggregates passing 600 μm Indian Standard (IS) sieve.

Fakhri and Amoolsoltani [40] studied the effect of Portland cement content on the compressive strength of RCCP mixes containing 25%, 50%, and 100% RAP, respectively. Based on their study, increasing the cement content up to 350 kg/m^3 , the 50% RAP mix could achieve the minimum strength benchmark of 27.6 MPa, whereas it could not meet the requirements for the mix containing 100% RAP aggregates.

2.4 Effect of RAP on Flexural Strength

The mix design of RCCP is mainly based on the flexural strength at 28 days of normal curing age. Similar to compressive strength results, incorporation of RAP aggregates

(in different proportions) could reduce the flexural strength of the RCCP mixes irrespective of any curing ages [8, 15, 38, 40]. A study conducted by Modarres and Hosseini [8] revealed that coarse RAP mixes exhibited the highest flexural strength followed by fine RAP and total RAP mixes w.r.t. the control mix (see Fig. 4). This finding by the authors is in line with other researchers reporting coarse RAP as a better potential than fine RAP mixes for preparation of conventional Portland cement concrete (PCC) mixes [19, 20, 29]. Similarly, in another study carried out by Debbarma et al. [15], coarse RAP mixes were noted to perform 10% and 24% better than the fine and total RAP mixes, respectively (see Fig. 5). Field emission scanning electron microscope (FESEM) images also revealed a closely packed and denser interfacial transition zone (ITZ) in the coarse RAP mixes, whereas a weaker ITZ was observed in the fine RAP mixes (see Fig. 6). But in another study carried out by Debbarma et al. [38], it was observed that the fine RAP performed better than coarse RAP mixes, and this was primarily due to the fact the fine RAP in the authors study was gap graded in nature and, hence, was filled by natural fine (passing 600 μm IS sieve), and hence, the resultant fine RAP used in the investigation was only 30%. This

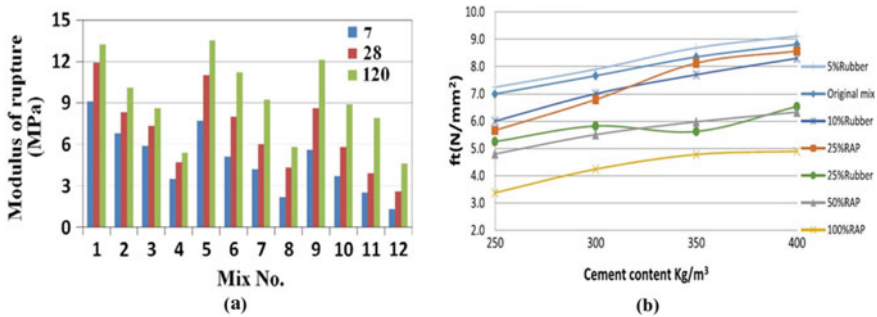


Fig. 4 Effect of RAP on flexural strength **a** Modarres and Hosseini [8]; **b** Fakhri and Amoolsotani [40]. Note Numbers in the x-axis (Fig. 1) represent different mix proportions; 1 = control mix; 2 = 100% coarse RAP; 3 = 100% fine RAP, 4 = 100% total RAP; and 5–12 = RAP mixes containing rice husk ash [8]

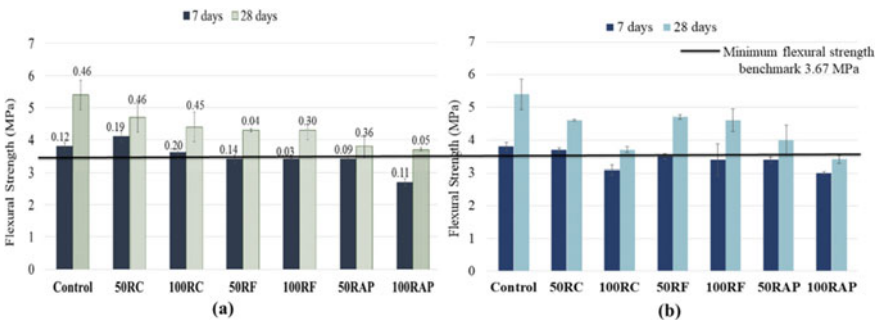


Fig. 5 Effect of RAP on flexural strength **a** Debbarma et al. [15]; **b** Debbarma et al. [38]

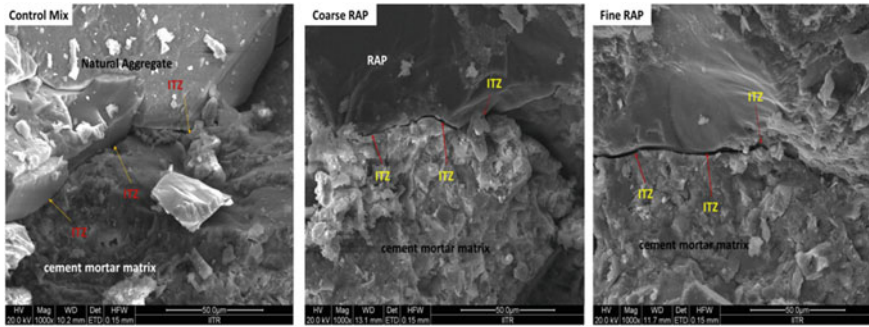


Fig. 6 SEM images revealing the ITZ of control and RAP mixes [15]

Table 2 Influence of RAP on the split tensile strength of RCCP mixes

Mix	Split tensile strength							
	Settari et al. [9]			Ferrebee et al. [39]	Debbarma et al. [15]		Debbarma et al. [38]	
	7 days	28 days	90 days	14 days	7 days	28 days	7 days	28 days
Control	1.5	2.1	2.8	4.16	3.2	4.2	3.2	3.6
16 fractionated RAP	–	–	–	3.50	–	–	–	–
50 coarse RAP	–	–	–	–	2.7	3.6	1.7	2.1
100 coarse RAP	1.2	1.6	1.3	–	2.0	3.3	1.6	1.7
50 fine RAP	–	–	–	–	1.9	2.6	2.5	2.6
100 fine RAP	1.0	1.4	1.4	–	1.9	2.8	1.9	2.5
50 total RAP	1.7	2.5	2.3	–	2.0	2.8	2.0	2.2
100 total RAP	1.0	1.3	1.3	–	1.6	2.2	1.4	1.6

reason may be held responsible for higher flexural strength of fine RAP (~4.7 MPa at 28 days) than its corresponding dust-contaminated fine RAP (~4.3 MPa) mixes. Despite reduction in the flexural strength w.r.t. the control mix, all mixes (except 100 total RAP) achieved the minimum flexural strength benchmark of 3.67 MPa as per ACI [10, 11] guidelines, and the authors recommended an optimum proportion of 50% total RAP as replacement of virgin aggregates to be used for the construction of RCCP.

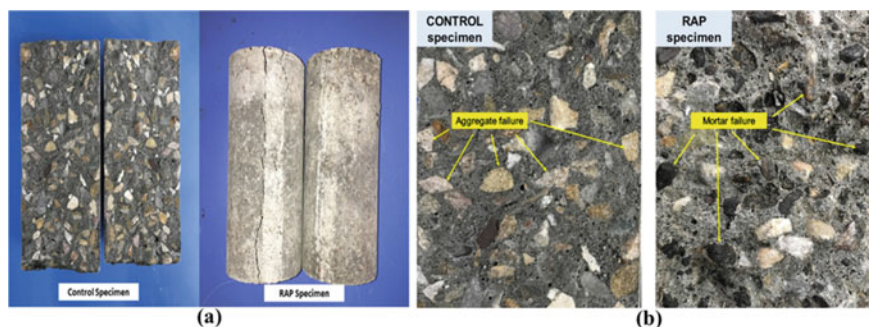


Fig. 7 a Split specimens after test [38], b failure mode in natural and RAP mix [15]

2.5 Effect of RAP on Split Tensile Strength

Table 2 illustrates the effect of incorporations of different fractions of RAP in the split tensile strength of RCCP mixes based on studies conducted by several researchers. As expected, Settari et al. [9] observed that the incorporation of RAP aggregates reduced the split tensile strength of the RCCP mixes irrespective of any curing ages. For instances, replacing 100% virgin aggregates by RAP aggregates reduced the tensile strength by about 26%, whereas incorporation of 50% total RAP had a lesser reduction of about 23% only due to which the authors recommended the utilization of 50% total RAP for RCCP mixes.

In a study conducted by Ferrabee et al. [39], a 16% decrease w.r.t. the control mix was noted when virgin aggregates were partly replaced by 16% of fractionated coarse RAP aggregates. A similar observation was made by Debbarma et al. [15, 38] wherein incorporation of RAP aggregates reduced the split tensile strength of the RCCP mixes. Despite the significant reduction, it was observed that the toughness increases when RAP is added in RCCP [40] as well in PCC mixes too [29]. The RAP specimens after split tensile test do not break apart (see Fig. 7) even after the maximum peak load was achieved indicating that RAP aggregates would greatly contribute in the load-carrying capacity of RCC pavements even after failure [38].

2.6 Effect of RAP on Abrasion Resistance

ACI 2001 [10] recommends a compressive strength of 27.6 MPa at 28 days if RCCP is to function as a surface layer, and when RAP is further added into the RCCP mixture, its suitability and resistance to abrasive forces need to be properly addressed. The incorporation of RAP was observed to reduce the abrasion resistance of the RCCP mixes as reported by Debbarma et al. [15, 38]. Strong linear relationship (see Fig. 8) between abrasion loss in mass and compressive strength of the RCCP mixes (containing soft asphaltic-coated RAP) was observed at 28 and 91 days, whereas

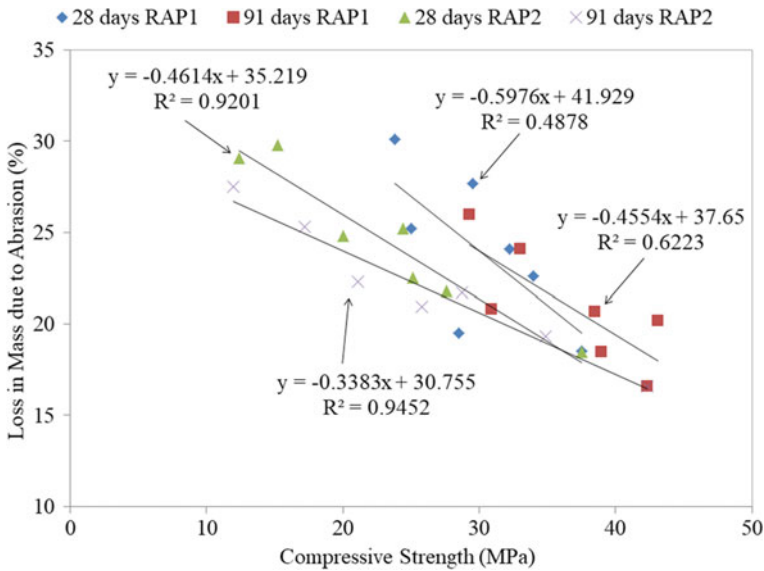


Fig. 8 Relation b/w compressive strength and loss in mass due to abrasion. *Note* RAP1 = dust-contaminated stiffened asphalt-coated RAP [15]; RAP2 = soft asphaltic-coated RAP [38]

fair relationships (see Fig. 8) were observed in the case of RCCP mixes containing dust-contaminated stiffened asphalt-coated RAP aggregates. This indicates that the abrasion resistance of RAP-RCCP mixes can be improved by increasing the Portland cement content [15, 38, 41, 42]. As far as the suitability of RAP-RCCP blend as the surface layer is concerned, incorporation of 50% coarse and 50% fine RAP individually may be recommended since these mixes provided adequate abrasion resistance to function as a surface layer [38].

2.7 Effect of RAP on Modulus of Elasticity

Modulus of elasticity (MOE) concrete is an important parameter in determining the concrete stiffness to tolerate loads [40]. Higher the MOE, more will be the ability of the concrete to carry more loads in less deformation. This means that the concrete will become brittle but stiff in nature. Settari et al. [9] investigated the effect of RAP on the modulus of elasticity of RCCP mixes wherein they found that more the amount of RAP added, lower is the MOE value. Fakhri and Amoolsoltani [40] also observed similar findings in their study. A meaningful relationship was found between RAP replacement level and MOE as shown in Fig. 9 indicating that the MOE of RCCP mixes tends to decrease (w.r.t. control mix) at a linear rate when RAP is added in higher doses. In contrast, increasing the cement content was found to somewhat improve the MOE at various RAP replacement levels.

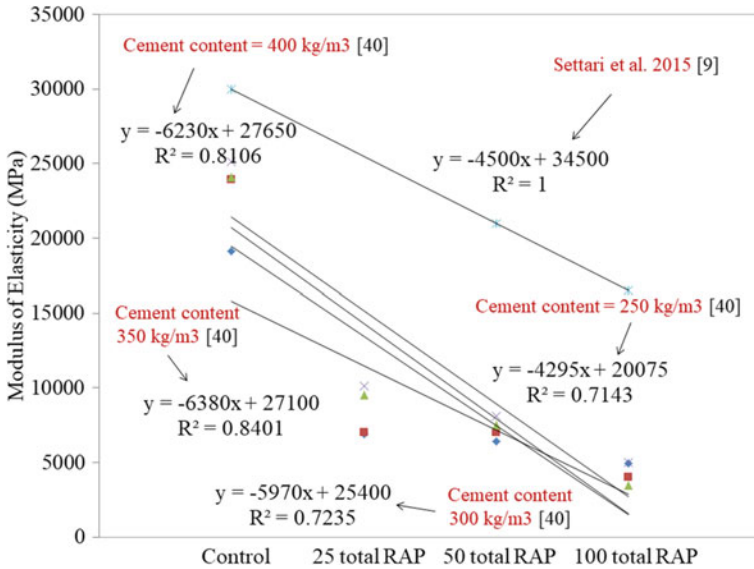


Fig. 9 Relationship b/w RAP replacement levels and modulus of elasticity [9, 40]

2.8 Effect of RAP on Porosity and Water Absorption

Incorporation of RAP aggregates was observed (by few authors) to lower the porosity values of the hardened RCCP specimens irrespective of any curing ages [9, 15, 38]. Table 3 summarizes the findings in the porosity and water absorption values by a few available literatures. Settari et al. and Debbarma et al. [9, 15, 38] noted a significant decrease in the total concentration of permeable voids on the addition of RAP, and this was mainly due to the melting of asphalt at higher temperatures. This condition eventually filled the empty pores that remained after hydration and subsequently restricted the ingress of water in the concrete matrix. This indicates that RAP aggregates if added in RCCP mixes would prove to be beneficial in terms of its durability aspects.

2.9 Effect of Miscellaneous Wastes on RAP-RCCP Properties

Very limited studies pertaining to the utilization of industrial/agricultural wastes such as silica fume, fly ash, sugarcane bagasse ash, and rice husk ash for enhancing the RAP-PCC properties have been characterized [30, 43, 44]. In the case of RAP-RCCP, only one such study (as per the authors' knowledge) has been investigated so far [8]. Modarres and Hosseini [8] added rice husk ash (RHA) as replacement of Portland cement in proportions of 3% and 5%, respectively. Based on their study,

Table 3 Porosity and water absorption of RAP-RCCP mixes

Mix →	Control	50 coarse RAP	100 coarse RAP	50 fine RAP	100 fine RAP	50 total RAP	100 total RAP
<i>Porosity (%)</i>							
Age ↓	Settari et al. [9]						
28 days	18.5	–	18.0	–	9	13.5	8
	Debbarma et al. [15]						
28 days	8.5	5.6	4.4	6.8	6.4	5.8	5.1
91 days	4.8	3.6	3.3	3.4	2.7	2.8	2.4
	Debbarma et al. [38]						
28 days	8.5	5.0	6.0	6.7	6.7	5.2	4.6
91 days	4.8	2.7	2.9	3.6	3.7	3.2	2.6
<i>Water absorption (%)</i>							
	Debbarma et al. [15]						
28 days	4.2	3.2	3.0	3.7	3.9	3.3	2.6
91 days	3.5	2.8	2.6	3.1	3.3	2.8	2.2
	Debbarma et al. [38]						
28 days	4.2	2.4	2.7	3.2	3.4	5.0	2.5
91 days	3.6	2.3	2.5	2.8	2.8	3.2	2.2

the addition of 3% RHA was found to increase the OMC of the RAP-RCCP mixes, owing to its hygroscopic nature. Despite increase in water demand, it was able to enhance the compressive and flexural strength (Fig. 10a) and also caused a reduction in the porosity values of the RCCP mixes containing RAP aggregates (see Fig. 10b),

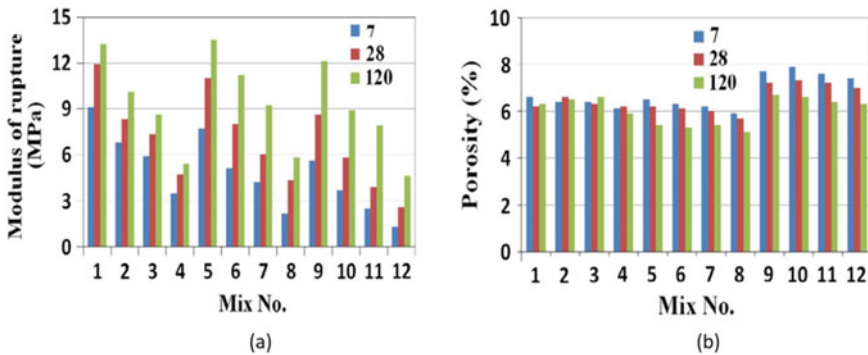


Fig. 10 a Effect of RHA on modulus of rupture. b Effect of RHA on porosity. *Note* RHA = rice husk ash. Numbers in the x-axis represent different mix proportions; 1 = control mix; 2 = 100% coarse RAP; 3 = 100% fine RAP; 4 = 100% total RAP; 5 = control + 3% RHA; 6 = coarse RAP + 3% RHA; 7 = fine RAP + 3% RHA; 8 = total RAP + 3% RHA; 9 = control + 5% RHA; 10 = coarse RAP + 5% RHA; 11 = fine RAP + 5% RHA; and 12 = total RAP + 5% RHA [8]

whereas higher doses of RHA (5%) resulted in lower strength and higher porosity of RAP-RCCP mixes (see Fig. 10b).

2.10 Effect of RAP on the Construction Cost of RCCP

Debbarma et al. [15] carried out economic analysis on the effect of RAP on RCCP. In their study, the authors considered only the costs related to materials and processing of RAP aggregates for the production of 1m³ of RCCP mix based on Central Public Works Department (CPWD), Govt. of India, rates [45]. Based on their study, incorporation of 100% total RAP helped in reducing the production cost of 1m³ RCCP mix by ~46%, whereas the suggested RAP replacement level of 50% (by several authors [9, 15, 25, 40]) could still provide cost savings of ~22%. This indicates that adding RAP into the RCCP system would definitely incur economic benefits.

3 Special Discussion and Recommendations

Analysis of the available literature indicates that incorporation of RAP for production of RCCP mixes affects the fresh, mechanical, and durability properties considerably. Also, the type of RAP (i.e., soft asphaltic coated/stiffened asphalt coated/dust contaminated) plays a vital role in the RCCP properties. Utilization of soft asphaltic-coated RAP aggregates was found to cause more strength reductions as compared to stiffened asphalt-coated RAP. Similarly, utilization of the same produced gap-graded fine RAP; however, introducing natural fine into the gaps increased the potential of fine RAP than coarse RAP. On the other hand, the presence of dust contaminants in the stiffened asphalt-coated RAP produced a relatively well-graded fine RAP which provided a better formation of mortar paste and strengthened the bond between RAP and mortar paste. But, the water-soaking nature of dust contaminants caused a significant increase in the water demand of the RCCP mixes. Based on the aforementioned findings, the following recommendations may be adopted for the higher potential of RAP-RCCP mixes:

1. Removal of asphalt film by solvents like petrol, kerosene, benzene, but this would rather increase the cost.
2. Puncturing of asphalt film by a simple and cost-effective technique commonly known as abrasion and attrition (AB and AT) method [16] may provide a higher window of interface for better bonding between RAP and mortar paste.
3. Part replacing Portland cement by supplementary materials having a high specific surface area such as silica fume and zinc waste (jarosite) may strengthen the microstructure of the hardened RAP-RCCP specimens.

4. Utilizing industrial and agricultural wastes such as fly ash, sugarcane ash, and rice husk ash that are rich in amorphous silica may help in improving the hardened RCCP properties up to some extent.
5. In order to truly understand the effect of RAP, fracture properties such as toughness, stiffness, and modulus of elasticity of hardened RCCP specimens need to be investigated in detail.
6. Life cycle assessment (LCA) needs to be carried out to study the economic and environmental impacts of RAP-RCCP blends in the long run.

4 Conclusions

From the literature, it can be concluded that RAP aggregates can be utilized as part replacement of virgin aggregates for production of RCCP mixes. However, more extensive research based on a comprehensive no. of experimental tests, statistical analysis, and micro-level studies needs to be carried out before determining the optimum RAP replacement level. The following inferences could be drawn from the current literature review carried out:

1. RAP-RCCP blends can be easily placed, compacted, and finished using conventional asphalt pavers/rollers.
2. Despite increase in OMC of RAP-RCCP mixes, an insignificant effect was observed in the MDD values indicating that the incorporation of RAP would not much affect the fresh density of RCCP mixes.
3. With the increase in RAP replacement level, strength properties (compressive, flexural, and split tensile strength) decrease linearly. Fine RAP mixes may also perform better than coarse/total RAP mixes indicating the higher potential of fine RAP for RCCP mixes. Nevertheless, any proportion of RAP (except 100% total RAP) may be suggested for RCCP mixes.
4. Incorporation of RAP aggregates was found to be profound in the durability properties with reduced porosity and lowered water absorption of the RCCP mixes. This indicates the restriction of ingress of harmful ions such as chloride and sulfate ions (coming from nearby aggressive environments) into the concrete matrix.
5. The literature recommends the utilization of 50% total RAP (combination of 50% coarse RAP and 50% fine RAP) for use as a surface layer of RCCP.
6. On the other hand, 100% total RAP can be used in base layers such as dry lean concrete (DLC), or the RCCP can act as a base layer.
7. The utilization of industrial and agricultural wastes to an optimum dosage may somewhat improve the mechanical and durability properties of RAP-RCCP mixes.
8. Adding RAP into the RCCP system would not only incur economic benefits but would also help environmentally by reducing the burden on landfills, and reduced carbon footprints, etc.

References

1. Aurangzeb Q, Al-Qadi IL, Ozer H, Yang R (2013) Hybrid life cycle assessment for asphalt mixtures with high RAP content. *Resour Conserv Recycl* 83:77–86
2. Shi X, Zollinger DG, Mukhopadhyay AK (2018b) Punchout study for continuously reinforced concrete pavement containing reclaimed asphalt pavement using pavement ME models. *Int J Pavement Eng* 1–14
3. Shi X, Mirsayar M, Mukhopadhyay A, Zollinger D (2019) Characterization of two-parameter fracture properties of Portland cement concrete containing reclaimed asphalt pavement aggregates by semicircular bending specimens. *Cement Concr Compos* 95:56–69
4. Shi X, Mukhopadhyay A, Zollinger D, Grasley Z (2019) Economic input-output life cycle assessment of concrete pavement containing recycled concrete aggregate. *J Clean Prod* 225:414–425
5. Shi X, Mukhopadhyay A, Zollinger D (2019c) Long-term performance evaluation of concrete pavements containing recycled concrete aggregate in Oklahoma. *Transp Res Record* 0361198119839977
6. Shi X, Mukhopadhyay A, Zollinger D, Huang K (2019) Performance evaluation of jointed plain concrete pavement made with Portland cement concrete containing reclaimed asphalt pavement. *Road Mater Pavement Design*. <https://doi.org/10.1080/14680629.2019.1616604>
7. Mukhopadhyay A, Shi X (2019) Microstructural characterization of Portland cement concrete containing reclaimed asphalt pavement aggregates using conventional and advanced petrographic techniques. *Advances in cement analysis and concrete petrography*, ASTM STP1613, D. Cong and D. Broton, Eds., ASTM International, West Conshohocken, PA, pp 187–206. <https://doi.org/10.1520/STP1613201800083>
8. Modarres A, Hosseini Z (2014) Mechanical properties of roller compacted concrete containing rice husk ash with original and recycled asphalt pavement material. *Mater Des* 64:227–236
9. Settari C, Debieb F, Kadri EH, Boukendakdji O (2015) Assessing the effects of recycled asphalt pavement materials on the performance of roller compacted concrete. *Constr Build Mater* 101:617–621
10. ACI (American Concrete Institute) (2001) Report on roller-compacted concrete pavements. ACI 325-95, Farmington Hills, MI
11. ACI (American Concrete Institute) (2014) Guide to roller-compacted concrete pavements. ACI 327R, Farmington Hills, MI
12. Harrington D, Abdo F, Adaska W, Hazaree CV, Ceylan H, Bektas F (2010) Guide for roller-compacted concrete pavements
13. Courard L, Michel F, Delhez P (2010) Use of concrete road recycled aggregates for roller compacted concrete. *Constr Build Mater* 24(3):390–395
14. Palmer WD (1987) Roller compacted concrete shows paving potential. *Roads & Bridges*, Scranton Gillette Communications Inc., Des Plaines, IL, USA, 40–43
15. Debbarma S, Ransinchung GD, Singh S (2019) Feasibility of roller compacted concrete pavement containing different fractions of reclaimed asphalt pavement. *Constr Build Mater* 199:508–525
16. Singh S, Ransinchung GD, Kumar P (2017) An economical processing technique to improve RAP inclusive concrete properties. *Constr Build Mater* 148:734–747
17. Singh S, Ransinchung GDRN, Kumar P (2017) Feasibility study of RAP aggregates in cement concrete pavements. *Road Mater Pavement Design* 20(1):151–170. <https://doi.org/10.1080/14680629.2017.1380071>
18. Singh S, Ransinchung RN GD, Debbarma S, Kumar P (2018) Utilization of reclaimed asphalt pavement aggregates containing waste from Sugarcane Mill for production of concrete mixes. *J Cleaner Prod* 174:42–52
19. Singh S, Ransinchung RN GD, Kumar P (2018b) Laboratory investigation of concrete pavements containing fine RAP aggregates. *J Mater Civil Eng* [https://doi.org/10.1061/\(ASCE\)MT.1943-5533.0002124](https://doi.org/10.1061/(ASCE)MT.1943-5533.0002124)

20. Singh S, Ransinchung GDRN, Monu K, Kumar P (2018) Laboratory investigation of RAP aggregates for dry lean concrete mixes. *Constr Build Mater* 166:808–816
21. Singh S, Ransinchung GD, Monu K (2019) Sustainable lean concrete mixes containing wastes originating from roads and industries. *Constr Build Mater* 209:619–630
22. Monu K, Ransinchung GD, Singh S (2019) Effect of long-term aging on properties of RAP inclusive WMA mixes. *Constr Build Mater* 206:483–493
23. Kumari M, Ransinchung GDRN, Singh S (2018) A laboratory investigation on Dense Bituminous Macadam containing different fractions of coarse and fine RAP. *Constr Build Mater* 191:655–666
24. Copeland A (2011) Reclaimed asphalt pavement in asphalt mixtures: state of the practice (No. FHWA-HRT-11-021)
25. Isola M, Betti G, Marradi A, Tebaldi G (2013) Evaluation of cement treated mixtures with high percentage of reclaimed asphalt pavement. *Constr Build Mater* 48:238–247
26. Farina A, Zanetti MC, Santagata E, Blengini GA (2016) Life cycle assessment applied to bituminous mixtures containing recycled materials: Crumb rubber and reclaimed asphalt pavement. *Resour Conserv Recycl* 117:204–212
27. Shi X, Mukhopadhyay A, Zollinger D (2018) Sustainability assessment for Portland cement concrete pavement containing reclaimed asphalt pavement aggregates. *J Clean Prod* 192:569–581
28. Said SEEB, Khay SEE, Loulizi A (2018) Experimental Investigation of PCC Incorporating RAP. *Int J Concr Struct Mater* 12(1):8
29. Huang B, Shu X, Li G (2005) Laboratory investigation of Portland cement concrete containing recycled asphalt pavements. *Cem Concr Res* 35(10):2008–2013
30. Huang B, Shu X, Burdette EG (2006) Mechanical properties of concrete containing recycled asphalt pavements. *Mag Concr Res* 58(5):313–320
31. Okafor FO (2010) Performance of recycled asphalt pavement as coarse aggregate in concrete. *Leonardo Electron J Pract Technol* 17:47–58
32. Al-Oraimi S, Hassan HF, Hago A (2009) Recycling of reclaimed asphalt pavement in Portland cement concrete. *J Eng Res* 6(1):37–45
33. Shi X, Mukhopadhyay A, Liu KW (2017) Mix design formulation and evaluation of Portland cement concrete paving mixtures containing reclaimed asphalt pavement. *Constr Build Mater* 152:756–768
34. Euch Khay SE, Euch Ben Said SE, Loulizi A, Neji J (2014) Laboratory investigation of cement-treated reclaimed asphalt pavement material. *J Mater Civil Eng*. [https://doi.org/10.1061/\(ASCE\)MT.1943-5533.0001158](https://doi.org/10.1061/(ASCE)MT.1943-5533.0001158)
35. Singh S, Ransinchung RN GD (2018e) Durability properties of pavement quality concrete containing fine RAP. *Adv Civil Eng Mater* 7(1): 271–290
36. MPRRDA (M.P. Rural Road Development Authority). Roller compacted concrete pavement. pilot project package No.Mp-0511 Project Implementation Unit, Bhopal, Madhya Pradesh
37. ASTM (American Society for Testing and Materials) (2012) Standard test methods for laboratory compaction characteristics of soil using modified effort (56,000 ft-lbf/ft³ (2,700 kN-m/m³)). ASTM D1557, West Conshohocken, PA
38. Debbarma S, Singh, Ransinchung RN GD (2019b) Laboratory investigation on the fresh, mechanical and durability properties of roller compacted concrete pavement containing reclaimed asphalt pavement aggregates. *Transp Res Record*. <https://doi.org/10.1177/0361198119849585>. Inpress
39. Ferrebee EC, Brand AS, Kachwalla JR, Roesler DJ, Gancarz, Pforr JE (2014) Fracture properties of roller-compacted concrete with virgin and recycled aggregates. *Transp Res Record J Transp Res Board* 2441(1):128–134
40. Fakhri M, Amoosoltani E (2017) The effect of reclaimed asphalt pavement and crumb rubber on mechanical properties of roller compacted concrete pavement. *Constr Build Mater* 137:470–484
41. Taha R, Ali G, Basma A, Al-Turk O (1999) Evaluation of reclaimed asphalt pavement aggregate in road bases and subbases. *Transp Res Rec* 1652(1):264–269

42. Taha R, Al-Harthy A, Al-Shamsi K, Al-Zubeidi M (2002) Cement stabilization of reclaimed asphalt pavement aggregate for road bases and subbases. *J Mater Civ Eng* 14(3):239–245
43. Singh S, Ransinchung GD, Kumar P (2017) Effect of mineral admixtures on fresh, mechanical and durability properties of RAP inclusive concrete. *Constr Build Mater* 156:19–27
44. Singh S, Dhawal S, Ransinchung GDRN, Kumar P (2018) Performance of fine RAP concrete containing flyash, silica fume, and bagasse ash. *J Mater Civ Eng*. [https://doi.org/10.1061/\(ASCE\)MT.1943-5533.0002408](https://doi.org/10.1061/(ASCE)MT.1943-5533.0002408)
45. CPWD (Central Public Works Department) (2016) Analysis of rates for Delhi, Part-1. New Delhi, India: CPWD

Design of Experimental Approach for Optimization of Foam Bitumen Characteristics



Fadamoro Oluwafemi Festus, Siksha Swaroopa Kar, and Devesh Tiwari

1 Introduction

Ladis Csanyi a university professor in Iowa State was the first to use foamed asphalt technique in 1956 [1]. Both in the lab and in the field, the efficiency of foam bitumen in stabilizing has been demonstrated that ungraded local aggregates such as gravel, sand, and loess could be used. Foamed bitumen was created by injecting saturated steam at 172 kPa which flows through a specifically built and calibrated nozzle [2]. Adding distilled water to hot bitumen and allowing it to spontaneously foam creates foamed bitumen, which is a combination of air, water, and bitumen. When injected water comes into touch with hot bitumen in the enlargement chamber, the bituminous physical properties are briefly altered. The injected water turns to vapor as it comes into touch with the heated bitumen, which is trapped in hundreds of small bitumen bubbles. The foaming process takes place in an expansion chamber, and it takes less than a minute for the foam to evaporate. Bitumen and water (plus air on certain systems) are injected at high pressure into expansion chambers, which are relatively small thick-walled steel tubes of 50 mm in depth and diameter [2]. When foam bitumen is blended into aggregates, the result is foam bitumen mix (FBM). The bitumen bubbles burst during the blending process, releasing microscopic particles containing bitumen and spread all through the mixture by sticking to the finer particles (fine sand and smaller) to form a mastic. During compaction, the bituminous granules in the mastic are mechanically forced against the bigger aggregate particles, leading to spot welds between the aggregates, increasing the granular pavement's shear strength while decreasing its permeability. The application of foam bitumen technology has helped in reducing greenhouse effects, as recent applications show that foam bitumen can be produced at a temperature as

F. O. Festus (✉) · S. S. Kar · D. Tiwari
Academy of Scientific and Innovative Research (AcSIR), Ghaziabad 201002, India
CSIR—Central Road Research Institute, Mathura Road, New Delhi 110025, India

© The Author(s), under exclusive license to Springer Nature Singapore Pte Ltd. 2022
D. Singh et al. (eds.), *Proceedings of the Fifth International Conference of Transportation Research Group of India*, Lecture Notes in Civil Engineering 218,
https://doi.org/10.1007/978-981-16-9921-4_29

397

low as 120 °C. The bitumen has a wide surface area and low viscosity in the foam state, making it perfect for combining with aggregates, boosting workability, raising surface tension (reducing water percolation), increasing fatigue, and increasing rut resistance [3, 4]. FBM only needs a small amount of bitumen (usually 1.7–2.5%) and can use a softer grade without compromising the mix's stability. Foam bitumen is classified by analyzing two factors: expansion ratio (ER) and half-life (HL). These two parameters are utilized to decide which bitumen qualifies to be used in an FBM. As a measurement of foam viscosity, expansion ratio may be used to assess how effectively bitumen will disperse in the mixture. Expansion ratio is evaluated by dividing the maximum volume of the expanded bitumen by the initial volume of fresh bitumen. Bitumen with a high expansion ratio has a low viscosity, making it more workable to coat the aggregate particles, particularly the fines [2]. Half-life can be used to determine the steadiness of the foam and the rate at which the froth collapses during mixing. It is the period of time between when the foamed bitumen gets to its highest volume and when it falls to half its original volume. It shows the foamed bitumen's stability in terms of effective surface contacts between aggregate particles. The ideal properties of foamed bitumen in this situation would be at a point where a fixed bitumen temperature and quantity of water injected gave the largest feasible expansion ratio while also giving foam bitumen the longest feasible half-life [2]. The distilled water injected into the enlargement chamber to produce foam is one of the most important factors influencing its properties [2]. A faster foamy water application rate causes more expansion (higher ER), but it also causes more rapid decay, resulting in a shorter half-life (HL) [2, 5]. The foamant water injection rate and temperature of bitumen are the foremost important factors influencing foam quality. Also, factors such as water content, viscosity, and temperature usually have various effects on the foam bitumen characteristics [6]. The expansion ratio increases as the water percentage in foam grows, while the half-life decreases, with the half-life being proportional to bitumen viscosity [7, 8]. Depending on its chemical makeup, the same penetration-grade bitumen might produce highly variable foaming qualities (expansion ratio and half-life) [9]. Physical and rheological bituminous properties were also influenced by the foaming process. It was observed that as the temperature of bitumen increases as well as the increase in water content, more bubbles are generated, resulting in a higher expansion ratio [10]. The influence of viscosity on foaming and stabilized mix qualities was also investigated. With increasing the viscosity of bitumen irrespective of the grade of binder, expansion ratio decreases, and high life increases [11]. Furthermore, statistical research demonstrated that the viscous behavior (loss modulus) of the foamed binder is highly associated with the amount of water in the foam (FWCs). The elastic behavior (elastic modulus) of foamed binder, on the other hand, was unrelated to FWCs [12]. A foamed binder has a lower viscosity than an unfoamed binder, and this tendency is dependent on FWC [12]. The effect of binder chemistry on foaming was also investigated, and it was found out that there is no significant effect of binder chemistry on the foaming parameter [13]. Several researchers have worked on the performance of FBM, but there have been fewer research works done on the optimization of foam bitumen characteristics with reference to foam water content, temperature, viscosity, and grade of bitumen using

a statistical approach with the application of design of experiment (DoE). This study is useful because it enables engineers to know the optimum requirement needed to produce the best foam that will be required for a bituminous mix. The broad objective of the paper is to optimize foam characteristics in terms of bitumen properties, temperature of foaming, and water content of foaming using the DoE approach.

2 Laboratory Investigation

2.1 Bitumen Physical Properties

The bitumen grade is used for the study includes VG-10 and VG-30. Properties of both grades of bitumen were determined as per Indian standard (IS 73: 2013) as shown in Table 1. Table 2 displays the outcome of a comparison of India's bitumen grading system with other types of grading systems.

Table 1 Physical properties of bitumen

Properties	Test results	Specification limit (IS 73: 2013)	Test results	Specification limit (IS 73:2013)
	VG-10		VG-30	
Penetration test (Min)	119	80	50.8	45
Softening Point °C (Min)	46	40	53	47
Viscosity (@60 °C) Poise	855	800–1200	2530	2400–3600
Viscosity (@135 °C) <i>cSt, min</i>	290	250	510	350
Viscosity at (@160 °C) <i>cSt, min</i>	125	–	135	–
Viscosity (@180 °C) <i>cSt, min</i>	100	–	115	–

Table 2 Different bitumen grading system

Penetration grade	Viscosity grade (Indian grade)	Atmospheric temp (°C)
30/40	VG-40	15 to 55
50/60	VG-30	10 to 50
60/70	VG-20	0 to 40
80/100	VG-10	–10 to 30

Fig. 1 Image showing the foam plant (WLB 10 S)



2.2 Characterization of Foam Bitumen

To test the foam characteristics, a foaming equipment (Wirtgen WLB 10S) was used to make the foam. Pre-heated bitumen is poured into the foaming plant (Fig. 1) to produce foam under the following constant foaming conditions:

- Bitumen temperature: 140 °C, 160 °C, 180 °C
- Foaming water content: 2% to 10% by weight of bitumen at an interval of 2%
- Water pressure: 500 kPa
- Air pressure: 550 kPa

The foaming conditions were chosen according to the mix design for foam bitumen characterization specified in TG-2, 2009.

Foam is generated in a bucket through the plant's nozzle, and the expansion ratio (ER) and half-life (HL) are recorded using a dipstick and a stopwatch, as illustrated in Fig. 2 for all temperature of the bitumen and water content of foam. Three replicas of ER and HL were measured for each combination, and the average values were taken. Tables 3 and 4 show the calculated expansion ratio and half-life values for VG-10 and VG-30 bitumen at various foaming water content and binder temperatures.

3 Discussion of Results

3.1 Laboratory Determination of Foaming Characteristic

Figure 3a, b depicts the effect of water content of foam bitumen and the temperature of the bitumen on the expansion ratio for VG-10 and VG-30 bitumen, respectively.

Fig. 2 Image showing foam bitumen with a dip stick (Wirtgen, 2004)



Table 3 Foam bitumen characteristics (VG-10)

Water content (%)	Foaming temperature					
	140 °C		160 °C		180 °C	
	ER	HL	ER	HL	ER	HL
2	6	16	8	13	4	18
4	9	12	10	10	8	16
6	11	10	12	8	10	14
8	12	8	13	7	11	13
10	13	6	15	5	12	10

Table 4 Foam bitumen characteristics (VG-30)

Water content (%)	Foaming temperature					
	140 °C		160 °C		180 °C	
	ER	HL	ER	HL	ER	HL
2	10	14	10	12	7	10
4	13	13	14	10	13	8.2
6	14	12	16	8	18	6
8	16	11	18	7.6	20	4
10	18	9.9	20	7	22	3.7

Similarly, Fig. 4a, b represents the effect of the foaming parameter on the half-life of foam for VG-10 and VG-30, respectively. The result shows that VG-30 produces higher ER compared to VG-10, whereas VG-30 produces lower stability compared to VG-10. This indicates that with increasing viscosity, the expansion ratio increases, and half-life decreases. This implies that at low viscosity, foam bitumen coats the aggregate particles more easily, especially the finer particles. A higher binder expansion ratio causes faster degradation, resulting in the half-life being reduced. With

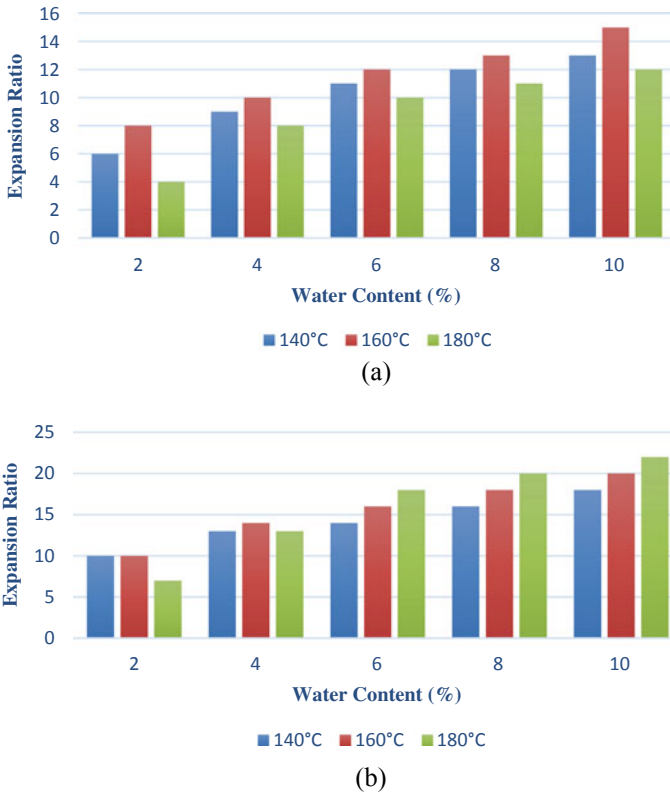


Fig. 3 Expansion ratio vs water content **a** VG-10, **b** VG-30

increasing the binder temperature, expansion ratio increases, and half-life decreases for both the binder and each foaming condition, except for VG-10 and 180 °C bitumen temperature condition. With increasing water content, the expansion ratio increases, and half-life decreases irrespective of foaming temperature and binder type. These findings corroborate with previous works of literature [2, 14, 15]

3.2 Optimization of Expansion Ratio and Half-Life Through Design of Experiment

Using the Design-Expert 11.1.2.0 software, an optimization technique was used to obtain the optimum value of expansion ratio and half-life at different temperatures and foam water content. The target goal for each input independent parameter (temperature and foam water content) was determined within the range displayed in Tables 5 and 6 during the software optimization process. These two parameters,

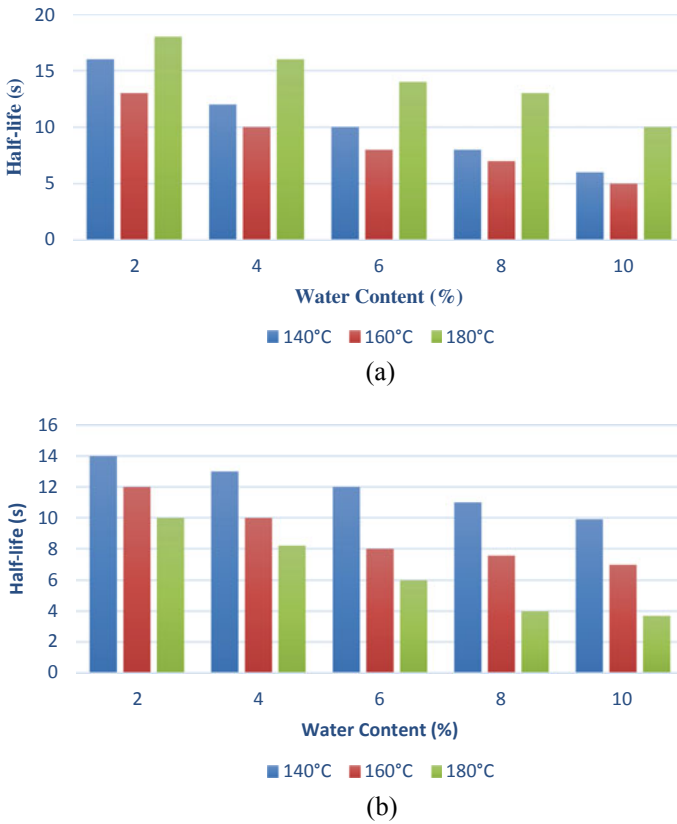


Fig. 4 Half-life versus water content **a** VG-10, **b** VG-30

along with their corresponding ranges, were chosen based on previous literature [8, 12]. Expansion ratio and half-life were considered the desirable mechanical dependent responses. Twenty experiments were carried out. To improve the precision of the trials and limit human and other possible sources of error, 15 alternative pairings were added with 5 duplicates of the mean case.

The regression models for expansion ratio and half-life were expressed by following second-order polynomial equations:

$$\begin{aligned} \text{Expansion ratio (VG-10)} &= 12.125 - 0.7 A + 3.7 B \\ &\quad + 0.25 AB - 2.125 A^2 - 1.125 B^2 \end{aligned} \tag{1}$$

$$\begin{aligned} \text{Half-life (VG-10)} &= 8.05 + 1.6 A - 4.4 B \\ &\quad + 0.5 AB + 3.75 A^2 + 0.75 B^2 \end{aligned} \tag{2}$$

Table 5 Experimental factors and experimental responses (VG-10)

	Factor 1	Factor 2	Response 1	Response 2
Run	A: Temperature	B: Foam water content	Expansion ratio	Half-life
	Degree	%		Seconds
1	160	6	12	8
2	160	10	15	5
3	160	6	12	8
4	160	6	12	8
5	140	2	6	16
6	140	10	13	6
7	140	6	11	10
8	160	2	8	13
9	180	2	4	18
10	180	6	10	14
11	160	6	12	8
12	180	10	12	10
13	160	6	12	8
14	160	6	12	8
15	180	2	4	18
16	160	6	12	8
17	180	10	12	10
18	140	10	13	6
19	160	6	12	8
20	140	2	6	16

$$\begin{aligned} \text{Expansion ratio(VG-30)} &= 16.075 + 0.6 A + 5.6 B \\ &+ 1.75 AB - 0.375 A^2 - 1.375 B^2 \end{aligned} \tag{3}$$

$$\begin{aligned} \text{Half-life (VG-30)} &= 8.11 - 2.64 A - 2.58 B \\ &- 0.55 AB + 0.45 A^2 + 0.95 B^2 \end{aligned} \tag{4}$$

where *A* is foaming bitumen temperature, and *B* is foam water content.

Contour plots showing the impact of foaming water content and bitumen temperature on foaming characteristics for VG-10 and VG-30 bitumen are presented in Figs. 5 and 6, respectively. The peak expansion ratio for both VG-10 and VG-30 is found at higher foaming temperature. As per the TG-2 requirement, the ER and HL should each be 8 and 6 s long. To achieve this value, FWC should not be less than 4% for all binder temperatures. The result of the expansion ratio shows that optimum binder temperature shifts to the right in the case of VG-30 if compared to VG-10.

Table 6 Experimental factors and experimental responses (VG-30)

	Factor 1	Factor 2	Response 1	Response 2
Run	A: temperature	B: foam water content	Expansion ratio	Half-life
	Degree	%		Seconds
1	140	10	18	9.9
2	160	10	20	7
3	180	10	22	3.7
4	160	6	16	8
5	160	6	16	8
6	180	10	22	3.7
7	160	6	16	8
8	160	6	16	8
9	140	2	10	14
10	160	2	10	12
11	140	6	14	12
12	180	6	18	6
13	140	2	10	14
14	160	6	16	8
15	160	6	16	8
16	180	2	7	10
17	180	2	7	10
18	140	10	18	9.9
19	160	6	16	8
20	160	6	16	8

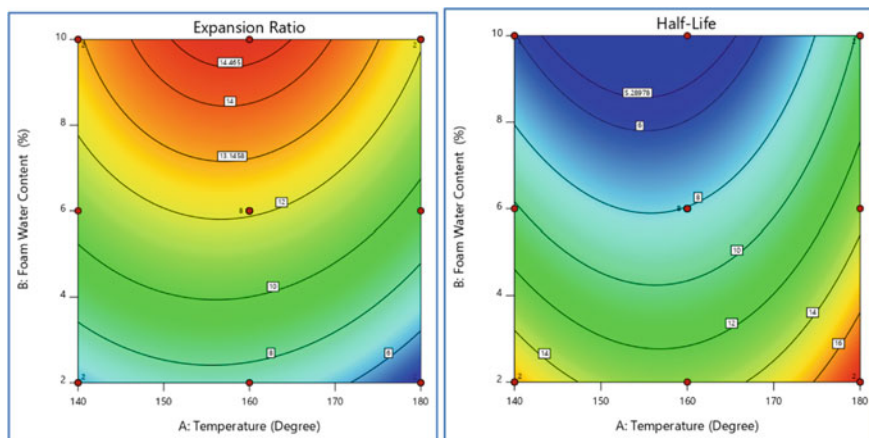


Fig. 5 Contour plots of foaming characteristics for VG-10 bitumen

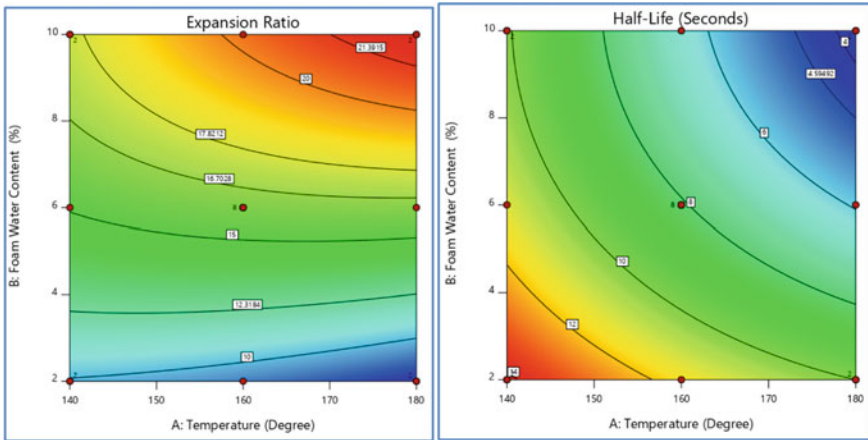


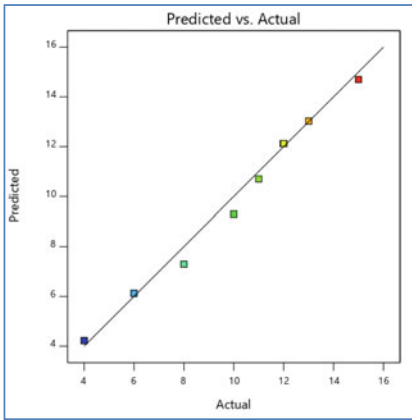
Fig. 6 Contour plots of foaming characteristics for VG-30 bitumen

Whereas, optimum binder temperature for obtaining higher half-life shifts toward the left in the case of VG-30 compared to VG-10.

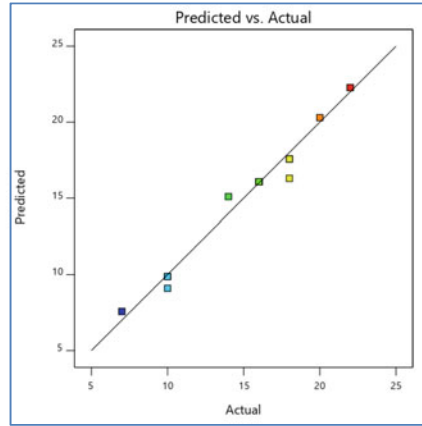
The actual versus projected expansion ratio and half-life data are shown in Fig. 7a–d. The actual data received during the experiment and the expected data are in reasonable accord. This validates the predicted model’s ability to navigate the CCD’s designated design space.

3.3 Statistical Analysis of Responses

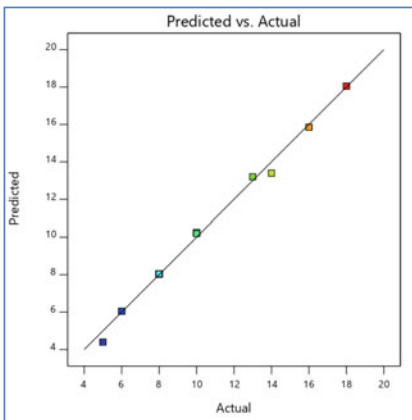
The reactions of foam bitumen properties were evaluated using statistical analysis. To make predictions, a quadratic model was created. The determination coefficient R^2 , as well as values of standard deviation, was used to assess the quality of the constructed model. Coefficient of determination was obtained as 0.99, 0.997, 0.98, and 0.99 for ER, HL of VG-10, and ER and HL of VG-30, respectively. The coefficient of determination should be at least 0.80 for a decent model fit. A high R^2 value, near to 1.00, indicates that the calculated and observed findings are in good agreement [16]. “Adequate precision” was another criterion utilized to assess the generated model (AP). The average prediction error is compared to the design point of the predicted values by AP. The AP values of the models in this situation were 59.4, 93.2, 40.17, and 62.36, respectively. They are all bigger than 4, indicating it is possible for the model to be utilized to navigate the CCD-defined space [17]. The ANOVA results in Table 7 reveal that both VG-10 and VG-30 have larger F values and lower P -values, indicating the statistical significance of the models. Because of noise, there is only a 0.01 percent chance that an F -value of this magnitude will occur in the model.



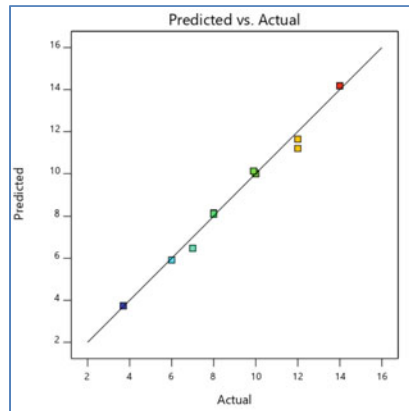
(a) Plot of Expansion Ratio Data for VG 10



(b) Plot of Expansion Ratio Data for VG 30



(c) Plot of Half-Life Data for VG 10



(d) Plot of Half-Life Data for VG 30

Fig. 7 Plot of design-experts (plot of predicted vs. actual values)

3.4 Optimization of Foam Bitumen Characterization

The optimum value of foaming temperature and foaming water concentration was determined using a numerical optimization method. To achieve the desired optimization goal (criteria), the best combination range of the independent variables for both bitumen grades as shown in Table 8 that will produce the optimized result was selected. The desirable performance response (ER and HL) was set at a target of 6 and 8, respectively as suggested by TG-2 (2009), while the FWC was set at a range between 2 and 10%, while the foaming temperature was set at a minimum value. Design-Expert software utilizes a desirability function to optimize the selected

Table 7 Result of ANOVA analysis

Source	Sum of squares	df	Mean square	F-value	p-value	Comment
<i>Response 1: Expansion ratio (VG-10)</i>						
Model	185.55	5	37.11	358.30	<0.0001	significant
A-temperature	4.90	1	4.90	47.31	<0.0001	SD = 0.3218 Mean = 10.50 $R^2 = 0.9922$ Adj. $R^2 = 0.9895$ Pred. $R^2 = 0.9791$ AP = 59.43
B-foam water content	136.90	1	136.90	1321.79	<0.0001	
AB	0.5000	1	0.5000	4.83	0.0453	
A ²	14.45	1	14.45	139.52	<0.0001	
B ²	4.05	1	4.05	39.10	<0.0001	
residual	1.45	14	0.1036			
Lack of fit	1.45	3	0.4833			
Pure error	0.0000	11	0.0000			
Cor total	187.00	19				
<i>Response 2: Half-life (VG-10)</i>						
Model	311.20	5	62.24	871.36	<0.0001	significant
A-temperature	25.60	1	25.60	358.40	<0.0001	SD = 0.2673 Mean = 10.30 $R^2 = 0.9968$ Adj. $R^2 = 0.9957$ Pred. $R^2 = 0.99$ AP = 93.24
B-foam water content	193.60	1	193.60	2710.40	<0.0001	
AB	2.00	1	2.00	28.00	0.0001	
A ²	45.00	1	45.00	630.00	<0.0001	
B ²	1.80	1	1.80	25.20	0.0002	
Residual	1.00	14	0.0714			
Lack of fit	1.00	3	0.3333			
Pure error	0.0000	11	0.0000			
Cor total	312.20	19				
<i>Response 3: Expansion ratio (VG-30)</i>						
Model	354.95	5	70.99	159.02	<0.0001	significant
A-temperature	3.60	1	3.60	8.06	0.0131	SD = 0.6682 Mean = 15.2 $R^2 = 0.9827$ Adj. $R^2 = 0.98$ Pred. $R^2 = 0.95$ AP = 40.17
B-foam water content	313.60	1	313.60	702.46	<0.0001	
AB	24.50	1	24.50	54.88	<0.0001	
A ²	0.4500	1	0.4500	1.01	0.3324	
B ²	6.05	1	6.05	13.55	0.0025	
Residual	6.25	14	0.4464			
Lack of fit	6.25	3	2.08			
Pure error	0.0000	11	0.0000			
Cor total	361.20	19				
<i>Response 4: Half-life (VG-30)</i>						

(continued)

Table 7 (continued)

Source	Sum of squares	df	Mean square	F-value	p-value	Comment
Model	146.77	5	29.35	314.19	<0.0001	significant
A-temperature	69.70	1	69.70	745.98	<0.0001	SD = 0.3057 Mean = 8.81 $R^2 = 0.9912$ Adj. $R^2 = 0.99$ Pred. $R^2 = 0.98$ AP = 62.34
B-foam water content	66.56	1	66.56	712.46	<0.0001	
AB	2.42	1	2.42	25.90	0.0002	
A ²	0.6480	1	0.6480	6.94	0.0196	
B ²	2.89	1	2.89	30.91	<0.0001	
Residual	1.31	14	0.0934			
Lack of fit	1.31	3	0.4360			
Pure error	0.0000	11	0.0000			
Cor total	148.08	19				

Table 8 Optimization criteria

Parameter	Unit	Desired goal	Lower limit	Upper limit
Foaming temperature	°C	Minimize	2	3.5
Foam water content	%	Range	2	10
Expansion ratio (ER)		Range	–	–
Half-life (HL)	s	Maximize	–	–

combination. The optimal value selected was based on the optimal solution with the highest desirability of 0.724 and 0.610 for VG-10 (Fig. 8) and VG-30 (Fig. 9), respectively. The maximum response for ER and HL was achieved under the conditions when foaming temperature was 140 °C, and foam water content was 5.2% for VG-10, while it was achieved when the foaming temperature was 150 °C, and foam water content was 4.9%.

4 Conclusion

This research work was carried out to maximize foam characteristics in relation to foaming temperature and foam water content using the design of experiment (DoE) approach. The determination of coefficient (R^2) which is less than 0.2 for both VG-10 and VG-30, respectively, indicates a good model fit between the actual and predicted values. The statistical analysis utilized in this study to determine the interaction between selected factors revealed that predicted and actual values were in good agreement, indicating that second-order response surface models are a good model for predicting the optimum expansion ratio and half-life values. The DoE desirability function with good desirability shows that the best response was achieved for ER

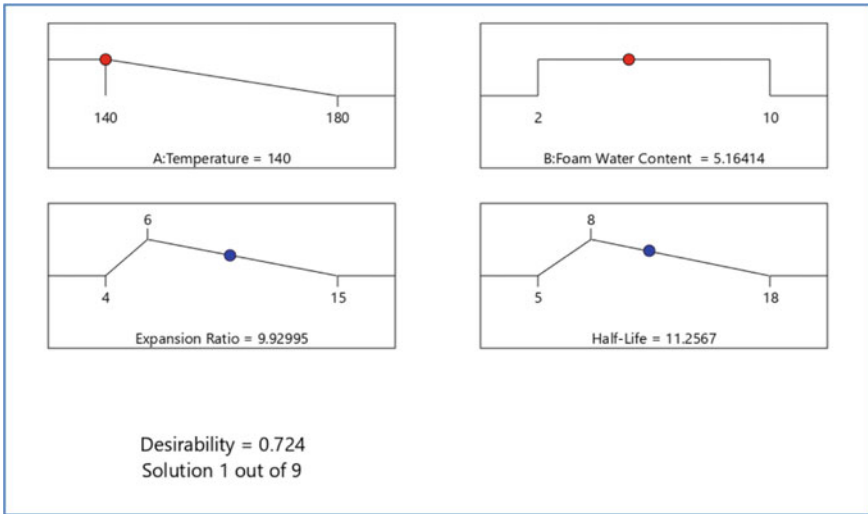


Fig. 8 Numerical optimization for VG-10

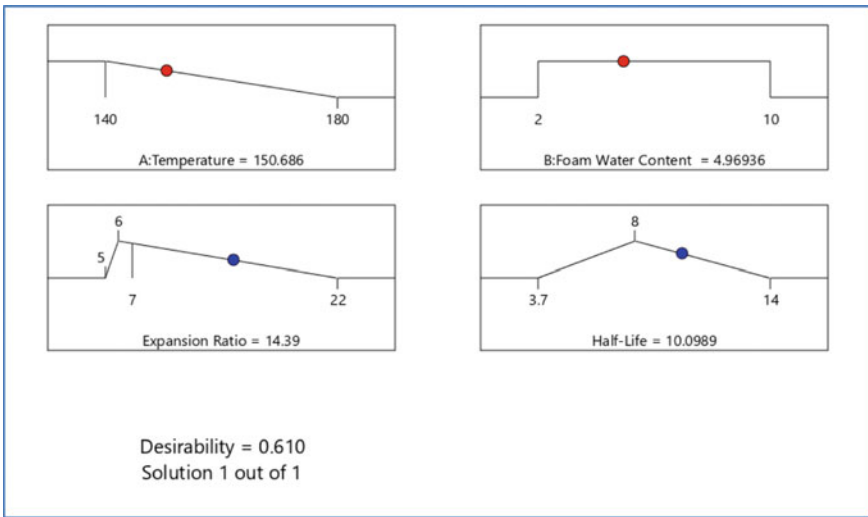


Fig. 9 Numerical optimization for VG-30

and HL under the following conditions: foaming temperature 140 °C and 150 °C for VG-10 and VG-30, respectively, and foam water content 5.2% and 4.9% for VG-10 and VG-30, respectively. DoE can easily be used to optimize large experiments of expansion ratio and half-life based on the analytical results (Design of experiment).

Conflict of Interest The authors state that they do not have any conflicts of interest.

References

1. Csanyi LH (1957) Foamed asphalt in bituminous paving mixtures. Highw Res Board Bull 160
2. Asphalt Academy (2002) Interim technical guidelines (TG2): The design and use of foamed Bitumen treated materials, CSIR, Pretoria, South Africa
3. Ashutosh T, Abhishek C (2016) Characterization and testing of foamed modified bitumen for quality assurance and feasibility for Indian condition and standards. *Int J Civil Eng* 3:14–19
4. Wirtgen (2005) Foamed Bitumen mix design procedure using the Wirtgen WLB 10 # 147 236.0001
5. Bairgi BK, Tarefder RA (2017) A synthesis of asphalt foaming parameters and their association in foamed binder and mixture characteristics, pp 256–267
6. Bairgi BK, Tarefder R (2017) Analysis of foaming properties of asphalt binder through a laser based non-contact method. ASME Int Mech Eng Congr Exposition 58455:V010T13A007
7. Sunarjono S (2008) The influence of foamed bitumen characteristics on cold-mix asphalt properties. Doctor of Philosophy, Nottingham Transportation Engineering Centre, the University of Nottingham, School of Civil Engineering
8. Wirtgen Cold Recycling Manual. Wirtgen GmbH, second Edition, Windhagen, Germany, November (2004)
9. Martinez-Arguelles G, Giustozzi F, Crispino M, Flintsch GW (2014) Investigating physical and rheological properties of foamed bitumen. *Constr Build Mater* 72:423–433
10. Namutebi M (2016) An investigation into some aspects for foamed bitumen technology (Doctoral dissertation, KTH Royal Institute of Technology)
11. Kar SS, Swamy AK, Tiwari D, Jain PK (2018) Impact of recycled asphalt pavement on properties of foamed bituminous mixtures. *Baltic J Road Bridge Eng* 13(1):14–22
12. Bairgi BK, Tarefder RA (2018) Effect of foaming water contents on high-temperature rheological characteristics of foamed asphalt binder. In: International conference on transportation and development 2018: airfield and highway pavements, pp 243–251
13. Namutebi M, Birgisson B, Bagampadde U (2011) Foaming effects on binder chemistry and aggregate coatability using foamed bitumen. *Road Mater Pavement Design* 12(4):821–847
14. Jenkins KJ (2000) Mix design considerations for cold and half-warm bituminous mixes with emphasis of foamed bitumen (Doctoral dissertation, Stellenbosch: Stellenbosch University)
15. Technology WCR (2012) Wirtgen GmbH, 1st edn. Windhagen, Germany
16. Noordin MY, Venkatesh VC, Sharif S, Elting S, Abdullah A (2004) Application of response surface methodology in describing the performance of coated carbide tools when turning AISI 1045 steel. *J Mater Process Technol* 145(1):46–58
17. Aldahdooh MAA, Bunnori NM, Johari MM (2013) Evaluation of ultra-high-performance fibre reinforced concrete binder content using the response surface method. *Mater Des* 52:957–965

Analysis of Short-Term Ageing Mechanism of Pyro-oil Modified Bitumen Compared to VG30 Based on FTIR Spectroscopy



Hemantkumar P. Hadole and Mahadeo S. Ranadive

1 Introduction

In pavement industries, asphalt is widely used due to its viscoelastic properties. In current trend, bitumen is widely obtained from crude petroleum as byproduct. As per Yao [1], 90–95% by weight of bitumen contains hydrogen, carbon, heteroatoms, and metals. Heteroatoms contain nitrogen, oxygen, and sulphur which replace carbon by heat and contribute to physical and chemical behaviour of bitumen. Metal atoms mainly include vanadium, nickel, and iron. Author also states that oxidation of bitumen is nothing but change in its properties due to change in temperature when it comes in contact with oxygen and oxidation of bitumen is also known as ageing of bitumen. Jahromi et al. (2009) stated that oxidation leads to stiffer and brittle bitumen and which results in rutting and fatigue cracking. This is the main reason that low- and high-temperature performance of bitumen should be improved, and for the same, many researchers are modifying the bitumen in different ways. Generally, fibres [2], styrene butadiene styrene (SBS), styrene butadiene rubber crumb rubber, etc., were used for improving the properties of bitumen [3]. Al Hadidy and Tan [4] explained that SBS improves low-temperature performance of bitumen. On the other hand, Thodesen et al. [5] and Bischoff and Toepel [6] explained that crumb tired rubber could improve viscosity, rheological, thermal cracking, and rutting of bitumen. Cheng et al. [7] studied the effects of addition of lime as the additive in warm mix asphalt to reduce moisture susceptibility. Ageing of bitumen is of two types of long-term ageing and short-term ageing. As per Hofko et al. [8], short-term ageing deals with chemical changes during mixing at elevated temperature of about 140–200 °C depending on type of binder. Long-term ageing of bitumen binder relates with bituminous mix in service over time in structure of flexible pavement. But as

H. P. Hadole (✉) · M. S. Ranadive
Civil Department, College of Engineering, Pune, Maharashtra, India
e-mail: msr.civil@coep.ac.in

per Nivitha et al. [3], the mechanism of ageing for modified bitumen supposed to be different when compared with long-term ageing and short-term ageing as production temperature for it is above 150 °C.

To conclude, HDPE pyro-oil is used to modify the base bitumen to form POMB. This modifier reacts with bitumen in unique way. Nivitha et al. [3] states that, such interaction leads to change in physical as well as chemical properties of base bitumen. Here, some general properties such as penetration, ductility, and viscosity were discussed before and after ageing. Along with this to analyze chemical properties, FTIR spectroscopy was used and results are discussed in detail. Primarily, functional groups associated with oxidation are focussed in the present research.

2 Literature Review

FTIR spectroscopy is generally adopted technique to examine the variation in chemical composition of binder before and after ageing and to analyze the end product after oxidation. As explained by Eberhardsteiner et al. [9] and Hafko et al. (2015), ageing of bitumen is a change takes place due to oxidation of bitumen and continued that oxidative ageing categories into two main types, such as short-term and long-term ageing. Oxidation of binder during production process, in which aggregate and binder are mix at temperature about 150–200 °C. When bituminous mix is in service over time, then corresponding oxidation of bitumen is known as long-term ageing. In general, the objective of FTIR is to collect results regarding absorptivity of infrared radiation at particular range of wavelength. As per Hofko et al. [10], only those vibrations are detected by infrared absorption for which the dipole moment is changing because of the movement in atoms. Author further states that, materials like bitumen having very high absorption coefficient, there is problem of very low transmission which leads to unacceptable low signal to noise ratio. Before finding out chemical properties of modified bitumen with different modifiers, it is necessary to firstly understand chemical structure of bitumen in aged and unaged condition. As per Chen et al. [11], asphalt binder consists of four fractions including aromatics, asphaltenes, saturates, and resins. Peterson (1975), Harnsberger et al. [12], Nivitha et al. [3] mainly focus on the FTIR spectroscopy results to study the variation in indices in chemical compounds before and after ageing for base and modified asphalt.

In present scenario, ageing is the main problem pavement engineers facing. Different research has been coming up to decrease the ageing of bitumen, and still, it is always hot topic for research. Hafko et al. (2015) and Eberhardsteiner et al. [9] explain about chemical sensitivity of bitumen. Shen et al. [13] concluded that ageing leads to decrease in penetration and ductility. On the other hand, viscosity, softening point, creep stiffness, and complex modulus increase. Further, author explains that this effect leads to elastic recovery, resistance to thermal cracking; thermal fatigue becomes poor leads to decrease in life of pavement. In the same manner, Petersen [14] and Masson et al. [15] stated that the oxidation of benzyl carbon leads to the formation of ketone functional group. The increase in viscosity of binder after ageing

is mainly due to the formation of ketones and asphaltenes. The ageing of asphalt is caused by the processes of steric hardening, oxidation, and volatilization. The literature review shows that there is need to work in the investigation of study of oxidation of HDPE pyro-oil modified binder compared to VG30 based on FTIR spectroscopy.

3 Objective

The primary objective of the study includes the study of physical properties of POMB, chemical changes in oxidation groups, and the effect of short-term ageing on POMB from physical and chemical point of view. Further, the analyzes of results with respect to FTIR are to be studied.

4 Experimental Work

4.1 Materials

In this study, the virgin binder, i.e. base binder VG30 and modified binder with the addition of Pyro-oil obtained from the pyrolysis of HDPE plastic waste was used. The HDPE waste was obtained from Municipal Solid Waste of Pune City. The specially designed Pilot Pyrolysis Plant at College of Engineering, Pune was used for the pyrolysis of HDPE plastic. For the process of pyrolysis, HDPE waste was selected of about 3 kg and 68.3% by weight of pyro-oil was produced at reactor temperature of about 730–750 °C.

The base bitumen VG30 was modified by mixing pyro-oil in it at a shear rate of 3000 rpm for 20 min at a temperature of about 160 °C. Due to this blending, composition of virgin bitumen undergoes chemical changes and these chemical changes were analyzed by FTIR. 5%, 10%, and 15% pyro-oil by weight of bitumen were added to VG30 for modification, and the resulting modified binders were abbreviated as POMB5, POMB10, and POMB15, respectively.

4.2 Bitumen Ageing

The RTFO ageing simulates the short-term ageing effect occurs during mixing of bituminous material, which is related with increases in viscosity and stiffness of binder. Each sample was aged by Rolling Thin Film Oven Tests (ASTM D2872) for short-term ageing at 163°C for 75 min to get short-term aged sample and denoted by AB5%, AB10%, and AB15%. The remaining of RTFO test samples further again tests for property characterization and ageing analysis.

4.3 FTIR

Fourier transform infrared spectrum plays a vital role in research work. FTIR test was used for chemical analysis. FTIR is a primary method used to for detecting infrared absorption, and spectral data were obtained for various wavelengths. In this study, FTIR conducted using Bruker FTIR.

4.4 Test Methods

The base binder VG30, POMB5, POMB10, and POMB15 samples were tested various properties such as penetration, viscosity, and ductility. The results of these tests are shown in Table 1.

The preparation of samples for FTIR test was done by dissolving sample in tetrahydrofuran (THF) of 10% w/v concentration. A spot of volume 20 μl of the solution was put on KBr disc and allowed to evaporate by hot air blow for three minutes. Spectra were recorded from 4000 cm^{-1} to 500 cm^{-1} . For each sample, three trials were performed for base and each modified bitumen. The test was conducted on base bitumen, modified bitumen, aged bitumen, aged modified bitumen, and HDPE pyro-oil. It is just to understand morphological changes when pyro-oil is used for modification of base bitumen.

Table 1 Physical properties of VG30 and POMB

Test	Reference	VG30	B5	B10	B15
		(Average value of 3 samples)			
Penetration at 25 °C (1/10 mm)	IS 1203/ASTM D5	58	78	89	107
Softening point (°C)	IS 1205/ASTM D36	66	52	46	38
Ductility (cm)	IS 1208/ASTM D113	80	86	96	108
Viscosity at 60 °C (poise)	IS 1206(2)	2850	–	–	–
Kinematic viscosity at 135 °C (cSt)	IS 1206(3)	480	–	–	–
Viscosity at 150 °C (poise)	IS 1206(1)	–	630	460	290
After rolling thin film oven test					
Loss in mass (%)	IS 9382	<1	<1	<1	<1
Softening point (°C)	IS 1205/ASTM D36	72	63	53	44

5 Results and Discussion

5.1 *Physical Properties of Bitumen and Pyro-oil*

Physical properties of base and modified bitumen are explained in Table 1. It reflects penetration value increases with increase in percentage of pyro-oil which implies POMB has less consistency than base bitumen. Softening point is an indicator for high-temperature performance of bitumen. Softening point decreases which implies high-temperature performance of POMB decreases. Ductility indicates low-temperature tensile deformation and asphalt flexibility. Higher the ductility better the low-temperature performance. Increase in ductility of POMB shows that POMB do not harm low-temperature performance of bitumen application. But it is also important to note that, from these results, we cannot arrive at a conclusion that the POMB has no application for high-temperature region until and unless conducting detail study of rheological properties of POMB. Loss of mass during short-term ageing is reported here, and it focusses on light weight volatile compounds. Zhao et al. [16], states that increase in loss of weight associated with increasing the average molecular weight and which leads to increase in asphalt viscosity. Yang et al. [17] conclude that loss of mass indicates the potential emission of volatiles from the bitumen binder during construction. Here, the loss in mass for base bitumen and POMB is less than 1%, which indicates that there was not much higher amount of light volatiles in pyro-oil as stated by Superpave guidelines. But light weight fractions are more than base bitumen which might be due to pyrolysis process. It can be further concluded that there are some light weight compounds in modified bitumen whose boiling point is lower than temperature in RTFO test.

Physical properties of HDPE pyro-oil are shown in Table 2.

5.2 *FTIR Analysis of Base Bitumen and HDPE Pyro-oil Modified Bitumen*

Figures 1, 2, 3 and 4 show FTIR spectra. In the figures, horizontal axis is wavenumber (cm^{-1}) and vertical axis is absorbance. From the graph, it is observed that the eminent peaks indicated for VG30 are crystal clear for bitumen. For the analysis of FTIR spectra, different groups of molecular bonds are categorized at different and specified wavelength of absorbance spectra. Four peaks in FTIR spectra of VG30 were observed in the range $2800\text{--}3000\text{ cm}^{-1}$, which mainly corresponds to the region of asymmetric and symmetric stretches of C–H in methane and methylene. The major band at 2877 cm^{-1} which typically represents hydrocarbon stretching vibrations, peak at 1458 cm^{-1} implies that C–H bond deformation vibrations. The peak at 1600 cm^{-1} known as vibrations in aromatics is corresponding to C=C bond in benzene, whereas the peak at 960 cm^{-1} corresponds to the same bond in non-benzene ring. Along with these prominent peaks, there are some other peaks like

Table 2 High density polyethylene pyro-oil physical properties

	Density at 15 °C (kg/m ³)	Kinematic viscosity at 60 °C (cSt)	Gross calorific value (kcal/kg)	Water content (% by vol.)	Pour point (°C)	Ash content (% by wt.)
Reference	IS 1448/ASTM D1298-12b	IS1448-25/ASTM D445-17a	IS 1448-P6/ASTM 240-17	IS1448-P40/ASTM D6340	IS 1448-P10/ASTMD7346-15	IS 1448-4/ASTM D482
sample	965.2	1.73	9840	0.63	24	Nil

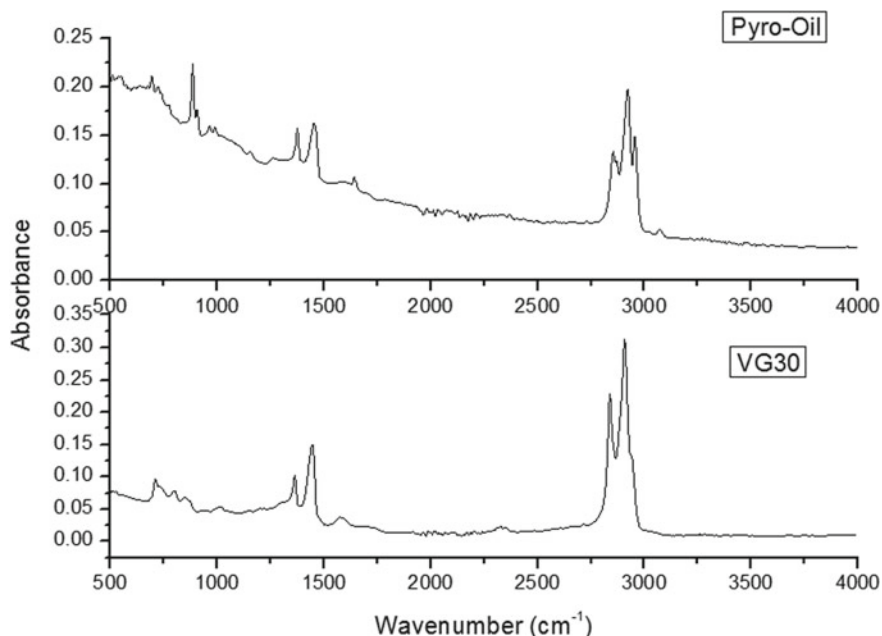


Fig. 1 FTIR spectra of VG30 and HDPE pyro-oil at room temperature

S=O, C=O which occur at 1032 cm^{-1} and 1700 cm^{-1} , respectively, and as discussed by Petersen (1986), S=O and C=O are generally used to characterize ageing in bitumen. Author continues that the strong bond 1030 and 1280 cm^{-1} indicates C–O stretching vibration, implies presence of ether, alcohols, and phenols. The weak peaks at absorbance of about $1370\text{--}1380\text{ cm}^{-1}$ described regarding C–H deformation vibration, this bonding also present in POMB. Figure 1 represents the variation in spectra for base bitumen VG30 and HDPE pyro-oil. One can observe the actual variation in spectra. Characteristics peak can be observed and identify the existence of pyro-oil by comparing the spectra from Fig. 1. For modification of base asphalt, HDPE pyro-oil was added and FTIR spectra for modified binder are observed and structural changes in base bitumen depends on the way in which modifier react with bitumen. Figure 2 gives spectra for base bitumen and POMB and it is observed that both samples show similar peaks, which show presence of same functional group, only the intensity of some peaks vary. From the Fig. 2, this is also be verified that oxidation peaks for carbonyl and sulphoxides group change and for all other peaks remain unaltered/ no prominent changes was observed. In general, it was noticed that this is common phenomenon for all types of modified bitumen.

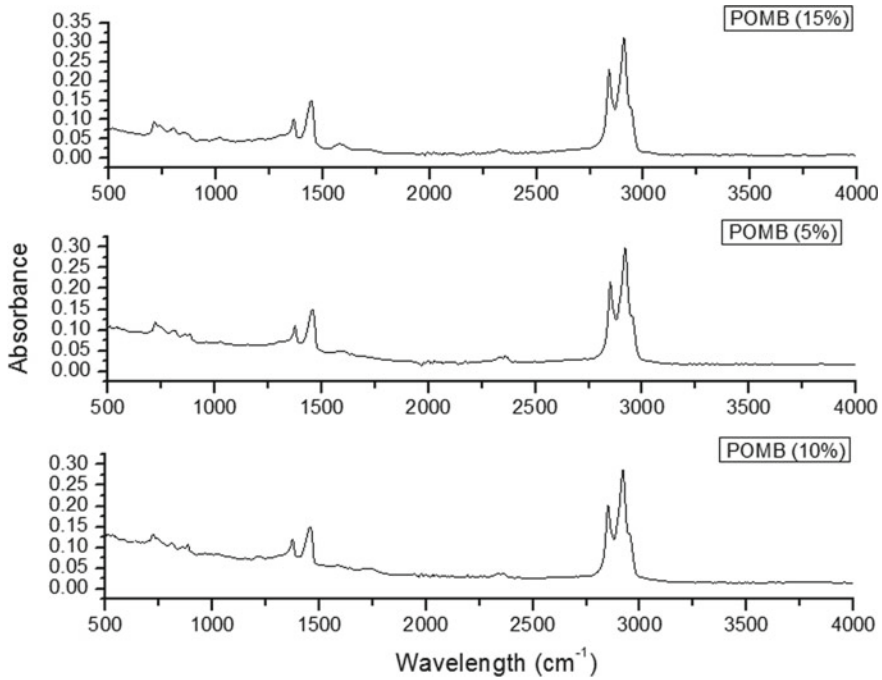


Fig. 2 FTIR spectra of POMB5, POMB10, and POMB15 modified bitumen at room temperature

5.3 Quantification of Ageing on Base and Modified Bitumen

As stated by Yang et al. [17], the ageing of bitumen during construction phase is mainly from two dimensions, such as loss of volatiles and oxidation of molecules. The loss in volatile calculated with the help of RTFO and already shown in Table 1. Along with this, oxidation of bitumen was also determined by chemical bondage such as C=O and S=O in FTIR test. As explained by Nivitha et al. [3], ageing effect monitored by peaks corresponding to carbonyl, sulphoxides, aliphaticity, and aromaticity. For the study of ageing, chemical modifications in base and modified bitumen were observed by analyzing FTIR spectra. As stated earlier, carbonyl (C=O) and sulphoxides (S=O) peaks change during oxidation of bitumen and same was observed from Fig. 3. As per the study done by Zhao et al. [16], Nivitha et al. [3], and Masson et al. [15], bitumen during modification subjected to temperature of about 160 °C for 2 h, oxidizes leading to considerable amount of hydroperoxide formation. So, the decrease in perhydroaromatic ring during the oxidation causes the absence of surge during short-term ageing in the modified binders. The results of FTIR graphs from Fig. 4 show that oxidation reaction led to the formation of unsaturated bonds which may be due to addition of HDPE pyro-oil. In order to analyze the variation in functional group during ageing process, absorption peaks are recorded. These all-transmission spectra converted into absorption peaks area of carbonyl, sulphoxides

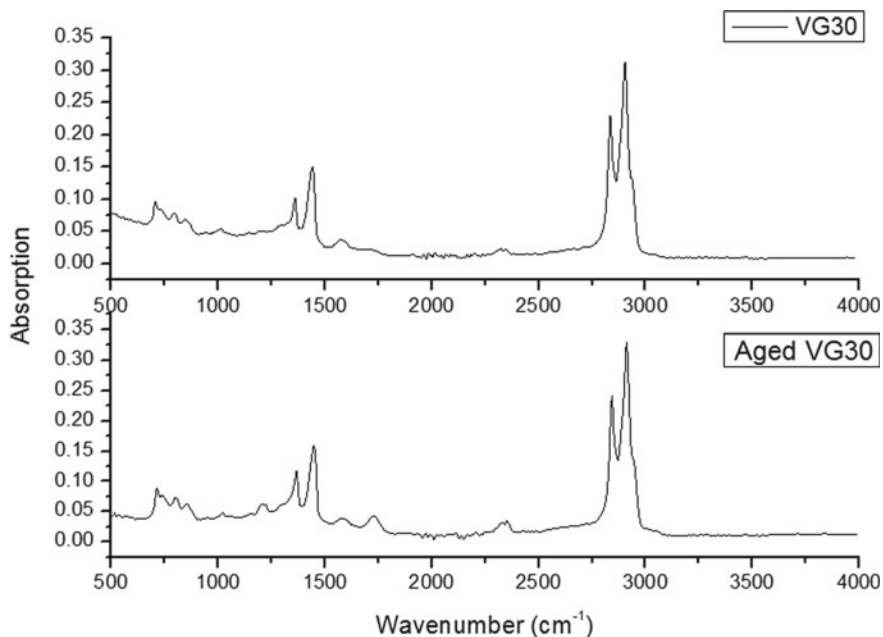


Fig. 3 FTIR spectra of VG30 (base bitumen) and short-term aged base bitumen at room temperature

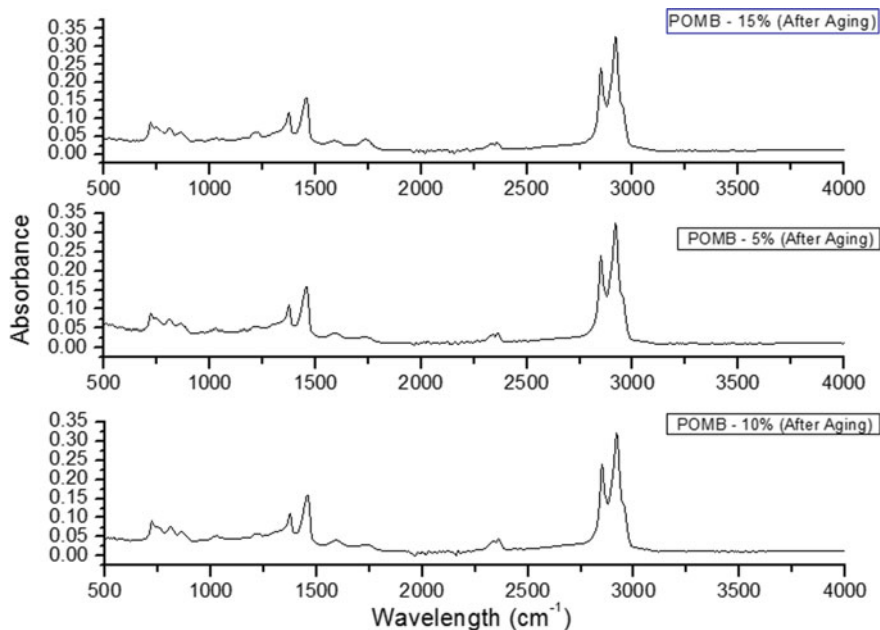


Fig. 4 FTIR spectra of short-term aged POMB5, POMB10, and POMB15 modified bitumen at room temperature

to calculate indices. The formation of C=O bond in carboxyl signifies the oxidation of carbon content and S=O bond is formed due oxygen absorption in sulphur content. But, the sulphoxides are mainly generated in short-term ageing. So, it is concluded that sulphur atom has more affinity towards oxygen than carbon atom. C=C index decreases which implies that C=C get affected or ruptured during ageing.

The carbonyl groups in modified bitumen are less than those of base bitumen when ageing occurs. This indicates that modification leads to less affinity towards oxygen of carbon. Table 3 shows important functional groups containing C=O in asphalt binder. It is found from the study of spectra that six functional groups, namely carboxylic acid, aldehyde, amide, anhydride, ester, and ketone contains carbonyl group in bitumen. This was also proved and explained by Yao et al. [18]. As per Superpave report bitumen contains around 1% of nitrogen and due to the same reason, the peak of N–H bond, i.e. amide group in bitumen is not so strong but detectable. As explained by Yao et al. [18], due to the coverage of strong bands, the peaks around anhydrides are not easily observed but evidence are found to support that anhydrides are present in bitumen. From spectra, it is found that ester formed during ageing of bitumen, and from study given by Silverstein and Bassler [19], carbonyl group in the ester is observed at range of 1735–1750 cm^{-1} . Absorbance spectra were drawn for all the cases and from that carbonyl and sulphoxides indices were calculated and shown in Table 4.

Table 3 Functional groups containing in asphalt binder

Functional group	Wave number (cm^{-1})
Carboxylic	
C=O	1700–1725
O–H	2500–3300
C–O	1210–1320
Aldehyde	
C=O	1720–1740
=C–H	2820–2850
Amid	
C=O	1640–1690
N–H	3100–3500 (stretching vibration)
N–H	1550–1640 (bending vibration)
Anhydride	
C=O	1800–1830
Ester	
C=O	1735–1750
C–O	1000–1300

Table 4 Carboxyl and sulphoxides indices

Sample	Carbonyl indices			Sulphoxides indices		
	Unaged	Aged	% Increase	Unaged	Aged	% Increase
VG30	0.298	0.484	62.449	0.702	0.816	16.24
POMB5	0.263	0.216	-17.936	0.737	0.784	6.416
POMB10	0.218	0.226	3.635	0.782	0.774	-1.014

6 Conclusions

In this study, HDPE pyro-oil was added to base bitumen (VG30) to study the effect of ageing. The base bitumen and modified bitumen were tested by FTIR to study the different functional groups under short-term ageing condition. Based on the results of FTIR for different bitumen samples, the following results are summarized.

1. From physical properties, it was found that POMB has better application in low-temperature region compared to hotter climate but this should be supported with rheological results.
2. It is found that POMB has loss in mass less than 1%, which is as per Superpave specifications provided for RTFO mass loss.
3. Six functional groups such as amide, anhydride, aldehydes, carboxylic acid, ketone, and esters contain carbonyl group.
4. Base binder and HDPE pyro-oil exhibit physical as well as chemical interaction as peaks of some functional groups changes and shift in position of peaks was recorded.
5. Modified bitumen undergoes less ageing compared with base bitumen as carbonyl functional group is less than base bitumen.

References

1. Yao H, You Z, Li L, Goh SW, Lee CH, Yap YK, Shi X (2013) Rheological properties and chemical analysis of nanoclay and carbon microfiber modified asphalt with Fourier transform infrared spectroscopy. *Constr Build Mater* 38:327–337
2. Ranadive MS, Hadole HP, Padamwar SV (2017) Performance of stone matrix asphalt and asphaltic concrete using modifiers. *J Mater Civ Eng* 30(1):04017250
3. Nivitha MR, Prasad E, Krishnan JM (2016) Ageing in modified bitumen using FTIR spectroscopy. *Int J Pavement Eng* 17(7):565–577
4. Al-Hadidy AI, Tan YQ (2010) The effect of SBS on asphalt and SMA mixture properties. *J Mater Civ Eng* 1(1):156
5. Thodesen C, Shatanawi K, Amirhanian S (2009) Effect of crumb rubber characteristics on crumb rubber modified (CRM) binder viscosity. *Constr Build Mater* 23(1):295–303
6. Bischoff D, Toepel A (2004) Tire rubber in hot mix asphalt pavements. Wisconsin Department of Transportation, Division of Transportation Infrastructure Development, Bureau of Highway Construction, Technology Advancement Unit

7. Cheng J, Shen J, Xiao F (2011) Moisture susceptibility of warm-mix asphalt mixtures containing nanosized hydrated lime. *J Mater Civ Eng* 23(11):1552–1559
8. Hofko B, Alavi MZ, Grothe H, Jones D, Harvey J (2017) Repeatability and sensitivity of FTIR ATR spectral analysis methods for bituminous binders. *Mater Struct* 50(3):1–15
9. Eberhardsteiner L, Füssl J, Hofko B, Handle F, Hospodka M, Blab R, Grothe H (2015) Towards a microstructural model of bitumen ageing behaviour. *Int J Pavement Eng* 16(10):939–949
10. Hofko B, Handle F, Eberhardsteiner L, Hospodka M, Blab R, Füssl J, Grothe H (2015) Alternative approach toward the aging of asphalt binder. *Transp Res Record J Transp Res Board* 2505(2505):24–31
11. Chen M, Leng B, Wu S, Sang Y (2014) Physical, chemical and rheological properties of waste edible vegetable oil rejuvenated asphalt binders. *Constr Build Mater* 66:286–298
12. Harnsberger PM et al (1993) Comparison of oxidation of SHRP asphalts by two different methods. *Fuel Sci Technol Int* 11(1):89–121
13. Shen J, Amirkhani S, Xiao F, Tang B (2009) Influence of surface area and size of crumb rubber on high temperature properties of crumb rubber modified binders. *Constr Build Mater* 23(1):304–310
14. Petersen JC (2009) A review of the fundamentals of asphalt oxidation: chemical, physicochemical, physical property, and durability relationships. *Transp Res Circular (E-C140)*
15. Masson JF, Pelletier L, Collins P (2001) Rapid FTIR method for quantification of styrene-butadiene type copolymers in bitumen. *J Appl Polym Sci* 79(6):1034–1041
16. Zhao Y, Gu F, Xu J, Jin J (2010) Analysis of aging mechanism of SBS polymer modified asphalt based on Fourier transform infrared spectrum. *J Wuhan Univ Technol Mater Sci Ed* 25(6):1047–1052
17. Yang X, You Z, Mills-Beale J (2015) Asphalt binders blended with a high percentage of biobinders: Aging mechanism using FTIR and rheology. *J Mater Civ Eng* 27(4):04014157
18. Yao H, Dai Q, You Z (2015) Fourier Transform Infrared Spectroscopy characterization of aging-related properties of original and nano-modified asphalt binders. *Constr Build Mater* 101:1078–1087
19. Silverstein RM, Bassler GC (1962) Spectrometric identification of organic compounds. *J Chem Educ* 39(11):546
20. ASTM (1995) Standard test method for softening point. ASTM D36, West Conshohoken, PA
21. ASTM (2007) Standard test method for ductility of bituminous material. ASTM D113, West Conshohoken, PA
22. ASTM (2013) Standard test method for penetration of bituminous materials. ASTM D5, West Conshohoken, PA
23. IS 1203. Methods of testing tar and-bituminous materials: determination of penetration
24. IS 1205. Methods for testing tar and bituminous materials: determination of softening point
25. IS 1206. Methods of testing tar and bituminous materials: determination of viscosity
26. IS 1206-Part2. Methods of testing tar and bituminous materials: determination of absolute viscosity
27. IS 1206-Part3. Methods of testing tar and bituminous materials: determination of kinematic viscosity
28. Petersen JC (1975) Quantitative method using differential infrared spectrometry for the determination of compound types absorbing in the carbonyl region in asphalts. *Anal Chem* 47(1):112–117
29. Ghaffarpour Jahromi S, Mortazavi M, Vosogh SH, Ahmadi NA (2009) Clay Impact on the Behavior of Fatigue and Permanent Deformation of Asphalt. *J Transp Eng* 11:51–65
30. Hofko B, Handle F, Eberhardsteiner L, Hospodka M, Blab R, Füssl J, Grothe H (2015). Alternative approach toward the aging of asphalt binder. *Transp Res Rec* 2505(1):24–31
31. Petersen JC (1986) Quantitative functional group analysis of asphalts using differential infrared spectrometry and selective chemical reactions--theory and application. *Transp Res Rec*, 1096

Impact on Resilient Modulus Values of the Bituminous Mixture Using Different Standard Methods



Aditya Singh, Devesh Tiwari, A. P. Singh, Tanuj Chopra,
and Anush K. Chandrappa

1 Introduction

India is known to have the second largest road network in the world. In India, majority of the roads present are the flexible pavements [1]. Flexible pavements deform under the application of repeated loading. The ability of the pavement to return to its original shape after being stressed is referred as the elasticity. Elasticity of the pavement materials plays an important role in the mechanistic design of the flexible pavement [2]. The resilient modulus is used for characterizing the bound and unbound pavement materials, including the asphalt mixtures [3]. The most common and current method of measuring the resilient modulus on the laboratory compacted samples of the bituminous mixture is the indirect tensile test conducted as per ASTM D 4123 [4] based upon the controlled stress loading procedure. In this standard, a compressive load varying between 10 and 50% of the indirect tensile strength of the specimen is applied as the peak load in the form of haversine loading, and the recoverable horizontal deformations are measured through the linear variable differential transducers (LVDT) for computing the resilient modulus of the bituminous mixture. However, there has been a recent addition of the European standard [5] for computation of the stiffness modulus of the bituminous mixture. The European standard describes the stiffness modulus of the bituminous mixture as the absolute value of the complex modulus irrespective of the type of the test considered [6].

A. Singh (✉) · T. Chopra

Department of Civil Engineering, Thapar Institute of Engineering and Technology, Patiala, Punjab, India

D. Tiwari · A. P. Singh

Pavement Evaluation Division, CSIR—Central Road Research Institute, New Delhi, India

A. K. Chandrappa

School of Infrastructure, Indian Institute of Technology, Bhubaneswar, India

In this standard, the indirect tension test, also known as the ITSM test (Indirect tension test on stiffness modulus), is conducted on the cylindrical specimens which imposes the vertical load pulse along with a rest period in a strain-controlled mode; thereby creating a haversine waveform form when the load is applied and a semi-sinusoid when unloading part takes place. Since this method does not make a sinusoidal waveform, which is a necessary observation for the complex modulus, the assumption of the complex is highly debatable. Further, there is no mention of phase angle in the standard. This problem was addressed by Brown and Cooper [7] who suggested using the concept of elastic stiffness modulus on which the European standard is based. In the study conducted by Santagata and Bassani [8], it was found that the standard does not take recoverable horizontal deformation into consideration, instead the peak horizontal deformation is used, and therefore, it is not correct to consider the modulus as resilient. It was further noted by Baldo and Passeto [6] that the controlled deformation is low for medium to high temperature which makes the measurement of the permanent deformation level insignificant. Therefore, the peak horizontal deformation can be used as recoverable deformation since the controlled deformation has an elastic nature. Hence, the stiffness modulus, as cited by the European standard, can be interpreted as a type of resilient modulus at the diametrical compression. This study therefore focuses on comparing both the standards for measuring the resilient modulus of the bituminous mixture and determining the standard best suited for our Indian conditions.

Further, the usage of the reclaimed asphalt pavement is gaining popularity in developing countries like India [9]. Reclaimed asphalt pavement materials are generated when the bituminous pavement is removed for the reconstruction or resurfacing. The material recovered can be used in the new bituminous mixture as the present in the RAP material still hold some value even when the pavement has reached their service life [10]. The RAP material can successfully reduce the use of the new aggregates and binders in the hot mix asphalt. The increase in the percentage of the RAP material results in increasing the stiffness and the rutting resistance of the mixture [11, 12]. However, a limitation of the amount of RAP is the decrease in the moisture resistance and the cracking resistance of the asphalt mixture [13, 14]. Many asphalt mixers designers choose RAP percentages that do not require any binder properties charts or equations because of time and the expense of the testing of the RAP binder properties. Therefore, in our study, 15% RAP material was chosen which requires no change in the binder selection.

2 Materials

The materials selected for the preparing the bituminous mixture should be of adequate quality and have sufficient strength. Therefore, it is important to test the materials individually present in the bituminous mixture. The details regarding the physical properties of the materials selected are discussed in detail in this section. The RAP sample was collected from the nearby site area near Delhi, and the bitumen content

Table 1 Physical properties of the aggregate

Properties	Test method	Obtained value	Requirement as per MORTH [15]
Aggregate impact value	IS 2386 IV [16]	19.40%	30 max
Abrasion value	IS 2386 IV [16]	26.08%	30 max
Specific gravity	IS 2386 II [17]	2.74	2.5–3.0
Water absorption (%)	IS 2386 III [18]	0.60%	2max
Combined (EI + FI) index (%)	IS 2386 I [19]	27.71%	30max
Stripping value (%)	IS 6241 [20]	99%	Min retained coating 95%
Soundness value	IS 2386 V [21]	10%	12%

of the sample was found out to be 4.4%. The bitumen was also recovered from the RAP sample, and their physical properties were also evaluated.

2.1 Aggregates

The aggregates selected in the study were granite, and it was obtained from the hot mix plant located near Delhi. The physical properties of the aggregate obtained after conducting various test are described in Table 1.

2.2 Bitumen

The bitumen selected for our study was VG-30 bitumen procured from the site near Agra. The properties of the bitumen are described in Table 2.

2.3 Filler

Hydrated lime was used as the filler material in the bituminous mixture to improve the moisture sensitivity of the bituminous mixture. In our study, 1.5% of the lime (aggregate weight) was selected and added to the aggregate prior to the introduction of the bitumen. Hydrated lime improves the adhesive bond between the aggregate and the asphalt, and it reacts with clay or the aggregates to minimize the moisture caused by the clay particles.

Table 2 Physical properties of the bitumen

Properties	Test method	Obtained value	Requirement as per IS 73 [22]
Penetration, (25 °C, 100 g, 5 s), 0.1 mm	IS 1203 [23]	51.3	>45
Softening point (R&B), °C	IS 1205 [24]	52	>47
Specific gravity	IS 1202 [25]	1.01	–
Flash point (clever hand open cup) (°C)	IS 1448 [26]	350	>220
Solubility in trichloroethylene, percent, Min	IS 1216 [27]	99.9	>99.0
Absolute viscosity at 60 °C, Poise	IS 1206 [28]	3082	2400–3600
Kinematic viscosity at 135 °C, cSt	IS 1206 [28]	519	> 350
Test on residue from rolling thin film oven test			
(a) Viscosity ratio at 60 °C	IS 1206 [28]	2.06	4.0
(b) Ductility at 25 °C	IS 1208 [29]	75	>40

2.4 RAP

In our study, RAP was taken from the site near Delhi, and the RAP material was found to be 4–5 years old. For all the levels of the RAP material, there is need of knowing the bitumen content. Hence, the bitumen content was found out by the centrifuge extraction method as per ASTM D2172-17 [30]. The bitumen contents of the sample were found out to be 4.4%. The binder was also recovered through rotary evaporator using ASTM D5404-17 [31]. The properties of the RAP material are further shown in Table 3.

Table 3 Properties of the RAP material

Properties	Test method	Obtained value	Requirement as per MORTH [15]
Aggregate impact value	IS 2386 IV [13]	23.12%	30max
Specific gravity	IS 2386 II [14]	2.63	2.5–3.0
Combined (EI + FI) index, %	IS 2386 I [16]	29.16%	30max
Penetration, (25 °C, 100 g, 5 s), 0.1 mm	IS 1203 [23]	6.2	–
Softening point, °C	IS 1205 [24]	97.3	–
Viscosity at 135 °C	IS 1206 [23]	15,425	–

3 Mix Design

The mix design for the virgin and the RAP mixes was carried out by Marshall method of mix design using ASTM D6927-15 [32]. The aggregate gradation adopted was for 50 mm thick bituminous concrete, and the gradation for both the type of mixes was performed in accordance with the desired gradation as per MORTH [15] specifications shown in Figs. 1 and 2, respectively.

The design bitumen content was selected based on the one whose aggregate structure and the binder content compacted to the designed number of blows resulted in four percent air voids, and it also satisfactorily meet all the other criteria by the MORTH and MS 2 standards. These criteria include voids in mineral aggregate (VMA), voids filled with bitumen (VFB), Marshall stability, and flow number. Based

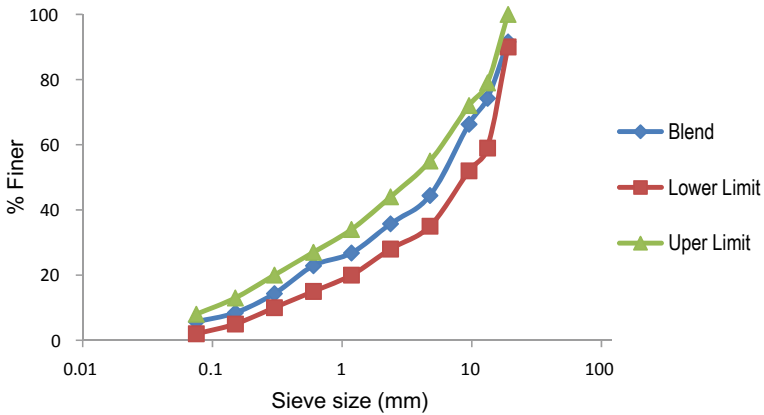


Fig. 1 Sieve gradation graph for mixture containing 0% RAP material

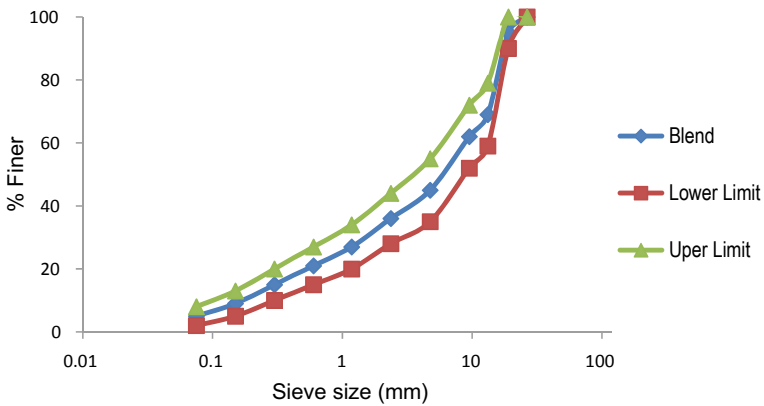


Fig. 2 Sieve gradation graph for mixture containing 15% RAP material

Table 4 Volumetric properties of the conventional mix and mix with 15% RAP

Mix type	Binder content (%)	Bulk density (gm/cc)	Air voids (%)	Voids in mineral aggregates (%)	Voids filled with bitumen (%)	Marshall stability (kN)	Flow (mm)
Virgin	5.65	2.38	4	16	74	12.15	3.10
15%RAP	5.65	2.39	4	15	73	13.40	3.35

upon this, the design bitumen content was selected as 5.65% for the conventional mix, and for the mix containing 15% RAP material, the bitumen content was also selected as 5.65% inclusive of the RAP binder in the mixture (Table 4).

4 Performance Testing

In this section, performance testing performed for both the type of the mixture is discussed. The performance testing performed was retained Marshall stability test, indirect tension test, and resilient modulus test as discussed in the section below.

4.1 Retained Marshall Stability Test

The retained Marshall stability test was conducted as per ASTM D1075-11 [33]. In this, the standard six Marshall samples of height 63.5 mm and 100 mm diameter were prepared. The samples were then further divided into two subsets, one set was unconditioned (dry), and the second set was conditioned by partially saturated in the water bath at 60 °C for 24 h. The Marshall stability was then conducted on both the samples of unconditioned and the conditioned sample after immersing the sample in thermostatically controlled water at 60 °C for 30–40 min. The ratio of the Marshall stability of the conditioned sample to the unconditioned sample will be the retained Marshall stability.

4.2 Tensile Strength Ratio

The tensile strength ratio was conducted as per ASTM D 4867-09 [34]. In this test, six prepared samples were divided into two subsets, one subset was unconditioned (dry), and the second set was conditioned by partially saturated with water. The ratio of the tensile strength of the conditioned sample to the unconditioned sample is defined as the tensile strength ratio which indicates the moisture damage to the sample. The unconditioned (dry) sample was immersed in a water bath for 20 min at 25 °C and

then tested. For the conditioned sample, the samples were first partially saturated with distilled water at the room temperature and then saturated partially by applying a partial vacuum of 525 mm for a shorter period until the degree of saturation comes in between 55 and 80% for both the samples. The samples are then kept in the water bath at 60 °C for 24 h and then placed in the water maintained at 25 °C for 1 h before testing in the tensile splitting test. The tensile strength is calculated as:

$$S_t = 2000P/\pi t D \quad (1)$$

where S_t = tensile strength, MPa, P = maximum load, kN, t = specimen height immediately before tensile test, mm, D = specimen diameter, mm.

The tensile strength ratio (TSR) of the specimen is calculated as:

$$\text{TSR} = \frac{S_{tw}}{S_{td}} * 100 \quad (2)$$

where S_{tw} = average indirect tensile strength of the conditioned specimens, kPa and S_{td} = average indirect tensile strength of the unconditioned samples, kPa.

4.3 Resilient Modulus Test

Resilient modulus of the bituminous mixture was determined by the indirect tension test conducted according to the ASTM and EN standards. The ASTM and the EN standards differ with respect to each other in terms of the loading procedure, loading time, and the rest period. The test was performed for both the types of mixtures, and at least, five samples were used for computing the resilient modulus at each temperature for both the standards. In the ASTM standard D7369, a compressive load varying between 10 and 50% of the indirect tensile strength of the specimen was applied in the form of haversine loading, and the recoverable horizontal deformations were measured through the transducers for computing the resilient modulus values. The samples were subjected to a repeated loading time of 0.1 s and a rest period of 0.9 s. The test was conducted at 15 °C, 25 °C, and 35 °C for both the types of mixtures, i.e., virgin and the RAP mixture and the specimens were kept in the environmental chamber for min 4 h before testing at the given temperature (Fig. 3).

In the EN standard 12697-26, Annex C which is based upon the controlled strain loading, the target horizontal deformation was fixed as 5 μm, and corresponding to this horizontal deformation, the resilient modulus of the sample was measured. The standards recommended a loading period of 125 ms. However, the specimen was subjected to a repeated loading time of 0.1 s as it is allowed to vary the parameter between 50 and 150 ms as recommended in the standard. The setup was same as shown in the ASTM standard above. The test was also conducted at same temperature of 15 °C, 25 °C, and 35 °C for both the type of mixtures, and the specimens were kept in the environmental chamber for min 4 h before testing at the given temperature.

Fig. 3 Resilient modulus test in progress



5 Results and Discussions

In this section, the test results of the various test conducted are discussed in the following sections for both the types of the mixture: virgin mixture and the mixture containing 15% RAP material.

5.1 Retained Marshall Stability

The results of the Marshall stability as depicted in Table 5 shows the average of three specimens. Moisture stability of the mix containing 15% RAP mix was found out to be better which indicates that the mix with the RAP found out to be less susceptible to moisture damage as compared to the virgin mix.

Table 5 Retained Marshall stability test results

Mix type	Marshall stability of unconditioned sample at 60 °C (kN)	Marshall stability of conditioned sample at 60 °C (kN)	Retained Marshall stability (%)
Virgin mix	12.15 (0.23) ^a	10.39 (0.41) ^a	85.56
15% RAP mix	13.40 (0.41) ^a	11.68 (0.56) ^a	87.20

^aThe number in parenthesis indicates one standard deviation

Table 6 Tensile strength ratio test results

Mix type	Indirect tensile strength of unconditioned sample at 25 °C (MPa)	Indirect tensile strength of conditioned sample at 25 °C (MPa)	Tensile strength ratio (%)	Requirement as per MORTH, 2013
Virgin mix	0.63 (0.02)	0.52 (0.01)	82.10	> 80%
15%RAP mix	0.69 (0.01)	0.58 (0.02)	83.85	> 80%

*The number in parenthesis indicates one standard deviation

5.2 Tensile Strength Ratio

The indirect tensile strength of the mixture containing 15% RAP was found out to be higher because of presence of some amount of oxidized binder in the mixture. The degree of saturation for both the samples was ensured between 55 to 80% before conditioning. The degree of saturation for the RAP mixture was found out to be less than the virgin mixture. The tensile strength ratio was also found out to be higher of the mix with 15% RAP which also depicts that it is found out to be less susceptible to the moisture damage and confirms the increases resistance of the RAP mixes toward the moisture damage as shown in Table 6.

5.3 Resilient Modulus Test

The resilient modulus test was conducted with respect to both the standards ASTM and EN. The EN standard was found out to have higher standard deviation as compared to the ASTM standard. This difference in the standard deviation was found out to be increasing with the increase in the temperature from 15 °C to 35 °C for both the type of mixture as shown in the figure. At temperature of 35 °C, the resilient modulus shown by the EN standard was found out to be very low and insignificant as compared to the Indian conditions mentioned in IRC 37 [35] for the VG-30 bitumen. The resilient modulus test of the mixture containing 15% RAP material was found out to be higher as compared to the virgin mixture. The reason behind this is the presence of some amount of aged binder present in the RAP mixture which stiffens the mixture thereby increasing their resilient modulus. The values measured by the both the standards were further compared with the values mentioned in the Indian Roads Congress (IRC) 37 standard. IRC 37 is the standard used in India for designing the flexible pavement, and the resilient modulus taken from IRC code is the values obtained from many field cores samples for BC mixture having VG-30 bitumen present in it (Figs. 4 and 5; Tables 7, 8).

In order to study the effect of RAP, temperature and test methods on the resilient modulus, three-way analysis of variance (3-way ANOVA) was conducted. The result

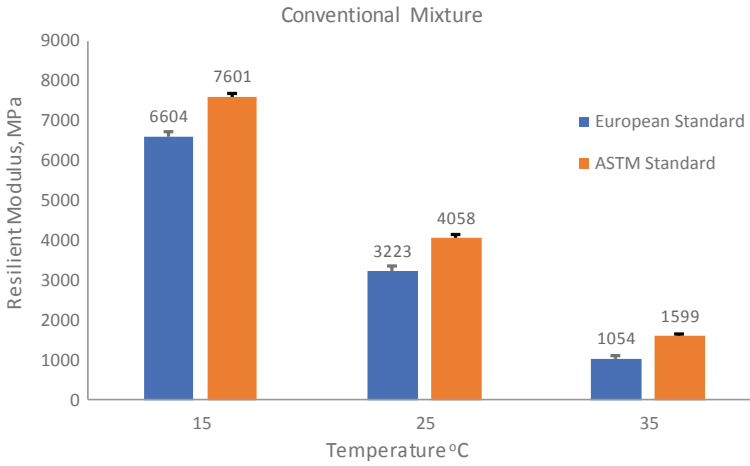


Fig. 4 Resilient modulus obtained at different temperature for conventional mixture by ASTM and EN standards

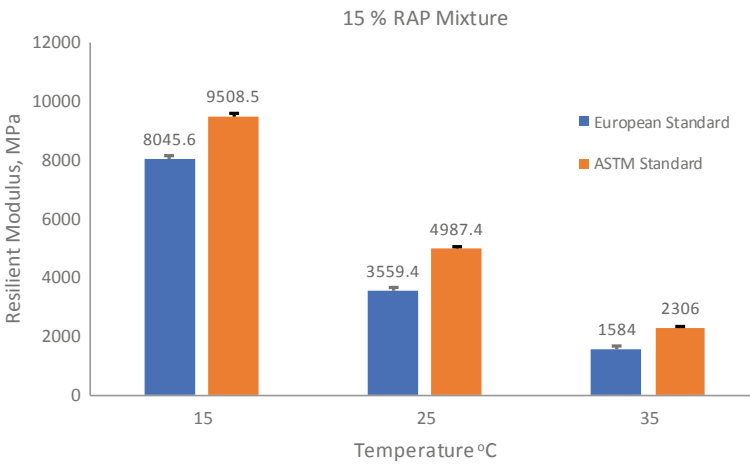


Fig. 5 Resilient modulus obtained at different temperature for 15% RAP mixture by ASTM and EN standards

Table 7 Resilient modulus compared between IRC and EN standard (virgin mixture)

Temperature (°C)	Resilient modulus IRC 37	Resilient modulus EN standard	R ²
15	4000	6604	0.984
25	3000	3323	
35	2000	1053	

Table 8 Resilient modulus compared between IRC and ASTM standard (virgin mixture)

Temperature (°C)	Resilient modulus IRC 37	Resilient modulus ASTM standard	R^2
15	4000	7601	0.989
25	3000	4058	
35	2000	1582	

Table 9 Three-way ANOVA for resilience modulus

Dependent variable: resilience modulus					
Source	Type III sum of squares	Degree of freedom	Mean square	F -value	p -value
Corrected model	402,706,577.9	4	100,676,644.473	956.985	0.001
Intercept	1,172,952,862.293	1	1,172,952,862.293	11,149.544	0.001
Test_Method	13,871,502.534	1	13,871,502.534	131.856	0.001
Temperature	381,512,901.450	2	190,756,450.725	1813.242	0.001
RAP	13,128,934.255	1	13,128,934.255	124.798	0.001
Error	5,575,699.003	53	105,201.868		
Total	1,569,696,928.000	58			
Corrected total	408,282,276.897	57			

R Squared = 0.986

of the test is shown in Table 9. Table 9 shows that all three variables affect the resilient modulus significantly. The test methods (EN and ASTM) result in significantly different resilient modulus values for same mixture. This indicates that the result obtained from these test methods shall be having design implications as they may result in different thicknesses of layers for same design conditions. Further, by adding 15% recycled asphalt, the resilient modulus values increased significantly implying recycled asphalt improves the stiffness of mixture resulting in reduced thickness of pavement.

6 Conclusions

In this study, the laboratory test was performed for both the types of the mixture, and it was founded from the study that the mixture with the 15% RAP material was found to perform better as compared to the virgin mixture. The usage of the 15% RAP in the mixture can be successfully utilized and help in saving the amount of aggregate and binder in the hot mix mixture.

Based on the results obtained from the laboratory studies, the following conclusions are made:

- The retained Marshall stability and tensile strength ratio increased with the inclusion of recycled asphalt (RA). However, the standard deviation was found to be higher in case of retained Marshall stability for RA mixtures.
- The modulus of resilience determined as per ASTM method showed consistently higher MR at all temperatures compared to EN method. The standard deviation was found to be higher in the case of resilient modulus determined from EN method at all temperature levels.
- At higher temperature, the difference in the modulus was found out to be increasing, and the values exhibited by the EN standard was found out to be insignificant. Therefore, the EN standard can be used for determining the resilient modulus at the lower temperature, but for conditions like country India, where average pavement temperature is close to 35 °C, the ASTM standard proves to be a better one.
- Recycled asphalt, temperature, and testing method had significant effect on the modulus of resilience. Resilient modulus obtained from different testing methods will have significant implications on pavement design.
- The resilient modulus values measured by the ASTM standard also demonstrated a better co-relation with the resilient modulus mentioned in IRC 37. Therefore, this paper recommends the use of the ASTM standard for measuring the resilient modulus of the bituminous mixture for our Indian conditions.

References

1. Singh A, Sharma A, Chopra T (2020) Analysis of the flexible pavement using falling weight deflectometer for Indian national highway road network. *Transp Res Procedia* 48:3969–3979
2. Swamy K, Das A (2006) Pavement design with central plant hot-mix recycled asphalt mixes. *Constr Build Mater* 21:928–936. <https://doi.org/10.1016/j.conbuildmat.2006.05.004>
3. Munoz JSC, Kaseer F, Arambula E, Martin AE (2015) Use of the resilient modulus test to characterize asphalt mixtures with recycled materials and recycling agents. *Transp Res Rec* 2506(1):45–53. <https://doi.org/10.3141/2506-05>
4. ASTM D 7369-11 (2011) Standard test method for determining the resilient modulus of bituminous mixtures by indirect tension test. ASTM International, West Conshohocken, PA, www.astm.org
5. EN 12697-26 Annex C (2012) Bituminous mixtures—test methods for hot mix asphalt—Part 26: Stiffness, British Standards Institution
6. Baldo N, Passeto M (2013) Indirect tensile test for the determination of the stiffness and the resilient modulus of asphalt concretes : experimental analysis of the EN 12697-26 and the ASTM D 4123 Standards proceedings 10th international conference on asphalt pavements, Québec, Canada
7. Brown SF, Cooper KE (1993) Assessment of the mechanical properties of asphaltic mixes on a routine basis using simple testing equipment. In: Proceedings of the 5th eurobitume congress, Stockholm, Sweden

8. Santagata E, Bassani M (1999) Improved use of the repeated load indirect tensile test. In: Proceedings of the 3rd European symposium on performance and durability of bituminous and hydraulic stabilised composites, Leeds, UK
9. Saride S et al (2016) Utilization of reclaimed asphalt pavements in Indian low volume roads. *Am Soc Civil Eng* 1–10. [https://doi.org/10.1061/\(ASCE\)MT.1943-5533.0001374](https://doi.org/10.1061/(ASCE)MT.1943-5533.0001374)
10. FHWA Report (2012) Introduction to pavement recycling. <http://www.fhwa.dot.gov/pavement/recycling/98042/01.cfm>
11. Tarbox S, Daniel J (2012) Effects of long-term oven aging on reclaimed asphalt pavement mixtures. *Transp Res Rec* 2249(1):1–10. <https://doi.org/10.3141/2294-01>
12. Hajj E et al (2011) Laboratory evaluation of mixes containing recycled asphalt pavement (RAP). *Road Mater Pavement Design* 10(3):495–517
13. Chen J et al (2007) Engineering characterization of recycled asphalt concrete and aged bitumen mixed recycling agent. *J Mater Sci* 42(23):9867–9876
14. Huang B et al (2010) Laboratory investigation of cracking resistance of hot-mix asphalt field mixtures containing screened reclaimed asphalt pavement. *ASCE* 23(11):1535–1543
15. MORTH (2013) Ministry of Road Transport and Highways Specifications for Road and Bridge Works, Section 500, Fifth Revision, Indian Roads Congress, New Delhi, India
16. IS 2386 IV (1963) Methods of test for aggregates for concrete mechanical properties, Bureau of Indian Standards, New Delhi
17. IS 2386 II (1963) Methods of test for aggregates for concrete estimation of deleterious materials and organic impurities, Bureau of Indian Standards, New Delhi
18. IS 2386 III (1963) Methods of test for aggregates for concrete specific gravity, density, voids, absorption and bulking, Bureau of Indian Standards, New Delhi
19. IS 2386 I (1963) Methods of test for aggregates for concrete particle size and shape, Bureau of Indian Standards, New Delhi
20. IS 6241 (1971) Method of test for determination of stripping value of road aggregates, Bureau of Indian Standards, New Delhi
21. IS 2386 V (1963) Methods of test for aggregates for concrete part V soundness, Bureau of Indian Standards, New Delhi
22. IS 73 (2013) Paving bitumen specification (fourth revision), Bureau of Indian Standards, New Delhi
23. IS 1203 (1978) Methods for testing tar & bituminous materials: determination of penetration, Bureau of Indian Standards, New Delhi
24. IS 1205 (1978) Methods for testing tar & bituminous materials: determination of softening point, Bureau of Indian Standards, New Delhi
25. IS 1202 (1978) Methods for testing tar & bituminous materials: determination of specific gravity, Bureau of Indian Standards, New Delhi
26. IS 1448 (1998) Determination of flash point by Abel Apparatus
27. IS 1216 (1978) Determination of solubility in carbon disulphide trichloroethylene, Bureau of Indian Standards, New Delhi
28. IS 1206 (1978) Methods for testing tar & bituminous materials: determination of viscosity Part III kinematic viscosity, Bureau of Indian Standards, New Delhi
29. IS 1208 (1978) Methods for testing tar & bituminous materials: determination of ductility, Bureau of Indian Standards, New Delhi
30. ASTM D 2172-17 (2017) Standard test methods for quantitative extraction of asphalt binder from asphalt mixtures. ASTM International, West Conshohocken, PA. www.astm.org
31. ASTM D 5404-17 (2015) Standard practice for recovery of asphalt from solution using toluene and the rotary evaporator. ASTM International, West Conshohocken, PA, 12(C):12–14. <https://doi.org/10.1520/D5404>
32. ASTM D 6927-15 (2015) Standard test method for Marshall stability and flow of asphalt mixtures. Designation, American Society for Testing Materials. <https://doi.org/10.1520/D6927-15.2>
33. ASTM D 1075-11 (2011) Standard test method for effect of water on compressive strength of compacted bituminous mixtures, ASTM International, West Conshohocken, PA. www.astm.org

34. ASTM D 4867-09 (2014) Standard test method for effect of moisture on asphalt concrete paving mixtures, ASTM International, West Conshohocken, PA. www.astm.org
35. IRC 37 (2018) Guidelines for the design of flexible pavements, Indian Roads Congress, New Delhi, India

Selection of Bitumen in Indian Condition



Swapan Kumar Bagui, Atasi Das , and Yash Pandey 

1 Introduction

Selection bitumen is an important aspect for the performance of bitumen mixes for long term. Bitumen has sufficient strength to sustain at highest air temperature and lowest temperature during summer and winter periods against bleeding and low temperature crack. Average of consecutive seven days maximum and minimum temperature considered for pavement design. There is wide variation of temperature in India from one location to another location.

Again temperature of bitumen varies along the depth of bitumen. Representative temperature presented at a depth of one-third location of thickness from top of the bitumen surface. For the case of high thickness of bitumen even in the case of deep strength bitumen and perpetual pavement, different grade of bitumen can be proposed. This paper presents a details discussion for selection of bitumen for Indian condition. Different models are presented in the next section.

2 Review Temperature Model

2.1 Han's Models

Chunhua Han in the study used the data from Mohseni to develop and evaluate models relating, the seven days average maximum air temperatures to the seven days

S. K. Bagui

CGM, Intercontinental Consultants & Technocrats Pvt. Ltd., Delhi 110016, India
e-mail: swapan.bagui@ictonline.com

A. Das · Y. Pandey (✉)

G R Infraprojects Limited, Gurugram 122015, India

© The Author(s), under exclusive license to Springer Nature Singapore Pte Ltd. 2022
D. Singh et al. (eds.), *Proceedings of the Fifth International Conference of Transportation Research Group of India*, Lecture Notes in Civil Engineering 218,
https://doi.org/10.1007/978-981-16-9921-4_32

439

average maximum temperature within the bituminous concrete, and, the minimum air temperature to the temperature within the bituminous concrete pavement [1]. The models developed by Hen were slightly different from those by Mohseni; however, both were having approximately similar results. The predicted temperatures from Han's and Mohseni's models result in approximately the same PG bitumen. Model equation developed by Han et al. [1] is:

$$T_{d(\text{Max})} = 0.52 + 6.225\varphi - 0.15\varphi^2 + 0.001\varphi^3 + 0.28T_{a(\text{Max})} - 8.37 \ln(d + 40) \quad (1)$$

where

$T_{d(\text{Max})}$ Maximum pavement temperature at depth d in °C;
 φ Latitude in degree; and
 d Depth in mm.

The R^2 for the above equation is 0.875 for 70 collected data points and the standard error for estimate is 2.2 °C. For the above model, latitude has much significance on temperature than air temperature. Similarly,

$$T_{d(\text{Min})} = -0.14 - 1.7\varphi + 0.06\varphi^2 - 0.0007\varphi^3 + 0.69T_{a(\text{Min})} + 4.12 \ln(d + 100) \quad (2)$$

The R^2 for this is 0.948 for 71 collected data points, and the standard error for the same is 2.6 °C. In this, air temperature has significant effect on minimum pavement temperature.

2.2 Mohseni's Models

Mohseni [2] also developed models for prediction of maximum and minimum temperatures as a function of latitude, temperature (air), and depth:

$$T_{d(\text{Max})} = 54.32 - 0.002468\varphi^2 + 0.77585T_{a(\text{Max})} + 6.264 \ln(d + 25) \quad (3)$$

The R^2 is 0.76 for 309 collected data points having standard error of 3.0 °C.

$$T_{d(\text{Min})} = -1.56 - 0.0039666\varphi^2 + 0.71819T_{a(\text{Min})} + 46.264 \ln(d + 25) \quad (4)$$

The R^2 is 0.96 on 411 collected data points having standard error 2.1 °C.

2.3 Robertson’s Models

Robertson in [3] studied the relation between minimum air and pavement surface temperatures on the assumption as proposed by SHRP that low air temperature has much effect on pavement temperature. Robertson collected the data for developed the simple relation between the minimum air and surface temperature:

$$T_s = 0.749T_a \tag{5}$$

where,

T_s is the minimum pavement surface temperature (°C)

T_a is the minimum air temperature (°C).

2.4 Erland’s Models

Erland et al. [1] proposed following equations for pavement temperature:

$$T_{d(\text{Max})} = 0.47 + 5.717\varphi - 0.127\varphi^2 + 0.0008\varphi^3 + 0.3078T_{a(\text{Max})} - 8.7 \ln(d + 40) \tag{6}$$

$$T_{d(\text{Min})} = -0.15 - 1.9\varphi + 0.06\varphi^2 - 0.0007\varphi^3 + 0.59T_{a(\text{Min})} + 5.2 \ln(d + 100) \tag{7}$$

IRC: 37-2018 [4] developed following equation for maximum temperature at depth 20 mm:

$$T_{20\text{mm}} = [(T_{\text{air}} - 0.00618\varphi^2 + 0.2289\varphi + 42.2) \times (0.9545)] - 17.7 \tag{8}$$

where

$T_{20\text{mm}}$ Pavement temperature at a depth of 20 mm

φ Latitude of the place

T_{air} Seven days maximum temperature average.

The equation was used for computing the maximum pavement temperature for Kharagpur. Corresponding to a maximum air temperature of 38 °C and 47 °C (a typical range of summer-time maximum temperatures) and feeding the latitude and longitude data of Kharagpur, the corresponding pavement temperatures are predicted as 61 °C and 69 °C, respectively. A better and more reliable input of temperature would be seven days average (mean) plus twice the standard deviation. Using this model, the maximum pavement temperature at any place can be predicted. A judicious assumption, however, could be that in most part of the country, the maximum pavement temperature may reach around 70 °C (IRC: 37-2018).

3 Limitation in Indian Scenario

Indian Roads Congress (IRC): 37-2018 presented an equation for pavement temperatures at 20 mm depth but no established equations are available for maximum and minimum temperature and temperature variation at different depth of flexible pavement. Again, life cycle cost of perpetual pavement perpetual pavement is least as compared to rigid pavement for design period of 40–50 years. Perpetual pavement requires heavy bituminous pavement thickness in the range of 400 mm or more. Different grade of bitumen is required at different depth, but there is no standard guideline for determination pavement temperature at minimum and maximum temperatures. Therefore, there is a need of research work on these aspects for Indian condition.

4 Hypothetical Case Study

Different cases considered varying latitude, air maximum and minimum temperature, and pavement temperatures are determined and presented here in.

Three methods are considered for determination of maximum and minimum temperatures as mentioned below.

Method 1: Han's method

Method 2: Mohsent's method

Method 3: Erland s method.

For 30 degree latitude, pavement temperature has been determined varying air temperature and presented in Fig. 1.

5 Case Study

Government of India recently start to construct perpetual pavement. Thickness of perpetual is found to be in the range 400 mm. Assuming, perpetual pavement will be constructed near Varanasi. Latitude, minimum and maximum temperatures are 25.318°, 3 °C, and 46.5 °C. Thickness of perpetual thickness of pavement is 400 mm.

From Fig. 7, it is found that maximum pavement temperature is around 62 °C. Therefore, top 50 mm BC shall be constructed with bitumen with softening point around 65 °C. Pavement temperature varies from 55° to 51 °C from depth 50 mm to 100 mm. Softening point for this 50 mm thickness will be more than 55°C. Pavement temperature varies from 51° to 45 °C from depth 100 mm to 250 mm. VG 40 bitumen may be used for this thickness. VG 30 will be used below 300 mm depth. Same is presented in Table 1.

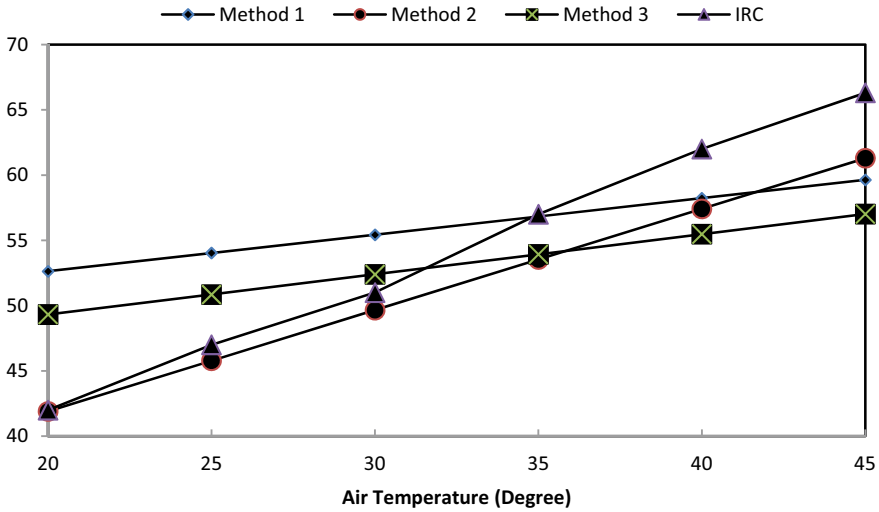


Fig. 1 Variation of pavement versus maximum air temperature for location with latitude 30°

Table 1 Softening point/type of bitumen for Varanasi

Depth of pavement (mm)	Softening point/bitumen type
0	Softening point >62 °C
50	
100	Softening point >55 °C
150	
200	
250	VG 40
300	
350	
400	
	VG 30

Pavement temperature varies from 62 to 3 °C. Performance grade bitumen PG 67-3 equivalent can be provided. MS 26 recommended different PG bitumen.

5.1 Second Case

Consider latitude, maximum, and minimum temperatures of Leh (34.15 °C, 25.3, and -14.3 °C). Maximum and minimum pavement temperatures are calculated from different methods and finally adopted maximum and minimum temperatures are 54 °C and -14.4 °C. Therefore, PG 54-15 is required.

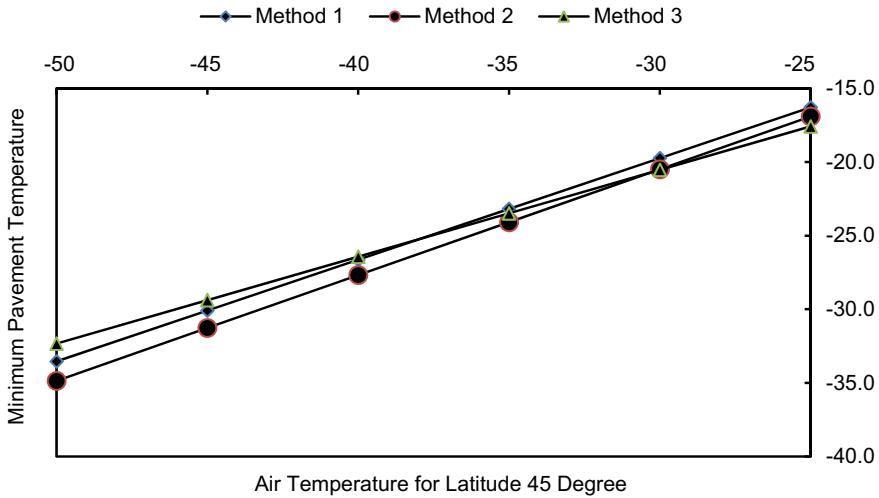


Fig. 2 Variation of pavement versus minimum air temperature for location with latitude 30°

6 Discussion of Results

From Fig. 1, it is found that maximum pavement temperature varies linearly with upward slope with air temperature. Therefore, higher order value of latitude mentioned in pavement temperature can be neglected and similar trend is also found in Fig. 2 for minimum temperature. Therefore, higher order value can be neglected in the equations mentioned. It is also found that pavement temperature obtained by Method 1 and Method 2 are close values. Equation proposed in IRC gives higher pavement temperature after 35°C as shown in Fig. 1.

Pavement temperature at various depths is determined for different maximum air temperatures for the location of latitude 30° N and presented in Figs. 3, 4, 5 and 6. It is observed that pavement temperature decreases gradually with depth nonlinearly. This suggests that different grades of bitumen are required for bituminous mix.

A case study for perpetual pavement at Varanasi has been adopted, and it is found that bitumen of different softening points is required (Fig. 7).

7 Conclusion

Following conclusions, regarding selection of bitumen consideration from the present study, may be drawn:

- Equation proposed in IRC yields higher temperature. This equation may be re-looked.

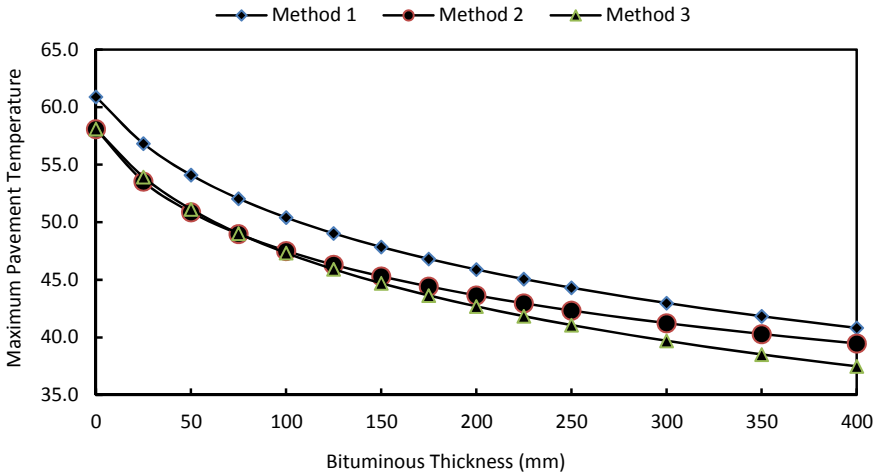


Fig. 3 Pavement temperature at different depth (mm) for air temperature 35° for latitude 30°

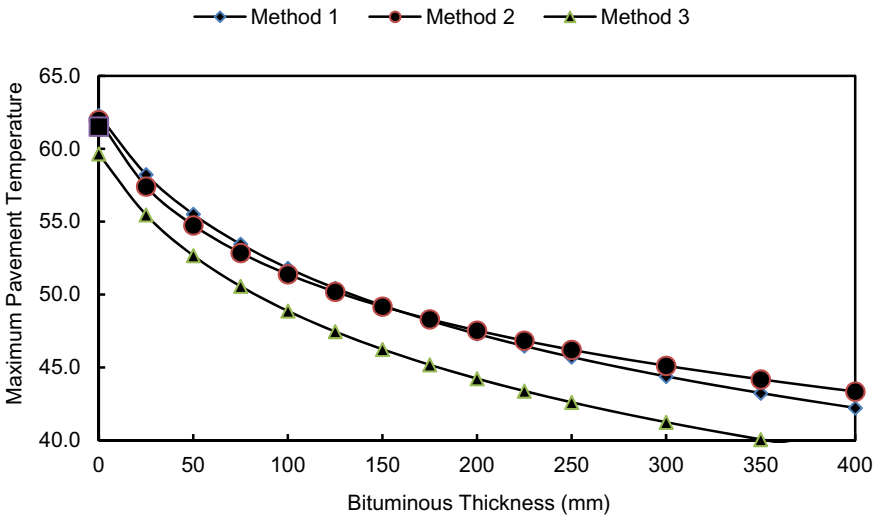


Fig. 4 Pavement temperature at different depth (mm) for air temperature 40° for latitude 30°

- Maximum and minimum pavement temperatures vary linearly with positive slopes. These equations may be revised.
- IRC do not recommend variation of pavement temperature with different depths of pavement. Therefore, this equation needs review for selection of bitumen.
- No pavement temperature equation is not available in India. Equation 5 may be adopted for minimum pavement temperature.

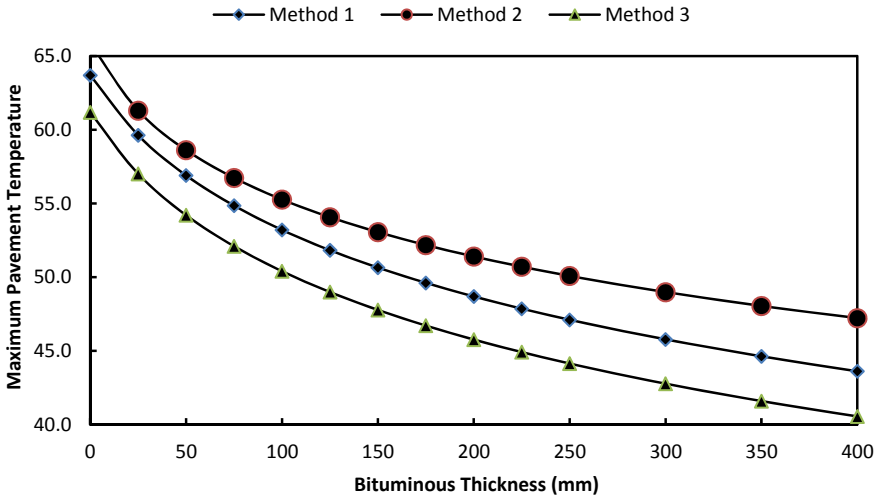


Fig. 5 Pavement temperature at different depth (mm) for air temperature 45° for latitude 30°

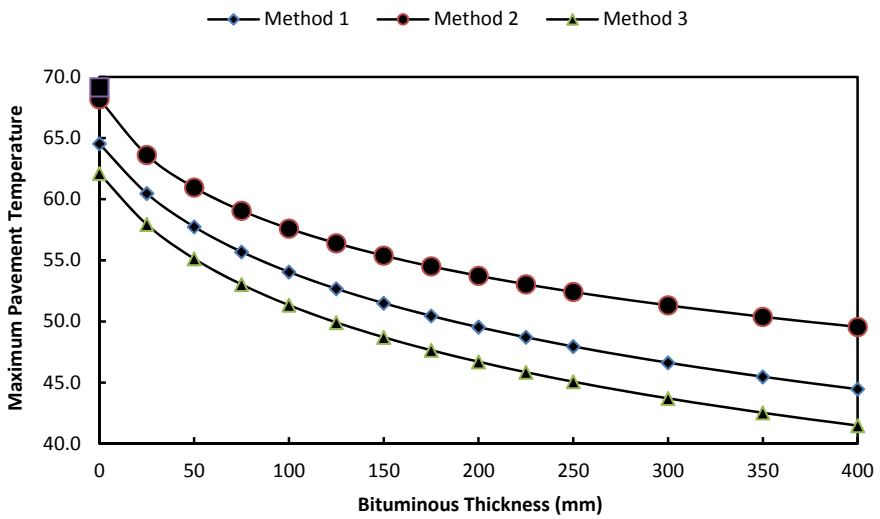


Fig. 6 Pavement temperature at different depth (mm) for air temperature 48° for latitude 30°

- Case study mentioned for Varanasi may be used for other location of India for selection of bitumen.
- P G bitumen may be considered where temperature variation is wide.

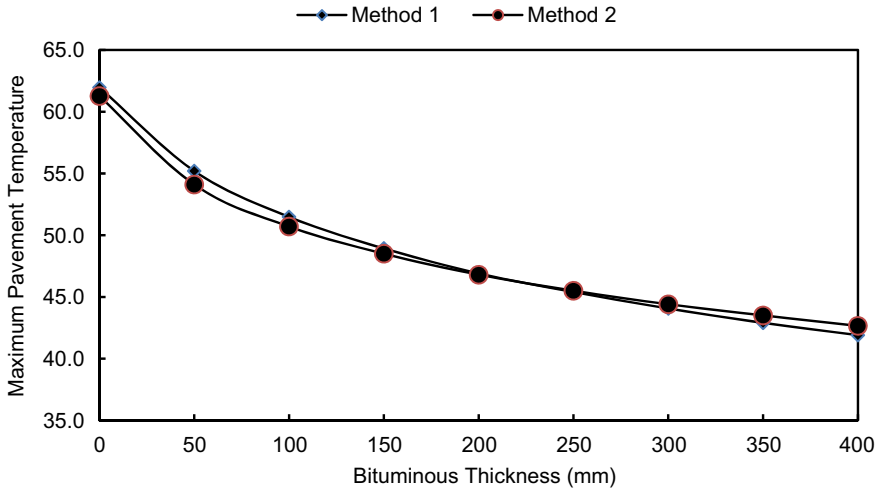


Fig. 7 Pavement temperature at Varanasi for perpetual pavement

References

1. Lukamem EO, Han C, Eugene L, Skok IR (1998) Probabilistic method of bitumen binder selection based on pavement temperature. TRR N0(1609):12–20
2. Mohseni A (1997) Seasonal AC pavement temperature (SAPT) database. Presented at meeting of the Transportation Research Board Data Analysis Working Group Meeting, Washington, D.C.
3. Robertson WD (1997) Determining the winter design temperature for bitumen pavements. Presented at annual meeting of the association of bitumen pavement technologists, St. Paul, Minn
4. IRC: 37-2017. Guideline for flexible pavement

Compaction Characteristics of Marshall Mould at Refusal Density



Swapan Kumar Bagui, Atasi Das , and Yash Pandey 

1 Introduction

Well-designed bituminous mixes, when compared to badly designed bituminous mixes, shall have higher strain tolerance levels; however, both of them will fail eventually. For the particular designed traffic loading, a good bituminous mix might fail at early stage if the road is too weak and strain values are quite high. So, premature cracking prevention involves both:

- Design of bituminous mixes
- Design of pavement.

Mix parameters, for well resistance to cracking, which are directly or indirectly involved are as follows:

- Bitumen properties, such as rheological properties, viscosity, penetration.
- Effective bitumen content (EBC).
- Asphalt film thickness (AFT).
- Voids in mineral aggregate (VMA).
- Voids filled with asphalt (VFA).

Bituminous mixes having continuous stone matrix and partially filled with sand asphalt, atmosphere has access to the individual coated particles of aggregate. In these types of bituminous mixes, it is probable that AFT will be useful if “enough” asphalt is ensured for mix durability.

S. K. Bagui
Intercontinental Consultants & Technocrats Pvt. Ltd., Delhi 110016, India
e-mail: swapan.bagui@ictonline.com

A. Das · Y. Pandey (✉)
G R Infraprojects Limited, Gurugram 122015, India

Table 1 Marshall hammer blows for different traffic levels

Traffic level	Number of blow for Marshall mould
Light (<0.4 MSA)	35
Medium (0.4–1 MSA)	50
Heavy (>1 MSA)	75

2 Literature Review

2.1 Compaction

Swanson et al. [1] define the compaction of bituminous concrete mix as, “the stage of construction which changes the mix from its loose state to a denser state, thus allowing it to carry traffic load”. Further, it is concluded that the efficiency of compaction depends on internal resistance of mix (viscous resistance, interlocking of aggregate and resistance to friction).

As per Smith [2], the reason for compaction of asphalt pavements is to make them impervious to air and water. A stronger mix is guaranteed with increase in mix density, but the same will not guarantee for the robust pavement.

Epps [3] studied that with the present system for laboratory compaction, it is not possible to simulate field condition.

Weak compactive effort [4] is suitable for low-volume road, and strong compactive effort is suitable for heavy traffic. The laboratory compaction needs to simulate field compaction. The number of blows of Marshall hammer required for bituminous surface at varying traffic level is shown in Table 1.

With the effort of external forces, in the mix compaction, volume of air decreases and density increases. The compaction mass should have sufficient air voids to allow the asphalt to expand without filling the voids resulting in flushing.

2.2 Refusal Density

For an asphalt mix to be successful, it must have sufficient asphalt to bind the aggregate particles and sufficient voids in mix (VIM) to avoid failure by means of plastic flow. Both of these two requirements are contradictory to each other. If we add enough asphalt for durability, there will not be sufficient VIM; if we leave enough VIM, there will not be sufficient asphalt to make durable mix. Thus, it is necessary to target more VMA that allows scope for ‘enough’ asphalt and ‘enough’ VIM both.

VIM drop below 3% asphalt mix [5] are prone to failure in plastic flow; data from roads observed in Indonesia, Kenya, Saudi Arabia and other countries confirm the probability of failure. Studies also advocates that gap-graded mixes, having more voids in mix, are slightly less prone to failure than threshold limit (VIM 2%) than well graded mixes (with VIM 3%).

There are some studies that also suggests that in ‘free flow’ conditions, the threshold in voids in mix is closer to about 2% than 3%, but is not yet certain. However, Asphalt Institute Manual Series No. 2 (MS-2)-1994, recommends the final void in mix after plying of traffic should be about 3%.

Marshall’s method of mix design procedures recommends 75 blows for sample preparation. Marshall’s sample, extracted from site, after trafficking required the voids in mix to be about 3%. The trouble is the density achieved by 35, 50, or even 75 blows on each face of the sample is less than that which occurs in the wheel paths of roads carrying severe traffic loads. Free falling of hammer was ensured in order to achieve best results whilst testing of samples.

To ensure that the in-situ void in mix should not drop <3%, additional test is desired to be performed, in which Marshalls moulds needs to be compacted to the refusal condition that is until the sample refuses to be further denser. An upper limit to this design binder content can be set corresponding to 3% voids in mix at refusal condition.

Refusal density test can be performed by the following two methods.

In the first method, it is recommended the use of vibrating hammer for compacting the samples in a CBR mould. The procedure as per BS 598 Part 1-1989, for percentage refusal density (PRD), test needs to be followed, with some improvement in hammer weight which shall be surcharged by hanging 30 kg extra on it. Due high cost of this equipment, this method is rarely used different projects in India although this method requires lesser bitumen content than that of conventional mix design.

In another method, it is the extended version of Marshall Test with about 400–500 or even more blows per face in place of 75 blows.

Cooper et al. [6], have reported that minimum 3% VIM shall be retained in the asphaltic mix after its service life in order to prevent any deformation.

Based on the available literatures, following points are highlighted:

- Marshall Method of compaction should be checked at refusal density for heavy traffic.
- Minimum air void/VIM of 3% should be maintained at the end of service life of mix.
- Marshall Mould should be checked at refusal density.

3 Objective and Scope of Works

Based on major findings of previous research works, the aim of the present study also includes development of empirical relationships to estimate maximum density of asphalt mix compaction control parameters, like compaction energy and asphalt content. These correlations may be very much useful to estimate the density at different values of compaction energy, density and binder content in the field.

In the present research work, an attempt has been made to investigate the effect of compaction characteristics of Marshall Sample on the vital Marshall’s parameter.

Table 2 Test result of aggregate

Test	Result	Limit
Flakiness and elongation	20%	30%
Aggregate impact value	13%	27%
<i>Water absorption</i>		
20 mm	0.50%	2%
10 mm	0.61%	2%
Less than 6 mm	0.66%	2%
Dust	0.75%	2%
<i>Specific gravity</i>		
20 mm	2.841	–
10 mm	2.821	–
Less than 6 mm	2.801	–
Dust	2.780	–
Stripping	>95%	Min 95% coated

4 Laboratory Test

The aggregate was collected from Jhansi. The physical properties are shown in Table 2. Polymer modified bitumen (PMB 70) was used for construction of asphalt layer.

5 Brief Methodology of Mix Design

Mix design has been carried out as per guidelines of MS-2, selecting aggregate, asphalt content as per specification, and finalised asphalt content after preparing following graphs against percent asphalt content:

- a. Stability of mix
- b. Flow
- c. Air void in mix
- d. Unit weight of mix
- e. Voids in mineral aggregate (VMA)
- f. Void filled with bitumen (VFA)

Final asphalt content is found 4.5%. Actual bitumen content may be increased by 0.5 or 0.6% above optimum bitumen content to increase fatigue life three times. This reduces the crack which increases fatigue life/reduces bottom-up crack, and top-down crack formation may be controlled by proving mix rut resistance. Top-down cracking develops on high volume road in India due to excessive tensile strain developed at surface. Top-down cracking shall be eliminated by proving high modulus rut and fatigue resistance mix, i.e. proving 0.5% more bitumen above optimum bitumen

content. Ravelling may be occurred in the non-wheel path. This may be eliminated by using new mix on the existing surface or applying slurry seal, cutback bitumen.

6 Compaction Characteristic of Marshall Mould

Types of aggregate used in this study have been procured from the Jhansi. The values of the physical properties of all the aggregates as obtained from the laboratory tests are presented in Table 2.

To investigate the compaction characteristics of asphalt mix, compaction tests were conducted in the laboratory. The hammer of Marshall Mould as used to compact Marshall Mould of 101.6 mm diameter 75.0 mm height and free fall of this hammer has been maintained as 457 mm in all the tests. In the present study initially, moulds were casted 75 number of blows both faces with varying asphalt content (3.9, 4.2, 4.5, 4.8 and 5.1%). Optimum asphalt content (OAC) is determined as per Sections 5.1 4 and 5.15 of MS 2.

After determine OAC, 75 moulds were casted at OAC, above and below OAC at 200, 300, 400, 500 and 600 blows each face of the Marshall moulds. The compaction energy per unit volume of Marshall Mould has been calculated by the standard formula as follows:

$$E = \frac{W \times h \times N}{V} \quad (1)$$

where

- V is the volume of compacted mix in the moulds;
- W is the weight of hammer;
- N is the number of blows imparted to the mix, and
- h is the height of fall of the hammer.

Mixing temperature was 163 °C, and compaction temperature varies from 155 to 85 °C. From Eq. 2, it may be concluded that compacting energy is proportional to number of blows. Different graphs have been plotted against number of blow, and same graphs may be applicable for compacting energy.

7 Analysis of Results

7.1 Influence of Compaction Energy on Density of Mix

The density versus compactive energy graphs for various asphalt contents are shown in Fig. 1.

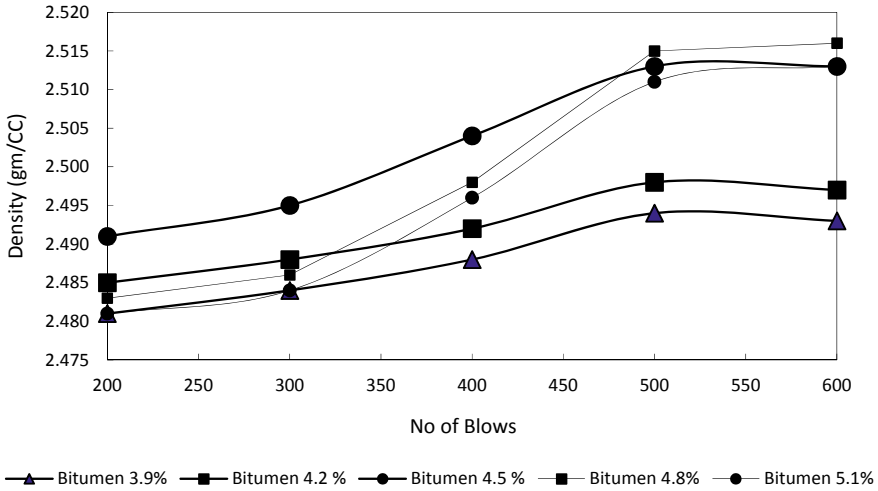


Fig. 1 Density versus compaction energy

From Fig. 1, it is noticed that with increase in compaction energy/no of blows (200, 300, 400, 500 and 600) Marshall Density increases at particular blow with increasing bitumen content. A semi-logarithmic plot (Fig. 1) of Marshall Density versus no of blow/compaction energy shows that their relationship is linear. The equation of the trend line is as follows:

$$\gamma = C_1 + C_2 \times \ln(E) \tag{2}$$

where

- γ Density of mix;
- E Compactive energy, and
- C_1 and C_2 Regression coefficients.

The regression coefficients, C_1 , C_2 and R^2 values for various asphalt content are shown in Table 3.

Table 3 Values of regression coefficients C_1 , C_2 , and R^2 at various asphalt content

Asphalt content (%)	C_1	C_2	R^2
3.9	2.4477	0.0124	0.926
4.2	2.4517	0.0124	0.926
4.5	2.4301	0.0226	0.937
4.8	2.3898	0.0339	0.900
5.1	2.3918	0.0325	0.910

7.2 Influence of Compaction Energy on Maximum Mix Density

In compaction of Marshall Mould, no. of blow/compaction energy is one of the vital parameters to achieve maximum mix density. From Fig. 2, it is revealed that the maximum mix density of all the mould samples of this study increases with increase in asphalt content up to certain limiting value for a given compacting energy. With further increase of asphalt content, the density decreases. Compacting energy varies from 5.13 to 41.5 kJ/Cum. But, this improvement of mix density of mould is prominent both at lower compaction energy level compared to higher compaction energy level. Maximum density was found at 4.5% asphalt content for all compactive energies. To study the trend for variation of maximum mix density with compaction energy, graph on maximum mix density versus compaction energy is plotted in Fig. 2. The trend line for all samples of this study may be presented in the following form:

$$\gamma_{\max} = Ax^3 + Bx^2 + Cx + E \tag{3}$$

The values of regression coefficients *A*, *B*, *C*, *E* along with *R*² (determination coefficient) are shown in Table 4.

From Fig. 2, data points clearly seem to have a sigmoidal shape. It seems to be that a plausible explanation for this exists in the breakdown of aggregate. Going from 200

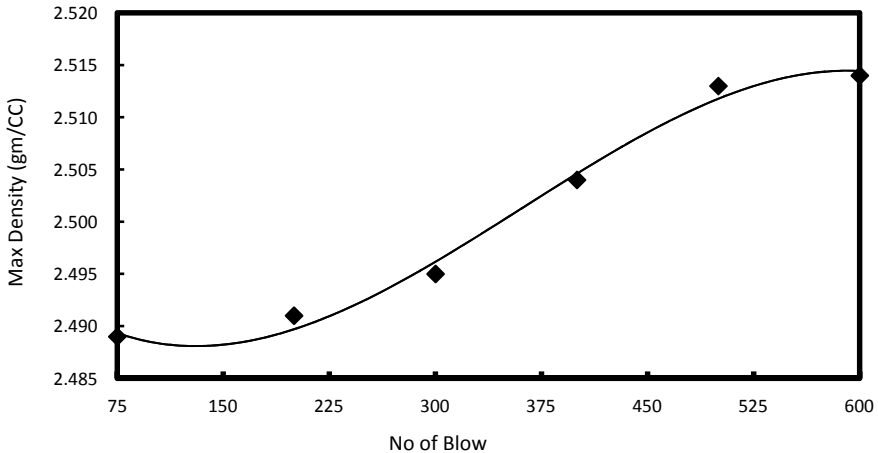


Fig. 2 Maximum mix density versus compactive energy at optimum asphalt content

Table 4 Values for regression coefficients (*A*, *B*, *C*, *E*) and determination coefficient (*R*²)

<i>A</i>	<i>B</i>	<i>C</i>	<i>E</i>	<i>R</i> ²
-2×10^{-6}	0	-0.001	2.495	0.991

blows to 300 to 400 to 500, it may be possible that aggregate particles are breaking, thereby allowing density to increase. From 500 to 600 blows, the aggregates are packed so tightly that further increase in density is not possible. It has been observed from extracting the specimens after compaction; breakdown of aggregate was not noticed. This may be due to specific gravity is high, and the water absorption is low. Together this suggests the aggregate is quite resistant to breakdown.

From Fig. 2, it has been found that with an increase in compaction energy maximum mix density (MMD) increases. This increase in maximum mix density may be due to closer packing of the particles at high energies. Equation 4 can be used to estimate MMD for a given compaction energy. However, if compaction energy at 75 number blows (E_{75}) and maximum density at 75 blows (MMD_{75}) for mix are known, MMD for mix can be estimated for any compaction energy E_n , by Eq. 5, given below:

$$MMD_n = MMD_{75} \times \left(0.9972 + 0.0017 \times \frac{E_n}{E_{75}} \right) \tag{4}$$

The values of estimated maximum mix density obtained from the above expression are also plotted in Fig. 3. Relevant statistical coefficients like, multiple coefficient of determination (R^2) is determined. The values of $R^2 = 0.92$ show the validity of the Eqs. (4, 5) for practical purposes.

Air void versus compaction energy for various asphalt content is shown in Fig. 4.

Air void (AV) decreases with increase of compaction energy (E) for a given asphalt content. Air void is higher at lower asphalt content and vice versa. At lower asphalt content, the graph is more or less linear and transition between linear and nonlinear at higher asphalt content. The best fit curve can be defined as mentioned below:

$$AV = G + H \times E \tag{5}$$

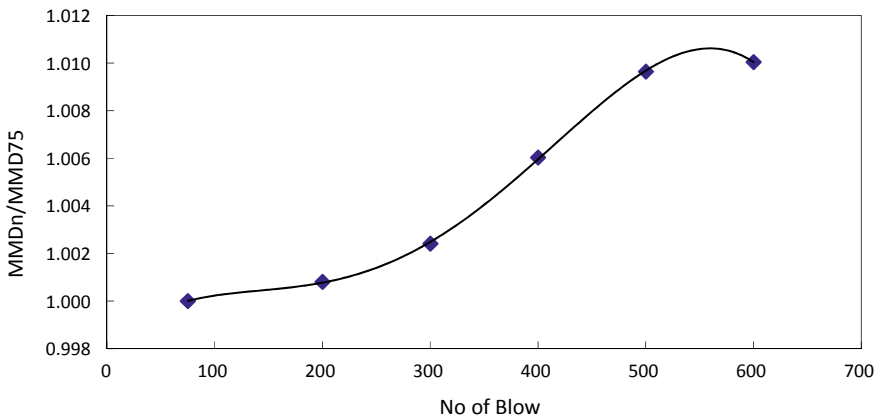


Fig. 3 MD_n/MD_{75} versus no of blow (E_n/E_{75}) at optimum asphalt content

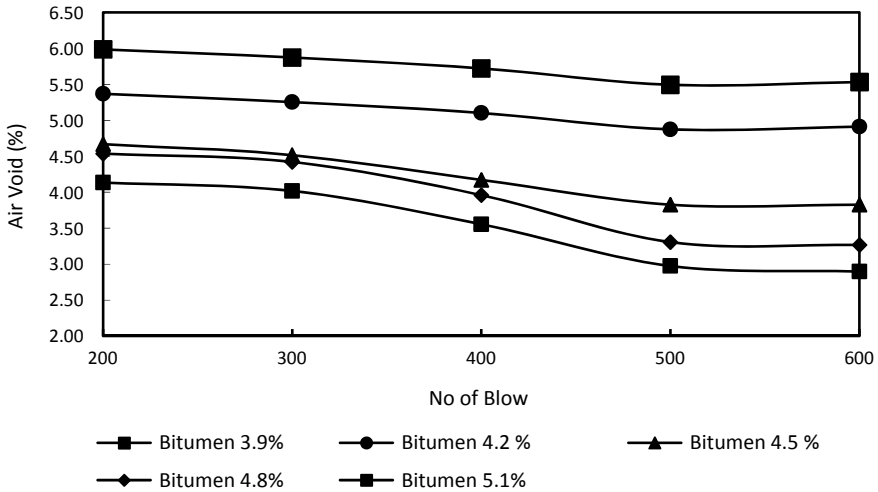


Fig. 4 Air void versus no of blow

where G, H are constant.

The values for G, H, R^2 for different asphalt per cent are shown in Table 5.

Air void has been found more or less same, i.e. constant between compaction energy between 35 and 41.5 kJ/Cum for all asphalt content.

Figure 4 shows that 4.5% asphalt binder content, the ‘correct’ content from the 75 blow Marshall Mix density reduces from 4.5% air voids at 100 blows to only 3.1% air voids at 600 blows. So that would say that even 600 blows adequately describe compaction that occurs under traffic.

Marshall Compaction has similarity to traffic compaction of mix on the road. The Marshall hammer produces very high pressure for short time periods (0.001 s or less), and truck tyres compact with a pressure a little higher than the tyre inflation pressure, may be 0.6 MPa. The pressure is applied for about 0.01 s (at 100 kph), longer time of loading for slower moving trucks, and there is shear forces induced. Thus, refusal density simulates field compaction at the end of design period.

From Fig. 4, it is also found that excess asphalt decreases air void at refusal density than that of less asphalt of optimum asphalt content. This means that asphalt content

Table 5 Values for G, H, R^2

Asphalt content (%)	G	H	R^2
3.9	6.2372	-0.0188	0.9175
4.2	5.6207	-0.0189	0.9175
4.5	5.1512	-0.0347	0.9403
4.8	5.3595	-0.0534	0.9312
5.1	4.9227	-0.0514	0.9432

less than optimum asphalt content (within permissible tolerance) will produce better performance of the road than excess asphalt content.

It will be advisable to construct road with asphalt content optimum asphalt content minus 0.3% as permitted specification. Minimum asphalt will also be checked.

Table 5 and Eq. 5 shall be used to determine air void at refusal density for practical purposes during execution of the work for known value of air void of Marshall Mould at laboratory or core from field. The value of *G* and *H* may be interpolated linearly for the asphalt content lying between two consecutive asphalt contents.

Similarly, VMA, VFA curves are plotted and shown in Figs. 5 and 6.

From Fig. 5, it is found that VMA decreases with increasing no of blow/compacting energy non-linearly, and variation is very small for compacting

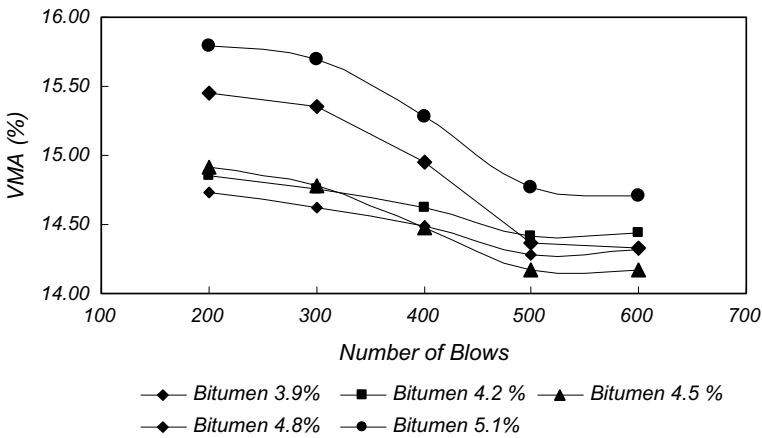


Fig. 5 VMA versus blows

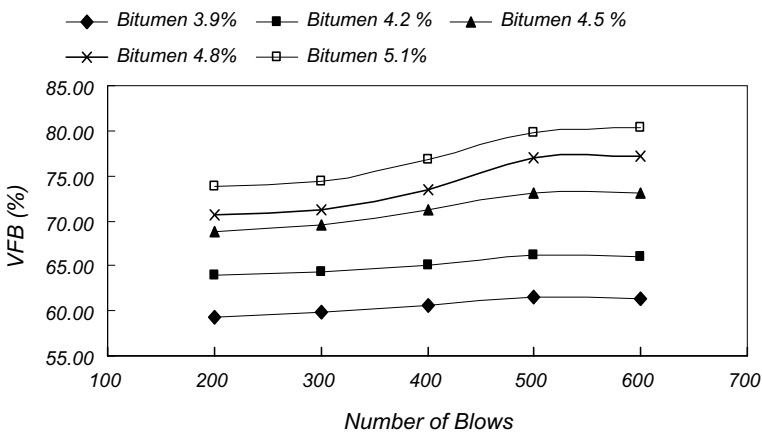


Fig. 6 VFA versus blows

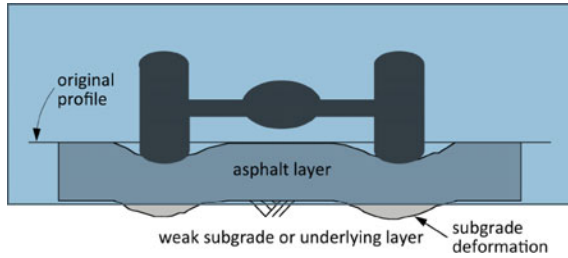


Fig. 7 Rut failure in subgrade layer. Source MS 2 2014

energy varying from 35 to 41 kJ/Cum/(500–600 blow). Similarly, from Fig. 7, it is found that VFA increases with increasing compacting energy non-linearly, and variation is very small for compacting energy varying from 35 to 41 kJ/Cum/(500–600 blows).

8 Requirement of Refusal Density During Mix Design Stage

Pavement mode of failures is rutting failure or fatigue failure. Rutting failure occurs in heavily traffic road through the world. Rut can be occurred in bituminous layer, granular layer, or subgrade layers of any combination of these. It is an important aspect to find out mode of failure using visual inspection. Typical photographs are shown in Figs. 7, 8, 9 and 10.

It is noticed that many projects in India rutting is one of the failure modes. These are found in several sections of NH 2. Mix design has been checked, and it is noticed



Fig. 8 Rut failure in bituminous layer. Source MS 2 2014

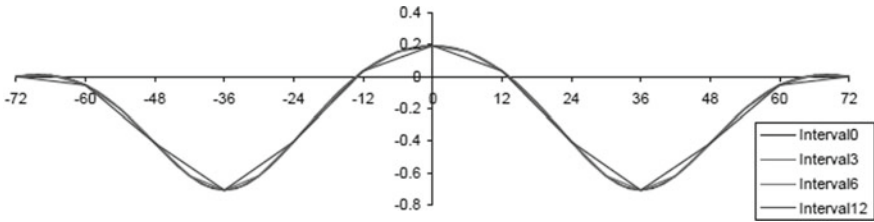


Fig. 9 Base failure

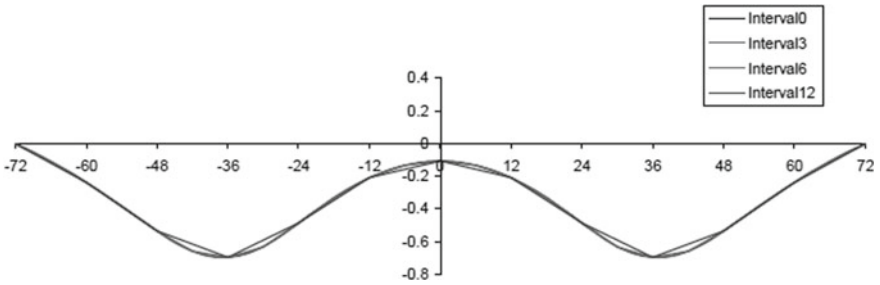


Fig. 10 Sub-base failure

that air void is found to be below 3% at refusal density, and subgrade failure occurred where CBR value is below 5%.

Transverse trench shall be excavated up to subgrade level to find out causes of rut as shown in Fig. 11, and rectification will be carried out accordingly.

Therefore, refusal density test should be conducted during preparation of mix design, or rutting should be checked via wheel rut testing equipment available at market/research institute.

Fig. 11 Excavation of transverse at rut location



9 Conclusions

From the study, for the particular mix with PMB 70, it may be concluded (similar trend may be obtained for other similar mix which may be confirmed during particular tests):

- Mix design of bituminous concrete can be checked at refusal density.
- Density varies linearly with compaction energy (semi log graph), or number of hammer blows with positive slope up to refusal density. After refusal density, density does not increase because of extreme packing of the particle.
- Compaction energy per cubic metre volume can be determined as mentioned in Eq. 2.
- Maximum density at any blow can be determined by developing similar formula as mentioned Eq. 5.
- Air void at known compaction energy can be determined by developing similar formula mentioned in Eq. 6.
- Laboratory and field compaction can be simulated using the methodology described in the present paper.
- Asphalt content should be optimum asphalt content minus tolerance of 0.3% for good future performance of the road.

References

1. Swanson RC, Nemej J Jr, Tons E (1966) Effect of asphalt viscosity on the compaction of bituminous concrete. Highway Research Record No. 117, Highway Research Board, Washington DC
2. Smith RW (1979) Purposes and reasons for compacting asphalt mixtures. Improved asphalt performance through effective compaction
3. Epps JA, Gallaway BM, Scott WM Jr (1970) Long term compaction of asphalt concrete pavement. Highway Research Record No. 313, Highway Research Board, Washington DC
4. Asphalt Institute Manual Series No 2 (MS 2), Sixth Edition (1997) Mix design methods for asphalt concrete and other hot—mix types
5. Sridhar R, Sunil B, Nilanjan S, Girish S (2006) Refusal density concept for design of dense bituminous mixes. Highway Research Bulletin, Highway Research Board, Indian Roads Congress, Number 74, April Issue
6. Cooper KE, Brown SF, Pooley GR (1985) The design of aggregate grading for asphalt base course. In: Proceedings of the association of asphalt paving technologies, vol 54

Experimental Investigation on the Effect of Microwave Heating Technique on the Healing Characteristics of Bituminous Concrete Mixtures



Satya Lakshmi Aparna Noojilla and Kusam Sudhakar Reddy

1 Introduction

India, with a wide road network of 56.03 lakh kilometer [1], has majority of its roads constructed as flexible pavements with bituminous mixtures used in binder and surface courses. Major distresses in these pavements include fatigue cracking originating either from top or bottom of the bituminous layers and permanent deformation (rutting) along the frequently used wheel path. Fatigue cracking occurs mainly due to the repeated application of loads that induces micro cracks and these micro cracks coalesce to form macro cracks visible to naked eye. It not only reduces the load carrying capacity of the pavement but also aggravates the damage due to ingress of moisture into the pavement through the cracks. Thus, these cracks need to be sealed/repared periodically for better performance of pavement.

Bituminous mixtures have the intrinsic property of healing the damage during the resting time available between vehicular loads and with an increment in temperature of the mixtures and thus are expected to heal by themselves during hot summers and long rest periods resulting in the extension of service life. Bitumen, being a thermoplastic material, it behaves as a Newtonian fluid when heated above certain threshold temperature. This causes it to flow and diffuse across the cracks and recovers the strength [2, 3].

However, self-healing of bituminous mixtures depends on several factors which mainly include the climatic condition of the pavement which is practically difficult to control. Thus, improving the self-healing capability of bituminous mixtures by external means (supplying thermal energy and providing rest period by controlling the

S. L. A. Noojilla (✉) · K. S. Reddy
Department of Civil Engineering, Indian Institute of Technology, Kharagpur, India
e-mail: aparnanoojilla@iitkgp.ac.in

K. S. Reddy
e-mail: ksreddy@civil.iitkgp.ernet.in

traffic) is an interesting area that is being explored actively [4–6]. Heating by means of induction heating [5, 7], microwave heating [8–11], and infrared heating [12] has been explored by researchers to enhance the healing characteristics of bituminous mixtures. Cracking of surface layers and their repair and rehabilitation is major concerns for pavement engineers. If timely interventions can be made to decrease/heal the fracture damage in the layer, its life can be extended significantly. Heating the layer is a practical approach that can help the mix heal from fracture damage. Different heating techniques such as infrared heating method are currently being used for hot in place recycling method. Alternative methods of heating the pavement can prove to be beneficial, if found to be economically feasible. Thus, the present study aims at using microwave heating, a faster heating method and which produces smaller thermal gradients [8], for healing of bituminous mixtures with different rest periods.

2 Literature Review

2.1 *Healing of Bituminous Mixtures*

Healing of asphalt mixtures can be improved by active and external enhancement technologies [8]. Active enhancement technology can improve the healing ability through optimization of the materials and structure of asphalt. Whereas, external enhancement technology can improve the healing ability of mixture through delivering rejuvenating material [13] or thermal energy. Current work focuses on supplying thermal energy to bituminous mixture, thereby increasing the temperature of the mixture to a level that the binder can attain Newtonian behavior, thereby filling the cracks with a subsequent recovery of its initial strength. This is in accordance with the research done by Bhasin et al. [4] stating that providing external energy will significantly increase the rate of intrinsic healing and promote overall healing. The authors proposed intrinsic healing function which depends on material properties such as molecular weight, activation energy, and extrinsic properties such as pressure and temperature. A threefold increase in the healing rate was observed when the testing temperature was increased from 10 to 15 °C [14]. Bhasin et al. [4] reported that intermittent application of the thermal treatment, i.e., mixture heated to 50 °C for 20 min resulted in approximately 50% increase in the fatigue life of the mixture. Observations made on the effect of temperature on healing of asphalt mixtures thus made the researchers to adopt heating technologies that utilize the principles of electromagnetic induction, absorption of microwaves, and infrared waves for healing. This paper focuses on the enhancement in the healing of asphalt mixtures by supplying microwave energy.

2.2 Utilizing Microwaves

Researchers explored the usage of microwave technology for deicing the surface courses of roads and bridge decks during winter and for the recycling of road materials [15, 16]. As microwaves produce heat, the healing ability of bituminous mixtures by supplying microwave energy is being considered as an alternative heating technique [6, 8–11]. But, for the heating to be possible in the bituminous mixture, presence of microwave absorbing material (such as metallic minerals (magnetite, hematite)) is necessary. Most of the studies were carried out by adding suitable microwave absorbing additives (steel slag, graphite powder, ferrite powder, steel fiber, and carbon fiber) in the bituminous mixture and studying its healing ability under static and dynamic loading conditions and by considering several factors such as extent of damage, rest periods, and temperatures [2]. Most of the existing literatures highlight the healing behavior of the mixes when a microwave absorbing additive is added. However, for healing the cracks in existing pavements without any additives, the heating behavior of the bituminous mix when exposed to microwaves needs to be studied. Also, healing is observed to be dependent on the binder and gradation used to prepare mixture. At last, in all the previous laboratory studies, the specimen was exposed to microwaves from all the sides, however, if a suitable piece of equipment is made to deliver microwave radiation to the existing road surface, only top surface of the road will be exposed to microwave. This was considered in present study.

3 Objectives and Scope

The broad objective of the present study is to evaluate the microwave induced heating and healing behavior of bituminous mixtures. For this purpose, the following scope was selected.

- Bituminous concrete gradation (dense graded) specified by MoRTH, (2013) [17] with a nominal maximum aggregate size (NMAS) of 13.2 mm which is commonly used as a surface layer was selected for preparing mixes in combination with VG40 as binder.
- Heating studies were performed using microwave oven at different levels of power, and heating parameters were calculated to understand the heating behavior of bituminous mixtures.
- A three-step cycle of breaking–heating–healing of Marshall samples was performed and healing indices at different rest periods were obtained to understand the effect of rest period on the healing ability of the mix.

Table 1 Properties of binder used in the study

Property	Value	Test method
Penetration, pen	38	IS 1203 (1978) [19]
Softening point, °C	55	IS 1205 (1978) [20]
Complex modulus as ($G^*/\sin\delta$) as min. 1.0 kPa at 10 rad/s, at a temperature, °C	76	ASTM D7175 (2008) [21]
Mixing temperature (°C) at η of 170 cP	170	
Compaction temperature (°C) at η of 280 cP	157	

Table 2 Properties of aggregates used in the study

Property	Value	Test method
Combined flakiness and elongation index (%)	25	BIS:2386 (Part IV)—1963 [22]
Los Angeles abrasion value (%)	22	BIS:2386 (Part IV)—1963 [22]
Aggregate impact value (%)	15	BIS:2386 (Part IV)—1963 [22]
Water absorption (%)	1.8	BIS:2386 (Part IV)—1963 [22]
Coating and stripping bitumen and aggregate mix (%)	95	IS 6241—1971 [23]
Retained tensile strength (%)	91	AASHTO 283—2003 [24]

4 Experimental Methods

4.1 Materials and Equipment Used

The binder used in this study was VG40 graded as per IS 73 [18] and was supplied by Jalnidhi bitumen specialties pvt. ltd., Kolkata. Basic properties of the binder are given in Table 1. Aggregates were procured from a quarry located in Rampurhat, West Bengal and are of Basaltic in nature. Physical properties of aggregates are given in Table 2. A microwave oven (Bajaj 1701MT DLX), capable of producing microwaves with 2.45 GHz frequency, rated 700 W at full power was used to heat the mixture.

4.2 Calibration of Microwave Oven

As it is very difficult to measure the accurate output power of microwave utilized in heating any material, a simple method was adopted. At full power level of the oven, known quantity of double distilled water was kept inside the microwave for 15 s. The change in temperature was kept as the standard to determine microwave absorption ratio (MAR) of the aggregate (as defined in Eq. 1). Along with aggregates, graphite powder (metal with high microwave absorption) was also heated separately

Table 3 Microwave absorption ratio

Material	Heating time, <i>t</i> (s)	<i>T</i> _i (°C)	<i>T</i> _f (°C)	$\Delta T = T_f - T_i$ (°C)	$\Delta T/t$ (°C/s)	MAR
Distilled water	15	23.4	47.6	24.2	1.61	1
Graphite powder	15	25.4	104	78.6	5.24	3.25
Aggregate	15	25	30	5	0.33	0.207

*T*_i—Initial temperature; *T*_f—final temperature; ΔT —rise in temperature

to understand the relative extent of microwave absorption of aggregates. Table 3 shows the corresponding MAR values of water, graphite powder (metal with high microwave absorption), and aggregates. It is observed that the value of MAR of aggregates is comparatively lesser than that of water and graphite powder. However, the aggregates have a little microwave absorbing ability and when longer durations of exposure to microwaves are provided, required amount of heat can be produced in the mix containing aggregates.

$$MAR = \frac{(\Delta T/t) \text{ material}}{(\Delta T/t) \text{ distilled water}} \tag{1}$$

4.3 Preparation of Specimens

Bituminous mixture prepared with VG40 as binder and midpoint gradation of bituminous concrete (prescribed to be used as top surfacing layer for high traffic volume roads in India) with a nominal maximum aggregate size of 13.2 mm specified by MoRTH [17] was considered in this study. Marshall method of mix design with a compaction effort of 75 blows on each face was adopted and the optimum binder content was selected corresponding to a design air void content of 4%. Details about the volumetric parameters of design mix are given in Table 4.

Table 4 Volumetric parameters from Marshall method of design

<i>G</i> _{mm} [*]	Binder content (%)	VMA [*] (%)	VFB [*] (%)
2.592	5.66	14.94	72.7

*G*_{mm}—Theoretical maximum mix specific gravity, VMA—voids in mineral aggregate, VFB—voids filled with bitumen

4.4 Experiments

Heating characteristics: Heating studies on the mix were done by heating the cylindrical specimens using microwave oven (Bajaj 1701MT DLX) which works at a frequency of 2.45 GHz and rated at a maximum power of 700 W (Fig. 1) and various heating parameters such as heating rate and heating uniformity were observed. Thermal images were captured using FLIR thermal camera. An aluminum mold was used to enclose the samples while heating is carried out to insulate the sides of the sample from getting exposed to microwaves.

Healing cycle: Experiments involved in this study consist of three phases. They are testing of virgin samples to measure indirect tensile strength (ITS), heating, and further healing the failed samples and testing the healed samples to measure ITS.

Cylindrical samples were prepared at the corresponding optimum binder content, and their indirect tensile strength (ITS) values were obtained at 25 °C. This test temperature is chosen to have a convenient crack width in all mixes and to prevent any sample fail from brittle failure. The characterization of bituminous mixtures in terms of indirect tensile strength is evaluated by loading a Marshall specimen along diametric plane with a compressive load at a constant rate of 51 mm/min as per ASTM D 6931 [25]. The failed samples were heated using the microwave oven to attain a maximum temperature ranging from 95 to 100 °C measured over the top surface of the sample. A split mold fabricated with 1.5 mm thick aluminum sheet with a suitable base plate was used to hold the specimens for keeping them in the microwave oven so that only the upper surface is exposed to the penetration of microwaves and thus simulating the practical condition of heating in the field.

Parameters evaluated from the experiments

- i. *Indirect tensile strength:* Indirect tensile strength of bituminous mixtures is obtained by loading a cylindrical specimen across its vertical diametrical plane



Fig. 1 Sample with aluminum mold kept in microwave oven used in present study

at a specified rate of deformation and test temperature. The peak load at failure is recorded and used to calculate the indirect tensile strength (ITS) of the specimen as follows.

$$ITS = 2P/(\pi t D) \text{ in kPa} \tag{2}$$

where

- ITS Indirect tensile strength, kPa
- P Maximum load, N
- t Specimen height immediately before test, mm
- D specimen diameter, mm.

- ii. *Heating rate*: Heating rate is defined as the raise in temperature of the mixture per unit time of exposure to microwave irradiation. This parameter indicates the efficiency of the microwave source and microwave absorbing capability of the mixture as well.

Heating rate

$$\Delta = (T_f - T_i)/t \text{ in } ^\circ\text{C/s} \tag{3}$$

where

- T_f Final temperature on the surface exposed after time “ t ” seconds
- T_i Initial temperature on the surface exposed.

- iii. *Heating uniformity*: It is defined in terms of the temperature gradient that exists between top surface and the bottom surface of the sample (along the thickness) when it is exposed to microwaves

$$\text{Heating gradient} = (T_{\text{top}} - T_{\text{bottom}})/h \text{ in } ^\circ\text{C/mm} \tag{4}$$

where

- T_{top} Average temperature on the top surface of the sample
- T_{bottom} Average temperature on the bottom surface of the sample.

- iv. *Healing index*: The healing index of each sample at the end of healing cycle, HI is defined as the percentage of ITS recovered at the end of healing cycle.

$$HI = (ITS_f/ITS_o) \times 100 \tag{5}$$

where

- ITS_f ITS of the sample after healing cycle
- ITS_o ITS of virgin sample.

5 Analysis and Discussion

5.1 Heating Studies

Samples of bituminous mixture (without any microwave absorbing additive) were getting heated when exposed to microwaves. Thus, heating tests were separately conducted on both bitumen and aggregates and it was observed that the aggregates possess microwave absorbing ability and thus the bituminous mixes were getting heated as the aggregates absorb heat and transfer the heat to binder by thermal conduction. Though microscopic structural analysis of the aggregates was not performed in this study, there is a clear evidence of presence of hematite (Fe_2O_3) mineral in the basalt-based aggregates procured from the rocks in Rampurhat, West Bengal [26, 27]. As these minerals absorb microwaves and thereby, the aggregates were getting heated.

Table 5 shows the details of heating times and cooling times taken by the samples. Heating was studied at three different power levels of the oven (33, 66, and 100% of full level power) to understand the effect of power on the absorption of microwaves. It can be observed that, at higher power level, the heating gradient was reduced due to the increase in penetration depth of microwaves. Theoretically, penetration depth of the waves increases with increase in power level. In the present study, a general trend of increase in gradient with the power level was observed at higher power levels. Also, at lower power level, samples took more time to reach the considered temperature. Another parameter cooling time is defined as the time taken by the top surface of sample to reach till 60 °C (softening point of the binder). This will indicate the quantum of time during which the temperature of the mixture is above its softening point and at all power levels, it was observed to be approximately 20 min.

Efficiency of heating of the mixtures under microwave was quantified in terms of rate and uniformity of heating. The top surface of the sample was getting heated at a rate of 0.13 °C/s which is less than the heating rate of pure aggregates as bitumen by itself is non-responsive to microwaves, and transfer of heat was taking place from aggregates to the bitumen.

Uniformity of heating along the depth was measured in terms of the temperature gradient from top surface to bottom surface. There exists an average gradient of 30 °C

Table 5 Heating studies

Power level (%)	Heating time (min)	Heating gradient		
		Maximum temperature at surface (°C)	Maximum temperature at bottom (°C)	Gradient (°C/mm)
33	10	110	76	0.56
66	7.5	110	72	0.688
100	5	109	70	0.624

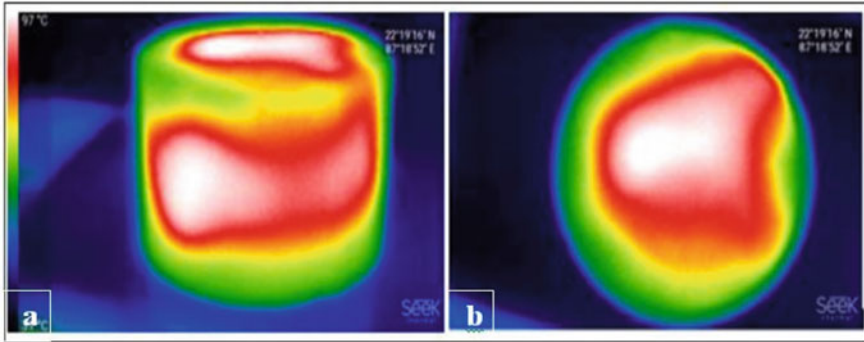


Fig. 2 Infrared images of heated samples **a** distribution of temperature along thickness, **b** distribution of temperature across the top surface of the sample

over a depth of 60 mm. Also, infrared images were taken on the top surface of the samples when the heating process was complete. Figure 2 shows the images which clearly indicate the presence of gradient in temperature on the surface and along the depth of the sample. The central portion of the sample has higher temperature (indicated by white color) than the surrounding portion which reinforces the fact that microwaves generate heat starting from the central portion and propagate to the surrounding portion.

5.2 Effect of Heating Only from Top Surface

Samples were enclosed in the aluminum collar (for the insulation purpose) and are heated to simulate the practical heating condition of pavement exposed to microwaves only on the top surface. The temperatures achieved by this process and the heating times required to achieve the required temperatures are compared with those of the samples heated without enclosure. Table 6 shows the details of the same. Though the heating time and gradient are higher for the sample with enclosure, it simulates the realistic condition of heating.

Table 6 Heating studies carried out with and without using insulation setup

Heating condition	Heating time (s)	Heating gradient (°C/mm)
Sample heated without mold	180	0.512
Sample heated with mold	300	0.624

5.3 Healing Studies

Figure 3 shows the images of samples before and after healing cycle. It can be clearly identified that the crack width was reduced after the healing cycle. After a cycle of breaking–heating–healing of the samples, average healing indices were calculated and reported in Table 7. There is a clear indication of increase of the healing ability with increase in rest period. Also, there is a statistically significant (95% level of confidence interval— p value <0.05) increment in healing index for a mix healed at 3 h compared to a mix healed at 24 h. However, there is no significance difference



Fig. 3 Crack width before and after heating and healing cycle

Table 7 Healing indices with different rest periods

Rest period (h)	ITS ₀ *	ITS _f *	HI*	Average HI % (SD*)
3	13.01	4.42	0.34	0.34 (0.072)
	11.72	4.90	0.42	
	12.42	3.40	0.27	
6	12.41	4.82	0.39	0.36 (0.021)
	10.71	3.72	0.35	
	11.54	4.15	0.36	
12	13.58	6.14	0.45	0.45 (0.026)
	11.59	5.35	0.46	
	13.12	5.4	0.41	
24	12.3	5.25	0.43	0.46 (0.039)
	11.7	5.92	0.50	
	11.58	5.4	0.46	

ITS₀—Indirect tensile strength of the sample before healing; ITS_f—indirect tensile strength of the sample after healing; HI—healing index; SD—standard deviation

between the healing indices at 12 and 24 h. Thus, based on the results obtained in the study, a rest period range of 6–12 h is being recommended.

However, heating ability of the mix varies with the change in aggregate type (different chemical composition). Thus, for healing a specific mix using microwave heating, first, its heating properties need to be checked and power level of the microwave needs to be adjusted to heat the specimen within a specified heating time.

In-place heating of pavements by techniques such as infrared heating is already in practice for applications such as hot in-place recycling. The cost of milling or completely removing the cracked bituminous layers is expected to make the proposed method of heating an economically feasible option. As the microwave heating method can be used for the mixes without any special additives for absorbing microwaves, the cost required for heating is the only issue to be considered. However, the transferability of this laboratory study to field implementation needs further studies so as to fix the heating time and power levels required. In that case, life cycle assessment of the pavement needs to be further performed to know the economic viability.

6 Conclusions

The main conclusions of this work are summarized below.

- The feasibility of heating bituminous mixes without additives by microwave method was demonstrated in this study.
- Bituminous mixtures prepared without any microwave absorbing additive were able to absorb the microwaves due to the presence of hematite mineral in the aggregates. Thus, this heating technique can be used for the pavements without adding any additives.
- Microwave heating produces non-uniform heating in the mixtures as the average temperature gradient of 0.5 °C/mm was observed along the depth of the specimen.
- Effect of power level on the heating properties was studied and it was observed that at higher power levels, heating uniformity is improved due to the deeper penetration of microwaves.
- In this study, the field condition of heating the pavement layer through its surface was mimicked by insulating all the sides except top surface of the sample by single split aluminum collar and heating by applying microwaves at the top surface. This resulted in exact estimation of the time required for heating the mixtures using microwaves.
- The duration of healing period has been found to have an effect on the healing characteristics of the mixes. The information generated from the present study will be useful for identifying the conditions to be adopted for microwave heating and healing of the cracks in field bituminous layers. For this, it is, however, required that a more detailed laboratory investigation is to be done followed by field validation of this recommended conditions.

References

1. Basic Road statistics of India, published by Ministry of Road Transport Highways, Transport research wing (2015–2016)
2. Sun D, Sun G, Zhu X, Guarin A, Li B, Dai Z, Ling J (2017) A comprehensive review on self-healing of asphalt materials: mechanism, model, characterization and enhancement. *Adv Colloid Interface Sci* CIS-01887
3. Sun D, Sun G, Zhu X, Pang Q, Yu F, Lin T (2017) Identification of wetting and molecular diffusion stages during self-healing process of asphalt binder via fluorescence microscope. *Constr Build Mater* 132:230–239
4. Bhasin A, Narayan A, Little DN (2009) Laboratory investigation of a novel method to accelerate healing in asphalt mixtures using thermal treatment, No. SWUTC/09/476660-00005-1. Southwest Region University Transportation Center, Center for Transportation Research, University of Texas at Austin
5. Liu Q, Schlagen E, García A, van de Ven M (2010) Induction heating of electrically conductive porous asphalt concrete. *Constr Build Mater* 24:1207–1213
6. Norambuena-Contreras J, Garcia A (2016) Self-healing of asphalt mixture by microwave and induction heating. *Constr Build Mater* 127:369–382
7. Garcia A (2012) Self-healing of open cracks in asphalt mastic. *Fuel* 93:264–272
8. Gallego J, Val MA, Contreras V, Paez A (2013) Heating asphalt mixtures with microwaves to promote self-healing. *Constr Build Mater* 42:1–4
9. Franesqui MA, Yepes J, García-González C (2017) Top-down cracking self-healing of asphalt pavements with steel filler from industrial waste applying microwaves. *Constr Build Mater* 149:612–620
10. Zhu X, Cai Y, Zhong S, Zhu J, Zhao H (2017) Self-healing efficiency of ferrite-filled asphalt mixture after microwave irradiation. *Constr Build Mater* 141:12–22
11. Wang Z, Dai Q, Porter D, You Z (2016) Investigation of microwave healing performance of electrically conductive carbon fiber modified asphalt mixture beams. *Constr Build Mater* 127:1012–1019
12. Breixo Gómez-Mejide V, Ajam H, Lastra-González P, Garcia A (2017) Effect of air voids content on asphalt self-healing via induction and infrared heating. *Constr Build Mater* 126:957–966
13. Micaelo R, Al-Mansoori T, Garcia A (2016) Study of the mechanical properties and self-healing ability of asphalt mixture containing calcium-alginate capsules. *Constr Build Mater* 123:734–744
14. Grant TP (2001) Determination of asphalt mixture healing rate using the superpave indirect tensile test. Master thesis of the University of Florida
15. Wang Z, Wang H, An D, Ai T, Zhao P (2016) Laboratory investigation on deicing characteristics of asphalt mixtures using magnetite aggregate as microwave-absorbing materials. *Constr Build Mater* 124:589–597
16. Benedetto A, Calvi A (2013) A pilot study on microwave heating for production and recycling of road pavement materials. *Constr Build Mater* 44:351–359
17. MoRTH Ministry of Road Transport Highways (2013) Specifications on road and bridge works, fifth revision. Indian Roads Congress, New Delhi
18. IS: 73 (2013) Paving grade bitumen. Indian Standards, New Delhi
19. BIS: 1203 (1978) Determination of penetration. Bureau of Indian Standards, New Delhi
20. BIS: 1205 (1978) Determination of Softening Point. Bureau of Indian Standards, New Delhi
21. ASTM D7175–15 (2008) Standard test method for determining the Rheological properties of asphalt binder using a Dynamic Shear Rheometer, West Conshohocken, United States
22. BIS: 2386 (1963) Methods of test for aggregates for concrete, Part 1V, mechanical properties. Bureau of Indian Standards, New Delhi
23. IS: 6241 (1971) Methods of test for Determination of stripping value of road aggregates. Indian Standards, New Delhi

24. AASHTO T 283 (2003) Standard method of test for resistance of compacted asphalt mixtures to moisture-induced damage. American Association of State Highway and Transportation Officials, Washington, DC
25. ASTM D 6931-07 Standard test method for Indirect Tensile (IDT) Strength of asphalt mixtures. American Society for Testing and Materials International
26. Patra PK, Mandal B, Chakraborty S (2010) Hydro geochemistry of fluoride rich groundwater in Birbhum District of West Bengal, India. *Eco Scan* 4(2&3):209–211
27. Ghosh S, Guchhait SK (2015) Characterization and evolution of primary and secondary laterites in northwestern Bengal Basin, West Bengal. *J Palaeogeogr* 4(2):203–230

Utilization of Waste Ethylene-Propylene-Diene-Monomer (EPDM) Rubber Modified Binder in Asphalt Concrete Mixtures



Ankush Kumar, Rajan Choudhary, and Abhinay Kumar

1 Introduction

Asphalt binder used in bituminous pavements is expected to show good waterproofing, durability, and bonding properties. The damage and deterioration of pavements caused due to heavy axle loads and tire pressures, high-temperature variations, and the substantial increase in the traffic volume have necessitated high-performing asphalt binders and mixtures. The most often utilized modifiers to asphalt binders are polymers and rubber. The polymers used to modify asphalt binders are categorized into elastomers and plastomers. Most common elastomers include styrene-butadiene-styrene (SBS) and polybutadiene, whereas commonly used plastomers are ethylene-vinyl-acetate (EVA), polypropylene (PP), polyethylene (PE), etc. [1–3]. Thermosetting rubbers such as crumb rubber obtained from scrap tires are also used in asphalt binder modification [4]. A polymer used in asphalt binder modification as a modifier should be compatible, not degrade at the mixing temperatures, and improve thermal sensitivity of the modified binder [5]. Because of the high cost of virgin polymers, sustainable and recyclable/waste polymers are also being explored for possible applications in the domain of pavement engineering.

The use of crumb rubber as an asphalt binder modifier has been widely studied [4, 6, 7]. However, rubber wastes generated from other non-tire automotive parts have garnered little attention so far. The non-tire automotive rubber parts account

A. Kumar · R. Choudhary (✉) · A. Kumar
Department of Civil Engineering, Indian Institute of Technology Guwahati, Guwahati, Assam,
India

e-mail: rajandce@iitg.ac.in

A. Kumar
e-mail: ankus174104035@iitg.ac.in

A. Kumar
e-mail: abhinay.kumar@iitg.ac.in

for about 30% of the total rubber consumed in a medium-sized vehicle [8]. This study is conducted to evaluate the characteristics of an asphalt binder prepared with waste ethylene-propylene-diene-monomer (EPDM) rubber. EPDM accounts for 50% of the non-tire automotive rubber parts such as weather strips and window seals [8]. A substantial quantity of EPDM rubber is produced as residual/waste from manufacturing units. This motivated the present study to explore the possible usage of EPDM rubber waste for its reutilization in asphalt binder modification.

The effect of adding EPDM rubber waste to asphalt binders on rutting, fatigue, and cracking resistance is discussed in this study. Rutting characterization of the binders is performed through Superpave and Shenoy rutting parameters and zero shear viscosity (ZSV). For fatigue evaluation, a dynamic shear rheometer (DSR)-based elastic recovery test is done at intermediate temperatures. The Glover-Rowe (*G-R*) parameter has been used to determine the asphalt binders' performance against cracking. Following the characterization of unmodified and EPDM modified binders, the asphalt mixture performance testing is conducted on mixture specimens fabricated with and without EPDM rubber modified binders. Marshall stability, tensile strength ratio (TSR), and resilient modulus tests are used to assess the influence of EPDM rubber waste on asphalt mixture characteristics. The stability test evaluates the resistance to deformation of the mixtures at high-service temperatures. TSR test is employed to measure the potential against moisture-induced damage, while resilient modulus test is employed to determine the stiffness characteristics of the mix specimens at intermediate and high-service temperatures.

2 Materials and Experiment

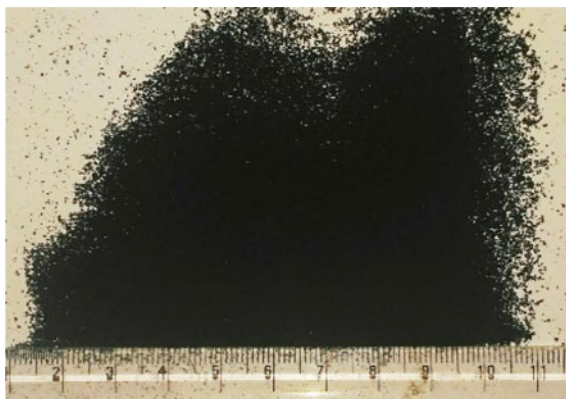
2.1 Materials

In this study, a virgin/neat viscosity graded 30 (VG-30) asphalt binder was adopted as the base binder. The physical parameters of the VG-30 binder satisfied the requirements stipulated in the Indian standard IS 73 [9] on paving bitumen. EPDM waste rubber granules used as the asphalt modifier were sourced from post-industrial residuals and were obtained from an industry in Delhi (India). The EPDM particles utilized were able to pass through a 300 μm sieve, and the specific gravity was found to be 1.16. Figure 1 shows the physical appearance of EPDM particles.

2.2 Formulation of Modified Binder

EPDM dosages between 0 and 8% (at an increment of 2% by binder weight) were used. For the preparation of modified asphalt blends, the neat/base binder was first heated up to 160 °C before blending with the desired quantity of EPDM granules. A

Fig. 1 Physical appearance of EPDM rubber waste particles



high shear mixer with rotor–stator arrangement was employed to prepare the blends at 8000 rpm for a blending duration of 45 min, and then, sulfur (0.3% by base bitumen weight) was introduced into the heated blend, and the blending was further continued for 15 min. Sulfur was used as a crosslinking agent in the modified binders.

2.3 Aging of Asphalt Binders

Asphalt binders were subjected for short-term aging for 85 min at the temperature of 163 °C in a rolling thin film oven (RTFO) following ASTM D2872 [10]. To obtain long-term aged binders, the RTFO-aged binders were further submitted to aging in a pressure aging vessel (PAV) at 100 °C under 2.1 MPa air pressure for 20 h as per ASTM D6521 [11].

2.4 Rheological Tests

The influence of adding EPDM to the base asphalt on rutting, fatigue, and cracking resistance of asphalt binder was evaluated through rheological tests. For high-temperature performance evaluation, a parallel plate geometry with a 25 mm diameter plate and 1 mm gap was utilized, while for intermediate temperature performance evaluation, an 8 mm diameter plate with 2 mm gap was employed for testing on a DSR. Various rheological tests used are described next.

Shenoy Rutting Parameter: As an alternative to the Superpave rutting parameter ($G^*/\sin \delta$), Shenoy [12] introduced a novel parameter termed as the Shenoy rutting parameter and is given by Eq. 1:

$$\text{Shenoy rutting parameter} : \frac{G^*}{1 - \frac{1}{\tan \delta \sin \delta}} \quad (1)$$

A higher value of this parameter is desirable as it corresponds to lower unrecovered (or plastic) strain in the binder [12]. Complex modulus (G^*) and phase angle (δ) were measured at 60 °C temperature and 10 rad/s frequency on RTFO-aged binders. Using Eq. 1, the Shenoy rutting parameter was determined for control and EPDM modified binders to understand their stiffness characteristics and rutting performance. The results of the Shenoy parameter were also compared with the Superpave rutting parameter ($G^*/\sin \delta$).

Zero Shear Viscosity: The viscoelastic nature of asphalt binders plays a pivotal role in the permanent deformation of flexible pavements. Change in the viscous behavior of asphalt material is a function of loading time and temperature. Zero shear viscosity (ZSV) of an asphalt binder has been put forward as a parameter that helps to compare the rutting resistance of asphalt binders. The ZSV represents dissipated movements in equilibrium “no-flow” structures that have been marginally perturbed [13]. In a frequency sweep test, mathematical models are commonly employed to predict viscosity at zero shear conditions using viscosity measurements. A frequency sweep test over a range of frequencies was performed at 60 °C with 0.1% strain, on RTFO-aged control, and EPDM modified asphalt binders. Cross-Sybilski model was used to estimate ZSV from frequency sweep data. Mathematically, the Cross-Sybilski model can be expressed as shown in Eq. 2:

$$\eta^* = \frac{\eta_0}{1 + (K\omega)^m} \quad (2)$$

Here, η^* = complex viscosity at frequency ω , η_0 = zero shear viscosity, K and m = model coefficients. Non-linear regression was performed on frequency sweep data to estimate the model parameters of Eq. 2.

DSR-Based Elastic Recovery (DSR-ER): The DSR-ER test measures the elastic response of asphalt binders at intermediate service temperatures under a monotonic loading. The test was carried out in line with AASHTO TP 123 [14] on PAV aged asphalt binders at 25 °C. The test consisted of the application of a constant strain rate (2.315% s⁻¹) for about 2 min until a strain of 277.78% was achieved. Thereafter, the binder sample was allowed to recover for 30 min under no shear loading. A typical DSR-ER output is depicted in Fig. 2. DSR-based elastic recovery is computed from Eq. 3:

$$\text{ER} = \frac{\varepsilon_2}{\varepsilon_1} \times 100 \quad (3)$$

Here, ε_1 = strain after two minutes and ε_2 = recovered strain.

Glover-Rowe Parameter: Glover-Rowe parameter determined on a DSR has been widely used as a method for investigating asphalt binders' cracking potential. This

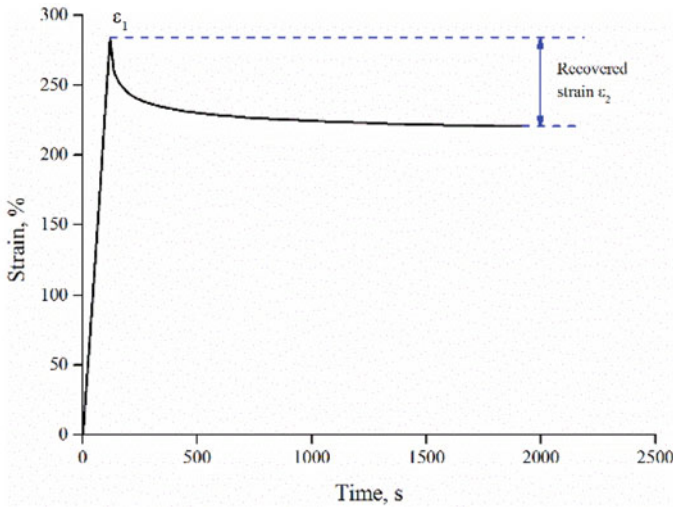


Fig. 2 A typical DSR-ER output

parameter is named after Glover et al. [15] who originally presented the parameter and Rowe [16] who simplified it in its present form. Glover et al. [15] presented a DSR function in the form of $G' / (\eta' / G')$ at 15 °C and 0.005 rad/s where G' is the storage modulus and η' is the dynamic viscosity and Rowe [16] further rearranged the version of Glover’s parameter to its present form given in Eq. 4:

$$G-R = \frac{G * (\cos \delta)^2}{\sin \delta} \tag{4}$$

The $G-R$ parameter is computed on PAV aged asphalt binders using G^* and δ at 15 °C and 0.005 rad/s. Because DSR testing at a low frequency of 0.005 rad/s is impractical, it has been recommended to execute the test at a temperature of 44.7 °C with a frequency of 10 rad/s [15, 17]. Two damage zones are identified based on Kandhal [18] durability thresholds, namely the beginning of the cracking zone with 180 kPa value of $G-R$ parameter equivalent to the ductility of 5 cm and significant damage zone with 600 kPa value of $G-R$ parameter equivalent to the ductility of 3 cm [19, 20].

2.5 Design and Evaluation of Bituminous Concrete Mixtures

Bituminous concrete (BC) Gradation II with 13.2 mm nominal maximum aggregate size (NMAS) was used for the preparation of asphalt mixtures (Fig. 3). In India, BC-II is a widely used flexible pavement wearing course and the mix design was performed using the Marshall method with a minimum of three specimens prepared at 4.5, 5.0,

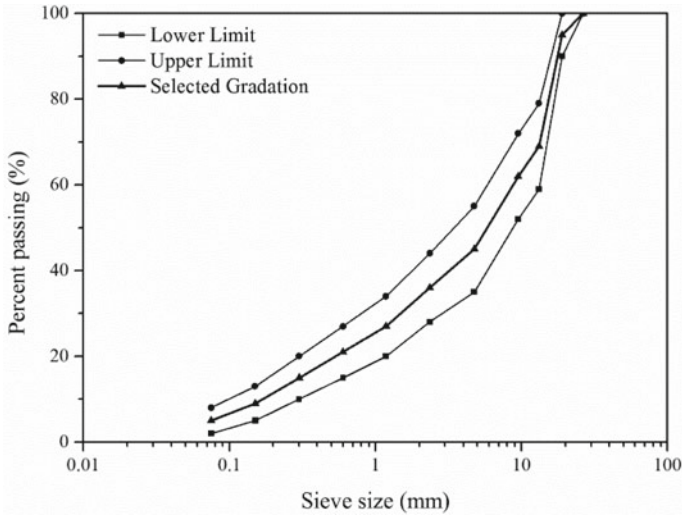


Fig. 3 Bituminous concrete (BC-II) gradation with specification limits

5.5, 6.0, and 6.5% binder contents (by weight of mix). The Marshall compactor was used to compact the specimens with 75 blows. At each binder content, Marshall parameters (stability and flow) and volumetric parameters (air voids, voids filled with asphalt (VFA), and voids in mineral aggregate (VMA)) were determined. Binder content to achieve 4% air voids and was selected as the optimum (found as 5.5%), which was then checked for other mix design requirements specified by MoRTH [21] that include Marshall stability (minimum 9 kN); Marshall flow (2–4 mm); VMA (minimum 14%); VFA (65–75%); and air voids (3–5%). Mix specimens containing EPDM modified binders were also prepared with the same OBC, with the intention that this approach allowed the comparison of all mixtures without binder content as an additional variable.

Stability and Flow: Marshall stability and flow tests were conducted as per ASTM D6927 [22]. Specimens were conditioned at 60 °C in a water bath for 30 min before testing in a digitalized Marshall machine (Fig. 4). After the conditioning period, specimens were removed, wiped dry with a towel, and promptly loaded in the Marshall testing head and the loading ram applied the load at a rate of 50.8 mm/min (2 in./min) until the maximum load was attained. The maximum load to failure was reported as the stability and the deformation at the point when load began to drop was considered to be the flow.

Tensile Strength Ratio: To assess the potential for moisture damage in compacted bituminous mixes, a tensile strength ratio (TSR) test was performed in compliance with AASHTO T 283 [23]. For each EPDM content, six mix specimens were compacted to achieve an air void content of $7 \pm 0.5\%$ and tested for evaluating unconditioned and conditioned indirect tensile strength (ITS) as per ASTM D6931

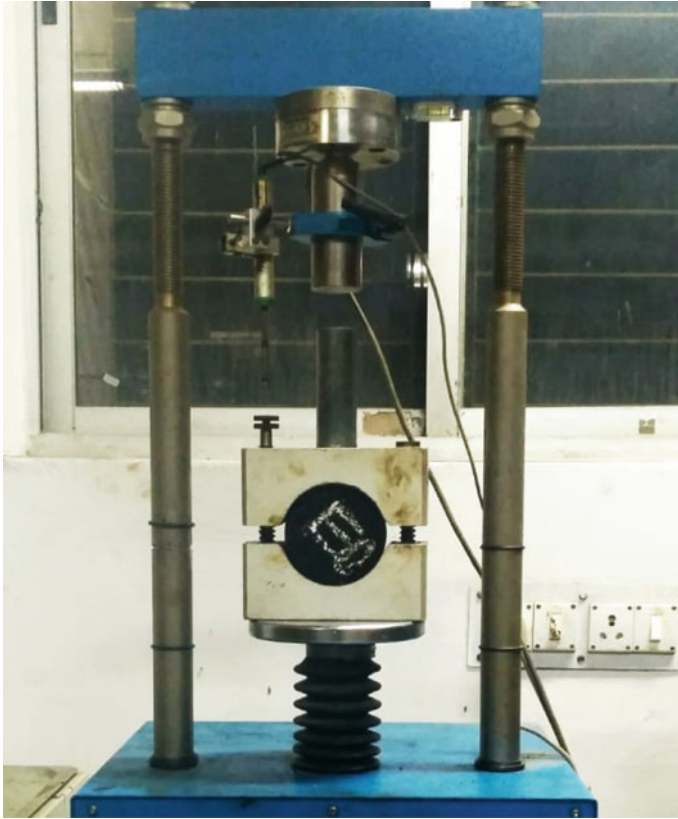


Fig. 4 Digitalized Marshall machine

[24]. Three specimens in the first set were partially saturated by the application of vacuum pressure. After that, the saturated samples were frozen at $-18\text{ }^{\circ}\text{C}$ for 16 h, then thawed for 24 h at $60\text{ }^{\circ}\text{C}$. The second set (the other three samples) remained unconditioned. All samples were kept at a constant temperature for 2 h in a water bath set at $25 \pm 0.5\text{ }^{\circ}\text{C}$. The ITS was then measured on both dry (unconditioned) and conditioned specimens. TSR was calculated using Eq. 5:

$$\text{TSR} = \frac{\text{ITS}_{\text{Conditioned}}}{\text{ITS}_{\text{Unconditioned}}} \quad (5)$$

Here, $\text{ITS}_{\text{Unconditioned}}$ = tensile strength for dry specimens, kPa; $\text{ITS}_{\text{Conditioned}}$ = tensile strength for freeze-thawed specimens, kPa.

Resilient Modulus: The resilient modulus (M_R) test predicts how a bituminous material will react to a repeated impulse or moving load imposed by a traffic/vehicle tire. The resilient modulus test was done in line with AASHTO TP 31 [25] at two

temperatures of 25 and 40 °C. To perform the test, four specimens were prepared at air voids in the range of $4 \pm 0.5\%$. One of the four Marshall samples was tested for ITS at 25 °C as per ASTM D6931 [24] to determine repetitive load level. The load levels at 25 and 40 °C were 15% and 5% of ITS, respectively. The resilient modulus test assembly is shown in Fig. 5 with a mix sample positioned between the top and bottom loading plates, and the mix samples were pre-conditioned prior to testing. A compressive repetitive load pulse (0.1 s load and 0.9 s rest) in the form of haversine wave was applied on the vertical diametric plane of the cylindrical specimen, and the horizontal deformation responses were recorded. At each test temperature, the first 100 repetitive load pulses were used for conditioning and the next 5 repetitive load pulses were used for calculating resilient modulus using Eq. 6.



Fig. 5 Test assembly for resilient modulus test

$$M_R = \frac{P(\mu + 0.27)}{H_r h} \tag{6}$$

where M_R = resilient modulus, MPa; P = repeated vertical load, N; H_r = total recoverable horizontal deformation, mm; h = mean thickness of specimen, mm; μ = Poisson’s ratio (0.35). After a 90° axial rotation, the test was repeated for each specimen and the final resilient modulus of one specimen was calculated as the mean of the observed modulus values.

3 Results and Discussion

3.1 Results on EPDM Modified Asphalt Binders

Shenoy Rutting Parameter: Fig. 6 shows the variation of Shenoy ($G^*/(1-1/(\tan \delta \sin \delta))$) and Superpave ($G^*/\sin \delta$) rutting parameters at 60 °C for EPDM modified asphalt binders. Both rutting parameters show an increasing trend as the EPDM rubber contents are increased. The $G^*/\sin \delta$ value of the control binder is 17.8 kPa, which increases to 30.0 kPa at 8% EPDM dosage. Further, $G^*/(1-1/(\tan \delta \sin \delta))$ value of the control binder is 29.9 kPa, which increases to 72.8 kPa at 8% EPDM dosage. These results indicate that adding EPDM to asphalt binder improves stiffness

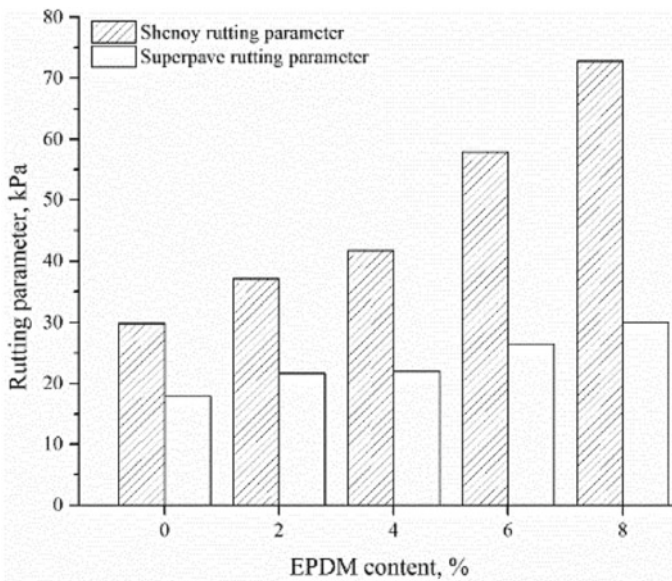


Fig. 6 Results of Shenoy and Superpave rutting parameters

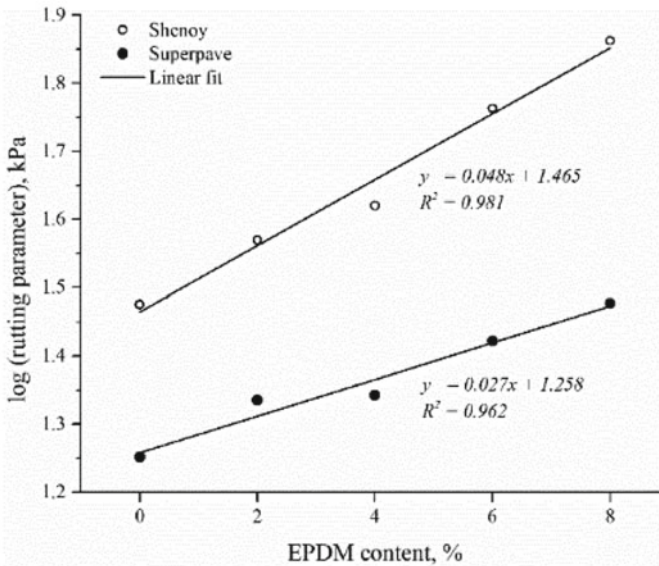


Fig. 7 Logarithmic plot of Shenoy and Superpave rutting parameters

and hence the resistance against rutting. It is also noted that higher values of Shenoy parameter are obtained compared to Superpave parameter at all EPDM dosages. Results indicate that the Shenoy parameter is more sensitive to EPDM dosage than the Superpave parameter. This finding is verified by comparing the slopes of the logarithm of the rutting parameter versus EPDM content plots shown in Fig. 7. The slope for the Shenoy parameter is greater than that for the Superpave parameter. Similar results have also been reported in the literature for other modified asphalt binders where both Shenoy and Superpave rutting parameters were investigated [26, 27].

Zero Shear Viscosity: The Cross-Sybilski model fit for the data produced in the frequency sweep test at 60 °C is shown in Fig. 8. It is observed that the model fits the experimental data well ($R^2 = 0.99$) for all the binders. The addition of EPDM to the binders produces a significant increase in the complex viscosity in the whole frequency domain which indicates the enhancement of stiffness characteristics of asphalt binders. The computed ZSV for the control and EPDM modified asphalt binders is shown in Fig. 9. The incorporation of the rubber modifier to the base binder increases the ZSV significantly. As EPDM is introduced, ZSV increases by 52, 78, 175, and 267% for sequential modifier dosages of 2, 4, 6, and 8%, respectively, when compared to the control binder. The increase in ZSV can be attributed to the EPDM rubber–asphalt interaction. After rubber–asphalt interaction, the development of an entangled network in the asphalt binder matrix enhances the viscosity and molecular weight of the asphalt binder [28]. The trend observed is desirable as the higher

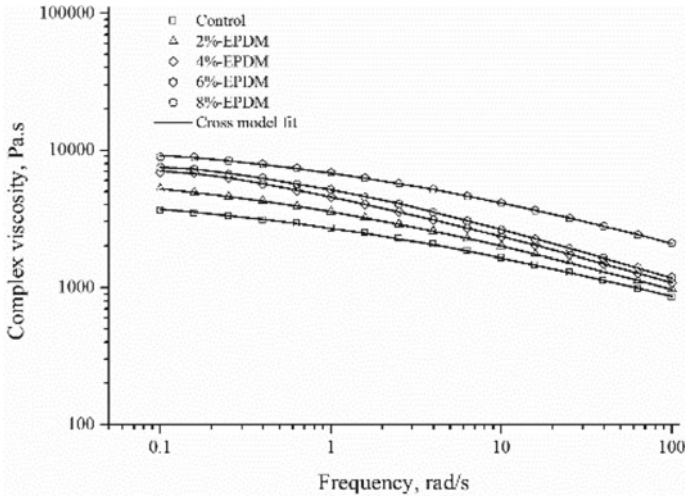


Fig. 8 Cross-Sybilski model fit

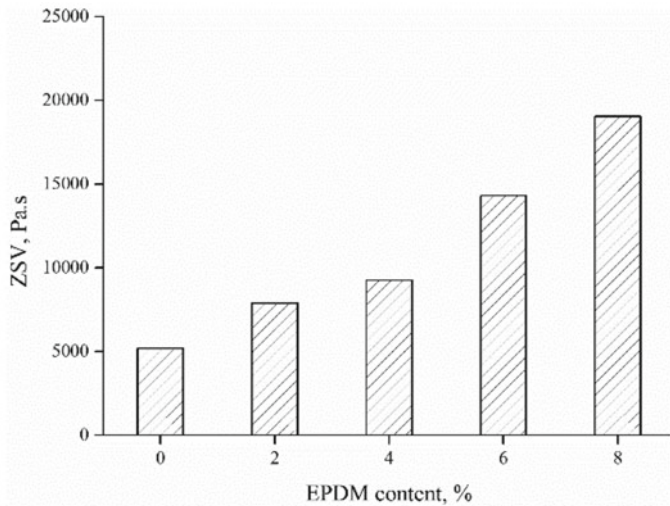


Fig. 9 Results of ZSV

ZSV for short-term aged asphalt binders indicates improved resistance to permanent deformation [29].

DSR-Based Elastic Recovery: Fig. 10 shows the outcomes of DSR-based elastic recovery. The incorporation of EPDM rubber waste improves the ER values, indicating that EPDM-modified asphalt binders have a better ability to recover from

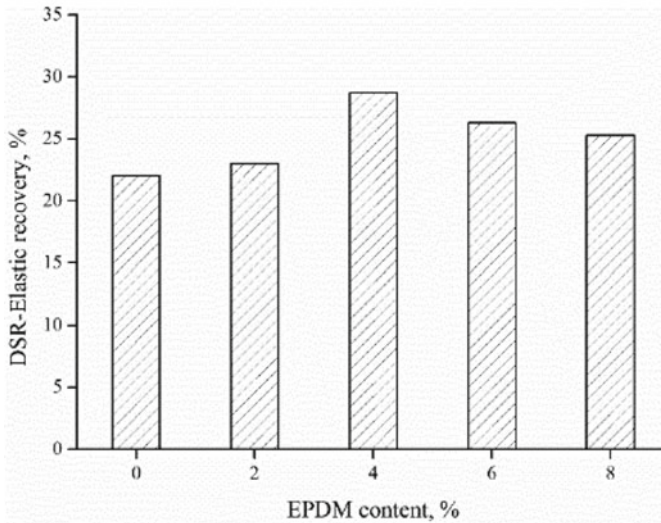


Fig. 10 Results of DSR-based elastic recovery

deformation. Maximum enhancement in ER is observed for 4% EPDM modified binder, with an increase of 30% in ER compared to the control. It has been reported that higher elastic recovery values indicate better fatigue performance [30]. The previous study revealed that DSR-ER has good correlations with the mixture fatigue performance [31]. A slight reduction in ER values beyond 4% EPDM dosage is observed and may be attributed to the over-stiffening of the binders at higher dosages. Fatigue performance of the mixtures would be useful in arriving at definite conclusions.

Glover-Rowe Parameter: The results of the $G-R$ parameter are presented in Fig. 11 with $\log G^*$ on the y -axis and δ on the x -axis. The figure also shows limiting curves identifying the beginning of the cracking zone and significant cracking zone. No significant cracking damage is expected for binders with $G-R$ parameter plotting below the significant cracking zone. The $G-R$ parameter plots below the significant cracking damage zone for all binders as shown in Fig. 11. It can be observed that with an increase in EPDM content the $G-R$ parameter plots toward low cracking risk zone, which suggests that the increasing EPDM content in PAV aged asphalt binders reduces their brittleness and therefore enhances the resistance of the modified binders to cracking. Thus, increasing the EPDM rubber component yields a decrease in the cracking susceptibility of the binders.

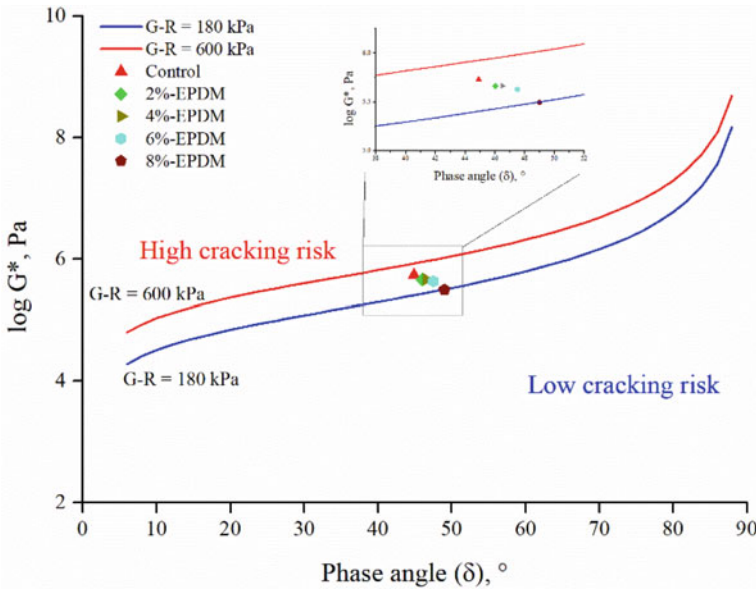


Fig. 11 Results of the *G-R* parameter on black space

3.2 Results on Asphalt Mixtures with EPDM Modified Binders

Stability and Flow: Fig. 12 shows results of Marshall stability and flow of the bituminous concrete specimens. The inclusion of the rubber modifier improves Marshall stability at 60 °C (a high in-service temperature). A maximum increment of 17% in stability is observed for 8% EPDM content as compared to the control mix. Higher stability values indicate improved strength and resistance to deformation of an asphalt mixture. All the mixes passed the minimum 9 kN stability requirement as per MoRTH specifications [21]. A decrease in flow is also observed with an increase in EPDM content. However, the mixes exhibited flow value in the recommended range of 2–4 mm as per MoRTH specifications [21].

Tensile Strength Ratio: Fig. 13 presents the tensile strength ratio (TSR) results. A low TSR indicates that the asphalt mixture is damaged by stripping and disintegration due to the freezing and thawing processes. As observed from the TSR test results shown in Fig. 13, mixes with EPDM modified asphalt binders showed greater resilience to moisture-induced damage than those with control binder. EPDM modified binders thus form a good bond with aggregates and have higher resistance to cohesive and adhesive damage. All mixtures including the control meet the limiting criteria of a minimum 80% TSR as per MoRTH specifications [21].

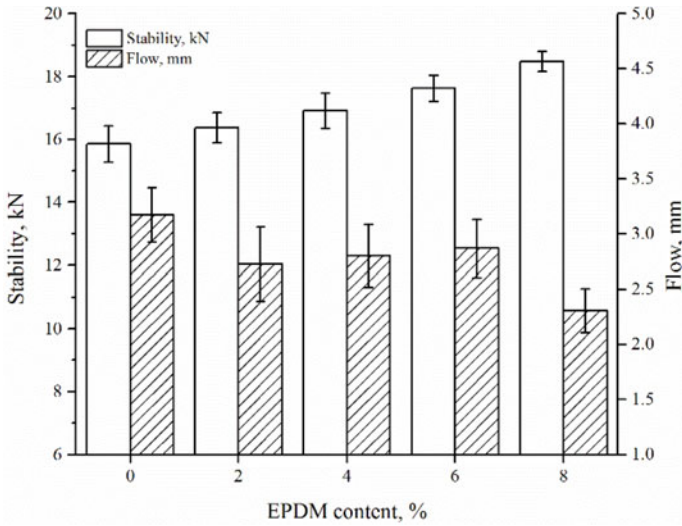


Fig. 12 Results of Marshall stability and flow

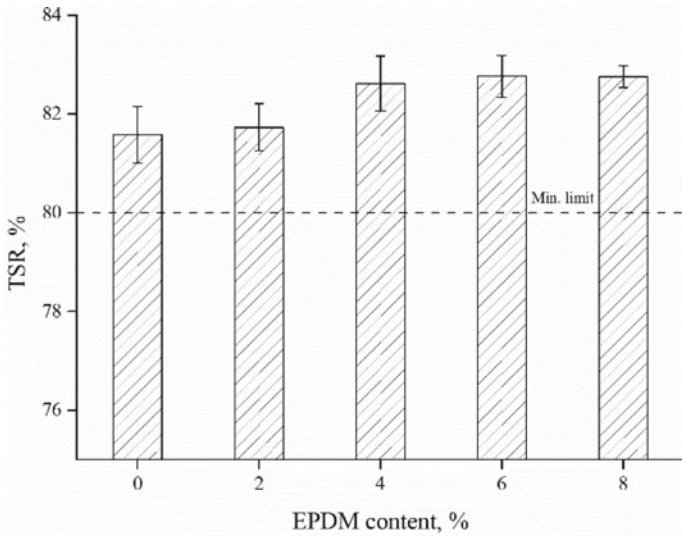


Fig. 13 Results of TSR

Resilient Modulus: Fig. 14 presents the results of resilient modulus determined at 25 and 40 °C test temperatures. At both test temperatures, the specimens produced with EPDM modified asphalt binders have greater M_R values than the control mixes. When tested at 25 °C, M_R values for EPDM content of 2, 4, 6, and 8% are slightly higher than the control mix by a margin of 1, 2, 7, and 10%, respectively. However,

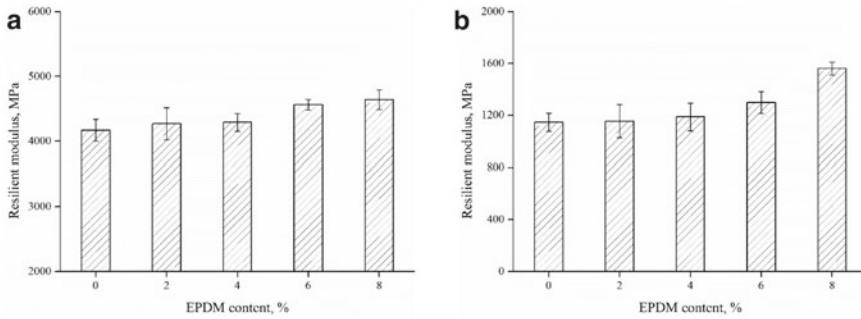


Fig. 14 Resilient modulus of mixes **a** at 25 °C; **b** at 40 °C

mixes containing EPDM modified asphalt binders exhibited 1, 4, 13, and 36% higher M_R values for 2, 4, 6, and 8% dosages of modifier, respectively, when tested at 40 °C. A higher M_R implies that the combination has a stronger capacity to recuperate the strains exerted by the loads. EPDM is a high-quality rubber that helps to enhance the stiffness and elastic behavior of asphalt binder and mixes. A high M_R value at intermediate to high temperatures (25–40 °C) is a desirable attribute to produce better performance for the bituminous mixes. Figure 14 also shows decrease in M_R values as the test temperature changes from 25 to 40 °C, which is likely due to reduced stiffness of binder that allows free movement of aggregate particles in the mix.

4 Conclusions

The present study investigated the influence of EPDM rubber waste sourced from the automobile industry as an asphalt binder modifier and its impact on the characteristics of mixes. The following conclusions are reached based on the findings and analyzes:

- Results of the high-temperature rheological tests showed that the rutting resistance of the binders improved with the incorporation of EPDM and further enhanced with increment in EPDM contents.
- Based on DSR-based elastic recovery results, it was found that the EPDM modified binders had higher elastic recovery than neat/unmodified binders. Fatigue resistance of the EPDM modified binders was optimum at 4% dosage.
- The Glover-Rowe parameter revealed that increasing the EPDM rubber dosages in the base asphalt resulted in a decrease in the cracking susceptibility of the binders.
- Mixture testing results showed that EPDM rubber waste enhanced Marshall stability and resilient modulus of the asphalt mixtures, indicating better performance against permanent deformation.

- Mixtures with EPDM also demonstrated better resistance against the effects of moisture with an enhanced tensile strength ratio obtained in the modified Lottman test.

References

1. Murphy M, O'mahony M, Lycett C, Jamieson I (2000) Bitumens modified with recycled polymers. *Mater Struct* 33(7):438–444
2. Airey GD (2002) Rheological evaluation of ethylene vinyl acetate polymer modified bitumens. *Constr Build Mater* 16(8):473–487
3. Kalantar ZN, Karim MR, Mahrez A (2012) A review of using waste and virgin polymer in pavement. *Constr Build Mater* 33:55–62
4. McNally T (2011) Introduction to polymer modified bitumen (PmB). Woodhead Publishing, Cambridge
5. Polacco G, Filippi S, Merusi F, Stastna G (2015) A review of the fundamentals of polymer-modified asphalts: asphalt/polymer interactions and principles of compatibility. *Adv Colloid Interface Sci* 224:72–112
6. Kandhal PS (2006) Quality control requirements for using crumb rubber modified bitumen (CRMB) in bituminous mixtures. *J Indian Roads Congr* 67(1):99–104
7. Sienkiewicz M, Borzędowska-Labuda K, Wojtkiewicz A, Janik H (2017) Development of methods improving storage stability of bitumen modified with ground tire rubber: a review. *Fuel Process Technol* 159:272–279
8. Fukumori K, Matsushita M (2003) Material recycling technology of crosslinked rubber waste. *R&D Rev Toyota CRDL* 38(1):39–47
9. IS 73 (2013) Paving Bitumen—specification. Bureau of Indian Standards, New Delhi
10. ASTM D2872 (2012) Standard test method for effect of heat and air on a moving film of asphalt (rolling thin-film oven test). ASTM International, West Conshohocken, PA
11. ASTM D6521 (2018) Standard practice for accelerated aging of asphalt binder using a pressurized aging vessel (PAV). ASTM International, West Conshohocken, PA
12. Shenoy A (2001) Refinement of the Superpave specification parameter for performance grading of asphalt. *J Transp Eng* 127(5):357–362
13. Liao MC, Chen JS (2011) Zero shear viscosity of bitumen-filler mastics. *J Mater Civ Eng* 23(12):1672–1680
14. AASHTO TP 123 (2016) Standard method of test for measuring asphalt binder yield energy and elastic recovery using the dynamic shear rheometer. American Association of State and Highway Transportation Officials, Washington, DC
15. Glover CJ, Davison RR, Domke CH, Ruan Y, Juristyarini P, Knorr DB, Jung SH (2005) Development of a new method for assessing asphalt binder durability with field validation. *Tex Dept Transp* 1872:1–334
16. Rowe GM (2011) Prepared discussion following the Anderson AAPT paper cited previously. *AAPT* 80:649–662
17. Anderson RM, King GN, Hanson DI, Blankenship PB (2011) Evaluation of the relationship between asphalt binder properties and non-load related cracking. *J Assoc Asphalt Paving Technol* 80:615–664
18. Kandhal PS (1977) Low-temperature ductility in relation to pavement performance. In: Marek C (ed) *Low temperature properties of bituminous materials and compacted bituminous paving mixtures*. ASTM International, West Conshohocken, PA, pp 95–106
19. Elkashef M, Williams RC, Cochran E (2018) Investigation of fatigue and thermal cracking behavior of rejuvenated reclaimed asphalt pavement binders and mixtures. *Int J Fatigue* 108:90–95

20. Garcia Cucalon L, Kaseer F, Arámbula-Mercado E, Epps Martin A, Morian N, Pournoman S, Hajj E (2019) The crossover temperature: significance and application towards engineering balanced recycled binder blends. *Road Mater Pavement Des* 20(6):1391–1412
21. MoRTH (2013) Specifications for road and bridge works (Fifth Revision). Indian Roads Congress, Govt. of India, Ministry of Road Transport and Highways, New Delhi
22. ASTM D6927 (2015) Standard test method for Marshall stability and flow of asphalt mixtures. West Conshohocken, PA
23. AASHTO T 283 (2003) Standard method of test for resistance of compacted asphalt mixtures to moisture-induced damage. American Association of State and Highway Transportation Officials, Washington, DC
24. ASTM D6931 (2017) Standard test method for indirect tensile (IDT) strength of asphalt mixtures. ASTM International, West Conshohocken, PA
25. AASHTO TP 31 (1991) Standard test method for determining the resilient modulus of bituminous mixtures by indirect tension. American Association of State and Highway Transportation Officials, Washington, DC
26. Nejad FM, Gholami M, Naderi K, Rahi M (2015) Evaluation of rutting properties of high density polyethylene modified binders. *Mater Struct* 48(10):3295–3305
27. Ashish PK, Singh D (2019) Effect of carbon nano tube on performance of asphalt binder under creep-recovery and sustained loading conditions. *Constr Build Mater* 215:523–543
28. Ragab M, Abdelrahman M (2014) Effects of interaction conditions on internal network structure of crumb rubber-modified asphalts. *Transp Res Rec* 2444(1):130–141
29. Morea F, Agnusdei JO, Zerbino R (2010) Comparison of methods for measuring zero shear viscosity in asphalts. *Mater Struct* 43(4):499–507
30. Clopotel CS, Bahia HU (2012) Importance of elastic recovery in the DSR for binders and mastics. *Eng J* 16(4):99–106
31. Kumar A, Choudhary R, Kandhal PS, Julaganti A, Behera OP, Singh A, Kumar R (2018) Fatigue characterisation of modified asphalt binders containing warm mix asphalt additives. *Road Mater Pavement Des*

Assessing the Suitability of Polyethylene Terephthalate (PET) in Bituminous Concrete Mixes



Mohit Chaudhary, Nikhil Saboo, and Ankit Gupta

1 Introduction

Due to their efficiency as well as their versatility, plastics have become an integral part of today's lifestyle. One cannot imagine any shelf in the house without a plastic product [1]. Plastic usage in India has increased from 0.061 million tonnes in 1996 to 13.5 million tonnes in 2011 and this figure is increasing every year indicating a very serious problem [2]. Around 55% of the plastic is being used for packing. They are littered after their use which is then mixed with domestic waste, making the disposal of municipal waste difficult [3]. Polyethylene terephthalate (PET) is a semi-crystalline polymer. It is thermoplastic and is produced from the synthesis of ethylene glycol and terephthalic acid. The rigorous use of PET in the last few decades makes it the most important plastic material [4]. It is light, safe, chemical resistant, and economical. Most commonly found in drinking bottles, the proper disposal of such enormous polymer waste has not been discovered. There are mainly two conventional methods to get rid of waste, i.e. incineration and landfilling. But both methods have adverse impacts on the environment in the case of plastic wastes. The incineration of plastic waste causes air pollution whereas landfilling may result in soil and water pollution. Hence, due to these issues, an alternate use for plastic wastes is highly essential.

The swift increase in traffic in the last few decades, as well as the change in vehicular characteristics such as maximum axle loads, has significantly increased

M. Chaudhary (✉) · N. Saboo · A. Gupta
Department of Civil Engineering, IIT (BHU), Varanasi 221005, India
e-mail: mohitchaudhary.rs.civ18@iitbhu.ac.in

N. Saboo
e-mail: nikhilsaboo.civ@iitbhu.ac.in

A. Gupta
e-mail: ankit.civ@iitbhu.ac.in

the stresses on the pavement [5]. The performance of flexible pavements can be affected by the changing climatic conditions, increasing tire pressure, wheel loads, and everyday wear and tear [6]. The severe stresses in the pavement can lead to premature failure with distresses such as rutting, ravelling, and fatigue cracking [7]. Therefore, the conventional methods of mix design which were designed decades ago for the traffic of that time need to be improved. Every pavement engineering research aims to improve pavement quality [8]. Considering the present scenario, the improvements in the quality of the pavement through modification of conventional material is the need of the hour. Out of various modification techniques, polymer modification has been considered as an effective technique to ameliorate the performance of the pavement. PET is a polymer that can also be used as a modifier in pavement application.

The two methods which are used to add the plastic to the asphalt mixture are the dry process and the wet process. In the dry process, the plastic is mixed with aggregate before adding bitumen, whereas in the wet process, the plastic is mixed with a binder before adding the binder into the mixture. In dry process, waste plastic in shredded form is added to the aggregates and mixed for 5–10 min. After that the bitumen in the required amount is added to the mix (Fig. 4). In wet process, firstly the bitumen is heated in the required amount on a controlled heating medium, and then the shredded waste plastic is added to the hot bitumen so that it is mixed properly and homogeneously with bitumen. After properly mixing bitumen and plastic, it is added to the aggregates (Fig. 5).

Parker and Gharaybeh [9] evaluated tensile strength ratios (TSR) to measure the performance of various hot mix asphalt (HMA) mixtures against stripping and concluded that TSR values can probably be a valid indicator of stripping performance. Vasudevan et al. [10] modified the rural and arterial road network by utilizing polypropylene and polyethylene bags in bitumen. A higher value of Marshall stability shows better performance of polymer modified bitumen. Rajan et al. [11] studied the effect of three variables, i.e. PET size, PET content, and mixing process in terms of volumetrics, Marshall parameters, and moisture susceptibility characteristics on the asphalt mixes. They concluded that the aforementioned properties are significantly affected by the variables.

Awwad and Shbeeb [12] added low density polyethylene (LDPE) and high density polyethylene (HDPE) to coat the aggregates by 6, 8, 10, 12, 14, 16, and 18% by weight of optimum binder content. It was concluded that HDPE enhances the asphalt mixture properties far more than those by LDPE. The optimum PE content was 12% by weight of bitumen as it provides the highest stability, bulk density, and minimum air voids. Ahmadinia et al. [13] suggested that 4–6% PET can be added to decrease drain down, and better rutting properties. Ebrahim and Behiry [14] used hydrated lime and Portland cement as anti-stripping additives and showed the better performance of hydrated lime. Quesada et al. studied the mechanical behaviour of asphalt mixtures using the Marshall stability, Marshall flow, and resilient modulus test by incorporating PET. The results showed that the performance of PET modified mixtures was much better than the traditional mixtures [15]. Attaelmanan et al. [16] incorporated 5% of high density polyethylene (HDPE) by asphalt weight as the modifier and

concluded that the moisture susceptibility and temperature susceptibility of the modified asphalt mixtures were reduced. Sui and Chen observed that the water resistance, low temperature cracking resistance, and high temperature stability were improved by using polyethylene as a modifier by dry method. The effects of incorporating waste polyethylene terephthalate (PET) on the properties of the bituminous mixture were studied by Moghaddam et al. [17]. They observed the increment in rutting properties under dynamic loading and decrement under static loading. The application of PET also decreased the Marshall quotient and indirect tensile strength values. Rahman and Wahab [18] replaced fine aggregates using recycled PET in modified asphalt and concluded that the addition of PET helps in decreasing rutting and the lowest permanent deformation is observed with 20% PET. Usman et al. [19] examined the stripping in aggregates by reinforcing recycled plastics in bituminous mixtures. The results showed that bituminous mixtures with 0.5% plastic fibre are the most effective in improving stripping resistance. Rodrigues et al. [1] suggested that the gradual addition of PET increased pulp consistency and elastic response. Higher oxidation levels resulted in anti-aging action.

This study has been taken up to assess and compare the effect of the wet and dry process of PET addition in bituminous mixes.

The principle objectives of this research are:

- To incorporate the waste plastic in shredded form in the bituminous concrete (BC) mix by the dry method as well as the wet method.
- To study the effects of adding polyethylene terephthalate (PET) as a partial bitumen replacement in bituminous concrete mixes.
- To analyse the performance of BC mixes in terms of Marshall stability, Marshall flow, and moisture susceptibility.

2 Experimental Work

2.1 Materials

The materials that are used in this research are:

- (a) Aggregates.
- (b) Bituminous binder.
- (c) Mineral filler.
- (d) Plastic drinking water bottles (waste PET).

The aggregates were collected from the quarry located at a short distance from Varanasi. The selected gradation of aggregates as per MORTH-2013 grading-I has been used. Bitumen of viscosity grade VG30 is used in this research. The same bitumen is used for all the mixtures so that the type and grade of the bitumen remain constant for all. The bitumen was collected locally from the Public Works Department (PWD) storehouse at Rajghat Varanasi. The filler used in this research was stone

dust. The shredded waste plastic drinking water bottles were used in preparing the samples. The drinking water bottles were collected from the conference held in the college (Fig.2) They were put in hot water for 3–4 h for cleaning after which they were allowed to dry. The waste plastic drinking water bottles (PET) were shredded manually in the size 1 cm * 1 cm with the help of cutters (Fig. 3) and then used in the mix for partial bitumen replacement. The aggregate gradation has been shown in Fig. 1. The conventional aggregate and binder properties as per Indian standards are shown in Tables 1 and 2, respectively.

The waste PET was used as a partial bitumen replacement by 0, 2, 4, 6, 8, and 10% by weight of bitumen. At each bitumen content, six samples corresponding to each plastic content are prepared. Therefore, a total of 216 samples were made, i.e. 108 each for dry as well as the wet process.

The samples are prepared according to the Marshall method of mix design which includes designing as well as evaluating properties of bituminous mixes. The

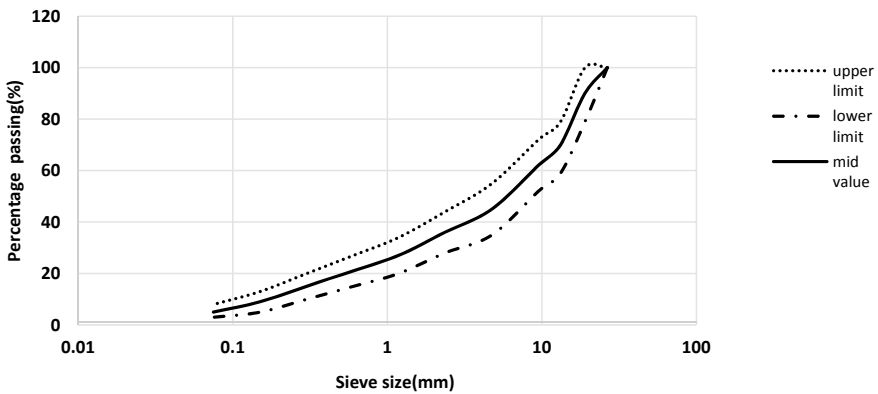


Fig. 1 Aggregate gradation

Table 1 Evaluated properties of aggregates

Type of test	Obtained values	IS specifications	Indian standards
Crushing	25%	MAX 30%	IS: 2386 (Part 4)
Los Angeles abrasion	26%	MAX 35%	IS: 2386 (Part 4)
Aggregate impact	20%	MAX 27%	IS: 2386 (Part 4)
Shape (combined flakiness and elongation)	21%	MAX 35%	IS: 2386 (Part 1)
Specific gravity (fine aggregates)	2.642	2.5–3.0	IS: 2386 (Part 3)
Specific gravity (coarse aggregates)	2.739	2.5–3.0	IS: 2386 (Part 3)
Water absorption	0.25%	MAX 2%	IS: 2386 (Part 2)

Table 2 Evaluated properties of bitumen (VG30)

Properties	Values	Specifications (IS: 73–2013)
Penetration	62	45 (minimum)
Softening point	55 °C	47 (minimum)
Absolute viscosity	3200 poise	2400–3600
Specific gravity	1.0134	0.97–1.02

**Fig. 2** Collected waste drinking water bottles

Marshall method is the most routinely used method to test the suitability of bituminous mixes. In the method, the compression test is carried out on a cylindrical specimen whose diameter is 101.6 mm and height is 63.5 mm. The test comprises measuring the resistance to plastic deformation of the specimen of the bituminous mix which is measured as the load taken at 50 mm/min till it fails. This resistance is known as the Marshall stability value. The deformation at the failure is also recorded in units of 0.25 mm which is known as the Marshall flow. The test procedure is repeated for no. of specimens having the same grade of aggregates with different PET contents and bitumen contents.

2.2 Moisture Susceptibility Test

The moisture susceptibility shows the sensitivity of the bituminous mixture towards moisture induced damage. The penetrated water weakens the bond between aggregate and binder which results in a many number of distresses such as cracking, potholes,



Fig. 3 Shredded PET bottles

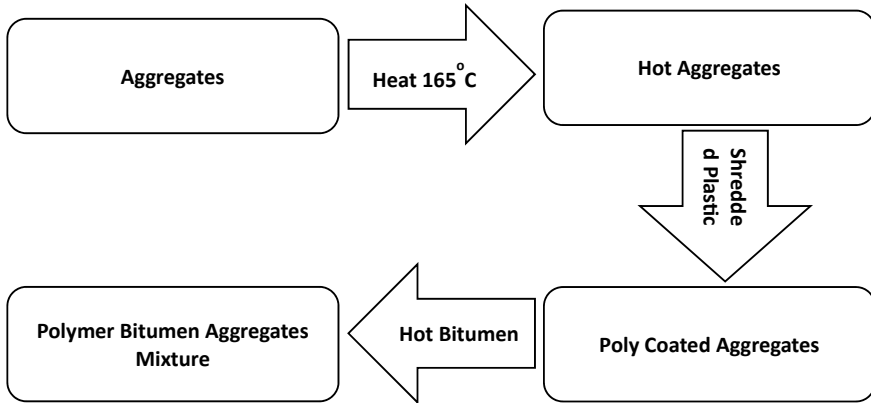


Fig. 4 Dry process of adding plastic

etc. Mineralogical and physical properties of aggregates, binder properties, improper construction practices, negligence of quality control during compaction, dynamic traffic loading effect, water quality are some of the factors behind the moisture induced damage.

The moisture susceptibility of the bituminous mixture is determined with the help of the indirect tensile strength (ITS) test as per ASTM D 4867. The tensile strength ratio (TSR) is a measure of moisture susceptibility which is the ratio of

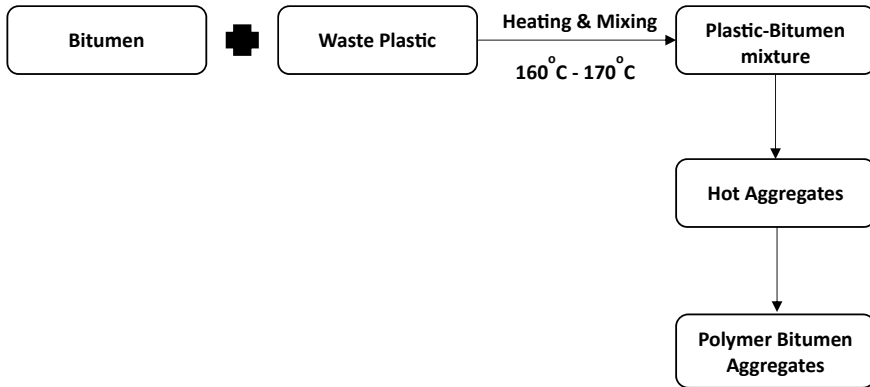


Fig. 5 Wet process of adding plastic

the tensile strength of water conditioned specimen (ITS wet, 60 °C, and 24 h) to the tensile strength of unconditioned specimen (ITS dry) expressed as a percentage. Conditioned and unconditioned specimens were tested for each group of mixtures. The unconditioned samples were kept in a water bath at 25 °C for 2 h and then the ITS test was conducted by loading the specimens at the suitable place in the Marshall stability test apparatus with a breaking head at a constant rate of 50 mm/min. Now measure the force required to fail the specimen and calculate indirect tensile strength (ITS) in dial gauge having a calibration factor of 3.455 and designate it as T_1 . The conditioning of specimens was done by vacuum-saturating for 30 min at 10–26 in. Hg partial pressure (13–67 kPa absolute pressure). The specimens were put in plastic bags containing 3 ml of water. The specimens were freezer for 16 h at – 18 °C to complete one freeze cycle and soaked for 24 h at 60 °C to complete one thaw cycle. After that the specimens were placed in water for 1 h at 25 °C and the ITS test was conducted and strength is designated as T_2 .

Now, the TSR is calculated by Eq. (1):

$$TSR = \frac{T_2}{T_1} * 100 \tag{1}$$

3 Results and Discussion

3.1 Marshall Stability

Figure 6a–c illustrate that the stability curve shows a similar trend approximately, i.e. first increasing, reaching a peak value, and then decreasing.

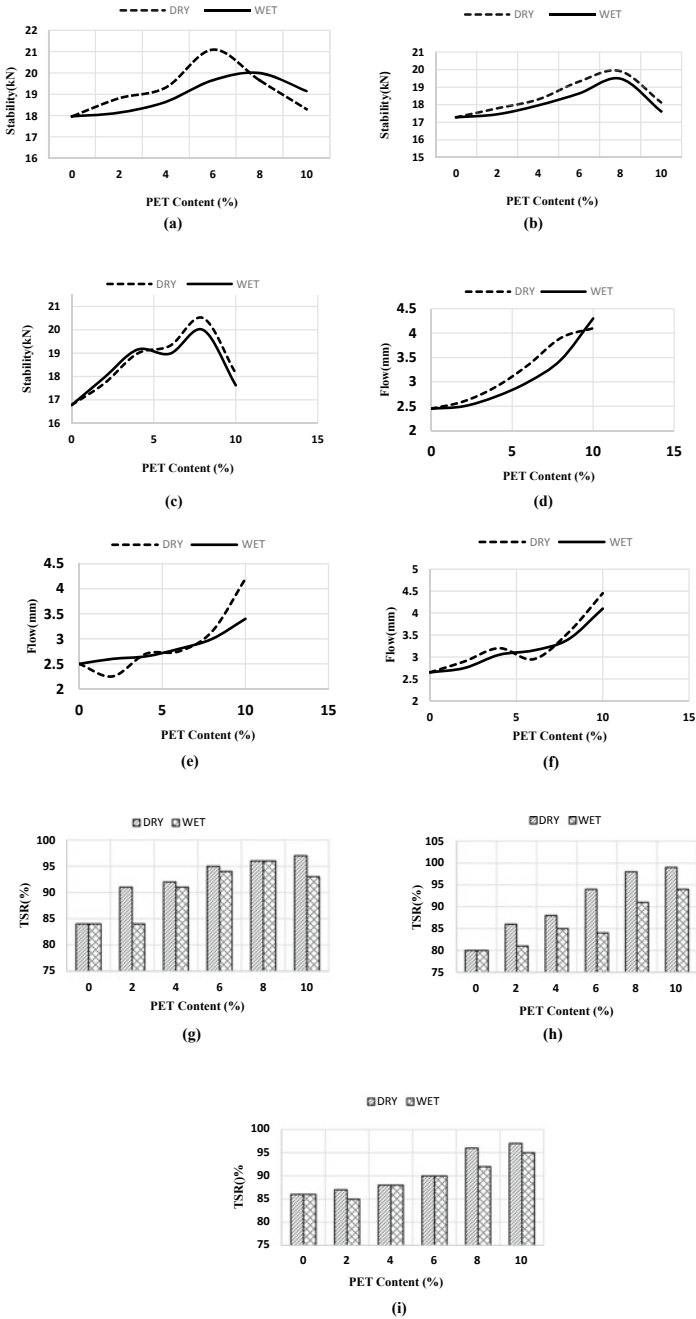


Fig. 6 Stability versus PET content at **a** 4.5% **b** 5% **c** 5.5% binder content, flow versus PET content at **d** 4.5% **e** 5% **f** 5.5% binder content, TSR versus PET content at **g** 4.5% **h** 5% **i** 5.5% binder content

At 4.5% bitumen content, when the PET is added, the stability value starts increasing with the increment in PET content. It follows the same increasing trend up to the 6% PET content in the dry process and 8% PET content in the wet process and reaches the peak value. After reaching the peak value, it again starts decreasing with an increment in PET content. This can be attributed to the fact that the increment in PET content improves the adhesion between aggregates and the binder but after a certain amount, the PET content becomes much more such that it starts hindering the bond between binder and aggregates. Hence, it starts decreasing after a certain plastic content because the cavities in the mixture become higher than before. The bitumen content is increased by an amount of 0.5% and reached to 5%. From Fig. 6b, it is observed that when the PET content is increased from 0 to 10% with an increment of 2% each time, the stability values also start increasing as the plastic content increased. The stability value starts increasing and continues to follow the increasing trend till the PET content reaches to 8% and reaches the peak value. It is noted that when the PET content is further increased after 8%, the stability value starts decreasing and continues to decrease for the remaining plastic contents which may be due to the slippery effect of the excess plastic content. The stability curves for both the dry process and wet process follow almost the same trend throughout the process. The stability curves corresponding to 5.5% bitumen content also show a similar trend to the above curves but in this case, the stability values corresponding to the wet process is greater than that of dry process at low PET content, i.e. up to 4% but after that as the PET content increases.

It is clear that the value of Marshall stability increases on the increment of PET content. This shows that the load bearing capacity of the specimen increases on partial replacing the bitumen with waste plastic. From the figures, it is evident that peak stability value generally reaches at 8% PET content. Therefore, it can be inferred that up to 8% of waste plastic can be used in bituminous concrete mixes for better strength. The peak value in the dry process is generally greater than that of in wet process because, in dry process, plastic forms a coating over aggregates to induce proper adhesion but in the case of the wet process, PET and binder are mixed first and then added to aggregates due to which there is unevenness and proper adhesion could not be provided by the plastic.

3.2 Marshall Flow

As displayed in Fig. 6d, an increase in PET causes the flow value to increase continuously up to 10% PET content for both the dry and wet process at 4.5% bitumen content. For 5% bitumen content, the flow value decreases slightly at 2%, but then it starts increasing and continues to increase up to the 10% plastic content in the dry process whereas for the wet process the flow value continuously follows the increasing trend with the addition of PET. The plastic when heated with mix becomes soft and in a molten state due to which it provides lubrication which increases the flow value.

According to Fig. 6f, for 5.5% bitumen content, the flow value for both dry process and wet process increases on increment in PET content except at 6% in the dry process where it shows a decreasing value then again increases further. All the Marshall flow values are within the permissible limits, i.e. 2–5 mm.

3.3 Tensile Strength Ratio (TSR)

From Fig. 6g, h, it is clear that the value of TSR increases with an increase in PET content for the dry process at each plastic content. Similarly, it also increases the wet process. The reason behind this is that the plastic forms coating on the aggregate in its molten state and strengthen the bond between aggregate and bitumen due to which the moisture fails to penetrate between and aggregate and hence the susceptibility of the modified mix decreases and it performs better. It shows a declining behaviour at 10% PET because the high plastic content does not allow a proper bitumen coating on the aggregates due to which the resistivity is slightly decreased.

For 5.5% bitumen content, the TSR value continuously follows the increasing trend with the addition of PET in the dry process. In the wet process, the TSR decreases slightly at 2%, but then it starts increasing and continues to increase up to the 10% plastic content. TSR value represents the moisture susceptibility of the mix and all the TSR values are above the minimum specified limits (80%) for both the dry process and wet process of adding plastic. Hence, it can be said that the addition of polyethylene terephthalate increases the moisture resistivity of the mixture. TSR values in the dry process of adding PET are always higher than the corresponding TSR values in the wet process because of the proper protective thin layer of plastic over aggregates in the dry process to resist the penetration of moisture as compare to the wet process.

4 Conclusions

This study presented the variation of Marshall stability, Marshall flow, and TSR of the bituminous concrete while replacing bitumen partially with polyethylene terephthalate (PET). The comparative analysis of both the mixing methods, i.e. dry method and wet method is also discussed. The primary conclusions drawn from the study are summarized as follows:

- (1) Test results showed that the value of Marshall stability increases on the increment of PET content. It is also evident that peak stability value generally reaches at 8% PET content. Therefore, it can be inferred that up to 8% of waste plastic can be used in bituminous concrete mixes for better strength.

- (2) The graphs of Marshall flow versus PET content show that the flow values increase on increasing the PET content. The values corresponding to the dry process are generally higher in comparison to the wet process.
- (3) All TSR values are more than 80% which indicates that all mixes can resist moisture induced damage to a good extent, therefore it is evident that the moisture resistivity of the mix increases with the addition of waste PET into it.
- (4) The values of Marshall stability, Marshall flow, and TSR are generally higher for the dry process in comparison to the wet process except at some PET content corresponding to bitumen content. Hence, it can be concluded that dry process of adding plastic to the mix is better than the wet process.



References

1. Rodrigues G, Carvalho MW, Costa DB (2015) Use of micronized polyethylene terephthalate (PET) waste in asphalt binder. *Pet Sci Technol* 33:1508–1515
2. Gawande A, Zamare G, Renge VC, Tayde S, Bharsakale G (2012) An overview on waste plastic utilization in asphalt of roads. *J Eng Res Stud* 3:1–5
3. Vasudevan R, Ramalinga Chandra Sekar A, Sundarakannan B, Velkennedy R (2012) A technique to dispose waste plastics in an ecofriendly way—application in construction of flexible pavements. *Constr Build Mater* 28:311–320
4. Hassani A, Ganjidoust H, Maghanaki AA (2005) Use of plastic waste (poly-ethylene terephthalate) in asphalt concrete mixture as aggregate replacement. *Waste Manag Res* 23:322–327
5. Sk AS, Prasad KSB (2012) Utilization of waste plastic as a strength modifier in surface course of flexible and rigid pavements. *Int J Eng Res Appl* 2:1185–1191
6. Kok BV, Yilmaz M (2009) The effects of using lime and styrene—butadiene—styrene on moisture sensitivity resistance of hot mix asphalt. *Constr Build Mater* 23:1999–2006
7. Gorkem C, Sengoz B (2009) Predicting stripping and moisture induced damage of asphalt concrete prepared with polymer modified bitumen and hydrated lime. *Constr Build Mater* 23:2227–2236
8. Sarang G, Lekha BM, Krishna G, Shankar AUR, Sarang G, Lekha BM, Krishna G, Shankar AUR (2016) Comparison of stone matrix asphalt mixtures with polymer-modified bitumen and shredded waste plastics. *Road Mater Pavement Des* 17:933–945
9. Parker F, Gharaybeh FA (1988) Evaluation of tests to assess stripping potential of asphalt concrete mixtures. National Research Council, Transportation Research Board, pp 18–26
10. Vasudevan R, Chandra AR, Sundarakannan B, Velkennedy R (2012) A technique to dispose waste plastics in an ecofriendly way—application in construction of flexible pavements. *Constr Build Mater* 28:311–320
11. Rajan C, Kumar, Murkute K (2018) Properties of waste polyethylene terephthalate (PET) modified asphalt mixes. Dependence on PET size, PET content, and mixing process. *Periodica Polytech Civ Eng* 3:685–693
12. Awwad MT, Shbeeb L (2007) The use of polyethylene in hot asphalt mixtures. *Am J Appl Sci* 4:390–396
13. Ahmadinia E, Zargar M, Karim MR, Abdelaziz M, Ahmadinia E (2012) Performance evaluation of utilization of waste polyethylene terephthalate (PET) in stone mastic asphalt. *Constr Build Mater* 36:984–989
14. Ebrahim A, Behiry AE (2013) Laboratory evaluation of resistance to moisture damage in asphalt mixtures. *Ain Shams Eng J* 4:351–363

15. Quesada M, Raposeiras AC, Olavarr J (2019) Effects of recycled polyethylene terephthalate (PET) on stiffness of hot asphalt mixtures. *Adv Civ Eng*
16. Attaelmanan M, Pei C, Ai A (2011) Laboratory evaluation of HMA with high density polyethylene as a modifier. *Constr Build Mater* 25:2764–2770
17. Moghaddam TB, Soltani M, Karim MR (2014) Experimental characterization of rutting performance of polyethylene terephthalate modified asphalt mixtures under static and dynamic loads. *Constr Build Mater* 65:487–494
18. Mohd W, Wan N, Rahman A, Fauzi A, Wahab A (2013) Green pavement using recycled polyethylene terephthalate (PET) as partial fine aggregate replacement in modified asphalt. *Procedia Eng* 53:124–128
19. Usman N, Idrus M, Masirin M, Ahmad KA, Nda M (2018) The use of plastic fiber for minimizing stripping potential of bituminous mixture. *Int J Integr Eng* 10:113–118

Experimental Investigation of Resilient Modulus of Various Bituminous Mixes



Swapan Kumar Bagui, Atasi Das , Yash Pandey , and Kishan Vachhani

1 Introduction

The development of economy of any country depends on the development of its infrastructure. Since India is a developing economy, which needs a smart and well-organized infrastructure development. The development in infrastructure can be possible with the practical and experience gained and implemented timely. The highway development is one of the vital streams. The Indian Roads Congress (IRC), a non-profit Government organization responsible for developing, implementing, and maintaining the guidelines and specifications for the roads and bridges in India. The design guidelines IRC: 37-2012 (current revised version 2018) is predominant for the design of flexible pavement and it proposes to adopt MR as the key parameter for the design of flexible pavements.

The IRC guidelines suggest MR values at different temperatures for different types of bituminous mixes (dense graded bituminous macadam (DBM) and bituminous concrete (BC)) with modified and unmodified specimens of bitumen binder. As per the Indian codal provisions IRC 37 [1, 2], the MR has been assigned a particular value for bituminous mix prepared with a different bitumen. It recommends the MR value of 3000 MPa for bituminous mixes prepared with VG 40 grade of bitumen, 2000 MPa with VG 30 grade of bitumen and 1600 MPa with polymer modified bitumen (PMB). However, the MR varies differently for mixes with different binder. Although, the MR value of the PMB mix comes higher than as specified and vice

S. K. Bagui

Intercontinental Consultants & Technocrats Pvt. Ltd., Delhi 110016, India

e-mail: swapan.bagui@ictonline.com

A. Das · Y. Pandey (✉)

G R Infraprojects Limited, Gurugram 122015, India

K. Vachhani

Aadharshila Infratech Pvt. Ltd., Udaipur 313001, India

versa for VG 40. Also, the National Highway Authority of India (NHAI) mandates the use of stone matrix asphalt (SMA) in the wearing course for all the upcoming projects. However, no proper guideline is provided for the MR value achievable with the use of the SMA. Addendums in the IRC guidelines on SMA specify the use of VG 40 forthwith, which earlier had been VG 30. Again, there is no proper testing regime available with the users as to the design MR achievable with use of VG 30, VG 40, or PMB. Keeping all these practicalities in mind for design of pavement, this paper has been embarked on to reaching a solution of adoptable MR after holistic testing regime in the laboratory. For the construction of pavement, the crushed aggregates are used. It is required that the shape and size of material, i.e. it should neither be much flakey nor much elongated for the BC and DBM. For the same aggregates are required to be crushed in the crusher with a special attachment that is vertical shaft impactor (VSI). The VSI attachment takes care for the proper shape and size of the aggregates to be crushed out from the crusher.

In this investigation, BC and DBM mixes with VG 30, VG 40, and PMB bitumen were prepared and tested for MR values at temperatures 35 °C as per ASTM D4123 [3].

Also, the effect of non-VSI and VSI crushed aggregates and bitumen on resilient modulus calculated as per ASTM D 4123 [3] is done. The other mechanical parameters, i.e. Marshall parameters and indirect tensile strength (ITS) of the mix are within the limits as specified in MoRTH 2013 [4]. Since, the design of flexible pavements affects a lot due to change in resilient modulus of bituminous mix (keeping other parameters constant) so this study provides comparison of elasticity modulus for different bitumen and aggregate type. The comparison of practical MR value with the MR value calculated with the help of ITS using the different empirical methods available is also done.

2 Literature Review

Resilient modulus of bituminous mixes can be determined by testing the mix in the laboratory or it can also be predicted from the properties of mix materials, i.e. bitumen and aggregate.

The MR is the elastic modulus used for pavement design purpose. Since hot bituminous mixes fall in the category of viscoelastic materials, after application of every load cycle, permanent deformation is being experienced by it. Moreover, if the load applied is very less, as compared with the material strength itself, and after comparatively large number of repetitions of load application, the deformation is almost recovered completely. As the applied load and the deformation are proportional and also the deformation is almost recovered completely, it may be considered as elastic deformation.

The carrying out of MR test is difficult, and the instrument is very expensive, so a number of empirical models have been developed for MR predictions using mix properties. The MR test can be conducted on the Marshall's sample prepared in

laboratory or core extracted from field. For design consistency, the MR test results estimated from the laboratory prepared Marshall specimen should match with that obtained from field extracted cores and as estimated from empirical models.

Aggregates for infrastructure construction are follows a general procedure that is first the blasting of rocks then rock is disintegrated in chunks of stones. These chunks of stones are fed into the crusher and the aggregates are produced. These produced aggregates differ in shape and sizes that is it contains flakey and elongated aggregates. For utilization in road construction, it is necessary that the aggregates should be properly shaped and sized for which vertical shaft impactor (VSI) type crusher is used. Anvils and high-speed rotor are utilized for energy, needed for size reduction, rather than compression force in VSI crushers. Centrifugal force applied by rotor in VSI crusher accelerates the material towards outer anvil ring which breaks the rock or mineral along the natural faults. The final product is consistent and comprising of cubical shape which is excellent for utilization in flexible pavement applications.

3 Materials

VG 30, VG 40, and PMB 40 bitumen, antistripping agent (liquid type) and silica, granite and marble mixed type aggregates (VSI and Non-VSI) of different sizes were obtained from the nearby quarry to perform the research work. The VG 30 and VG 40 bitumen confirming to Bureau of Indian Standards (BIS) code 73-2013 (IS-73:2013) [5] and PMB 40 confirming to IS 15462-2004 [6] & IS 53-2010 [7] and the physical properties of aggregate were studied as per IS 2386-1963 (Part 1-6) [8] and Ministry of Road Transport and Highways (MoRTH) [4] specifications, to evaluate its performance. The results of testing parameters for aggregates are presented in Table 1.

4 Mix Design

The present work is performed on DBM Grade 1 and 2 and BC Grade 1 and 2 mix in accordance with the provisions of MoRTH. The aggregate gradation adopted is shown in Tables 2, 3, 4, 5, and 6. The gradation curve is shown from Figs. 1, 2, 3, 4, 5, 6, 7 to 8. The optimum binder content (OBC) for the above-mentioned bituminous mixes was found to be 5.25, 5.45, 4.05, and 4.5%, respectively, for BC-I, BC-II, DBM-I, and DBM-II using Marshalls' method for design of bituminous mixes.

Table 1 Properties of VSI and non-VSI aggregates

Property	Test performed	Method of test	Specifications as per MoRTH 2013	Test results	
				VSI aggregates	Non-VSI aggregates
Cleanliness (dust)	Grain size analysis	IS:2386 Part I	Max. 5% passing 0.075 mm sieve	0.78%	0.96%
Particle shape	Combined flakiness and elongation test	IS:2386 Part I	Max 35%	18%	28%
Strength	Aggregate impact test	IS:2386 Part IV	Max 27%	15%	21%
Water absorption	Water absorption test	IS:2386 Part III	Max 2%	0.61 (40 mm) 0.92 (20 mm) 1.2 (10 mm) 1.4 (6 mm) 2.9 (dust)	0.57 (40 mm) 0.84 (20 mm) 0.98 (10 mm) 1.2 (6 mm) 2.5 (dust)
Specific gravity	Specific gravity test	IS:2386 Part III	–	2.64 (40 mm) 2.64 (20 mm) 2.63 (10 mm) 2.62 (6 mm) 2.57 (dust)	2.64 (40 mm) 2.64 (20 mm) 2.63 (10 mm) 2.62 (6 mm) 2.57 (dust)
Stripping	Coating and stripping of bitumen aggregate mix	IS:6241	Minimum retained coating 95%	98%	98%

5 Resilient Modulus Test

Elasticity modulus/resilient modulus (MR) is an important parameter of any material regarding its utilization in building infrastructure. The slope of the stress–strain curve for a given material, within its linear elastic region, is defined as material stiffness. On the other hand, MR is defined as evaluation of the modulus of elasticity based on recoverable strain under repeated stress (loading). The MR value of bituminous mixes changes with change in its skeleton, material properties (aggregate gradation, type and percentage of bitumen, etc.), compaction, etc. The MR value is tested in laboratory as per ASTM D4123/EN 12697-26 [3, 9]. The test procedure involves application of peak-to-peak load along the diametrical plane whose intensity is determined from indirect tensile strength with measurement of deformations in the horizontal direction only. The Poisson’s ratio is adopted as 0.35. The height and

Table 2 Gradation of aggregate for BC Grade 1 for VSI and non-VSI aggregates

IS sieve size (in mm)	% Passing		Specified limits (as per MoRTH 2013)	
	VSI aggregate	Non-VSI aggregate	Lower	Upper
26.5	100	100	100	100
19	95.45	97.02	90	100
13.2	70.23	72.07	59	79
9.5	58.37	55.05	52	72
4.75	45.20	45.12	35	55
2.36	36.40	38.07	28	44
1.18	26.52	28.90	20	34
0.6	20.80	22.11	15	27
0.3	13.48	16.14	10	20
0.15	7.56	11.33	5	13
0.075	4.69	3.9	2	8

Table 3 Gradation of aggregate for BC Grade 2 for VSI and non-VSI aggregates

IS sieve size (in mm)	% Passing		Specified limits (as per MoRTH 2013)	
	VSI aggregate	VSI aggregate	Lower	Upper
19	100	100	100	100
13.2	97.50	100	90	100
9.5	77.64	73.76	70	88
4.75	60.25	58.21	53	71
2.36	48.68	50.06	42	58
1.18	42.10	38.67	34	48
0.6	30.70	30.06	26	38
0.3	24.50	21.21	18	28
0.15	15.60	13.52	12	20
0.075	7.48	5.08	4	10

diameter of the samples were measured using digital vernier callipers. The sample is conditioned at the desired temperature before the application of peak load for about 6 h. The peak load is applied at frequency 1 Hz with 0.1 s loading and 0.9 s rest period. The LVDTs measure the horizontal deformations of the sample. The resilient modulus is calculated from the following formula, and the test results for bituminous mixes prepared with VSI/non-VSI aggregates with different types of bitumen are presented in Table 6, respectively.

Table 4 Gradation of aggregate for DBM Grade 1 for VSI and non-VSI aggregates

IS sieve size (in mm)	% Passing		Specified limits (as per MoRTH 2013)	
	VSI aggregate	VSI aggregate	Lower	Upper
45	100	100	100	100
37.5	96.40	97.79	95	100
26.5	77.62	77.47	63	93
13.2	63.10	63.42	55	75
4.75	47.58	46.52	38	54
2.36	34.23	36.08	28	42
0.300	15.20	13.43	7	21
0.075	4.20	4.32	2	8

Table 5 Gradation of aggregate for DBM Grade 2 for VSI and non-VSI aggregates

IS sieve size (in mm)	% Passing		Specified limits (as per MoRTH 2013)	
	VSI aggregate	VSI aggregate	Lower	Upper
37.5	100	100	100	100
26.5	94.60	100	90	100
19	81.70	91.78	71	95
13.2	66.30	74.79	56	80
4.75	44.25	43.28	38	54
2.36	36.40	34.5	28	42
0.3	12.60	11.61	7	21
0.075	4.20	4.31	2	8

Table 6 Resilient modulus test results

S. No.	Type of mix	MR test result (MPa) at 35 °C					
		VG 30 bitumen		VG 40 bitumen		PMB 40 bitumen	
		VSI aggregates	Non-VSI aggregates	VSI aggregates	Non-VSI aggregates	VSI aggregates	Non-VSI aggregates
1	BC 1	1970	1740	2120	1980	2340	2190
2	BC 2	1980	1860	2350	2120	2420	2305
3	DBM 1	1850	1680	2260	2110	2310	2120
4	DBM 2	1910	1790	2370	2190	2480	2360

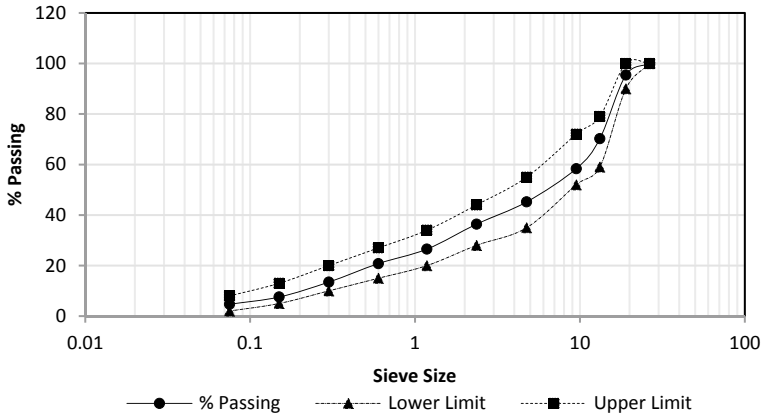


Fig. 1 Gradation curve for BC Grade 1 with VSI aggregates

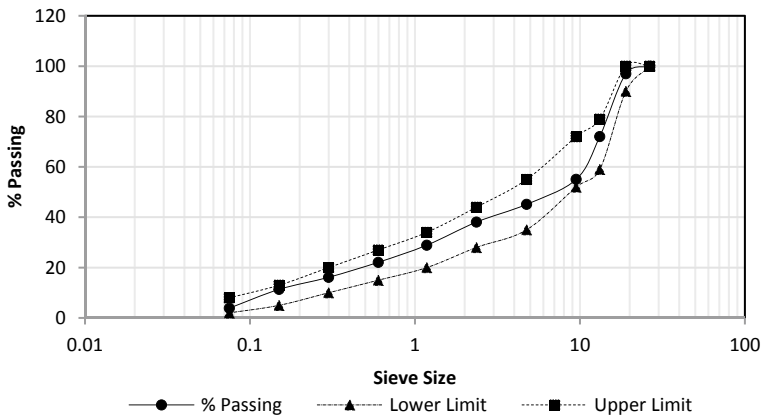


Fig. 2 Gradation curve for BC Grade 1 with non-VSI aggregates

$$M_R = \frac{P(0.23 + \mu)}{t \times \Delta h} \tag{1}$$

where

- P Peak load (N)
- t Sample thickness (mm)
- μ Poisson's ratio
- Δh Total horizontal deformation (μm)
- M_R Resilient modulus (MPa).

The resilient modulus test results are shown below in Table 6.

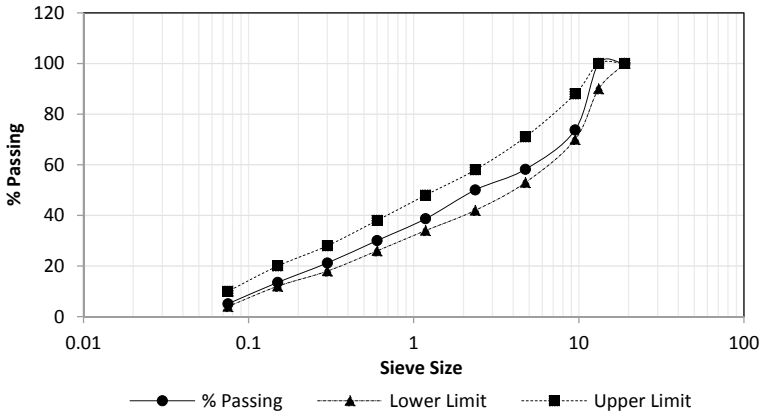


Fig. 3 Gradation curve for BC Grade 2 with VSI aggregates

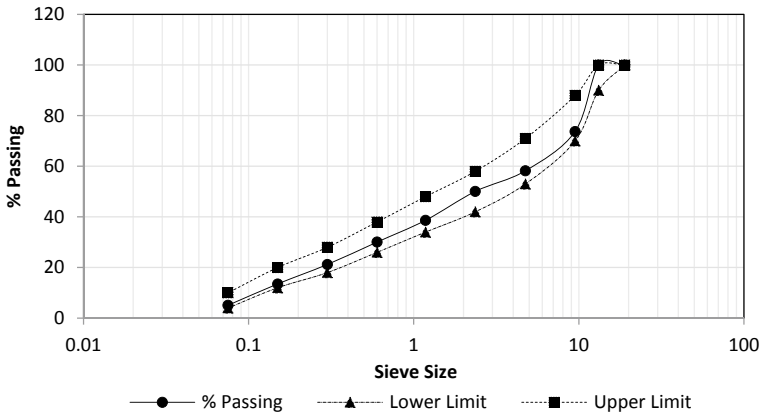


Fig. 4 Gradation curve for BC Grade 2 with non-VSI aggregates

6 Comparison of MR Test Results

The MR test results show that there is a comparable change in the elasticity modulus values in all the type of mixes. As the binder content increases, the MR value tends to increase. The bituminous mixes prepared with VSI crushed aggregates are showing better results in comparison with the non-VSI crushed aggregates. As the packing of the material changes to close grading, the MR value increase.

As specified in IRC 37-2018 [2], the MR value for bituminous mixes prepared with VG 30, VG 40, and PMB bitumen shall be 2000 MPa, 3000 MPa, and 1600 MPa, respectively, when tested at 35 °C. With respect to same, it can be seen that the MR test results to be comparable for VG 30 grade of bitumen. Figure 9 presents

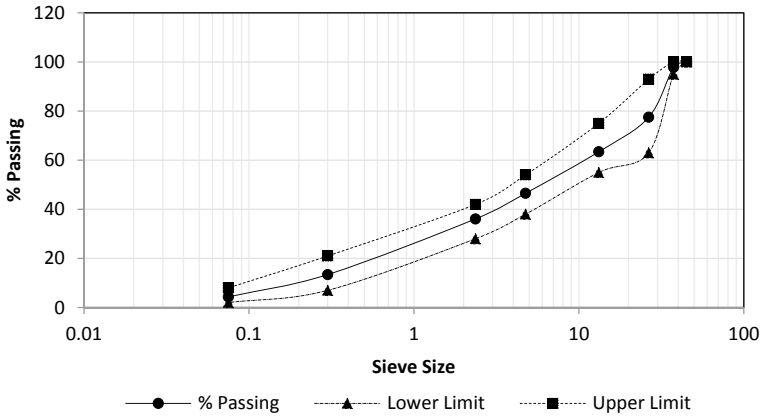


Fig. 5 Gradation curve for DBM Grade 1 with VSI aggregates

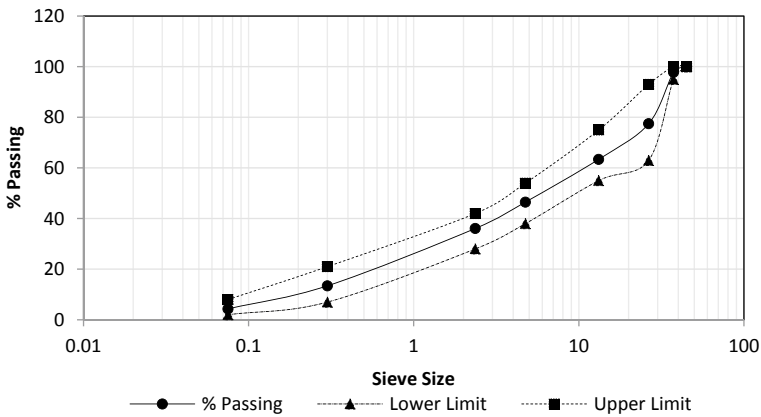


Fig. 6 Gradation curve for DBM Grade 1 with non-VSI aggregates

the comparison of MR test for different types of bituminous mixes prepared using different types of bitumen.

For mixes with VG 40 grade of bitumen, the MR value comes out to be much lesser than as specified 3000 MPa. And, for the mixes with PMB 40 bitumen, the MR value comes out to be much higher than 1600 MPa.

It is resulted that as the bitumen gets stiffer the elasticity modulus increases. The increase is more for the increased bitumen content. Also, as the packing of the aggregate mix gets proper, i.e. as the flakey and elongated aggregate reduced, the mix properties gets enhanced.

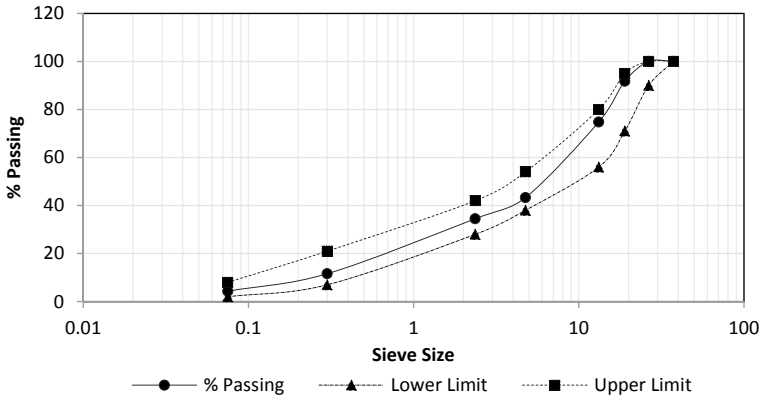


Fig. 7 Gradation curve for DBM Grade 2 with VSI aggregates

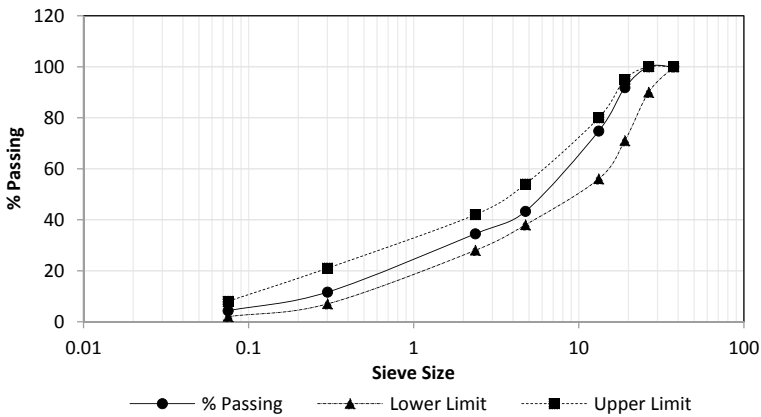


Fig. 8 Gradation curve for DBM Grade 2 with non-VSI aggregates

7 Conclusion

It is can be concluded that the MR value is an important and valuable parameter for the design purpose. The following are the vital points drawn from the study:

- The MR value changes with the percentage of binder content present in it.
- The MR is the combined property of bitumen and aggregate both as it is a viscoelastic material.
- With increase in viscosity of bitumen and bitumen content, MR value increases.
- The MR value of the mixes for PMB is comparatively greater than that with the VG grade bitumen.
- The properly shaped (VSI) aggregate shows better performance with respect non-VSI aggregates.

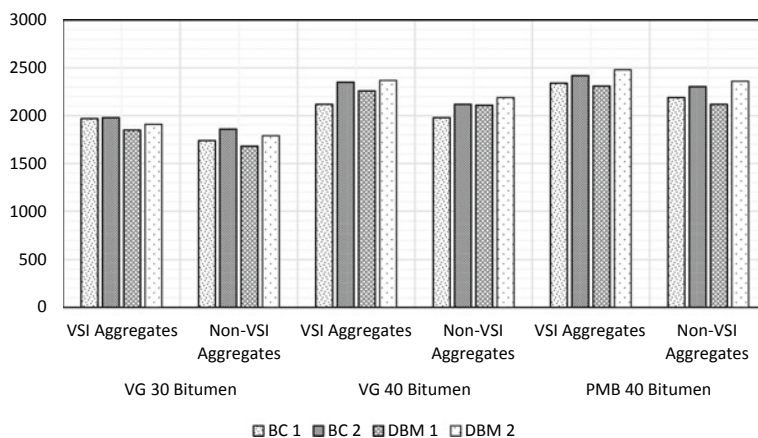


Fig. 9 Comparison of MR test for different types of mixes

- The MR value of bituminous mix with VG 40 grade of bitumen is not comparable to the value as provided in the guidelines. Also, for the mixes with PMB, the MR values come out to be more than as specified in the IRC 37. So, care should be taken whilst adopting the MR value for design.

8 Recommendation and Future Need

The increase in infrastructure construction is also affecting the environment which is leading towards the increase in the ambient temperatures. Considering the same, it is necessary to utilize the high viscous binder as per the temperature differences. There is a very little or few study available in the Indian environmental condition so it is of very much need to study about the elasticity modulus of the bituminous mixes prepared with high viscous bitumen besides adopting the particular value for design.

References

1. Tentative guidelines for the design of flexible pavements, 3rd revision, IRC 37. Indian Roads Congress, New Delhi (2012)
2. Guidelines for the design of flexible pavements, 4th revision, IRC 37. Indian Roads Congress, New Delhi (2018)
3. Standard test method for indirect tension test for resilient modulus of bituminous mixtures, ASTM D4123-82. American Society for Testing of Materials, USA (1995)
4. Ministry of Road Transport and Highway (2013) Specifications for road and bridge works- fifth revision. Indian Road Congress, New Delhi
5. Paving Bitumen- Specification, IS, No. 73. Bureau of India Standards, New Delhi (2013)

6. Polymer and Rubber Modified Bitumen- Specification, IS, No. 15462. Bureau of Indian Standards, New Delhi (2004)
7. Guidelines on the use of polymer modified binder specifications, IRC SP: 53. Indian Roads Congress, New Delhi (2010)
8. Methods of test for aggregates for concrete, Part 1, 3 and 4, IS, No. 2386. Bureau of Indian Standards, New Delhi (1963)
9. Bituminous mixtures test methods for hot mix asphalt, EN 12697 Part 26 stiffness. British Standard, UK (2004)